MACHINABILITY ANALYSIS OF DRILLING-INDUCED DAMAGE ON FIBRE-REINFORCED POLYMER COMPOSITES

Sikiru Oluwarotimi ISMAIL

PhD **August** 201**7**

MACHINABILITY ANALYSIS OF A DRILLING-INDUCED DAMAGE ON FIBRE REINFORCED COMPOSITES

by

SIKIRU OLUWAROTIMI ISMAIL

B.Eng. (Hons), M.Sc.

A thesis submitted to

The University of Portsmouth, England, United Kingdom

for the award of the degree of

DOCTOR OF PHILOSOPHY

School of Engineering, Faculty of Technology

The University of Portsmouth

August 2017

DECLARATION

I hereby declare that the research work presented in this thesis is original, to the best of my knowledge, understanding and belief, except as acknowledged within the text. The research was carried out in accordance with the rules and regulations of the University of Portsmouth and this report has neither been submitted in part nor in whole, for the award of any other degree in this or other university.

Name: Sikiru Oluwarotimi ISMAIL

Signature: 

Date: 24 – 08 - 2017

Word count: 56,891 (without ancillary data)

CERFIFICATION

I hereby certify that this research project was conducted by **Sikiru Oluwarotimi ISMAIL** under my thorough supervision and guidance. Therefore, it meets the requirements and standard that merits the award of **Doctor of Philosophy** (PhD) degree in Mechanical and Manufacturing Engineering, School of Engineering, Faculty of Technology, University of Portsmouth, England, United Kingdom.

……	……..
Dr Hom Nath DHAKAL	*Dr Ivan Eugeniev POPOV*
Director of Studies	Second Supervisor
……	……
Date	Date

…….

Prof Asa Barber

Head of School

……

Date

DEDICATION

This thesis is solely dedicated to the **Almighty God- the Author of life**, my late father and uncle in persons of Late Chief (Mr) Kareem Asekunola Ismail and Mr Omotola Aliu Ismail, respectively.

ACKNOWLEDGEMENTS

The humble author would like to deeply appreciate the Almighty Lord of heaven and earth, that rules and reigns in affairs of mortal man, created for His glory that through endowed wisdom, knowledge and understanding as well as gifts and talents His name may be praised among the living. His abiding power, supply, protection, love, mercy and caring throughout the duration of the Doctor of Philosophy degree programme in University of Portsmouth, England, United Kingdom, a place far away from home are gratefully acknowledged. He has proved His faithfulness and unalloyed supports throughout the programme, according to diversity of His names.

Gratitude remains the object of heart's memory which must be expressed, especially to those who their assistances and contributions in life have brought out desired dream of successes. Among these people are the first (Director of Study) and second supervisors in persons of Dr Hom Nath Dhakal and Dr Ivan Eugeniev Popov respectively, School of Engineering, Faculty of Engineering, University of Portsmouth, United Kingdom. The invaluable professional guidance, supervisory and mentoring skills of the Director of Study are uncommon, special, unparalleled and unalloyed. More also, the initial supervisions of Professor Eric Dimla and Dr James McMullen, before joining the Department of Mechanical Engineering, Institut Technologi Brunei, Brunei Darussalam and relocating to Australia respectively, are well acknowledged. Thank you (supervisors) very much for sharing your research experience and knowledge. I also appreciate the supports of both academic and non-academic staffs of the School of Engineering, University of Portsmouth, United Kingdom. Furthermore, my special, deepest and sincerest gratitude and appreciations are due to my dearest wife, Mrs Adenike ISMAIL for her love and total supports. I sincerely appreciate the parental love and supports of my family including, but not limited to, uncles, aunts, brothers, sisters (siblings) and their spouses. I am privileged to have you around me at every point of needs and throughout the journey.

In addition, I am indebted to the Niger-Delta Development Commission (NDDC) of Federal Government, Nigeria for the financial support under postgraduate overseas

scholarship award number NDDC/DEHSS/2013PGFS/OND/3. The author appreciates the provision of the study leaves with payment of monthly salary, granted by the University of Lagos, Akoka, Lagos State, Nigeria; the University of First Choice and Nation's Pride, as my employer, throughout the period of this PhD research. The incomparable supports of my Head of Department, Dean of Faculty of Engineering and Dr Sunday Joshua Ojolo (Associate Professor), among others are highly appreciated.

Also, I candidly acknowledge the helps rendered by Franc¸oise Berzin and Alain Lemaitre, INRA, France for the manufacture and provision of the fibre-reinforced polymer composite specimens. The technical supports of the technologists and technicians of the Schools of Engineering and Earth & Environmental Sciences, University of Portsmouth, United Kingdom as well as the technical crew of the D & T Precision Engineering Limited, Curbridge Botley, Hampshire, UK are significantly appreciated. The research collaboration and co-operation of Dr Anish Roy and Dr Dong Wang, Wolfson School of Mechanical and Manufacturing Engineering, Loughborough University, UK are highly thanked. Moreover, the technical and moral supports of Dr Saheed Olalekan Ojo and Ganiyu Soliu O., IMT School for Advanced Studies Lucca, Piazza San Francesco 19, 55100 Lucca, Italy, are gratefully appreciated. Pen-ultimately, my profound thanks are extended to the entire members of the Deeper Life Bible Church, Portsmouth and Borough Region, London, United Kingdom, especially the angels of the churches in Borough Region.

Lastly, all my PhD research and office mates in the School of Engineering and other schools are specially acknowledged. Thank you for helping me developing more inter-personal and research skills as we related together in the research offices and during Graduate School Development Programmes (GSDP) or workshops. Dear colleagues, thank you for being good friends and motivators. I look forward to seeing you all as a great achievers and successful researchers as we keep striving for an excellence in all things pertaining to life and godliness. Thank you all!

ABSTRACT

This research presents a comprehensive experimental investigation on the machinability effects of variable drilling parameters (feed rate, cutting speed and thrust force), drill diameters and chips formation mainly on delamination and surface roughness, in addition to other drilling-induced damage on both natural and synthetic fibre reinforced polymer (FRP) composites: hemp fibre reinforced polymer (HFRP) and carbon fibre reinforced polymer (CFRP) composite laminates respectively, using double-fluted coated high speed steel (HSS) drills under dry machining and compressed air cooling conditions. It also describes a thermo-mechanical models for predicting and analysing onset push-out delamination during FRP composite machining.

After a broad and critical literature survey on FRP composites and their drilling has been carried out, three principal stages of experimental, and an analytical works were conducted to investigate and analyse the influence of both conventional drilling (CD) and ultrasonically-assisted drilling (UAD) techniques on different specimens of HFRP and CFRP composites. Stage 1 involved the CD of 5 specimens of 197 x 197 mm, 7.5 mm thickness HFRP composite laminates of aspect ratios (AR) of 00 (neat), 19, 23, 30 and 38, using diameter holes of 5.0 and 10.0 mm for delamination and surface roughness respectively, among other drilling-induced damage. Taguchi's technique was used in the design of experiment. The results obtained show that increase in cutting speed reduced delamination factor and surface roughness of drilled holes. However, increase in feed rate caused an increase in both delamination factor and surface roughness. Feed rate and cutting speed had the greater influence on delamination and surface roughness respectively, when compared with aspect ratio, while an increase in fibre AR caused a significant increase in both delamination factor and surface roughness. The optimum results occurred at cutting speed and feed rate (drilling parameters) of 20 mm/min and 0.10 mm/rev, respectively, when drilling specimen of AR 19.

The stage 2 experiment described a comprehensive investigation on the machinability effects of CD parameters, drill diameters and chips formation on the same drilling-induced damage on an optimal specimen of 19-HFRP and MTM 44-1/CFRP composite laminates, using the same specimen dimensions, drills, drilling parameters and condition. The results obtained depict that an increase in feed rate and thrust force caused an increase in delamination and surface roughness of both specimens, different from cutting speed. But HFRP and CFRP specimens have greater surface roughness and delamination-drilling damage respectively. Also, increased drill diameter and types of chips formation caused an increase in both delamination and surface roughness of both specimens as the material removal rate (MRR) increased. Evidently, the minimum surface roughness and delamination factor of the two specimens for an optimal drilling are associated with feed rates of 0.05-0.10mm/rev and cutting speed of 30m/min. Stage 3 of the research focused on the benefits of UAD technique compared with the CD, initially on the first 5 hemp fibre/thermoplastic polycaprolactone (HF/PCL) composite specimens under similar drills, drilling parameters and condition. The results obtained show that UAD technique further confirmed and validated the optimal performance of specimen with AR of 19 (19-HF/PCL) composites, because of the minimum value of thrust force and machining time recorded, when compared with other aspect ratios and CD technique. The 19-HF/PCL laminate has maximum thrust force of 90N and 75N during UAD and CD respectively, which were the lowest force reduction at minimum drilling-induced damage, with the lowest machining time of 30 seconds for both. But comparatively, an improved drilled holes, optimal drilling and nearly 40 % of an average drilling forces (thrust and toque) reduction were recorded with UAD of hemp fibre/thermoset vinyl ester (HF/VE) composite specimens, when compared with both CD and HF/PCL specimens, respectively.

Conclusively, the stage 4 addressed the theoretical aspect of this research through application of analytical method. Hence, in this last stage, an analytical thermo-mechanical model is proposed to predict critical feed rate and critical thrust force at the onset of delamination crack on CFRP composite cross-ply laminates, using the principle of linear elastic fracture mechanics (LEFM), laminated classical plate theory (LCPT), cutting

mechanics and energy conservation theory. The delamination zone (crack opening Mode I) is modelled as an elliptical plate. The advantages of this proposed model over the existing models in literature are that the influence of drill geometry (chisel edge and point angle) on push-out delamination are incorporated, and mixed loads condition are considered. The forces on chisel edges and cutting lips are modelled as a concentrated (point) and uniformly distributed loads, resulting into a better prediction. The model is validated with models in the literature and the results obtained show the flexibility of the proposed model to imitate the results of existing models. Evidently, it can be summarily concluded that the quality of the drilled holes and total machinability of the FRP composites depend on the nature and properties of the composite specimens, drill designed geometry, drilling parameters, conditions and techniques.

TABLE OF CONTENTS

LIST OF FIGURES

LIST OF TABLES

NOMENCLATURE

$\underline{Q}_{ij}$: Elements of the transformed stiffness matrix

$\mathrm{v_i}$: Volume fraction of the fibre and matrix (%)

$[D]$: Elements of the bending stiffness matrix

E_i : Modulus of the fibre and matrix (*MPa*)

G_{IC} : Critical strain energy release rate for delamination (J)

G_c : Critical energy absorbed due to delamination propagation (J)

P^* : Critical thrust force (*N*)

P_L : Thrust force due to the uniformly distributed loads (*N*)

P_c : Thrust force due to the concentrated load (*N*)

U_L : Strain energy due to uniformly distributed loads (*J*)

U_c : Strain energy due to concentrated load (*J*)

W_L : Virtual work due to uniformly distributed loads (*J*)

W_c : Virtual work due to concentrated load (*J*)

f^* : Critical feed rate (mm/rev)

k_L : Specific energy at the cutting lips (*J*)

k_c : Specific energy at the chisel edge (*J*)

q_L : Uniformly distributed loads (*N*)

q_c : Concentrated load (*N*)

v_i : Poisson's ratio of the fibre and matrix

w_L : Deflection due to uniformly distributed load (*mm*)

α_1 : Coefficient of thermal expansion in the longitudinal direction (*/K*)

α_2 : Coefficient of thermal expansion in the transverse direction (*/K*)

α_x : Coefficients of thermal expansion in the x direction

α_y : Coefficients of thermal expansion in the y direction

γ_L : Average rake angle (^{o})

γ_c : Average chisel edge rake angle (^{o})

ε_0 : Reference point angle (^{o})

b : Size of the elliptical delaminated zone along the minor axis (*mm*)

d : Diameter of the fibre (*mm*)

D : Drill diameter (*mm*)

D_{max} : Maximum diameter of the delamination zone (*mm*)

D_o : Drilled hole diameter (*mm*)

E : Modulus of elasticity (*GPa*)

f : Feed rate (*mm/rev*)

F_c : Critical force (*N*)

F_d : Delamination factor, $\frac{D_{max}}{D}$

G_{IC} : Energy release rate (J/m^2);

h : Thickness of the uncut ply under the drill bit (*mm*)

H : Composite laminate thickness (*mm*)

K : Thermal conductivity (W/m^oC)

l : Length of the fibre (mm)

R_a : Average surface roughness (μm)

R_{max} : Maximum surface roughness (μm)

TD : Tool diameter (mm)

T_g : Glass transition temperature (^oC)

T_m : Melting temperature (^oC)

v : Poisson's ratio

V : Cutting speed (m/min)

VBB_{max} : Maximum flank wear (mm)

δU : Strain energy variation (J)

π : Constant (3.142)

σ : Tensile strength (MPa)

G : Strain energy release rate (J)

P : Total thrust force (N)

W : Total virtual work (J)

a : Size of the elliptical delaminated zone along the major axis (mm)

k : Laminate

β : Ratio between ε and ε_0

γ : Chisel edge ratio

δU_d : Energy absorbed due to delamination propagation (*J*)

δA : Infinitesimal increase in the delamination area (mm^2)

ε : Arbitrary point angle (^{o})

η : Ellipticity ratio, $\frac{a}{b}$

$\theta(z)$: Temperature variation along the thickness (*K*)

LIST OF ABBREVIATIONS

ANOVA	:	Analysis of variance
AR	:	Aspect ratio
AWJ	:	Abrasive waterjet
BS	:	Balzers
CAD	:	Computer aided design
CC	:	Cemented carbide
CCC	:	Coated cemented carbide
CD	:	Conventional drilling
CFRC	:	Carbon fibre reinforced composite
CFRP	:	Carbon fibre reinforced plastic
CMM	:	Coordinate Measuring Machine
CN	:	Cemecon
CNC	:	Computer numerically controlled
CrN	:	Chromium nitride
CT	:	Computed tomography
CVD	:	Chemical vapour deposition
DCC	:	Diamond coated carbide
DLC	:	Diamond-like carbon
EDM	:	Electroplated diamond micro

EP	:	Epoxy resin
ESC	:	Electro-spark coating
Exp. SS	:	Expected sum of squares
FEA	:	Finite element analysis
FIS	:	Fuzzy inference system
FRP	:	Fibre reinforced polymer
GFRC	:	Glass fibre reinforced composite
GFRP	:	Glass fibre reinforced plastic
HAZ	:	Heat affected zone
HFRP	:	Hemp fibre reinforced polymer
HNF	:	Hemp natural fibre
HSS	:	High speed steel
ICM	:	Inverse coefficient matrix
LEFM	:	Linear elastic fracture mechanics
MMC	:	Metal matrix composite
MMCs	:	Metal matrix composites
MRR	:	Material removal rate
MTM	:	Medium Temperature Material
NFRC	:	Natural fibre reinforced composite
OA	:	Orthogonal array
OM	:	Optical microscope/microscopy

OoA	:	Out of autoclave
PCBN	:	Polycrystalline cubic boron nitride
PCD	:	Poly-crystalline diamond
PCL	:	Polycaprolactone
PM HSS	:	Powder metallurgical high-speed steel
PMC	:	Polymer matrix composite
PVD	:	Physical vapour deposition
SEM	:	Scanning electron microscope/microscopy
SS	:	Sum of squares
TiAlN	:	Titanium aluminium nitride
TiN	:	Titanium nitride
TiN(C, N)	:	Titanium carbonitride
UAD	:	Ultrasonically-assisted drilling
UC	:	Uncoated carbide
UCC	:	Uncoated cemented carbide
UD	:	Unidirectional
VE	:	Vinyl ester

DISSEMINATION

A list of academic and scholarly publications that came out from the research is highlighted.

List of publications and awards

A. Journal Articles

- **Sikiru Oluwarotimi Ismail**, Saheed Olalekan Ojo, Hom Nath Dhakal. (2017). Thermo-mechanical modelling of FRP cross-ply composite laminates drilling: Delamination damage analysis. *Composites Part B: Engineering, 108*, 45-52.

- **Sikiru Oluwarotimi Ismail**, Hom Nath Dhakal, Eric Dimla, Johnny Beaugrand, Ivan Popov. (2016). Effects of drilling parameters and aspect ratios on delamination and surface roughness of lignocellulosic HFRP composite laminates. *Journal of Applied Polymer Science, 133* (7), 1-8.

- **Sikiru Oluwarotimi Ismail**, Hom Nath Dhakal, Eric Dimla, Ivan Popov. (2016). Recent advances in twist drill design for composites machining: A critical review. *Proceedings of Institution of Mechanical Engineers, Part B: Journal of Engineering Manufacture*, 1-16.

- **Sikiru Oluwarotimi Ismail**, Hom Nath Dhakal, Ivan Popov, Johnny Beaugrand. (2016). Comparative study on machinability of sustainable and conventional fibre reinforced polymer composites. *Engineering Science and Technology, an international Journal, 19*(4), 2043-2052.

- **Sikiru Oluwarotimi Ismail**, Hom Nath Dhakal, Anish Roy, Dong Wang, Ivan Popov. (2016). Machinability analysis of bio-composite: Conventional versus ultrasonically-assisted drilling. *Composites Part A: Applied Science and Manufacturing* (under review).

B. Conference Proceedings

- **Sikiru Oluwarotimi Ismail**, Hom Nath Dhakal, Anish Roy, Dong Wang, Ivan Popov. (2016). Machining of FRP composite laminates with conventional and ultrasonically-assisted drilling techniques: A comparative and experimental investigation. *Proceedings of the ASC 31st Technical Conference and ASTM Committee D30 Meeting,* September 19-22, Williamsburg, Virginia, USA.

- **Sikiru Oluwarotimi Ismail**, Hom Nath Dhakal, Ivan Popov, Johnny Beaugrand. (2016). Analysis and impacts of chips formation on hole quality during fibre-reinforced plastic composites machining. *Proceedings of the 14th International Conference on Manufacturing Research (ICMR 2016), incorporating the 31st National Conference on Manufacturing Research,* September 6-8, 2016, pp. 143-148, Loughborough University, Loughborough, Leicester, United Kingdom.

- **Sikiru Oluwarotimi Ismail**, Hom Nath Dhakal, Ivan Popov, Johnny Beaugrand. (2015). Experimental analysis of drilling-induced damage of lignocellulosic 19/hemp fibre-reinforced polycaprolactone and MTM 44-1/carbon fibre reinforced epoxy resin composites. *Proceedings of 5th Conference on Natural Fibre Composites for Industrial Applications,* 15-16 October 2015, pp. 1-6, Sapienza Universiti di Roma, Rome, Italy.

C. Edited Book Chapter

- **Sikiru Oluwarotimi Ismail** & Hom Nath Dhakal. (2017). Philosophical study on composites and their drilling techniques. *Functional Biopolymers.* Berlin, Germany: Springer Publisher (final acceptance for publication).

D. Awards

- June 2017: Paper Prize - First Place, Faculty of Technology, University of Portsmouth, England, United Kingdom.
- May 2017: Best Student Paper Award in the School of Engineering, Faculty of Technology, University of Portsmouth, England, United Kingdom.

- August 2016: Doctoral Assistance Grant, awarded by Faculty of Engineering, University of Lagos, Lagos State, Nigeria.
- June 2016: Journal Paper Price-Highly Commended, awarded by the Faculty of Technology at the Annual Faculty Research Conference, University of Portsmouth, England, United Kingdom.
- June 2014 - 2016: Partial Funding as a Representative of University of Portsmouth, England, United Kingdom, ICONS 2014, 2015 and 2016 Conferences.
- October 2013 - September 2016: Beneficiary of Niger-Delta Development Commission (NDDC) Overseas PhD Scholarship, Federal Government of Nigeria, Nigeria.

PART I

INTRODUCTION

CHAPTER ONE

INTRODUCTION

1.0 Introduction

This is the first chapter that introduces the content, focus and structure of the research. It discusses the background of the study, statement of problems, aims and objectives of the study, scope of the research, relevance (justification) and implication of the research, contributions to the knowledge (research novelty) and lastly, the structure of the entire thesis.

1.1 Background to the research

The kinematics of drilling is a process of using a rotating drill bit to create or enlarge existing round holes in a fibre-reinforced polymer (FRP) composite or workpiece. Drilling is one of the most frequently processes used in manufacturing industry among machining operations. It takes a considerable total machining time and operations of a manufacturing process. It is a preliminary step for many other machining operations, such as reaming, tapping and boring. Drill, as a rotary end cutting tool, has one or more cutting lips and flutes for the release of chips and the access of a cutting fluid. Presently, drill bits are the most frequently and extensively used material cutting tools (Faraz, Biermann & Weinert, 2009; Khashaba et al., 2010b; Ismail et al., 2016b; Ismail et al., 2016e; Ismail et al., 2017).

1.1.1 Composite materials and technology

Recently, there has been growing interest in the composite materials and technology. The composites technology has enabled the production of outstanding FRP composites with respects to better damage tolerance, impact resistance, toughness, sustainability, renewability, strength, electromagnetic transparency, biodegradability, environmental superiority, cost and ease of productions, part count reduction, stiffness, design flexibility, low weight, mechanical damping, strength properties as well as chemical, thermal, corrosion and wear resistance when compared with the conventional metallic

engineering materials. The conventional homogeneous materials such as metals and alloys can not only satisfy the growing demands on product capabilities and performance effectively, due to demand for an improved properties towards advancement in products design and materials engineering. Therefore, the FRP composites with better properties and desirable applications emerged. These enhanced qualities of the FRP composites have emphasised the crucial need for analysing their machinability for further improvement of performances and applications (Oksman, 2000; Faruk et al., 2012; Dhakal et al., 2015; Baghaei & Skrifvars, 2016; Bakare et al., 2016; Andrew et al., 2016; Ismail et al., 2016c.

In addition, the desirable general inherent and better properties of FRP composite materials have increased the areas of application of these heterogeneous materials as both functional and structural components. These areas of application include telecommunication, automotive, oil and gas, building and construction, sports and recreation, aviation, biomedical, marine, electronics, defense or military, power generation, food and packaging industries. Moreover, the environmental and economic global treats today have called for the production of natural fibre reinforced, bio-resourced and sustainable composite materials. Consequently, the attention of many product manufacturers has shifted to natural fibre reinforced composites (NFRC) due to the unease of production and increased tool wear from the use of synthetic or conventional fibre-reinforced composites (CFRC), due to the greater hardness and abrasiveness of CFRC.

One of the prominent types of NFRC is hemp fibre reinforced polycaprolactone composite. However, the application of some synthetic fibre reinforced composites has not been totally replaced with the natural fibre reinforced composites in engineering structures, because of the remarkable properties of the conventional FRP composites which include, but are not limited to, relative high tensile and impact strengths, strong fibre-matrix interface adhesion and high melting points. The hemp fibre is a bast lignocellulosic natural fibre, reinforced with a biodegradable thermoplastic and thermoset matrices, known as polycaprolactone (PCL) and vinyl ester (VE) separately, respectively. The carbon fibre is an inorganic and synthetic fibre, reinforced with a non-biodegradable thermoset matrix, known as Epoxy resin (EP). Therefore, the hemp fibre reinforced polymer

(HFRP) is an example of a natural (sustainable) fibre reinforced composite, while carbon fibre reinforced polymer (CFRP) is referred to as synthetic (conventional) composite. These (HFRP and CFRP) composites are the two main samples used as an experimental workpiece throughout this study (Ismail et al., 2015; Ismail et al., 2016a; Ismail et al., 2016c).

1.1.2 Composite machining (Drilling techniques)

After many decades of developments of FRP composites manufacturing (machining) technology with aid of a conventional drilling (CD) technique, the desire to improve the machining of these materials based on the numerous areas of application remains a challenge. This brought about the invention of the ultrasonically-assisted drilling (UAD) technique. The UAD is a non-traditional technique which involves the superimposition of a high frequency and low amplitude vibration, usually greater than 18 kHz and less than 20 µm respectively, on a drill bit along the feed direction when cutting (drilling) the workpiece under a certain drilling parameters and conditions. The CD is a traditional method whereby drilling is performed in the absence of frequency and amplitude vibration on the drill bits. The UAD reduces the drilling forces (thrust force and torque) better than the CD technique. Drilling force reduction improves the quality of the drilled holes, reduces power consumption rate and cost of production. However, UAD technique attracts greater expensiveness of experimental set-up, unpredicted results and chipping effects when compared with the CD. Both CD and UAD techniques are adopted during this study under a range of selected drilling parameters and dry machining environment. The vertical and horizontal drilling orientations were considered, based on the manufacturers' configuration of the computer numerical control (CNC) drilling machine centres used.

More also, a double-fluted uncoated high speed steel (HSS) drill bits of different diameters are utilised. The choice on the use of HSS drills is based on their availability, low cost and highest toughness, making them the most widely used tooling materials. The Taguchi and analytical methods are used for the design of experiment and theoretical analysis respectively. Taguchi is one of the latest machining optimisation techniques. It enhances job quality, saves experimental time and cost. The application of analytical

method has several benefits. Implementing this method in this research work increases the rate of understanding the mechanism of drilling and composite materials under a specified conditions. Similarly, it saves time, cost, materials and other resources when analysing performance and possible modifications, as an effective predictive analytical tool.

1.2 Problem Statement

The quality and the integrity of the holes obtained during drilling of various fibre reinforced composite laminates are quite different from that of drilled metals. The drilled metal surfaces are smoother and more regular than the drilled FRP composite surfaces under the same conditions, due to the abrasive nature, heterogeneity and anisotropy of the FRP composite materials. In addition, the combination of the poor thermal conductivity of the resin matrix as well as the tough and abrasive properties of some FRP composites cause their poor machinability. The effects of these properties on a drilled composites result in some severe drilling-induced damage, which include delamination, surface roughness, crack development, stress concentration, fuzzing, drill edge chipping and excessive wear, spalling, fibre uncut and pull-out, matrix sintering or burning and de-bonding. Among these damage, the delamination and surface roughness defects are the most critical flaws on drilled composite materials. Therefore, they are mainly considered in this research work.

Delamination is simply defined as the main form of failure of laminated composites whereby the laminates or layers separate along their interfaces. Delamination sometimes forms as a crack between the adjacent plies, it occurs often between two anisotropic and heterogeneous materials as an interface crack. Furthermore, it occurs under a tensile loading, bending loads, but it grows mostly under the critical compressive and fatigue loading conditions. Delamination is principally caused by an increase in feed rate and drilling forces (thrust and torque), unlike cutting speed, among other drilling parameters. Meanwhile, surface roughness is defined as the average mean of the deviation of the roughness profile from the average line within the estimated length. Surface roughness is a very vital quality in a drilled hole, because mechanisms of creep, wear, fatigue and corrosion depend on it.

Furthermore, due to the accurate solutions relevant to the application of an analytical method, when compared with the other approaches used in analysing theories of material failure such as numerical and finite element methods, an analytical method was adopted for further prediction and analysis of delamination drilling-induced damage on FRP composite laminates. The numerical method is approximate, while analytical is exact. Therefore, to eliminate the problem of delamination in drilling, calculation of the critical thrust force below which no damage occurs is important. To achieve this, classical plate theory approach is employed and assumption of linear elastic fracture mechanics (LEFM) mode I is invoked to determine the amount of work required to initiate and cause propagation of delamination drilling-induced damage in the composite laminates. In an attempt to simplify calculation of the critical thrust force, many analytical models in the literature focus more on the mechanics of the FRP composite laminates while ignoring the role of drill characteristics such as drill point geometry (drill diameter, rake angle, chisel edge angle), cutting mechanism, chip formation and cutting parameters such as feed rate, among others. In addition, the effect of machining temperature which may influence drilling damage is usually not accounted for. Properties of laminate composites are usually affected by high temperature and since drilling operation is associated with thermo-mechanical deformation, a theoretical model which accounts for critical thrust force with thermal effect is desirable.

While much research has concentrated on synthetic or conventional composites, but very little is known about the machinability of natural or sustainable FRP composites. Also, an improved analytical approach and comprehensive experimental studies of these two classes of composites; mainly on the material samples considered under the same CD and UAD parameters and condition, are very rare and scarce. Hence, this research presents the results of an experimental and theoretical analysis of the effects of some variable drilling parameters (feed rate, thrust force and cutting speed), drill designed geometry (chisel edge, cutting lips and diameters) and types of chips formation mainly on delamination and surface roughness in addition to other associated damage on the samples of HFRP and CFRP composite laminates, using Taguchi technique of design of experiment and analytical approach.

1.3 Aims and objectives of the study

1.3.1 Aim

The aims of this present research was to experimentally and analytically analyse the machinability of a natural (hemp) and conventional (carbon) fibre-reinforced polymer (FRP) composites as well as the causes of their drilling-induced damage, for the purpose of optimising the FRP composites drilling.

1.3.2 Objectives

The stated aims were successively implemented through the following highlighted objectives. Therefore, the specific objectives of the study were to:

i. Conduct a comprehensive and critical state-of-the-art review on FRP composite laminate materials and drilling of FRP composites;
ii. Conduct drilling operation experimentally and investigate damage characterisation of natural (hemp) and synthetic (carbon) fibre-reinforced polymer (thermoplastic and thermoset) composites;
iii. Carry out comprehensive study on drilling-induced damage on the two FRP composites using conventional and ultrasonically-assisted drilling (CD and UAD) techniques;
iv. Characterise the damage responses statistically and microscopically in an attempt to investigate and determine the causes of the drilling-induced damage on the FRP composites;
v. Develop predictive analytical thermo-mechanical models for the main drilling parameters and drill bit geometry, in order to clearly analyse the delamination drilling-induced damage; and
vi. Validate the proposed models and optimise the drilling operation.

1.4 Scope of the research

This research is broadly divided into two main sections: the experimental and the analytical. The analytical approach is based on the principle of linear elastic fracture

mechanics (LEFM), laminated classical plate theory, cutting mechanics and energy conservation theory. While, the experimental part comprises of three related stages. The two major classifications of FRP composite were used as samples. These include the natural (HF/PCL and HF/VE) and synthetic (CF/EP) composite laminates, with dimension of 197mm x 197mm, and 5.0mm and 7.5mm thicknesses.

This research is limited to the wide application of two drilling techniques. These techniques are conventional and non-conventional drillings. The conventional drilling (CD) involves the use of both vertical and horizontal drilling orientations only, while the non-conventional drilling attracts the ultrasonically-assisted drilling (UAD). The UAD was performed only on horizontal orientation due to the design configuration of the Computer numerically controlled (CNC) machine centres.

The double-fluted uncoated HSS drill bits were used throughout the experimental and theoretical works with dry machining condition, while the diameter of the drills and drilling parameters were varied. Also, drilling was performed with support pre-drilled aluminium plate at the back of the composite samples, to minimise the possibility of occurrence of push-out delamination drilling-induced damage. All drilling exercises was performed under dry machining environment.

The validation of the proposed analytical thermo-mechanical models was carried out using the data available in latest literature. Also, these data are relevant to the CFRP composite laminates because of the unavailability of the data for the natural, especially hemp fibre (both HF/PCL and HF/VE) reinforced polymer composites.

1.5 Relevance (Justification) and implication of the research

Drilling takes an indispensable role among the principal machining operations which include, but are not limited to, milling, turning and boring. Drilling is a final process during assembly stage of manufacturing processes. It attracts an average of 50 % of the total material removal operations (Isbilir & Ghassemieh, 2011; Yang & Sun, 2009). For instance, in the Airbus A350 aircraft, an estimate of about 55,000 holes are reported to have been

drilled to assemble the numerous intricate parts of the aircraft (Faraz et al., 2009). Also, more than 100,000 and 1 million holes are required for the assembly of a small single engine and a large transport aircrafts respectively (Khashaba et al., 2010a). With an advent of several modern manufacturing technology, many composite materials can be produced into a near-net shape, excluding the application of several machining operations, with an exception of a drilling operation. Drilling operation is inevitably and indispensably required during mating of engineering components, commonly referred to as an assembling or coupling, and installation stages of engineering activities. Therefore, the choice of drilling is hereby justifiable.

The CD and UAD techniques were used under experimental section, while analytical approach was also conclusively employed. CD has a very cheap cost of operation when compared with other non-conventional techniques. However, due to its adverse effect on some FRP composite materials, it was comprehensively studied concomitantly with the UAD. UAD has a better performance, though it requires huge capital investment to set-up, as an advanced technology. Also, high power consumption with unpredictable results are often gotten from the application of UAD technology, coupled with the misunderstanding of the working process and high rate of tool wear resulting from chipping effects, consequently leading to premature tool (drill) failure. Notwithstanding, UAD advantages supersedes its setbacks, especially in FRP composite drilling technology.

These benefits include ability to drill any type of materials, irrespective of their electrical conductivity, UAD can be used to machine hard materials of 40 HRC to 60 HRC like carbides, ceramics, and industrial diamonds, aspect ratio of about 40:1 can be achieved using UAD, holes of 76micron diameter with 51mm depth can be conveniently drilled, it produces better surface integrity and finish, absence of thermal, electrical and chemical effects is possible with use of UAD, and it can be simultaneously used with other non-conventional techniques such as electrical discharge drilling (EDD) technique (Thomas & Babitsky, 2007). There is an ease and possibility of interchanging of drilling techniques between CD and UAD on a single CNC drilling machine centre and on same material.

The quest of having materials with improved properties and structures of better load bearing capacity in the fields of materials science and engineering respectively, produced

the FRP composite materials of enhanced properties and for numerous applications. The application of FRP composite cuts across almost all facets of human endeavours. The structural performance of the synthetic CFRP composites is great, especially in transportation (automobile, marine and aerospace) sector. In other hand, recently, the applications of natural fibres as reinforcements in polymer composites are seriously considered in addition to the synthetic reinforcements such as carbon and glass fibres. These are based mainly on the sustainability, lower cost of production (lesser energy consumption), environmental friendliness due to the biodegradability and lower CO2 emission, greater modulus-weight ratio of natural fibre-reinforced polymer (NFRP) composites, among others, when compared with synthetic composites. In addition, based on the directive issued by the European Union requires that the greatest percentage of 85 %, followed by 10 % and just only 5 % of all new automobiles should be reusable (recyclable) by weight, for energy recovery and used in landfills respectively, starting from year 2015 (Paul, Kanny & Redhi, 2015). These enhanced properties, increasing application of the FRP composites and government directives have emphasised the need for a clear and deeper understanding of their machinability in order to further improve their functionality and applicability. Hence, these reasons have necessitated the choice of the composite materials (samples) used during this research study.

Lastly, delamination and surface roughness have been reported as most crucial drilling-induced damage on FRP composite materials. Also, up to 60 % reject of drilled composite products has been recorded at the stage of assembly of machined products, due to the delamination drilling-induced damage (Sakthivel et al. 2015; Ismail et al., 2016b). Therefore, revelation of optimal drilling parameters and conditions at which delamination could be drastically controlled or reduced, and proposed analytical thermo-mechanical models for the concerned FRP composites are of great academic relevance and industrial application. The models are capable of predicting minimum critical thrust force and critical feed rate under which delamination will not occur. Furthermore, the effects of drill bit geometry (chisel edge and cutting lips) and mixed (concentrated and uniformly distributed) loads considered on push-out delamination are also very important to researchers,

designers, manufacturers (manufacturing companies) and users of drill bits for FRP composite drilling.

1.6 Contributions to knowledge (research novelty)

Prior to the commencement of this experimental and analytical study on machinability analysis of drilling-induced damage on FRP composites, a wide comprehensive and critical state-of-the-art (review) on recent advances in twist drill design for composites drilling was conducted. The geometry, material and parametric drill design methods and their inherent challenges confronting composites machining are well discussed. The inter-dependable effects of thrust force, cutting speed, feed rate, cutting force and torque on drill designs are similarly reviewed in addition to the associated issues facing composites drilling include, but are not limited to, delamination, surface roughness, rapid tool wear and drill breakage. Well-designed drill geometry and good knowledge of drilling parameters afford the producers of polycrystalline diamond (PCD), Carbide and HSS tooling materials better opportunity of developing a drill that will minimise delamination of the reinforced composites, tool wear and produce a high quality surface. Twist drill designers, researchers, manufacturers and users stand to benefit from this research work as they seek to have well designed, improved drills and optimal drilling operation. Additionally, several manufacturing companies that use drill bits tend to be frequently patronised and hence, demand for more drill bits. Consequently, this will lead to high productivity and profitability.

In addition to the above highlighted contributions from the critical review of literature conducted, the following contributions both from the main experimental and theoretical works are thus stated:

- This research study presents a novel results of the effects of aspect ratios of natural (hemp) FRP composites on drilling-induced damage. These damage include the delamination effect, surface roughness, matrix melting or burning, fibre-uncut and pull-out, burrs formation and drill wear. The optimal drilling parameters, conditions and composite sample were determined.

- Several research works have been conducted on drilling of different types of synthetic composites, as shown in the next chapters of literature review, but much is neither yet reported nor known about the machinability of natural or sustainable FRP composite materials. Also, a comprehensive experimental study on drilling of both natural (hemp) and conventional (carbon) FRP composite material samples under the same drilling parameters and condition, is very rare and scarce. This is germane in order to draw a similarity and difference between them. To bridge these research gaps, this research work presents the results obtained from an experimental investigation on the influence of drilling parameters, drills diameters and types of chips formation principally on delamination and surface roughness drilling-induced damage on these samples.
- Furthermore, a thorough and comprehensive study on the influence of the CD and UAD techniques on two different natural (hemp) FRP composites are clearly revealed in this study. Hence, the limitations of each of these techniques and samples were found, at different specific drilling parameters, in terms of their response to the considered drilling-induced damage. The choice of technique for drilling and engineering application of these composite materials (samples) are based on their responses.
- The effects of the main compositions (matrices and fibres) of FRP composites on drilling operation and techniques has not been extensively studied. Therefore, the relevance of the composite constituents, mainly hemp and carbon fibres as well as polycaprolactone and vinyl ester matrices is experimented in this research work. The presence of polycaprolactone (PCL) matrix in HFRP composites resulted into poor machinability, particularly during UAD due to the high drill-composite interface temperature generated during drilling operation. Moreover, the low melting and glass transmission temperatures of PCL and decomposition temperature of hemp FRP composites were responsible for the poor performance. However, vinyl ester (VE) supported a better drilling performance in terms of higher hole quality and reduced damage.
- The effects of the drilling forces (thrust force and torque) on the quality of the FRP composites machining was experimented. As a part of the contributions to knowledge (novelty of this study), a highly significant drilling forces reduction, nearly 40% was achieved when drilling HF/VE composite samples with UAD technique. The application

of UAD technique for the remarkable reduction of drilling forces during natural (hemp) FRP composite drilling has not been reported. Though, recently very few research has been focused on CD of some natural FRP composites, such as jute, banana, among others. The considerable and available reports are mainly on conventional (glass and carbon, among others) FRP composites using CD, UAD and other non-traditional drilling techniques.

- A novel analytical thermo-mechanical models are proposed for analysing the FRP delamination drilling-induced damage, by predicting the critical feed rate and critical thrust force at the onset of delamination crack on CFRP composite laminates, using the principle of linear elastic fracture mechanics (LEFM), laminated classical plate theory, cutting mechanics and energy conservation theory. The advantages of this proposed model over the existing models in literature are that the influence of drill geometry (chisel edge and point angle) on push-out delamination are incorporated, and mixed (concentrated and uniformly distributed) loads condition are considered, as depicted in Figure 1. The forces on chisel edges and cutting lips are modelled as a concentrated (point) and uniformly distributed loads, resulting into a better prediction. The model is compared with models in the literature and the results obtained depict the flexibility of the proposed model to imitate the results of existing models.

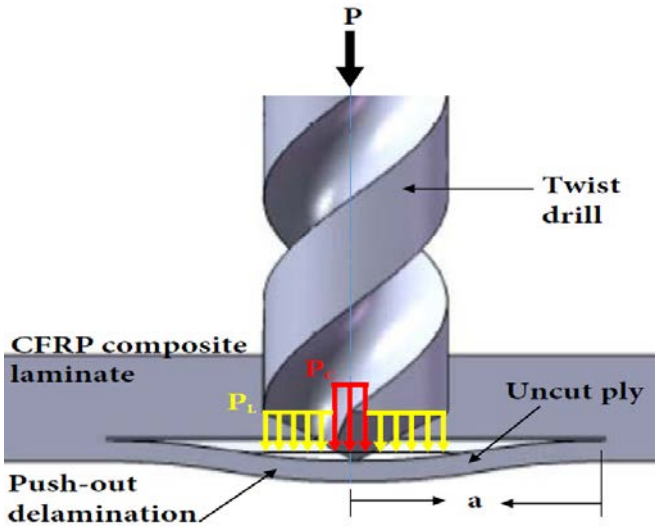

Figure 1: Thrust force models showing mixed loads on chisel edge and cutting lips (Ismail et al., 2017).

1.7 Structure of the thesis

The entire works in this thesis are discussed in nine distinctive chapters, under some parts. Table 1.1 simply and clearly outlines the arrangement and presentation of these chapters under some parts.

Table 1.1: Structure of the thesis.

PART I		INTRODUCTION
	Chapter 1	Introduction
PART II		LITERATURE REVIEW
	Chapter 2	Part A: Fibre-reinforced polymer (FRP) composites
	Chapter 3	Part B: Drilling of Fibre-reinforced polymer (FRP) composites
PART III		MATERIALS AND METHODOLOGY
	Chapter 4	Experimentation
	Chapter 5	Instrumentation
PART IV		ANALYTICAL APPROACH
	Chapter 6	Thermo- mechanical modelling of FRP composite laminates drilling: Delamination damage analysis
PART V		RESULTS AND DISCUSSIONS
	Chapter 7	Phase A: Experimental Works Phase B: Theoretical (Analytical) approach
PART VI		CONCLUSIONS AND RECOMMENDATIONS
	Chapter 8	Conclusions
	Chapter 9	Recommendations
PART VII		REFERENCES
		APPENDICES

After **chapter 1** where the whole concept of this thesis was introduced, chapter 2 follows. **Chapters 2 and 3** present a comprehensive and critical state-of-the-art review on FRP composite materials and machining (drilling) of FRP composite materials. It also covers the effects of drilling parameters, types of drill bits, various associated drilling-induced damage on FRP composites, to mention but a few. **Chapter 4** focuses on the exact FRP composite materials (samples) used and methodologies applied during the experimental stage of the research. Mainly, it emphasises the experimental work conducted. Also, this

chapter discusses the methods of samples manufacture, all the machine tool set-up (experimentation) conducted, experimental procedures and design of experiment (DOS). **Chapter 5** presents all the measurements taken before and after drilling operations in order to quantify the drilling-induced damage, adopted equations and equipment or instruments used (instrumentation). Meanwhile, **chapters 6** explains the theoretical approach using an analytical method to formulate a thermos-mechanical model that could predict and analyse ply exit (push-out) delamination. The whole results obtained for both experimental and analytical works are unambiguously presented and well discussed in **chapter 7**. Many statistical tools and sophisticated instruments for analysing microscopic material damage were used to analyse and present these results in a chronological order, before conclusions based on the results and discussions are drawn in **chapter 8**. Pen-ultimately, recommendations for the future works are highlighted in **chapter 9** respectively. The list of **references** is located immediately after the recommendations. It alphabetically contains all the citations used in this thesis. Lastly, other essential, supporting evidence and documents are collated and listed as an **appendices**.

1.8 Summary

This first chapter of the study has introduced the background, the theme and the structure of the research. It has explained the background of the study, statement of problems, aims and objectives of the study, scope of the research, relevance (justification) and implication of the research, contributions to the knowledge (research novelty) and lastly, the structure of the entire thesis. The background of the research revealed the general focus and context of the study. The problem statement presented the rationales, circumstances surrounding and the needs that necessitated the study. The aims and objectives of the research were unambiguously stated. The scope of the research was highlighted, as a study that embraced both experimental and theoretical investigations. The significance of the study was expressed under relevance (justification), implication and contributions of the research. Conclusively, the structure of the thesis outlined the path for the entire research work, chapter by chapter.

PART II

LITERATURE REVIEW

CHAPTER TWO

LITERATURE REVIEW

PART A: FIBRE-REINFORCED POLYMER (FRP) COMPOSITES

2.0 Introduction

The literature review is divided into two distinctive parts A and B. This present second chapter (Part A) of the research discusses extensive current and relevant literature on the materials aspect of this study, according to its title. It broadly covers the main aspect of fibre-reinforced polymer (FRP) composites, including different types of FRP composite materials as well as their reinforcements and matrices, and their properties, applications, advantages and limitations. The literature survey continued throughout the entire period of this research work, as many recent works are rightly elucidated.

2.1 Fibre-reinforced polymer (FRP) composites

The recent advancement in the field of composite materials technology has been traced to the product of synergic knowledge from sciences (materials, physics and chemistry) and engineering (mechanics and manufacturing) (Kim & Mai, 1998). The deep and thorough research on fibre-reinforced polymer (FRP) composites is an inter-disciplinary task (Mathews & Rawlings, 1994). The quest of having materials with high corrosion resistance and structures of better load bearing capacity in the fields of materials science and engineering respectively, produced the fibre FRP composites of different properties for numerous applications. Mechanical properties of FRP composites are considerably important during manufacturing and service stages, because they determine the performance, functionality and workability of the composites.

A better material with an improved performance produced from an amalgamation of two or more materials that are insoluble in one another and different in both physical and chemical properties, is referred to as a FRP composite material (Sridharan, 2008; Dandekar & Shin, 2012). It is formed by combining fibre and matrix, as a reinforcement

and a binder respectively, to form a single ply. The reinforcement is always bonded between the matrices, as shown in Figures 2.1 and 2.2.

A composite material is a heterogeneous solid consisting of two or more different individual materials which are held together by a mechanical bond. While each material within the composite can act independently without the bond, the overall property of a composite material is the combination of the varying characteristics of its component materials.

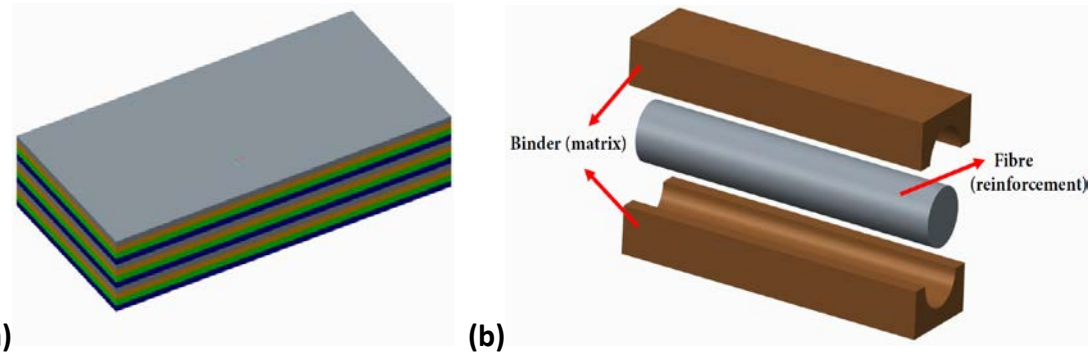

(a) **(b)**

Figure 2.1: (a) The FRP of several plies (represented by different colours), having (b) a typical arrangement (relationship) of reinforcement and matrix

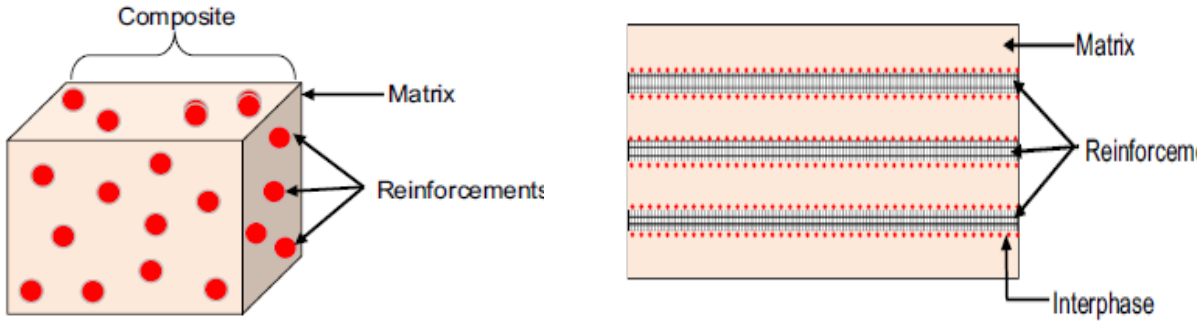

(a) (b)

Figure 2.2: Schematic diagram of a typical composite (a) Reinforcement and matrix representation; (b) Interfacial boundaries (Nirmal, Hashin & Ahmed, 2015)

This implies that both reinforcement and matrix carry the applied loads on the composite, but principally by the reinforcement, as a harder, tougher constituent and chief load carrier, while the binder (matrix) dissipates the load to the fibre (reinforcement); functioning as a load transfer member, retains the fibres firmly and protects the fibre surface against mechanical (abrasion) and environmental (moisture and chemicals) degradations (Mallick, 2008). The properties of FRP composites depend on the qualities of these two main constituents, their interfaces (boundaries) and microstructures. Furthermore, in a composite, several plies are arranged in different orientations and later cured or treated under a specific high temperature and pressure. The laminates are prominently used geometry for continuous FRP composites. Laminates comprise of a well arranged plies, of fibres in either the same or different orientations, such as [0/-45/90/+45/0/0/+45/90/-45/0] (Quartus, 2016), as shown in Figure 2.3. The strength of the fibre-reinforced composites depends on the mechanical properties of the material interface between the fibre and the matrix.

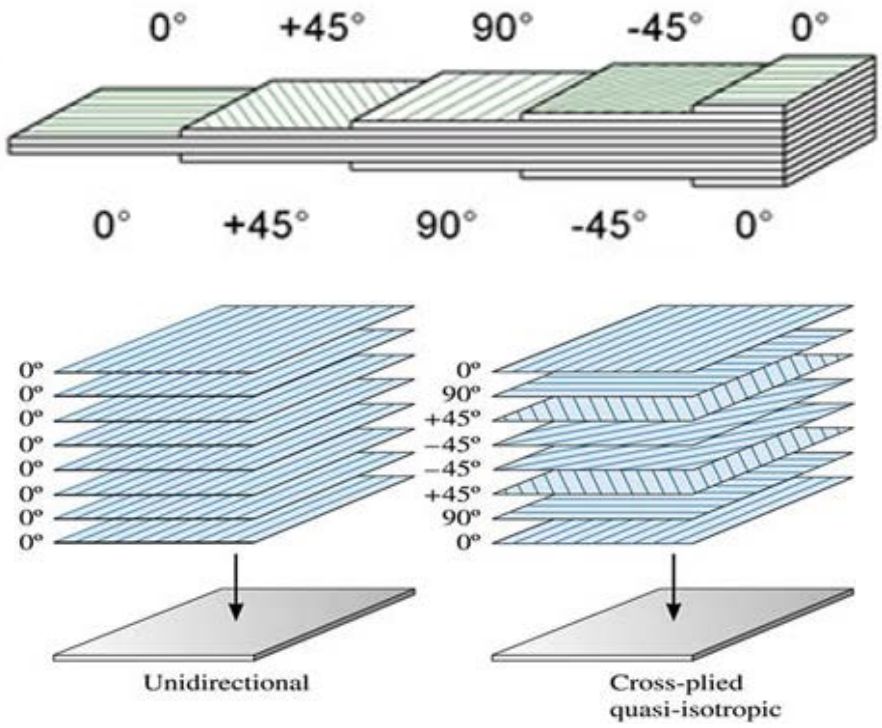

Figure 2.3: Composite laminate stacking and ply layup nomenclature (Quartus, 2016)

The evolution of composite materials was necessitated to overcome the individual shortcomings of conventional materials (metals and alloys). Considering the fact that diverse applications require varying material properties for functionality. The degree of property manipulation that composite materials afford automatically makes them a suitable choice in manufacturing science. Fibre reinforced composites (FRCs) are the most popular types of composite materials, possessing a unique level of specific strength and rigidity, as well as lightweight (Bagherpour, 2012). They are usually embedded with stiff fibres of different choice materials, with the main objective of achieving a resultant material with high rigidity and modulus (implies high strength and stiffness to weight ratio). Furthermore, the embedded fibres are arranged in a way to permit synergy between them. Fibre-reinforced composites consist of two main parts namely: reinforcement and matrix.

(i) **Reinforcement**: These are filaments of individual materials which make up the composite structure. They are usually arranged in a delicate way so as to achieve targeted properties of the finished composite material. Generally, the reinforcement occupies 30 – 70 % of the composite matrix volume (Bagherpour, 2012), and can be obtained from natural means or synthetic manufacturing. However, the most commonly employed reinforcing fibres in structural applications are carbon, aramid and fibreglass.

(ii) **Matrix**: This is the gluey part of the composite which is usually viscous but relatively weak. It is responsible for three basic functions within the composite material, namely: the mechanical bonding of the embedded reinforcements, the transmission of any imposed mechanical stress from the composite polymer to its reinforcements, and the protection of the composite surface from abrasion or chemical attack. The matrix is applied to the interfacial boundaries of the reinforcing fibres for bonding effects. Notable examples of composite matrices are epoxy resins, vinyl esters, and polycaprolactone, among others.

Generally, the performance of any fibre-reinforced composite is depended on a number of criteria, namely: (1) the characteristic properties of its component materials (2) the quality of the interfacial interaction that exists between the matrix and the

reinforcement; hence denoting the importance of interfacial bonding, and (3) the orientation of individual components (Bagherpour, 2012), as shown in Figure 2.4. While the mechanical properties such as off-axis strength and impact toughness of FRCs are governed by the properties of the reinforcing fibres and the adhesion strength of the matrix-fibre interface, other key properties such as thermal stability and chemical reactivity of FRCs are driven by the quality of the adhesive matrix (Liu et al., 2015). Fibre-reinforced composites are commonly employed in applications where a high strength to weight ratio and rigidity are required, such as the aerospace, automotive, structural industries, and a great deal of other consumer and technical applications.

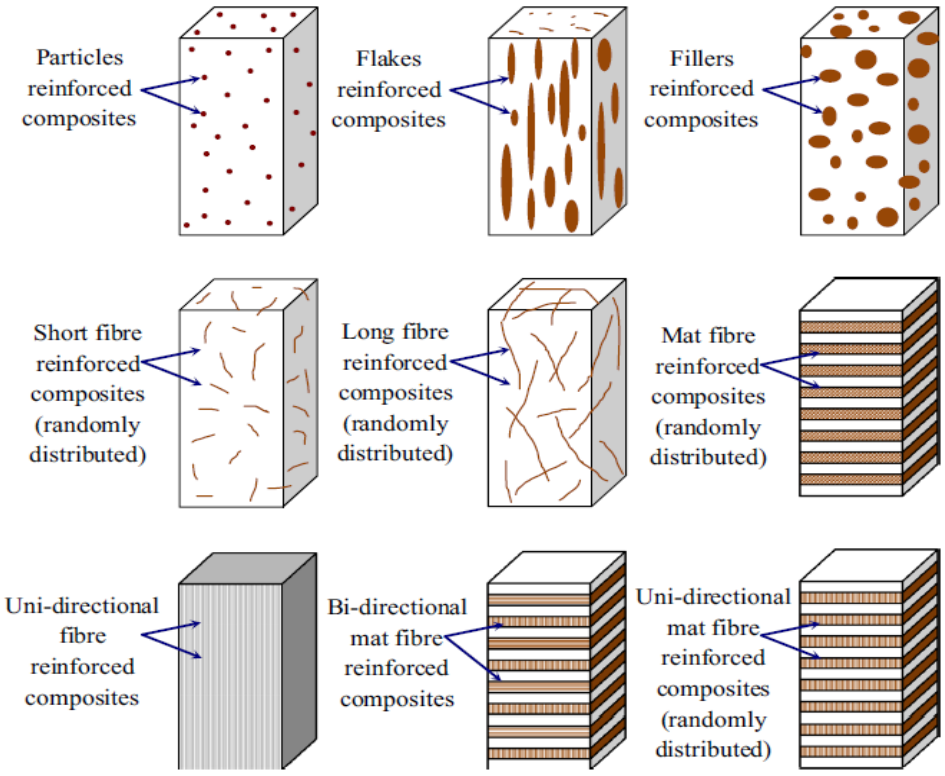

Figure 2.4: Types of reinforcements showing arrangement of their fibres, fillers and particles within various composites (Nirmal et al., 2015)

The fibre-reinforced composites are becoming the acceptable and desirable material system in many industrial applications today. They have better electromagnetic transparency, part count reduction, toughness, stiffness, design flexibility, low weight,

mechanical damping, strength properties as well as chemical, thermal, corrosion and wear resistance when compared with the conventional metallic engineering materials (Sridharan, 2008). These improved properties and increased application of the fibre-reinforced composites have emphasized the need for understanding their machinability in order to further improve their functionality.

2.2 Applications of fibre-reinforced polymer (FRP) composites

The increasing application of the FRP composites, as an effective engineering materials to meet the human insatiable needs in various areas, has encouraged many industrial sectors. The exhausting crude oil resources and quest for a perfect substitute for non-renewable (synthetic) composites have necessitated the advancing research on and use of FRP composites, most importantly, the renewable (natural) composites (Scarponi et al., 2015; Ismail et al., 2015). The list of the areas of application is not exhaustive, as it involves both commercial and industrial uses.

Also, the vast improvement in technology over the recent years has prompted the need for better and sustainable engineering materials. While it is commendable to actualize a design with cost optimisation, it is paramount to prioritise the most crucial aspects of its eventual usage, such as performance, environmental compatibility, and disposability or recyclability (Faris & Sapuan, 2014). In delicate engineering applications, such as that of the aerospace industries, lightweight materials with high strength and flexural stiffness are required (Swoffs et al., 2014). Though certain conventional materials possess some of these aforementioned qualities, however, a great deal of disadvantages associated with their engineering applications. Eventually, this contributes largely to their replacement. This makes proper material selection in engineering design a complex matter where adequate decisions are necessitated (Ashby & Cebon, 1992).

Hence, based on the detailed understanding of outstanding mechanical, thermal and physical properties of FRP composites, they are very demanded and useful, but are not limited to the following sectors (Figure 2.5):

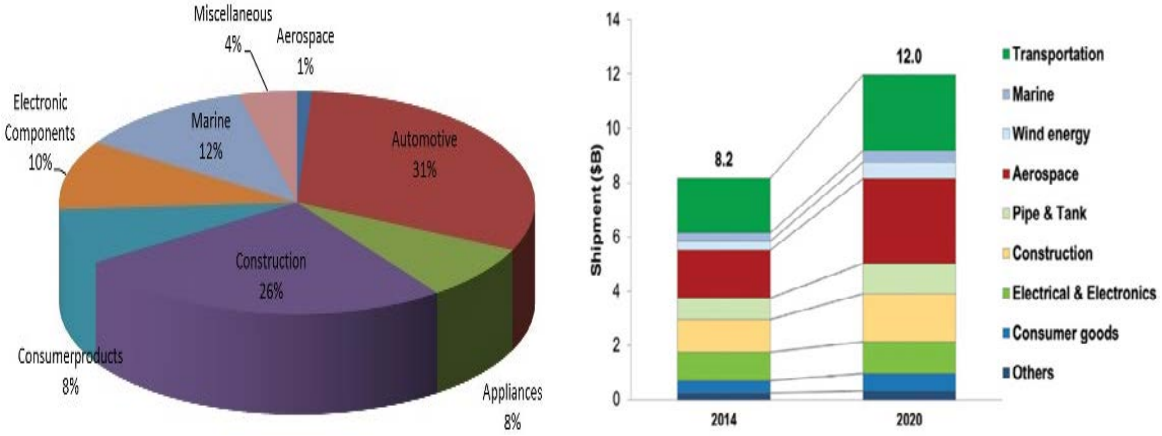

Figure 2.5: (i) Market share of FRP composite materials and (ii) US market forecast (ACMA, 2015)

▪ **Aerospace**: This sector mostly used FRP composites for structural purpose in this present times than other industries. The weight reduction through the application of FRP composites enhances higher speed and increased payloads. In 1987, Airbus commercial aircraft manufacturer used composite extensively to build A310 aircraft. Meanwhile, all-composite tail of aircraft was manufactured by Airbus A320 in the following year (Mallick, 2008). FRP composites are used for the manufacturing of the aircraft wings, floors, stabilisers, seats, fuselage, helicopter blades, landing gears, fuel tanks, tail-planes (Mathews & Rawlings, 1994) amongst others. Furthermore, FRP composites have their applications equally in building truss structures, door of payload bay, arm of remote manipulator and pressure vessels (Mallick, 2008).

▪ **Defense**: The application of FRP composites could be traced to the military during the early World War II. This resulted to the mass commercial exploitation. The military field has the second largest application of FRP composites after commercial aircrafts due to the necessity for weight reduction in order achieve higher speeds, lower fuel consumption as well as increased payloads. In addition, it enhances reduction in the production and assembly costs due to the decrease in components and fasteners, supports decrease in maintenance and repair costs because of the possibility of better fatigue and corrosion

resistance, and allows maneuverability, aero-elasticity and aero-dynamism of aircrafts, especially their aerofoil, tails and wings, through good design of the fibre orientation angles (Mallick, 2008).

- **Marine**: FRP composites are also used for the production of canoes, sail masks and boat hulls due to the outstanding property of corrosion resistance. Also, these marine vehicles have advantages of weight reduction, which aids acceleration (higher crusing speed). In addition, the fuel efficiency and ease of manoeuvrability of the marine vehicles are enhanced. Presently, glass fibre/polyester or vinyl ester resin composites are used for the manufacturing of approximately 90 % of all recreational boats (Mallick, 2008).
- **Automotive**: Basically, the use of FRP composites is divided into three categories. There are body, chassis and engine parts. The first two parts have been more successful than the later (Mallick, 2008). For the production of seats, car body in order to reduce the overall weight of the vehicle, resulting into an energy-efficient vehicles. Also, FRP composites are used for fuel storage tanks, floor and exterior structural panels, drive-shafts, hoods, spoilers, bumpers, gears, bearing, body panels, to mention but a few (Sridharan, 2008; Mathews & Rawlings, 1994).
- **Civil infrastructure/building construction**: The high strength, corrosion and vibration resistance and weight reduction properties of FRP composites have made them alternative materials over the use of concrete and steel for the construction of bridges and buildings among other civil infrastructures. FRP composites are also used for the production of floor beams.
- **Oil and gas**: They are used for the manufacturing of the platforms and oil sucker rods used in offshore and raising underground oils respectively.
- **Domestic**: The domestic materials which are produced from FRP composites include tables, ladders, chairs, bathroom panels, interior and external building materials, chair springs furniture, to mention but a few (Mathews & Rawlings, 1994).
- **Sports, leisure and recreation**: This application is based on the crucial issues of weight reduction, flexibility design as well as the vibration damping. They are used for the manufacturing of the fishing and pole-vaulting poles, bicycle frames, athletic shoes, diving

boards, archery bows baseball bats, golf club shafts, tennis and racquetball rackets, skis, surf and snowboards using advanced composite materials. Some parts of sport boats include hulls, interior panels, protective helmets, decks, engine shrouds and masts are made up of FRP composites (Mathews & Rawlings, 1994). The applications of FRP composites in sports, leisure and recreation are possible due to their (FRP composites) design flexibility, vibration damping, as well as commonly known property of weight reduction.

- **Electrical and electronics**: FRP composites are used for the fabrications of many electrical parts such as panels, connectors, insulators, transformer housing and such likes (Mathews & Rawlings, 1994).
- **Medical Science**: The bone plates are fabricated using FRP composites. These plates are used for fixing fracture, implants and prosthetics, amongst others.

2.3 Types of fibre-reinforced composites

Fibre-reinforced composites are normally grouped on the basis of the nature of their reinforcement (fibres), and not the matrix. The naming convention for each type follows after the source of the reinforcement. As a result, there are basically two types of fibre-reinforced composites namely: Natural fibre-reinforced composites (NFRC) and Synthetic fibre-reinforced composites (SFRC).

2.3.1. Natural fibre-reinforced composites

Natural fibre-reinforced composites are otherwise referred to as green composites or bio-composites, these are composites which contain embedded reinforcements of bio-fibres. In this type of composite, the fibre reinforcements are sourced from natural means of plants, animals, and minerals, as shown in Figure 2.6.

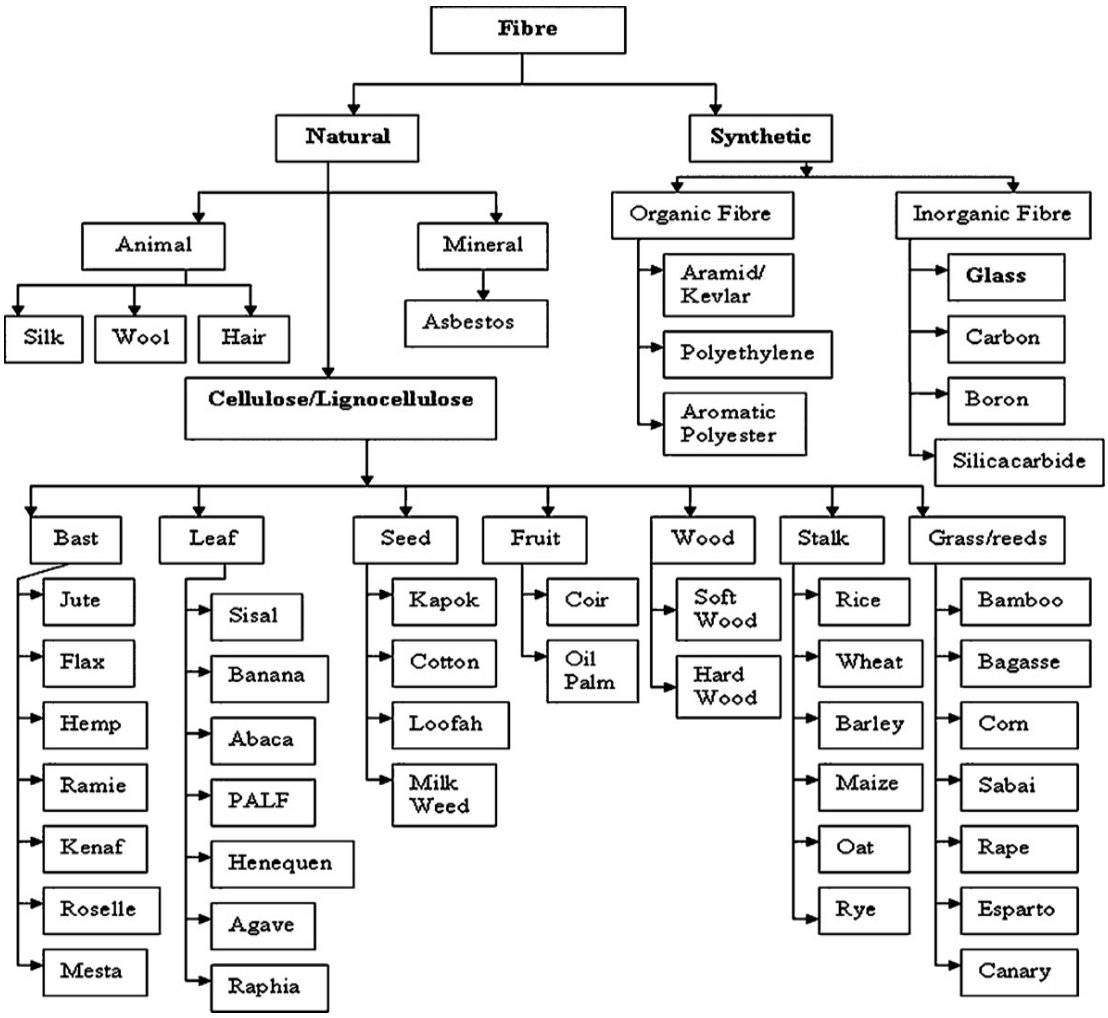

Figure 2.6: Classification of FRP composite fibres (Jawaid & Abdul Khalil, 2011)

2.3.1.1 Historical background of Natural Fibre-reinforced Composites

The utilization of natural fibres as reinforcement in composites has its history well documented. It is generally believed that composite materials evolved as biomaterials which had natural fibres as their primary reinforcement. As far back as the era of the Stone Age (6500 BC), history has it that hemp and linen textiles were utilized as fillers for ceramics (Pickering, 2008). Similarly, dating back as 3000 years ago, the Egyptians used straws and grasses as reinforcement for making clay bricks used for wall building (Bledzki, Sperber & Faruk, 2002). In the last century (1950), a major pick of product development was the manufacturing of an East German Trabant car, which had its frame constructed from cotton fibre-reinforced polyesters (Jawaid & Abdul Khalil, 2011).

2.3.1.2 Plant or vegetable fibres

Among all the sources of natural fibres used in the reinforcement of composites, plant fibres are mostly employed (Jawaid & Abdul Khalil, 2011). Commonly referred to as lignocellulosic fibres, these natural fibres are gaining research recognition in recent years due to a number of impressive advantages they possess over their synthetic counterparts. The mechanical properties of natural fibre-reinforced composite is largely depended on the chemical composition and physical properties of the embedded natural fibres. In the selection of natural fibres as choice materials for composite reinforcement, the most important mechanical properties of interest are the density, Young modulus, and the tensile strength.

2.3.1.3 Chemical properties of plant fibres

The chemical composition of plant fibres is notably made up of atoms of cellulose and lignin. The lignin acts as the glue which binds the fibre cells or cellulose together, thus having a direct bearing on the shape, structure and properties of any natural fibre (Terzopoulou et al., 2015). While the cellulose level in a natural fibre dictates the mechanical properties, especially the tensile strength, and the nature of the lignin layer accounts for the level of its chemical reactivity (Nirmal et al., 2015).

Natural fibres are selective in their matrix choice. This is due to their hydrophilic nature, implies a strong affinity for water absorption, and the hydrophobic quality of most composite matrices. As a result of these contrasting properties between the fibres and the binders, there is usually a high tendency for the formation of aggregates at the interfacial boundary; a condition which puts the composite's interfacial bonding at a failure threat (Kocsis, Mahmood & Pegoretti, 2015). In the selection of matrices for bio-fibres, thermoplastic materials are usually preferred to their thermosetting counterparts due to their high toughness and resilience properties. Up to 30 % of NFRCs with plant fibre reinforcement operate on thermosetting plastic matrices, while the rest are based on thermoplastics (Shah, 2013). Commonly used thermoplastic polymers for this purpose are the polypropylene (PP), polyethylene (PE) and polyamide (PA); while phenolic, epoxy (EP)

and unsaturated polyester resins are the notably used thermosetting matrices (Puglia, Biagiotti & Kenny, 2004; Ku et al., 2011).

2.3.1.4 Physical properties of plant fibres

The physical properties of plant fibres emanates from the variation of its sizes, shapes, and cell wall thickness. The aspect ratio (implies length to width ratio) is a crucial factor to evaluating the mechanical strength of natural fibres. A central hollow cavity known as "lumen" exists in the transverse axis of lignocellulosic fibres, which further translates to the reduction of the fibre's bulk density. While the hollow cavity accounts for the good thermal and acoustical insulation qualities of the fibres, the density reduction translates to their lightweight properties.

In a study conducted by Sapuan et al. (2011), 29 samples of natural fibres were weighed with respect to a number of design criteria such as Young Modulus, density and tensile strength. The results gotten from the study indicated the suitability of natural fibres for manufacturing the dashboard panel of automotives. Similarly, Cheung et al. (2009) studied the application potential of natural fibres of plants and animal residues in biomedicals, with regards to their mechanical and thermal strengths. The results achieved in the study showed that these natural fibres can be effectively employed in manufacturing materials suitable for biomedical applications.

Graupner, Herrman and Mussig (2009) studied extensively on the mechanical properties of various renewable fibres. The major evaluation criteria used for these natural fibres were the tensile strength, Young modulus, elongation at break, and the Charpy impact tests. The results obtained from the study showed the superiority of kenaf and hemp fibres in tensile strength and Young modulus values; as well as cotton exhibiting good impact strength, while lyocell fibres had the combination of high tensile strength, Young modulus, and impact strength.

The mechanical properties of NFRCs are influenced by a number of parameters such as fibre weight, processing techniques, fibre quality, and the adhesive matrix employed (Ku et al, 2011). The most common processing techniques for NFRCs are the extrusion-injection moulding and the compression moulding. Tungjitpornkull and Sombatsompop

(2009) researched on the variation of tensile properties of an E-glass fibre (GF) reinforced wood/PVC (WPVC) manufactured by the injection moulding and compression methods respectively. The results obtained from this study showed that a better tensile modulus of the composite was achieved in compression moulding technique, compared to its injection-extrusion counterpart due to its low fibre volume content comparing to the matrices, as shown in Figure 2.7.

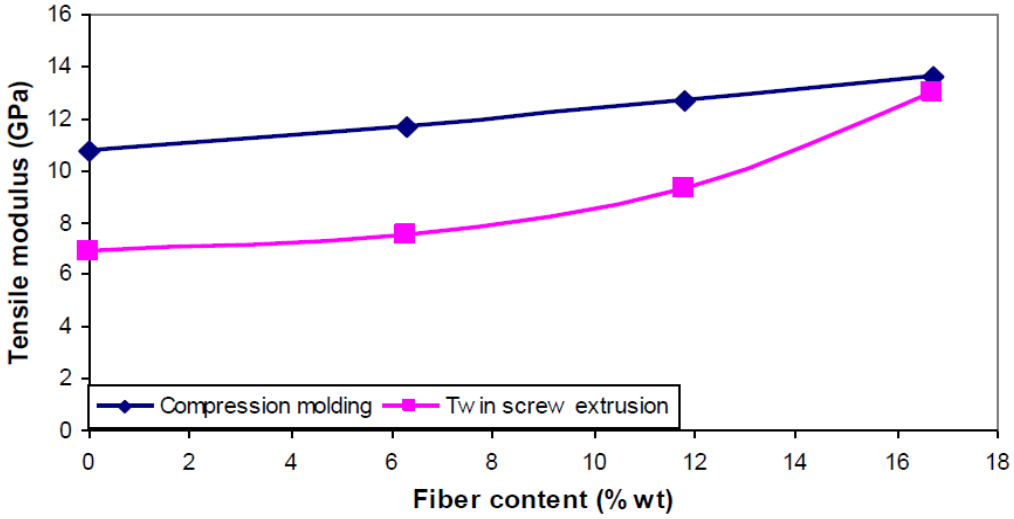

Figure 2.7: Tensile modulus variation for compression moulding and injection-extrusion processing techniques (Tungjitpornkull & Sombatsompop, 2009)

2.3.1.5 Examples of natural fibre-reinforced composites

Considering the wealth of natural fibres available for use in composite reinforcements, notable ones commonly employed in the manufacturing industries are as listed:

(i) Hemp fibre-reinforced composites.

(ii) Sisal fibre-reinforced composites.

(iii) Date-palm fibre-reinforced composites.

(iv) Coir fibre-reinforced composites.

(v) Flax fibre-reinforced composites.

2.3.1.6 Advantages of natural fibre-reinforced composites

Today, the applications of natural fibre-reinforced (NFRP) composites are increasing more than the uses of synthetic composites such as carbon and glass fibres reinforced

composites, mostly in the automotive company. This increase is based on the following highlighted merits:

(i) Relatively lesser production cost due to their universal availability and ease of processing or machining: less drill wear.

(ii) Greater modulus-weight ratio compared to E-glass fibres, resulting into greater specific strength and stiffness

(iii) Reduced risk of environmental pollution through their biodegradability, reusability, and recyclability properties, including possibility of thermal recycling. Environmental friendliness due to their biodegradability and lower CO_2 emission.

(iv) Irritation effects of composites on dermal and respiratory organs are not applicable to natural fibre composites.

(v) Lower density of 1.25 - 1.50gcm^{-3} compared to 1.80 – 2.10 gcm^{-3} and 2.54 gcm^{-3} for carbon and glass fibres, respectively.

(vi) Tool resistance, degradation, and wear commonly encountered in the machining of composites are largely reduced in the case of natural fibre composites.

(vii) Better electrical resistance, good thermal stability and acoustical balance makes them suitable for the automotive industry. Greater acoustic damping property/suitability for noise diminution (reduction).

(viii) Smaller energy consumption during production.

(ix) Minimal or no global warming potential, due to their enhanced carbon (IV) oxide sequestration ability. (Pickering, 2008; Wambua, Ivens & Verpoest, 2003; Faruk et al., 2012).

(x) Equal volume of carbon and glass fibres are much expensive than natural fibres (Mallick, 2008; Jawaid & Abdul Khalil, 2011), based on applications.

2.3.1.7 Disadvantages of natural fibre-reinforced composites

Conversely, natural fibres have some setbacks which limit their structural application in some engineering components. These disadvantages include:

(i) Non-uniformity in fibre geometry can result in structural instability of the finished composite.

(ii) Fibre breakage and thermal degradation during manufacturing processes.

(iii) Poor interfacial adhesion between hydrophilic reinforcing fibres and hydrophobic matrices often lead to poor mechanical properties of composite and fibre swelling (Yan et al., 2013a). High rate of moisture absorption (in some cases), which consequently results in product failure (Kabir et al., 2012). This implies weak fibre-matrix interface due to poor adhesion between fibre and matrix (Dhakal, Zhang & Richardson, 2007).

(iv) Susceptibility to pest infestation if not treated properly, as well as degradation by other natural interferences such as fire.

(v) Unsuitability for high temperature applications due to their low degradation temperatures (< 200 ^{o}C) makes them limited in effective usage (Abiola et al., 2014). It has been reported that the thermal degradation or decomposition of natural fibres begins at temperature just above 200 ^{o}C (Mallick, 2008), while carbon fibres starts at temperature greater than 900 ^{o}C (Wang et al., 2013).

(vi) Inability to resist fire.

(vii) Negative impacts of harvest results on price fluctuation (Jawaid & Abdul Khalil, 2011). Also, there is an instability of cost by harvest, being an agricultural produce unpredictably and easily affected by bad weather.

In summary, natural fibre composites are considered eco-friendly materials which are crucial to a sustainable product development, as a means of properly harnessing the potentials of the supposed waste materials of natural fibres, which will also aid in their complete disposal.

2.3.2 Synthetic fibre-reinforced composites

This is a class of composite materials with reinforcements of synthetic fibres. They are often employed in applications, where a great deal of strength to weight ratio is required. In this type of composite, the reinforcing fibres are processed filaments of conventional materials such as carbon, basalt, glass, among others. The notable examples of this

composite type commonly employed in manufacturing are Aramid fibre-reinforced polymer composite (AFRP), Basalt fibre-reinforced polymer (BFRP), Carbon fibre-reinforced polymer (CFRP) and Glass fibre-reinforced polymer (GFRP) composites (Kopeliovich, 2012).

2.3.2.1 Historical background of synthetic fibre-reinforced composites

The usage of synthetic fibres in composite reinforcement is a relatively new occurrence, compared to its natural counterpart. The evolution of synthetic fibres came as a result of the need to overcome the restraints of natural fibres, such as pest infestation and unsuitability for high temperature applications. The first success about this composite type was recorded in the last century, though efforts on this subject dated as far back as 200 years ago.

Swiss Chemist Audemars in the year 1855 developed the first patented artificial fibre in England. This was achieved by the dissolution of a fibrous inner bark of a mulberry tree with some chemicals to yield cellulose. As at the year 1924, successes were recorded on the production of rayon from cellulose, which was employed in a Celanese textile company. By the year 1965, synthetic fibres were totalled to have met 40 percent of US's fibre needs in composite reinforcing (Kopeliovich, 2012).

2.3.2.2 Advantages of synthetic fibre-reinforced composites

(i) Relatively high thermal stability and electrical conductivity (graphite types).
(ii) Good corrosion resistance and tribological properties.
(iii) Suitability for delicate applications such as wind turbines, aerospace, automotive, due to lightweight characteristics.
(iv) High degradation temperatures make them suitable for high temperature applications.

2.3.2.3 Disadvantages of synthetic fibre-reinforced composites

(i) Unstable or weak interfacial adhesion of the fibre and matrix often results in fibre pull out and matrix debonding during machining operations.

(ii) Inter-ply delamination is a major setback for some of these composites in some machining operations, particularly conventional drilling.

(iii) Relatively high cost of production and maintenance.

(iv) High level of toxicity makes them environmentally unfriendly, and makes them relatively unsafe for human health.

2.4 Comparison of natural and synthetic fibres

The comparison of physical and mechanical properties of natural fibres against synthetic fibre is illustrated in Table 2.1.

Table 2.1: Mechanical properties of natural and synthetic fibres (Saba, Paridah & Jawaid, 2015; Malkapuram, Kumar & Yuvraj, 2008)

Fibre	Density (gr/cm^3)	Tensile Strength (MPa)	Elastic Modulus (GPa)	Elastic at Break (%)
Jute	1.3	393 - 773	26.5	1.5 – 1.8
Sisal	1.5	511 - 635	9.4 – 22	2.0 – 2.5
Flax	1.5	500 – 1500	27.6	2.7 – 3.2
Hemp	1.47	690	70	2.0 – 4.0
Pineapple	1.56	170 – 1627	60 – 82	2.4
Cotton	1.5 - 1.6	400	5.5 – 12	7.0 – 8.0
Kenaf	1.45	930	53	1.6
E-glass	2.55	3400	71	3.4
Aramid	1.4	3000 – 3150	63 – 67	3.3 – 3.7
Carbon	1.4	4000	230 – 240	1.4 – 1.8

2.5 Hemp fibre-reinforced composites (HFRCs)

Hemp fibre-reinforced composite is a natural fibre composite embedded with reinforcement of hemp fibres. It is one of the examples of natural composites commonly employed in the manufacturing industries. The principal components of this composite are the reinforcement; the hemp fibre, and the matrix.

2.5.1 Hemp fibre

Hemp is a plant typical of Central Asia. It was first cultivated in China, about 4500 years ago. Hemp fibre is a natural lignocellulosic fibre similar to kenaf, jute and flax. It is a bast fibre plant which possesses an exceptional coefficient of specific stiffness and the most widely used bast fibre in the reinforcement of composites, due to the high level of its specific strength and durability (Mohanty, Misra & Drzal, 2005). Though, natural fibres are known for possessing similar properties in their usability, the peculiarity of hemp fibre lies in its excellent qualities of absorbency, fibre length, durability, and mildew resistance (Terzopoulou et al., 2015).

Hemp fibre is gotten from the bast of the plant *Cannabis sativa L.* and it is known to grow to a height of about 4m. The world production of hemp fibre is fast growing, with world trade results showing a drastic 40000 tonnes rise in its production figures between the years 2000 (50000 tonnes) and 2006 (90000 tonnes). The world's leading producer of this fibre is China, though a number of major producers also exist such as UK, Germany, and France, while tangible production of this fibre is also gotten from Chile and Democratic Republic of Congo (FAO, 2009).

2.5.2 Physical properties of hemp fibres

Hemp fibre possesses distinct physical features which makes them appealing for use in diverse applications, particularly in composite reinforcement.

(i) **Length**: The average length of hemp fibres lies in the range of 4 to 6.5 feet. For applications where fibre length is considered crucial, such as the textile industries, the hemp fibre is a suitable option.

(ii) **Colour and Glossiness**: Hemp fibres are usually yellowish grey to dark brown in colour, with a highly bright luster, as shown in Figure 2.8.

(iii) **Tensile Strength**: Hemp fibres have a relatively higher tensile strength; 20 % higher than that of flax, as well as when compared to most natural fibres.

(iv) **Moisture recovery**: Hemp fibres have a 12 % moisture regain value, higher than that of cotton and linen (Terzopoulou et al., 2015).

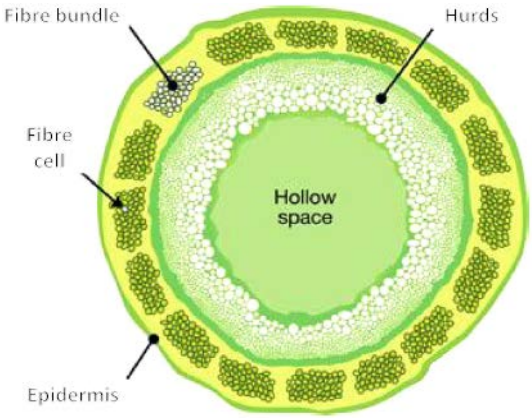

Figure 2.8: Cross sectional view of a hemp stem (Ingrao et al., 2015)

(v) **Elongation**: Hemp fibres possess a higher yield point in manufacturing. They can be easily stressed without undue failure.

(vi) **Acoustical insulation**: The hollow cavity in the stem of hemp fibres equips them with good acoustical balance.

2.5.3 Chemical properties of hemp fibres

Hemp fibres contain 55 – 72 % cellulose, 8 – 19 % hemicellulose and a low level of lignin (8 – 10 %). Some hemp fibre has 7 %, 22 % and 71 % of lignin, hemicellulose and cellulose respectively, as well as tensile strength of 460 MPa (Matthews & Rawlings, 1994). Consequently, this higher cellulose content translates into their toughness and strength peaks. In addition, they have special chemical properties which make them suitable for reinforcement purposes.

(i) **Alkali effects**: Hemp fibre is resistant to alkalis.

(ii) **Acid effects**: Cold concentrated and hot dilute acids have degradation effects on hemp fibres.

(iii) **Insect attack**: Unlike some other natural fibres, hemp is unaffected by infestation of insect pests such as beetles and moth-grubs (FAO, 2009).

(iv) **Ultraviolet radiation resistance**: Hemp fibre has the unique ability to resist the infiltration of ultraviolet radiation, thus enhancing its product life and overall performance (Abiola et al., 2014).

Hemp fibre-reinforced composites are subjects of recent research studies. Placet (2009) studied the improvements in the mechanical properties of hemp reinforced composite with respect to pristine. The results obtained show an increase in the Young Modulus to about 1.9 GPa, and a minute decrease in the ultimate strength to 19 MPa. In another research on the acoustical insulation property of epoxy-matrix hemp fibre-reinforced composite, conducted by Buksnowitz et al. (2010), the results from the study clarified the superior suitability of hemp fibres in acoustical applications.

Similarly, Yan et al. (2013a) studied the possibility of improving the mechanical properties of a polypropylene HFRC by resin modification and fibre treatment. The results obtained from the study showed improvements in the interfacial bonding of the composite, thus depicting the effectiveness of fibre treatment and resin modification in enhancing the mechanical properties of HFRCs. The variation in the tensile strength and Young Modulus of HFRCs with different fibre weight and orientation has been researched by Hajnalka, Racz and Anandjiwala (2008). The results obtained from this study showed the linear variation of tensile strength with fibre weight in the parallel fibre orientation, and the opposite case in the perpendicular direction, while results for the Young Modulus showed a linear variation with fibre weight up to 50 %, and a slight decrease at 70 % in the parallel fibre orientation, and perpendicular orientation showed a reduction in Young modulus with increasing fibre weight (maximum reduction of 34 % was recorded at 70 % fibre weight) as depicted in Figure 2.9.

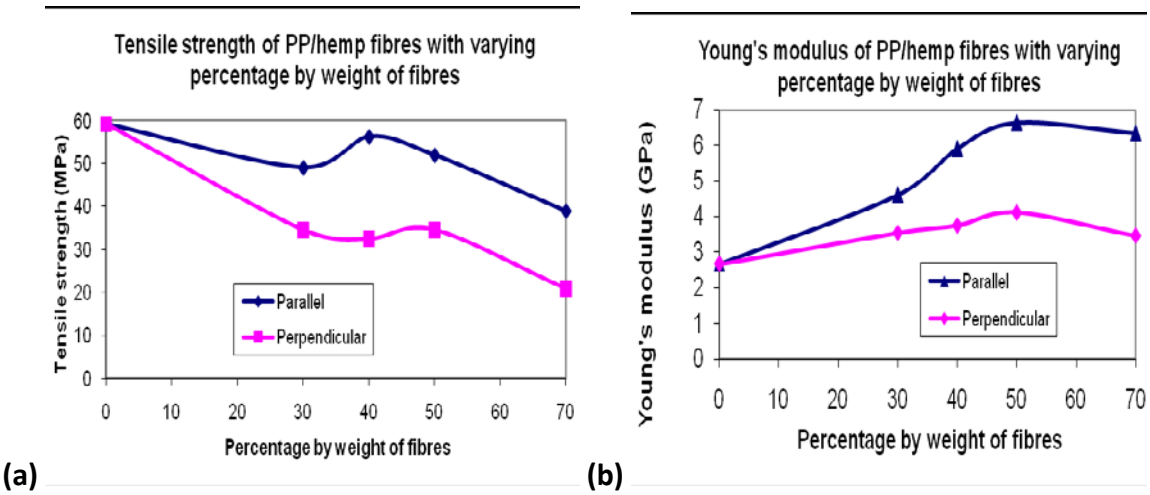

Figure 2.9: (a) Tensile strength variation with hemp fibre weights (b) Young modulus variation with hemp fibre weights (Hajnalka et al., 2008)

2.5.4 Advantages of hemp fibre-reinforced composites

(i) Relatively lower cost of production due to its universal availability.

(ii) It is environmentally conducive and eco-friendly, with high recyclability and disposability potential.

(iii) Toxicity level to human health is little or nil.

(iv) Relative high tensile strength.

(v) Structural stability due to the impervious nature.

(vi) Suitability for indoor air regulation due to good thermo-acoustic, transpirability, and hygroscopicity properties.

2.5.5 Disadvantages of hemp fibre-reinforced composites.

(i) Incompatibility with different composite binders makes it limited in design consideration.

(ii) The distribution of the composite's structural strength may be affected by non-uniformity in the geometry of hemp fibres.

2.6 Carbon fibre-reinforced composites (CFRCs)

Carbon fibre-reinforced composite is an example of synthetic fibre composites with extremely high values of rigidity, tensile strength, and flexural stiffness. It has been the core of research studies on synthetic fibre composites since 1960s (Liu et al., 2015). Like every other typical composite, it is consisted of two main parts, namely: the reinforcement, and the matrix. In CFRCs, the reinforcement is made from carbon or graphite filaments, though other additive fibres such as aluminium, glass, kevlar, twaron, glass, aramid, and ultra-high-molecular-weight polyethylene (UHMWPE) are often used to enhance the composite overall performance. The reinforcement; being carbon fibre, is responsible for the supply of the composite strength and structural performance (Wang et al., 2015). On the other hand, the matrix is usually a polymer resin, such as epoxy, although other polymers such as polycaprolatone, nylon, polyester, vinyl are also sometimes used to aid the binding effect of the reinforcing fibres together.

2.6.1 Carbon fibres

As earlier stated, carbon fibres are the bedrock of any CFRC. These are filaments made from carbon crystals which contain at least 92 % carbon weight. By a process known as carbonization, they are shapened into desired geometries, with structural patterns ranging from crystalline, partly crystalline, to amorphous. The overall properties of the carbon fibre are largely depended on the degree of its carbonization, as well as the orientation of its crystal lattice (Bagherpour, 2012).

There are basically three grades of commercial carbon fibre available for composite reinforcement, as shown in Table 2.2.

Table 2.2: Properties of carbon fibres (Bagherpour, 2012; Kim & Mai, 1998)

Property	Type I High Strength (HS)	Type II Intermediate Modulus (IM)	Type III High Modulus (HM)	Unit
Special strength	17.5 - 32.7	28.2	15.7	10^6cm
Tensile strength	3000 - 5600	4800	2400 - 3000	MPa
Specific modulus	1370 - 1720	1740	1850 - 2790	10^6cm
Young's modulus	235 - 295	296	345 - 520	GPa
Elongation at break	1.0 - 1.8	2.0	0.38 - 0.5	%
Density	1.7 - 1.8	1.74	1.85 - 1.96	gcm^{-3}
Diameter	6 - 8	6 - 9	7 - 9	μm
Co-efficient of thermal expansion (Axial & Radial)	-0.5 & 7.0	---	-1.2 & 12.0	10^{-6}/K

2.6.1.1 General properties of carbon fibres

The anisotropic properties of the carbon fibres are directly replicated from the structure of the graphite, being an allotrope (amorphous) of carbon. The carbon fibres have been classified into three groups, namely; high strength, high modulus and ultra-high modulus, represented by Types I, II and III respectively. Table 2.2 depicts the detailed properties of each of the types (Kim & Mai, 1998). Carbon fibre possesses a number of admirable characteristics which makes it competitive for reinforcement purposes in manufacturing science. These include:

(i) **Thermal and Electrical conductivity**: Carbon fibre has extremely high conductivity values, both for heat energy, and for electricity. As a result, it turns out to be suitable reinforcement option for applications where a great deal of conductivity is required.

(ii) **Fatigue and Corrosion resistance**: Cyclic stresses which induce fatigue failure in engineering materials have little or no effects on carbon fibre, due to its high levels

of static strength and stiffness. Similarly, the inertness of carbon fibre makes it less responsive to corrosion effects. Consequently, it is not affected by the adverse conditions of corrosion, and hence affords a guarantee for long term usage.

(iii) **High Tensile Strength**: As presented in Table 2.2 above, carbon fibre has extreme strength peaks. It can withstand a heavy amount of shock, as well as repeated cyclic loadings.

(iv) **Brittleness**: Layers of carbon fibres are formed from strong covalent bonding typical to carbon atom, and thus allow easy crack propagation. This translates to a low strain peak value for the carbon fibres, causing it to fail at relatively lower amount of bending (Tong et al., 2002).

(v) **Smoothness**: Due to the smoothness property of carbon, the adhesion strength of the polymer resin at the matrix-fibre interface is regularly under failure threat. This is as a result of the low coefficient of static friction which exists at the fibre surfaces.

(vi) **Chemical inertness**: The inert nature of carbon atom makes for a near impossible bonding reaction at the interfacial boundaries of the fibre-matrix in the composite. Since the chemical reactivity of carbon is very low, it is usually unaffected by the adhesive effects of the polymer resins necessary to actualize mechanical bonding, and consequently makes the fibre-matrix bonding a difficult-to-achieve process (Chukov et al., 2015; Liu et al., 2015).

2.6.1.2 Properties of carbon fibre-reinforced composites

CFRCs have distinguishable properties from other fibre reinforced composites such as the aramid fibre and glass fibre. While some of the properties are advantageous to product design, a number of them prove disadvantageous for consistent usage. A summary of these properties are:

(i) High stiffness and hardness.

(ii) High strength to weight ratio.

(iii) High flexural strength.

(iv) High level of abrasivity.

(v) Heat resistance (for glass additives).

(vi) High elastic modulus (for aramid additives).

(vii) Relatively expensive production cost.

2.6.1.3 Advantages of carbon fibre-reinforced composites

(i) **Lightweight**: The relatively lower weight of CFRCs compared to other synthetic composites such as fibre glass and aramid reinforced composites makes it a choice material in most engineering applications. In industries such as aerospace, automotive, and structural; weight is usually considered a disadvantage due to the delicate nature of the applications. This makes lightweight materials a major preference for the product designs. In the comparison of CFRCs to light metals such as steel and aluminium, a decent rule of thumb is that a CFRC which will provide equivalent strength as that of a steel material will usually weigh less than 1/5th of that steel. Similarly, an aluminium structure with equivalent strength as that of a CFRC will usually weigh 1.5 times the weight of the CFRC.

(ii) **Tensile Strength**: The high tensile strength quality of the embedded carbon fibres in CFRCs automatically makes it a strong, rigid material which can satisfy the shock resistance of almost any engineering application. This advantage of CFRCs is usually complemented by its lightweight property, thus making it a manufacturer's choice in robust designs.

2.6.1.4 Disadvantages of carbon fibre-reinforced composites

(i) **Cost**: CFRCs are the most expensive composites among notable synthetic composites comprising of aramid, fibre glass, and carbon fibres (Bagherpour, 2012). The cost prohibition of CFRCs has been one of the major reasons for its inconsistent usage in engineering applications. On a per pound scale, raw carbon is estimated to be in the range of 5 to 25 times more expensive than fibre glass. Similarly with steel, CFRCs have a greater price tag than their steel counterparts.

(ii) **Thermal and Electrical Conductivity**: While the extreme conductivity values of CFRCs in heat energy and electricity makes it advantageous in applications that are reliant on these mechanisms, in other applications where insulation is paramount, CFRCs seem disadvantageous for usage. Utility industries for instance, ensure that their products are made from fibre glass, so as to reduce the risk of electrocution or fire outbreak which is often associated with prolonged hours of usage.

2.6.1.5 Applications of carbon fibre-reinforced composites

CFRC is one of the most demanded materials in the manufacturing world today. The increasing use of CFRCs comes at a promising rate due to its superior mechanical properties. The demand figures of CFRCs in recent years, and a forecast of the future demand is shown in Figure 2.10.

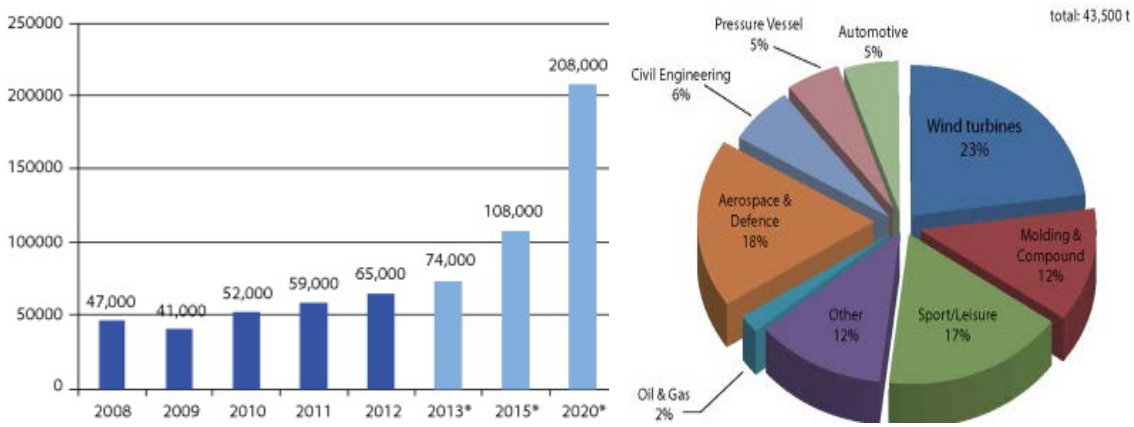

(i) Demand in tonnes (*estimated) (ii) Consumption (tonnes) by application (2012)

Figure 2.10: Global demand for and application of CFRP composites (Holmes, 2014)

CFRCs have wide range of applications. These include, but are not limited to:

(i) **Automotive industries**: CFRCs are preferred in automotive industries due to their damage tolerance and lightweight properties, as a means of reducing accidental impacts on human lives.

(ii) **Wind turbines**: Reports claimed that the wind turbine market has the second highest consumption rating for CFRCs (Jacob, 2014). It is often used in the manufacturing of the turbine blades, due to its lightweight properties.

(iii) **Aerospace and defence**: Aircraft manufacturers such as Boeing and Airbus are constantly in demand for CFRCs, considering the suitability of this composite to aerospace applications.

(iv) **Construction industries**: The enormous strength of CFRCs makes it a major demand for structural industries.

(v) **Sports/Leisure goods**: CFRCs have found their way into the sporting world, majorly used for the manufacturing of sporting products such as golf clubs, bicycle frames, and tennis rackets.

(vi) **Biomedical**: Properties such as X-ray permeability and non-poisonous attributes of CFRCs make it a suitable choice in biomedical applications. It is often used in the manufacture of surgical instruments, heart valve components, and X-ray accessories (Edie & McHugh, 1999; Mallick, 2008; Harris, 1999).

2.7 Comparison of HFRCs and CFRCs.

In comparing composites, it is necessary that the basic general properties are made as the reference notes.

(i) **Weight**: HFRCs and CFRCs possess a lightweight frame which has been the primary reason for their recognition in the manufacturing world. Hemp fibre has a gross density of 1.47 gr/cm^3, while carbon has 1.4 gr/cm^3.

(ii) **Tensile Strength**: The tensile strength of HFRCs and CFRCs can be deducted from their respective fibre strength. Hemp fibre has a tensile strength of 690 MPa, while carbon has an enormous 4000 MPa strength value.

(iii) **Safety in usage**: HFRCs are relatively safer to human health than CFRCs due to their eco-friendly nature. Though CFRCs are non-poisonous, yet the carbon fibres can be quite irritating to the human skin after prolonged exposure. Similarly, the matrix employed in CFRCs (epoxy or polyester) can be toxic if not properly handled.

(iv) **Conductivity**: CFRCs are better conductor of heat and electricity than HFRCs. The extreme conductivity values of carbon fibre-reinforced epoxy (24 W/m K) points out its preference in applications which depend on such mechanisms.

(v) **Wear resistance**: Both CFRCs and HFRCs have admirable resistance to effects such as wear, abrasion, fatigue and corrosion. HFRCs are impervious in their structure, while CFRCs are damage tolerant (Mallick, 2008; Harris, 1999).

2.8 Composite matrices (binders)

These are matrix materials responsible for the compactness of reinforcing fibres in FRCs. Otherwise referred to as resins; these materials form an integral part of any FRC, and influence the overall performance of the composite. They perform three basic functions in the composite structure, namely:

(i) The adhesion of reinforcing fibres in the composite.
(ii) The transfer of mechanical stress from composite surface to its reinforcement.
(iii) The protection of composite surface from abrasive and chemical attacks.

Binders play an important role in ensuring the interfacial bonding of the fibres, which consequently decides the mechanical properties of FRC. Importantly, in the selection of a resin system, the major properties of consideration are: tensile strength, modulus and strain, compression strength and modulus, notch sensitivity, impact resistance, glass transition temperature, ease of availability, and price. Though resins make up about 40 – 50 % of the composite weight, they usually contribute lesser to the overall composite cost, and are majorly assessed based on the quality of their stiffness and tensile strength (SP Systems, 2001). As shown in Table 2.3, according to the chemical nature of binders, they can be classified into two groups, namely:

(i) **Thermosets**: These are polymers which cure irreversibly, usually at temperatures above 200 ^{o}C. They are designed to be either moulded to their final shape, or used directly as adhesives. Major examples of thermosets commonly encountered in manufacturing are amino, epoxy and phenolic.

(ii) **Thermoplastics**: These are polymers which can be re-melt back into their liquid state, even after curing. They have excellent level of toughness, resilience, and corrosion resistance, but elevated curing temperatures. Polypropylene (PP), Polyethylene (PE), Poly Vinyl Chloride (PVC) and Polystyrene (PS) are the most commonly encountered thermoplastic polymers in practice.

Table 2.3: Thermo-mechanical properties of thermoplastic and thermoset polymer matrices (Matthews & Rawlings, 1994)

Property	**Polymer Matrix**		**Unit**
	Thermoplastics	**Thermosets**	
Young's modulus	1.0 - 4.8	1.3 - 6.0	GPa
Tensile strength	40 - 190	20 - 180	MPa
Fracture toughness:			
K_{IC}	1.5 - 6.0	0.5 - 1.0	MPa $m^{1/2}$
G_{IC}	0.7 - 6.5	0.02 - 0.2	KJ/m^2
Maximum service temperature	25 - 230	50 - 450	^oC

2.8.1 Epoxy resins

These are thermosetting composite matrices which belong to the general reactive group of $ECHOCH_2$. Also referred to as polyepoxides, these polymers are the most commonly used binders in composite reinforcement, due to a number of admirable properties which they possess (Singla & Chawla, 2010). They have a wide range of applications in metal coatings, electrical insulations, structural adhesives, encapsulates, and binders. They offer a unique combination of properties which are unattainable with other thermoset resins. Similarly, they come in diverse forms; from low viscosity liquids to high-melting solids, and the ease at which they wet surfaces makes them a perfect choice for composites applications (Boyle, Martin & Neuner, 2001). Epoxy resins are majorly derived from petroleum products nowadays, although some are gotten from plant sources such as glycerol. It is compatible with most common reinforcing fibres such as carbon, fibreglass, aramid, and basalt.

In a research conducted by Vautard and Drzal (2009), the positive influence of epoxy coatings on a vinyl ester CFRC was investigated. The results obtained from the study showed a sharp increase in the quality of the composite's interfacial adhesion and mechanical properties, subject to the addition of epoxy resin. In another research conducted by Hepworth and Bruce (2000), the superiority of epoxy resin matrices was evaluated by the mechanical strength of hemp and flax fibre composites. The results indicated the production of a composite with a mean stiffness of 26 GPa and mean modulus of 378 MPa at 80 % volume fraction of flax fibres in epoxy resins. On the other hand, similar fibre combination with phenolic resin resulted in a poor composite of mean stiffness 3.7 GPa, and mean modulus of 27 MPa.

2.8.1.1 General properties of Epoxy resins

(i) Good adhesion characteristics to other materials.
(ii) High strength and resilience.
(iii) Low shrinkage during cure.
(iv) Good electrical insulation.
(v) Resistance to solvents and chemicals.
(vi) Toxicity and poisonous quality.
(vii) Low cost of production or purchase.
(viii) Long shelf life.
(ix) General applicability due to their compatibility with most substrates.

2.8.2 Vinyl esters

This is an example of thermosetting plastic polymer, produced from the esterification of an epoxy resin with an unsaturated monocarboxylic acid. It is a dependable matrix which is commonly employed in the composites industry. It is known for its excellent strength, water absorption resistance, and corrosion resistance, and as a result, gained preference over other composite matrices in marine environments, energy and infrastructural industries.

In comparison with epoxy resins and polyesters, vinyl esters have higher tensile strength than polyesters and epoxy, and a lower resin viscosity (approximately 200 cps) than polyester (approximately 500 cps) and epoxy (approximately 900 cps). It is often used in the manufacture of FRC tanks and vessels, fabricating tanks, pipes and process equipment. It can be applied by hand, or by spraying on occasional purposes (Mallick, 2008).

2.8.2.1 General properties of vinyl esters

(i) High temperature capabilities.
(ii) Good solvent resistance.
(iii) High level of resistance to corrosive substances such as acids, alkalis, and oxidizing chemicals.
(iv) High tensile strength.

The effects of ultraviolet radiation on the environmental durability of vinyl ester FRCs was investigated by Signor and Chin (2002) using exposure durations of 1000 h and 4000 h. The results obtained from this study showed a decline of 60 % in the toughness of the vinyl ester FRC after prolonged exposure to ultraviolet radiation, as well as a slight transition from ductile to brittle behaviour, and a decrease of 40 % in the strain-to-failure.

2.8.3 Polyester resins

Polyester resin is another strong adhesive used in composite binding. It is made up of dicarboxylic acids, glycols, and monomers. In the presence of high heat (up to 430 ^{o}F) and long exposure time (usually 14 – 24 hours), the glycols and dicarboxylic acids react together to form an ester; a reaction which is commonly referred to as esterification reaction.

Unsaturated polyester resins (UPE) are used in a wide range of industrial and consumer applications. It is commonly used for reinforcement adhesion in FRCs, due to

their ability to positively influence the overall mechanical properties of FRCs through stronger interfacial bonding. Polyester resins when reinforced with structural fibres such as glass fibre gives rise to a strong composite material.

2.8.3.1 General properties of polyester resins

Table 2.4 shows the mechanical properties of polyester resins. In a research conducted by Girisha, Anil and Akash (2014), the comparison of polyester and epoxy resins in a hybrid composite of hemp and jute fibres was conducted. The results obtained from this study showed the advantages of polyester resins over their epoxy counterparts, in the areas of tensile, structural, and impact strengths of the composite.

Table 2.4: Mechanical properties of unsaturated polyester resins (Alaa, Kasim & Mohammed, 2014)

Property	**Unit**
Density	1200 (kg/m^3)
Thermal conductivity	0.17 ($W/m.^oC$)
Tensile strength	70.3 – 103 (MPa)
Modulus of elasticity	2.06 – 4.41 (GPa)
Fracture toughness	0.6 ($M.Pa.m^{0.5}$)

2.8.4 Polycaprolactone (PCL)

Polycaprolactone is a biodegradable, non-cytotoxic polyester commonly employed in composite binding, food packaging, and tissue engineering. It is used for improving the processing characteristics and properties of resins due to its ability to impart water, oil and solvent resistance on resins.

It is one of the long existing polymers used in composite binding, around the year 1930 (Van Natta, Hill & Carruthers, 1934). It became neglected in engineering because of its susceptibility to decay by micro-organisms, but has been resurged back into the

Bio-materials/arena through tissue engineering. Though it is relatively inexpensive to manufacture, compared to other aliphatic polymer matrices, yet it lacks the mechanical properties required for high load bearing applications.

2.8.4.1 General properties of polycaprolactone

(i) Low melting temperature in the range 59–64 ^{o}C and a glass transition temperature of -60 ^{o}C (Liu et al., 2011).

(ii) Good solubility.

(iii) Blend compatibility (Woodruff & Hutmacher, 2010).

2.9 Comparison of composite matrices

(i) **Resin Structure**: A post cured epoxy resin typically exhibit tensile strength and stiffness which is approximately double to that of a non-post cured vinyl ester or polyester.

(ii) **Shrinkage**: While vinyl esters and polyesters have a volumetric shrinkage tendency of about 7 %, epoxies have a relatively lower value of 2 %. This constitutes to the relative stability of epoxy resins than its ester counterparts.

(iii) **Fatigue resistance and micro-cracking**: Relatively more brittle resins such as polyesters and vinyl esters have lower failure strain levels. This resulted in poor fatigue tolerance, and the easy formation of cracks, which subsequently led to eventual component failure. Epoxy resin has the superior ability to withstand cyclic stresses which induce fatigue failure, and this is the reason why it is given higher preference in aircraft applications.

(iv) **Adhesive quality**: The lower volumetric shrinkage ability of epoxy resin makes it a better adhesive than its ester counterparts. As a result of this property, it is highly preferred for use in NFRCs and SFRCs applications.

(v) **Tensile strength**: Polyester and vinyl ester resins have relatively higher tensile

strength and elastic modulus than epoxy resins. However, the property of an epoxy resin can be easily improved by using appropriate reinforcing fibres in composite laminate, as shown in Figures 2.11 and 2.12. It is observed that after lower time of 5 hours at higher temperature of 176 ^{o}F, epoxy recorded highest tensile strength of 8 MPa as well as highest tensile modulus of nearly 3.5 GPa. The epoxy tensile modulus increased after 7 days at 68 ^{o}F.

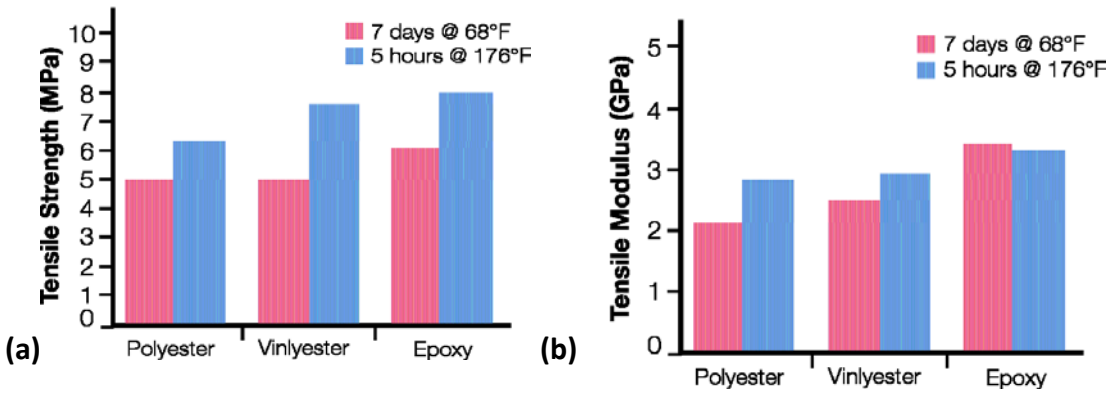

Figure 2.11: (a) Comparative tensile strength and (b) Comparative stiffness of resins (SP Systems, 2001)

(i) **Water resistance**: All resins absorb water to a certain extent, causing an increase in the composite weight. The degradation impact of water on composite binders is crucial to evaluating their stability and shelf life potential. While polyesters and vinyl esters can only retain about 65 % of their initial shear strength after water infiltration, epoxy resin can retain a massive 90 % of its initial shear strength. This makes epoxy resins more suitable for marine applications and other applications where a great deal of water interference is frequently encountered (SP Systems, 2001).

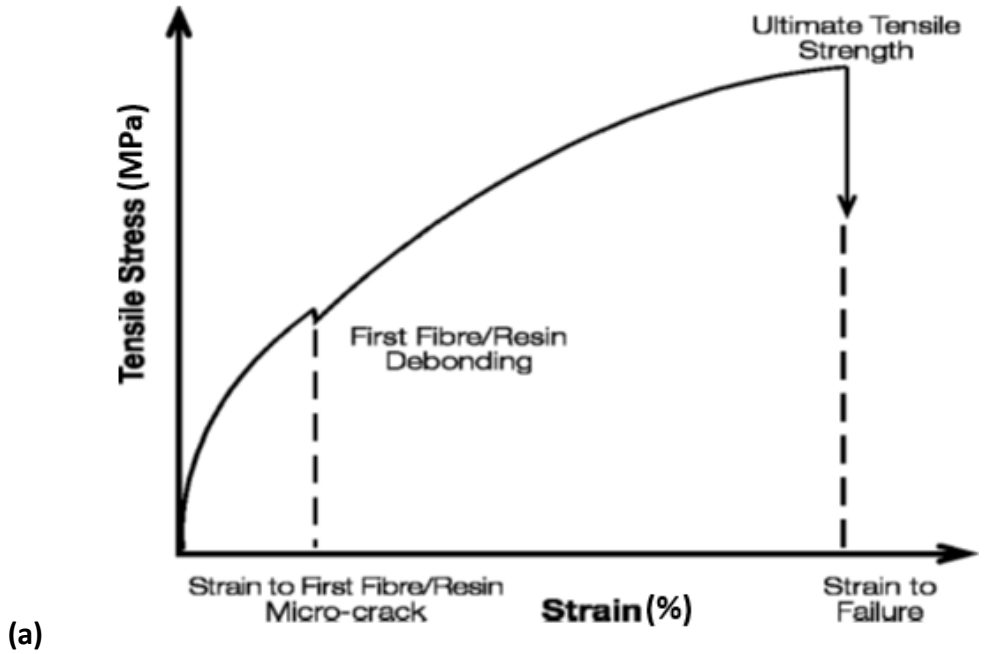

(a)

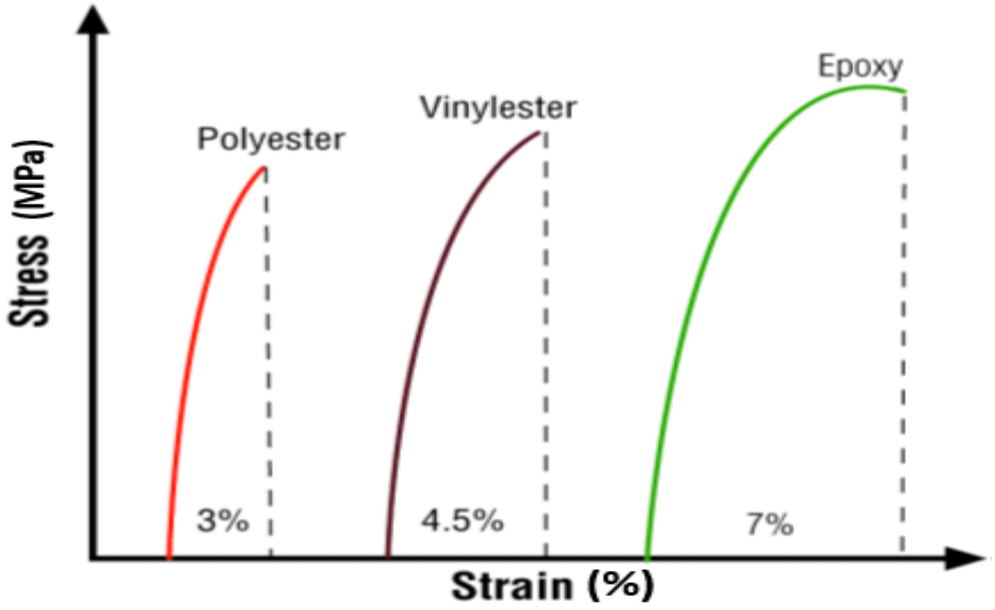

(b)

Figure 2.12: (a) Stress-Strain curve for a typical FRC (b) Typical resin Stress-Strain curves (post cured for 5hrs & 176˚F) (SP Systems, 2001)

A summary of the mechanical properties of notable composite binders is shown in Table 2.5.

Table 2.5: Mechanical properties of some thermoset polymers (Malkapuram, Kumar & Yuvraj, 2008; Holbery & Houston, 2006)

Property	Polyester Resin	Vinyl ester Resin	Epoxy Resin
Density (g/cm^3)	1.2 – 2.5	1.2 – 1.4	1.1 – 1.4
Elastic modulus (GPa)	2.0 – 4.5	3.1 – 3.8	3 – 6
Tensile strength (MPa)	40 – 90	69 – 83	35 – 100
Compressive strength (MPa)	90 – 250	100	100 – 200
Elongation (%)	2	4 – 7	1 – 6
Cure shrinkage (%)	4 – 8	N/A	1 – 2
Water absorption (24 h@ 20 ^{o}C)	0.1 – 0.3	0.1	0.1 – 0.4
Izod impact strength (J/m)	0.15 – 3.2	2.5	0.3

2.10 Summary

This chapter has reviewed the main concepts of fibre-reinforced polymer composites as a material workpiece throughout this study. These included natural (hemp) and synthetic (carbon) reinforced polymer (mainly epoxy, vinyl ester and polycaprolactone) composite materials. Based on the requirement of the application, an appropriate FRP composite material having a certain properties could be rightly selected. Moreover, this chapter considered desirable properties, applications, advantages and limitations of FRP composites, when compared with each other, engineering metallic materials and alloys. These characteristics and detailed analysis will guide all the FRP composites users, manufacturers and researchers in their choice of composite materials, design, manufacturing and applications, as they all depend on the machinability (ease of drilling) of the FRP composites. Therefore, the broader concepts of drilling of FRP composite materials continues in the next review chapter (three).

CHAPTER THREE

LITERATURE REVIEW (Part B)

PART B: DRILLING OF FIBRE-REINFORCED POLYMER (FRP) COMPOSITES

3.0 Introduction

This is a continuation of chapter two, as part B. This third chapter of the research discusses extensive current and relevant literature on the machinability aspect of this study, as the title indicates. It broadly covers experimental and theoretical concept of FRP composite machining (drilling), associated problems of drilling-induced damage on both conventional and conventional FRP composites and drill bits (tools), importance of tooling materials, drill types, geometry and design, drilling conditions, techniques and parameters. In addition, this literature review chapter contains pertinent literature on analytical modelling of delamination prediction and analysis. The literature survey covers the entire research work, as many current recent works are rightly elucidated.

3.1 The concepts of drills and drilling operation

The kinematics of drilling is a process of using a rotating drill bit to create or enlarge existing round holes in a workpiece (Toolingu, 2013). Drilling is one of the most frequently processes used in manufacturing industry among machining operations (Wang & Zhang, 2008). Tonshoff et al. (1994) noted that drilling takes about 25 % of the total machining time and 33 % of all the total machining operations of a manufacturing process. It is a preliminary step for many other machining operations, such as reaming, tapping and boring (Sanjay, 2006; Wen, Soon & Sivarao, 2004).

Drill, as a rotary end cutting tool, has one or more cutting lips and flutes for the release of chips and the access of a cutting fluid. Presently, drill bits are the most frequently and extensively used material cutting tools (DrillDr, 2011). Geometrically, a twist drill is a complex material cutting tool, as depicted in Figure 3.1. Both the geometrical shape and dimensions of a twist drill determine the cutting performance; influence the cutting

forces, tool wear, cutting dynamics and, the quality and integrity of drilled holes (Xiong, Fang & Shi, 2009; Shaw, 2005; Webb, 1993; Harris et al., 2003). These make the design of twist drill of a critical importance. A poorly designed cutting edge results in an undesired distribution of the cutting angles along the drill cutting edge (Bhattacharyya et al., 1971; Kaldor & Lenz, 1982; Selvam & Sujatha, 1995; Paul, Kapoor & Devor, 2005), causing inefficient performance, loss of cutting ability and increase in total manufacturing cost.

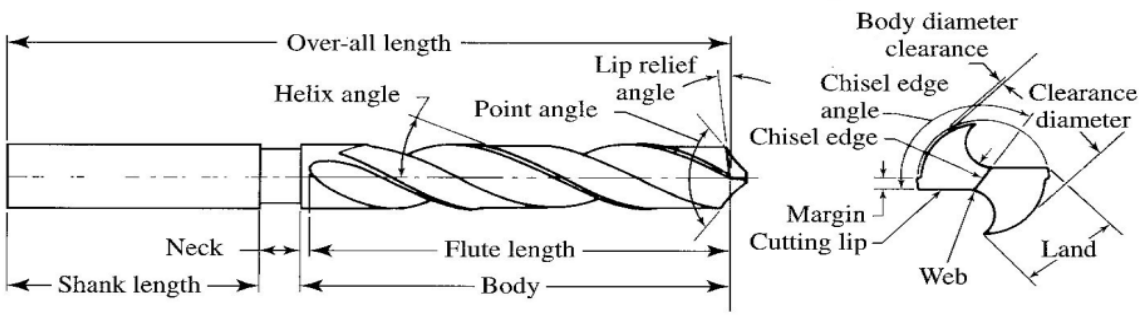

Figure 3.1: Characteristics of a typical double fluted drill (Stephenson & Agapiou, 1996; Chao et al., 2009; Marinov, 2010, Ismail et al., 2016b)

3.1.1 Twist drill geometric design concept

The complexity of the geometry of a twist drill requires careful design consideration. The cutting dynamics, drilling forces and tool wear strongly depend on the drill dimensions and geometry (Tsao & Hocheng, 2004; Tsao & Hocheng, 2005; Shyha et al., 2009; El-Sonbaty et al., 2004; Abrão et al., 2008; Brinksmeier & Janssen, 2002). The machine tool requires much more energy and power when its cutting tool is poorly designed, in addition to tendency of damage on the machine.

Fetecau et al. (2009) reported that the efficient approach to reduce drill wear in order to increase the drill performances is to have well defined geometry of the main cutting edge only, such that it could lead to a constant unitary energetic load along the main cutting edges. In an attempt to redesign a drill for an optimum performance, the flute profile has often been designed by incorporating 'forward' and 'backward' simulation analyses, to decide on an optimum geometry of the flute grinding process (Armarego & Kang, 1998). A straight lip and parabolic heel flute profiles, computer-aided design/

manufacture software were used to establish a design flute profile from the drill specification. The application of the software and model to flute showed that the required wheel profile parameter with respect to the diameter could be represented by simple regression equations.

Piquet et al. (2000) studied the drilling of thin carbon/epoxy laminates with two types of drills: a helical drill and a drill without chamfer on the cutting edge, made up of HSS and “micrograin” tungsten carbide (K20 rating) respectively. It was concluded that both drills caused damage at the entrance of the wall and the exit of the hole, but K20 tungsten carbide geometry drill produced reduction in the final damage.

3.1.1.1 Cutting edges and angles

The design of cutting edges has focused on point design with consideration of cutting forces for arbitrary cutting geometries (Audy, 2008a), stress analysis (Hinds & Treanor, 2000), and design and optimisation using simplified drill geometry models (Yan & Jiang, 2013; Chen & Ni, 1999; Schulz & Emrich, 2000; Schulz & Emrich, 2001; Herbert et al., 2002). Majority of the drill geometrical improvements has often been limited to the chisel edge region. This proved to be effective in reducing the total thrust force, but marginally reduced the torque and the power which are major determinants of the tool performance (Wang & Zhang, 2008). Furthermore, significant design features such as reverse web taper and internal cooling channels, cutting lips and chisel edge geometries including verification of grindability which is important for the drill cross sectional design has been reported to be considered in an acceptable drill geometry model (Abele & Fujara, 2010).

Thinned purpose and faceted point together with the patented 'circular centre edge' designs have been developed, using predictive force models (Armarego & Zhao, 1996). The predictive mechanics of cutting models for thrust and torque were numerically and experimentally tested, and found that the drill designs substantially reduced the thrust force when compared to un-thinned drills and differences in the forces for the three designs were minimal after comparison.

A practical method to determine the cutting edges and rake angles has been carried out by Li, Zhang and Xiong (2010). Cutting edge points and the rake angles were examined using 2D tool microscope and image-based instrument and numerical computation respectively. This method proved effective compared with common unaffordable labourious analysis required in rake angle determination, because it does not require high level of co-ordinates transformation and mathematical competence.

3.1.1.2 Lip Geometry

A methodology to model the geometry and cutting forces of drills with generic point has been established (Sambhav, Tandon & Dhande, 2012a; Sambhav, Dhande & Tandon, 2012b). With the aid of non-uniform rational basis spline, CAD geometric models were used for a fluted drill in terms of bi-parametric surface patches. Generic and mechanistic models were presented for the cutting lip and chisel edge, and prediction of the forces respectively. The mechanistic model was applied to calculate the forces for each element and determined the drill total thrust and torque. Similarly, a new paradigm to model various twist drill geometries in terms of three-dimensional parameters was established (Tandon, Gupta & Dhande, 2008). Their work outlined the construction of a detailed CAD model for a fluted tool. A new well detailed and broad 3D definition of the drill geometry was established.

3.1.1.3 Point Angle

Durão et al. (2010) experimental techniques showed that the most effective tool was 120^{o} point angle drill for minimal delamination and at higher feed rates. They reported that a good alternative could be a step drill designed for a particular composite though presently, not yet available commercially. Vijayaraghavan (2006) reported a tool which could generate automated 3D CAD drill geometric models and manufacturing parameters as a required component of numerical/finite element analysis models of FRP drilling. The outputs of the tool gave variety of solid geometry formats of drills and through meshing,

it was used in different FEA analysis packages.

Drilling of thick fabric woven CFRP composite laminates was experimentally performed, using uncoated carbide (UC) and diamond coated carbide (DCC) twist drills. The effects of the geometries of double pointed angle drills were investigated (Karpat, Deger & Bahtiyar, 2012). The UD, DCC-I and DCC-II have 6.35, 6.91 and 6.38mm diameters; 140-60^{o}, 130-60^{o} and 140-60^{o} drill tip angles respectively, with rake, clearance and helix angles of 7^{o}, 11^{o} and 30^{o} respectively. The geometries of both UD and DCC-II drills were the same, while the tip angles, primary and secondary cutting edge lengths of DCC-I and II drills were different. The diamond particles size as well as the coating condition and thickness determined the performance of the drills. It was concluded that the geometry of DCC-II was appropriate than the DCC-I drill during high feed drilling of the composite material, producing critical hole diameter tolerance than delamination drilling-induced damage.

Chao et al. (2009) stated that edge radius has the greatest effect on the interface stresses by deposition. Tensile radial normal stresses affected the reliability of the coating bond and changed helix angle, point angle and web-thickness. These stresses influenced a difference in drill tip from 100 to 200 point angles. Meanwhile, point angle increased with the normal stresses unlike helical angle, as shown in Table 3.1, where σmax is the maximum stress, though depends on the tooling material, but decreased with delamination (Durão et al., 2010; Jain & Yang, 1994). Stresses on the tool reduce its life. Kilickap (2010) observed that increase of HSS drill point angle leads to decrease in delamination effect during unidirectional-ply GFRP composite laminate conventional drilling. During drilling (high speed and conventional) of woven-ply CFRP, Gaitonde et al. (2008) reported that cemented carbide K20 point angle increased with increase in delamination damage.

Table 3.1: Effects of different drill point angles and helical angles on interface normal stresses (Chao et al., 2009)

Normal stress (GPa)	Point angle (degree)			Helical angle (degree)		
	90	**118**	**135**	**20**	**30**	**40**
σ_{rmax}	1.217	1.227	1.234	1.24	1.23	1.21
$\sigma_{\Theta max}$	2.78	2.89	2.94	3.05	2.89	2.73

3.1.1.4 Lip flute profile

Armarego and Kange (1998) reported that the generated lip and heel flute profiles closely formed the ideal profile for the creation of straight lip and a parabolic curve respectively, with the curve being tangential to the web diameter and passing through the corresponding heel corner. A multi-objective geometry optimisation was realised by implementing meta-heuristic algorithms (Sardin˜as, Reis & Davim, 2006). The subsequent geometry was validated and verified by constraint functions including chip flute grindability verification.

3.2 Tooling material selection

Tooling material influences drilling-induced damage, such as delamination effect (Tsao & Hocheng, 2004; Tsao & Hocheng, 2005; Kim & Ramulu, 2004a), and variation in cutting forces (Min et al., 2001) have significant effects on both drill life and the structural integrity of composite materials.

3.2.1 Drill tool materials

The life of a drill depends mainly on hardness, toughness, wear and thermal resistance. A good drill must possess ability to resist wear, fracture, quick rupture and retain hardness

at the state of hot hardness. The major properties of different tool materials are shown in Figures 3.2 and 3.3.

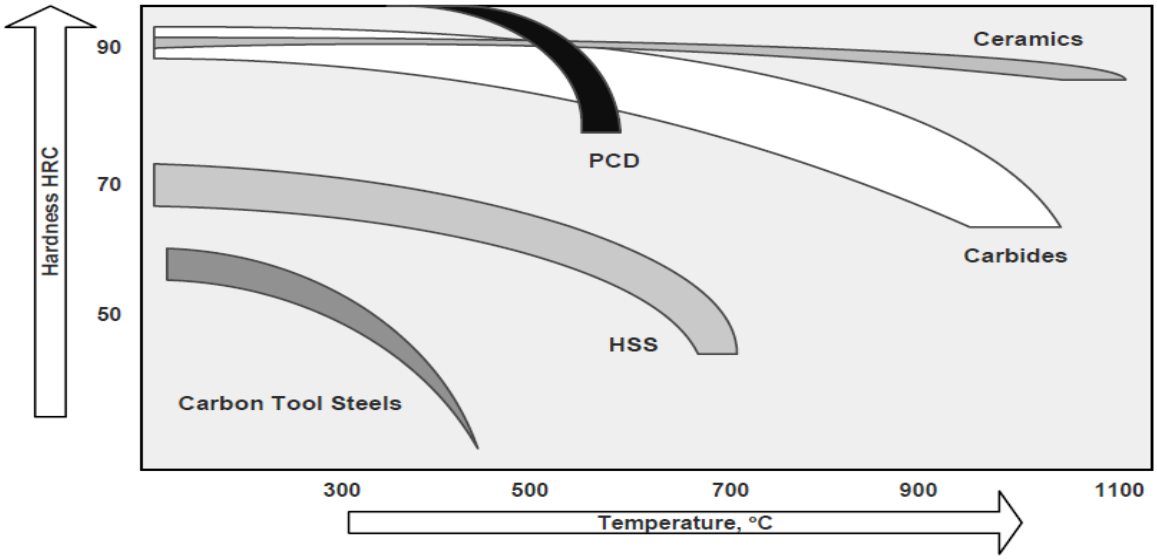

Figure 3.2: Relationship between hardness and temperature of drill materials (Astakhov & Davim, 2008; Ismail 2016b)

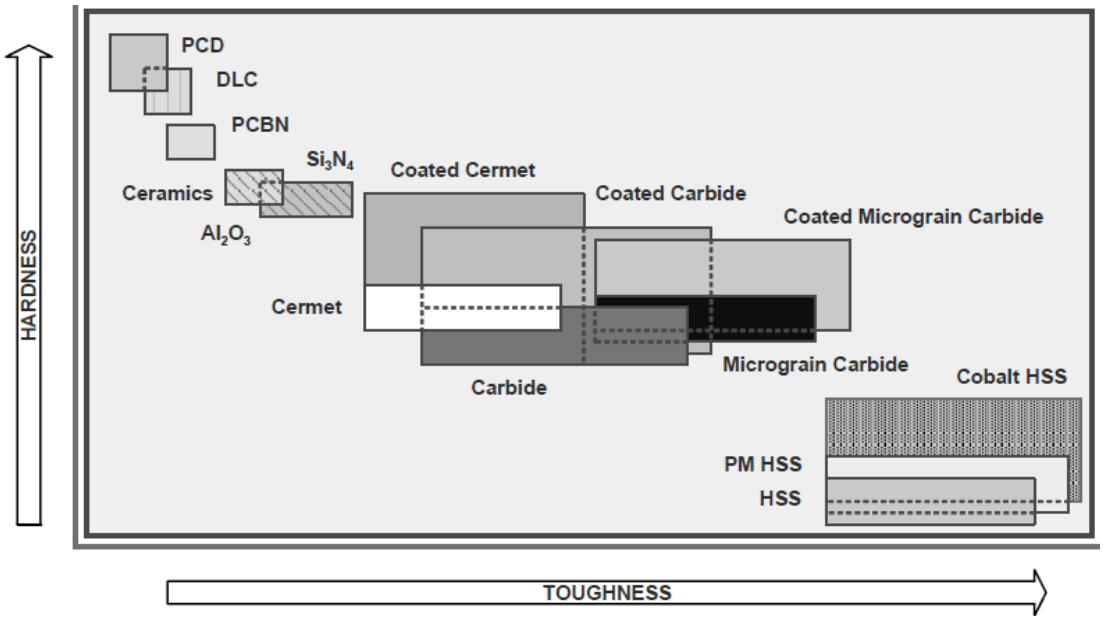

Figure 3.3: Relationship between hardness and toughness of drill materials (Astakhov & Davim, 2008; Ismail 2016b)

From these Figures, hardest tooling material; PCD possesses least toughness property as its sharp deformation occurs around a temperature of 600 ^{o}C unlike HSS with the best toughness, but deforms around 700 ^{o}C when compared with other tooling materials.

3.2.1.1 High speed steel

Table 3.2: Various twist drill materials for drilling composite laminates: 2000-2012 (Ismail et al., 2016b)

Tooling materials	Reference	No of articles
PCD	Madhavan & Prabu, 2012; Garrick, 2007; Ghidossi, El Mansori, & Pierron, 2004; Heath, 2001; Park et al., 2011.	05
CCC	Shyha et al., 2009; Chao et al., 2009; Park et al., 2011; Iliescu et al., 2010; Dharan & Won, 2000; Liu et al., 2010; Shyha et al., 2010; Shyha et al., 2011; Mohan, Ramachandra & Kulkarni, (2005).	09
UCC	Brinksmeier & Janssen, 2002; Sardin˜as, Reis & Davim, 2006; Kim & Ramulu, 2004a; Madhavan & Prabu, 2012; Davim, Reis & Antonio, 2004a; Wang, Wang & Tao, 2004; Ramulu, Branson & Kim, 2001; Zitoune & Collombet, 2007; Davim & Reis, 2003a; Lazar & Xirouchakis, 2011; Singh & Bhatnagar, 2006; Velayudham, Krishnamurthy & Soundarapandian, 2005a; Velayudham & Krishnamurthy, 2007.	13
HSS	Harris et al., 2003; Tsao & Hocheng, 2004; Tsao & Hocheng, 2005; El-Sonbaty et al., 2004; Abrao et al., 2008; Kim & Ramulu, 2004a; Liu et al., 2012; Capello, 2004; Hocheng & Tsao, 2003; Davim & Reis, 2003a; Che, 1997; Madhavan & Prabu, 2012; Wang et al., 2004; Ramulu et al., 2001; Singh & Bhatnagar, 2006; Karpuschewski, Byelyayev & Maiboroda, 2009; Raju et al., 2008; Kilickap, 2010; Zhang, Wang & Wang, 2003; Khashaba, 2004; Ramkumar et al., 2004a; Ramkumar, Malhotra & Krishnamurthy, 2004b; Tsao & Hocheng, 2007; Singh, Bhatnagar & Viswanath, 2008.	24
Total		**51**

It was reported in a review study of drilling composite laminates that HSS or Carbide drill bits have primary attraction based on better performance at high cutting speed compared with other drill bits (Liu, Tang & Cong, 2012). Some studies (Hocheng & Tsao, 2003, Davim & Reis, 2003a; Che, 1997) used HSS drills frequently; making it the most widely used tooling material due to its availability, low cost and highest toughness, as shown in Table 3.2. It has a highest percentage (47 %) of applications; 24 applications out of 51 research works considered from years 2000-2012 inclusive, as depicted in Figure 3.4.

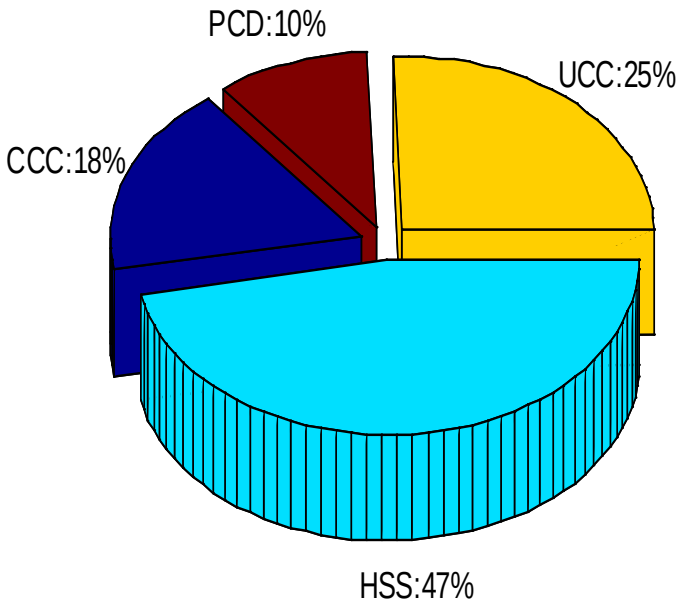

Figure 3.4: Percentage application of drill tool materials

3.2.1.2 Cemented carbide

Carbide drills performed better in terms of wear resistance, delamination effect and surface finish when compared with HSS under comparative low speed and feed at high temperatures when drilling the same composite materials (Abrão et al., 2008; Kim & Ramulu, 2004a; Davim & Reis, 2003a; Madhavan & Prabu, 2012; Davim et al., 2004a; Wang, Wang & Tao, 2004; Ramulu et al., 2001), as indicated in Figures 3.2 and 3.3. When

the radius apart from the corner was measured, almost null wear land was shown in the flank surface of carbide drills, while HSS drill had considerable wear (Davim & Reis, 2003a).

3.2.1.3 Polycrystalline diamond

Garrick (2007) reported producing a veined drill that was capable of drilling carbon composites and its stack with titanium. However, he observed that, after 200 holes had been successfully drilled, a wear land was formed on the cutting edge of the 86 series PCD veined drill which necessitated re-sharpening of the drill. In addition, it was reported that in order to strengthen its cutting edge and make PCD drills viable, it might require modification with k-lands. Also, further suggestion was made, that an assessment of the drill process and delamination would be useful in the design and optimisation of new PCD drill geometry that might give a better output. Investigation of the effect of the cutting parameters on drilling carbon/epoxy and carbon/peek was done by Chambers and Bishop (1995). They concluded that the drilling of carbon composites is depended on the characteristics of the matrix. The helical PCD drill geometry gave the best overall performance when compared with other cemented carbide drills, but more reactive to feed rate changes, when delamination was considered (Madhavan & Prabu, 2012).

Heath (2001) reported that PCD being a stronger tool material could be used for machining of composites because of its ability to withstand the severe abrasion of the carbon fibre reinforced composites. However, PCD is found to be too fragile to withstand the high cutting forces required for metal such as titanium (Heath, 2001) especially when stacked with composites. Furthermore, the configuration of the core drill had been proved better the traditional twist drill. Therefore, the outstanding advantages of core drilling, using a solid PCD drill has been reported by Butler-Smith et al. (2015). A novel designed core drill produced 26 % reduction in thrust force, reduced drill surface clogging, cutting force and drilling temperature, producing reduced delamination damage possibility during composites drilling. The novel micro PCD core drill possessed laser generated cutting micro-teeth formed onto a tungsten carbide backing. The performance

of this novel drill was experimentally compared with electroplated diamond tool during micro-core drilling. The electroplated diamond micro (EDM) core drill produced cutting forces that were 36 % and 190 % greater than PCD core drill at new state of the tool and after 216 drilled holes, resulting to terrible composite delamination. Similarly, up to 11 % and 25 % greater drilling temperatures were generated by the EDM core drill than the PCD core drill at new state of the tool and after 216 drilled holes. Also, at 216th hole 1.8 times higher thermal spread was produced by EDM core drill than the PCD core drill.

3.3 Problems associated with drills

3.3.1 Rapid tool wear

Tool wear is an unwanted phenomenon in machining process, whereby tool lost an amount of matter. It affects the quality of the drilled surfaces (holes) and geometry of the material workpiece. The chip produced during the drilling of carbon composites is abrasive dry powder. The ineffective extraction of these chips is one of the major reasons for high tool wear rates. The most common type of wear; crater wear occurred to a major extent as a result of discontinuous chip formation, caused flagging of the tool which propped up cutting edge chipping (Madhavan & Prabu, 2012). The cutting force increased with the workpiece-drill tool interface temperature, followed by the increased drill wear, resulted to workpiece deflection and drill bit breakage (Sivarao, 2005). The flank wear decreased near the corner of the drill chisel edge, while the maximum flank was common at the drill outer corner. Increase in thrust force, torque on the drill bit and the number of drilled holes caused a proportional increase in the drill tool wear (Sivarao, 2005).

There have been some research on the tool wear processes during drilling of carbon composites, as well as the effect of tool wear on the drilling forces and quality of the holes produced. Some investigated the drilling process and correlated it with delamination, while others correlated the drill geometry and feed rate to delamination (Jain & Yang, 1994; Davim et al., 2004a; Tsao & Hocheng, 2007; Veniali, Dillio & Tagliaferri, 1995; König et al., 1984; Hocheng & Dharan, 1990; Jain & Yang, 1993).

Karpuschewski et al. (2009) reported that consistent rounding of the drill cutting edges improves the quality of the corner edges and tool surfaces that form the cutting edge, citing that rounded corners allow the avoidance of run-in periods. Consequently, the high wear of the drill is reduced which leads to 80 % increased tool life. Ramkumar et al. (2004a; 2004b) and Zhang et al. (2003) stated that vibration assisted twist drill could be used to improve drilling operations and reduce wear. Lin and Chen (1996) concluded in their study on drilling CFRC materials at high speed that an increase in the cutting velocity led to an increase in the drill wear which directly caused a rise in the thrust force. Furthermore, an analysis and monitoring of occurrence of a flank wear on a 10mm diameter twist drill tool had been carried out effectively by Sivarao (2005), using Mamdani fuzzy inference system (FIS). He reported the reliability of the Fuzzy application as a tool condition monitoring technique.

Statistical and mathematical methods have been used comparatively, to determine the wear on two 10mm diameter twist drills during drilling operation (Sivarao & Wen, 2004). The drill tools X and Y experienced the same process parameters, but slightly different in specification. Drill tool X had 57 HRc, 86 mm and 136 mm, while tool Y possessed 55 HRc, 87 mm and 133 mm of hardness, flute and overall lengths respectively. Drilling operations were carried out with and without lubricant conditions. Tool wear analysis was performed by applying regression analysis and inverse coefficient matrix (ICM) method, considering these drilling variables: thrust force, feed rate, cutting speed and drilling time. In both drilling conditions and within drilling parameters selected, the results obtained from the statistical analysis were much better in terms of accuracy and reliability, when compared with the expected values got from the mathematical analysis. Also, Tool X proved superior to tool Y in terms of design, quality and functionality.

Wear mechanisms of PCD and tungsten drills when drilling CFRP stacked on top of titanium (Ti) has been studied by Park et al. (2011). The wear rate and progression of the tool surface were periodically monitored by using a scanning electron microscope and a con-focal laser scanning microscope. Micro-chipping was observed at the cutting edges

near the PCD drill margin which reduced the tool performance. Major chipping was observed at the cutting edges when drilling titanium as a part of the constituents of the stacked composite due to the brittle nature of the PCD. However, the PCD drill was comparatively better than a tungsten drill tool in terms of wear resistance.

3.3.2 Edge chipping and breakage

Edge chipping is a process whereby small pieces of the drill is removed or cut off as a result of high cutting and thrust forces, as depicted in Figures 3.5 and 3.6 (Rahman, Mamat & Wagiman, 2009; Ertunc, Loparo & Ocak, 2001). An Ineffective removal, control of the various chip formation, poor cooling of the drill and improper selection of the drill point angle, helical angles, chisel edge and inadequate knowledge of the composite materials could lead to reduction in tool life and eventually, tool breakage. These occur when there is no effective space between the tool and workpiece due to poor design of drill geometry and thermal resistance, causing catastrophic rise in drill temperature.

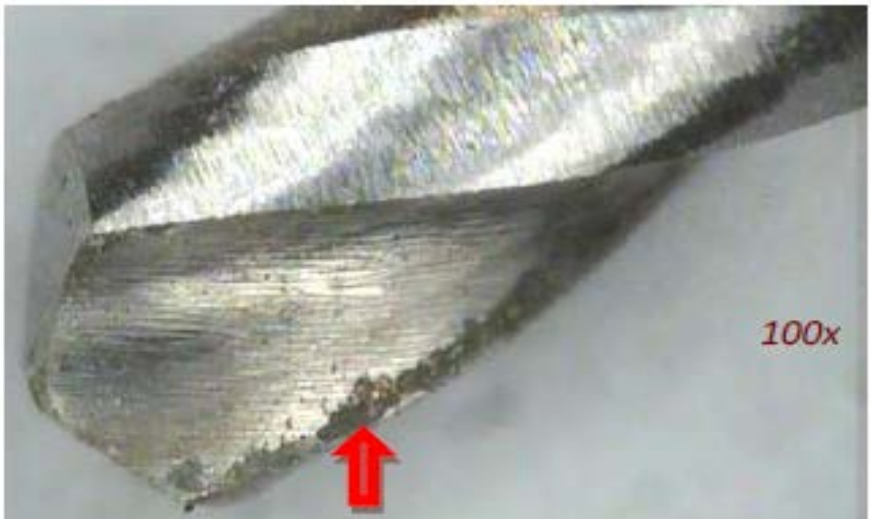

Figure 3.5: Twist drill edge chipping type of wear at lip (Rahman et al., 2009)

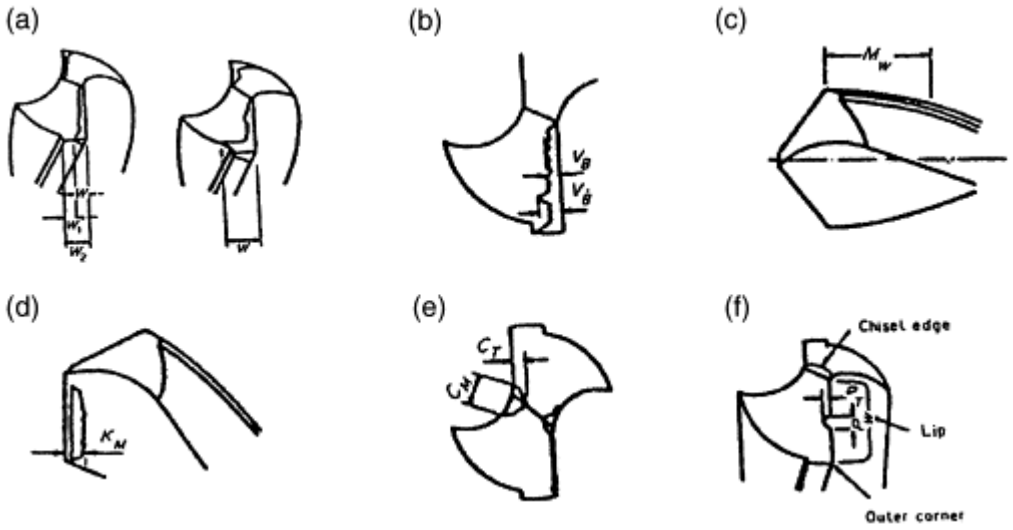

Figure 3.6: Types of drill wear: (a) Outer corners; (b) Flank; (c) Margin; (d) Crater; (e) Chisel edge and (f) Chipping (Ertunc et al., 2001)

3.4 Tool coatings

Improvement and better performance of twist drill life could be achieved, especially at high cutting parameters such as cutting speed and feed rate, and during dry machining, by coatings (Astakhov & Davim, 2008). Coating increases wear resistance, surface quality of drilled composites, corrosion resistance and oxidation resistance. Factors include coefficients of friction, interface temperature and thermal energy that aids wear could also be reduced using appropriate coatings on correct drill bits. Coatings are rampant on both cemented carbide and HSS drills.

3.4.1 Coated cemented carbide

Drill geometry effects on the deposition residual or interface stresses in diamond coated carbide drills has been investigated by Chao et al. (2009), through the performance of a solid modelling of diamond-coated two-fluted twist drills. They concluded that diamond-coated drills have a potential for high performance drilling and for drilling of difficult-to-machine materials. Researchers have concluded that coated drills performed better than

the uncoated, as a result of their increased wear resistance and consequently, improved tool life (Liu et al., 2010; Shyha et al., 2010a; Shyha et al., 2011; Thomas et al., 2012).

3.4.2 Coated high speed steel

Investigation on effectiveness of WC-8C_O electro-spark coating on HSS drills has been reported by Raju et al. (2008). They stated that ESC performance enhances the drill bit life, as high as 5 fold compared to the uncoated HSS drills, based on the machining conditions of variable spindle speed at fixed feed. In comparison to bare drill bit, ESC coated drills performed better in terms of tool life even when drilling at higher speeds.

3.5 Performance and effects of tool coatings

The better or improved performance of drill bits are achieved through coating. In machining technology, several processes have been used in coating cutting tools. In the past nearly 40 years, the thermal diffusion and thin-film processes have been well and rampantly used. Also, it could be chemical and physical vapour deposition (CVD and PVD, respectively) coatings. Contemporarily, 40 % and 50 % of high speed steel and super hard tools, while 85 % of carbides utilised in company are subjected to coating, either on the substrates or entire tools (Astakhov & Davim, 2008). The later application attracts more cost. The coating method could be combination of multiple layers. Among the tooling materials, carbides have been found to be an excellent substrates, irrespective of the types of coatings, including solid lubricant, soft, hard or super-hard, single and multi-layer coatings, as well as PVD: Chromium nitride [CrN], Titanium nitride [TiN], Titanium aluminium nitride [(Ti,Al)N)] and Titanium carbonitride [TiN(C,N)], to mention but a few (Astakhov & Davim, 2008). Audy (2008b) performed a comparative experimental and quantitative investigations on TiN, Ti (C,N) and Ti (Al,N) coatings and found that Ti (Al,N) coating produced the lowest force components and 'edge' forces, using cathodic arc evaporateds PVD coatings. Sivarao et al. (2007) have reported in their experimental work that the TiAlN coated 8mm diameter twist drill tool performed better when compared

with the TiN coated type, under the same dry drilling conditions and parameters in terms of reduction in burrs formation (height). However, using 5mm diameter drill tool, TiN coating proved better when considered the caps formation. The characteristic performances of these coatings are based on their ability to function at high speed, high temperature and dry or semi-dry condition of machining.

In addition, Iliescu et al. (2010) had modelled and experimented the uncoated and Balzers (BS) and Cemecon (CN) diamond coated twist drills wear in CFRP drilling. The drills were manufactured by Diager and Sofimag manufacturer. The results obtained revealed that higher life expectancy of the CN diamond coated drills than the BS coated type, while the Diager and CN coatings were better than the Balzers coating. Furthermore, in a single shot conventional drilling operation on 30 mm thick Ti-6Al-4V/CFRP/Al-7050 stacks, a comparative experimental evaluation of the effects of diamond-like carbon (DLC) and chemical vapour-deposited (CVD) diamond tool coatings on drill wear modes and quality of drilled holes were carried out by Kuo et al. (2014). The DLC and CVD diamond coated drills experienced abrasion (and brittle fracture) wear mechanism initially and untimely flaking or delamination of the coating primarily, respectively. They concluded that the holes drilled with CVD diamond coated drills were clearly better than holes produced with DLC coated drills, in terms of burrs reduction and when circularity was considered.

3.6 The drilling operation

Drilling is a machining process that involves the cutting out or enlargement of holes in a solid material. It is a versatile manufacturing operation which forms an integral part of any machine assembly and component mating. Mostly used as a finishing process, drilling requires a great deal of precision and accuracy for effective usage. The functionality of any mechanical structure is largely depended on the quality of mating between its interconnecting parts, which is achieved through the use of mechanical fasteners such as rivets, pins, screws, among others.

It has been reported that an approximately 25 % of the machining operations used among manufacturing industries are drilling-associated, with an estimate of about 55,000 drilled holes used to assemble the numerous parts of the Airbus A350 aircraft **(**Faraz et al., 2009**).**Therefore, in order to achieve the effective mating of machine parts through the use of fasteners, proper provision of grooves/holes for their installation must be adequately made, and this can only be achieved through drilling.

Mechanical fasteners; usually available in standard sizes, are required to create perfect fit into grooves for which they are designated for use. Therefore, it is necessary to ensure that bolted or riveted joints are accurately drilled, so as to prevent the slackness of the fasteners on the machine members, or their excessive tightness. Consequently, drilling is a crucial machining operation which constitutes largely to the success or failure of any machine assembly **(**Makhdum et al., 2014**).**

Different engineering materials such as metals, woods, plastics, polymers and composites have all been machined through drilling. More so, a variety of drilling processes are available in the world today, depending on the target finish and the nature of the workpiece. Furthermore, drilling engineering is not limited to the aforementioned engineering materials and industries, as it is also a major operation used in the oil and gas industry. Drilling operations in the oil and gas industry takes the form of well drilling for potential exploration sites; the earth crust being the workpiece in this regard. As a result, drilling is a versatile manufacturing operation which spans across a vast past or majority of the engineering world.

3.7 Types of drilling processes

There are basically two types of drilling processes under which all drilling techniques and methods can be appropriately classified. These are:

- Conventional or Traditional Drilling (CD), and
- Non-Conventional or Non-Traditional Drilling (NCD).

Different techniques and methodologies to achieve a damage-free drilling output of these composites have been studied in extant literatures, such as conventional drilling (Abrate & Walton, 1992; Tagliaferri, Caprine & Diterlizzi, 1990; Bongiorno et al., 1998), high speed drilling (HSS) (Rubio et al., 2008; Arul et al., 2006) vibration assisted drilling (VAD) (Arul et al., 2006**;** Sakthivel et al., 2015; Ramkumar et al., 2004a; 2004b), grinding drilling (Park et al., 1995), and other specially designed non-conventional drilling techniques (Abrate & Walton, 2016).

3.7.1 Conventional drilling

Advancement in materials science over the years has prompted the evolution of new tools and the discovery of newer energy sources for effective materials processing. While tools made from crude materials of stone and iron were effective in materials processing some decades ago, twentieth century products featured sophisticated, durable, and consequently the most difficult materials to machine using the pre-existing tools. Therefore, in order to overcome the challenges posed by these materials, new processing tools such as carbide, diamond, and steel were introduced, while new methods of machining were developed to ensure satisfactory levels of materials processing.

Initially, conventional or traditional techniques were pioneering methods used in the drilling of materials. These techniques usually involve the use of prime movers to mechanically energize crude cutting tools against a work-piece material surface. Typical prime movers used in these pre-existing techniques were electric motor, gravity, and hydraulics, with iron-made materials being the main cutting tools.

3.7.1.1 Mechanics of conventional drilling

The conventional drilling operation is actualized by the high speed rotary impact of a cutting tool; the drill bit, against the surface of a work-piece, which is guided by the influence of a mechanical thrust for the generation of drilling effects. The cutting edge of the drill bit which rotates at high speed; usually in the range of hundreds to thousands of

revolutions per minute then cuts off chips from the workpiece material by shear deformation.

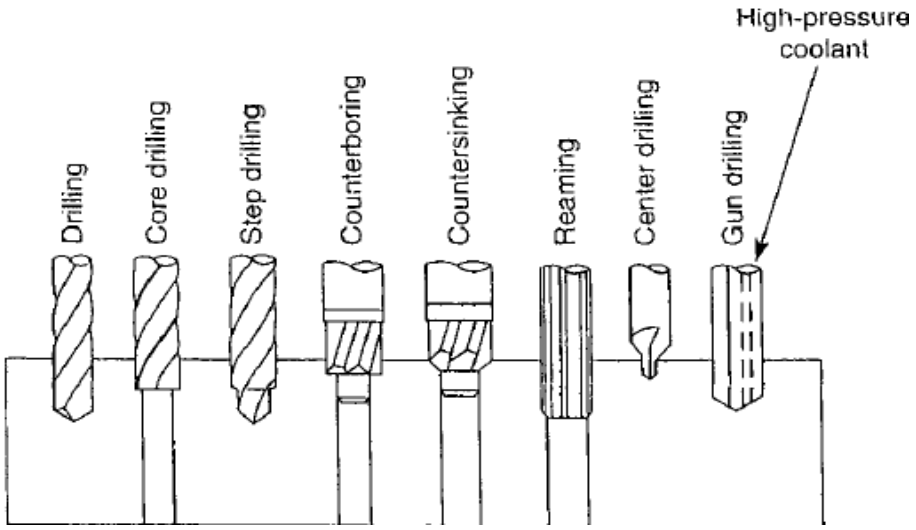

Figure 3.7: Various types of drills and drilling operations (Kalpakjian & Schmid, 2003)

Various drill bits are available in the manufacturing world of today, such as the twist drill bit, step drill bit, hole saws, among others, for different drilling operations, as depicted in Figure 3.7. Also, the twist drill bit remains the most common type of drill bit used for drilling purposes, with reports which showed that the United States' manufacturing industries consume about 250 million twist drills per annum **(**DeGarmo, Black & Kohser, 2003**).** The twist drill bit is made up of a cylindrical shaft with helical flutes and a cutting edge at its end, with other designed geometry (Figure 3.1). The drilling effect of the twist drill bit is achieved by the rotary action of the cylindrical shaft against the work-piece, primarily caused by the impact of the helical flutes with the sharp cutting edge.

Furthermore, the governing parameters of drilling mechanics are the cutting speed, feed rate, cutting force, and the material removal rate (MRR). These are further discussed as thus:

Cutting Speed: This is the rate at which the outside or the periphery of the tool moves relative to the workpiece, usually measured in mm/min. It is the largest of all the relative

velocities developed in drilling operation. Respectively, the peripheral and rotational velocities of a cutting tool are given by the relations:

$$\mathrm{V} = \frac{\pi \mathrm{DS}}{1000} \tag{3.1}$$

Where V is the peripheral velocity measured in mm/s, D is the diameter of the drill bit in mm, and N is the rotational speed; otherwise referred to as spindle speed, measured in revolutions per minute (rpm).

Consequently, the spindle speed:

$$S = \frac{1000V}{\pi D} \tag{3.2}$$

The optimum cutting speeds can be adjusted for better performance, depending on factors such as:

- Material composition, hardness, and thermal stability.
- Nature of cutting fluid.
- Depth of hole, as well as the finish quality desired.
- Stiffness of cutting tool, and orientation.

Feed Rate: This refers to the rate at which the drilling tool advances along the workpiece geometry, usually measured in mm/min. It signifies the rate at which the workpiece material is fed into the drill bit without causing a jam, and is given by the equation:

$$F = S \times f \times N \tag{3.3}$$

Where *S* = spindle speed, *f* = feed per tooth, and *N* is the number of flutes on the cutting tool.

Furthermore, the feed rate is a standardized parameter for different drill diameters, and highly depended on the strength nature of the workpiece material. A good rule of thumb

for drilling operation is to use lower feed rates for harder materials, and higher feed rates for their softer counterparts.

Cutting Force: This refers to the contact force generated by the tool tip against the workpiece surface, as shown in Figure 3.8.

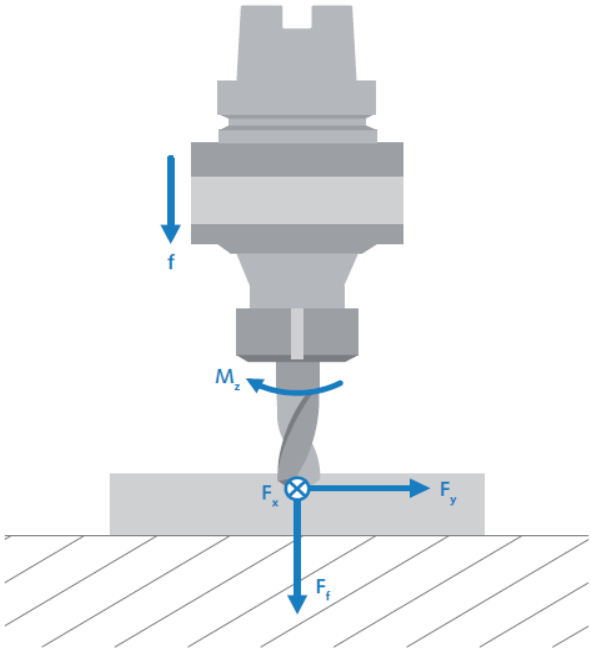

M_z = Drilling Moment.

F_x = Deflective force in the x-axis.

F_y = Deflective force in the y-axis.

F_f = Feed force.

Figure 3.8: Cutting forces in drilling operation

Thrust Force: This is the normal force exerted by the cutting tool on the workpiece, for the generation of drilling effects. It can be estimated according to the equation:

$$F = \frac{k' \times k_c \times f \times D}{2} \qquad (3.4)$$

Where k_c = specific cutting force, measured in N/mm^2, depending on the material being drilled.

f = feed per rotation (mm), D = tool diameter (mm), and k is a drilling coefficient, depending on the tool tip geometry (typically considered as an average of 0.5).

Material Removal Rate: This is the volume of workpiece material removed per minute, given by:

$$MRR = V \times f \times D \quad (3.5)$$

3.7.1.2 Conventional drilling of fibre-reinforced polymer (FRP) composites

Conventional drilling refers to any material removal process for hole generation, which involves the formation of chips from a work-piece by the direct contact of a wedge shaped cutting tool which is harder than the workpiece material, under machining conditions. It is characterized by a macroscopic chip formation; achieved by the shear deformation of the work-piece material, a mechanical energy domain for cutting effects, and a tool which is stronger than the workpiece at room temperature and machining conditions.

The thrust and torque applied to a bit during drilling operation is depended on the drilling speed, feed rate, tool geometry and the rate of tool wear, as illustrated in Table 3.3 (Abrate & Walton, 1992). Wong, Wu and Croy (1982) reported that the thrust increased steadily at the entrance until a constant value necessary to initiate drilling is ultimately reached, followed by a sharp decrease in the thrust value, as the tool finally exits the opposite side of the workpiece. As a result, there is a sharp decline in the feed force at the entrance of the workpiece, resulting in a “peeling-out” phenomenon; commonly referred to as delamination. Owing to the abrasive, inhomogeneity and anisotropic nature of FRPs, the actualization of a damage-free output in their conventional drilling approach has proven quite ineffective (Arul et al., 2006).

Table 3.3: Typical machining parameters for drilling composite materials (Abrate & Walton, 1992)

Workpiece material	Tool material	Hole diameter (mm)	Material thickness (mm)	Cutting speed (m min^{-1})	Feed rate (mm rev^{-1})
Unidirectional graphite–epoxy	Carbide	4.85–7.92	0–12.7	42.7	0.0254–0.0508
		4.85–7.92	12.7–19.1	33.5	0.0254
	PCD	4.85–7.92	0–12.7	61.0	0.0508–0.0889
		4.85–7.92	12.7–19.1	51.8	0.0508–0.0889
Multidirectional graphite–epoxy	Carbide	4.85–7.92	0–12.7	61.0	0.0254–0.0508
		4.85–7.92	12.7–19.1	42.7	0.0254
	PCD	4.85–7.92	0–12.7	68.6	0.0508–0.0889
		4.85–7.92	12.7–19.1	61.0	0.0508–0.0889
Graphite–epoxy	Carbide	4.85	6.35	60.9	0.0254
Glass–epoxy	HSS	—	12.5	15.0	0.028
Glass–epoxy	HSS	3	10	33.0	0.05
Carbon–epoxy	Carbide	3	10	33.0	0.05
Glass–epoxy	HSS	8	1.2	0–40.2	20–460 mm min^{-1}
Boron–epoxy	PCD	6.35	2.0	91–182	25.4 mm min^{-1}
		6.35	25.4	91–182	25.4 mm min^{-1}
MMC	PCD / Carbide	6	19.2	15–75	0.05
Boron–epoxy	PCD	6.35	10.4	79	41.91 mm min^{-1}
Kevlar–epoxy	Carbide	5.6	—	158	0.05

3.7.1.3 Problems associated with FRP composite conventional drilling

The mechanism of drilling composites is a process different from that of conventional materials (especially metals and their alloys) for a good quality hole to be obtained (Rubio, Panzera & Scarpa, 2015). It has been stated that due to the coexistence of hard abrasive fibres and a soft matrix, there is need for an appropriate selection of cutting conditions (Velayudham, Krishnamoorthy & Soundarapandian, 2005b). Carbon fibre composites have a challenge of poor machinability as a result of their highly abrasive nature, which limits its applications. This causes its fast replacement with natural fibre composites. There are damage caused on drilled composite materials as a result of their composition such as delamination, hole dimensional inaccuracy, surface roughness, fuzzing and composite fibre-pull out or uncut fibres (Mišković & Koboević, 2011; Rubio et al., 2015; Wang et al., 2014). The damaged composite materials are susceptible to fatigue strength and load bearing capacity (Wang et al., 2014).

Conventional drilling of FRPs often results in a variety of damage on the composite laminates, which affects the load-bearing capacity of the composite joints, and consequently leads to their eventual discard. Due to the complex nature of the materials, some of these damage may not be observable by visual inspection, thus leading to the need for conducting Non-Destructive Testing (NDT) of the composite materials, in order to assess their safety towards industrial usage **(**Durão et al., 2014**)**. Notable material damage and tool effects commonly encountered in the conventional drilling of composite materials are outlined.

Additionally, Kim and Ramulu (2004a) reported that for years, carbon fibre composites have been drilled using the same methods applied in drilling metals. These have resulted in poor finish quality and excessive tool wear (Kim & Ramulu, 2004a). Abrasive, heat sensitivity and heterogeneous nature of composite materials make its drilling a complex operation (Davim & Reis, 2003a). For applications where quality demand is high, drilling of the composite structures remains a major challenge, especially where carbon reinforced composite is stacked to metal parts (Brinksmeier & Janssen, 2002; Kim & Ramulu, 2004a). This scenario increased the severity of the problem, and hence it requires a more robust specially designed drill and better drilling processes.

Importantly, drilling of carbon fibre laminates has several common problems. These setbacks include surface scorching, delamination, excessive tool wear, fibre cratering, matrix- melting and softening (Coromant, 2011). Among these, delamination is the most critical defect as it has the highest level of impact on accuracy and quality of a drilled hole (Madhavan & Prabu, 2012; Wang et al., 2014).

3.7.1.3.1 Delamination

This is a drilling-induced damage on composites, typically exhibited at the inter-laminar boundaries between the adjacent fibres. Delamination is simply defined as the main form of failure of laminated composites whereby the laminates or layers separate along their interfaces (Sridharan, 2008). Consequently, its occurrence during drilling is

depended on the nature of composite fibres, the polymer matrix, and the mechanical properties; such as toughness, Poisson ratio, or the elastic modulus of the interfacial boundaries. It is the major drilling damage on composite materials (Kavad et al., 2014). Reports from Wong et al. (1982) and Sakthivel et al. (2015) also showed that about 60% of composite rejects in the aerospace industry are traced to delamination defects, as highlighted in Figure 3.9.

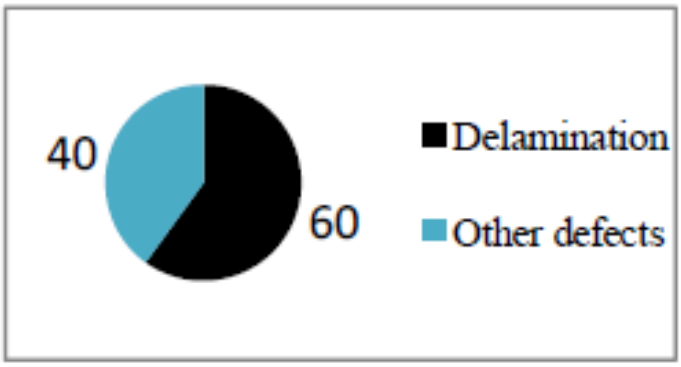

Figure 3.9: Composite rejection reasons in many manufacturing companies, mainly in the aerospace industry (Sakthivel et al., 2015)

Delamination in a composite material occurs whereby reinforced fibre plies separate, either by peel-up or push-out phenomenon. This defect occurs at the upper most layer of laminate from the rest of the body and/or on the drill bit's tip which pushes the bottom layers of the laminate respectively (Khashaba, 2004; Hocheng & Tsao, 2005). In drilling, delamination occurs mainly at the critical entry and exit locations of the drill bit when the thrust force is greater than a threshold value (Dharan & Won, 2000; Zitoune & Collombet, 2007; Velayudham & Krishnamurthy, 2007; Mišković & Koboević, 2011). Delamination depends on many factors such as composite fibre nature, drilling parameters, drill design and laminate orientation. When the drill tip exerts compressive thrust force on the uncut composite laminate plies, and the point loading is greater than the inter-laminar bond strength of the composite, delamination occurs. It reduces composite dimensional accuracy, structural integrity, surface quality and durable applications (Davim & Reis, 2003a; Madhavan & Prabu, 2012; Mišković & Koboević, 2011). In other words,

delamination decreases the assembly tolerances, reduces the bearing strength of engineering materials and reduces the components performances at a long term when subjected to fatigue loads.

Madhavan and Prabu (2012) indicated that an increase in cutting speed reduced the delamination for HSS drills, whereas an increase in feed rate increased the delamination effect in case of carbide drills. An analysis of the differences in delamination mechanisms has been carried out by Capello (2004) when drilling laminate composites with and without a support device placed under the workpiece. His results showed that the proposed device drastically reduced delamination.

An analytical approach to identifying the process window of chisel edge length concerning drill diameter for delamination-free drilling has been studied by Tsao and Hocheng (2003). The approach was based on linear elastic fracture mechanics of fibre reinforced composites. An optimal range of diameter of pilot hole associated with chisel edge length was derived. They concluded that composite laminates drilling at higher feed rate without delamination damage could be conducted by controlling the ratio of chisel edge length and preferring medium to large hole. Isbilir and Ghassemieh (2013) studied that the delamination-free drilling process might be obtained by the proper selections of drill point geometry and the process parameters: high spindle speed and lower feed rate. They showed that effective tool choice could minimize delamination effect. Importantly, the use of higher feed rates is achievable provided there is sufficient knowledge of the effects on thrust force and delamination for each selected drill.

3.7.1.3.2 Mechanics of delamination

Delamination is caused by a number of drilling parameters, namely: the thrust force, feed and the thermal stress mode on the material. Experimentally proven by Stone and Krishnamurthy (1996) as well as Tsao (2012), the delamination potential is directly related to the thrust force developed during drilling. The drilling evolution as well as the axial drilling force and time taken are shown in Figure 3.10. The possibility of delamination damage is rampant at a peak or critical thrust force, after the knee region.

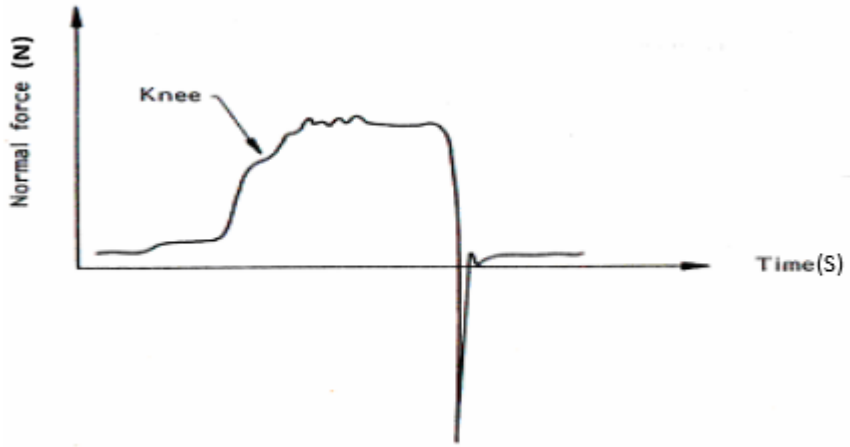

Figure 3.10: Typical axial force history during composite drilling (Abrate & Walton, 1992)

Delamination sometimes forms as a crack between the adjacent plies, it occurs often between two anisotropic and heterogeneous materials as an interface crack. Delamination occurs under a tensile loading, bending loads, but it grows mostly under the critical compressive and fatigue loading conditions (Sridharan, 2008). It is a microscopic defect. It describes the weakest inter-laminar fracture and most rampant life-limiting crack propagation mode occurred in a good number of composite laminates and structures. Usually, it is a mixed-mode (opening, sliding shear and tearing modes) fracture phenomenon (Kim & Mai, 1998; Sridharan, 2008), as shown in Figure 3.11.

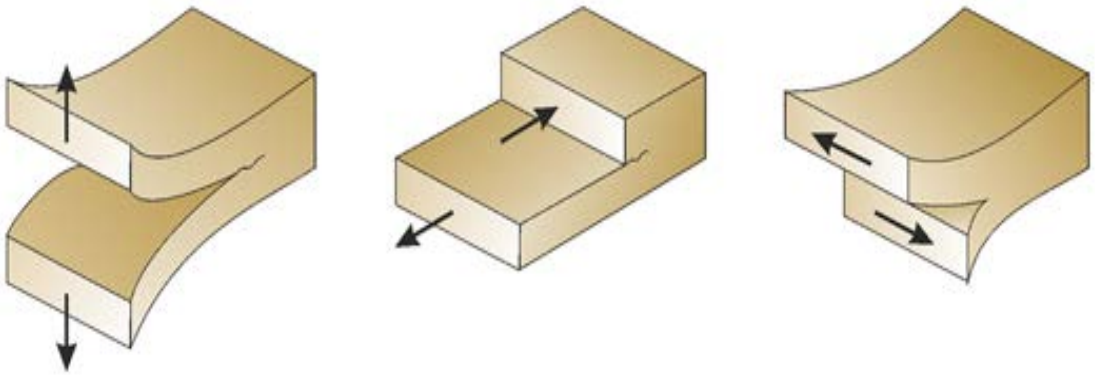

(a) Mode I (Opening or peeling) (b) Mode II (Sliding shear) (c) Mode III (Tearing shear)

Figure 3.11: The basic fracture modes in delamination

Several research (studies) have been carried out towards the understanding and description of its nature as well as improving the machining parameters, conditions and drills design against occurrence of this drilling-induced failure. The possibility of delamination strongly depends on the thrust force, residual stress and the properties of the fibre-matrix material/interface. Delamination occurs when the critical thrust force exerted by the drill bit on the composite material is exceeded. Irrespective of the base: ceramic, polymer or metal matrices, residual stresses are innate in nearly all the fibre-reinforced composite materials. Other factors responsible for delamination are illustrated in Figure 3.12. Primarily, the thermal and mechanical are the two basic sources of residual stresses common in fibre-reinforced composites. The thermal type caused by the difference in co-efficient of thermal expansion (CTE) is mostly rampant. The curing pressure and elevated temperature dissimilar from process temperature induces and builds up residual stresses in the fibre-composites. The CTE depends on the constituents of the composite. The thermal residual stress could be either micro or macro. It depends on the geometry of the composite and scale (Kim & Mai, 1998).

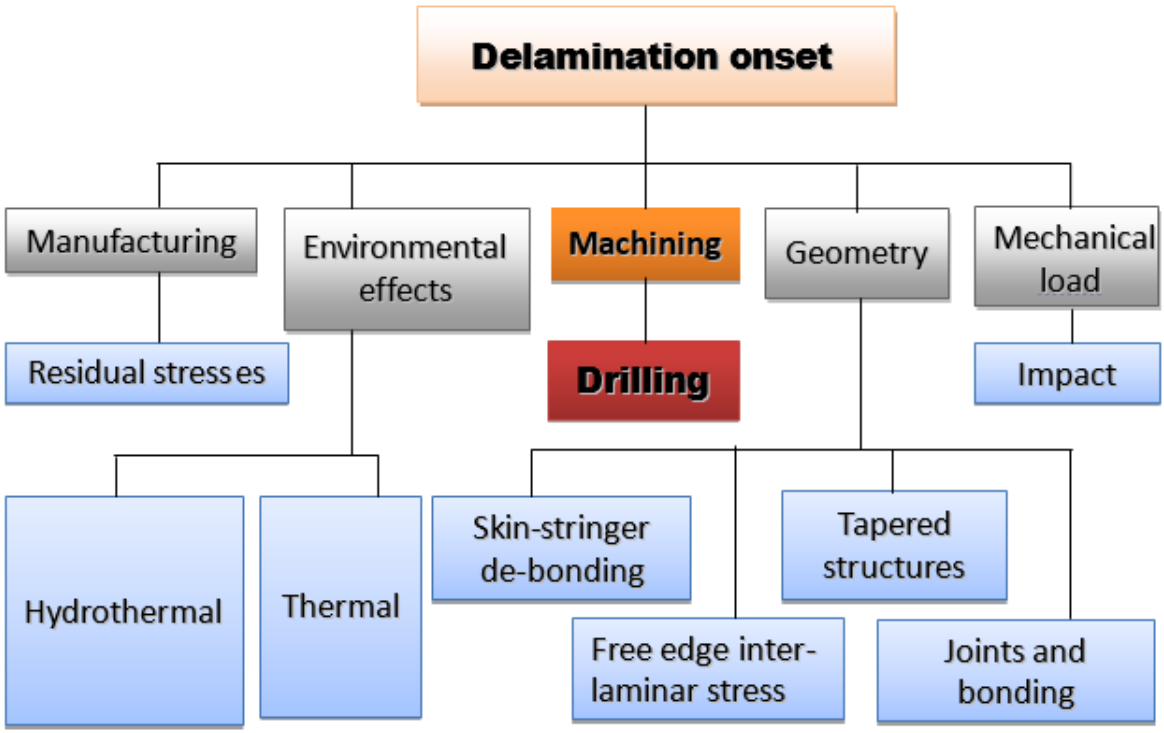

Figure 3.12: The principal causes of delamination onset (Sridharan, 2008)

Khashaba **(**2004**)** showed that delamination size increased linearly with feed, and inversely with cutting speed. The thrust force; being the normal force on the drill bit, is the major cause of delamination, and a critical thrust force is usually reached before the onset of crack propagation. While the ability to transmit the thrust force developed during drilling from the tools to the composite material is depended on the tool geometry (Figure 3.13), the evaluation of delamination onset is also subject to the type of drill bit employed in the drilling operation.

Numerical models to evaluate the relationship between thrust force and delamination damage during drilling have been developed (Hocheng & Tsao, 2005; Hocheng & Dharan, 1988; Upadhyay & Lyons, 1999). The first model which was developed by Hocheng and Dharan (1988) assumed a circular delaminated region and a rigid circular plate which was clamped on its contour to the cut portion of the laminate. More so, they treated the critical thrust as a single concentrated load through the drill tip, and found that it was depended on the composite properties (quasi-isotropic) and the thickness of the uncut plies. Noticeably, Hocheng and Tsao (2005) developed a more comprehensive model by considering the influence of tool geometry (across a variety of drill bits such as brad point, slot, step and core drill bits) in the generation of the critical thrust. Further mathematical models are presented in Table 3.4. Similarly, Upadhyay and Lyons (1999) improved the model of Hocheng and Dharan (1988) by treating the thrust force as a uniformly distributed load, rather than a single concentrated. This is because, the thrust force does not act as a single concentrated load through the tool tip, but as a distributed load over the entire chisel edge of the drill bit.

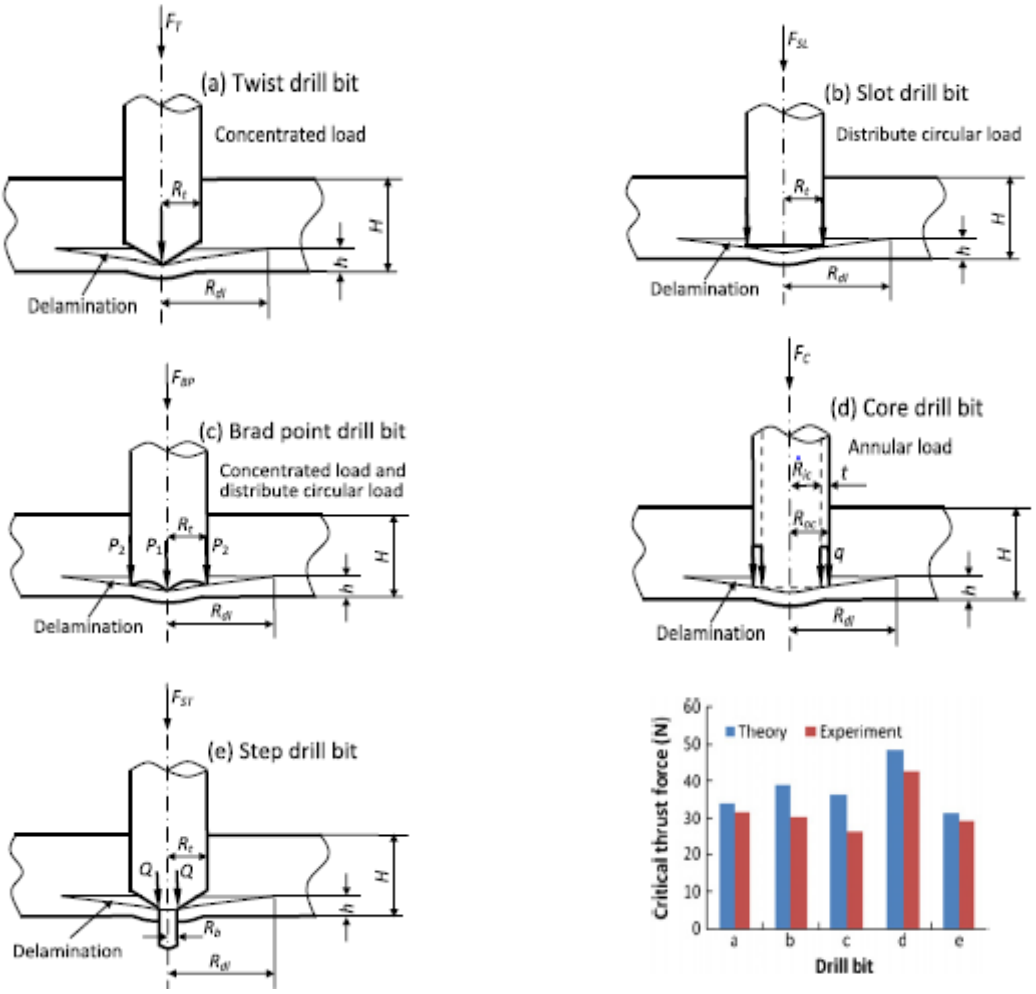

Figure 3.13: Schematics of delamination for various drill bits (Liu et al., 2012)

Table 3.4: Critical thrust force models for delamination onset in various drill bits

S\N	Drill bit type	Critical Thrust force model	Remarks	Author
1	Twist drill	$F_{CT} = \pi \left[\frac{8G_{IC}Eh^3}{3(1-\nu^2)}\right]^{1/2}$	E = Elastic modulus, G_{IC} = Critical strain energy, h = uncut plies thickness under drill bit	Hocheng & Dharan [27] Abrate & Walton [11] Sakthivel et al. [16]
2	Brad drill bit	$F_{CSL} = \frac{1}{\sqrt{1 - 2S^2 + S^4}} F_{CT}$	$S = R_t/R_{dl}$, where R_t = drill bit radius, and R_{dl} = Delamination radius	Hocheng & Tsao [10]
3	Slot drill bit	$F_{CBP} = \frac{1+\alpha}{\sqrt{1+\alpha^2 (1 - 2S^2 + S^4)}} F_{CT}$	α = Ratio of concentrated load (P_1) and peripheral circular load (P_2)	
4	Step drill bit	$F_{CBP} = \frac{\beta(2-\beta)}{\sqrt{[1-(1-\beta)^4] - (1/2)S^2[1-(1-\beta)^6]}} F_{CT}$	$S = R_{oc}/R_{dl}$, and $\beta = t/R_{oc}$ t = Thickness of core drill bit, and R_{oc} = Outer radius of core drill bit	
5	Core drill bit	$F_{CST} = \left\{\frac{[(1-\nu)+2(1+\nu)\xi^2]^2}{\sqrt{(1+\nu)[2(1-\nu)(1+2\nu^2) - 12(12 - 4\nu + 3\nu^2 + 3\nu^3)\xi^2 \ln \xi]}}\right\}^{1/2} F_{CT}$ $\xi = R_b/R_t$		

3.7.1.3.3 Delamination Assessment

In the evaluation of delamination damage in drilled materials, a number of assessment models have been developed to measure the extent of material damage. The most common evaluation is shown in Figure 3.14. For clear understanding, they are clearly illustrated in Table 3.5. Analytically, delamination factor, F_d has been generally used (Tsao, & Hocheng, 2004; Davim & Reis, 2003a; Madhavan & Prabu, 2012; Davim & Reis, 2003b) to describe the intensity of damage on the composite both at the drill entry and exit. It is expressed as $F_d = \frac{D_{max}}{D}$, where D_{max} and D are the maximum diameter of the delamination zone and the drill diameter (Ismail et al., 2016a; Ismail et al., 2015) respectively (Figure 3.14b). A typical microscopic result of the delamination defect is depicted in Figure 3.14(b), showing how this damage was measured and analysed. The higher the F_d, the greater the delamination effect (Tsao & Hocheng, 2004; Davim & Reis, 2003b; Ismail et al., 2016a).

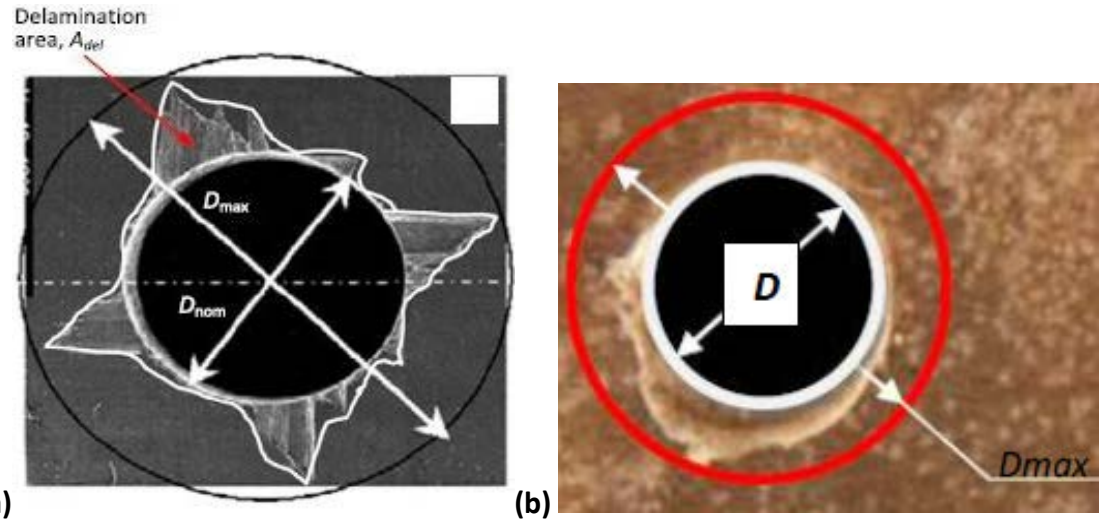

(a) **(b)**

Figure 3.14: (a) Surface image of delamination in CFRP drilling (Liu et al., 2012) and (b) analysis or determination of delamination factor (Ismail et al., 20115; Ismail et al., 2016a)

Table 1.5: Delamination factor assessment models

S\N	Delamination factor (D_f) Assessment	Analysis	Remarks	Author
1.	$\frac{D_{max}}{D_{min}}$	One dimensional	D_{max} = Major diameter D_{min} = Minor diameter	Arul et al. (2006); Sakthivel et al. (2015); Abrate and Walton (1992)
2.	$\frac{D_{MAR}}{A_{AVG}}$	Two dimensional	D_{MAR} = Hole Peripheral Damage Area A_{AVG} = Nominal Drilled Hole Area	Mehta et al. (1992)
3.	$\left(\frac{A_{del} - A_{nom}}{A_{nom}}\right)$	Two dimensional	A_{del} = Damaged area A_{nom} = Nominal area of hole	Faraz et al. (2009)
4.	$\alpha\frac{D_{max}}{D_{nom}} + \beta\frac{A_{max}}{A_{nom}}$	Adjusted two dimensional	A_{max} = Area of maximum diameter in delamination zone, α and β are delamination coefficients.	Davim et al. (2008)

3.7.1.3.4 Types of Delamination

Delamination effects can be classified into two, depending on the side of its occurrence and the nature of force involved in its mechanics. These include:

Peel-up Delamination: This type of delamination effect is caused by the tensile impact of the cutting thrust which pulls the laminate surface towards the helical flutes of the drill bit at hole entrance, as shown in Figure 3.15a. Consequently, this results in the separation of the upper laminate surface from the adjacent layers beneath, leading to a cavity within the composite material. The peel-up delamination is depended on the tool geometry and the friction between the tool and workpiece.

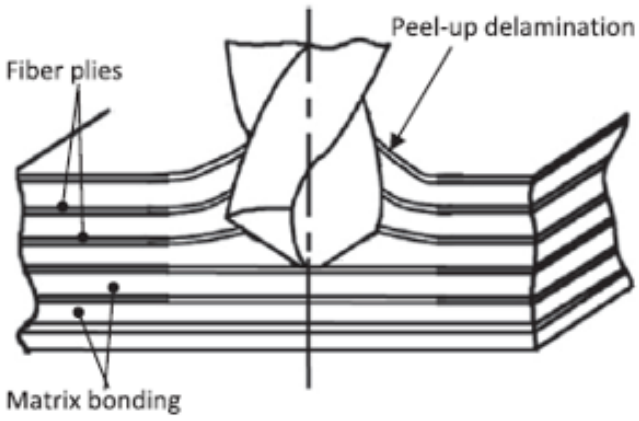

Figure 3.15a: Peel-up delamination in FRP composite laminate (Liu et al., 2012)

Push-out Delamination: The push-out delamination is generated by the compressive action of the drill bit on the adjacent layers of the laminate, usually at the exit side of the composite material (Figure 3.15b). It is the most prominent and severe delamination damage in composite machining (Khashaba, 2004; Hejjaji et al., 2016)**.** As the drill bit approaches the exit side of the laminate, the uncut plies gradually become thinner and more prone to deformation. With constant thrust force coupled with reduced laminate

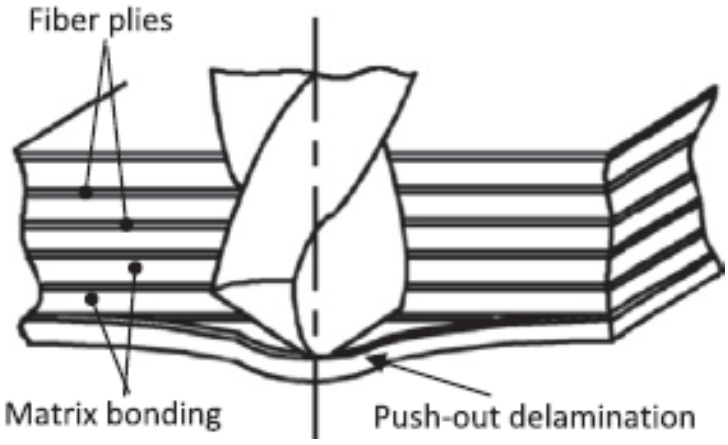

Figure 3.15b: Push-out delamination in FRP composite laminate (Liu et al., 2012)

thickness, the interfacial bonding strength of the composite is eventually exceeded by the thrust, leading to the push-out delamination at the periphery of exit. It is quite possible to have both types occurred in a single FRP composite material, at the same time and in a single hole, as depicted in Figure 3.16.

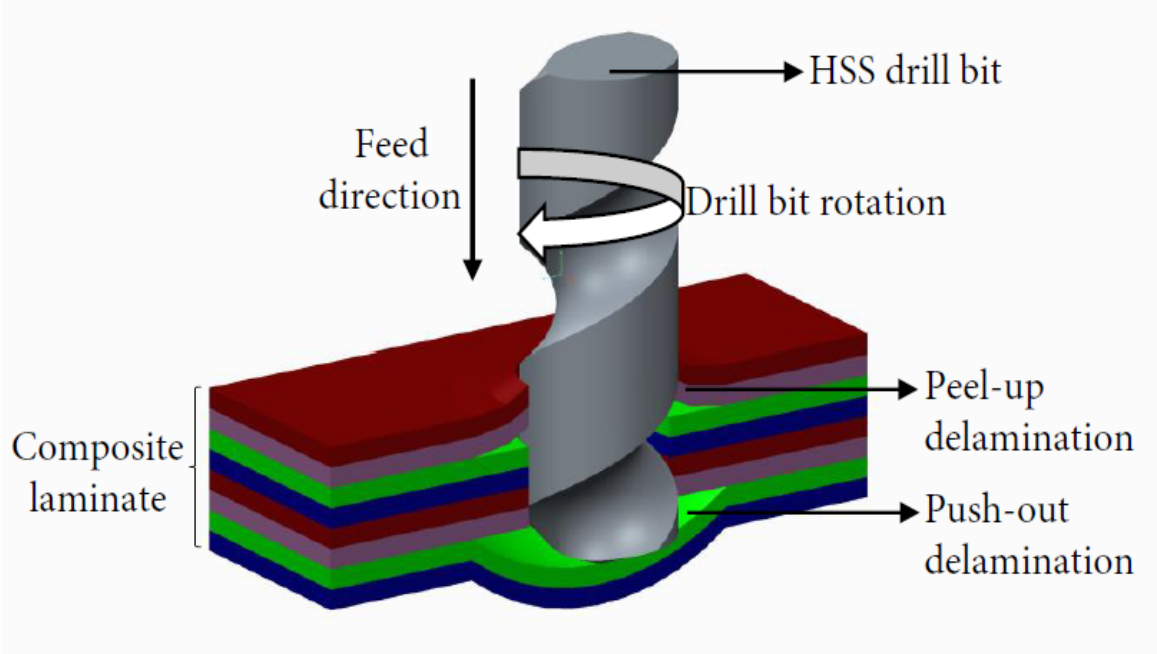

Figure 3.16: Combined peel-up and push-out delamination in a FRP composite laminate (Ismail et al., 2016c)

Temperature-induced damage in conventional drilling techniques takes the form of localized heating which results in burning, melting, or micro-cracks within the composite structure. Due to the highly abrasive nature of FRPs, high thermal energy resulting from excess friction is usually developed at the interface between the tool tip and the composite. While it is not recommended to employ cutting fluids during composite drilling due to the nature of their fibres, the distribution of the generated heat becomes quite concentrated (Durão, 2005).

Basically, the heat distribution during drilling operation differs with workpiece materials. For metals, 75 % of the heat generated during drilling is eliminated by the chips, 7 % is absorbed by the workpiece material and 18 % by the tool. However, in the case of

carbon-epoxy composites, half of the heat generated is absorbed by the tool, while the other half is trapped within the composite and conveyed by the chips. With machining temperatures reaching as high as 200 ^{o}C during composite drilling and in the absence of cutting fluids, the risk of thermal damage via localized heating increased significantly (König & Graβ, 1989).

3.7.1.4 Tool (drill bit) Wear

Conventional drilling of composite materials is usually accompanied by relatively higher cutting thrust sufficient to damage the tool tip by flaking and chipping mechanisms. Tool damage is usually characterized by excessive wear and frictional heat; in cases of composites with hard and abrasive fibres and tool edge dull by clogging; in cases of soft and sticky polymer matrix (Chen, 1997). Experimental investigations on the wear mechanisms of drill bits such as high speed steel (HSS), cemented carbide and diamond coated carbides have been extensively studied (Abrão et al., 2007; Rawat & Attia, 2009) to prove this subject. Much on this has been earlier discussed under sub-title 3.3.1.

3.7.1.5 Surface roughness and dimensional inaccuracy

The importance of surface integrity, quality, dimensional and geometric tolerances of holes when drilling CFRP composites can never be compromised. Surface roughness is basically measured using two distinctive methods: direct and indirect methods. The former involves the use of stylus (contact) instruments and the later depends on optical (non-contact) instruments (Wen et al., 2004). As a result of the nature of some composite materials, very little has been accomplished to improve on surface roughness and dimensional integrity (Abrão et al., 2008; Brinksmeier & Janssen, 2002; Davim et al., 2004a; Shyha et al., 2011; Singh & Bhatnagar, 2006; Velayudham & Krishnamurthy, 2007). The roughness of the drilled surface has not been accounted for as a major issue based on its application (Abrão et al., 2007). In addition, formation of burrs and caps are another causes of dimensional inaccuracy, as reported by Sivarao et al. (2007). They both reduced the fatigue life of the assembly components. Burr occurred as a resultant effect of a plastic deformation of a material under machining process (drilling). Practically, the burrs formed

at the entrance of a drilled hole are usually smaller than the exit burrs (Sivarao et al., 2007). The surface roughness in drilling with two different tools has been comparatively analysed and modelled, using regression analysis and ICM method (Wen et al., 2004). It was concluded that the statistical (regression) analysis produced better results than the mathematical analysis (ICM). The evaluation was based on the proximity of their results to the actual values.

Poor surface finish as well as delamination occurs due to the heat generation (friction) between drill edges and the composite. The heat aids the softening of the matrix. Also, poor surface finish could be aided by improper selection of drilling parameters and tooling materials. Ogawa et al. (1997) reported that surface roughness varies at different speeds, but speed is only of minor influence. They also stated that feed rate seems to affect the surface roughness most. Thereby, it is a great task to obtain the required surface quality for accurate assembly of some structural parts (Brinksmeier & Janssen, 2002; Madhavan & Prabu, 2012). Ogawa et al. (1997) observed that smoothest surfaces of almost 0.1 µm were produced with PCD drills, followed by Carbide drill at the same speed of 100 mm/min which produced good appearance holes but with high roughness of 6.5 µm while HSS has the highest surface roughness of 8.0 µm. Cutting speed increased with decrease in surface roughness. Comparatively, PCD drills provided good surface finish at high cutting speed and feed rate (Madhavan & Prabu, 2012). It was concluded that the surface roughness of drilled holes on composites increased with increase in feed rate irrespective of the drill diameters unlike the spindle speed which has a small effect on surface roughness. Meanwhile, the dimensional accuracy of drilled hole decreased with an increase in machine spindle speed, drill diameter and feed rate (Rahman et al., 2009), as shown in Figure 3.17, where TD represents the tool diameter. Hence, hole diameter inaccuracy increased with an increase in drill diameter. This is attributed to the high drilling force impacted on the surface of the hole when cutting at high values of the afore-mentioned parameters, as both entry and exit parts of the hole are significantly impaired. The experimental numbers 1 to 9 refer to the number of experiment tests conducted.

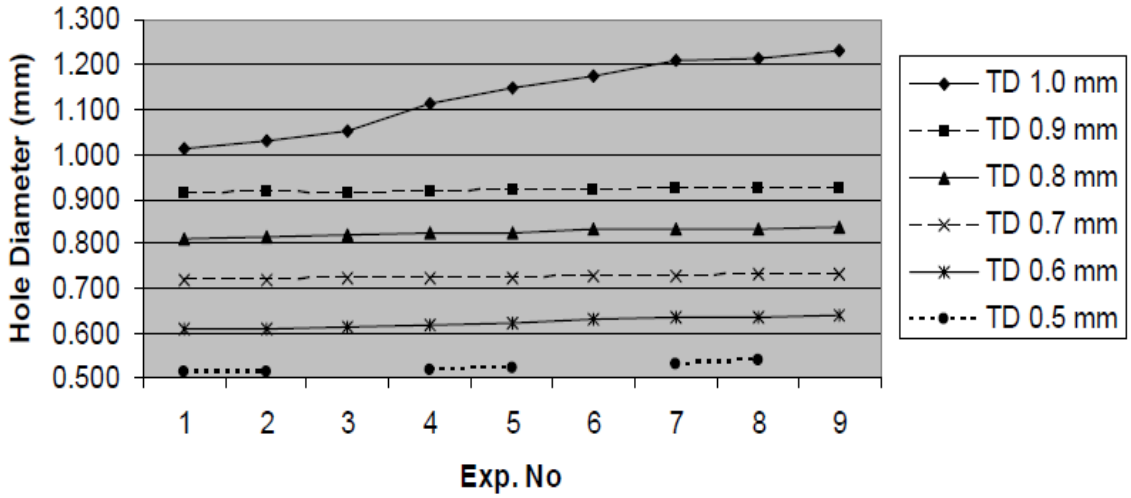

Figure 3.17: Effect of different tool diameters on drilled hole dimensional accuracy (Rahman et al., 2009)

From Figure 3.17, the experimental numbers increased with the diameters of the drilled holes. Importantly, increase in the TD caused a significant increase; deviation in form of errors in the desired hole diameter. This was more evident at 0.6 and 0.8 mm TD immediately after experimental number 5, at most in 1.0 mm TD progressively. Dimensional errors ranging between 5 to 10 % were recorded (Rahman et al., 2009). Summarily, it has been reported that the surface roughness of a drilled hole depended on the hardness of the workpiece and drill, geometry of the drill, drilling parameters and machine rigidity (Wen et al., 2004).

3.7.1.6 Matrix de-bonding, fibre pull-out, fibre-uncut and other associated problems

Due to the quasi-isotropic nature of FRPs, the high cutting thrust developed during their drilling operation destroys the interfacial adhesion energy between the fibres and the matrix, resulting in matrix de-bonding, and eventually fibre pull-out. Abrão et al. (2007) suggested in their review paper that the cutting speed should be kept below 60 m/min; due to the fact that high cutting speed values led to higher cutting temperatures, which caused composite matrix softening, followed by matrix cratering and thermal damage of its constituents, particularly the binders.

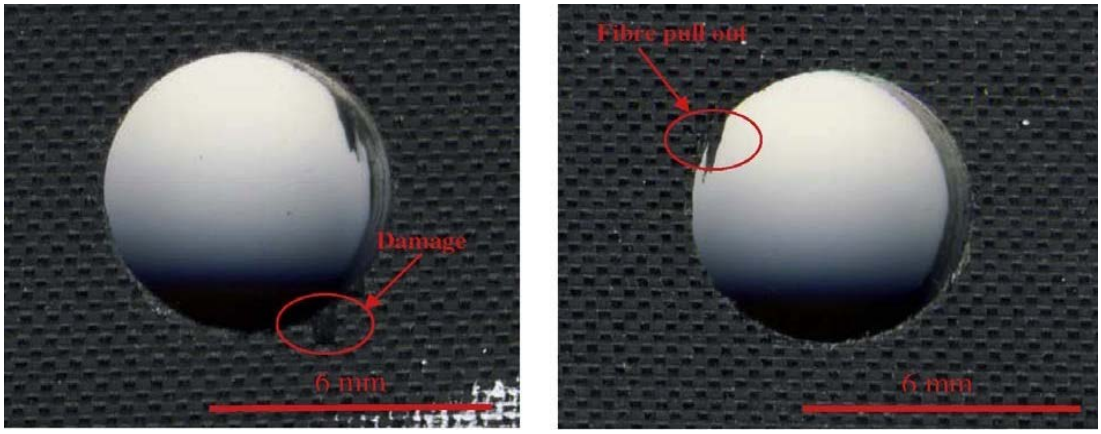

Figure 3.18: Fibre pull-out and fibre-uncut defects at hole entry and exit (Zitoune et al., 2010)

Fibre pull-out and uncut fibre (Figure 3.18) are separate relevant problems. The significance of correct choice of process parameters especially when drilling multi-material stack has been reported (Zitoune, Krishnaraj & Collombet, 2010). Their experimental results depicted that the quality of drilled holes could be improved by proper selection of cutting parameters as the drilled hole circularity increased with feed rate: around surface roughness, R_a of 6 µm (at low feed rates) to 25 µm in CFRP. From drill wear test results, they showed that thrust force significantly increased to 90 % in CFRP compared with 6 % in aluminum after the first 30 holes were drilled. When the number of holes increased to 60, composite fibre pulled out and parts of the fibres remained uncut (Figure 3.18), due to the drill wear caused by an increased workpiece-tool interface temperature and friction.

3.7.2. Non-conventional drilling

With regards to the sophisticated characteristics of the new age materials, the conventional drilling techniques became relatively ineffective in materials processing. More so, a great deal of restrictions associated with the use of traditional drilling techniques for materials processing rendered them relatively unsatisfactory for reliable usage, as outlined:

- Very hard fragile materials difficult to clamp are unsuitable for traditional drilling methods.
- Extremely slender or flexible work-piece are prone to failure in traditional drilling.
- The inability to satisfactorily drill complex shaped workpiece materials; particularly fibre reinforced composites.

As a result of the aforementioned limitations of traditional drilling, there arose the need to develop better, fast and reliable processing techniques, which are collectively referred to as the Non-Conventional Drilling (NCD) processes.

Non-Conventional Drilling refers to a group of advanced drilling processes employed to remove excess material by various individual or combinatory techniques of mechanical, electrical, chemical, or thermal energy domains, usually in the absence of a sharp cutting tool which is typical of the conventional counterparts. Unlike the conventional drilling processes, chip formation in Non-conventional drilling is not achieved solely by shear deformation which results in macroscopic chip volumes. Rather, chips formed in these advanced drilling processes are microscopic in size, or completely dissolute at atomic levels. Other differences are summarised in Table 3.6.

Table 3.6: Summary of differences between CD and NCD techniques

S\N	Conventional Drilling	Non-Conventional Drilling
1.	Energy domain for drilling effects is solely mechanical.	Drilling energy can be sourced from mechanical, chemical, electrical, or thermal means.
2.	A sharp solid cutting tool is required for material removal.	Cutting tool could be solid, liquid, or gaseous.
3.	Chip formation is visible with macroscopic volumes.	Chip formation is microscopic in size, or completely dissolute at atomic levels.

Non-Conventional Drilling processes are classified based on the nature of their energy domains, under which we have the mechanical, electrical, thermal and chemical:

Mechanical Energy: Water Jet Drilling (WJD), Abrasive Jet Drilling (AJD), Ultrasonic Assisted Drilling (UAD).

Electrical Energy: Electrical Discharge Drilling (EDD).

Thermal Energy: Laser Beam Drilling (LBD), Plasma Arc Drilling (PAD).

Chemical Energy: Chemical and Electro-Chemical Drilling (ECD).

Simply, these classifications are further divided into the following drilling methods:

3.7.2.1 Laser beam drilling (LBD) of FRP Composites

The LBD is an advanced drilling technique, as depicted in Figure 3.19, which utilizes high-temperature radiation to produce drilling effects. It is a non-conventional technique, one of the few used for drilling high aspect holes with depth-to-diameter ratio greater than 10:1 (Forsmann et al., 2007).

3.7.2.1.1 Mechanics of laser beam drilling

The term LASER is an acronym for Light Amplification by Stimulated Emission of Radiation. In this technique, drilling is achieved by the impact of a short laser pulse with high power density on the workpiece surface (Fig. 3.18). The process is based on the conversion of electrical energy to light energy, and then to heat energy. It is typically generated by a transducer, the laser beam transmits high heat energy sufficient to thermally degrade the workpiece and cuts through the material by melting and vapourisation mechanisms. The power developed by the laser (P) is thus given as:

$$P = \delta V_m \, \delta t \qquad (3.6)$$

Where δ is the material parameter, which depends on the specific heat of vapourisation, the specific heat and the vapourisation temperature of the material, V_m is the maximum transverse speed, and δt is the material thickness.

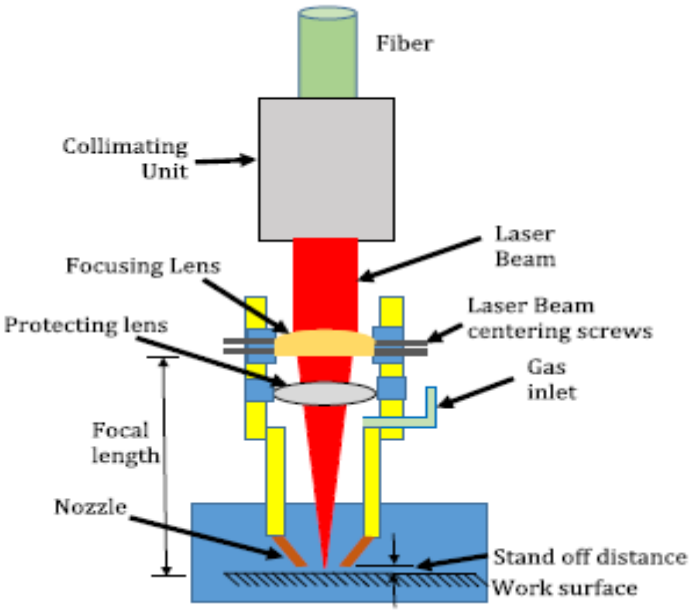

Figure 3.19: Schematics of laser head and workpiece arrangement in LBD (Hejjaji et al., 2016)

Lasers are promising alternatives in composite machining processes. The chips formed are expelled from the hole by the generated vapour pressure, usually in dissolved gaseous forms. While air is mostly used as the assist gas; due to its ability to neutralize oxidation, other gases such as CO_2 and helium have been used for glass and boron-epoxy composites respectively.

Chips are formed by material melting and expelled via vapourisation from the drilled region. 90 % of the drilled material is removed as small particles of diameter less 0.1 µm. The vapourization of carbon-epoxy composites at temperatures of about 4000 ^oC produces CO and CO_2 gases, while aramid-epoxy composites produced fragments of diameter range 50-100 µm, with 35 % of the removed material being recovered as gases with high amounts of Hydrogen Cyanide (HCN) gas, and small amounts of organic

compounds. Lasers can be focused to a spot of about 0.018-0.30 mm in diameter, with beam power output as high as 125-20000 W. However, a spot size of 0.013 mm in diameter can be achieved in laser cuts, while a hole diameter of as low as 0.005 mm can be produced in LBD, which may be unachievable by other drilling techniques (Abrate & Walton, 2016**)**.

Heat Affected Zone (HAZ): This is defined as the region in which the localized temperature exceeds the vapourisation temperature of the polymer matrix **(**Abrate & Walton, 2016**).** It is the major defect of LBD technique, particularly with thermoset polymers. In most cases, the HAZ can be eliminated by post-heat treatment, but there is a risk of distortion.

Kerf: This is the portion of the material removed by the laser when it cuts through a workpiece. Usually, it ranges from 0.08-0.45 mm, depending on the type of material and other conditional factors.

Furthermore, the applicability of the laser drilling technology to a material is depended on the microstructural interactions within the material's lattice. With regards to composite materials, the workability of FRPs with lasers is subject to the type of polymer matrix used for interfacial bonding. Generally, lasers are effective for drilling plastics; due to their high absorptivity for infra-red radiation, and low thermal conductivity which allows high heat retention (Abrate & Walton, 2016). As a result, the LBD technique is best used for drilling composites with thermoplastic polymer matrices, as opposed to their thermosetting counterparts. This is because thermoplastics have a linear chain of monomers with a simpler lattice fusion, while thermosets have a three dimensional lattice structure. Therefore, in order to break the strong fusion bond present in the lattice structure of thermosetting plastics, relatively higher energy levels (vapourisation temperatures of about 3000 ^{o}C for thermosets, compared to 1000 ^{o}C for thermoplastics) are required. However, with higher energy levels in laser drilling, there is a greater risk of HAZ formation, and thermal degradation via burnout (Caiazzo et al., 2005).

In addition, the wide differences in the thermal conductivities, vapourisation temperatures, and heat of vapourisation of the constituents of a composite makes laser

drilling complicated (Table 3.7). Generally, polymer resins; which make up for about 50-60 % of FRPs, usually have low thermal properties, when compared to the reinforcing fibres. Therefore, in order to use the LBD technique on FRPs, the laser power requirements need to be based on the type and volume of fibres used, thus leading to high energy levels which can chemically degrade the polymer resins.

Table 3.7: (a) Typical thermal properties of fibre-reinforced material constituents, and (b) Unidirectional composites (Komanduri, 1997)

(a)

MATERIAL	ρ, g cm^{-3}	K, W m^{-1} K^{-1}	C, J kg^{-1} K^{-1}	κ, (cm^2 s^{-1})10^{-3}	T_v, °C	H_v, J g^{-1}
Resin	1.25	0.20	1200	1.30	450	1000
Aramid Fibers	1.44	0.05	1420	0.24	950	4000
Carbon Fibers	1.85	50	710	380	3300	43000
Glass	2.55	1.0	850	4.6	2300	31000

(b)

COMPOSITE	ρ, g cm^{-3}	K, W m^{-1} K^{-1}	C, J kg^{-1} K^{-1}	κ (cm^2 s^{-1})10^{-3}
Aramid/resin	1.35	0.13	1300	0.74
Graphite/resin	1.55	25	950	170
Glass/resin	1.90	0.60	1000	3.2

Taking reference from the numerical differences in the vapourization temperatures of the prominent resins and fibres above, it can be inferred that the laser drilling of aramid FRPs will produce lesser HAZ effects than the glass and carbon counterparts. Conclusively, in the laser drilling of FRPs, the order of workability (measured with respect to HAZ effects) goes from Aramid to Glass to Carbon composites (Komanduri, 1997).

Caiazzo et al. (2005) investigated the applicability of CO_2 laser for cutting three polymeric thermoplastics; namely polyethylene (PE), polypropylene (PP) and polycarbonate (PC). Using a thickness range of 2-10 mm, he obtained results which showed that high cutting speeds are not always related to good process efficiency, as there exists optimum values of cutting speeds for each material type. Similarly, using a wide range of power settings (200-1400 W), he discovered that the use of CO_2 with the

laser beam was quite unnecessary, as the same cutting effects on the thermoplastics could have been achieved with a few hundred watts. From the results achieved, the workability of the polymers; measured relative to their kerf widths, melted transverse area, melted volume per unit time, surface roughness values, was ranked as PC-high, PP-medium high and PE-lower.

In a similar research by Davim et al. (2008), the effect of laser processing parameters on the quality of cut (HAZ dimension and surface finish) for several thermoplastic polymers; namely PP, PC and Polymethyl methacrylate (PMMA), was conducted. Using a CO_2 laser, he obtained results which ranked the workability of the polymers as PMMA-very high, PC-high, and PP-high/medium, and thus confirmed the results by Caiazzo et al. (2005). It was found that the HAZ increased with laser power and decreased with cutting velocity. Consequently, attempts to apply the laser cutting technique on thermosetting plastics produced results with high HAZ effect, and surface burnout.

Choudhury and Shirley (2010) also investigated the use of CO_2 laser to cut PP, PC and PMMA thermoplastics. The workability of each polymer; measured relative to the HAZ, roughness, and dimensional accuracy, presented results which showed close conformity with that by Davim et al. (2008). From the results, PMMA had the least HAZ, followed by PC, and PP. However, in terms of dimensional accuracy, PMMA had the best surface finish, followed by PP and PC. For all the three polymers investigated, it was also found that the HAZ dimension was directly proportional to the laser power, and inversely proportional to the cutting speed and compressed air pressure.

A research conducted by Anarghya et al. (2015) explored the use of lasers in the drilling operation of CFRPs. Using a series of Scanning Electron Microscope (SEM) images, he obtained the optimum machining parameters which produced good surface finish with the least HAZ effects. The results from the research study showed that the HAZ effect increased proportionally with increase in laser frequency, hole diameter and laminate thickness as shown in Figure 3.20. The optimum machining parameters obtained are:

1. Frequency Range: 200-250 Hz

2. Diameter of the Hole: 0.4 mm

3. Drilling Speed: 200 m/sec

4. Thickness of specimen: 3 mm

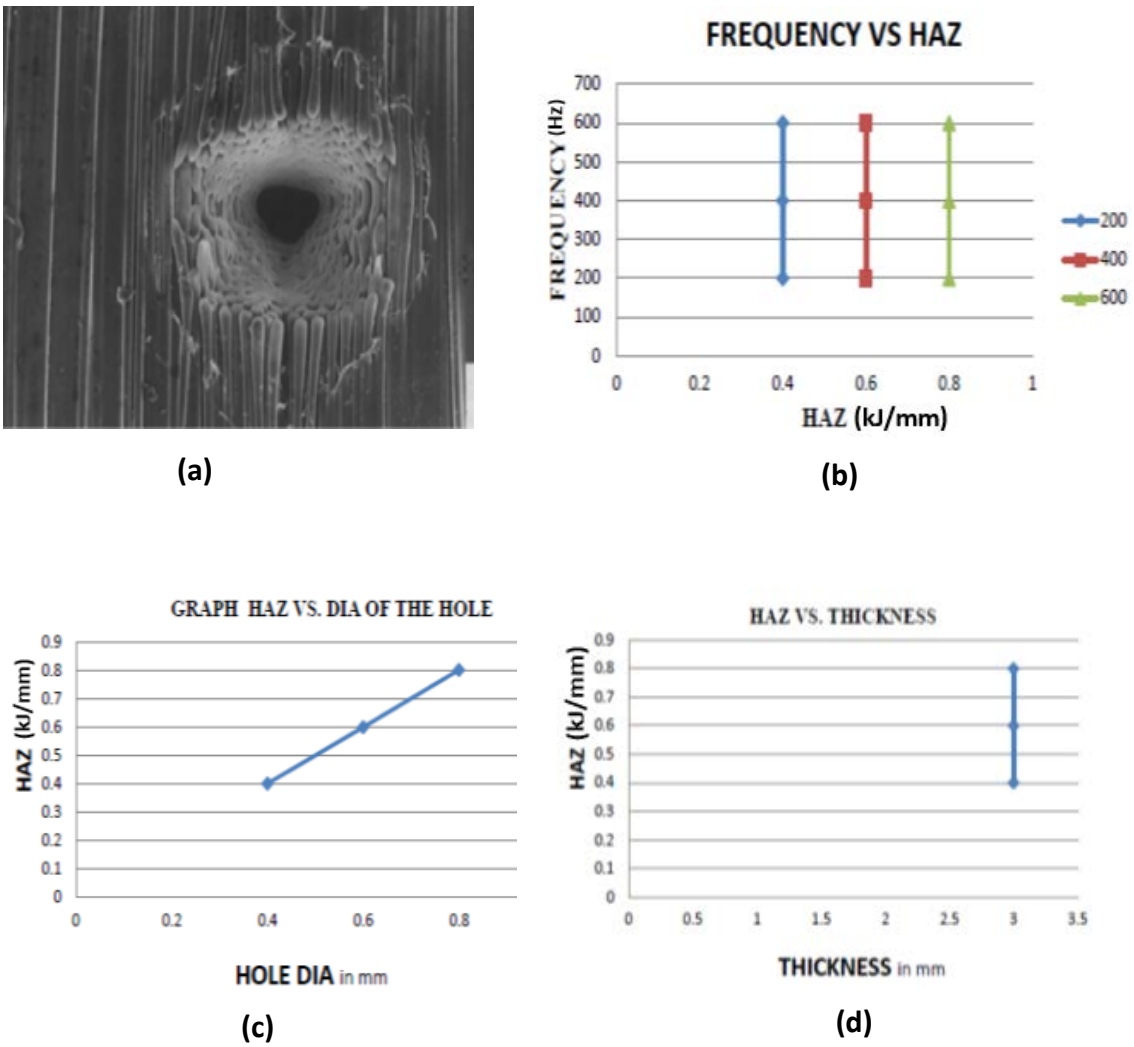

Figure 1.20: (a) Scanning Electron Microscope (SEM) of a laser drilled hole; (b) Graphs of frequency vs HAZ; (c) HAZ vs hole diameter; and (d) HAZ vs laminate thickness (Anarghya et al., 2015)

3.7.2.1.2 Advantages of laser beam drilling

1. Relatively lesser cutting thrust is developed in this technique, leading to reduced delamination potential. Hejjaji et al. (2016) studied the damage characterisation of FRPs comparatively in conventional and fibre laser drilling techniques. While the CD technique produced a finer finish quality on the composite, the machining damage; measured with respect to the delamination effect on the composite, was relatively greater in CD than the laser counterpart.
2. Fragile, slender and delicate materials can be conveniently drilled because of the non-contact relationship between laser and workpiece (Chryssolouris et al., 2014).
3. High aspect ratio holes, as high as 30:1 depth-to-diameter ratios can be drilled.
4. It is accurately fast, and can be easily automated.
5. Bevelled holes; that is, holes at shallow angles from the workpiece surface are best achieved with this technique.

3.7.2.1.3 Disadvantages of laser beam drilling

1. LBD requires a huge capital investment to set-up.
2. Accumulation of dross build-up at hole entry and exit may be present, due to the melting and vapourisation mechanisms. Consequently, this defect reduces the hole quality.
3. A considerable taper may be present in holes with large depth-to-diameter ratios.
4. Unsuitability for drilling thermoset FRPs; such as glass and carbon-epoxies, makes it limited for wider application in composite machining.

The thermal energy often induces a HAZ around the drilled hole, leading to micro-cracks in some materials. Abrate and Walton (2016) studied the applicability of laser drilling on composites, and obtained results which highlighted the major setbacks of this advanced technology as HAZ formation, and the destructive interference of material thickness on laser beam focus. Consequently, this caused a higher energy levels and resulted in charring or burning (Figure 3.21).

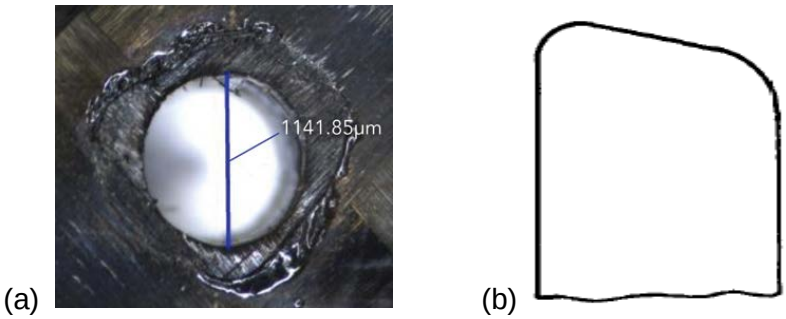

Figure 3.21: (a) Charring and (b) rounded-corner effects in excessive power laser drilling of FRP composite (Abrate & Walton, 2016)

3.7.2.2 Water jet and Abrasive Jet Drilling (AJD) of FRP Composites

The AJD is an advanced drilling technique which employs extremely high fluid pressures to mechanically energise a jet of abrasive particles on to a material surface for drilling effects (Figure 3.22). The high velocity impact of the abrasive jet produces a micro-cutting action which automatically erodes the material surface for drilling to occur. The abrasive particles are typically in the range of 10-50 µm in size, with flow velocity reaching as high as 300 m/s, depending on the MRR desired (Mohamed, 2014).

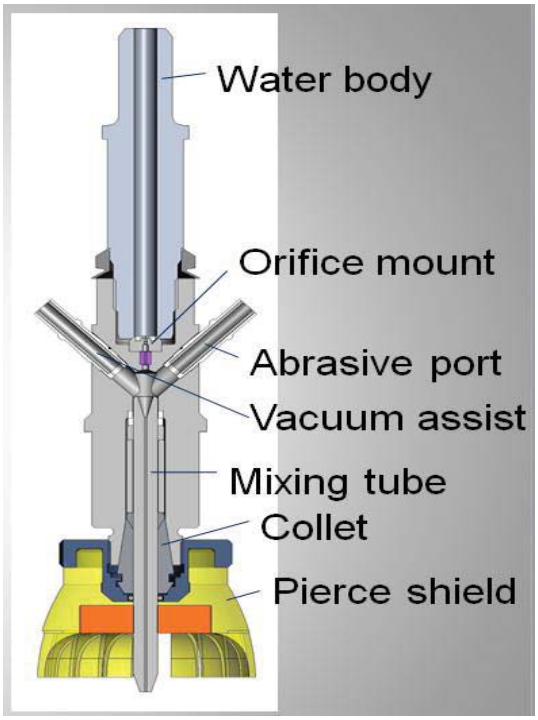

Figure 3.22: Schematic of the abrasive water jet drilling tool (Mohamed, 2014)

3.7.2.2.1 Mechanics of AJD

A nozzle of injection diameter of about 0.5 mm, positioned at a stand-off distance in the range of 0.5-15 mm, and at a deflection angle of 60-90^{o} is used to supply the pressure needed to drive the abrasive jet to the workpiece surface (Mohamed, 2014). The kinetic energy developed by the abrasive particles in the transport process is then converted to produce the drilling effects, via erosion degradation and brittle fracture of the workpiece. Notable transport fluids commonly employed in the AJD technique are air, carbon (iv) oxide, Nitrogen gas, inert gases, and in some cases, water. In processes where water is used as the transport fluid, the technique is otherwise known as Abrasive Water Jet Drilling (AWJD). Similarly, in the absence of abrasives, the technique is referred to as Water Jet Drilling (WJD).

AWJD is a relatively new manufacturing technology which addresses various limitations of pre-existing techniques. In AWJD, material removal rate (MRR) depends on the operating parameters and the properties of the target material. Similarly, the taper of machined surface increased with decrease in hardness of abrasives. However, abrasives with high level of hardness have detrimental effects like accelerating tool wear. Thus, garnet abrasives are the often used in AWJ machining industries due to their favourable effects like low nozzle wear rate, good machinability and economical availability (Doreswamy et al., 2015). Other commonly used abrasives are Al_2O_3, silicon carbide and glass beads.

In addition, Hocheng and Dharan (1990) investigated the mechanics of exit-ply delamination during WJD of graphite-epoxy composite laminates. Using fracture mechanics and plate theory, he developed a numerical model to optimize the water pressure needed for zero delamination effects in WJD. While the water jet force was adjudged to be the most significant factor towards the onset of delamination, it was noticed that at some points during WJD, the water jet force appears bent. Therefore, as the water jet continues drilling towards exit, the decrease in thickness of the uncut plies resulted in lesser resistance to deformation. Consequently, the interfacial bonding

strength breaks off and delamination sets in. Conclusively, a better machining performance on FRPs is possible with WJD, given that the significant process parameters such as water jet pressure and jet diameter are optimised.

Shaikh and Jain (2012) studied the cutting mechanisms of FRPs (such as cotton fibre polyester composites), using CO_2 laser, water jet and diamond saw cutting techniques. The results obtained from experimental analysis showed the preference of laser cutting over water jet and diamond saw cutting, due to failure effects; such as fibre pull-out during diamond saw cutting, and fibre pull-out in many directions and fibre curling experienced during water jet machining of composites. More so, the tendency of degradation of reinforcing fibres; in this case, cotton fibres with moisture, automatically limits the applicability of water jet cutting technique.

In a recent research by Unde, Gayakwad and Ghadge (2014), the machinability of FRPs using AWJ technique was critically reviewed. They discovered that the most important process parameters for tuning purposes in AWJ machining are the transverse speed, stand-off distance, abrasive water pressure and the mass flow rate. Due to the absence of HAZ via thermal distortion in AWJ machining of FRPs, he concluded that it is the most suitable method for machining composite materials. More so, the prevalent problems of other machining techniques, such as burr formation and delamination was found to be almost negligible in AWJ machining, thus making it a good preference for composite machining.

Ramulu and Arola (1993) investigated the micromechanical behaviour of the reinforcing fibres and matrix of a unidirectional graphite-epoxy composite, to water jet machining (WJM) and abrasive water jet machining (AWJM) techniques. The results obtained from experimental analysis showed that the AWJM produced a finer surface finish than WJM, due to its combinatory material removal mechanisms of shearing, erosion and micro-machining. Consequently, AWJM was considered feasible for machining FRPs.

3.7.2.2.2 Advantages of Abrasive Jet Drilling

1. Complex, intrinsic mechanical parts can be easily drilled using this advanced technique.
2. Material wastage is largely reduced by the smaller kerf size.
3. Requires no secondary finishing operation.
4. Strain hardening effects; typical of conventional methods, is minimally reduced due to the cooling effects of the transport fluids.
5. Absence of thermal distortion via HAZ.
6. Chip formation is microscopic and unattached to material surface, due to the cleaning effects of the transport fluid. Consequently, this aids drilling performance and enhances tool life.
7. Low cutting thrust levels in this technique reduces tool wear and delamination damage.

3.7.2.2.3 Disadvantages of Abrasive Jet Drilling

1. High capital investment is required to set-up this advanced technique.
2. Noise levels during operation is relatively high.
3. Unsuitability for materials with high moisture degradation potential.
4. Inability to drill flat bottomed holes.

3.7.2.3 Electrical Discharge Drilling (EDD)

EDD is thermoelectric material removal process between a tool and the workpiece, usually in the presence of a dielectric fluid (Figure 3.23). It is a non-conventional drilling technique that is largely depended on electrical conductivity.

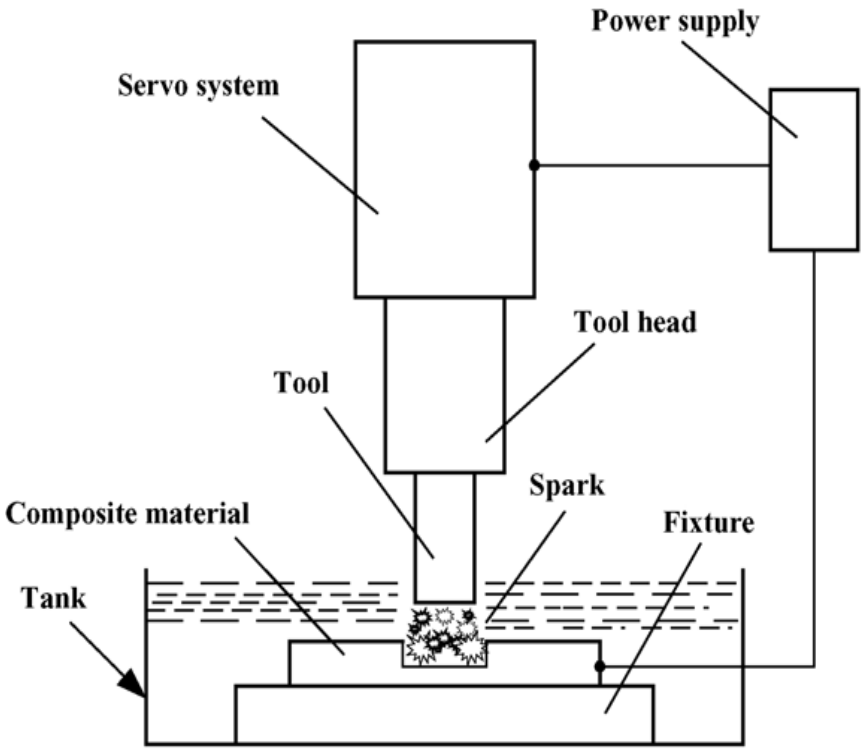

Figure 3.23: Schematics of electrical discharge machining (Hocheng & Tsao, 2005)

3.7.2.3.1 Mechanics of EDD

In this technique, drilling is achieved by the impact of recurring electrical sparks used to thermally erode the workpiece surface in order to remove the undesired materials. While the tool serves as the electrode in this technique, the workpiece is deployed for use as the anode, along with a conductive dielectric fluid (Figure 3.24). The cathode; in this case, the tool, gradually erodes the anode until the desired material geometry is ultimately achieved.

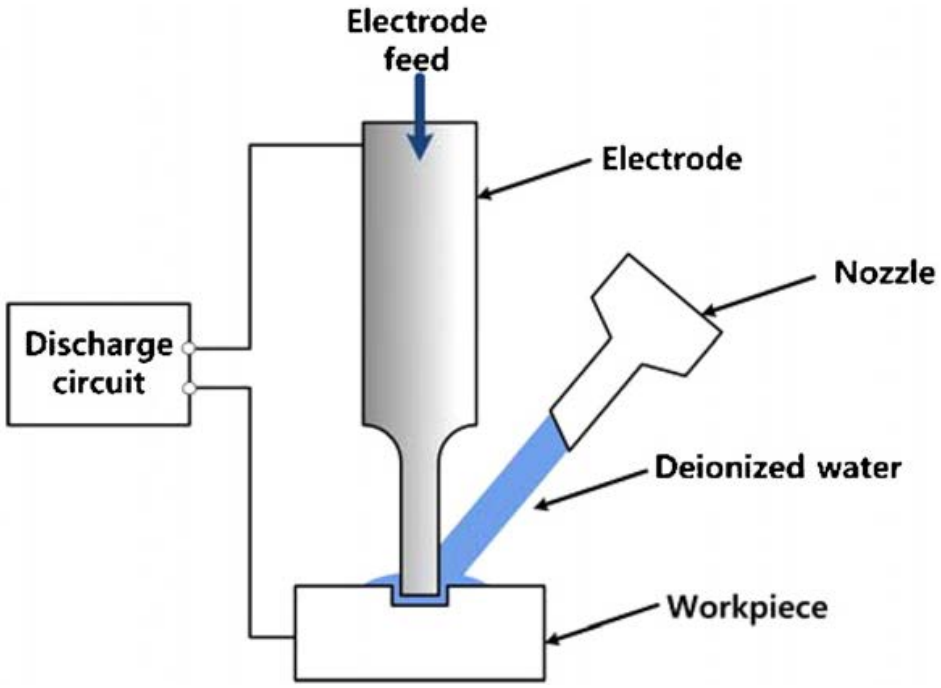

Figure 3.24: Basic EDM system (Song et al., 2009)

At the start of the EDD process, a high voltage electric spark is applied across the small gap between the tool and workpiece, in the presence of a dielectric fluid. This voltage creates an electric field which agitates the particles within the dielectric fluid, and causes them to settle at the points where the electrical field is strongest. As the potential difference between the tool and the workpiece becomes considerably high, the dielectric fluid breaks down, and recurring sparks which gradually removes material from the workpiece surface are discharged through the dielectric fluid. Material removal rate (MRR) in EDD process is given by this expression:

$$MRR = 40\ I/{T_m}^{1.23} \tag{3.7}$$

Where *I* is the current ampere, and T_m is the melting temperature of workpiece.

In EDD process, the dielectric fluid serves three purposes, as described:

- Acts as an insulator between the tool and workpiece.
- Regulates the temperature generated at the tool-workpiece interface, by acting as a coolant.

- Acts as a flushing medium for chip removal.

Typical dielectric fluids commonly used in EDM processes are hydrocarbon oils, kerosene and deionised water.

Moreover, Vaxevanidis et al. (2006) investigated the applicability of EDD to FRPs, using PAN-epoxy, Hexcel satin carbon-epoxy and PAN-carbon composites with copper electrodes. From the experimental results obtained, the feasibility of EDD to FRPs was found to be largely depended on the selection of optimum machining parameters, namely positive tool polarity, small pulse-on times and small pulse currents. Also, the surface finish of the hole entrance was better than the exit in this technique due to the influence of the small pulse-on times, while machining damage on the composites were reported as craters, valleys, as well as delamination and cracking.

Guu et al. (2001) investigated the feasibility of machining CFRPs by electrical discharge machining (EDM) technique. Using a series of generated empirical formulas for process assessment, they obtained the optimised machining parameters for the composite under test.

$$D_f = 0.815{I_p}^{0.0681}{\tau_{on}}^{0.0579} \quad (3.8)$$

$$d_t = 13.696{I_p}^{0.534}{\tau_{on}}^{0.204} \quad (3.9)$$

$$MRR = 0.378{I_p}^{0.216}{\tau_{on}}^{0.041} \qquad \tau_{on} \leq 100\mu s \quad (3.10)$$

$$MRR = 4.400{I_p}^{0.134}{\tau_{on}}^{-0.428} \qquad \tau_{on} > 100\mu s \quad (3.11)$$

$$R_a = 1.326{I_p}^{0.224}{\tau_{on}}^{0.216} \quad (3.12)$$

Where D_f is the delamination factor, d_t is the recast layer thickness, MRR is the material removal rate, R_a is the surface roughness, I_p is the pulse current, and τ_{on} is the pulse duration.

From the results obtained (Figure 3.25), it was found that both peel-up and push-out delamination defects can be prevented by using smaller pulse energy for electrical discharge. Similarly, higher discharge energy was characterized with high

temperatures which constituted to surface roughness, larger recast layer, and delamination on the cutting edge.

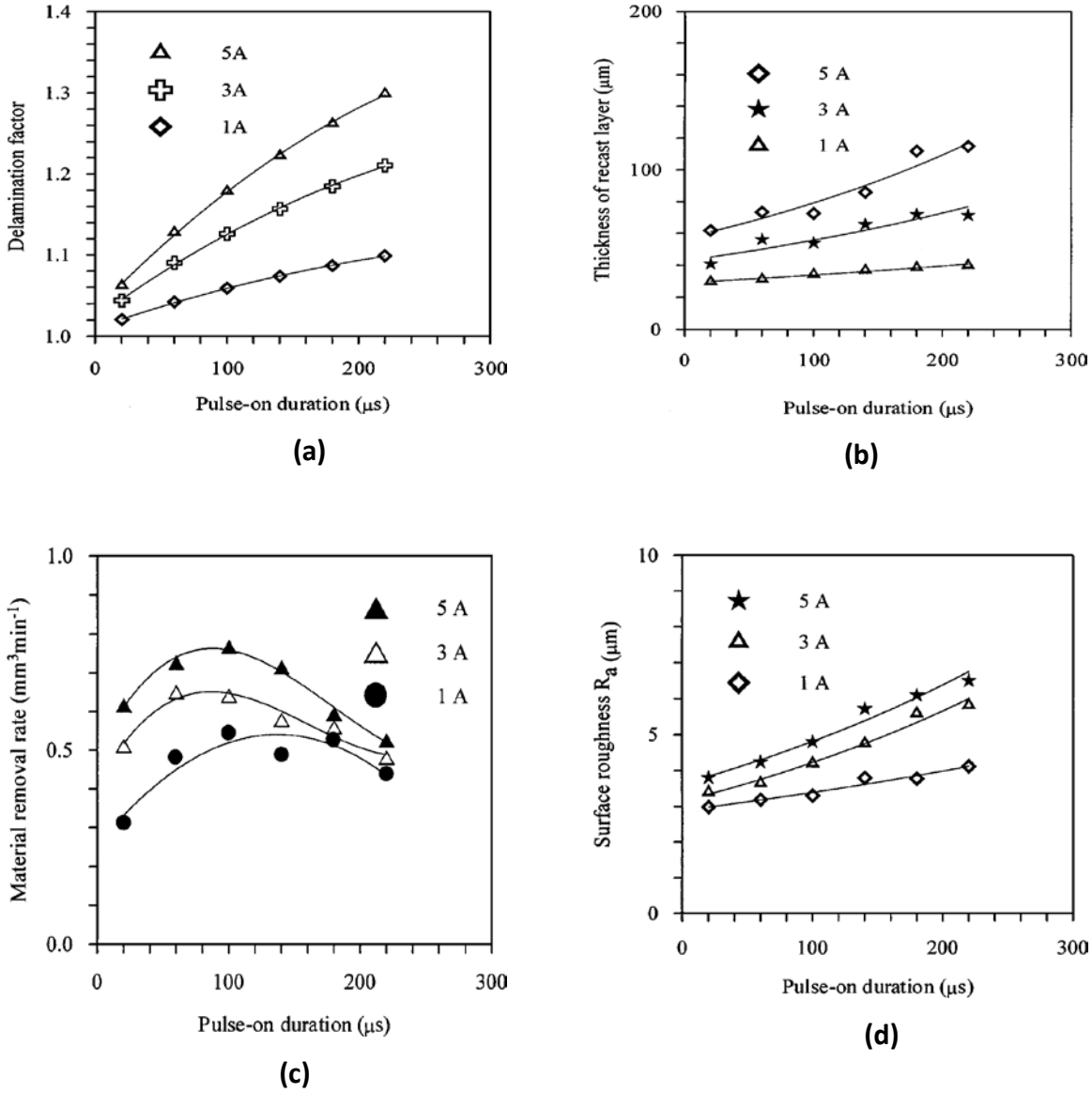

Figure 3.25: Graphs of correlation between (a) delamination factor and machining conditions; (b) recast layer under various machined conditions; (c) material removal rates for various pulse current and duration; (d) surface roughness against various pulse durations (Guu et al., 2001)

Using the optimised pulse current of 5 A, and pulse-on duration of 100 μs, MRR was found to be as high as 0.768 mm^3/min in this technique. Conclusively, and with the

selection of appropriate process parameters, the EDM technique was considered feasible for machining CFRPs.

3.7.2.3.2 Advantages of EDD

1. Thin and fragile workpiece materials can be accurately drilled without distortion, using EDD.
2. Absence of burrs on machined surface.
3. Electrically conductive materials of any hardness can be machined using EDD.

3.7.2.3.3 Limitations of EDD

1. EDD is limited to machining electrically conductive materials only.
2. Low MRR makes it relatively slow to conventional techniques.
3. Increased MRR can lead to rough surface finish.
4. Higher risk of erosion and over cutting is a major concern in this technique.

3.7.2.4. Ultrasonic Assisted Drilling (UAD) of FRP composites.

This is a non-conventional drilling technique which utilizes high mechanical vibration to produce drilling effects. It involves the superimposition of a high frequency vibration on a drill bit at the feed direction.

3.7.2.4.1 Mechanics of UAD

In this technique, the drill bit is mechanically excited in the torsional or axial direction by the super-imposed vibration (the axial excitation being preferred in many applications) to remove undesired materials. It involves the combinatory mechanisms of conventional drilling and ultrasonic oscillation (Figure 3.26), and is applicable to drilling both ductile and brittle materials (Azarhoushang & Akbari, 2007).

The ultrasonic vibration (with frequency typically in excess of 20 kHz and balanced

with a low amplitude of tens of micrometers) can be sourced from piezoelectric actuators such as transducers. The use of ultrasonic vibration in machining operations has its history documented for more than 50 years (Graf, 1975). The results obtained from this technology over the years of discovery has proven successful in applications where conventional drilling techniques were ineffective.

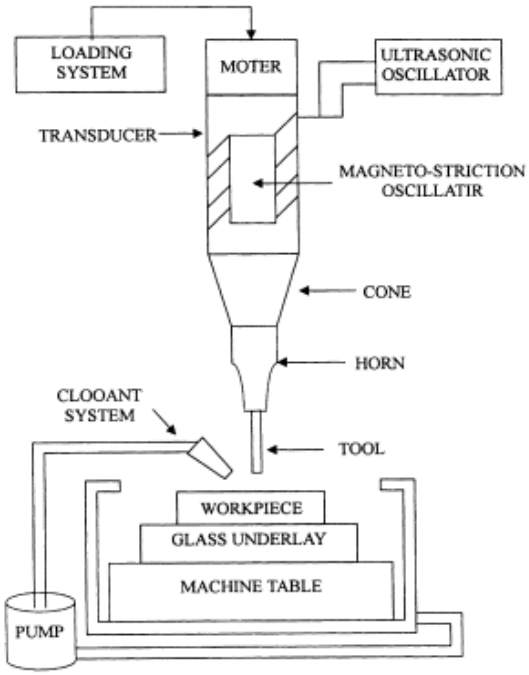

Figure 3.26: Set-up of Ultrasonic Machining (HoCheng, Tai & Liu, 2000)

Fundamentally, UAD being an advanced technology, has different mechanics of material removal compared to CD. While material removal is continuous in CD, UAD utilizes the impact of a low amplitude intermittence between the tool and workpiece interface to achieve high deformation rates. Consequently, the drilling process in UAD is achieved by the high-frequency hammering effect of the abrasive grains at the tool's cutting edge on the surface of the workpiece (Hocheng et al., 2000).

Importantly, drilling parameters in UAD include the following:

Thrust Force and Torque: The thrust force developed in UAD has an optimal value, and is

significantly lower than that of CD techniques at all vibration frequencies (Thomas & Babitsky 2007; Makhdum et al., 2014). In some cases, such as reports from Gupta et al. (2014), thrust force in CD and UAD techniques were nearly equal at all cutting speeds with constant feed rates (in the absence of cutting fluids), but with slight reduction in the thrust force during UAD at specific lower cutting speeds. Similarly, the torque on the tool in UAD was comparatively lower than that developed during CD techniques over the period of tool engagement.

Cutting Speed: The cutting speed varied linearly with thrust force in UAD, and was similar to that of CD. The thrust force reached its maximum value at the lowest cutting speed and vice-versa, as shown in Figure 3.27. Consequently, it is recommended to employ high cutting speeds during UAD **(**Phadnis et al., 2012a**).**

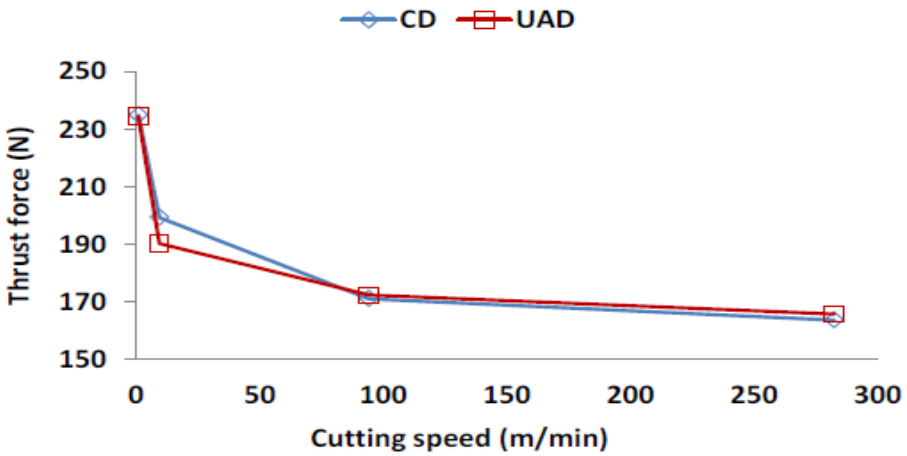

Figure 3.27: Average thrust force recorded in CD and UAD (Gupta et al., 2014)

Feed Rate: Feed rate varies linearly with MRR in UAD, as well as to the amount of workpiece material removed by one abrasive grain **(**Cong et al., 2012**).**

Cutting Temperature: The temperature developed at the tool-workpiece interface during UAD is similar to that of CD at lower cutting speeds (< 10 m/min), but greater in UAD at higher cutting speeds (< 200 m/min) (Gupta et al., 2014). Meanwhile, the cutting temperature increased linearly with feed rate in CD, the high temperature in UAD remained constant irrespective of the feed rate (for < 20 mm/min), due to the repeated

vibratory cycles to which the drill bit is constantly subjected. Using a feed rate of 16 mm/min, cutting temperatures of 90.2 ^{o}C and 290.8 ^{o}C were respectively reported for CD and UAD technologies by Makhdum et al. (2014). Comparatively, with CD, Pujana et al. (2009) reported that tool tip temperature was relatively higher in the UAD of Ti6Al4V material, and observed the linear relationship between vibration amplitude and tool tip temperature.

Many studies have been carried out on application of UAD on FRP composite materials. To start with, Phadnis et al. (2012a) investigated the drilling of CFRP laminate using UAD and CD techniques. The results obtained from experimental analysis showed the effectiveness of UAD over CD in terms of reduction in the average thrust force. An excellent correlation between experimental data and numerical analysis models portrayed the feasibility of UAD over CD techniques in composites machining. At certain drilling conditions, comparative reduction in the average thrust force was as high as 30%. Considering the linear relationship between thrust force and delamination potential in drilling operation, the safe workability of composites with UAD was thus verified.

Similarly, the relationship between cutting speed and thrust force was studied in both UAD and CD techniques by Phadnis et al. (2012a; 2012b), using both experimental data and numerical analysis on a CFRP composite. The results showed that thrust force decreased with increase in cutting speed, as a decrease in thrust force was considerably higher in UAD than CD (31.1 % at 1700 rpm against 15.8 % at 216 rpm) at higher cutting speeds. Furthermore, the intermittent vibration oscillation in UAD was adjudged to reduce the frictional effect at the tool-workpiece interface, by increasing the sliding velocity. This translated into a tangible reduction in the overall thrust force at the tool-workpiece interface, and thus suggested the need to employ higher rotational speeds during the UAD of CFRPs.

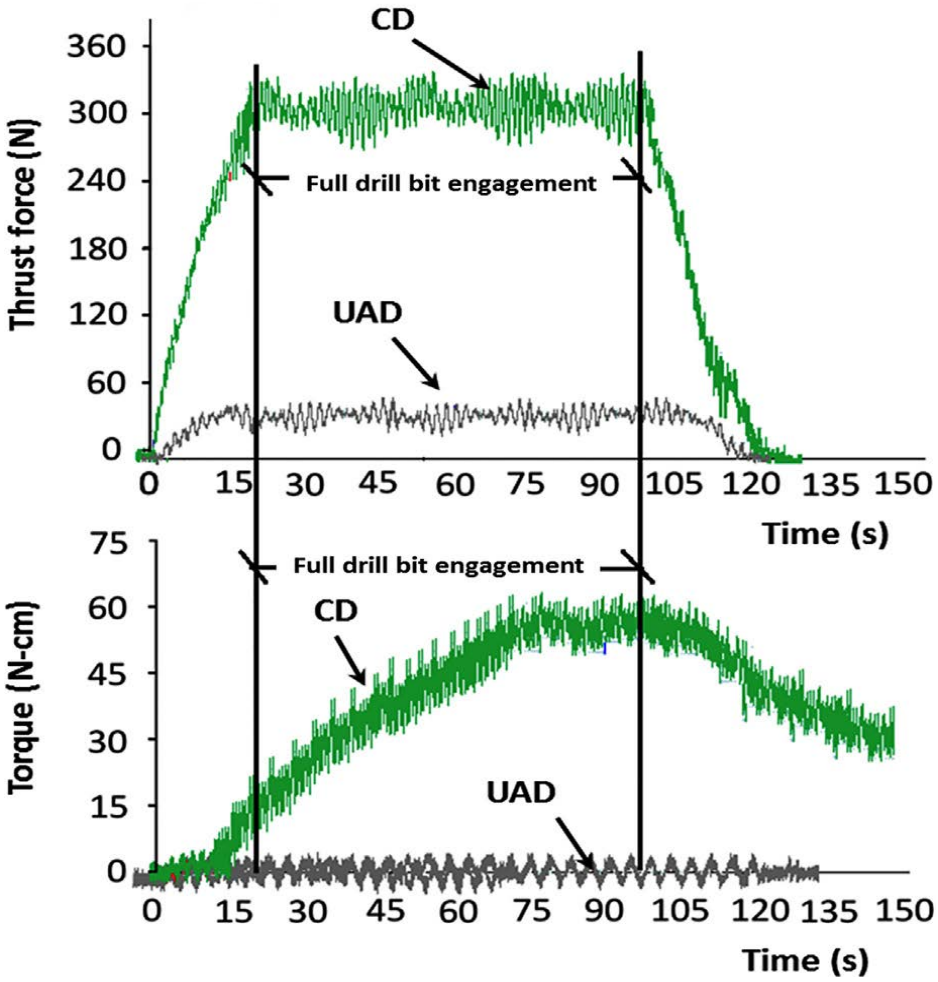

Figure 3.28: Drilling forces: (a) thrust force and (b) torque evolution in UAD and CD (Makhdum et al., 2014)

Makhdum et al. (2014) studied the mechanics involved in the UAD of CFRPs. Using a combination of experimental data and mathematical models; the drilling forces, cutting temperature, chip formation, surface finish, circularity, delamination and tool wear were investigated. The results obtained from the study showed significant reduction in drilling forces during UAD, as high as 80 % for aluminium workpiece (Figure 3.28), as well as general improvements in the drilling output, relative to conventional drilling. Furthermore, the softening effects of UAD on CFRPs was accounted for in the numerical model of this research, and the results obtained from this demonstrated the reason behind the much desired reduction of thrust forces in this advanced method of drilling.

3.7.2.4.2 Advantages of UAD

1. Ability to drill any type of materials, irrespective of their electrical conductivity.
2. UAD can be used to machine hard materials of 40 HRC to 60 HRC like carbides, ceramics, and industrial diamonds.
3. Aspect ratio of about 40:1 can be achieved using UAD.
4. Holes of 76 micron diameter with 51 mm depth can be conveniently drilled.
5. Produces surface integrity and finish.
6. Absence of thermal, electrical, and chemical effects.
7. Can be conjunctively used with other non-conventional techniques like EDD.

3.7.2.4.3 Disadvantages of UAD

1. UAD is an advanced technology, and so requires huge capital investment to set-up.
2. High power consumption
3. Unpredictable results are often gotten from the application of this technology, due to the misunderstanding of the working process.
4. High rate of tool wear may result from chipping effects, leading to premature tool failure (Thomas & Babitsky, 2007).

3.7.2.4.4 Summary of UAD

Below are the documented summary of the characteristics of Ultrasonic Assisted Drilling over Conventional Drilling:

1. Reduced drilling reaction force and torque: This enhances the ease of drilling thin structures without deformation.
2. Increased positional accuracy; better precision.
3. Improved chip expulsion.
4. Reduced or eliminated burr formation on the exit side of drilled holes.
5. Improved hole roundness and size.
6. Extended drill bit life due to the reduction in the rate of tool wear.

7. Increased material removal rate.
8. Improved hole surface finish.
9. Reduced or eliminated built up edge.

As a result of the above reasons, UAD has proven to be better than conventional drilling and some NCD techniques, based on other drilling and material factors. Hence, these advantages necessitated its choice for this research, among others. In addition, UAD enhanced the drilling of FRP composite because of the following under-listed reasons:

1. No de-burring operations are required after drilling.
2. No spot drilling operation is required when drilling into an inclined surface,
3. Improved hole quality/roundness automatically eliminates the need for subsequent post-machining operations such as reaming operation, and thus saves production cost.

Lastly, Tables 3.8 and 3.9 summarise the differences in process capabilities of the two techniques and material response for various NCD techniques.

Table 3.8: Summary of differences in process capabilities of NCD and CD techniques (Singh, 2008)

S\N	Process	MRR (mm^3/min)	Tolerance (μ)	Surface finish (μ)	Depth of surface damage (μ)	Power consumption (Watts)
1	USD	300	7.5	0.2 – 0.5	25	2400
2	AJD	0.8	50	0.5 – 1.2	2.5	250
3	EDD	800	15	0.2 – 1.2	125	2700
4	LBD	0.1	25	0.5 – 1.2	125	2 (average)
5	Conventional Drilling	50000	50	0.5 – 50	25	3000

Table 3.9: Summary of material applicability for various NCD techniques (Singh, 2008)

S\N	Process	Steel	Ceramics	Plastics	Glass	Refractory material
1	USD	Fair	Good	Fair	Good	Good
2	AJD	Fair	Good	Fair	Good	Good
3	EDD	Good	–	–	–	Good
4	LBD	Fair	Good	Fair	Fair	Poor

3.8 Effects of conventional drilling input variables or parameters (Parametric design)

Drilling parameters are the machining variables and conditions that affect the entire drilling process. They are machine capacity and function-dependents. Among them include cutting force, thrust force, torque, feed rate, material removal rate, coolant flow resistance and cutting speed. It has been reported that thrust force and torque increased with the size of the drill bits. Also, increase in feed rate caused an increase in both thrust force and torque, while both decreased with the spindle speed (Sivarao, 2005). The effects of drill wear and composite thickness on thrust force and torque has been investigated by using 'one shot' drill bit (Kilickap, 2010; Fernandes & Cook, 2006). They concluded that the thrust force increased with number of drilled holes for twist drill bit, unlike torque. Decrease in composite thickness caused increase in thrust force due to wear, while increase in feed affected thrust force causing increase in the rate of the tool wear. Hence, thrust force and torque significantly depends on drill feed rate, bit, wear and composite thickness.

3.8.1 Tooling materials

Experimental results of CFRP composite drilling using Carbide, HSS and PCD drills conducted by Madhavan and Prabu (2012) and Mohan et al. (2005) revealed the effect of feed rates, drill geometry and cutting speeds on chip formation, delamination, surface roughness and cutting forces. They stated that feed rate increased with delamination

factor and surface roughness. Chip formation increased with increase in cutting force. Similarly, variations of cutting forces with or without onset of delamination during the drilling operations has been studied by Chen (1997) and concluded that the delamination-free drilling processes might be obtained by the proper selections of tool geometry and drilling parameters such as cutting force.

3.8.2 Thrust force

During drilling, thrust force is the applied force on workpiece by the machine tool through speed and feed in downward direction. It is the plunging force of the drill bit unlike cutting force which is rotating force. Delamination effect, occurred principally at the drill exit in composite materials, has been reported to be mainly caused by the thrust force (Tsao & Hocheng, 2008; Wang et al., 2014). An optimisation of twist drill point geometries in order to minimise thrust and torque in drilling has been carried out by Paul et al. (2005), using conical, racon and helical drill point geometries. Racon drill showed a marked reduction in thrust while the optimised helical drill reduced thrust by over 40 % when compared with conical. Lazar and Xirouchakis (2011) experimentally determined the axial and tangential cutting loads distribution by analysing the thrust on drilling CFRP composites with three different types of drills. It was shown that the maximum thrust forces occurred on the fibre plies in contact with the drill tip. Analysis of delamination in various drills: saw, candle stick, core and step drills has been analytically and compressively carried out by Hocheng and Tsao (2003). They predicted the critical thrust force that caused the initiation of delamination mathematically. They concluded by comparing the results obtained with that of a twist drill for all the available drills and predicted the decrease of critical thrust for the different drills and the points at which they were reduced to the twist drill. Theoretical predictions of critical thrust force at the inception of delamination, of different special drill bits have been carried out by Hocheng and Tsao (2006) using experimental investigations. Their results on critical thrust forces were confirmed and agreed with both the analytical findings of critical thrust forces and

industrial experiences, that drill geometry has significant effect on the thrust force, as supported by works of Madhavan and Pradu (2012) and Wang et al. (2004).

Moreover, formulation of a detailed analysis for the critical thrust force ratio related to the peripheral drilling moment has been conducted by Tsao and Hocheng (2008). Special drill bits such as saw, core and candle stick were used for the composites drilling. It was concluded that the special drill bits possessed a lower critical thrust force at peripheral drilling moment than without peripheral moment. This indicated that at the exit of drill bit in the composite materials, the peripheral moment caused bigger delamination drilling-induced damage. Prediction of thrust force during All 100/10 % SiC metal matrix composites (MMCs) drilling has been performed (Doomra, Debnath & Singh, 2015). Both experimental method and ABAQUS/Explicit FEA were used, with close agreement in their results. Drilling the typical MMCs with a low cutting speed and feed rate, for reduction in thrust force, were recommended.

3.8.3 Torque

Xiong et al. (2009) used mapping method to develop 81 major mathematical equations in a new methodology for designing a curve-edged twist drill. They distributed the cutting angles along the tool cutting edge randomly. Their results were validated experimentally, and the drilling torque and the thrust force were compared. It showed that the new curve-edged drill reduced the drilling torque and thrust force by 28.5 % and 24.6 % on average respectively. Nagaraja et al. (2013) reported that an increase in spindle speed and feed rate led to increase in torque, delamination and thrust force when drilling carbon fibre epoxy composite using HSS drill. They concluded that spindle speed has insignificant effect on torque and thrust force.

3.8.4 Feed rate

Liu et al. (2012) stated that feed rate had the greatest influence on drill wear, thrust force and delamination (Basavarajappa, Chandramohan & Davim, 2008). Low feed rate

coupled with high cutting speed reduced delamination and prolonged drill life (Liu et al., 2012). Research on the development of suitable models with intelligent control scheme in the machining of composite laminates has been carried out by Dharan and Won (2000). Drilling experiments were conducted using carbide-tipped twist drills on composite material to obtain thrust force and torque responses for a wide range of feeds in high-rate drilling. Empirical expressions relating the thrust force and torque to the feed and drill diameter were obtained from the results of the experiment. Isbilir and Ghassemieh (2013) declared vividly that the detailed understanding of the effects of higher feed rate on delamination and thrust force is essential before embark on its application. They concluded that step drill reduced torque and thrust force (delamination) when compared to twist drill at similar feed rate and speed.

3.8.5 Material removal rate

Material removal rate (MRR) is another drilling parameter that determines the efficiency of a drill. A good designed drill should be able to evacuate chips easily and rapidly. An attempt to determine the drilling process for carbon laminates, Sardiñas et al. (2006) proposed a multi-objective optimisation of the drilling process. Two mutually contradictory objectives were optimised: material removal rate and delamination factor, which represented the productivity and characterised the superficial quality respectively as jointly contradictory objectives were optimised. Increase in cutting speed and feed led to increase in MRR while delamination factor increased with decrease in MRR.

3.8.6 Coolant flow rate

During wet machining, flow rate of coolant is imperative. Abele and Fujara (2010) designed a drill geometry performance characteristic model and used it to obtain drill performance characteristics, numerical simulation of 3D FEA models and calculated coolant flow resistance. Their models also captured prediction of coolant flow, effects of coolant channel diameter and its surface roughness.

3.8.7 Cutting speed

The cutting speed of a drill determines the rate of production of holes in composite materials. Cutting speed has less effect on delamination when compared with feed rate (Liu et al., 2012). HSS drill supported a high cutting speed when compared with carbide (coated and uncoated types) and PCD (Madhavan & Prabu, 2012). Isbilir and Ghassemieh (2012) stated that surface roughness and delamination damage reduced with increase in cutting speed when drilling CFRP composite with multi-layer TiAlN/TiN PVD tungsten carbide tools. They concluded that drilling parameters influenced drilling outputs significantly. Gaitonde et al. (2008) investigated process parametric effects on delamination during high-speed thin woven-ply CFRP composite drilling. Cutting speed, one of the process parameters considered, was used to analyse the delamination-damage factor. Their investigations showed that the delamination tendency decreased with cutting speed and further suggested that combined low values of feed rate and point angle would reduce the damage (Rubio et al., 2015). Conversely, Sardiñas et al. (2006), Davim and Reis (2003a) and Kilickap (2010) studied delamination during conventional drilling of composite laminates and optimisation of cutting parameters using genetic algorithms, design experiments and Taguchi methods respectively. They reported that delamination increased with cutting speed. Lastly, High spindle speed as well as lower feed rate favoured delamination-free composite drilling. Thus, thrust force and delamination go together and depend on other drilling parameters such as cutting Speed (Kilickap, 2010), feed rate (as illustrated in Figure 3.29), drill geometry and wear (El-Sonbaty et al., 2004; Liu et al., 2012; Ramulu et al., 2001; Rubio et al., 2015). From the 3D plot of Figure 3.29, the highest thrust force of more than 500 N was recorded at highest feed rate of 0.8 mm/rev and lowest cutting speed of 24 m/min. These results evidently implied that the thrust force of the drills increased as the feed rate increased, but decreased as the cutting force increased during CFRP composite (conventional) drilling. Also, a lowest feed rate of 0.1 mm/rev and thrust force of nearly 25 N were recorded at maximum cutting speed of 235 m/min.

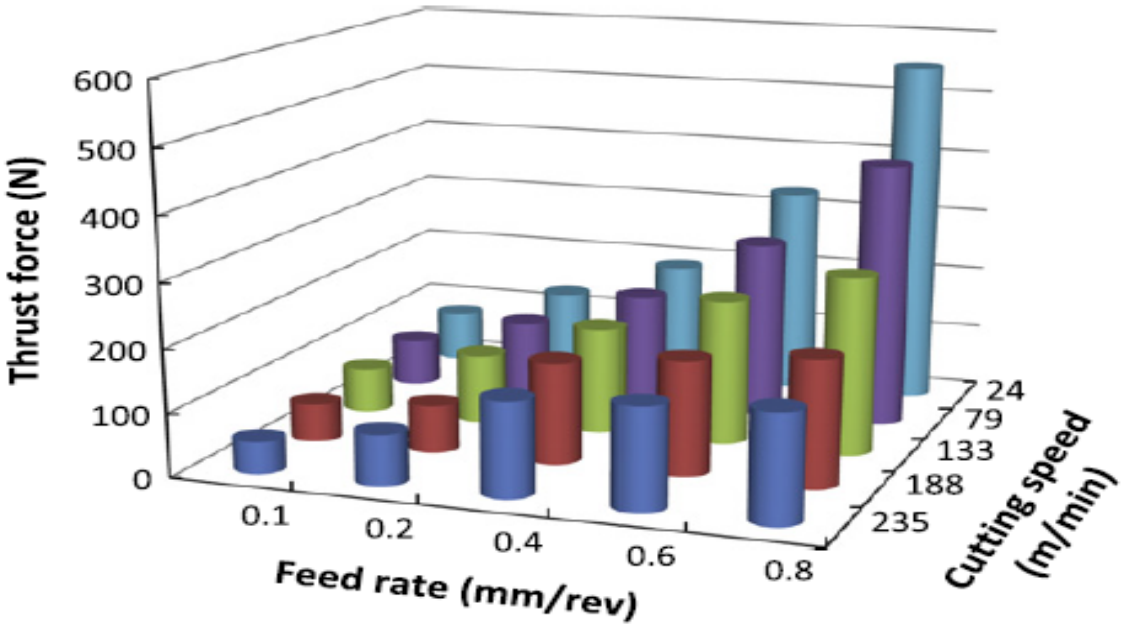

Figure 3.29: Parametric effects of cutting speed and feed rate on thrust force in CFRP composite drilling (Liu et al., 2012)

3.8.8 Chip formation and separation

Composite fibre orientation determines chip formation during machining**.** The chip formed on the drill increased as cutting speed increased during composites drilling (Lin & Chen, 1996). FEA drilling model that showed chip formation at the exit surface has been developed by Min et al. (2001). The model was used to simulate the formation of both crown and homogeneous chips which were formed at higher and lower feeds respectively. They based the failure criterion governing the chip formation on the equivalent discrete element-plastic strain. Also, the same plastic failure criterion was used to model chip separation by Klocke, Raedt and Hoppe (2001).

3.9 Pertinent survey on comparison of CD with UAD of FRP composites

The possibility of drilling damage-free composite materials, especially a synthetic carbon fibre-reinforced plastics (CFRP) and glass fibre-reinforced plastics (GFRP), still

remains a challenging task in manufacturing industries (Sun & Zhou, 2014). Several drilling methods have been used in an attempt to reduce or solve drilling-induced damage on conventional composites (CFRP and GFRP). These damage include, but are not limited to, thermal degradation, inter-ply delamination, spalling, surface roughness, burrs formation, hole shrinkage, fibre-matrix de-bonding, fuzzing, cracking, fibre-uncut and pull-out (fibre deformation or cratering) (Khashaba et al., 2010b). Recently, a few modern drilling techniques such as electrical discharge, laser, abrasive jet, rotary and ultrasonically-assisted drilling have been used to drill several categories of a conventional fibre-reinforced polymer (FRP) composite materials. In many cases, these techniques performed better than the traditional or conventional drilling technique, though it depends on the properties of material workpiece, drilling parameters, conditions and techniques (Makhdum et al., 2014; Hocheng & Tsao, 2005; Phadnis et al., 2012a; Phadnis et al., 2012b ; Hejjaji et al., 2016). Among these recent techniques, ultrasonically-assisted drilling (UAD) technique has a numerous outstanding performances, especially when compared with the CD.

3.9.1 Brief overview of CD and UAD techniques

Over the years, CD has been the norm of manufacturing operations, but it has a quite limitation in working applicability to some newly introduced FRP composite materials. Hence, there is a need for a better technique of drilling. The CD technique involves the process of creating or enlarging already existing hole in a solid material, using a rotating drill bit that is operated under the concomitant action of drilling forces (thrust and torque), feed rate and cutting speed. The UAD is a hybrid technique that combines a conventional drilling and ultrasonic oscillation. It is a non-traditional technique of drilling whereby a drill bit is excited under a superimposed high frequency (typically >18 kHz) and a low-amplitude (< 20 μm) vibration, on a drill bit along the feed or axial direction, causing drilling action (Makhdum et al., 2014). UAD has a remarkable advantages over the CD, especially its drilling forces (thrust and torque) reduction. The thrust force is the axial force required by the drill bit to initiate the drilling process, while the torque is the

developed force that causes the drill bit rotation. The quality of the drilled holes, reduced power consumption rate and consequently, low cost of production are enhanced with reduction of these forces. However, the setbacks of modern UAD technique include expensiveness of set-up, unpredicted results and chipping effects on the drill bits.

Furthermore, UAD has been effectively used for drilling of both brittle and ductile materials (Azarhoushang & Akbari, 2007). It has been reported that UAD decreased drilling forces and burr formation when drilling metal matrix composites, causing reduction in both delamination and surface roughness defects respectively (Kadivar et al., 2014). They examined these parameters and demonstrated that the drilling force developed in UAD was significantly lower relative to the conventional drilling technique. Similarly, the drilling force developed in UAD has been found lower than CD at all vibration frequencies and has optimal quantity (Thomas & Babitsky, 2007). However, similar values of thrust force in CD and UAD at all the cutting speeds and at constant feed rates in the absence of coolant have been obtained in another experimental study (Gupta et al., 2014). Though, a small reduction in thrust force of 9.1 N was obtained at a cutting speed of 9.42 m/min. They concluded that the thrust force was maximum at the lowest cutting speed and minimum at the highest cutting speed. Also, they demonstrated that the cutting temperature was similar in CD and UAD at lower cutting speeds, but different in CD and UAD at higher cutting speeds.

3.9.1.1 Chips formation and morphology

In addition, with respect to the morphology of chip formation in UAD and CD techniques, it was demonstrated that the cutting speed was influential to the morphology of the chips generated in the UAD. From the results obtained, it was observed that the largest type of chip fragments were formed at both the lowest and highest cutting speeds of 0.942 m/min and 282.6 m/min respectively (Gupta et al., 2014). At almost all variations in the cutting speed, the most common type of chips formed in the UAD technique was a short broken chip fragments. A similar conclusion has also been reported (Phadnis et al.,

2012a, Phadnis et al., 2012b). They reported a significant decrease in thrust force with an increased cutting speed, and thus recommended the need to employ UAD at a high cutting speeds. Moreover, it was reported that the CFRP chips formed in UAD were long, helical, curled continuous chips, similar to chip generation during CD of ductile metals (Makhdum et al., 2014). This observation displayed a sudden transformation of the brittle fibre-reinforced composite to a ductile material. This was primarily due to the acoustic softening effect of the vibratory cycles of excitation in UAD. On the other hand, the CD technique produced a small sized crumpled chip which indicated the brittle nature of the CFRP composite. The dissimilarity in the chip formation and morphology of the UAD was attributed to a various factors; the major one among a list of them being the effect of the ultrasonic excitation at the interface of the tool and workpiece. Similarly, it was reported that the feed rate had a direct influence on chip formation, as a lower feed rates produced longer chips, whereas a higher feed rates yielded the shorter ones (Makhdum et al., 2014).

3.9.1.2 Feed rate

Meanwhile, an increase in feed rate of UAD technique led to an increase in the material removal rate (MRR), as well as material volume removed by one abrasive grain (Cong et al., 2013). They noted that a linear relationship existed between the feed rate and the material removal rate in UAD. Also, it has been stated that the temperature gradient in UAD was relatively higher than CD (Makhdum et al., 2014). In the CD, the cutting temperature varied linearly with the feed rate as expected. However, in UAD the temperature rise was almost constant irrespective of the feed rate. This constant rise in cutting temperature experienced in the latter was attributed to the consequence of the effect of vibratory cycles to which the tool was constantly subjected. A maximum temperature of 90.2 ^{o}C and 290.8 ^{o}C was reported for CD and UAD techniques respectively, using the same feed rate of 16 mm/min (Makhdum et al., 2014). Similarly, the tool tip temperature was higher in the UAD of Ti6Al4V than CD, and a linear

relationship existed between the vibration amplitude and the temperature variations at the tool tip (Pujana et al., 2009).

3.9.1.3 Surface integrity

Considering the surface roughness of holes drilled with UAD, it was observed that the feed rate had no direct bearings on the surface regularity, as the surface roughness improved significantly even for a feed rate that showed no improvement on drilling forces in UAD. This independence of the end result of surface finish was concluded to have been based on the positive effect of the multiple vibration excitations to which the drilling system was constantly subjected. Consequently, the drill bit generated the necessary polishing effect over the workpiece surface (Makhdum et al., 2014). Similarly, the microstructure of internally drilled holes has been analysed (Gupta et al., 2014), using the scanning electron microscopy (SEM) method. It was observed that there was no significant difference between UAD and CD techniques, when viewed at a lower magnification of 40 x. However, at the exit side of the drilled holes, the fibre pull-out defect was reported which was peculiar to the conventional drilled hole.

3.9.1.4 Drilling forces (thrust and torque) and parameters

Moreover, an effectiveness of UAD over CD was demonstrated in terms of reduction in average thrust force (Phadnis et al., 2012a). An excellent correlation between an experimental and a numerical analysis of model was achieved, as both the generated simulation results and the experimental data showed a greater advantage of UAD over CD. It should be noted that the thrust force developed during drilling operation plays a major role in obtaining the surface integrity and minimising the delamination tendency. They also studied the effect of cutting speed on the drilling thrust force on both UAD and CD, using both experimental methods and numerical models on a CFRP composite. It was observed that in both UAD and CD, the thrust force decreased with an increase in the cutting speed, as experimental results showed that the decrease in relative average thrust

force encountered in UAD was considerably higher; 31.1 % at 1700 rpm against 15.8 % at 260 rpm, with an increased cutting speed. The contribution of frictional force in UAD has been studied (Phadnis et al., 2012b). It was reported that the generation of intermittence in UAD, caused by the vibration effect was a favourable condition which reduced the effective frictional coefficient at the cutting interface. This reduction of frictional coefficient can be attributed to the increase in relative (sliding) velocity, translated into a tangible reduction in the overall thrust force at the tool-workpiece interface. The results evaluation therefore recommended the need to employ higher rotational speeds when drilling CFRPs (Phadnis et al., 2012a; Phadnis et al., 2012b). The acoustic softening effect of UAD has been modelled using numerical simulations (Phadnis et al., 2013b). It was reported that the vibration effect on the tool in UAD generated an adiabatic heat transfer which further translated into a plastic deformation of the workpiece (CFRP). As a result of this phenomenon, this phenomenon caused a softening effect. It was then ensured that a minimum thrust force and torque were used by the tool in this method of drilling, compared to the CD counterpart. Also, it was observed that these favourable conditions of plasticity and reduced thrust forces were crucial, to ensuring a better drilling output, as well as to preserve the tool life for a longer period. Some vital information about the effects of UAD on CFRPs have been equally reported (Makhdum et al., 2014), using a combination of experimental data and mathematical models. The drilling forces, temperature, chip formation, surface finish, circularity, delamination and tool wear were investigated in UAD of CFRPs. The remarkable results presented show that a significant reduction in drilling forces, often in the excess of 80 % compared to the CD. Summarily, general improvements on the UAD outputs were achieved, relative to CD.

From the extensive literature reported above, it is evident that in the recent years, metal matrix and conventional FRP composites have been extensively machined using both UAD and CD methods. But, there is no a single report on UAD of a natural FRP composite materials, especially on a HF/VE bio-composite sample. The only very few reports available on machining of a natural FRP composites are based on only CD technique. For instance, a lowest conventional drilling-induced damage (delamination

and surface roughness) were observed on the HFRP composite, when compared with banana, glass and jute fibre-reinforced composites (Babu et al., 2013a). An experimental investigation of the effects of drilling parameters (feed and speed) on the damage (delamination) factor during CD of glass, hemp and sandwich fibres of 10 %, 20 % and 30 % fibre volume fractions have been conducted (Naveen, Yasaswi & Prasad, 2012). They reported that fibre-uncut defect was observed at a high feed, and an increase in feed rate caused an increase in the damage factor. The optimum results were associated with a volume fraction and speed of 30 % and 40 m/min respectively, coupled with a lower feed rate. Similarly, the effects of a conventional drilling parameters (feed rate and cutting speed) and aspect ratios (00, 19, 23, 30, 38) on delamination and surface roughness damage responses of HFRP composites have been experimentally reported (Ismail et al., 2016a). From their results, it was evident that the feed rate and the fibre aspect ratio have a significant influence on both damage responses. Also, these damage responses decreased with the cutting speed, while an increase in feed rate significantly caused an increase in both damage responses. They concluded that both damage responses were increased with the fibre aspect ratios.

The enhanced properties and increased application of HFRP composites have emphasised the need for an innovative and a novel understanding of their machinability in order to further improve their functionality and applicability. The natural FRP composites tend to gain wider application when compared with a synthetic FRP composites. This is due to the low energy consumption, sustainability, biodegradability, tailorability, recyclability, high fatigue, thermal, acoustic, electrical and corrosion resistance, ease of production process, low cost, repairability, high strength to weight ratio, low density and environmental friendliness of the natural FRP composites (Baghaei & Skrifvars, 2016; Bakare et al., 2016; Oksman, 2007; Dhakal et al., 2015; Andrew et al., 2016; Faruk et al., 2012; KC et al., 2016). These advantages call for a better and novel technique of drilling natural FRP composites.

3.10 Morphological damage characterisation (response measurement and analysis)

In an attempt to effectively observe, detect, monitor and characterise the drilling-induced surface integrity and delamination flaw in a several types of composite materials, quite a lot of non-destructive examinations (NDE), techniques and methods have been conducted. These examinations include, but are not limited to, the application of *scanning electron microscope* (Gilchrist & Svensson, 1998; Svensson, Shishoo & Gilchrist, 1998; Svensson & Gilchrist, 1998; Gilchrist, Svensson & Shishoo, 1998; Oguni & Ravichandran, 2001; Khashaba, 2010a; Khashaba, 2010b; Rawat & Attia, 2009; Kumar et al., 2014), *X-ray micro computerised tomography* (Chen, 1997; Durão et al., 2008; Durão et al., 2010; Hocheng & Tsao, 2007; Tsao & Hocheng, 2005), *ultrasonic C-scan* (Tsao & Hocheng, 2004; Tsao & Hocheng, 2007; Tsao, 2008; Hocheng & Tsao, 2006; Hocheng & Tsao, 2007; Velayudham & Krishnamurthy, 2007), *electric resistance change method* (Todoroki & Tanaka, 2002; Todoroki, Tanaka & Shimamura, 2002), *shadow moiré laser based imaging technique* (Seif, Khashaba & Rojas-Oviedo, 2007), *fibre Bragg grating sensor system* (Takeda, et al., 2003; Takeda, Okabe & Takeda, 2002; Ling, Lau & Cheng, 2004; Lee, Lee & Yun, 1995), *optical microscope* (Kim & Ramulu, 2004a; Gaitonde et al., 2008; Davim & Reis, 2003a; Davim & Reis, 2003b; Davim et al., 2004a; Davim et al., 2004b; Rawat & Attia, 2009; Karnik et al., 2008; Kilickap, 2010; Kim & Ramulu, 2004b; Makhdum et al., 2014), *stere-microscope* (Faraz et al., 2009), *vibration-based methods/techniques* (Saravanos & Hopkins, 1996; Williams & Addessio, 1998; Lee, 2000), *digital photography technique* (Khashaba, 2004; Khashaba, 2010a; Khashaba, 2010b) and *piezo-electric sensors/actuators* (Teboub & Hajela, 1992; Keilers & Chang, 1993; Keilers & Chang, 1995a; Keilers & Chang, 1995b; Saravanos, Birman & Hopkins, 1994). Other emerging NDE methods applying to characterise delamination and surface integrity of composite materials in this contemporary days include *radioscopy, infrared thermography, acoustic emission, eddy current, modal data-based analysis, computerised vibro-thermography* (Sridharan, 2008), amongst others.

3.11 Description of gaps in research literature

Based on several research works that have been earlier and extensively reported under chapters two and three (literature review), it is evident that much research has concentrated on synthetic or conventional (mainly on carbon and glass) FRP composites, but very little is known about the machinability of natural or sustainable FRP composites. Importantly, drilling of HFRP material samples under the same CD and UAD parameters and conditions, are very rare and scarce. Though, in the recent years, metal matrix and conventional (mainly carbon and glass) FRP composites have been extensively machined using both UAD and CD methods (Thomas & Babitsky, 2007; Pujana et al., 2009; Phadnis et al., 2012a; Cong et al., 2013; Phadnis et al., 2013a; Phadnis et al., 2013b; Gupta et al., 2014; Kadivar et al., 2014; Makhdum et al., 2014). But, there is no a single report on UAD of a natural FRP composite materials, especially on a HF/VE bio-composite samples. Consequently, possibility of reducing drilling forces (thrust and torque) with application of UAD technique on natural (HFRP) composite materials has not been reported.

In addition, the quantity of these drilling forces determine the quality of the drilled holes of the concerned FRP composites. The only very few reports available on machining of a natural FRP composites are based on only CD technique (Naveen et al., 2012; Babu et al., 2013a; Babu et al., 2013b; Ismail et al., 2016a). Also, their drilling-induced damage (especially delamination and surface roughness) on both fibres and matrices (thermoplastic and thermoset), using UAD technique, have not been analysed and characterised.

Furthermore, the advantages of aspect ratio of fibre as a reinforcement in a FRP composite materials can never be overlooked. It determines the mechanical properties of the FRP composites, which depends on stiffness and fibre-matrix interface bond (strength). Other properties of fibres such water absorption (Dhakal, Zhang & Richadson, 2007), fracture behaviour and toughness (Liu & Hughes, 2008; Almansour et al., 2015), to mention but a few, have been extensively studied. Therefore, the effects of these properties are available in the extant literature, with exception of fibre aspect ratios. Consequently, there is no report on optimal aspect ratio, drilling parameters and conditions for a natural (HFRP) composite materials.

More also, the quality of a drilled hole, delamination defect of composite materials and rapid tool wear depend greatly on the drill geometry and drilling parameters. There is need for improvement on the drill geometry (chisel edge, point angles and cutting lips, material and drilling conditions (Tsao & Hocheng, 2004; Tsao & Hocheng, 2005; Basavarajappa et al., 2008) in order to optimise the entire drill design. According to Isbilir and Ghassemieh (2013), delamination free drilling process might be obtained by the proper selections of drill point geometry and the process parameters. Hence, efficient point angle, helix angle and chisel edge that will not increase normal stresses (wear) and delamination at the drill tip are required. Chisel edge and point angle increased with delamination effect and normal stress respectively. There is need for the correct selection and optimisation of the chosen drill bit geometry and tooling material as point angle increased with normal stress depending on the tooling material (Chao et al., 2009). Though, Wang and Zhang (2008) had worked on drill chisel edge region. Other parts of the drill geometry such as diameter, cutting lips and point angles should be considered in addition to chisel edge region.

Moreover, substantial studies (Gururaja & Ramulu, 2009; Karimi, Heidary, & Minak, 2016; Lachaud et al., 2001; Zhang, Whang & Liu, 2001; Saoudi et al., 2016; Ko¨ nig et al., 1985; Upadhyay & Lyons, 1999; Timoshenko & Woinowsky-Krieger, 1959; Jones, 1975) have addressed modelling of some parts of FRP composite machining. But, predictive thermo-mechanical models for analysing the FRP delamination drilling-induced damage, by predicting the critical feed rate and critical thrust force at the onset of delamination crack on CFRP composite laminates models as well as incorporating drill geometry (especially the cutting lips, chisel edge and point angles), mixed loads (concentrated or point and uniformly distributed forces), experimentally based assumptions and machining parameters have not yet been formulated, validated and optimised.

Lastly, all these research gaps look as challenging tasks that provide direction and focus to this reported research work.

3.12 Summary

This chapter reviewed the experimental and theoretical concept of FRP composite machining (drilling), associated problems of drilling-induced damage on both FRP composites and drill bits (tools), the importance of tooling materials, drill types, geometry and design, drilling conditions, techniques and parameters. Furthermore, it explained pertinent literature on analytical modelling of delamination prediction and analysis.

The workability of FRPs with various non-conventional drilling technologies has been discussed in this paper. Decisions on process suitability for machining FRPs were based on the ability to produce a damage-free drilled laminate, measured with respect to the delamination potential, thermal degradation effects and operational costs involved. Among all the five processes discussed in this chapter, abrasive jet and ultrasonic assisted drilling demonstrated capabilities for effective machining of FRPs. This is reflected in their quality of machined holes, coupled with their flexibility in the choice of workpiece materials.

Laser beam technology proved highly promising due to the ease of process automation, but with limited applicability to FRPs due to the tendency of HAZ formation and unsuitability for thermosetting polymer matrices such as epoxy and polyester resins. Abrasive jet drilling showed lesser delamination damage on FRPs, but with undue high noise level during operation and process costs involved in setting up this technology. Water jet drilling, though extensively used in manufacturing industries, has restrictions due to its possibility of introducing delamination and its incompatibility for materials with water degradation potential; of which some FRPs, such as natural (cotton, hemp, jute, to mention but a few) fibre reinforced composites are inclusive. Electrical discharge drilling technology, though most suitable for generating precision holes (holes without distortion), has its applicability to FRPs reduced by the total dependence on materials' electrical conductivity and low material removal rates.

However, ultrasonic assisted drilling proved highly applicable to FRPs by its relatively lesser delamination potential and lower thermal build-up at tool-workpiece interface.

While operational costs for this technology were reportedly high comparing with other non-conventional processes, favourable results obtained from this technology suggests its suitability for machining several FRP composite materials, regardless of their electrical conductivity levels, hardness or slenderness. Conclusively, non-conventional drilling technologies showed greater effectiveness towards machining FRPs over their conventional counterparts.

Conclusively, a well-designed drill geometry, good choice of drill materials and knowledge of drilling parameters, conditions and techniques afford better opportunity of minimising drilling-induced damage, especially delamination of the fibre-reinforced polymer composites, tool wear, and producing a high quality surface. These are the focuses of the next chapter four.

PART III

MATERIALS

&

METHODOLOGY

CHAPTER FOUR

MATERIALS AND METHODOLOGY (EXPERIMENTATION)

4.0 Introduction

This chapter details with the different types of materials and methodology used for the experimentation. Two main classes of FRP composite specimens were fabricated for the investigation of machining characteristics. These include natural (hemp) and synthetic (carbon) fibre-reinforced polymer composite specimens, as experimental work pieces. The account of their properties and fabrication or manufacturing procedures are well stated. Importantly, the experimental works (part A) of this study is also discussed in this chapter under three distinctive stages as outlined, whereby methods, techniques and procedures taken during the drilling experiments are explained.

Stage 1: *Effects of drilling parameters and aspect ratios on delamination and surface roughness of lignocellulosic HFRP composite laminates.*

Stage 2: *Comprehensive study on machinability of natural fibre-reinforced bio-composites and conventional fibre-reinforced polymer composites.*

Stage 3: *Machinability of bio-composites: Conventional versus ultrasonically-assisted drilling techniques.*

4.1 Composite specimens

Three different important and different fibre-reinforced polymer composite work piece materials were used throughout this research work. Two of them are classified as a natural FRP composite specimens. These were hemp fibre-reinforced polymer with polycaprolactone and vinyl ester matrices, designated as HFRP/PCL and HFRP/VE respectively. The third specimen was a synthetic or conventional carbon fibre-reinforced with epoxy resin (CFRP/EP), as a reference specimen. Hemp fibre is a bast lignocellulosic natural fibre, reinforced with a biodegradable thermoplastic matrix, known as

polycaprolactone (PCL). The carbon fibre is an inorganic and synthetic fibre, reinforced with a non-biodegradable thermoset matrix, known as Epoxy resin (EP). Therefore, the hemp fibre reinforced polymer (HFRP) is an example of a natural (sustainable) fibre-reinforced composite, while carbon fibre-reinforced polymer (CFRP) is referred to as synthetic (conventional) composite. In addition, the main constituents, properties and architecture of these three FRP composite laminates used, as workpiece specimens are illustrated in Figure 4.1. As discussed in the subsequent sub-chapters, the experiment began with utilisation of HFRP/PCL specimens, followed by CFRP/EP and lastly, HFRP/VE composite specimens were used. The hemp fibre is not expensive in terms of cost of production (planting) and process among other bast natural fibres. It is ready available in Europe and Asia in a very large quantity. It is classified as one of the high lignocellulosic fibre, with high mechanical properties, making it a good reinforcement of many fibre-reinforced composites (FRCs) (Scarponi et al., 2015; Ismail et al., 2015), while a carbon fibre is a synthetic material with higher stiffness, brittleness and cost of fabrication, when compared to hemp fibre.

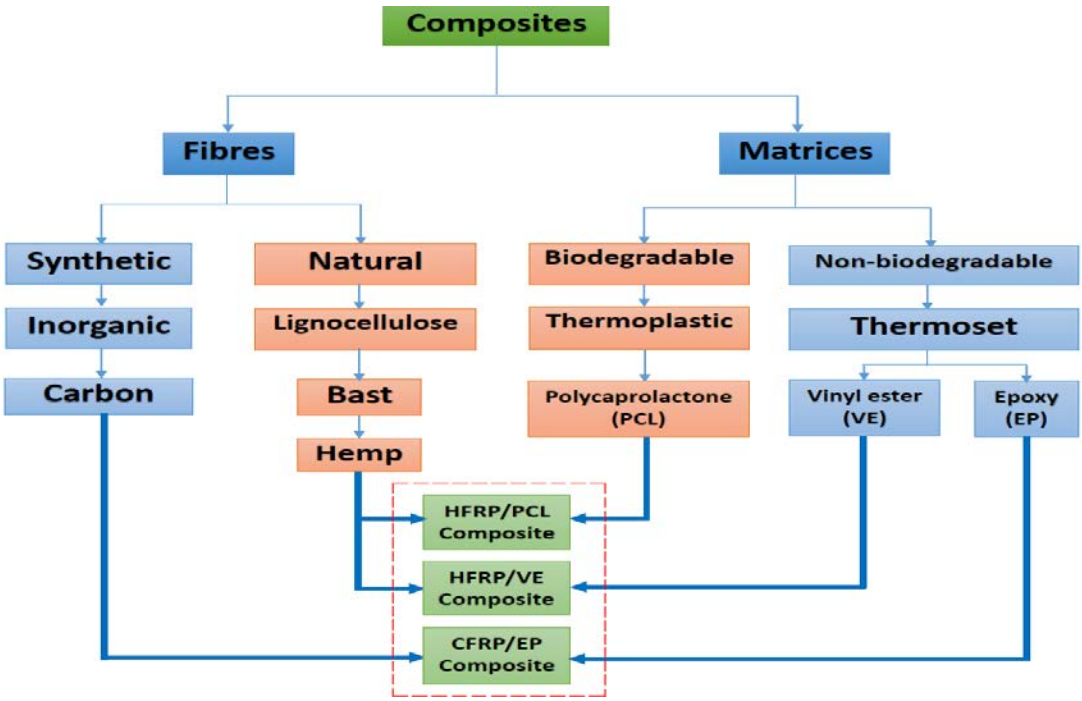

Figure 4.1: The main compositions, properties and architecture of the FRP composite laminates used

4.1.1 Stage 1: Fabrication of HFRP/PCL composite laminates

In an attempt to investigate the effects of drilling parameters and aspect ratios on delamination and surface roughness of lignocellulosic HFRP composite laminates, five squared 197 x 197 mm, thickness 7.5 mm HFRP/PCL composite laminates designated as specimens A, B, C, D and E made up of different aspect ratios, AR of 0 (neat, control and reference sample), 19, 26, 30 and 38 respectively were used as test specimens for this experiment. These specimens are shown in Figure 4.2. The first specimen (neat) has no hemp fibre reinforcement. Aspect ratio is the ratio of the hemp fibre length, L to the diameter, D. All the diameters of the fibre elements present in the HFRP were in the same order of magnitude (Table 4.1), close to 22 µm. This means that majority of fibre elements were small bundles size elements or individualised fibres. Therefore, the aspect ratio (L/D) of the specimens varied due to the length, L only.

(a) A typical bast hemp fibre

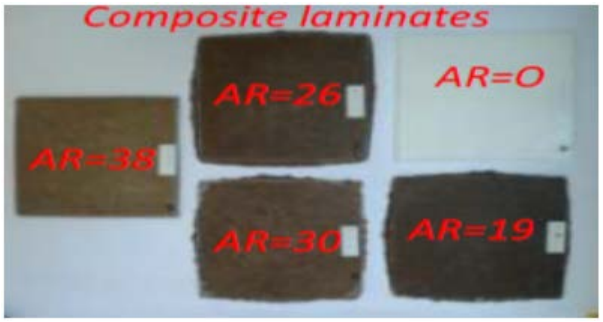

(b) HFRP/PCL composite laminate specimens

Figure 4.2: (a) A typical bast hemp fibre before fabrication and (b) fabricated HFRP/PCL composite laminate or specimens with different aspect ratios

Table 4.1: Analysis of the fibre aspect ratios (Ismail et al., 2016a)

Aspect ratio (L/D)	19	26	30	38
Mean fibre element length, L (μm)	432	568	708	845
Mean fibre element diameter, D (μm)	22.4	21.7	23.6	22.5

An extrusion process was used to prepare the specimens using a resin bio-binder; PCL possessing a specific gravity of 1.1 at 60 ^{o}C and flash point of 275 ^{o}C (open cup method). The composites were prepared using a laboratory-scale twin screw extrusion (TSE) Clextral BC 21 (Firminy, France). The extruder has a diameter (D) of 25 mm and a length (L) of 900 mm (L/D ratio: 36). Hemp fibres elements and PCL were introduced either all together in the hopper or in two location. In all cases, a venting zone for water steam evacuation was included. The fibres were mixed with PCL at a concentration of 20 wt. %. This is the fibre volume fraction, which implies the percentage of hemp fibre volume in the whole volume of the HFRP composite sample. The barrel temperature was set at 100 ^{o}C, and the experiments consisted of varying parametric setup of the extruder: feed rate and screw speed. A triplicate of data sheet from both extrudate neat PCL or 20 % wt. hemp fibre/PCL composites differing in their average L/D ratio were obtained by Press moulding. The press is a two-column automatic laboratory hydraulic press (Carver, Wabash, IN USA) equipped with heating platens. Three types of moulds (MGTS, La Neuvillette, France) of all 20 cm x 20 cm length but differing in their thickness: 5; 6.5 and 8 mm (approx. 340; 280 and 220 g on average respectively), were filled with specimens and preheated 5mins at 135 ^{o}C before 1 Ton pressing for 3mins. Data sheets were then cooled down by immersion in distillate water, dry and stored at 65 % RH before testing.

4.1.2 Stage 2: 19-HFRP/PCL and MTM 44-1/CFRP/EP composite specimens

Figure 4.3 depicts the 197 x 197 mm, thickness 5 mm MTM 44-1/CFRP/EP and 19-HFRP/PCL specimens used as experimental specimens, simply referred to as CFRP and HFRP respectively. These specimens were used to conduct a comprehensive study on machinability of sustainable and conventional fibre reinforced polymer composites. The

choice of 19-HFRP/PCL specimens among other aspect ratio was based on its optimal performance after the first phase of the experiment (sub-section 4.1.1). The HFRP was made up of aspect ratio (AR) of 19. The HFRP composite laminate specimens were fabricated using an extrusion process. A resin bio-binder; PCL, a semi-crystalline polymer having a specific gravity of 1.1 at a low melting temperature of 60 ^{o}C Aas well as a flash point of 275 ^{o}C was used. It was provided by Perstop (UK) (Capa© 6800). The hemp fibre used was Fedora 17 specie, delivered by FRD©. The hemp fibre is a very strong lignocellulosic natural fibre that requires less processing energy. The mechanical properties of natural hemp fibre and PCL are highlighted in Table 4.2 in addition to the afore–mentioned properties under sub-section 4.1.1, especially in Figure and Table 4.1.

(a) MTM 44-1 CFRP/EP laminate. (b) 19-HF/PCL laminate.

Figure 4.3: The specimens used for the second experiment

Table 4.2(a): Mechanical properties of a natural hemp fibre and polycaprolactone (Shah, 2013; Naveen et al., 2012; Asokan, Firdoous & Sonal, 2012)

Properties	**Value**	
	Hemp fibre	**Polycaprolactone**
Density (g/cm^3)	1.0 – 1.48	1.13
Tensile Modulus (GPa)	30 –70	0.4
Moisture content (wt. %)	10.8 –14.5	–
Tensile (Fracture) strength (MPa)	310 – 900	16–23
Elongation to failure (%)	1.6	>700

The low pressure vacuum bag Out–of-Autoclave (OoA) moulding with 0 % void content, prepreg form, oven cure (OC) and unidirectional (UD) methods were used for the manufacture of the CFRP composite laminate specimens. The MTM (Medium Temperature Material) 44-1 CFRP laminate specimen is one of the carbon fibre composite laminates, with a reactive formulation and low exothermic risk, used in manufacturing of primary and secondary aircraft or space structures. It has a high damage tolerance, excellent mechanical properties, superior temperature performance, superb drape and tack, controlled matrix flow in processing, excellent translation of fibre properties, availability on different reinforcements and excellent impact resistance. Also, the CFRP prepreg contained 18 plies hand lay-up with a high strong EP (matrix) acting as a binder. The process was carried out under a minimum of 980 mbar (29 ”Hg) vacuum bag pressure with 1 to 2 ^{o}C (1.8 to 3.6 ^{o}F) per minute ramp rate. The UD CFRP composite laminates were supplied by Umeco Structural Materials Company. The brief and main compositions, properties and architecture of the two composite laminates (specimens) used for this second experimental investigation have been earlier illustrated in Figure 4.1.

Table 4.2(a): Mechanical properties of UD carbon prepregs

Test	UD Carbon Prepregs	Units
0° Tensile Strength	2538	MPa
90° Tensile Strength	92	MPa
0° Tensile Modulus	163	GPa
90° Tensile Modulus	10	GPa
0° Compression Strength	1690	MPa
0° Compression Modulus	150	GPa
0° ILSS (Shortbeam shear)	94	MPa
In-plane Shear Strength	106	MPa

The effective cure cycles used were 2 hours at 130 ^{o}C and another 2 hours at 180 ^{o}C. The cool down was observed at maximum of 3 ^{o}C per minute to 60 ^{o}C. The storage took 21 days, which was the accumulated time before the part is cured at 70 ^{o}F. Tables 4.2(a) and (b) depict the mechanical properties of the UD carbon and MTM 44-1 epoxy resin, as adapted from the material data sheets. The values highlighted in Table 4.2(b) account for the surface weight. Other properties can be found in the Appendices B and C.

Table 4.2(b): Mechanical properties of MTM 44-1 epoxy resin

Test (0^{o} & In-plane)	**268 g/m^2 24k UD**	**Unit**
Tensile modulus	174.6	GPa
Tensile strength	2738	MPa
Compressive modulus	147.2	GPa
Compressive strength	1459	MPa
Shear modulus	3.60	GPa
Shear strength	76.0	MPa
Flexural modulus	154.9	GPa
Flexural strength	1874	MPa
Inter-laminar shear strength (ILSS)	109.4	MPa

4.1.2.1 SEM morphological characterisation of matrices of the specimens

The morphological and micro-structural examinations of both binders of the two specimens were performed using Scanning Electron Microscopy (SEM) method. This non-destructive examination was performed before they were affected or burned by the composite-drill interface temperature generated during drilling operations. The micrographs were taken at the surfaces of the specimens for a better comprehensive study. The epoxy resin is stronger, and has a greater adhesive force, as well as higher glass transition temperature (T_g) between 60 ^{o}C and 110 ^{o}C (Techtip, 2012) than the polycaprolactone of −60 ^{o}C T_g (Kumbar, Laurencin & Deng, 2014), which depends on the cure schedule. Glass transition temperature is the temperature zone where the polymers

(epoxy and polycaprolactone resins) transition from a glassy and hard material (matrix) to a rubber-like and soft material. It plays a very significant role in analysing the properties of matrix. Hence, epoxy resin produces a stronger bond expected between the carbon fibre and the resin, as shown in Figure 4.4. In addition, the TGA results discussed under results and discussion chapter depicted that CFRP composite samples were stronger than the HFRP samples. The effects of these properties will be further and detail discussed under results and discussion chapter.

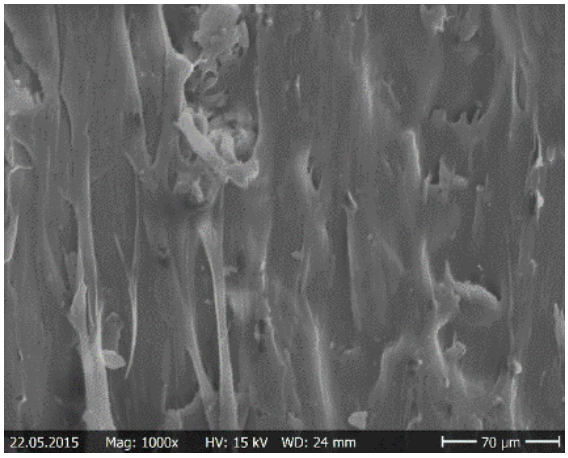

(a) HFRP polycaprolactone

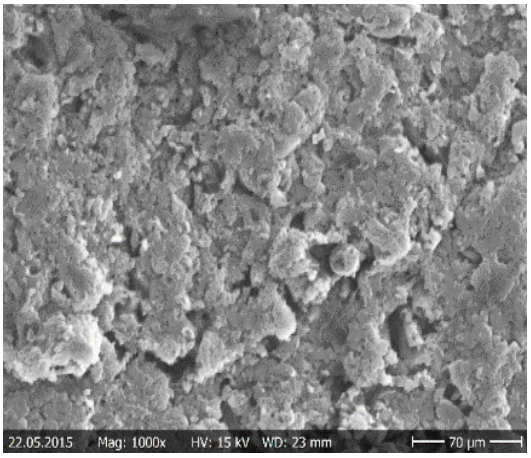

(b) CFRP Epoxy resin

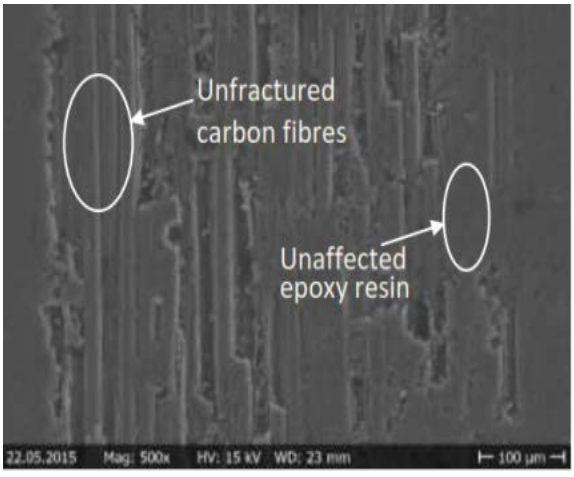

(c) Fibre and matrix

Figure 4.4: SEM micrographs showing: (a) & (b) their matrices and (c) strong CFRP-EP interfacial bond

4.1.2.2 Thermogravimetric analysis of the specimens

The thermogravimetric analysis (TGA) of the two HFRP and CFRP specimens were conducted, using a TGA Q50 V 6.1 (Figure 4.5) produced by TA Instruments, available in the advanced polymers and composites (APC) laboratory of University of Portsmouth, UK. The platinum crucible of the instrument accommodated the samples before they were heated in an environment filled with nitrogen. The samples were subjected to a heating rate of 20 ^{o}C/min starting from an ambient temperature to 500 ^{o}C. The samples have an initial weights of nearly 8 mg. The data obtained from the specimen test are presented as TG and DTG, denoting the weight loss due to the temperature rise and weight loss rate due to the temperature rise, respectively. Relevant results obtained for the two specimens have been discussed later under results and discussion chapter.

Figure 4.5: A Q50 V 6.1 Thermogravimetric analyser

4.1.3 Stage 3: 19-HFRP/PCL and 19-HFRP/VE composite specimens

Squared workpiece of overall dimensions of 140 x 140 mm x 4 mm of HFRP composite specimens made up of aspect ratios, AR of 19 were used for this experiment. The choice of the AR of 19, as an optimal specimen among other hemp fibre ARs, was based on the results of the recently reported work (Ismail et al., 2015; Ismail et al., 2016a), as afore-mentioned. Each specimen contained 4 layers, and a lay-up process was used to prepare

the HFRP specimens, using two different resins, which are bio-binder (PCL) and a thermoset matrix, known as vinyl ester resin (VE) for the fabrication of another 19-HF/VE bio-composite specimen (Figure 4.6). Figure 4.3 shows 19-HF/PCL laminate specimen.

Figure 4.6: A typical fabricated Hemp fibre-reinforced/vinyl ester (19-HF/VE) composite laminate

The VE matrix possessed a specific gravity of 1.04 g/ml and flash point of 23–29 ^{o}C (74-84 ^{o}F). The machinability of these two bio-composites (19-HF/PCL and 19-HF/VE) was conducted using a conventional and ultrasonically-assisted drilling techniques. The failure of the 19-HF/PCL due to the presence of PCL matrix under ultrasonically-assisted drilling technique necessitated its replacement with VE resin for the same 19-HF.

4.2 Methodology (Experimentation)

The first and second experiments were conducted using L_{16} (4^5) and 4^2 orthogonal array of *Taguchi technique or method of design of experiments* for stages 1 and 2 respectively. This method has been reported as a modern design and optimisation technique extensively used to show the influence of machining parameters on variable experimental responses. It saves experimental period and cost as well as improves the quality of outputs. The orthogonal array has suitability to express the inter-dependent connections among the drilling factors considered (Dhavamani & Alwarsamy, 2011). In

stages 1 and 2, both cutting speed and feed rate were mainly selected for investigation being the two most notable drilling parameters that influence the quality of drilled holes, apart from the aspect ratio of the composite laminates. The array selected has sixteen rows equivalent to the test number with two factors at four different levels. The experimental plan is made of sixteen tests: first and second columns were allocated to the cutting speed, *V* (*m/min*) and feed rate, *f (mm/rev)* respectively, and the remaining were allocated to the iterations or five specimens. Surface roughness, R_a *(µm)* and Delamination factor, F_d are the two responses (outputs) to be studied with respect to five aspect ratios, *AR* of HFRP composite laminates. Analysis of average and variation were used to analyse the results of experiments. The drilling operation for stages 1 and 2 was carried out without coolant due to the adverse effects of some wet coolants. This dry machining environment is required for the proper analysis of the considered responses: the delamination and surface roughness effects.

The last stage 3 of the experimental work was conducted using the same orthogonal array of Taguchi technique of design of experiment. But, the aim was on the measurement of principal drilling forces (thrust and torque) for the prediction and analysis of drilling-induced damage, especially delamination. Conventional and ultrasonically-assisted drilling techniques were used. Drilling operation was performed under compressed air cooling environment. In addition, all the drilling operations for stages 1-3 were performed with the support of an aluminium plate at the back of the composite specimens.

Details of all the machines and methods used are hereby discussed in the succeeding sub-sections of this chapter.

4.2.1 Process parameters of drilling operation

The fishbone (or Ishikawa cause-effect) diagram, as depicted in Figure 4.7 is constructed to illustrate the drilling process parameters that have effect on the quality of the drilled holes of FRP composite laminates. Each of these parameters was addressed during the experimental plan. Hence, the highlighted blue fonts were experimentally investigated within the scope of this research while, other parameters were considered

based on optimal results reported in literature. Among them, workpiece materials have been discussed in sub-section 4.1 of this chapter, while other drilling process parameters such as cutting tool (drill bit) properties, drilling environment and parameters are thus elucidated.

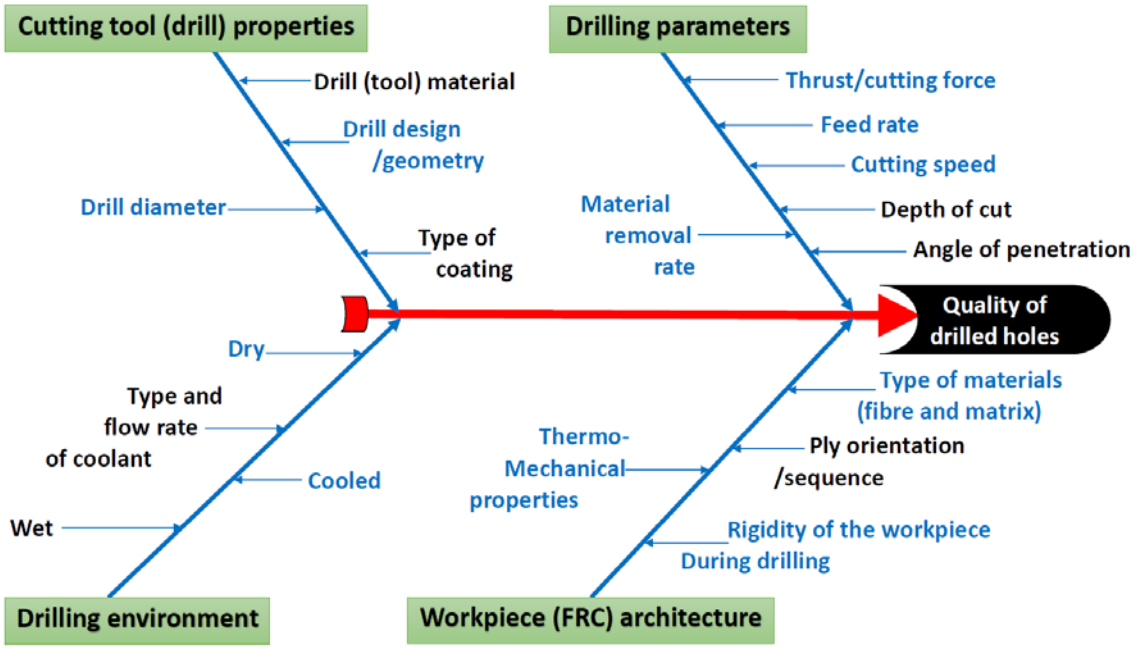

Figure 4.7: The Ishikawa (cause-effect) diagram of a drilling process

4.2.2 Experimental Procedures (design and test arrays) for Stages 1 and 2

The subsequent sub-sections explain the experimental procedures and related test arrays adopted in the experimental stages 1 and 2. Both stages have similar experimental set-up and conditions.

4.2.2.1 Drilling tools: High speed steel (HSS) drill bits

Two (diameters 5.0 and 10.0mm) double-fluted standard HSS twist drills were used for the drilling, details are presented in Table 4.3 and Figure 4.8. Sharp and new double fluted drills were used in order to reduce delamination effect and surface roughness.

Table 4.3: Twist drills specification (Ismail et al., 2016a)

Set	Diameter (mm)	Length (mm)	Description
1	5.0	115.30	High speed steel (HSS) twist drills of different diameters, point angle 118^{o}, two cutting edges and manufactured by DORMER.
2	10.0	206.64	

(a)

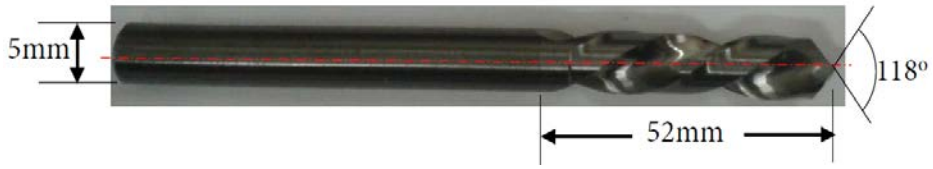

(b)

Figure 4.8: HSS twist drills used: (a) 10.0 mm and (b) 5.0 mm diameters

4.2.2.2 Drilling design and set-up

A design software, known as Pro-Engineer (Creo 2 version) was used to produce the CAD drawing (Figure 4.9a), programmed into the CNC drilling machine (Figure 4.9b), before drilling operation was carried out to produce drilled composite specimens (Figure 4.9c). Taguchi method of design of experiment used for feed rates and cutting speeds to produce the spindle revolution is an efficient technique for obtaining near optimal design of experimental parameters for cost effective, better time management, performance, optimisation and accuracy of experimental results (Pattanaik, Satpathy & Mishra, 2016;

Gupta & Kumar, 2015).

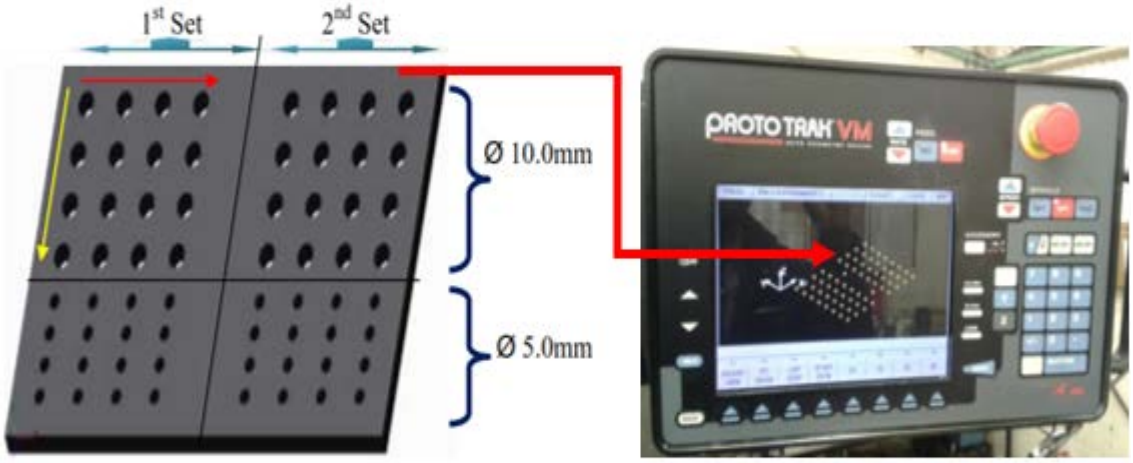

(a) CAD drawing for CNC programming **(b)** CNC programming stage

HFRP specimen

CFRP specimen

(c) Drilled specimens showing drilled holes of Ø 10.0 and 5.0 mm

Figure 4.9: Drilling experimental plan

The operational set-up, especially appropriate tooling calibration and gauging, as illustrated in Figure 4.10 were performed in order to avoid errors, accidents, dimensional and programming inaccuracies. This is done by placing the drill bit, already fitted on the CNC drilling machine and ensure that the drill bit is properly fitted, aligned and perpendicular to the flat surface of the gauge.

In an attempt to further reduce the drilling-induce damage that are associated with drilling of FRP composite materials, the specimens were supported at the back using a pre-drilled aluminum plate, as depicted in Figure 4.11(a).

Figure 4.10: Calibration and gauging of the drilling set-up

In addition, this method is required in order to prevent bending of the specimens (Figure 4.11b), due to the high thrust force developed during drilling process and the considerable small thickness 5.0 mm of the specimens used.

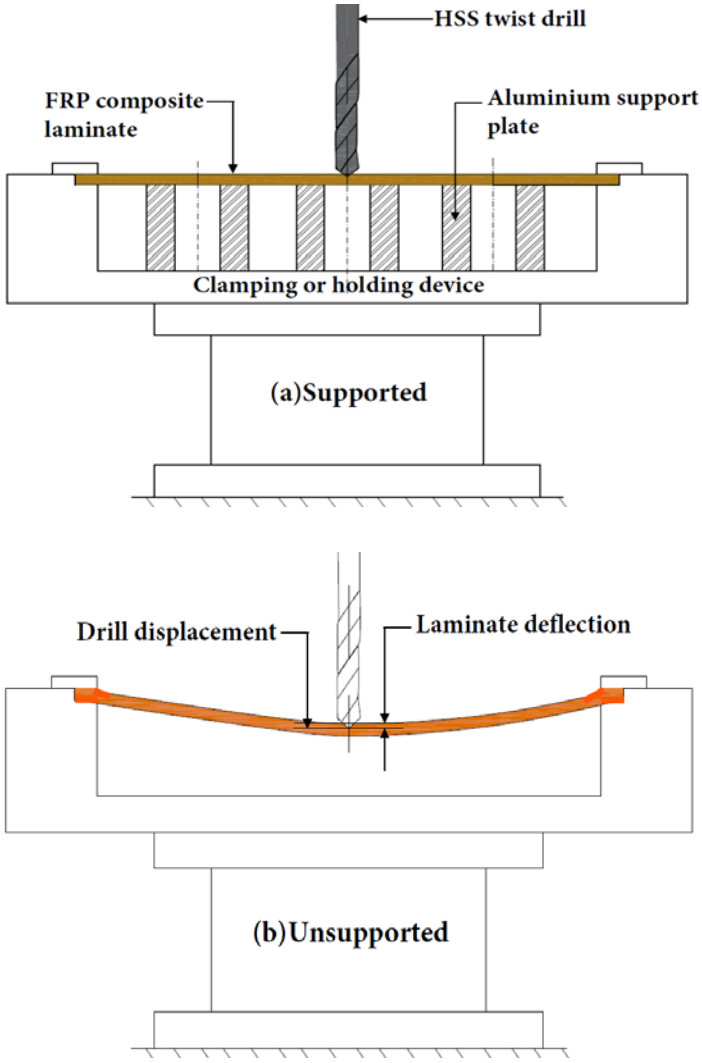

Figure 4.11: The drilling set-up of: (a) supported and (b) unsupported FRP composite specimen (Ismail et al., 2016e)

4.2.2.3 Machining set-up and conditions

Vertical conventional drilling of the HFRP composite specimens was carried out on a HURCO VM10 CNC machining centre (Figure 4.12a) available in the Mechanical Laboratory, University of Portsmouth, UK, with a maximum spindle speed of 10,000rpm. The composites were clamped firmly to avoid movement of test specimens (Figure 4.12b) and achieve zero degree of freedom throughout the drilling operation. Machining was performed under dry conditions throughout. The machining conditions implemented are shown in Table 4.4.

Figure 4.12(a): The HURCO VM 10 CNC machining centre

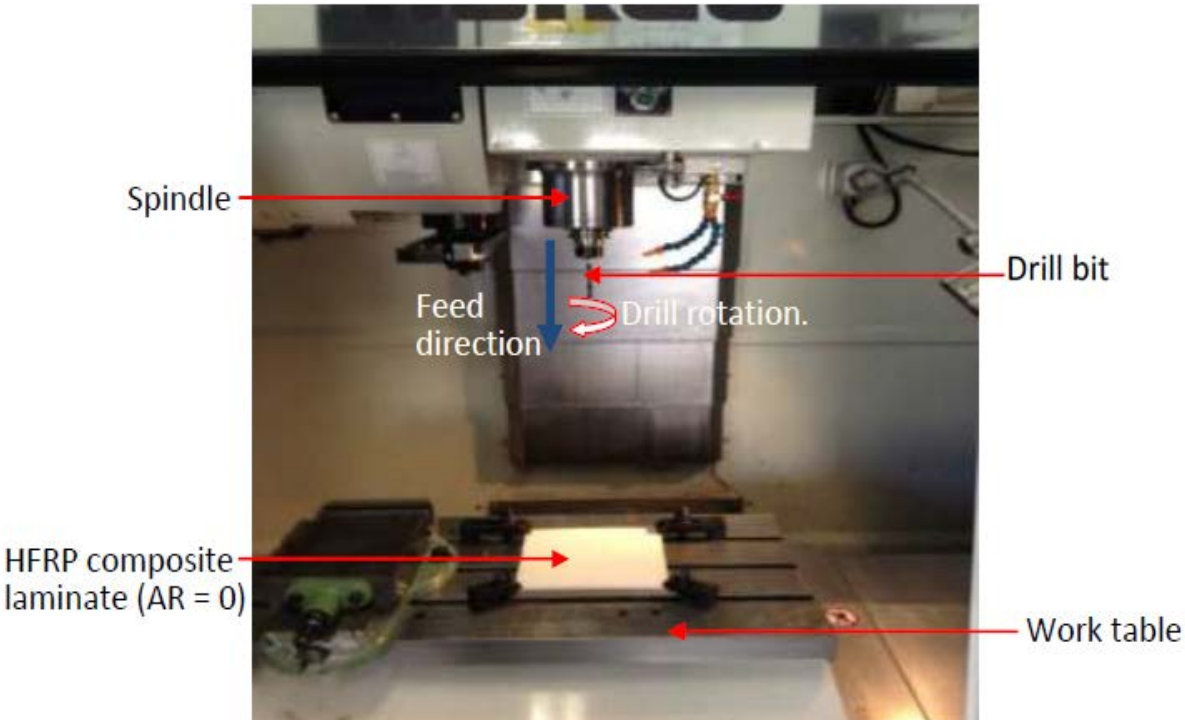

Figure 4.12(b): Stage 1 machining experimental set-up (Ismail et al., 2016a)

Table 4.4: Machining conditions considered (Ismail et al., 2016c)

Drilling Parameters	Symbol	Level				Unit
		1	2	3	4	
Feed rate	f	0.05	0.10	0.15	0.20	mm/rev
Cutting speed	v	10	20	30	40	m/min
Spindle revolution	N_5	637	1273	1910	2546	rpm
	N_{10}	318	637	955	1273	rpm

Furthermore, due to the unavailability of vacuum extractor in the HURCO VM10 CNC machining centre, stage 2 experiment which involved CFRP specimens was performed on a Proto TRAK VM CNC machining centre (Figure 4.13), available in D & T Precision Engineering Limited, Curbridge Botley, Hampshire, UK. This machine is required for the

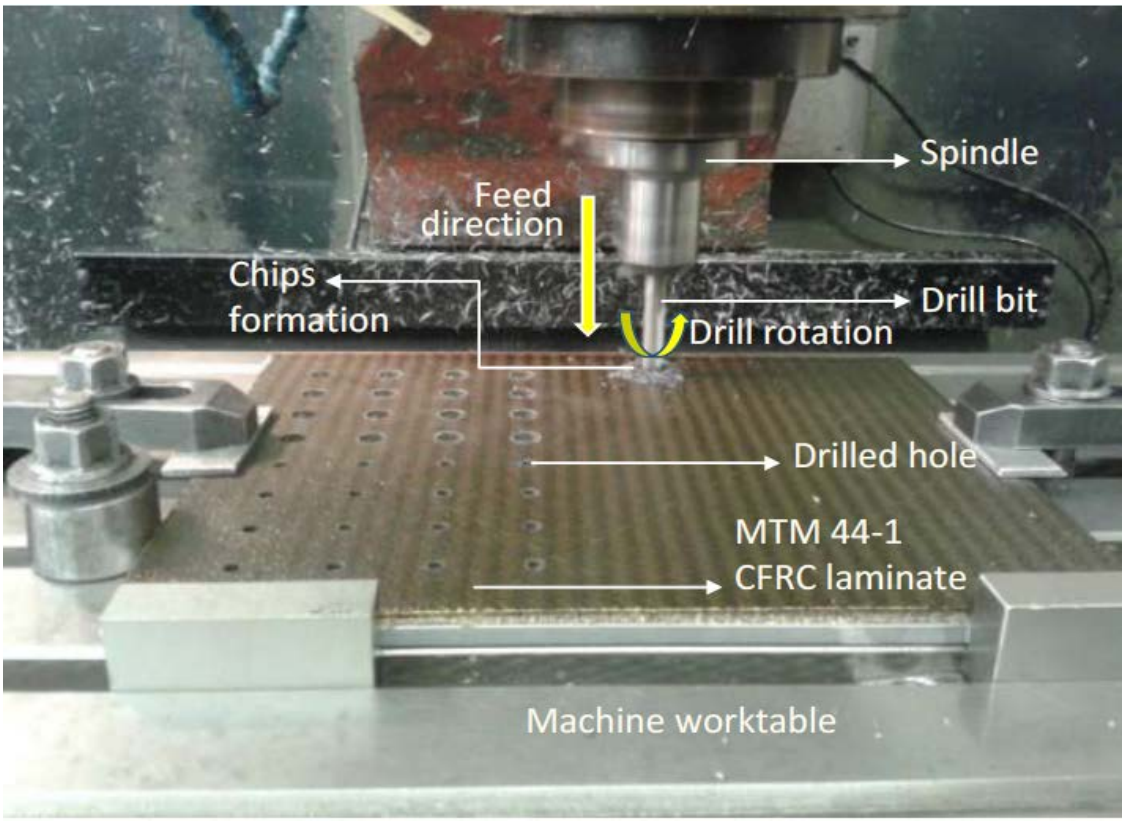

Figure 4.13: Stage 2 machining experimental set-up (Ismail et al., 2016a)

removal of the powder-like or dusty chips formed during drilling of CFRP specimens. This decision was made after risk assessment of the CFRP specimens was conducted, showing the possibility of inhaling a poisonous gas, particles (chips) that could cause cancer disease among other lethal diseases. The Proto TRAK VM CNC machine was used for the drilling of the two (HFRP and CFRP) specimens, under the same conditions. It has a maximum variable spindle speed and motor power of 5,000 rpm 7.5 HP (5.75 KW) respectively.

The cutting speed and feed rate were selected for the investigation as indicated in Table 4.4, being the two most notable drilling parameters that influence the quality of drilled holes. The spindle revolution of drill bits of diameters 5.0 mm and 10.0 mm, denoted as N_5 and N_{10} was also included respectively. The HSS twist drill bits of diameters 5.0 mm and 10.0 mm were used for the drilled holes for delamination and surface roughness analyses, respectively. These drilling parameters were programmed into the two CNC drilling machine centres for an uninterrupted operation for both first and second sets. Observations were made immediately after completion of each set and stage, followed by the measurement of the delamination factor and surface roughness in the laboratory.

4.2.3 Experimental Procedures (design and test arrays) for Stage 3

The machinability of bio-composites (HF/PCL and HF/VE) are compared using a conventional and ultrasonically-assisted drilling techniques. The ultrasonically-assisted drilling (UAD) technique was introduced in a bid to further reduce the possibility of occurrence of drilling-induced damage, especially the delamination as the thrust force reduced. Other advantages of UAD techniques have been earlier stated in the literature review chapter. The operational technique of UAD is quite different from conventional drilling (CD). UAD has standard tools and equipment suitable for its operation. Therefore. These led to some inevitable changes in drilling parameters, tools, conditions and set-ups, as subsequently discussed.

4.2.3.1 Drilling tool

Drilling experiments were conducted using a similar standard TiN-coated HSS two-flute Ø3 mm Jobber carbide twist drill, with a point and helix angles of 135^{o} and 28^{o} respectively. TiN coating is applied to help reduce tool wear and provide longer tool life. Vibrations were applied in the direction at the drill tip for UAD experiment only.

4.2.3.2 Drilling methodology

Drilling tests were carried out, as earlier arranged in Figure 4.11 based on Taguchi method of design of experiment, using an initial trial parameters stated in Table 4.5, before using an optimal parameters such as drill bit Ø3 mm, a constant feed rate of 0.03 mm/min and three spindle speeds of 85 rpm, 540 rpm and 1200 rpm. Detailed discussions are included in the results and discussion chapter. CD test was firstly carried out followed by UAD. This was repeated three times for each machining condition, to ensure accuracy and repeatability of the experimentations. Drill bits were changed after completion of each drilling test to ensure drill wear did not affect the results. The composite specimens were equally supported with a pre-drilled aluminum support plate, as depicted in Figure 4.14.

Table 4.5: Drilling parameters and conditions considered

Drilling Parameter	Symbol	Machining Technique		Unit
		CD	UAD	
Drill bit diameter	Ø	6.00	6.00	mm
Spindle speed	N	40.00	40.00	rev/min
Feed rate	f	0.1 (10%)	0.1 (10%)	mm/rev
Cutting speed	v	0.75	0.75	m/min
Vibration frequency	F	-----	24.75	kHz
Vibration amplitude (peak to peak) at the tip of drill bit	α	-----	8.00	µm
Condition	----	Dry (no coolant)	Dry (air)	-----

4.2.3.3 Drilling Condition or environment

The dry machining (drilling) condition was considered throughout this experiment due to the limiting effects of wet machining on the structural quality and integrity of FRP composites. The use of liquid coolant known as wet machining was discouraged, because it supports the high possibility of absorption of liquid coolant or cutting fluid by the FRP composites, especially the hydrophilic nature of natural fibre-reinforced composites (HFRP specimens) at high temperature, though with the exception of Cindolube V30ML liquid coolant, as reported by Turner, Scaife and El-Dessouky (2015). At high tool-workpiece interface temperature, rapid chemical reaction of hydrophobic matrix and liquid coolant is enhanced as their molecules gain more heat. Consequently, the fibre-matrix interfacial bond is weakened and the mechanical properties of the FRP composites are compromised. This is one of the limitations of composites machining under wet condition, unlike metals.

4.2.3.3 Experimental set-up

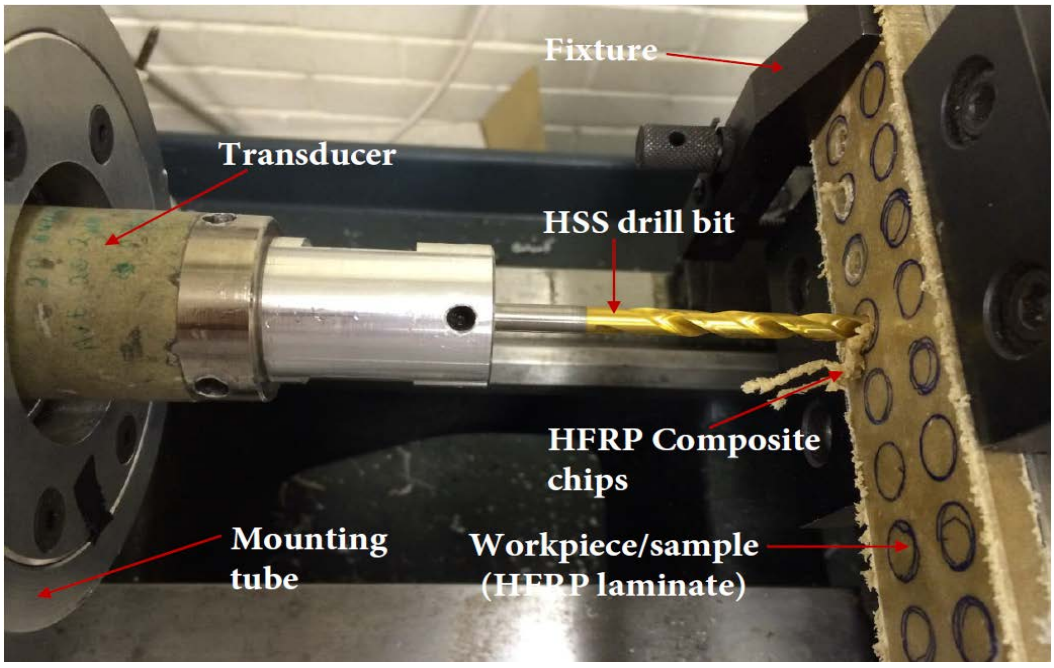

Figure 4.14(a): The full CD (machining) experimental set-up (Ismail et al., 2016e)

Experiments were conducted on a universal Harrison M-300 lathe machine (Figure 4.14a), effectively adapted to integrate an ultrasonic transducer with a 2.24 kW spindle power, as shown in Figure 4.14(b). A Langevin-type piezoelectric transducer was mounted in its three-jaw universal chuck. The transducer was typically composed of piezoelectric ceramics rings, a front mass, a backing mass and a central bolt. A Ø3 mm Jobber carbide TiN- coated twist drill was fixed on the front mass with a modified design to improve its waveguide and maximise the amplitude of the axial mode of vibration. The transducer produced the mechanical vibration by converting a high-frequency alternating voltage based on the piezoelectric effect.

A dynamometer Kistler 9345b piezoelectric 2-component sensor force link was placed on the cross slide of the lathe, fixed on an angle plate to measure thrust force and torque in the process of drilling. The force data measured by the dynamometer were obtained using charge amplifiers, by converting and transmitting the data through an analog-digital converter (digital oscilloscope Picoscope) connected to the computer. A thermal camera was mounted on the lathe and connected to the computer to monitor the temperature of the tool tip while drilling the material, as shown in Figures 4.14(b) and (c). The cooling system consisting of cold air gun vortex tube, pressure regulator and gauge meter.

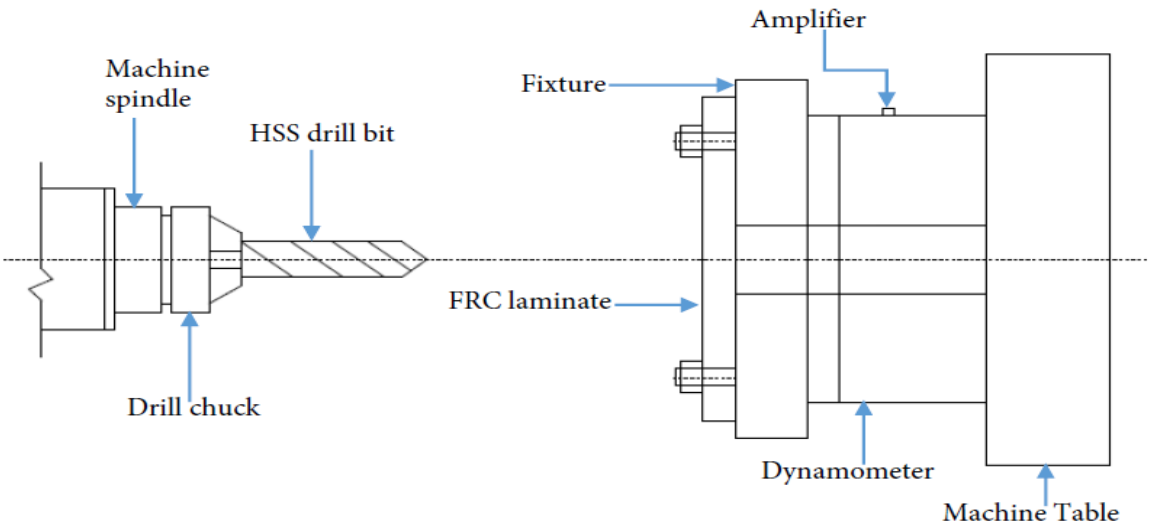

Figures 4.14(b): Schematic illustration of the drilling set-up (Adapted from Tsao & Hocheng, 2004; Tsao, 2008)

Therefore, compressed air was used to serve as a coolant to the tool tip and drilling surface. The complete UAD experimental set-up is shown in Figure 4.14(c).

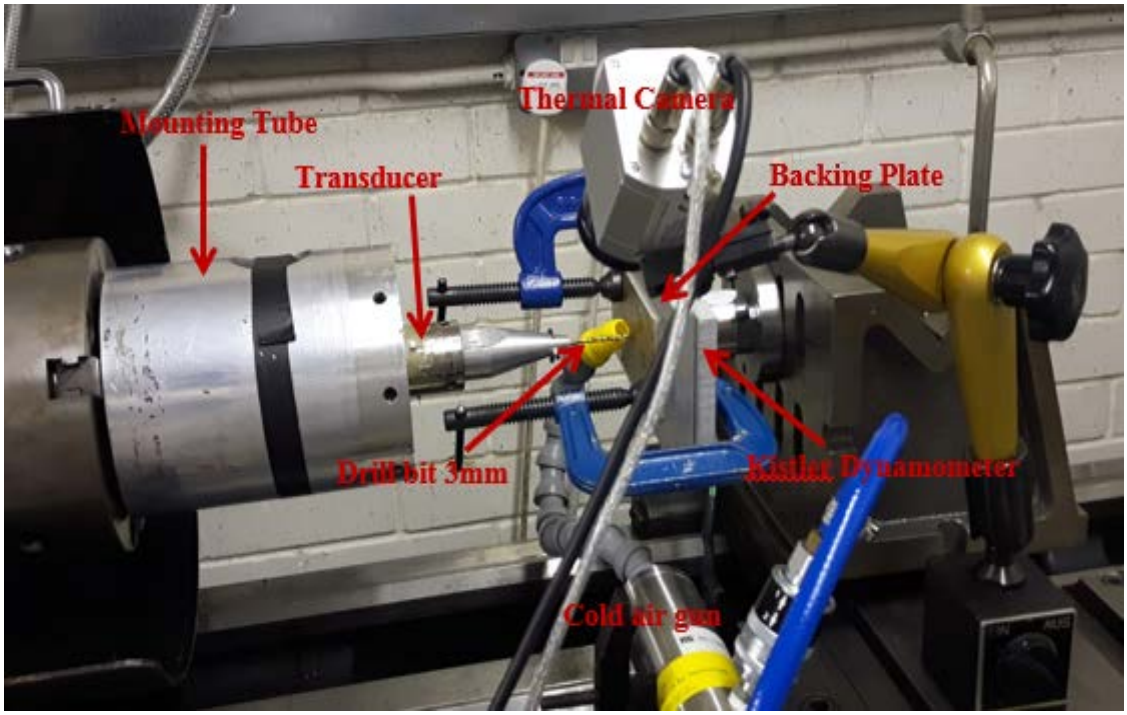

Figure 4.14(c): The full UAD (machining) experimental set-up showing the strategic positions of both thermal camera and cold air gun

4.3 summary

This chapter accounted for the properties and fabrication or manufacturing procedures of the hemp (HFRP/PCL and 19-HFRP/VE) and MTM 44-1 carbon (CFRP/EP) fibres-reinforced polymer composite specimens used as experimental workpieces. These properties included hemp fibre aspect ratios and mechanical properties of the specimens. In addition, this chapter further detailed all the experimental works conducted in this study, under three distinctive stages. Furthermore, fish bone diagram was employed to illustrate important inter-dependent process parameters of drilling operation which determine the quality of drilled holes. The methods, techniques and procedures (methodology) and machine centres, tools and equipment involved, as well as their experimental set-up and procedures have been explained.

Moreover, the SEM morphological analysis of the matrices (PCL and EP) was conducted, showing stronger fibre-matrix interfacial bond of CFRP/EP than HFRP/PCL composite specimens. Also, the thermogravimetric results of the two specimens were presented, depicting that CFRP specimen has a higher decomposition or disintegration temperatures than the HFRP specimen, and it has a greater glass transition than the HFRP specimen (Appendix C). Finally, the peculiarity of UAD technique in terms of drilling forces (thrust and torque) that necessitated its choice as well as its easy experimental set-up and procedures were discussed in comparison to the CD. A dry machining environment coupled with compressed air cooling system was applied during CD and UAD. The use of wet machining in form of liquid coolant was absolutely discouraged throughout this experimentation, because of the hydrophilicity of the FRP composite specimens, especially their fibres. Many instruments and measuring procedures were used to examine and analysis (instrumentations) the drilling-induced damage after these experiments. The next chapter (5) seeks to explain these instrumentations.

CHAPTER FIVE

INSTRUMENTATION

5.0 Introduction

This present chapter deals with the measurement of all concerned drilling parameters, drilling-induced damage and responses. Mainly, these involve measurement (instrumentation) of delamination, surface roughness, vibration amplitude, drilling forces (thrust and torque), tool-workpiece interface temperature, compressed air pressure (for cooling), to mention but a few. Instrumentation means the use or application of instruments for observation, measurement or control. Furthermore, damage characterisation, surface metrology, data conversion, processing and statistically presentations are much included in this chapter. It covers the names of different kinds of instruments used, their capacities, specifications, operating parameters, techniques and measuring procedures. Some mathematical expressions or equations used for the measurements, and operational or governing equations are stated. Concisely, stages 1 and 2 experiments have similar instrumentation, while stage 3 has a slight different instrumentation due to the application of UAD technique. Hence, instrumentation for stage 3 is hereby treated separately from stages 1 and 2.

5.1 Stages 1 & 2: Measurement of drilling-induced damage responses

The two main damage measured and analysed under stages 1 and 2 are delamination and surface roughness, in addition to others such as fibre-uncut, minimal burrs formation, matrix sintering (melting/burning) and fibre-uncut, crack, de-bonding, defects.

5.1.1 Delamination

The composite laminates drilling-induced and major damage known as delamination has been explained as the occurrence of failure at the inter-ply, whereby reinforced fibre plies or laminates or layers separate along their interfaces, either by peel-up (entrance) or push-out(exit) delamination (Durão et al., 2010; Liu et al., 2012; Ismail 2016b; Ismail

2016c), as illustrated in Figure 5.1. The measurement of the surface delamination was carried out considering the push-out type occurred at the exit of the drill only, has been reported that it has a greater effect (or value) than the peel-up type at the drill entry, irrespective of the drilling parameters (Shyha et al., 2010b; Khashaba et al., 2010a; Eneyew & Ramulu, 2014; Khashaba, 2004; Khashaba et al., 2010b**),** under the same material and drilling condition. Therefore, instrumentation of push-out delamination only was considered throughout this stages 1 and 2 experiments.

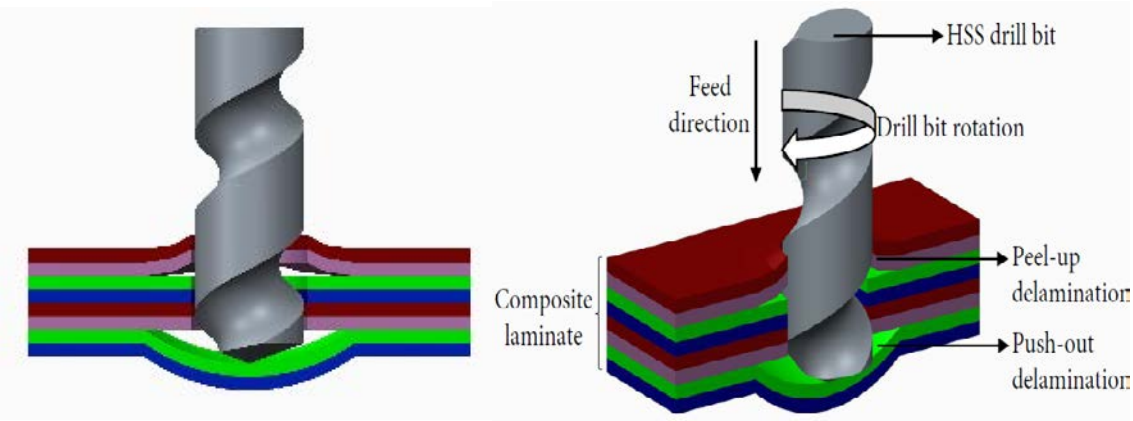

Figure 5.1: Peel-up and push-out delamination phenomena, showing their effects on the structural integrity and quality of the FRP composite laminate (Ismail et al., 2016c)

5.1.1.1 Measurement of delamination factor using optical microscope

The delamination drilling-induced damage around the circumference of a drilled hole remains a microscopic phenomenon. Therefore, the internal structure of the delaminated zone of the drilled holes of the FRP composite laminates were observed with the aid of the optical microscope (OM). An OLYMPUS BX 40 optical microscope with 25x magnification and 1.0 µm resolution was used to measure the delamination damage around the 5.0 mm drilled holes using Olympus DP software and Camera Leica Application Suite version 3.4.0, build 433, as depicted in Figure 5.2(a). The choice of the capacity of the lens used was based on the size of hole diameters that are necessary required to be analysed. The digital microscope was used to determine the longest diameter of delaminated zone. This

instrumentation (Figure 5.2b) is necessary in order to determine the delamination factor, which quantifies the magnitude of this damage.

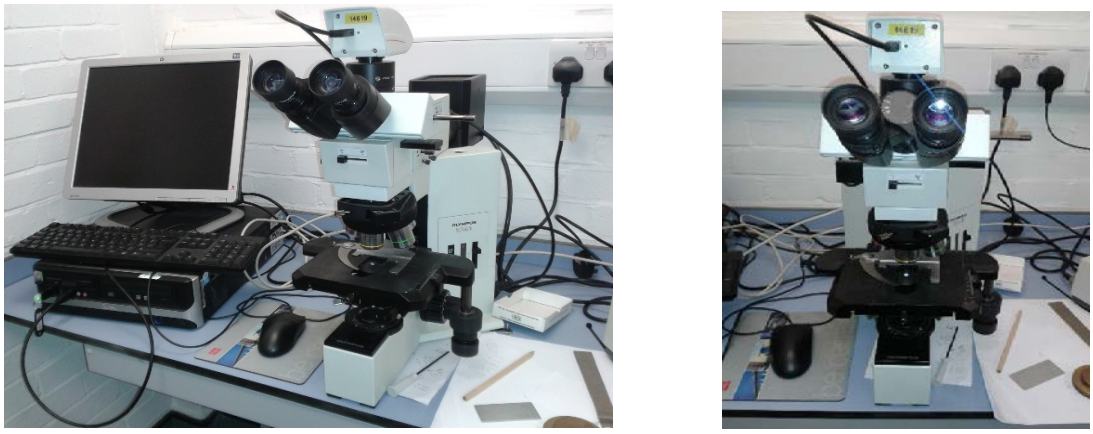

Figure 5.2(a): A typical OLYMPUS BX 40 computerised optical microscope

Figure 5.2(b): Set up showing measurement of delamination zone

The calibration of the microscopes was carefully carried out before the OM was used for the measurement (micro-graphing). Then, each of the drilled holes was mounted on the stand with the stage clip of the OM. Technically, the view was done using the eyepiece lens (ocular lens), and the objective lens was adjusted until the best sharp and clearest micrographic images were obtained, aided by the light and fitted camera (Figure 5.2b). The best images and data were captured and sent to the computer system connected to

(beside) the OM for further analysis, download or storage of the results obtained. Similarly, this process was repeated for all the concerned holes of the FRP specimen materials.

Moreover, in an attempt to further effectively detect, observe and characterise the drilling-induced damage such as surface integrity, delamination flaw, fibre-uncut and pull-out, on the FRP specimens, more non-destructive examination techniques were conducted. These include X-ray micro micro computed tomography (X-ray micro CT) and scanning electron microscopy (SEM).

5.1.1.2 Detection of delamination using X-ray micro computed tomography (X-ray micro CT) Scanner

Computed Tomography (CT) uses a single line of density data transferred during the X-ray micro bombardment to provide a shadow image in 3-D that helps in visualising the interior of a material whenever the X-ray micro is rotated in degrees (NDT, 2015). The X-ray micro CT is a non-destructive X-ray micro testing with three-dimensional visualisation of objects (Ketcham & Carlson, 2001), this digital process of defect detection creates images that allows variation, convenient, non-invasive analysis and are often easy to interpret by measuring X-ray micro as electric current and representing the images as a linear attenuate co-efficient (Xu et al., 2012). This information generated using attenuated X-ray micro slices are due to the beam hardening effect, the linear attenuation coefficient of the material changes as functions of material thickness and X-ray micro tube voltage (Kanno et al., 2015). Therefore, Van Geet, Swennen and Wevers (2000) described the linear attenuation co-efficient, μ using Equation (5.1).

$$\frac{I}{I_0} = \exp(-\mu h) \tag{5.1}$$

Where *I* and I_0 are intensity between attenuated and incident X-ray micros respectively, and μ is dependent on two predominant features which are the material photoelectric absorption and Compton scatter at voltage (energy) levels less than 200 kV. The features of a typical tomography system consists of two juxtaposed modules (an X-ray source and object holder module and a detector module) with a nominal spatial resolution of about

1000-2000x and an angular resolution of up to 0.5° (Kharfi, Yahiaoui & Boussahoul, 2015). This modern technology can do multiple slicing of image in axial and spiral scanning simultaneously within minimal time. The advantages of the CT include non-destructive and no specimen preparation is required for material testing. However, the major setback of this technology is the large data volume required for 3D visualisation. The visualisation technique comprises of physics, mathematical and computation techniques incorporated in an advance algorithm for quantification and analysis.

X-ray micro CT in material science and engineering is used within solid objects to understand information: 3D geometries and properties. This technique allows the object examination; understanding of the exact size, location and feature of the defect (delamination) present in the object internally. Few internal and inter-lamina delamination were observed. Therefore, the Nikon XT H 225 X-ray micro CT scanner used in this research work is shown in Figure 5.3(a) available in Materials Laboratory of University of Portsmouth, UK, with the inside part depicted in Figure 5.3(b).

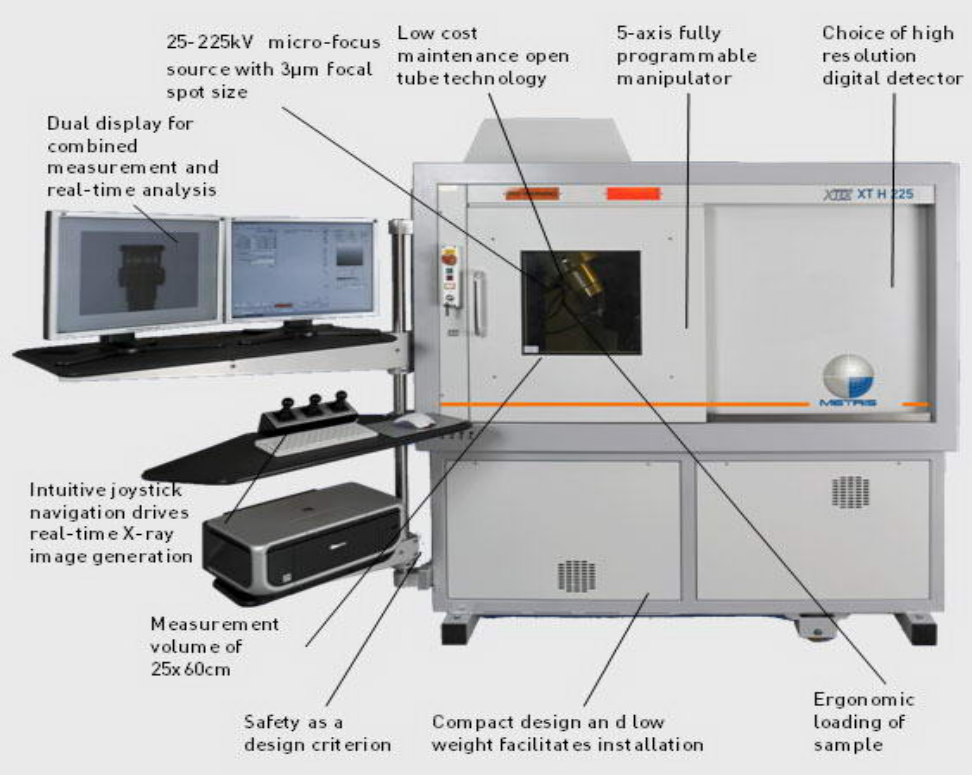

Figure 5.3(a): The XT H 225 X-ray micro CT Machine (Scanner)

This scanner has better advantages of rapid visual examination and in-depth analysis by X-ray micro and CT respectively, better resolution processing and digital imaging, high operational safety, production of an improved quality images and rapid data capture. It has a maximum capacity of 250 x 330 mm scan area with 160x and 400x geometric and system magnifications respectively.

Figure 5.3(b): Scanning FRP specimen with Metric XT H 225 Microfocus X-ray micro CT Scanner

Table 5.1: The scanning parameters used for the X-ray micro CT examination

Parameter	Magnitude	Unit
Current	178	µA
Exposure time per project	2000	ms
Scan time	33.33	min
Voxel size	920 x 965 x 416	μm^3
Energy (or voltage)	36	kV
Pixel size	0.02	mm
Resolution	22.981	µm
Angular increment	0.360 (360/1000)	degree
Scan size	21.1421 x 22.1763 x 9.5599	mm

The X-ray micro CT scanner was operated based on the scanning parameters expressed in Table 5.1. Also, the inter-lamina delamination micrographs obtained from the concerned specimens examined are hereafter presented and discussed in the under results and discussions chapter.

5.1.1.3 Analysis (or quantification) of delamination factor

The delamination factor is the ratio of the maximum diameter of the delamination zone, D_{max} to the drill diameter, D_o (Tsao & Hocheng, 2004; Davim & Reis, 2003b; Madhavan & Prabu, 2012; Bandhu et al., 2014; Ismail et al., 2015, Ismail et al., 2016a, Ismail et al., 2016c). Therefore, it (push-out delamination) was quantified by delamination factor, F_d, mathematically expressed in Equation (5.2):

$$F_d = \frac{D_{max}}{D_0} \tag{5.2}$$

Where F_d = Delamination factor;

D_{max} = Maximum delamination zone (mm); and

D_o (or D) = Drill bit diameters (5.0mm), as shown in Figure 5.4.

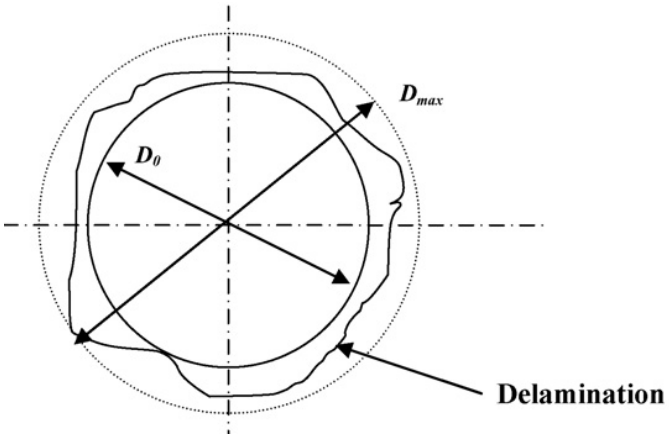

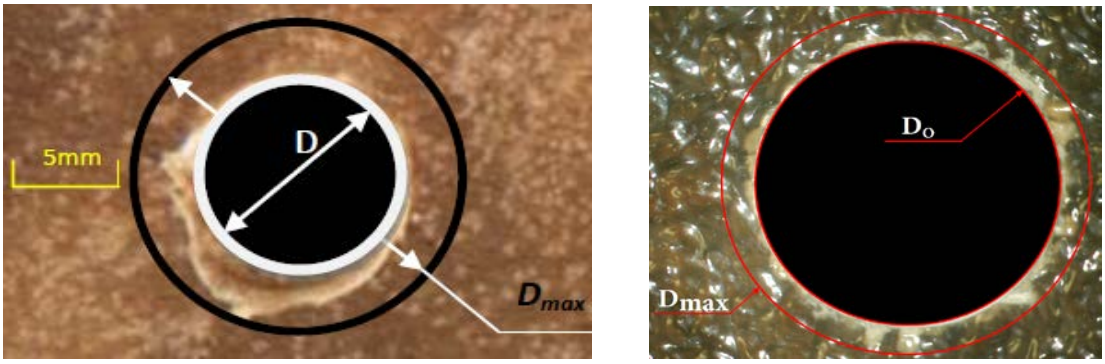

Figure 5.4: Determination of delamination factor (Ismail et al., 2016a & c)

Moreover, increasing delamination factor implies that the delamination effect is also increasing. The analysis of averages was performed after the readings were taken four times, with trials of the delamination factor before the average values as process outputs were calculated. The details of the results obtained are discussed under experimental results and discussion chapter.

5.1.2 Surface roughness

The surface roughness indicates the level of irregularity on the machined holes' circumferential walls. It is the degree of roughness on the circumferential walls of the drilled holes. Average surface roughness is the arithmetic mean of all the vertical deviations from the datum or reference line of the roughness contour (Bandhu et al., 2014). This is measured in standard unit, usually in microns (μm). During the instrumentation process, the average surface roughness, commonly denoted by R_a was adopted throughout this analysis.

5.1.2.1 Measurement of surface roughness using profilometer

The measurement of the roughness of the surface walls of all the drilled holes was performed using a profilometer; a Mitutoyo surface measuring instrument (Figure 5.5a), with SURF software having capacity and minimum surface length of 300.0 µm and 2.4 mm respectively. This software was able to measure the depth of the drilled hole since a specimen of 5.0 and 7.5 mm thickness each was considered. This instrument was properly calibrated before putting into use.

The surface roughness of the drilled 10.0 mm holes were measured. Figures 5.5(b) and (c) depict the magnitude of deviations of the roughness structure from the datum within the measured length, *l*. Surface roughness measurement was carried out along the direction of drilling at different locations which were axially parallel to the drill direction based on ANSI standard. These techniques were similarly used by Eneyew and Ramulu (2014). Analysis of averages, according to Equation (5.4), was used and readings were taken four times, with first trials of the surface roughness before the average values of other three actual readings as a process outputs were determined. Also, analysis of variance was carried out using IBM SPSS and Minitab 16 software to determine the drilling parameter that has the higher performance contribution and effect.

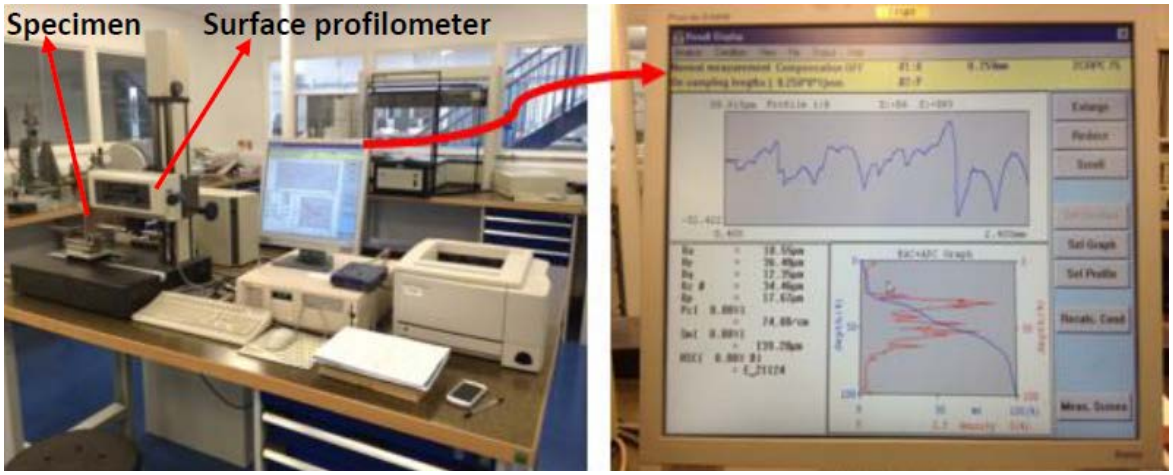

(a) Set-up **(b)** Readings

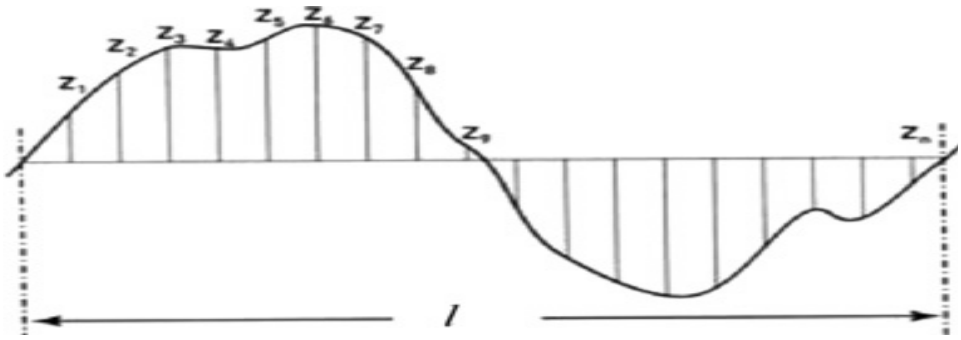

(c) Surface profile

Figure 5.5: Measurement of surface roughness using Mitutoyo Surface measuring instrument (Ismail et al., 2016c)

The surface profile and average surface roughness were measured, mathematically represented in Equations (5.3) and (5.4) respectively.

$$R_{a*} = \frac{1}{l}\left\{\int_0^l |z(x)|dx\right\} \quad (5.3)$$

$$R_a = \frac{1}{3}\sum_{j=2}^{3}|y_j| \quad (5.4)$$

Where R_{a*} = surface profile;

z(x) = y = measured roughness contour;

j =1 (for trial readings), 2, 3 & 4 (for actual readings);

R_a = arithmetical average surface roughness (µm);

and l = specimen measured length (mm).

5.1.2.2 Analysis of surface roughness using SEM

The use of SEM is necessary for deeper analysis, better and clearer micrographs as a result of its higher magnification capacity. The sectional view (two halves) of the drilled hole surfaces was obtained by cutting with the aid of the band saw cutting machine, as shown in Figure 5.6(a). This process was necessary in order to prepare the specimens for SEM examinations in an attempt to further study the surface conditions of the drilled holes of the concerned HFRP and CFRP composite specimens.

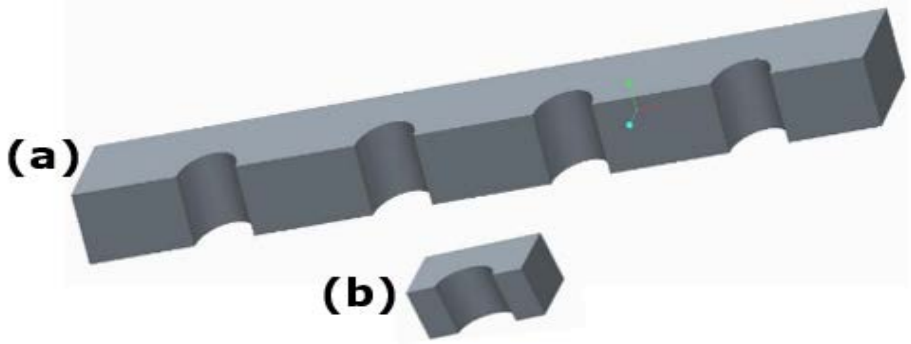

Figure 5.6 (i): The CAD drawings of the sectioned drilled holes of the specimens for SEM examination (Ismail et al., 2016c)

The specimens (Figure 5.6b) were prepared and mounted on the Scanning Electron Microscope stands, as shown in Figure 5.6(c) before (a) and after (b) SEM observations. The specimen preparation involved sputtering of the drilled hole surfaces of the specimens with an approximately 10 nm thick layer of platinum before scanning process commenced, for the conductivity of electrons during the SEM examination.

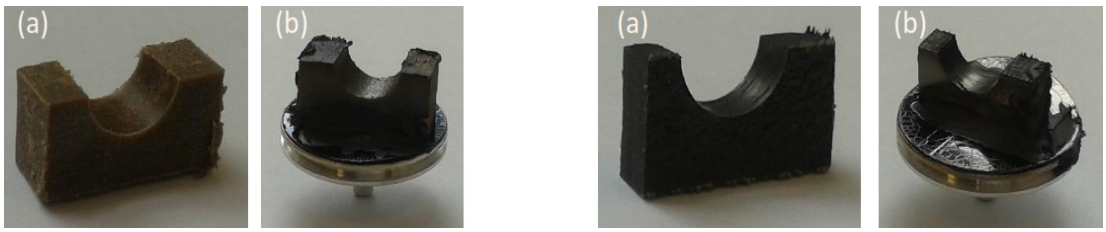

19/HFRP specimen MTM 44-1/CFRP specimen

Figure 5.6(ii): Method of preparing specimens showing specimens: (a) before and (b) after SEM Examinations

The JSM-6100 Scanning Electron Microscope (Figure 5.7), manufactured by JEOL Company, was used to examine the microstructure of the surfaces of the sectioned holes. The SEM machine has a highest magnification and resolution capacity as much as x100, 000 and up to approximately 40 A for imaging the areas of interest, respectively. Summarily, the parameters used for the SEM examination are summarised and presented in Table 5.2. SEM technique further revealed the micrographs of the damage areas, especially the crack propagation, cavity or void as a result of melted or burning matrix and fractured fibres. The micrographic results obtained are discussed later.

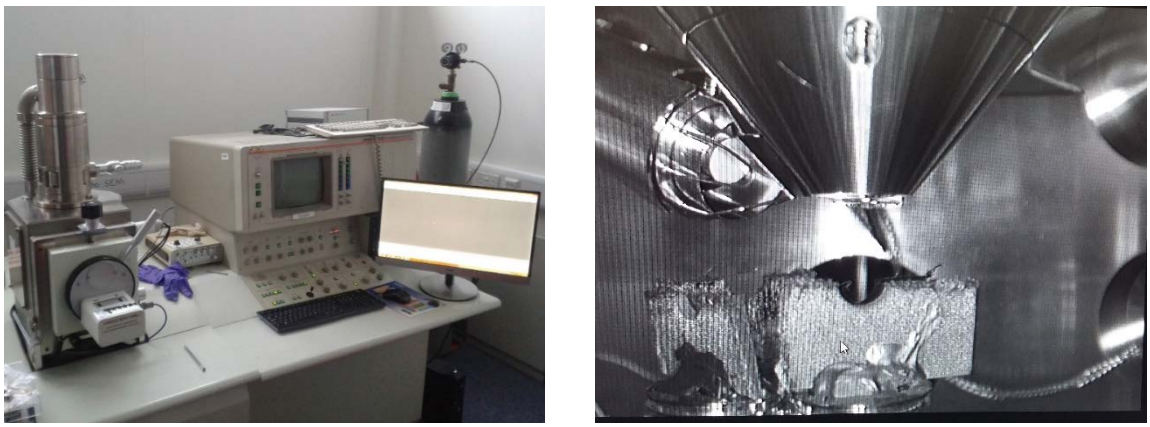

Before scanning During scanning

Figure 5.7: The JEOL JSM-6100 Scanning Electron Microscope

Table 5.2: The operational parameters used for the SEM examination

Parameter	Magnitude	Unit
Current	100	mA
Exposure time per scanning	1.30	min
Voltage	15	kV
Working distance (WD)	22-24	mm
Magnification	50 – 1000x	----
Speed	Slow 2000 (52.2%)	SE

5.2 Stage 3: Measurement of machining (drilling) responses

The application of the UAD technique resulted into the use of some special instruments. This has necessitated the measurement of the drilling responses, which is hereby discussed.

5.2.1 Measurement of vibration amplitude

The vibration amplitude of the tool in UAD was measured using Polytec^{TM} laser vibrometer (OFV-3001), as depicted in Figure 5.8, which was capable of measuring vibration at a velocity up to 10 m/s with the resolution of 0.08 µm/s. This process involved tuning the frequency and amplitude of the drill tip in free vibration. For UAD, the system was tuned at 37.9 kHz with the vibration amplitude of 3.7 µm peak-to-peak.

Figure 5.8: Polytec OFV 3001 vibrometer controller for higher accuracy measurement

5.2.2 Measurement of thrust force

A Kistler (9345b) Force link^{TM} (Figure 5.9) was attached to an angle plate on the cross-slide of the lathe machine. The thrust force and torque ranges up to 10 kN and 25 Nm during the drilling process. The force link had a high natural frequency of 41 kHz. The operating temperature ranges from -40 ^{o}C to 120 ^{o}C. The raw data acquired with the dynamometer via the attached Picoscope, was processed in Matlab, without filtering, to obtain average cutting forces and torques.

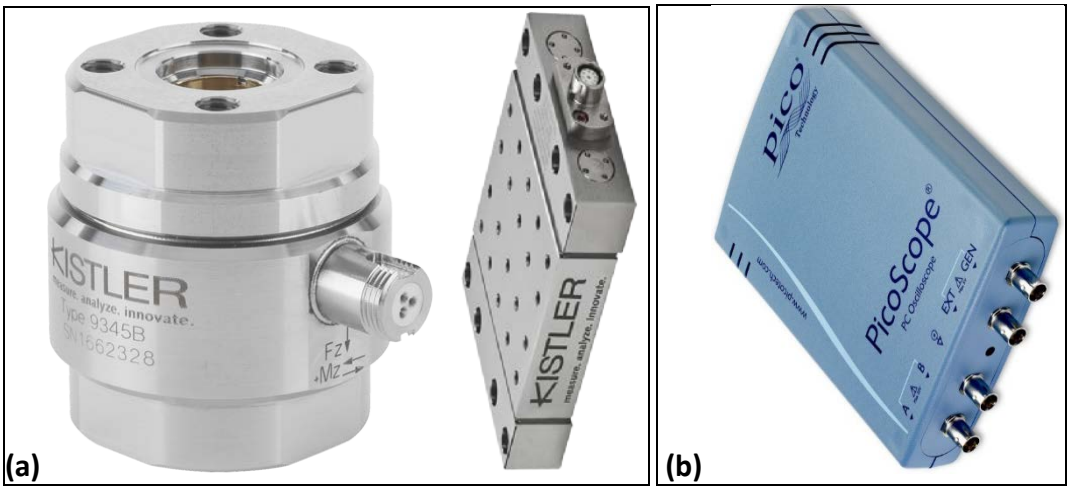

Figure 5.9: (a) A Kistler dynamometer and (b) Picoscope

5.2.3 Temperature measurement

Measurement of the drilling temperature was obtained from a thermal camera (MICRO-EPSILON thermoImager TIM 400), as depicted in Figure 5.10 during the drilling process in real-time. The thermal camera was calibrated using a K-type thermocouple to ensure accuracy of measurement, considering the FRP workpiece material and the setup including ambient lighting conditions. Measurements were analysed using software, namely TIM Connect. Also, the thermal decomposition temperature of the HFRP composite was measured by thermos-gravimetric method. This has been well explained in previous

chapter under sub-section 4.1.2.2 (Thermogravimetric analysis of the specimens).

Figure 5.10: A thermal camera (MICRO-EPSILON thermosImager TIM 400)

5.2.4 Cooling system

A vortex air gun Figure 5.11(a) was connected to the compressed air line using a regulator and gauge to measure the pressure of the air. This was ejected onto the work piece cutting zone and tip of drill bit through the nozzle of the air gun. This setup allowed for an efficient cooling system (Figure 5.11b), capable of maintaining temperature as low as 34 ^{o}C below compressed air temperature. Air cooling condition was adopted due to the hydrophilic nature of FRP composite materials, especially the bio-composites, and to prevent the structural integrity of the specimen.

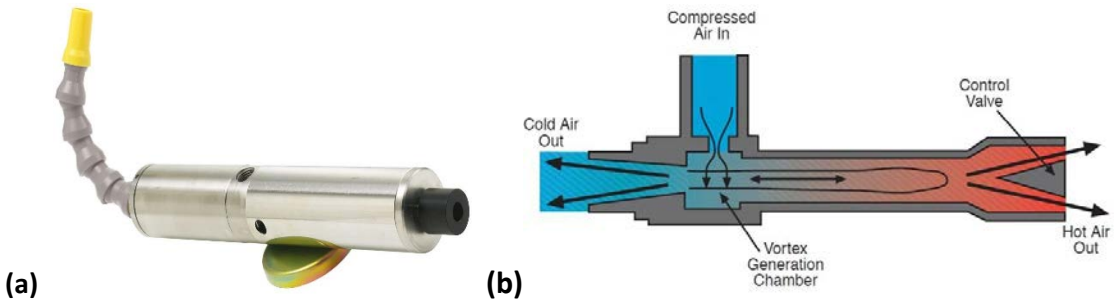

Figure 5.11: (a) A vortex air gun and (b) its cooling system

5.2.5 Damage characterisation

Principally, the drilling forces (thrust and torque) are measured and analysed within the scope of this experimental work in order to predict the possibility of occurrence of drilling-induced damage. For the reason that some of the critical damage, especially delamination and fibre pull-out are mainly caused by the thrust force and torque developed during FRP composite drilling (Ismail 2016b; Ismail 2017). Fibre pull-out was detected visually on each of the specimens after drilling exercise using an Alicona InfiniteFocus microscope (Figure 5.12). The micrographic results obtained are later shown and discussed under the chapter of results and discussion.

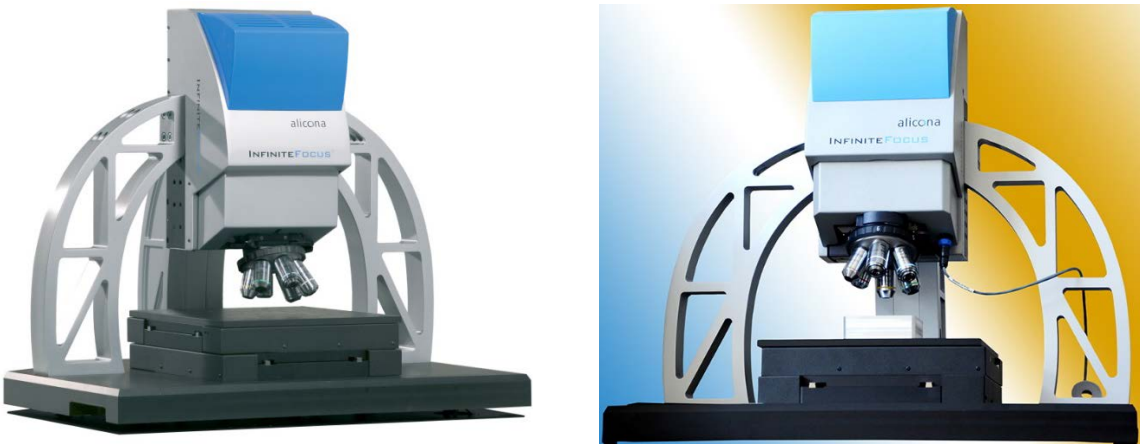

Figure 5.12: An Alicona InfiniteFocus microscope

5.2.6 Surface Metrology

The drilled holes were analysed to assess the quality of the drilling process. Metris LK Ultra 627134 coordinate measuring machine (CMM) with SP25 Ø1mm was used to measure the circularity of the hole and surface roughness of the hole. The test workpiece was place on the base-table of the CMM machine with the entry facing upward. Hole circularity were measured at three different depths of, 0.5mm, 2mm and 3mm from the entry surface of the hole. Similarly, the results obtained are later tabulated and discussed under the chapter of results and discussion.

5.3 Measurement of material removal rate using analytical approach

Practical measurement of material removal rate (MRR) was very difficult to carry out. Therefore, mathematical formulation was employed. The material (composite chips) removal rate model was developed starting from Equation (5.5).

$$N_i = \frac{1000V}{\pi D} \tag{5.5}$$

Where *N* = spindle revolution (rpm);

i = *D* = drills diameters (5.0 and 10.0mm);

V = cutting speed (m/min),

and π = a constant.

Therefore, the rate of the composite removal rate is calculated using the model formulated by Lee, Liu and Tarng (1998) for metal, as stated in Equation (5.6).

$$MRR = \frac{\pi D^2 f N_i}{4} \tag{5.6}$$

By substituting the value of N_i from Equation (5.5) into Equation (5.6) to obtain the results presented later, hence the MRR for the composites machining can be expressed as in Equation (5.7).

$$MRR = 250\ DfV \tag{5.7}$$

Where *f* = feed rate (mm/rev). The simulation results obtained are discussed under results and discussion chapter.

5.4 Summary

This chapter has firstly discussed measurement of drilling-induced damage for stages 1 and 2 experiments. These damage included delamination, surface roughness, fibre uncut and pull-out, crack, matrix melting, burr formation and dimensional inaccuracy (hole circularity or roundness). Calibration of all the instruments used was performed before

measurement began in order to avoid errors. Measurement and analysis of surface delamination flaw and delamination factor were conducted using optical, scanning electron microscopy and X-ray micro computed tomography for the internal inter-lamina delamination. Similarly, average surface roughness was measured and analysed using surface profilometer and scanning electron microscopy. Mathematical or analytical governing expressions for the measurement of these damage responses were stated with explanations.

Stage 3 experiment was likewise explained under measurements of vibration amplitude, thrust force, temperature, compressed air pressure, among other special UAD parameters and instruments used in addition to CD. Drilling-induced damage were well characterised and the surface metrology was explained. Lastly, material removal rate model was established for the measurement of the FRP composite specimen chips removed during drilling operation. Material removal rate was not easy to measure practically. This is the reason why analytical approach was adopted, because its effects on quality of drilled holes could never be overlooked. Therefore, other aspect of this research that requires detailed analytical models is hereby addressed in the next chapter six.

PART IV

ANALYTICAL APPROACH

CHAPTER SIX

ANALYTICAL APPROACH

6.0 Introduction

Due to the advantages of theoretical method of solving engineering problems, an analytical approach is used in this chapter to predict and analyse drilling-induced delamination damage on FRP composite laminate. The exact, accurate, cost and time-efficient solutions of an analytical models necessitate the choice of this approach among all other numerical and theoretical methods of solving problems. Therefore, this chapter chronologically discusses the process of model formulation, assumptions made and proposed analytical models for critical thrust force as well as the effects of drill bit geometry (mainly point and chisel edge angles) and feed rate on minimum critical thrust force below which ply exit or push-out delamination-free drilling of FRP composite is possible.

6.1 Thermo-mechanical modelling of FRP composite laminates drilling: Delamination damage analysis

Owing to inherent anisotropy and structural inhomogeneity in the FRP composite laminates (Chebbi, Wali & Dammak, 2016), drilling operation may cause delamination in the structural parts which in turns lowers the bearing strength and stiffness of the structure (Gururaja & Ramulu, 2009; Tagliaferri, Caprine, & Diterlizzi, 1990). This consequently impairs the load bearing capacity of the structure. In this context, exit-ply delamination has been identified as the most critical damage phenomenon for structural components (Gururaja & Ramulu, 2009; Saoudi, Zitoune, Gururaja, Mezlini, & Hajjaji, 2016). The drilling operation is performed by a cutting tool, commonly known as a drill bit. Drill bit, such as twist drill has a multi-cutting parts with different designed complex geometry (Ismail et al., 2016b). The geometric design of drills determines their efficiency and durability (tool life). Consequently, the total quality of the drilled holes depends on the geometry of the drill used. The geometric parts of drill include the point angle, chisel edge/angle, cutting lip (Heisel & Pfeifroth, 2012; Sambhav et al., 2012a; Paul et al., 2005;

Ahmadi & Savilov, 2015), helix angle, diameter, and web (Ismail et al., 2016b). The resultant effects of these parts are directly on the drilling variables or parameters. These parameters include, but are not limited to, drilling forces such as thrust force and torque (Feito, Diaz-Álvarez, López-Puente, & Miguélez, 2016), cutting force (Arola & Ramulu, 1997), cutting speed, feed rate (Ismail et al., 2016b), material removal rate (MRR) and depth of cut (Harris et al., 2003; Webb, 1993; Xiong et al., 2009). Among these variables, feed rate plays a crucial role in determining the quality of drilled holes of FRP composite laminates. It determines the magnitude of a thrust force during drilling operation; thrust force mainly depends on feed rate and chisel edge (Jain & Yang, 1993).

6.2 Rationale for the proposed model

To eliminate the problem of delamination in drilling, calculation of the critical thrust force below which no damage occurs is important. To achieve this, classical plate theory approach is employed and assumption of linear elastic fracture mechanics (LEFM) mode I is invoked to determine the amount of work required to initiate and cause propagation of delamination drilling-induced damage in the composite laminates (Gururaja & Ramulu, 2009; Karimi et al., 2016; Lachaud et al., 2001; Zhang et al., 2001; Saoudi et al., 2016; König et al., 1985; Upadhyay & Lyons, 1999; Timoshenko & Woinowsky-Krieger, 1959; Jones, 1975). In an attempt to simplify calculation of the critical thrust force, many analytical models in the literature focus more on the mechanics of the FRP composite laminates while ignoring the role of drill characteristics such as drill point geometry (drill diameter, rake angle, chisel edge angle), as illustrated in Figure 6.1, cutting mechanism,

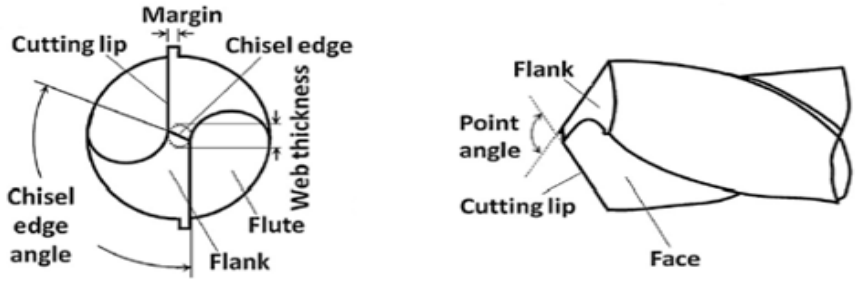

Figure 6.1: A twist drill bit showing its tip and geometry (Stephenson & Agapiou, 1996; Chao et al., 2009; Marinov, 2010; Ismail et al., 2016b; Ismail et al., 2017)

chip formation and cutting parameters such as feed rate, among others. In addition, the effect of machining temperature which may influence drilling damage is usually not accounted for. Properties of laminate composites are usually affected by high temperature (Ojo & Paggi, 2016a; Ojo & Paggi, 2016b) and since drilling operation is associated with thermo-mechanical deformation, a theoretical model which accounts for critical thrust force with thermal effect is desirable.

To improve the understanding of the influence of machining parameters on delamination drilling-induced damage and in line with the realities mentioned above, based on the works of Jain and Yang (1993) as well as Gururaja and Ramulu (2009), a new thermo-mechanical formulation for the prediction of minimum critical thrust force and feed rate for analysis of delamination in composite laminates is proposed. The current formulation accounts for the total thrust force by part contributions from the cutting lips and chisel edge of the drill using the principle of superposition.

The proposed model allows to analyse the effect of drill point angle on the critical values of the thrust force and feed rate. To determine the relationship between the feed rate and the thrust force, the general form of the model in Langella et al. (2005) is employed.

6.3 Model formulation

According to classical laminate theory, stress in the laminate k, as depicted in Figure 6.2 may be calculated using the relation:

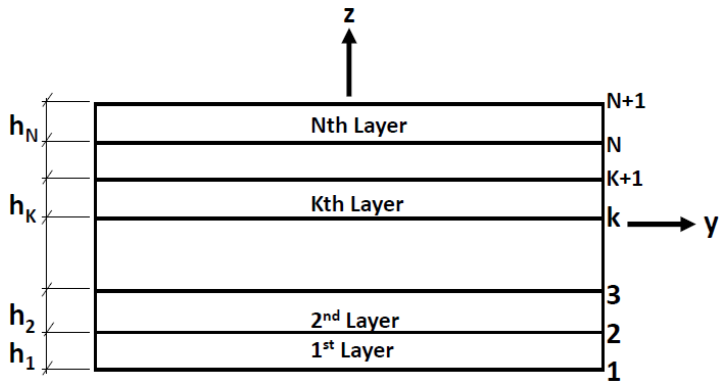

Figure 6.2: Laminate geometry (Ismail et al., 2017)

$$\begin{Bmatrix}\sigma_x\\ \sigma_y\\ \tau_{xy}\end{Bmatrix}=\begin{bmatrix}\underline{Q}_{11} & \underline{Q}_{12} & \underline{Q}_{16}\\ \underline{Q}_{12} & \underline{Q}_{22} & \underline{Q}_{26}\\ \underline{Q}_{16} & \underline{Q}_{26} & \underline{Q}_{66}\end{bmatrix}\left\{\begin{Bmatrix}{\epsilon^0}_x\\ {\epsilon^0}_y\\ {\gamma^0}_{xy}\end{Bmatrix}+z\begin{Bmatrix}k_x\\ k_y\\ k_{xy}\end{Bmatrix}-\begin{Bmatrix}\alpha_x\\ \alpha_y\\ 2\alpha_{xy}\end{Bmatrix}\theta(z)\right\}, \quad (6.1)$$

where $\underline{Q}_{ij}\ (i,j=1,2,6)$ are the elements of the transformed stiffness matrix and $\theta(z)$ is the temperature variation along the thickness. ${\epsilon^0}_i\ (i=x,\ y)$, ${\gamma^0}_{xy}$ and $k_i\ (i=x,\ y,xy)$ are the mid-plane strains and the curvatures of the ply which can be expressed as:

$$\begin{Bmatrix}{\epsilon^0}_x\\ {\epsilon^0}_y\\ {\gamma^0}_{xy}\end{Bmatrix}=\begin{Bmatrix}\frac{\partial u^0(x,y)}{\partial x}\\ \frac{\partial v^0(x,y)}{\partial x}\\ \frac{\partial u^0(x,y)}{\partial y}+\frac{\partial v^0(x,y)}{\partial x}\end{Bmatrix},\begin{Bmatrix}k_x\\ k_y\\ k_{xy}\end{Bmatrix}=\begin{Bmatrix}-\frac{\partial^2 w}{\partial x^2}\\ -\frac{\partial^2 w}{\partial y^2}\\ -2\frac{\partial^2 w}{\partial x\partial y}\end{Bmatrix}. \quad (6.2)$$

Here, u^0, v^0 and w are, respectively, the mid-plane displacements in the x and y directions and the deflection of the laminate ply. The resultant moments, according to classical Kirchhoff's assumption neglecting the mid-plane strains ${\epsilon^0}_x$, ${\epsilon^0}_y$ and ${\gamma^0}_{xy}$ are expressed as:

$$\begin{Bmatrix}M_x\\ M_y\\ M_{xy}\end{Bmatrix}=\begin{bmatrix}D_{11} & D_{12} & D_{16}\\ D_{12} & D_{22} & D_{26}\\ D_{16} & D_{26} & D_{66}\end{bmatrix}\begin{Bmatrix}k_x\\ k_y\\ k_{xy}\end{Bmatrix}-\begin{Bmatrix}{M_x}^T\\ {M_y}^T\\ {M_{xy}}^T\end{Bmatrix}, \quad (6.3)$$

Where elements of the bending stiffness matrix $[D]$ are given as:

$D_{ij}=\sum_{k=1}^{n}\left(\frac{{z_k}^3-{z_{k-1}}^3}{3}\right)\left({\underline{Q}_{ij}}^k\right)$.

If we assume a linear temperature variation through the thickness of the laminate as:

$$\theta(z)=\Delta T z\ , \quad (6.4)$$

then the thermal moments can be expressed as:

$$\begin{Bmatrix} {M_x}^T \\ {M_y}^T \\ {M_{xy}}^T \end{Bmatrix} = \Delta T \sum_{k=1}^{n} \left(\frac{{z_k}^3 - {z_{k-1}}^3}{3} \right) \begin{bmatrix} \underline{Q}_{11} & \underline{Q}_{12} & \underline{Q}_{16} \\ \underline{Q}_{12} & \underline{Q}_{22} & \underline{Q}_{26} \\ \underline{Q}_{16} & \underline{Q}_{26} & \underline{Q}_{66} \end{bmatrix} \begin{Bmatrix} \alpha_x \\ \alpha_y \\ 2\alpha_{xy} \end{Bmatrix} =$$

$$\Delta T \begin{bmatrix} D_{11} & D_{12} & D_{16} \\ D_{12} & D_{22} & D_{26} \\ D_{16} & D_{26} & D_{66} \end{bmatrix} \begin{Bmatrix} \alpha_x \\ \alpha_y \\ 2\alpha_{xy} \end{Bmatrix}. \tag{6.5}$$

Considering a general cross-ply laminates, the bending stiffness terms $\underline{Q}_{16}$, $\underline{Q}_{26}$ are zeros. So the constitutive relation (6.3) becomes:

$$\begin{Bmatrix} M_x \\ M_y \\ M_{xy} \end{Bmatrix} = \begin{bmatrix} D_{11} & D_{12} & 0 \\ D_{12} & D_{22} & 0 \\ 0 & 0 & D_{66} \end{bmatrix} \begin{Bmatrix} k_x \\ k_y \\ k_{xy} \end{Bmatrix} - \begin{Bmatrix} {M_x}^T \\ {M_y}^T \\ {M_{xy}}^T \end{Bmatrix}, \tag{6.6}$$

$$\begin{Bmatrix} {M_x}^T \\ {M_y}^T \\ {M_{xy}}^T \end{Bmatrix} = \Delta T \begin{bmatrix} D_{11} & D_{12} & 0 \\ D_{12} & D_{22} & 0 \\ 0 & 0 & D_{66} \end{bmatrix} \begin{Bmatrix} \alpha_x \\ \alpha_y \\ 2\alpha_{xy} \end{Bmatrix}, \tag{6.7}$$

Where α_x and α_y are coefficients of thermal expansion in the x and y directions respectively. These coefficients follow the same transformation laws as that followed by the strain vector. Accordingly,

$$\begin{Bmatrix} \alpha_x \\ \alpha_y \\ 2\alpha_{xy} \end{Bmatrix} = \begin{bmatrix} \cos\theta^2 & \sin\theta^2 & -2\sin\theta\cos\theta \\ \sin\theta^2 & \cos\theta^2 & 2\sin\theta\cos\theta \\ \sin\theta\cos\theta & -\sin\theta\cos\theta & \cos\theta^2 - \sin\theta^2 \end{bmatrix} \begin{Bmatrix} \alpha_1 \\ \alpha_2 \\ 0 \end{Bmatrix}. \tag{6.8}$$

α_1 and α_2 are the coefficient of thermal expansion in the longitudinal and transverse directions of the laminate ply. According to Schapery (1968), α_1 and α_2 can be expressed in terms of the matrix and fibre properties as:

$$\alpha_1 = \frac{\mathrm{E_f}\alpha_\mathrm{f}\mathrm{v_f} + \mathrm{E_m}\alpha_\mathrm{m}\mathrm{v_m}}{\mathrm{E_f}\mathrm{v_f} + \mathrm{E_m}\mathrm{v_m}}, \tag{6.9a}$$

$$\alpha_2 = (1 + v_\mathrm{f})\alpha_\mathrm{f}\mathrm{v_f} + (1 + v_\mathrm{m})\alpha_\mathrm{m}\mathrm{v_m} - \alpha_1(v_\mathrm{f}\mathrm{v_f} + v_\mathrm{m}\mathrm{v}_m), \tag{6.9b}$$

where $\mathrm{E_i}$, α_i, $\mathrm{v_i}$ and v_i $(\mathrm{i} = \mathrm{f}, \mathrm{m})$ are the modulus, coefficient of thermal expansion, volume fraction and Poisson's ratio of the fibre and matrix respectively.

The equilibrium equation for the thin composite plate is given as:

$$\frac{\partial^2 M_x}{\partial x^2} + 2\frac{\partial^2 M_{xy}}{\partial x \partial y} + \frac{\partial^2 M_y}{\partial y^2} + q = 0\,, \tag{6.10}$$

where $q = q_L$ is the uniformly distributed load from drilling operation and it is related to the thrust force P from the drilling machine by Zhang et al. (2001):

$$q_L = \frac{\eta P_L}{\pi a^2}, \qquad \eta = \frac{a}{b}\,. \tag{6.11}$$

P_L is the thrust force due to the distributed load, a and b denote the size of the elliptical delaminated zone along the major and minor axes as shown in Figure 6.3. Substituting the constitutive relation for moments in Equation (6.6) into the equilibrium Equation (6.10) gives:

$$-D_{11}\frac{\partial^4 w}{\partial x^4} - 2(D_{12} + 2D_{66})\frac{\partial^4 w}{\partial x^2 \partial y^2} - D_{22}\frac{\partial^4 w}{\partial y^4} - 4D_{16}\frac{\partial^4 w}{\partial x^3 \partial y} - 4D_{26}\frac{\partial^4 w}{\partial y^3 \partial y} + \frac{4\eta P_L}{\pi a^2} = 0 \tag{6.12}$$

According to Zhang et al. (2001), the boundary condition for the delamination zone is clamped i.e. $w = 0,$ at the elliptic boundary represented by the equation, as shown in Figure 6.3:

$$\frac{x^2}{a^2} + \frac{y^2}{b^2} - 1 = 0\,. \tag{6.13}$$

The solution which satisfy the boundary equation is given as (Timoshenko & Woinowsky-Krieger, 1959):

$$w = w_0\left(1 - \frac{x^2}{a^2} - \frac{y^2}{b^2}\right)^2\,, \tag{6.14}$$

where w_0 is a constant to be determined.

Substituting Equation (6.14) into Equation (6.12) gives:

$$D_{11}w_0 + \frac{2}{3}(D_{12} + 2D_{66})\eta^2 w_0 + D_{22}\eta^4 w_0 = \frac{a^2\eta P_L}{24\pi} \tag{6.15}$$

It follows from Equation (6.15) that:

$$w_0 = \frac{P_L a^2 \eta}{24\pi D^*}, \tag{6.16}$$

where $D^* = D_{11} + \frac{2}{3}(D_{12} + 2D_{66})\eta^2 + D_{22}\eta^4$.

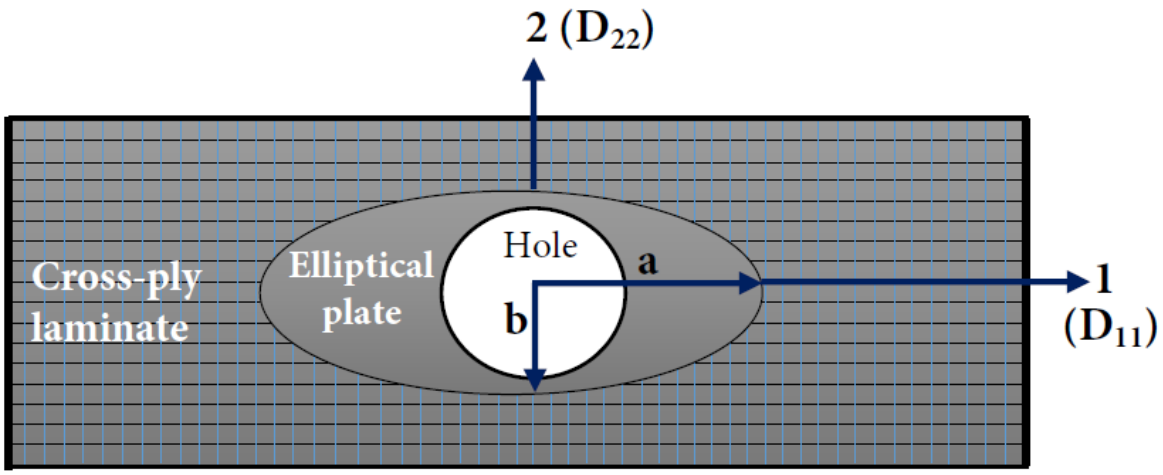

Figure 6.3: Delamination zone on a cross-ply laminate modelled as an elliptical plate (Ismail et al., 2017)

Equation (6.14) can now be rewritten as:

$$w = \frac{P_L a^2 \eta}{24\pi D^*}\left(1 - \frac{x^2}{a^2} - \frac{y^2}{b^2}\right)^2 . \tag{6.17}$$

w in Equation (6.17) is henceforth denoted as w_L to indicate deflection due to distributed load.

Based on the theorem of virtual work, the total energy balance equation for the propagation of delamination during drilling operation is expressed as:

$$\delta W = \delta U + \delta U_d , \tag{6.18}$$

where $\delta U_d = G_c \delta A$ is the energy absorbed due to delamination propagation. G is the strain energy release rate and δA is the infinitesimal increase in the delamination area given as:

$$\mathrm{d}A = 2\pi b \delta a . \tag{6.19}$$

δU is strain energy variation. The strain energy due to uniformly distributed load U_L is expressed as:

$$U_L = \frac{1}{2}\int \boldsymbol{\sigma}:\boldsymbol{\varepsilon}\,\mathrm{dV}\,, \tag{6.20}$$

Where

$$\boldsymbol{\varepsilon} = \begin{Bmatrix}\varepsilon_x\\ \varepsilon_y\\ \varepsilon_{xy}\end{Bmatrix} = \left\{ z\begin{Bmatrix}k_x\\ k_y\\ k_{xy}\end{Bmatrix} - z\begin{Bmatrix}\alpha_x\\ \alpha_y\\ \alpha_{xy}\end{Bmatrix}\Delta T\right\} \text{ and } = \begin{Bmatrix}\sigma_x\\ \sigma_y\\ \tau_{xy}\end{Bmatrix} = \begin{bmatrix}\underline{Q}_{11} & \underline{Q}_{12} & \underline{Q}_{16}\\ \underline{Q}_{12} & \underline{Q}_{22} & \underline{Q}_{26}\\ \underline{Q}_{16} & \underline{Q}_{26} & \underline{Q}_{66}\end{bmatrix}\begin{Bmatrix}\varepsilon_x\\ \varepsilon_y\\ \varepsilon_{xy}\end{Bmatrix}.$$

Expansion of Equation (6.20) leads to:

$$\begin{aligned} U_L = \frac{1}{2}\int_{-a}^{a}\int_{-b\sqrt{1-x^2/a^2}}^{b\sqrt{1-x^2/a^2}}\int_{-z}^{z}\Big[& z^2\underline{Q}_{11}\left(k_x{}^2 - 2k_x\alpha_x\Delta T + \alpha_x{}^2\Delta T^2\right)\\ & + +z^2\underline{Q}_{22}\left(k_y{}^2 - 2k_y\alpha_y\Delta T + \alpha_y{}^2\Delta T^2\right)\\ & + 2z^2\underline{Q}_{12}\left(k_yk_x - 2\left(k_y\alpha_y + k_x\alpha_x\right)\Delta T + \alpha_y\alpha_x\Delta T^2\right)\\ & + z^2\underline{Q}_{66}\left(k_{xy}{}^2 - 2k_{xy}\alpha_y\Delta T + \alpha_{xy}{}^2\Delta T^2\right)\\ & + 2z^2\underline{Q}_{16}\left(k_xk_{xy} - \left(k_x\alpha_{xy} + k_{xy}\alpha_x\right)\Delta T + \alpha_x\alpha_{xy}\Delta T^2\right)\\ & + 2z^2\underline{Q}_{26}\left(k_yk_{xy} - \left(k_y\alpha_{xy} + k_{xy}\alpha_y\right)\Delta T + \alpha_y\alpha_{xy}\Delta T^2\right)\Big]\,\mathrm{dV} \end{aligned} \tag{6.21}$$

Evaluating the integral term over the laminate thickness gives:

$$\begin{aligned} U_L = \frac{1}{2}\int_{-a}^{a}\int_{-b\sqrt{1-x^2/a^2}}^{b\sqrt{1-x^2/a^2}}\Big[& D_{11}\left(k_x{}^2 - 2k_x\alpha_x\Delta T + \alpha_x{}^2\Delta T^2\right)\\ & + D_{22}\left(k_y{}^2 - 2k_y\alpha_y\Delta T + \alpha_y{}^2\Delta T^2\right)\\ & + 2D_{12}\left(k_yk_x - 2\left(k_y\alpha_y + k_x\alpha_x\right)\Delta T + \alpha_y\alpha_x\Delta T^2\right)\\ & + D_{66}\left(k_{xy}{}^2 - 2k_{xy}\alpha_y\Delta T + \alpha_{xy}{}^2\Delta T^2\right)\\ & + 2D_{16}\left(k_xk_{xy} - \left(k_x\alpha_{xy} + k_{xy}\alpha_x\right)\Delta T + \alpha_x\alpha_{xy}\Delta T^2\right)\\ & + 2D_{26}\left(k_yk_{xy} - \left(k_y\alpha_{xy} + k_{xy}\alpha_y\right)\Delta T + \alpha_y\alpha_{xy}\Delta T^2\right)\Big]\,\mathrm{dS} \end{aligned}$$

(6.22)

Rearranging Equation (6.22) gives:

$$U_L = \frac{1}{2}\int_{-a}^{a}\int_{-b\sqrt{1-x^2/a^2}}^{b\sqrt{1-x^2/a^2}}\left[D_{11}{k_x}^2 + D_{22}{k_y}^2 + 2D_{12}k_yk_x + D_{66}{k_{xy}}^2 + 2D_{16}k_xk_{xy} + 2D_{26}k_yk_{xy}\right]\mathrm{dS}$$
$$-\frac{1}{2}\int_{-a}^{a}\int_{-b\sqrt{1-x^2/a^2}}^{b\sqrt{1-x^2/a^2}}\left[D_{11}k_x\alpha_x + D_{22}k_y\alpha_y + 2D_{12}\left(k_y\alpha_y + k_x\alpha_x\right) + D_{66}k_{xy}\alpha_{xy} + 2D_{16}\left(k_x\alpha_{xy} + k_{xy}\alpha_x\right) + 2D_{26}\left(k_y\alpha_{xy} + k_{xy}\alpha_y\right)\right]\Delta T\,\mathrm{dS}$$
$$+\frac{1}{2}\int_{-a}^{a}\int_{-b\sqrt{1-x^2/a^2}}^{b\sqrt{1-x^2/a^2}}\left[\overline{D}_{11} + \overline{D}_{22} + 2\overline{D}_{12} + 4\overline{D}_{16} + 4\overline{D}_{26} + 4\overline{D}_{66}\right]\Delta T^2\,\mathrm{dS}$$
$$= \frac{{P_L}^2\eta a^2}{144\pi D^*} + \frac{D'\pi a^2}{2\eta}$$

(6.23)

Where $D' = (\overline{D}_{11} + \overline{D}_{22} + 2\overline{D}_{12} + 4\overline{D}_{16} + 4\overline{D}_{26} + 4\overline{D}_{66})\Delta T^2$

$$\overline{D}_{ij} = \sum_{k=1}^{n}\left(\frac{{z_k}^3 - {z_{k-1}}^3}{3}\right)\left({\underline{Q}_{ij}}^k{\underline{\alpha}_i}^k{\underline{\alpha}_j}^k\right) \text{ for } i,j = 1,2,6 \quad (6.24)$$

6.3.1 Critical thrust force

To calculate the critical thrust force, the following assumptions are considered:

1. The uncut laminate under the drill bit exhibits an anisotropic nature.
2. The delamination zone around the exit drilled hole, with clamped boundary condition is considered elliptical.
3. Self-similar growth of the crack or inter-laminar delamination, hence the suitability of the application of LEFM approach.
4. The chisel edge force is modelled as a concentrated (point) load, while the cutting lip force is modelled as a uniformly distributed load.

The thrust force is a component of cutting (drilling) force along the drill bit axis. In accordance with Karimi et al. (2016), the total thrust force for the uncut ply is accounted for by part contributions from the chisel edge and the cutting lips of the drill, as detailed in Figure 6.4. Investigation shows in Won & Dharan (2002) that the chisel edge force has a greater contribution than the cutting lips and is hereby modelled as a concentrated (point) load q_c while the cutting edge is modelled as a uniformly distributed load q_L. The uniformly distributed load is considered, because the downward thrust force spread out over the chisel edge and it does not pass through the centre of the drill bit during the first phase of delamination and drilling operation as a point (concentrated) load. Also, the distributed load profile has a closer agreement with the experimental results (Gururaja & Ramulu, 2009). Since the linear elastic regime is considered, the total thrust force can be obtained using the law of superposition as:

$$P = P_c + P_L \,, \tag{6.25}$$

Where P_c and P_L are, respectively, thrust force contributions due to concentrated and distributed loads. Let us define a ratio to express the relationship between P_c and P_L as:

$$\alpha = \frac{P_c}{P_L} \quad , \qquad \text{for} \geq 0 \,. \tag{6.26}$$

Using the α parameter and considering Equation (6.25), the thrust forces P_c and P_L can be expressed as:

$$P_c = \left(\frac{\alpha}{1+\alpha}\right) P = \gamma P \,, \tag{6.27a}$$

$$P_L = \left(\frac{1}{1+\alpha}\right) P = (1-\gamma) P \,, \tag{6.27b}$$

Where $\gamma = \left(\frac{\alpha}{1+\alpha}\right)$ is the chisel edge ratio for $0 \leq \gamma \leq 1$.

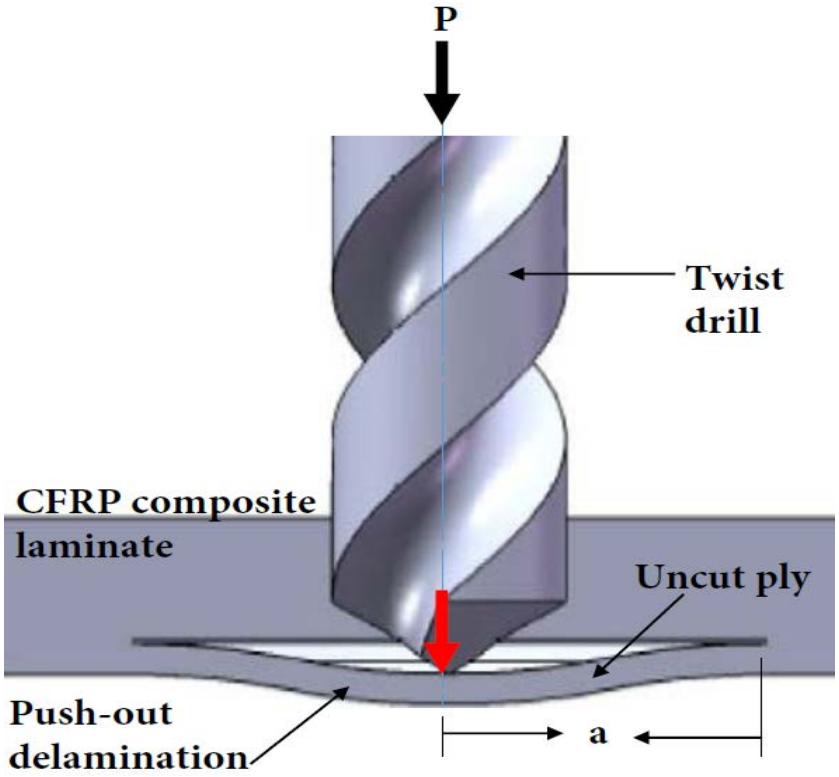

(a) Concentrated load on chisel edge

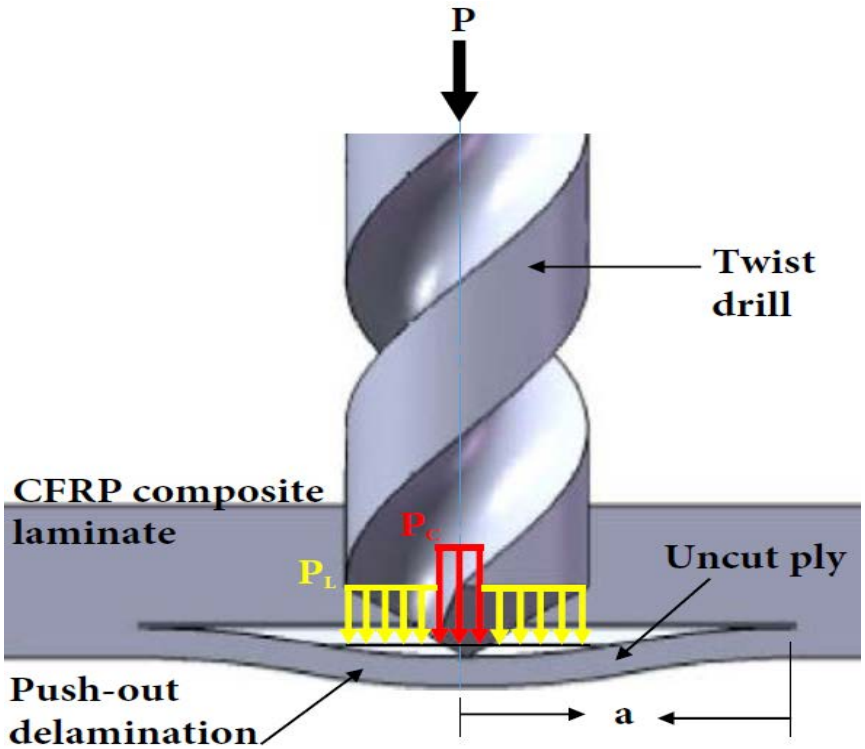

(b) Distributed loads on chisel edge and cutting lips.

Figure 6.4: Thrust force models (Ismail et al., 2017)

The strain energy derived based on superposition principle also involves part contributions from concentrated and uniformly distributed loads so that the total strain energy is given as:

$$U = U_c + U_L \, . \tag{6.28}$$

The expression for strain energy U_c due to concentrated load can be determined by repeating the same procedure as in Section 6.3 taking q in Equation (6.7) as $q_c = \frac{4\eta P_c}{\pi a^2}$. Accordingly, we get:

$$w_c = \frac{P_c a^2 \eta}{6\pi D^*}\left(1 - \frac{x^2}{a^2} - \frac{y^2}{b^2}\right)^2, \tag{6.29a}$$

$$U_c = \frac{{P_c}^2 \eta a^2}{9\pi D^*} + \frac{D'\pi a^2}{2\eta} \, . \tag{6.29b}$$

Substituting Equations (6.23) and (6.29b) in Equation (6.28) gives:

$$U = U_c + U_L = \frac{{P_c}^2 \eta a^2}{9\pi D^*} + \frac{{P_L}^2 \eta a^2}{144\pi D^*} + \frac{D'\pi a^2}{\eta} \, , \tag{6.30a}$$

$$U = \frac{P^2 \eta a^2}{72\pi D^*}(16\gamma^2 + (1-\gamma)^2) + \frac{D'\pi a^2}{\eta} \, . \tag{6.30b}$$

From Equation (6.18),

$$\delta U = \frac{\partial U}{\partial a}\delta a = \left(\frac{P^2 \eta a}{72\pi D^*}(16\gamma^2 + (1-\gamma)^2) + \frac{2D'\pi a}{\eta}\right)\delta a \, . \tag{6.31}$$

The virtual work of external loads corresponding to the work of distributed load q_L and concentrated load q_c may be expressed as:

$$W_L = \int_{-a}^{a}\int_{-b\sqrt{1-x^2/a^2}}^{b\sqrt{1-x^2/a^2}} q_L w_L \, dx\mathrm{d}y = \int_{-a}^{a}\int_{-b\sqrt{1-x^2/a^2}}^{b\sqrt{1-x^2/a^2}} \frac{\eta P_L}{\pi a^2}\frac{P_L a^2 \eta}{24\pi D^*}\left(1 - \frac{x^2}{a^2} - \frac{y^2}{b^2}\right)^2 dydx, \tag{6.32a}$$

$$W_c = P_c w_L(x = 0, y = 0) \, . \tag{6.32b}$$

Evaluating Equation (32) gives:

$$W_L = \frac{{P_L}^2 a^2 \eta}{72\pi D^*}, \tag{6.33a}$$

$$W_c = \frac{{P_c}^2 a^2 \eta}{6\pi D^*}. \tag{6.33b}$$

The total virtual work W is now expressed as:

$$W = W_C + W_L = \frac{P^2 a^2 \eta}{72\pi D^*}(12\gamma^2 + (1-\gamma)^2). \tag{6.34}$$

From Equation (6.18),

$$\delta W = \frac{\partial W}{\partial a}\delta a = \frac{P^2 a\eta}{36\pi D^*}(12\gamma^2 + (1-\gamma)^2)\delta a \quad . \tag{6.35}$$

Based on Equations (6.28)-(6.35), Equation (6.18) can now be evaluated as:

$$\frac{P^2 a\eta}{36\pi D^*}(12\gamma^2 + (1-\gamma)^2)\delta a = \left(\frac{P^2 \eta a}{72\pi D^*}(16\gamma^2 + (1-\gamma)^2) + \frac{2D'\pi a}{\eta}\right)\delta a + 2G\pi b\delta a \tag{6.36}$$

The critical thrust force can be obtained from Equation (6.36) as:

$$P^* = \frac{12\pi}{\eta}\sqrt{\frac{2D^*(D'+G_c)}{(16\gamma^2+2(1-\gamma)^2)}}. \tag{6.37}$$

According to Gururaja and Ramulu (2009), the minimum critical thrust force corresponds to a value of $\eta = (D_{11}/D_{22})^{\frac{1}{4}}$, as shown in Figure 6.3. With this realization, Equation (6.37) becomes:

$$P^* = 12\pi\left(\frac{D_{22}}{D_{11}}\right)^{\frac{1}{4}}\sqrt{\frac{2{D_c}^*(D'+G_c)}{(16\gamma^2+2(1-\gamma)^2)}}, \tag{6.38}$$

where ${D_c}^* = 2D_{11} + \frac{2}{3}(D_{12} + 2D_{66})\left(\frac{D_{11}}{D_{22}}\right)^{\frac{1}{2}}$.

Equation (6.38) gives the minimum critical thrust force below which delamination will not occur. Based on the model Equation (6.38), the total thrust force is bounded as a unit of the sum of P_L and P_c.

6.3.2 Effect of point angle (ε)

It is remarked here, according to Langella et al. (2005), that the point angle ε significantly affects the thrust force and analysis of total thrust force due to contributions of the cutting lips and the chisel edge shows that the risk of material damage during drilling increases proportionally to the feed rate and point angle. For a drill with an arbitrary point angle, Equation (6.25) becomes:

$$P(\varepsilon) = P_c(\varepsilon) + P_L(\varepsilon) \quad . \tag{6.39}$$

$P_c(\varepsilon)$ and $P_L(\varepsilon)$ according to Karimi et al. (2016) is given by:

$$P_L(\varepsilon) = \frac{k_L(\varepsilon)}{\exp(\alpha_L \gamma_L)} \sqrt{f} \quad , \tag{6.40a}$$

$$P_c(\varepsilon) = \frac{k_c(\varepsilon)}{\exp(\alpha_c \gamma_c)} \sqrt{f} \, . \tag{6.40b}$$

where γ_L and γ_c are the average rake angle and the chisel edge rake angle. k_L and k_c are parameters related to specific energies at the cutting lips and chisel edge respectively and can be determined by means of a single test described in (Langella et al., 2005).

$$\alpha_L = 1.089 \ln 10 = 2.51 \, . \tag{6.41}$$

With respect to the procedure described in Langella et al. (2005), it is remarked that the mechanistic model (6.40) is best suited for drills with 160º point angle. Using this as a reference point angle ε_0, Equation (6.39) can be rewritten as:

$$P(\varepsilon_0) = P_c(\varepsilon_0) + P_L(\varepsilon_0) \, . \tag{6.42}$$

Considering the relationship between chisel edge and cutting lips thrust forces and the total thrust force in Equation (6.27), the chisel edge and cutting lips thrust forces for a drill with an arbitrary point angle ε can be written in terms of the total thrust force P as:

$$P_c = \gamma^{\beta} P \,, \tag{6.43a}$$

$$P_L = \left(1 - \gamma^{\beta}\right) P \,, \tag{6.43b}$$

Where $\beta = \frac{\varepsilon}{\varepsilon_0}$ is the ratio between the arbitrary point angle ε and the reference point angle ε_0.

Given Equation (6.43), and repeating the procedure in Section 6.3.1, the equation for the critical thrust force is given as:

$$P^* = 12\pi \left(\frac{D_{22}}{D_{11}}\right)^{\frac{1}{4}} \sqrt{\frac{2{D_c}^*(D' + G_c)}{\left(16\gamma^{2\beta} + 2\left(1 - \gamma^{\beta}\right)^2\right)}} \,. \tag{6.44}$$

6.3.3 Feed rate

Feed rate plays a vital role in determining delamination. Thrust force is a function of feed rate. Therefore, emphasis must be placed on feed rate because it can be controlled as an input and independent drilling parameters, unlike thrust force. Since the total thrust force is a sum of contributions due to the cutting lips and the chisel edge, the relationship between the critical thrust force and the critical feed rate can be obtained based on Equations (6.39)-(6.40) and (6.43) as:

$$P^* = \frac{k_c}{\exp(\alpha_c \gamma_c)} \sqrt{f^*} + \frac{k_L}{\exp(\alpha_L \gamma_L)} \sqrt{f^*} \,. \tag{6.45}$$

Substituting for P^* in Equation (6.42), the critical feed rate is expressed as:

$$f^* = \frac{144\pi^2}{\varphi^2} \left(\frac{D_{22}}{D_{11}}\right)^{\frac{1}{2}} \left[\frac{2{D_c}^*(D' + G_c)}{\left(16\gamma^{2\beta} + 2\left(1 - \gamma^{\beta}\right)^2\right)}\right] , \tag{6.46}$$

Where $= \frac{k_c}{\exp(\alpha_c \gamma_c)} + \frac{k_L}{\exp(\alpha_L \gamma_L)}$.

6.4 Summary

Drilling operation plays an important role as a final process during assembly stage of manufacturing processes. Machining of fibre-reinforced polymer (FRP) composite laminates without drilling-induced delamination damage, as a main problem, remains a quest in the field of composite technology. Among other factors, thrust force and feed rate as well as twist drill bit chisel edge and point angle are the principal drilling and geometric responsible factors during thermo-mechanical deformation. Hence, in this chapter, an analytical thermo-mechanical model has been proposed to predict critical feed rate and critical thrust force at the onset of delamination crack on CFRP composite cross-ply laminates, using the principle of linear elastic fracture mechanics (LEFM), classical plate theory, cutting mechanics and energy conservation theory. The delamination zone (crack opening Mode I) was modelled as an elliptical plate. The advantages of this proposed model over the existing models in literature are that the influence of drill geometry (chisel edge and point angle) on push-out delamination were incorporated, and mixed loads condition were considered. The forces on chisel edges and cutting lips were modelled as a concentrated (point) and uniformly distributed loads, resulted into a better prediction. The model was validated with models in the literature and the results obtained, as discussed in the later part of the next chapter, show the flexibility of the proposed model to imitate the results of existing models.

PART V

RESULTS

&

DISCUSSIONS

CHAPTER SEVEN

RESULTS AND DISCUSSIONS

7.0 Introduction

This present chapter focuses on the results and discussion of both the experimentations and analytical approach. All the experimental works and theoretical results are sequentially presented and discussed. The raw data obtained are plotted using statistical software include, but are not limited to, Minitab 16, Matlab, Python, IBM SPSS, Microsoft Excel and analogue-digital converter. Also, the results obtained are divided into two phases A and B, namely: experimental and analytical works respectively. Phase A (experimental works) comprises three different stages, while second phase B hereby discusses the results of the proposed analytical models.

7.1 PHASE A: EXPERIMENTAL WORKS

The experimental aspect of this research involved three main stages. Stage 1 investigates the effects of drilling parameters (cutting speed and feed rate) and fibre aspect ratio on delamination and surface roughness of drilled holes of HF/PCL composite specimen. The optimised drilling parameters and specimen were obtained. Stage 2 involves the convectional drilling of optimised HF/PCL specimen with a reference to the CF/EP composite specimen. Lastly, stage 3 describes a comparative experiment on both HF/PCL and HF/VE composite specimens, using a dry conventional drilling (CD) and a novel ultrasonically-assisted drilling (UAD) techniques.

7.1.1 Stage 1: Effects of drilling parameters and aspect ratios on delamination and surface roughness of lignocellulosic HFRP composite laminates

Both drilling parameters (feed rate and cutting speed) and hemp fibre aspect ratios, AR (0, 19, 26, 30, 38) were variables considered in stage 1 to determine their influences on delamination and surface roughness damage of five different HFRP composite specimens, designated as specimens A-E respectively.

7.1.1.1 Influence of the drilling parameters on delamination factor

In order to have most effective tool and minimise delamination effect, HSS drill point angle 118^o was used, very close to 120^o used experimentally by Durão et al. (2010) and Kilickap (2010), been reported to be more efficient. Therefore, the results of delamination factors obtained from the HFRP specimens were evidently reduced due to the type of drill bit and related drilling parameters used, when compared with similar bio-composites and CFRP composites (Tsao & Hocheng, 2004; Davim & Reis, 2003a; Mišković & Koboević, 2011). Delamination factor increased from 1.0022 to 1.0456 across the five specimens, as shown in Table 7.1.

Table 7.1: Effects of drilling parameters on delamination of HFRP composite laminates

Test No	Cutting Speed, V(m/min)	Feed Rate, f(mm/rev)	Aspect Ratio (AR) 0	19	26	30	38
			Delamination Factor , F_d A	B	C	D	E
1	10	0.05	1.0046	1.0114	1.0154	1.0148	1.0154
2		0.10	1.0054	1.0108	1.0189	1.0166	1.0192
3		0.15	1.0062	1.0124	1.0198	1.0216	1.0310
4		0.20	1.0092	1.0128	1.0290	1.0422	1.0456
5	20	0.05	1.0040	1.0090	1.0136	1.0138	1.0150
6		0.10	1.0042	1.0119	1.0182	1.0186	1.0168
7		0.15	1.0052	1.0122	1.0211	1.0196	1.0284
8		0.20	1.0070	1.0133	1.0233	1.0396	1.0420
9	30	0.05	1.0036	1.0075	1.0118	1.0080	1.0148
10		0.10	1.0040	1.0092	1.0147	1.0158	1.0166
11		0.15	1.0058	1.0094	1.0159	1.0182	1.0306
12		0.20	1.0058	1.0079	1.0189	1.0234	1.0440
13	40	0.05	1.0022	1.0031	1.0051	1.0074	1.0150
14		0.10	1.0040	1.0038	1.0058	1.0090	1.0152
15		0.15	1.0044	1.0051	1.0090	1.0176	1.0270
16		0.20	1.0046	1.0056	1.0164	1.0190	1.0408

The effects of cutting speed, feed rate and aspect ratio on delamination factor are presented in sub-section 7.1-7.3, using the data in Table 7.1. Firstly, Figures 7.1-7.3 depict that an increase in cutting speed reduced the delamination factor, whereas increase in feed rate caused an increase in delamination factor, which is a close agreement with the results of Madhavan and Prabu (2012), Mohan et al. (2005), Liu et al. (2012), Naveen et al. (2012) and Gaitonde et al. (2008). Though, they did not consider the fibre AR. It was also noted that feed rate had greater influence on delamination when compared with cutting speed which is in agreement with the report of Liu et al. (2012), using analysis of variance method.

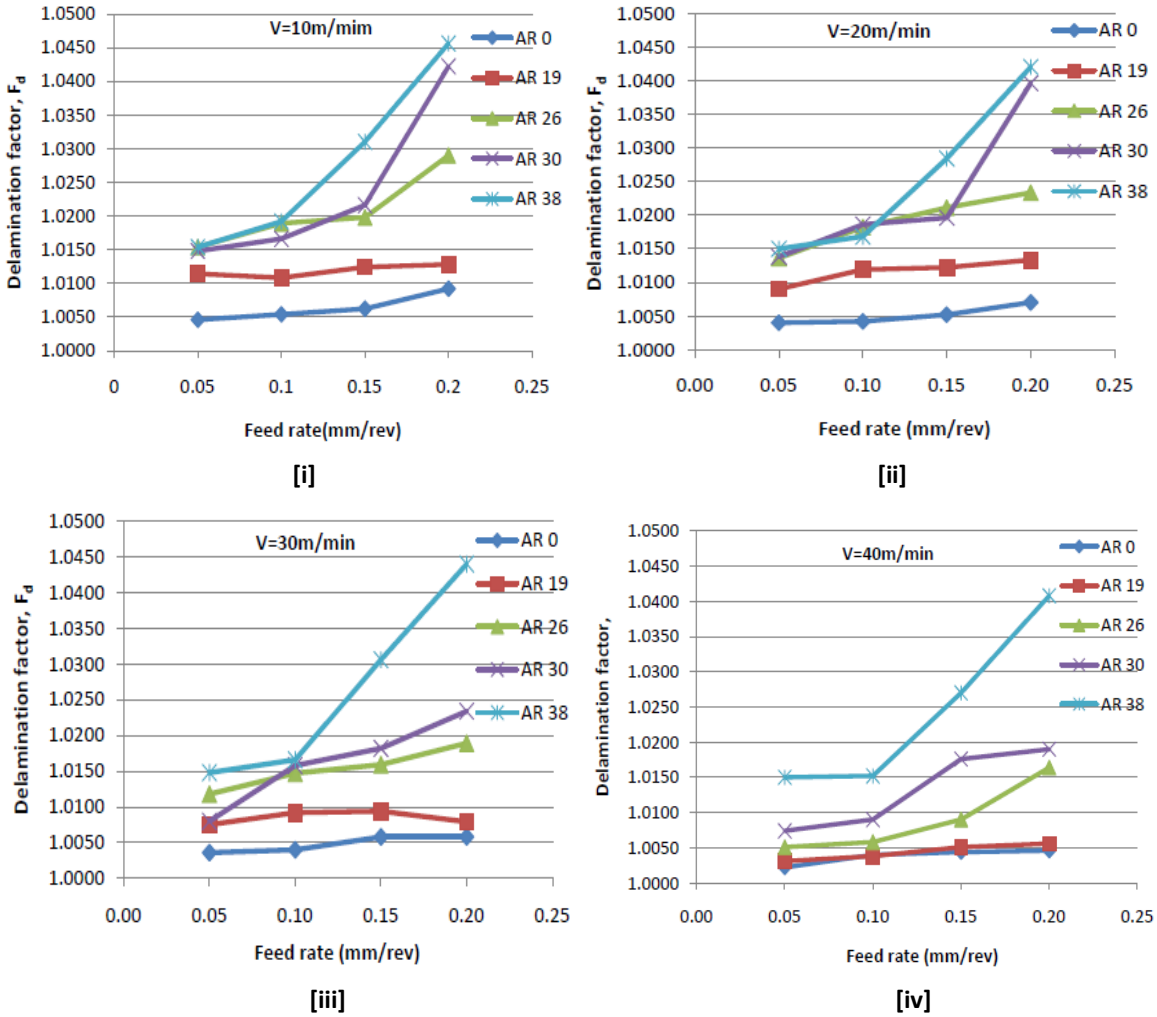

Figure 7.1: Effects of drilling parameters on delamination factor, showing that both increase in feed rate and decrease in cutting speed caused an increase in delamination factor

Furthermore, the responses of specimens A and B to delamination are very similar as the differences in their delamination factors were very close. This implies that they both responded slowly to the delamination when compared with both specimens D and E, which have a sharp response of delamination factor as the feed rate increased and cutting speed decreased. The specimen C has an average response to delamination effect. The specimen E has the highest values of delamination factor and aspect ratio. The variation in the responses of these specimens to delamination can be traced to the proportionality of their aspect ratios.

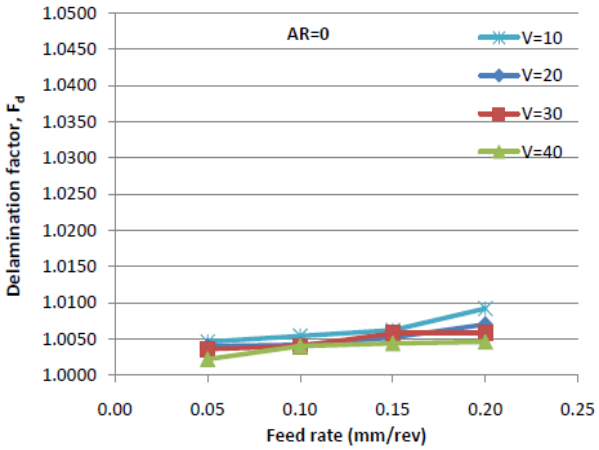

[A]

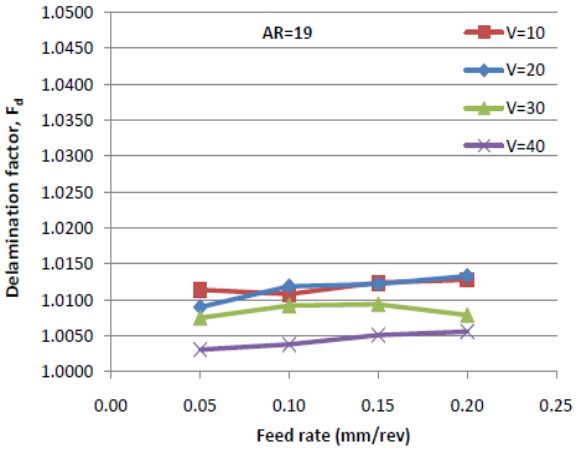

[B]

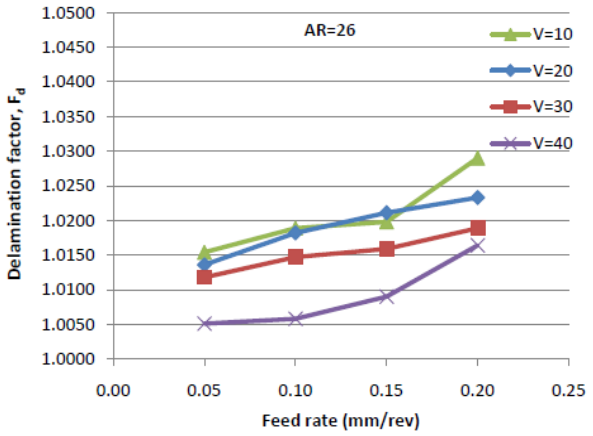

[C]

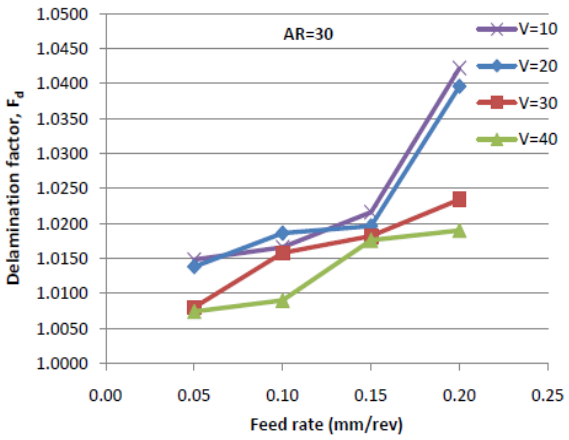

[D]

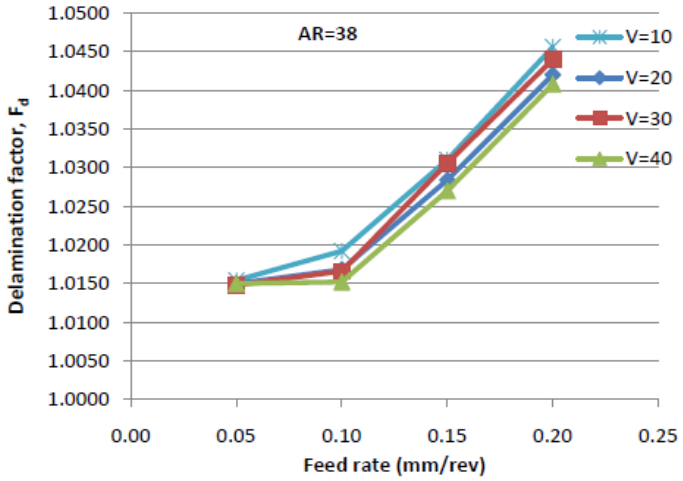

[E]

Figure 7.2: Effects of feed rate and aspect ratio on delamination factor, showing that delamination factor increased with both feed rate and aspect ratio

It was also observed that feed rate has greater influence on delamination when compared with cutting speed, as shown in specimen E with almost parallel graphs between two successive cutting speeds (Figure 7.3). Furthermore, specimens C, D and E clearly show the significant effects of the increased feed rate when compared with the first three specimens of similar response. This is indicated with the wide gap difference (scatter) in delamination factor at a certain cutting speed.

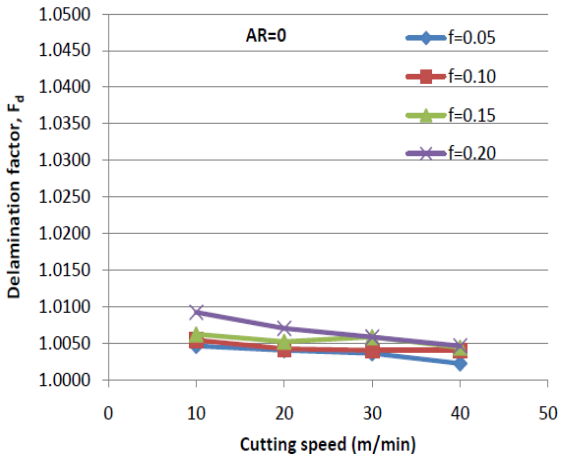

[A]

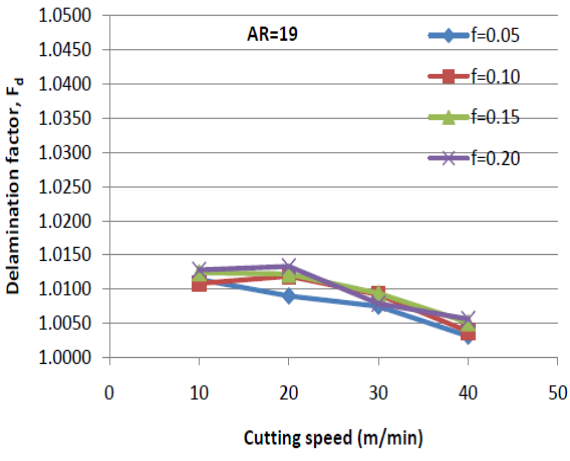

[B]

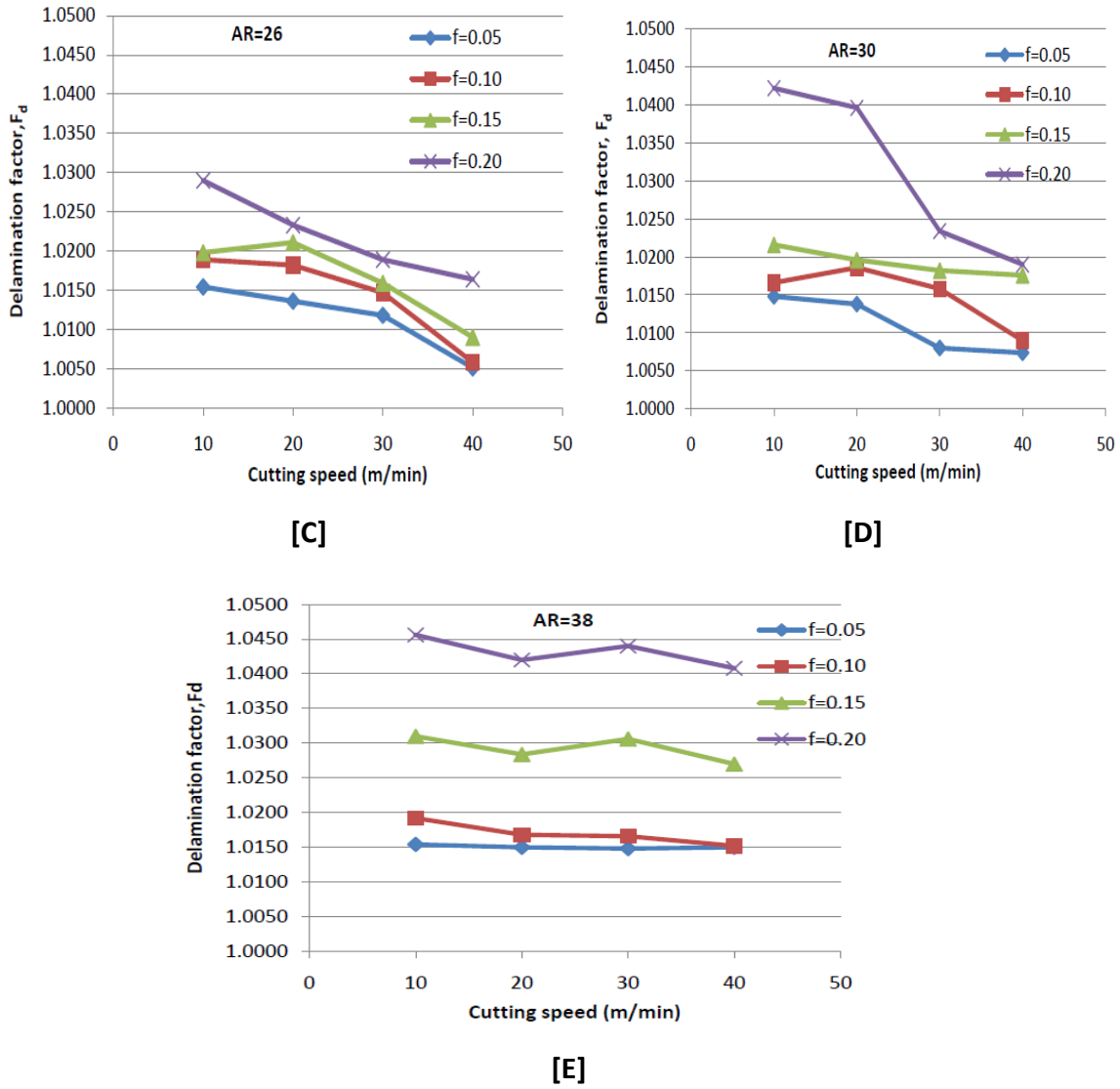

Figure 7.3: Effects of cutting speed and aspect ratio on delamination factor, showing that both increase in aspect ratio and decrease in cutting speed caused an increase in delamination factor (Ismail et al., 2016a)

7.1.1.2 Influence of the drilling parameters on surface roughness

Surface roughness, R_a has been explained as the average mean of the departures of the roughness profile from the mean line within the evaluation length. Surface roughness factor increased from 4.02 to 11.14 µm across the five specimens, as shown in Table 7.2.

Table 7.2: Effects of drilling parameters on surface roughness of HFRP composite laminates

Test No	Cutting Speed, V(m/min)	Feed Rate, f(mm/rev)	Aspect Ratio (AR)				
			0	19	26	30	38
			Surface Roughness , R_a (μm)				
			A	B	C	D	E
1	10	0.05	4.97	7.24	8.05	10.07	10.23
2		0.10	5.32	7.33	9.10	10.30	10.39
3		0.15	6.23	7.69	9.18	10.98	10.44
4		0.20	6.43	8.30	9.96	11.05	11.14
5	20	0.05	4.66	7.08	7.71	8.29	8.48
6		0.10	5.12	7.24	7.89	8.60	8.62
7		0.15	5.92	7.40	8.40	9.07	9.39
8		0.20	6.35	8.24	8.45	9.78	9.72
9	30	0.05	4.02	5.65	6.31	7.54	7.45
10		0.10	4.32	6.70	6.94	7.40	7.62
11		0.15	5.57	6.95	7.09	7.91	7.92
12		0.20	5.75	7.09	7.24	7.99	8.01
13	40	0.05	4.09	5.70	6.35	7.57	7.48
14		0.10	4.11	6.88	6.99	7.77	7.86
15		0.15	5.71	7.07	7.19	7.94	8.00
16		0.20	5.96	7.15	7.25	8.05	8.14

The R_a data obtained are presented in Figures 7.4 and 7.5. The relationship between surface roughness and cutting speed, at increasing feed rate and aspect ratio are illustrated in Figures 7.4 and 7.5. The results obtained show that R_a increased with an increase in feed unlike the cutting speed which has a smaller effect; R_a decreased with an increased cutting speed. In addition, the same Figures 7.4 and 7.5 show that at composites A with AR = 0 (neat; no reinforcement) has the lowest value of surface roughness at highest value of cutting speed and lowest value of feed rate. This trend increased along the five composite specimens, with laminate E having the highest surface roughness of 11.14 µm at lowest cutting speed of 10 m/min and highest feed rate of 0.20 mm/rev. Each of the

specimens has close response to surface roughness, but increased with an increasing aspect ratios as feed rate increased and cutting speed reduced.

These results are in close agreement with the results of Ogawa et al. (1997), Madhavan and Prabu (2012) and Rahman et al. (2009), though without influence of AR. Surface roughness increased with an increasing fibre AR. This increase was greater when compared with an increase of delamination with an increasing AR. This may be due to the fibre orientation and concentration within the area drilled and stylus measured length. At highest cutting speed, a small increase in R_a was observed across all the five drilled composite laminates, especially in D and E.

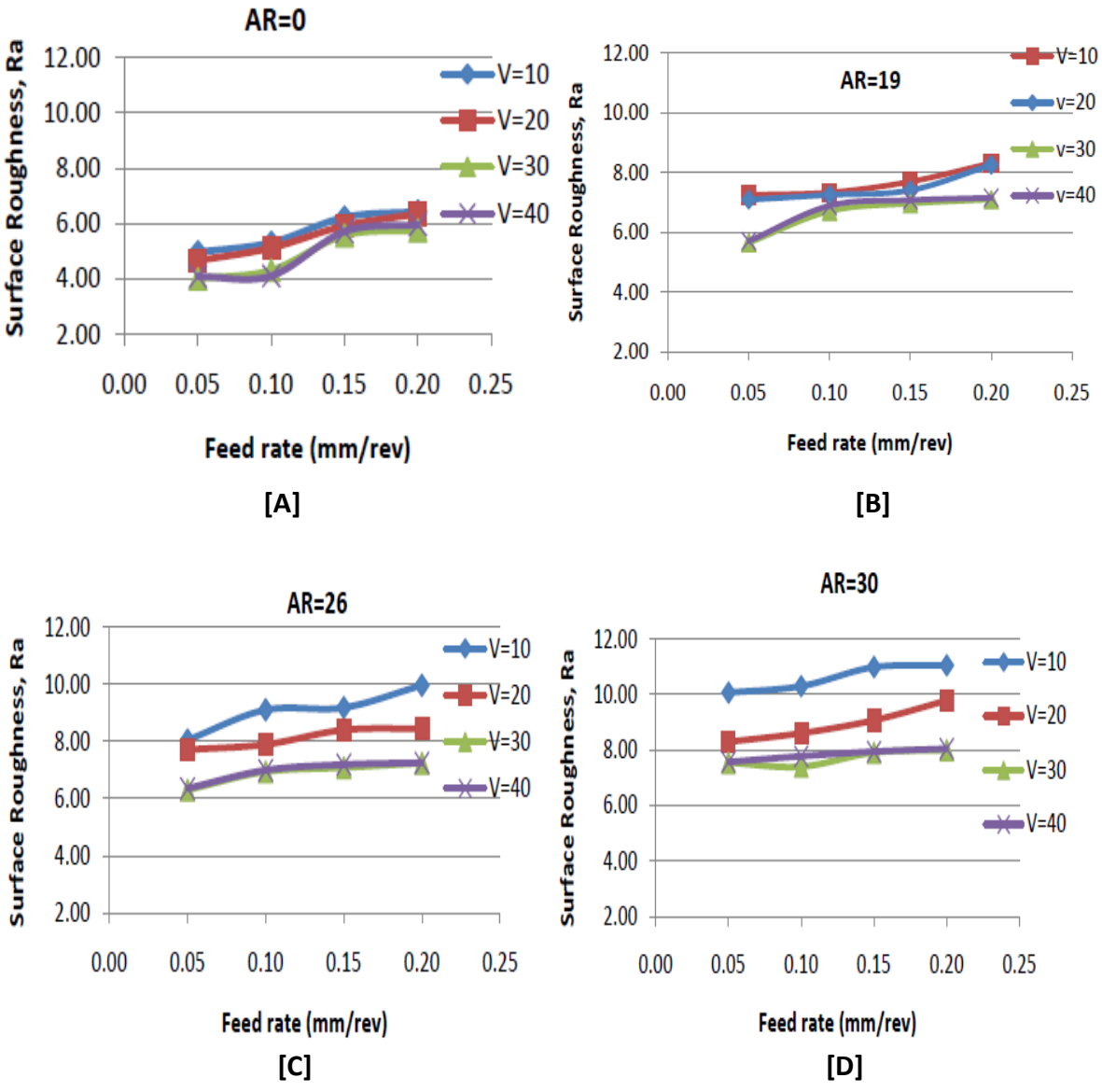

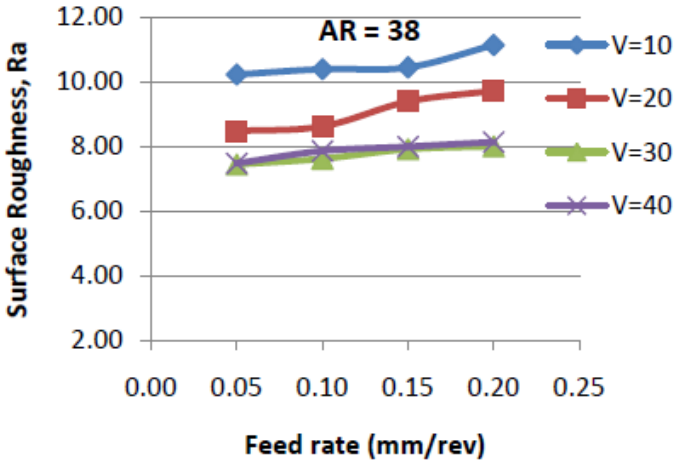

[E]

Figure 7.4: Effects of feed rate and aspect ratio on surface roughness, showing that surface roughness increases with both feed rate and feed rate

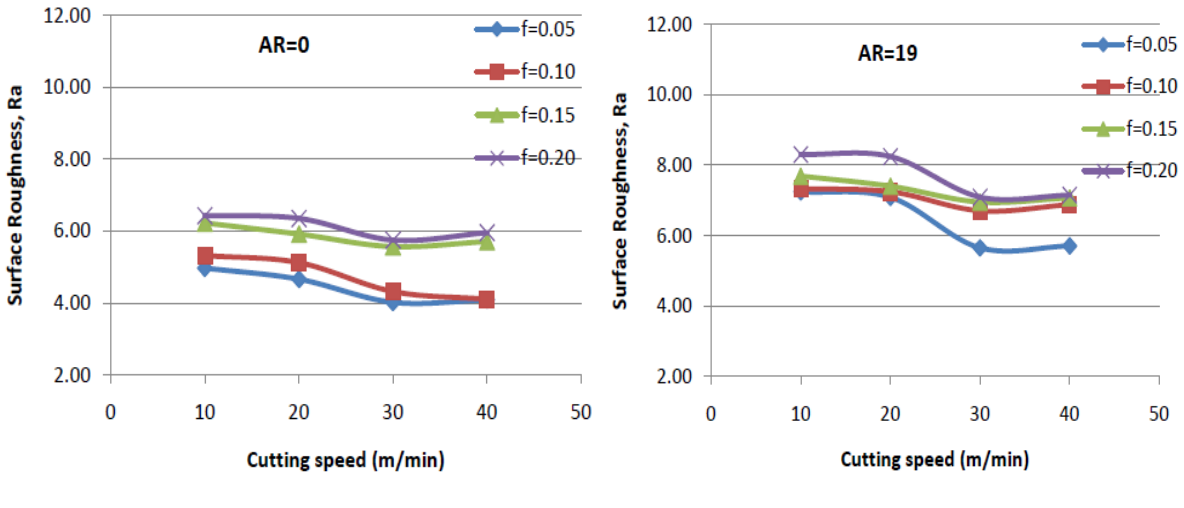

[A]

[B]

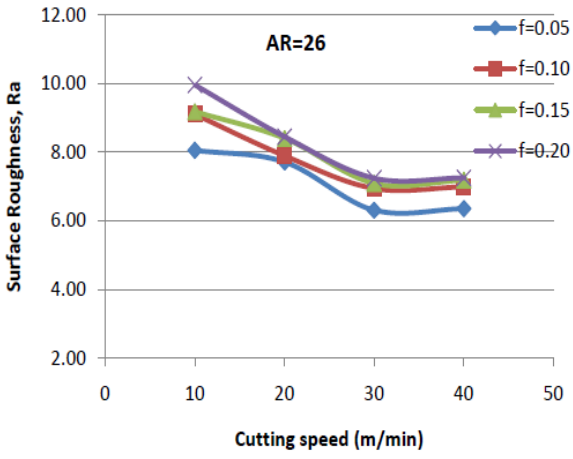

[C]

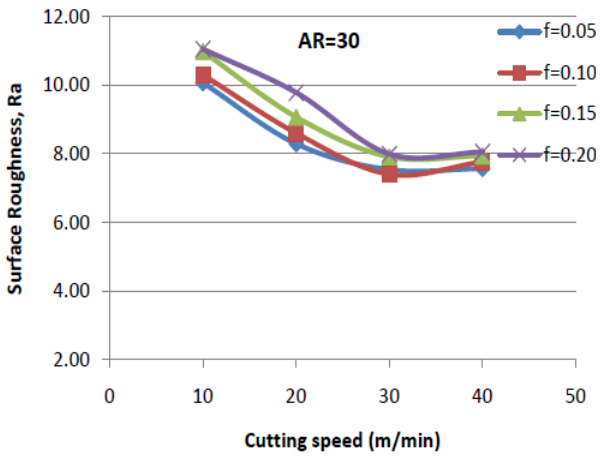

[D]

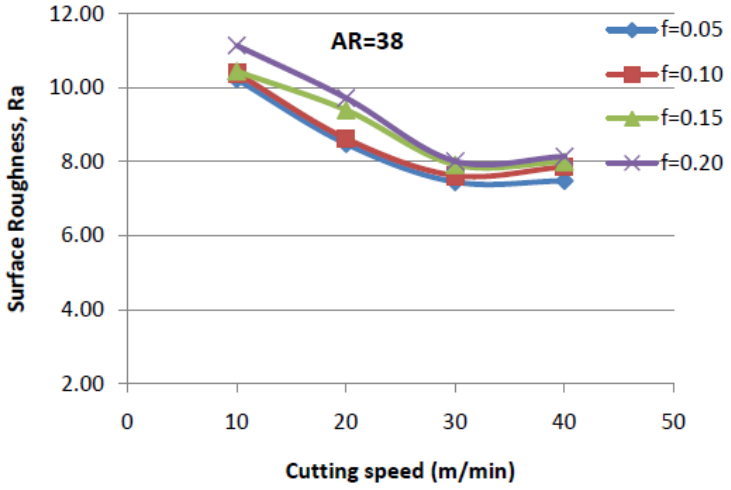

[E]

Figure 7.5: Effects of cutting speed and aspect ratio on surface roughness, showing that increase in aspect ratio and decrease in cutting speed caused an increase in surface roughness (Ismail et al., 2016a)

In addition, for further analysis, interpretation of data (results) and necessary decision making, a statistically based and objective decision making tool known as analysis of variance (ANOVA) technique was used. ANOVA detects variations in the mean performance of a set of factors considered in order to give validated and reliable conclusions from the analysis. Therefore, ANOVA was performed using 95.0 % confidence Interval and 2-way method, Minitab 16 and IBM SPSS software, as shown in Appendix E3. Before ANOVA analysis was performed, the normal distribution of all the data was checked and confirmed. The summary of the results is presented in Table 7.3., while detailed and other ANOVA results can be found in Appendices E4-E6. From Table 7.3, Feed rate, f has a greater maximum F-value of 669.83 on delamination factor, F_d versus 95.01 on surface roughness, R_a while cutting speed, v has a greater maximum F-value of 161.14 versus 58.35 on delamination. Importantly, it is clearly evident that the feed rate and cutting speed have a greater statistically contributions to the occurrence of delamination and surface roughness drilling-induced damage respectively. Also, the effect delamination was greater.

It was observed that the maximum F_d F-value of 669.83 occurred in specimen E, with highest AR of 38. At this value, specimen B (AR=19) has the lowest F_d value of 4.74. This implies that an increase in AR of hemp fibre resulted into an increase in F_d. Similarly, the

maximum R_a F-value of 161.14 occurred in same specimen E (AR = 38). At this value, same specimen B (AR=19) has the lowest R_a value of 14.23. This implies that an increase in AR of hemp fibre resulted into an increase in F_d , while the lower the AR of hemp fibre, the lower the R_a value. These results support or agree with the graphical results presented in Figures 7.1-7.5. Hence, due to the lowest values of both surface roughness and delamination drilling-induced damage responses at specimen B (AR = 19), specimen B (19-HFRP) composite specimen is hereby referred to as an optimal specimen.

Table 7.3: Summary of the ANOVA results of damage response for specimens A-E

Damage Response	Drilling parameter	ANOVA F-Value		P-Value
		Maximum	Minimum	
F_d	f	669.83	4.74	0.030
	v	58.35	4.85	0.028
R_a	f	95.01	11.67	0.002
	v	161.14	14.23	0.001

7.1.1.3 Influence of aspect ratio on delamination and surface roughness

The fibre aspect ratio is another factor that determines the delamination damage and surface roughness of the composite specimens. Figures 7.1 – 7.5, especially Figure 7.1 depict that an increase in aspect ratio caused an increase in delamination factor and surface roughness. The increase in delamination factor and surface roughness across the specimens depended on the ratio of their aspect ratios. The aspect ratio has no influence on delamination and surface roughness of specimen A, as a neat specimen. Therefore, the effects of both delamination and surface roughness damage responses were least and insignificant; almost negligible in case of delamination (Table 7.1). This trend increased with an increasing aspect ratio. Specimen E with highest value of aspect ratio has the maximum values of delamination factor and surface roughness. The increase in fibre aspect ratios caused a significant increase in both delamination factor and surface roughness, but an increase in surface roughness with an increasing fibre aspect ratio was found greater when compared with an increase in delamination with an increasing aspect ratio. This may be

due to the type of drill used, fibres orientation, dimension, concentration and matrix or inhomogeneous arrangement within a specific composite laminate, especially within the area drilled and stylus measured length (El-Sabbagh et al., 2014). In addition, the threshold fibre aspect ratio took place at 19, which is less than 20 (regarding as a low AR) according to El-Sabbagh et al. (2014). This implies that when drilling HFRP at cutting speed and feed rate above 20 m/min and 0.10 mm/rev respectively, to avoid greater delamination effect and surface roughness, the choice of the aspect ratio of the HFRP should be below 19.

7.1.1.4 Other drilling-induced damage (fibre-uncut, fibre pull-out and burrs formation)

Few uncut fibre and fibre pull out were observed in 5.0 mm holes especially at feed rates of 0.05 and 0.10 mm/rev with cutting speeds of 10 and 20 m/min respectively. Also, minimal burrs occurred at the entrance of the 10.0 mm holes at feed rate of 0.05 mm/rev with 30 and 40 m/min cutting speeds.

7.1.1.5 Chips formation and morphology

Short and melted chips formed at lowest feed rate and cutting speed, as depicted in Figure 7.6(a). Meanwhile, continuous ribbon-like chips formed at 0.20 mm/rev and 40 m/min feed rate and cutting speed respectively (Figure 7b); the higher the feed rate and cutting speed, the wider, longer and lighter the chips.

(a)  **(b)** 

Figure 7.6: Chips morphology showing melted chips at (a) f = 0.05 mm/rev & v = 10 m/mm and ribbon-like chips at (b) f = 0.20 mm/rev & v = 40 m/mm (Ismail et al., 2016a)

Almost no wear land was observed in the flank surface of the drill due to the nature of the composite and moderate cutting parameters used.

7.1.2: Stage 2: Comprehensive study on machinability of sustainable and conventional fibre reinforced polymer composites

In this stage 2 of the experimental work, the optimal 19-HFRP/PCL composite specimen was selected and subjected to further analysis using MTM 44-1 CFRP/EP composite specimen as a reference specimen under the same conventional drilling technique, parameters and conditions. These specimens are simply referred to as HFRP and CFRP composite specimens. This stage aimed at considering the degree of differences and similarities in damage responses, mainly delamination and surface roughness, between these HFRP and CFRP composite specimens. Later in this same stage 2, the effects of material removal rate (MRR) using two different diameters 5.0 and 10.0 mm in addition to drilling parameters (feed rate and cutting speed) were investigated.

7.1.2.1 Evolution and effects of drilling (thrust) force

The drilling force, mainly thrust, induced by the twist drill bit on the composite specimens was noted during the conventional drilling technique used with a different drilling parameters, as earlier discussed under experimentation. The complete evolution of the process is depicted in Figure 7.7; illustrating thrust force profile, and characterised by six distinctive main drilling operational steps.

Step 1: At inception, the thrust force increased drastically because of the increasing force required by the twist drill bit to gain the initial contact and entry into the composite (specimen), immediately after the penetration of the chisel edge and the point angle of the drill bit into the composite specimen. There was a gradual increase in the contact length between the composite laminate and the cutting edges. Later, the engaged radius increased from initial zero to the drill bit radius. The developed thrust force during penetration depended on the engaged radius. The step 1 is sometimes characterised with

peel-up type of delamination (Figure 7.8), caused by the rapid increased force and tool-composite interface temperature (Ismail et al., 2016a; Ismail et al., 2016b).

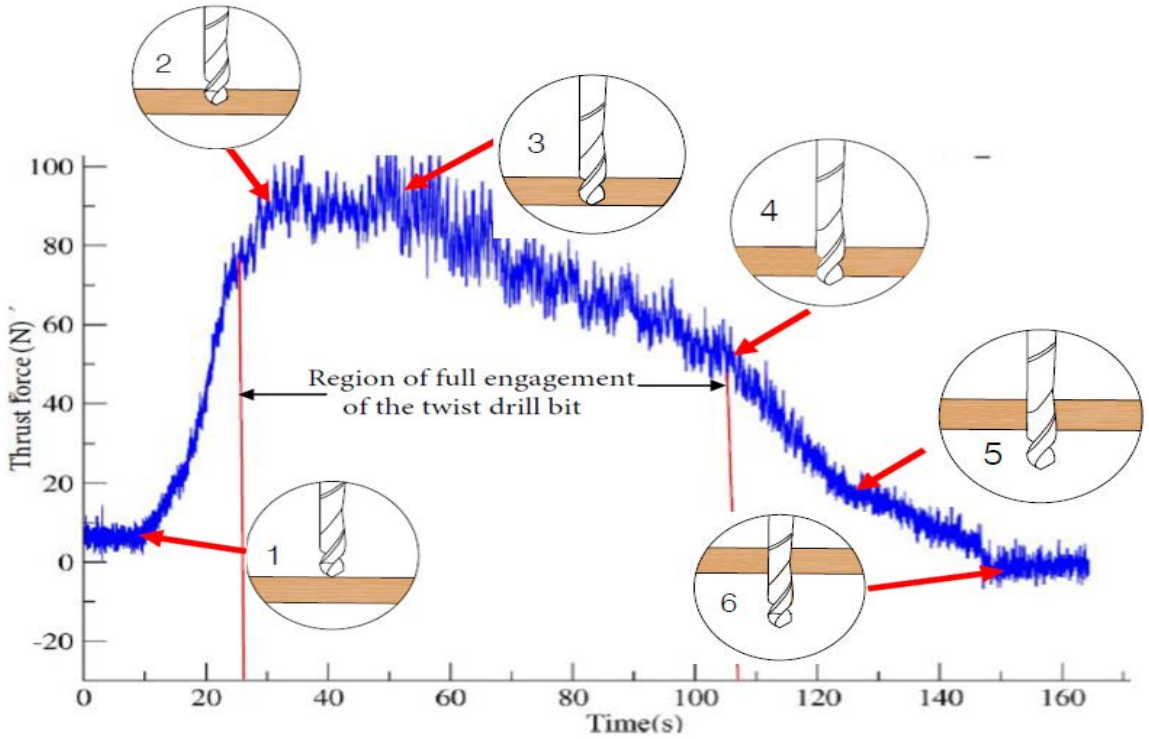

Figure 7.7: Phenomenal penetration of the drill bit showing the interaction between the thrust force and time during drilling operation or evolution (Ismail et al., 2016c)

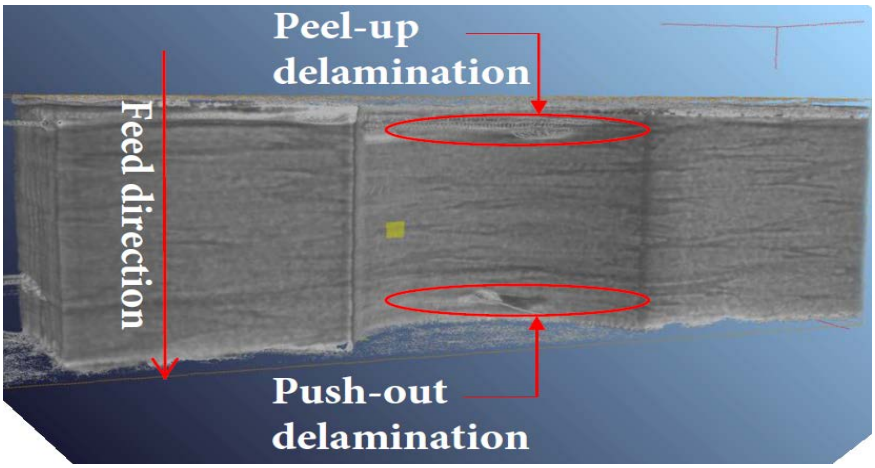

Figure 7.8: X-ray micro CT CFRP specimen micrograph showing inter-laminar delamination at steps 1 (peel-up) & 3 (push-out) when drilling at f = 0.20 mm/rev & v =10 m/min (Ismail et al., 2016c)

Step 2: Secondly, the force increased further as the second cutting edge of the drill bit gained full entrance to the composite specimen. The creation of a blind hole occurred at this drilling step concomitantly with an increased material removal (chip formation) rate.

Step 3: This is a crucial step that determines the quality of the drilled holes, whereby the highest force was recorded at the drill bit's tip due to the exceeded critical thrust force. The forced started decreasing at this steady state region. This can be attributed to the material properties such as the softening phenomenon of HFRP specimen, especially at high cutting interface temperature, though both specimens have a similar force signal. The drilling tool cut through the last or bottom ply or plies of the composite laminate, tending to push the last plies down. The possibility of a drilling-induced damage, known as the push-out delamination, is very high at this step (Figure 7.8).

Step 4: Immediately after step 3, a sharp decrease in the force was observed in step 4. This occurred because of the drill bit's tip has just penetrated through the last ply of the back of the composite laminate. Step 4 shows further sharp reduction in the force at increased time, while the drill bit gained more exit from the specimen.

Step 5: At step 5, where there was decrease in the contact length of the cutting edge of the drill bit, and caused more gradual decrease in the force.

Step 6: Lastly, the force reduced to zero at step 6. At this final step, there was no drilling operation, rather the reaming operation occurred. These phenomena have been similarly reported by Murphy et al. (2002), Khashaba (2012) and Ramesh et al. (2014).

7.1.2.2 Effects of feed rate and cutting speed on delamination and surface roughness drilling-induced damage

The increase in feed rate caused an increase in delamination and surface roughness of both specimens, unlike the delamination and surface roughness of both specimens which increased with a decrease in cutting speed, as depicted in both Tables 7.4 and 7.5. A bigger forms of both Tables 7.4(a) and 7.5(a) are presented in Appendices E1 and E2.

Tables 7.4(b) and 7.5(b) show the effects of drilling parameters on delamination of concerned HFRP and CFRP composite specimens. Delamination occurred mainly by an exceeded thrust force, resulted from feed rate. Therefore, further analysis of the influence of thrust force on the drilling process has just been presented under sub-section 7.1.2.1.

Table 7.4(a): Effects of drilling parameters and material removal rate on delamination of different aspect ratios of HFRP and CFRP composite specimens

Test No	Cutting Speed, v(m/min)	Feed Rate, f(mm/rev)	Delamination Factor, F_d						MRR (mm^3/min)	
			HFRP					CFRP	Drill Diameter (mm)	
			A	B	C	D	E			
			0	19	26	30	38	MTM 44-1	5.0	10.0
1	10	0.05	1.0046	**1.0114**	1.0154	1.0148	1.0154	**1.2860**	625	1250
2	10	0.10	1.0054	**1.0108**	1.0189	1.0166	1.0192	**1.2960**	1250	2500
3	10	0.15	1.0062	**1.0124**	1.0198	1.0216	1.0310	**1.3100**	1875	3750
4	10	0.20	1.0092	**1.0128**	1.0290	1.0422	1.0456	**1.3280**	2500	5000
5	20	0.05	1.0040	**1.0090**	1.0136	1.0138	1.0150	**1.2440**	1250	2500
6	20	0.10	1.0042	**1.0119**	1.0182	1.0186	1.0168	**1.2560**	2500	5000
7	20	0.15	1.0052	**1.0122**	1.0211	1.0196	1.0284	**1.2680**	3750	7500
8	20	0.20	1.0070	**1.0133**	1.0233	1.0396	1.0420	**1.3120**	5000	10000
9	30	0.05	1.0036	**1.0075**	1.0118	1.0080	1.0148	**1.2200**	1875	3750
10	30	0.10	1.0040	**1.0092**	1.0147	1.0158	1.0166	**1.2580**	3750	7500
11	30	0.15	1.0058	**1.0094**	1.0159	1.0182	1.0306	**1.2540**	5625	11250
12	30	0.20	1.0058	**1.0079**	1.0189	1.0234	1.0440	**1.2820**	7500	15000
13	40	0.05	1.0022	**1.0031**	1.0051	1.0074	1.0150	**1.0840**	2500	5000
14	40	0.10	1.0040	**1.0038**	1.0058	1.0090	1.0152	**1.1020**	5000	10000
15	40	0.15	1.0044	**1.0051**	1.0090	1.0176	1.0270	**1.1200**	7500	15000
16	40	0.20	1.0046	**1.0056**	1.0164	1.0190	1.0408	**1.1680**	10000	20000

Table 7.4(b): Effects of drilling parameters on delamination of optimal 19-HFRP and CFRP composite specimens only

Test No	Cutting Speed, v(m/min)	Feed Rate, f(mm/rev)	Delamination Factor, F_d	
			HFRP (AR 19)	CFRP (MTM 44-1)
1	10	0.05	1.0114	1.286
2		0.10	1.0108	1.296
3		0.15	1.0124	1.310
4		0.20	1.0128	1.328
5	20	0.05	1.0090	1.244
6		0.10	1.0119	1.256
7		0.15	1.0122	1.268
8		0.20	1.0133	1.312
9	30	0.05	1.0075	1.220
10		0.10	1.0092	1.258
11		0.15	1.0094	1.254
12		0.20	1.0079	1.282
13	40	0.05	1.0031	1.084
14		0.10	1.0038	1.102
15		0.15	1.0051	1.120
16		0.20	1.0056	1.168

Table 7.5(a): Effects of drilling parameters and material removal rate on surface roughness of different aspect ratios of HFRP and CFRP composite specimens

Test No	Cutting Speed, V(m/min)	Feed Rate, f(mm/rev)	Aspect Ratio (AR)						MRR (mm^3/min)	
			A	B	C	D	E			
			Surface Roughness , R_a (μm)							
			HFRP					CFRP	Drill Diameter (mm)	
			0	19	26	30	38	MTM 44-1	5.0	10.0
1	10	0.05	4.970	**7.240**	8.050	10.070	10.230	**1.609**	625	1250
2		0.10	5.320	**7.330**	9.100	10.300	10.390	**1.250**	1250	2500
3		0.15	6.230	**7.690**	9.180	10.980	10.440	**1.664**	1875	3750
4		0.20	6.430	**8.300**	9.960	11.050	11.140	**1.160**	2500	5000
5	20	0.05	4.660	**7.080**	7.710	8.290	8.480	**2.495**	1250	2500
6		0.10	5.120	**7.240**	7.890	8.600	8.620	**1.648**	2500	5000
7		0.15	5.920	**7.400**	8.400	9.070	9.390	**1.793**	3750	7500
8		0.20	6.350	**8.240**	8.450	9.780	9.720	**1.544**	5000	10000
9	30	0.05	4.020	**5.650**	6.310	7.540	7.450	**1.546**	1875	3750
10		0.10	4.320	**6.700**	6.940	7.400	7.620	**1.298**	3750	7500
11		0.15	5.570	**6.950**	7.090	7.910	7.920	**1.762**	5625	11250
12		0.20	5.750	**7.090**	7.240	7.990	8.010	**1.197**	7500	15000
13	40	0.05	4.090	**5.700**	6.350	7.570	7.480	**1.703**	2500	5000
14		0.10	4.110	**6.880**	6.990	7.770	7.860	**1.457**	5000	10000
15		0.15	5.710	**7.070**	7.190	7.940	8.000	**1.615**	7500	15000
16		0.20	5.960	**7.150**	7.250	8.050	8.140	**1.211**	10000	20000

Table 7.5(b): Effects of drilling parameters on surface roughness of 19-HFRP and CFRP composite specimens only

Test No	Cutting Speed, v (m/min)	Feed Rate, f(mm/rev)	Surface Roughness, R_a (μm)	
			HFRP (AR 19)	CFRP (MTM 44-1)
1	10	0.05	7.24	1.609
2		0.10	7.33	1.250
3		0.15	7.69	1.664
4		0.20	8.30	1.160
5	20	0.05	7.08	2.495
6		0.10	7.24	1.648
7		0.15	7.40	1.793
8		0.20	8.24	1.544
9	30	0.05	5.65	1.546
10		0.10	6.70	1.298
11		0.15	6.95	1.762
12		0.20	7.09	1.197
13	40	0.05	5.70	1.703
14		0.10	6.88	1.457
15		0.15	7.07	1.615
16		0.20	7.15	1.211

Comprehensively, from the results obtained on delamination factors, it is evident that the HFRP composite specimens have a smaller and close values while the values of CFRP specimens are higher and wide. The smaller and close values of delamination factors are rampant in bio-composites that are similar in properties (Naveen et al., 2012; Abdul Nasir et al., 2015), under the same drilling parameters, machining conditions (with supported back plate and dry environment) and type of drill bit. It was observed that an increase in the cutting speed caused a gradual reduction in the delamination factor. However, the delamination factor of the two specimens increased with an increase in the feed rate, as shown in Figures 7.9(a) and (b).

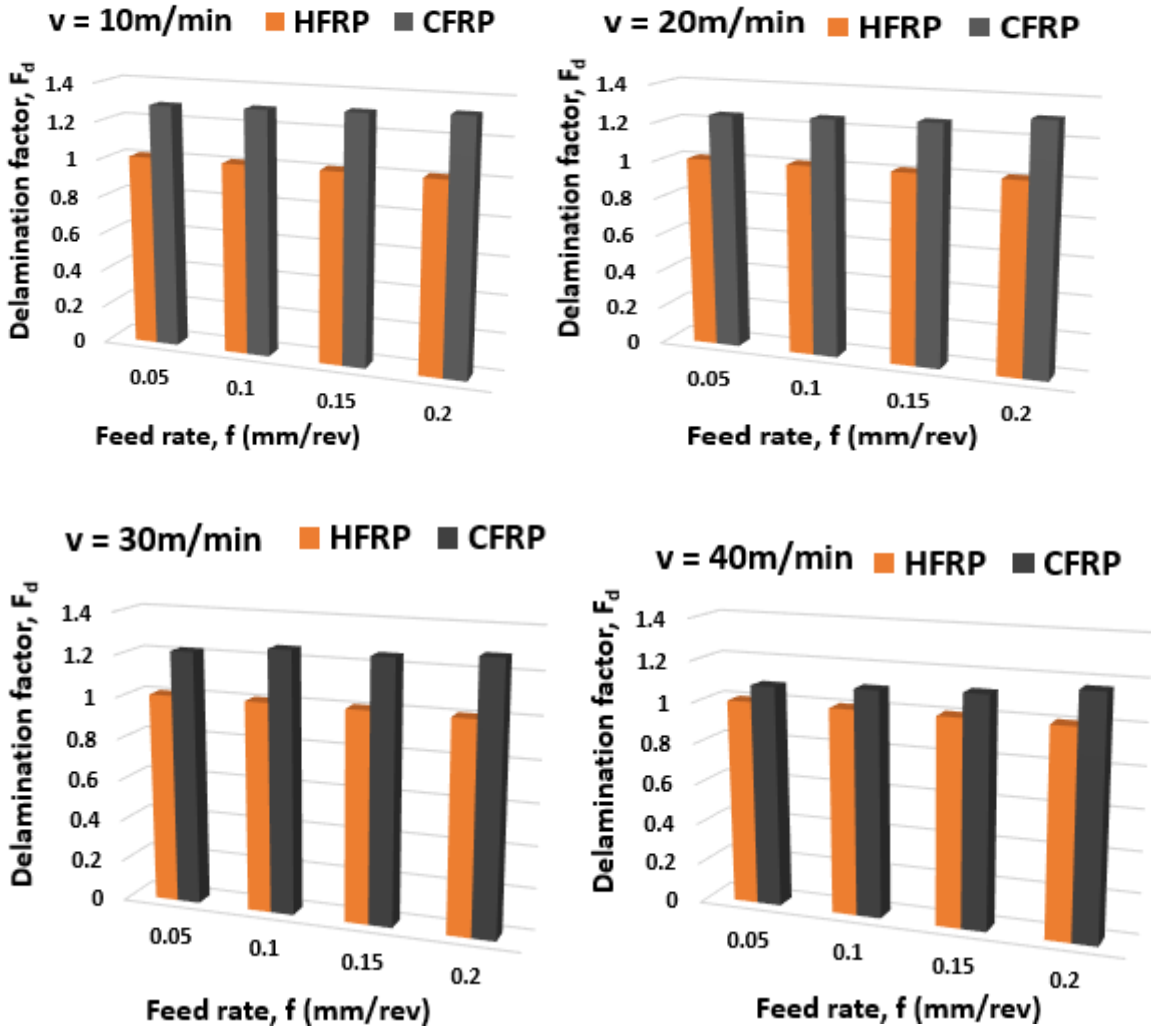

Figure 7.9(a): Effects of the drilling parameter (feed rate) on delamination, showing that delamination factor increased with feed rate (Ismail et al., 2016c)

An increase in feed rate caused an increase in drilling (thrust) force. Also, the optimum drilling conditions, hole surface finish and total quality are associated with a low feed rate (0.05 - 0.10 mm/rev) and high cutting speed (30 m/min), as further shown in Appendices E9 and E10. These experimental results are in close agreement with that of Ramesh et al. (2014) and Shunmugesh and Panneerselvam (2016).

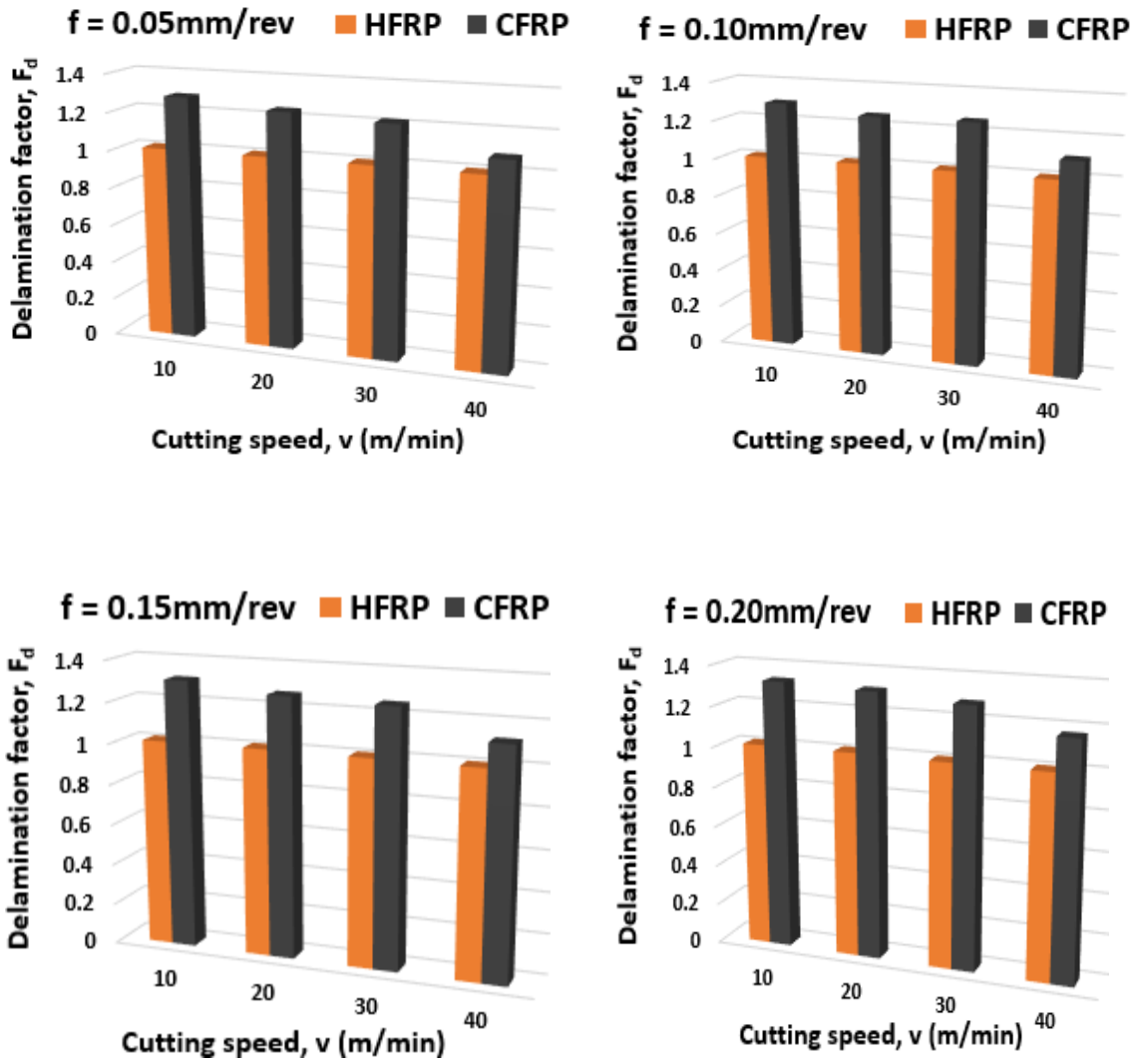

Figure 7.9(b): Effects of the drilling parameter (cutting speed) on delamination, showing that an increase in cutting speed caused a decrease in delamination factor

Evidently, an increase in the feed rate led to a proportional gradual increase in the surface roughness. However, an increase in cutting speed caused a non-linear decrease in the surface roughness of the two specimens, but very inconsistently in CFRP specimens, as shown in Figures 7.10(a) and (b). This may be attributed to the location of the fibre and the nature of the measured area of the drilled holes.

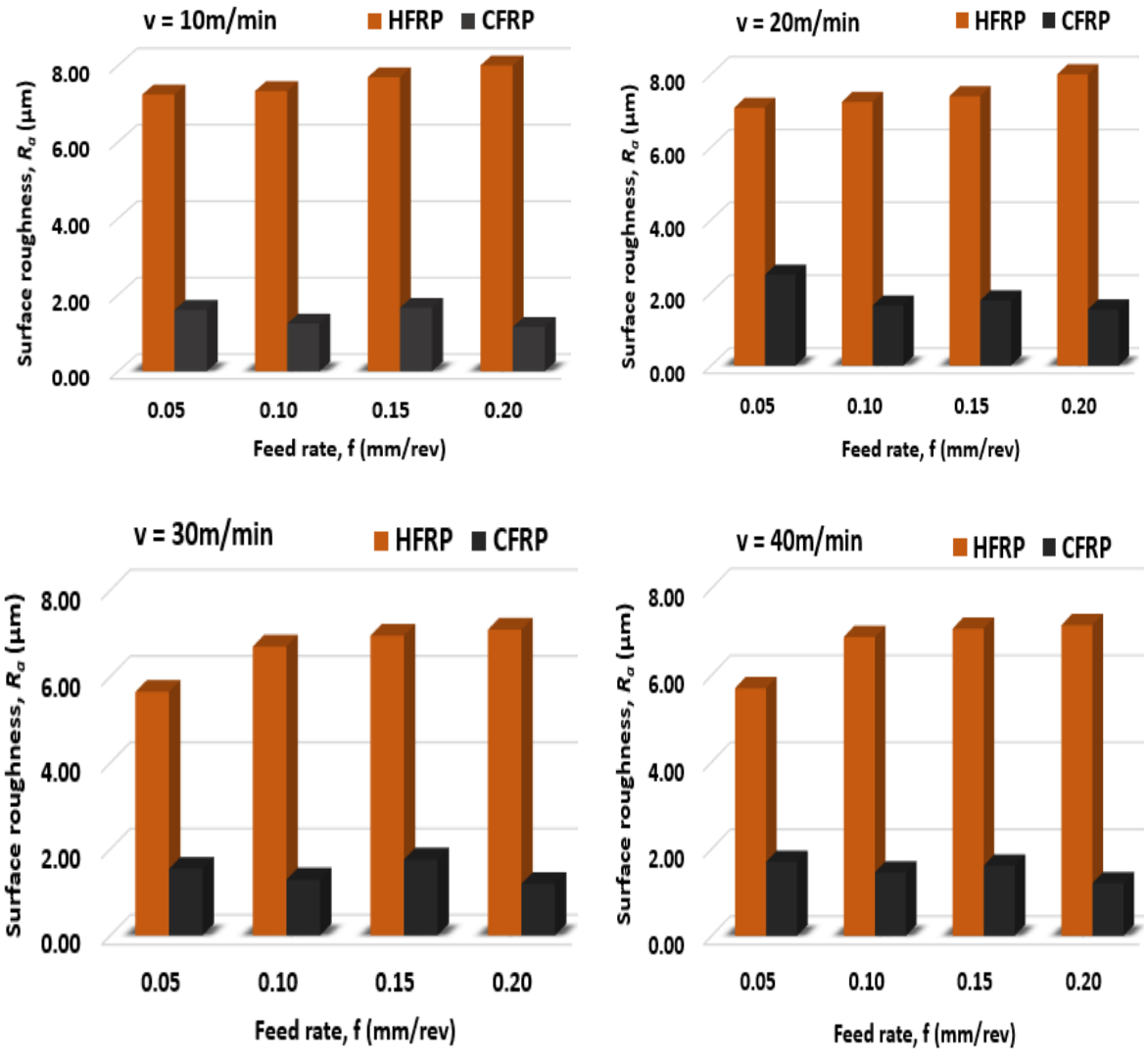

Figure 7.10(a): Effects of the drilling parameter (feed rate) on surface roughness, showing that surface roughness increased with feed rate (Ismail et al., 2016c)

Moreover, Figures 7.9 and 7.10 depict that better drilled hole surface roughness was obtained with a combination of low feed rate and high cutting speed for the HFRP

composite laminate (Appendices E9 and E10), while high feed rate and low cutting speed tend to favour the drilling of CFRP composites.

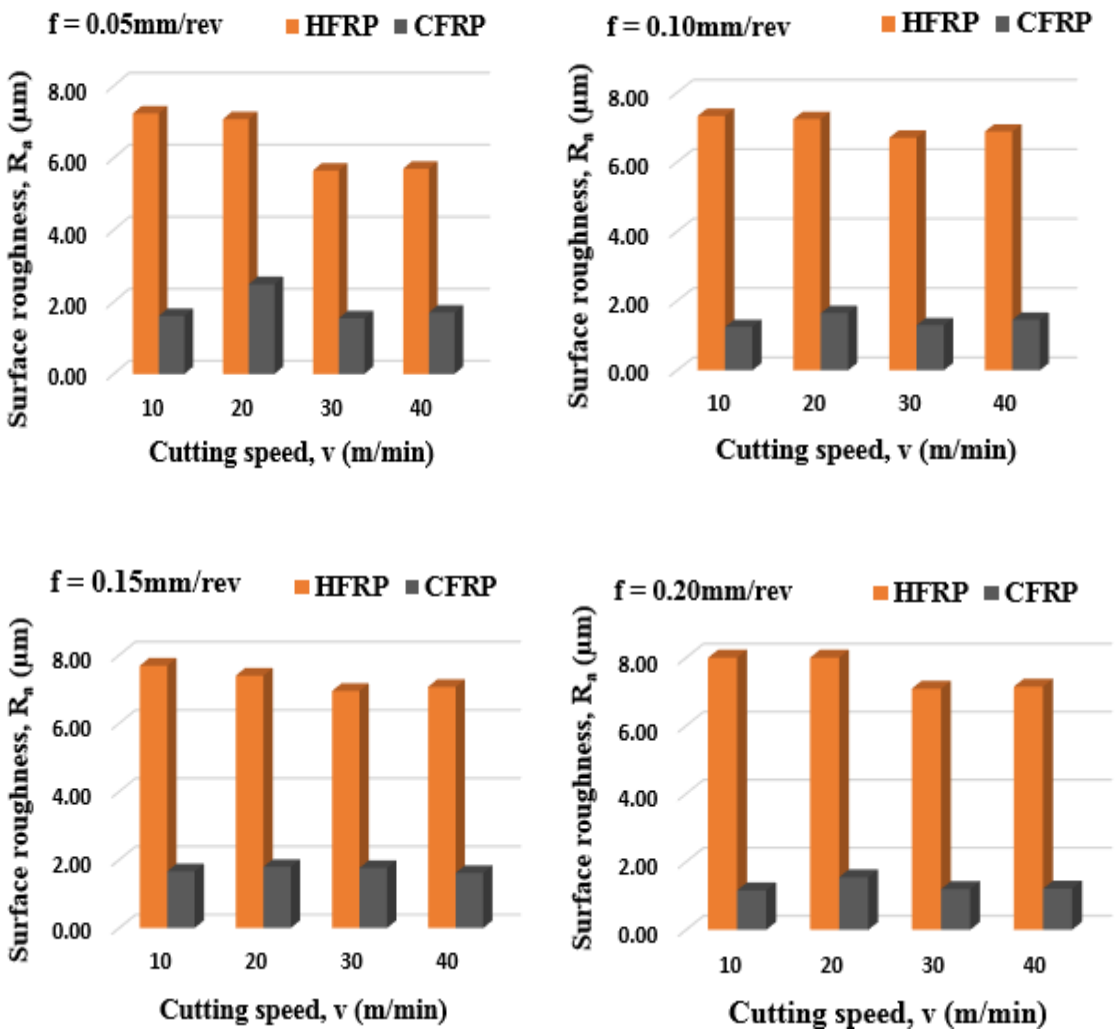

Figure 7.10(b): Effects of the drilling parameter (cutting speed) on surface roughness, showing that decrease in cutting speed caused an increase in surface roughness (Ismail et al., 2016c)

In addition, the ANOVA was applied for the identification of the important factors, their relations and influences as they function dependently. It was also used to evaluate the effects of the variables considered on the delamination and surface roughness analysed. With the aid of ANOVA, combination of the drilling parameters that gave better contribution, performance and greater influence were obtained. Using the same 95.0 %

confidence Interval and IBM SPSS statistical software or tool, the standardised coefficients, extracted from the ANOVA results obtained show the effects of drilling parameters on both composite specimens. These are summarily illustrated in Table 7.6 and represented in Figure 7.11. Other detailed ANOVA results are presented in Appendix E6. Comparatively, from these results, it is evident that feed rate has a greater effect (value of 0.302) on CFRP composite specimen, which consequently resulted into higher delamination factor. However, the lower value (-0.888) of effect of cutting speed on HFRP composite specimen resulted into a greater surface roughness damage. These ANOVA results agree closely with Figures 7.9 and 7.10.

Table 7.6: Comparison of effects of drilling parameters on both specimens

Drilling parameter	HFRP-19	CFRP	Difference
Cutting Speed, v (m/min)	-0.888	-0.860	0.028
Feed Rate, f (mm/rev)	0.255	0.302	0.047

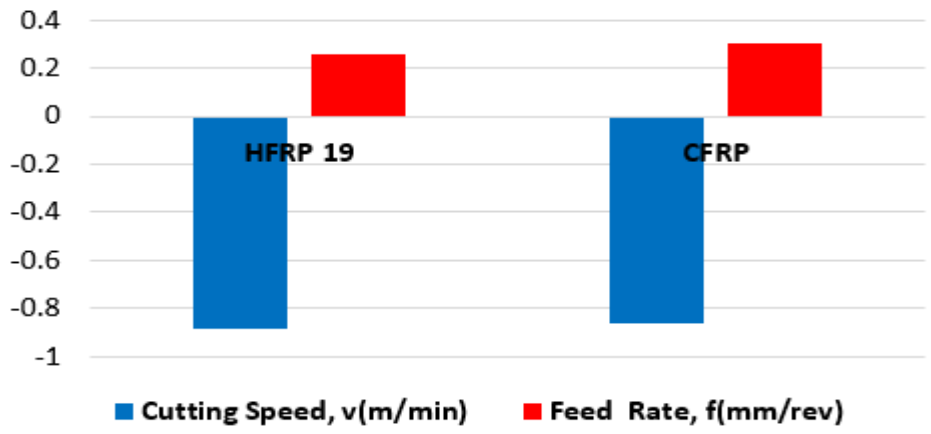

Figure 7.11: Comparison of effects of drilling parameters on both specimens, showing greater effect on CFRP than HFRP specimen

It has been established that feed rate affected delamination more than cutting speed, while cutting speed has a greater effect on the surface roughness of composite materials (Ismail et al., 2016a; Ismail et al., 2016b; Ismail et al., 2016c). These phenomena could be traced to the fact that at a low cutting speed, the workpiece-tool interface temperature could not dissipate off as much ribbon-like and curly chips clogged the twist drill flute and

hole. This could have resulted into burning PCL matrix and disintegration of the hemp fibre, causing a higher surface roughness in HFRP when compared with CFRP specimen. While, higher feed rate produced higher critical thrust force that caused higher delamination flaw on CFRP composite specimen. Summarily, these imply that delamination greatly depends on higher feed rate, while surface roughness significantly depends on lower cutting speed.

7.1.2.3 Effects of the drill diameter, feed rate and cutting speed on material removal rate

Using the equation 5.7 of sub-section 5.3 (Chapter 5: Instrumentation), the MRR results obtained for diameters 5.0 and 10.0 mm are presented in Table 7.7.

Table 7.7: Experimental drilling parameters and material removal rate performance

Serial No	Cutting Speed, V(m/min)	Feed Rate, f(mm/rev)	Material Removal Rate, MRR (mm^3/min)	
			Diameter (mm)	
			5.0	10.0
1	10	0.05	625	1250
2		0.10	1250	2500
3		0.15	1875	3750
4		0.20	2500	5000
5	20	0.05	1250	2500
6		0.10	2500	5000
7		0.15	3750	7500
8		0.20	5000	10000
9	30	0.05	1875	3750
10		0.10	3750	7500
11		0.15	5625	11250
12		0.20	7500	15000
13	40	0.05	2500	5000
14		0.10	5000	10000
15		0.15	7500	15000
16		0.20	10000	20000

Figure 7.12 depicts that the MRR has a direct proportionality to diameter, feed rate and cutting speed; it shows that the MRR increased with these drilling variables. The MRR has a great influence on the rate, efficiency and cost of production. Due to the abrasive and powdery nature of the CFRP composite laminates as well as the discontinuous chip formation during drilling operation, there was a tendency of much chips clogging on the flute of twist drills, increased at higher feed rate, cutting speed and when using bigger drill diameter (10.0 mm). This resulted into much surface damage. An insufficient chips removal and air cooling between the specimen and drill bit interface, when there are too much of blockage on the drill flank and narrow helical flutes of a twist drill, increased the interface temperatures which aided the delamination (cracks) propagation and compound void formation.

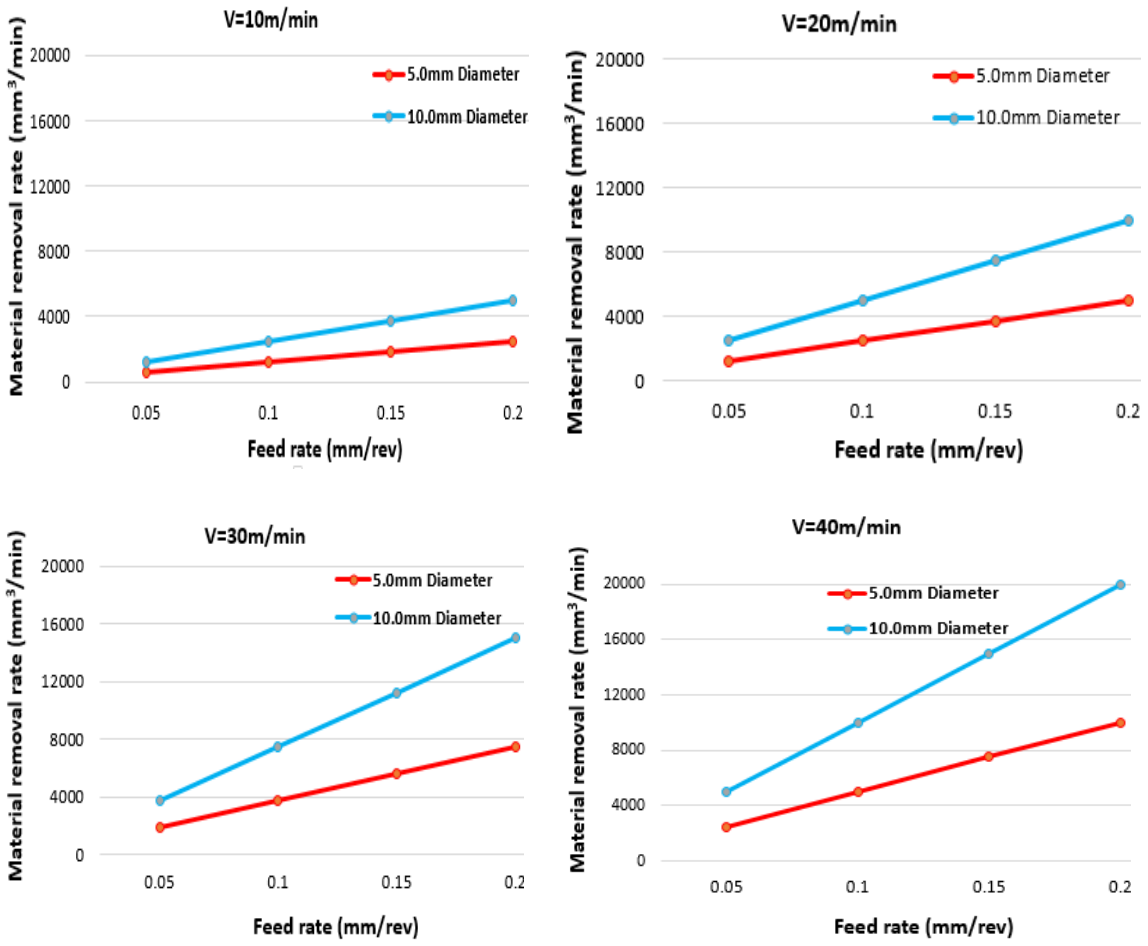

Figure 7.12: Effects of the drill diameter, feed rate and cutting speed on MRR, showing that MRR increased with drill diameter, feed rate and cutting speed

Furthermore, the outcomes (Pareto's front) of the research study conducted by Sardiñas et al. (2006), using genetic algorithm clearly showed the relationship between the MRR and the maximum delamination factor. It was reported that the MRR increased with the maximum delamination factor. The greatest value of MRR, also known as the point of maximal productivity produced the greatest value of delamination factor (point of worst surface roughness or quality). The lowest value of MRR was produced at a point of corresponding value of a lowest delamination factor. Therefore, a lower MRR produced by a smaller diameter, lower feed rate and cutting speed favoured the reduction of delamination drilling-induced damage on CFRP composite materials. In addition, the application of a low feed rate coupled with a small diameter drills favoured minimum delamination, for an improved quality holes, especially on CFRP specimens, as recently reported by Abilash and Sivapragash (2016). Comparatively, the optimum drilling conditions and better hole surface quality were associated with the use of the smaller drill diameter 5.0 mm. In order to reduce these resultant challenges of poor surface quality and delamination defects, among others, it is advisable and better to begin drilling operation with a drill bit of smaller diameter than the exact drill diameter for final expected hole, and progressively increasing the diameter of hole for the quantity of the material/chip removal rate to be minimised. Though, this proposed method is not really cost effective.

Additionally, a severe fractured carbon and hemp fibres as well as the burnt matrices, causing porosity on the drilled surfaces of the holes were observed when using higher drill diameter, as shown in Figure 7.13. These defects occurred at the lowest feed rate of 0.05 mm/rev and cutting speed of 20 m/min, this was expected due to the effect of an increased drill diameter on the surface integrity. The bigger 10.0 mm diameter drill bit has a greater chisel edge, web thickness and area of cut. Consequently, these increased drill bit geometries produced a higher drilling forces (thrust force and torque). Therefore, the defects observed especially in Figure 7.14(a) would have been caused by the increased drilling forces, induced by the greater drill bit diameter 10.0 mm used. Furthermore, with the use of greater diameter, more dust or powder-like chips are formed. The formation of

more chips supported a high interface-temperature between the composites and cutting edges of the drill bit, as the chips evacuation reduced at the averagely lower cutting speed and dry machining environment. Resultantly, this frictional generated temperature weakened the fibres and melted the binders greatly, as indicated in Figure 7.14(b). This high temperature is produced around the primary cutting region, most prominently when the drilling is performed in a dry environment. The increased temperature facilitated the drill wear as more molecules of the drill gained more kinetic energy to aid diffusion and adhesion mechanisms of tool wear. The drill wear increased with drilling parameters include cutting force, feed rate and thrust force. These parameters are the major causes of delamination and surface roughness (Ismail et al., 2016b; Ismail et al., 2016c). Consequently, an increase in drill wear caused an increase in delamination and surface roughness defects of CFRP composite laminates. The delamination defect was greater in the MTM 44-1 CFRP (synthetic) composites when compared with the HFRP (Natural) composite laminates, under the same drilling conditions. This shows that the CFRP is more brittle as it deformed under the combination of shearing and rupturing (Rajasekaran et al., 2012). In addition, the increased interface temperature scarcely caused another drilling-induced damage, known as fibre/matrix catering, fibre pull-out and matrix/binder thermal softening or de-bonding effects. These phenomena could also be traced to the dry machining (drilling) condition that was considered throughout this experiment due to the limiting effects of wet machining on the structural quality and integrity of FRP composites, especially natural or sustainable type.

More also, the diffusion and adhesion mechanisms of wear formation led to the minimal drill wear observed at the drill flank after drilling CFRP specimens when compared with insignificant wear on drill after drilling the same 64th hole on the HFRP specimens. The drill wear plays an important role in formation of these drilling-induced defects. Also, this can be attributed to the higher hardness, abrasive and brittle nature of the CFRP specimen, and relative softness and ductility of the HFRP specimen. The wear comparison between the used (worn) drill and the new type was observed by mere physical and visual inspection.

7.1.2.4 SEM quantification of delamination and surface quality (roughness)

The micrographs (Figures 7.13 and 7.14) depict the roughness developments, fibre and matrix damage in form of peaks and valleys, at the same drilling conditions.

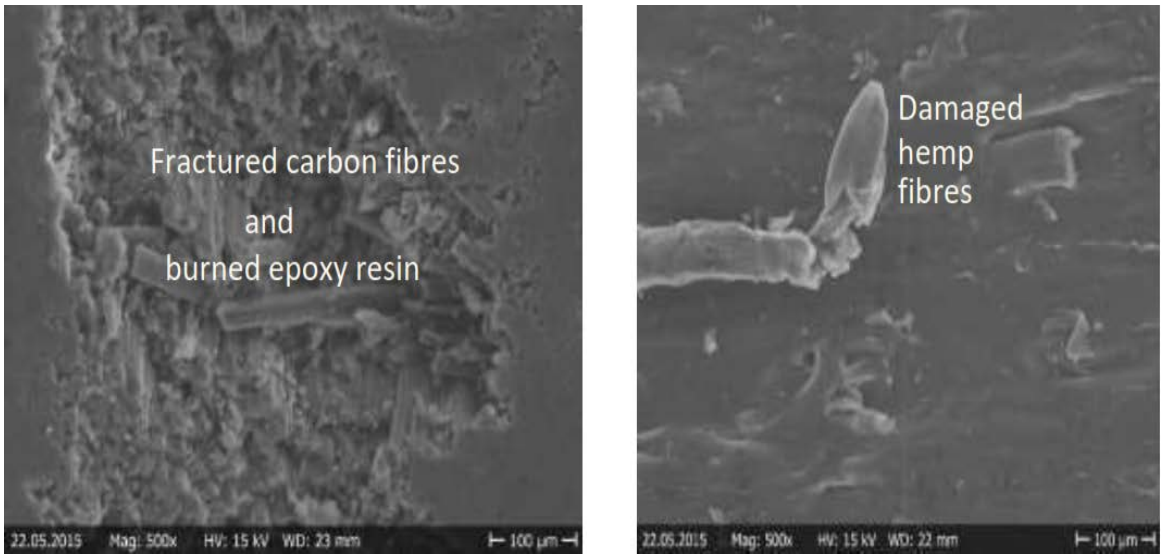

(a) CFRP **(b)** HFRP

Figure 7.13: SEM micrographs of the specimens with 10.0 mm diameter hole drilled at f = 0.05 mm/rev and v = 20 m/min (Ismail et al., 2016c)

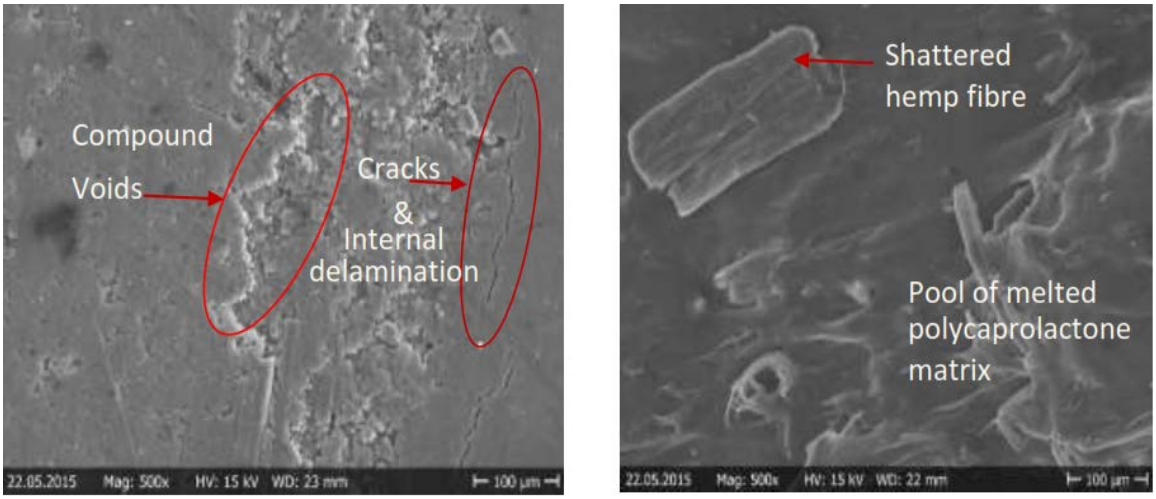

(a) CFRP **(b)** HFRP

Figure 7.14: SEM micrographs of the specimens holes of 5.0 mm diameter drilled at f = 0.15 mm/rev and v = 30 m/min (Ismail et al., 2016c)

The deep valleys and the high peaks illustrate the melted or burnt matrix and waved lumpy textured fibres, causing voids (or cavities), resultantly produced higher roughness and delamination defects on the surface of the HFRP and CFRP holes, respectively. These defects occurred prominently at a low feed rate of 0.05 mm/rev and a cutting speed of 0.20 m/min with a bigger drill diameter of 10 mm (Figure 7.13) as well as at a high feed rate of 0.15 mm/rev and a cutting speeds of 30 m/min with smaller drill diameter of 5.0 mm (Figure 7.14). Therefore, the cracks propagated in Figure 7.14(a) occurred due to the high feed rate of 0.15 mm/rev and cutting speed of 30 m/min used. In addition, thrust force and torque increased with the feed rate. Therefore, both thrust force and torque are the responsible factors for the occurrence of the compound voids, cracks, internal delamination and matrix melting of the two specimens, as depicted in Figures 7.14 (a) and (b).

Moreover, Figures 7.13(a) and 7.14(a) show a compound void and cracks propagated in the CFRP composite by delamination and de-bonding phenomena respectively. The propagation of the cracks was more prominent in a brittle materials than the ductile materials. The CFRP composites are more brittle than the HFRP composite due to their different reinforcements (carbon and hemp fibres) and binders (epoxy and polycaprolactone) respectively. The PCL matrix of HFRP is a ductile material, which increased the toughness of its constituent composite and consequently, reduced the possibility of having cracks and internal delamination drilling-induced problems, unlike the CFRP composites when subjected to the same drilling condition and parameters. The EP of CFRP composites is a thermoset polymer matrix, while PCL of HFRP is a thermoplastic polymer matrix. Typically, thermosets are relatively brittle, but they possess better chemical resistance and stronger interfacial bonds. Also, the decomposition and glass transition temperatures of EP are greater than PCL matrix. EP resin is stronger, and has a greater adhesive force as well as glass transition temperature (T_g) between 60 °C and 110°C (Techtip, 2012) than the polycaprolactone of −60 °C T_g (Kumbar et al., 2014), which depends on the cure schedule. These thermo-chemical properties of EP resin would have contributed towards the lower surface roughness of the CFRP composite laminates. Also,

epoxy resin produced a tougher bond expected between the carbon fibre and the resin.

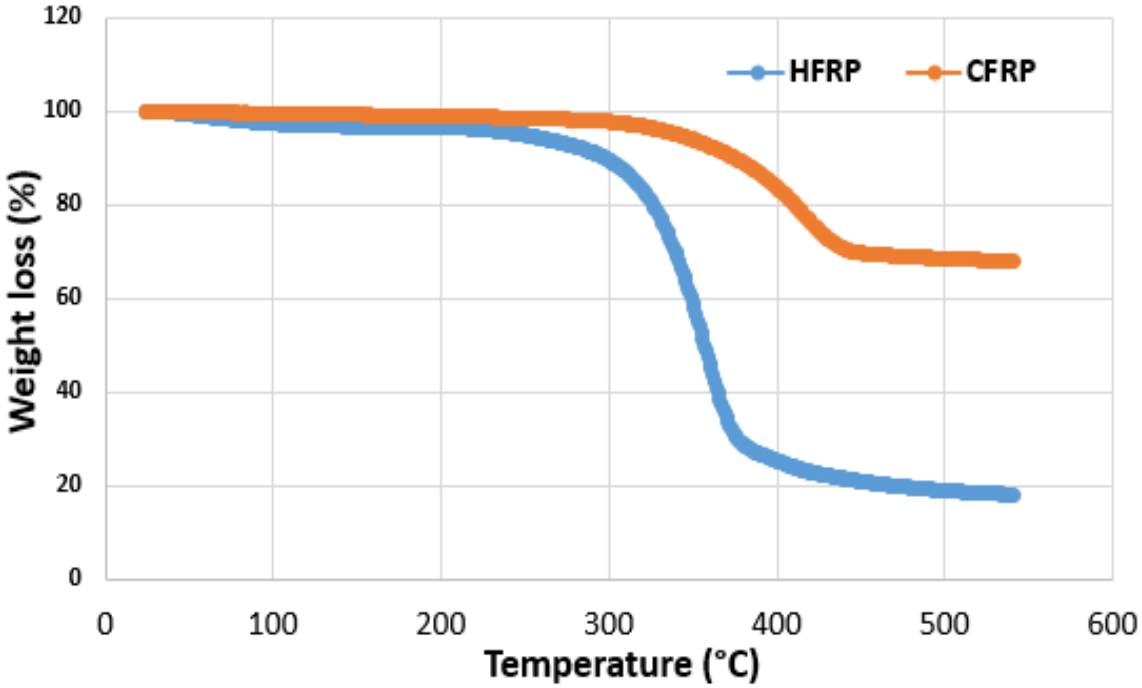

Figure 7.15(a): Thermogravimetric analysis of the specimens showing difference in their decomposition temperatures

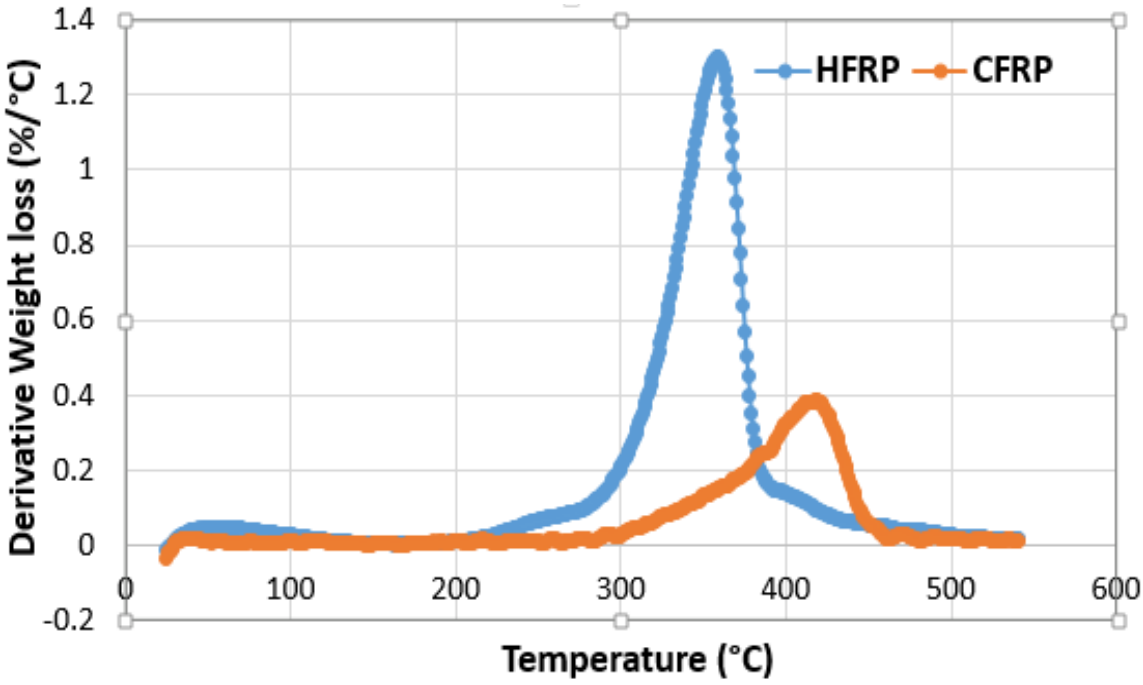

Figure 7.15(b): Thermogravimetric analysis of the specimens showing comparison between their derivative weight loss and temperature

Furthermore, the thermogravimetric analysis of the two specimens were conducted, both Figures 7.15(a) and 7.15(b) depict their behavioural results in terms of weight loss under increasing temperature. The procedures for this analysis have been detailed in the preceding chapters. It is evident that CFRP has higher decomposition temperature, under the same conditions, while the HFRP specimens have a lower decomposition temperature of around 200 ^{o}C (above T_g of PCL, but higher than CD temperature), when compared with nearly 300 ^{o}C for CFRP composite specimens, as shown in Figures 7.15 (a) and (b). The damage observed in the CFRP composite specimens are point concentrated defects, while that of HFRP are uniform damage, mainly caused by the melted and sintered PCL matrix.

7.1.2.5 Chip formation morphology and characterisation

Chips are generated immediately when the composite materials undergo a plastic deformation, generally at the drill-material slipping interface within a shearing region. During the chip formation, neither a dust-like nor a very long continuous chips is encouraged during drilling operations. The powdery chips from the CFRP composites are not easily evacuated from the drill flutes, causing a chip clogging due to high friction and forces developed, while a long continuous chips often results into a serious chip evacuation predicaments. These problems have a high propensity of causing decrease in drilled holes quality, tool (drill) life and drill breakage, if they are not properly managed.

The chips formation increased during drilling of both specimens at an increased feed rate and cutting speed, which was well prominent at 0.20 mm/rev and 40 m/min feed rate and cutting speed respectively. A continuous brown ribbon-like chips formed during the drilling of HFRP specimen, while the size of the CFRP discontinuous black powder-like chips generated was very small, fine, powdery and abrasive in nature, due to the properties of their fibres and matrices. The higher the feed rate and cutting speed, the wider, longer, more ribbon-like and lighter the HFRP chips and conversely, the powdery or dusty, smaller and darker the CFRP chips formation, as shown in Figure 7.16. These types of chips formation produced a lower surface roughness in the CFRP specimens, delamination and drill wear in HFRP specimens. Conclusively, the type of chips formation also directly and

indirectly affected the mode and possibility of formation of drilling-induced damage both on the specimens and the drill bit used.

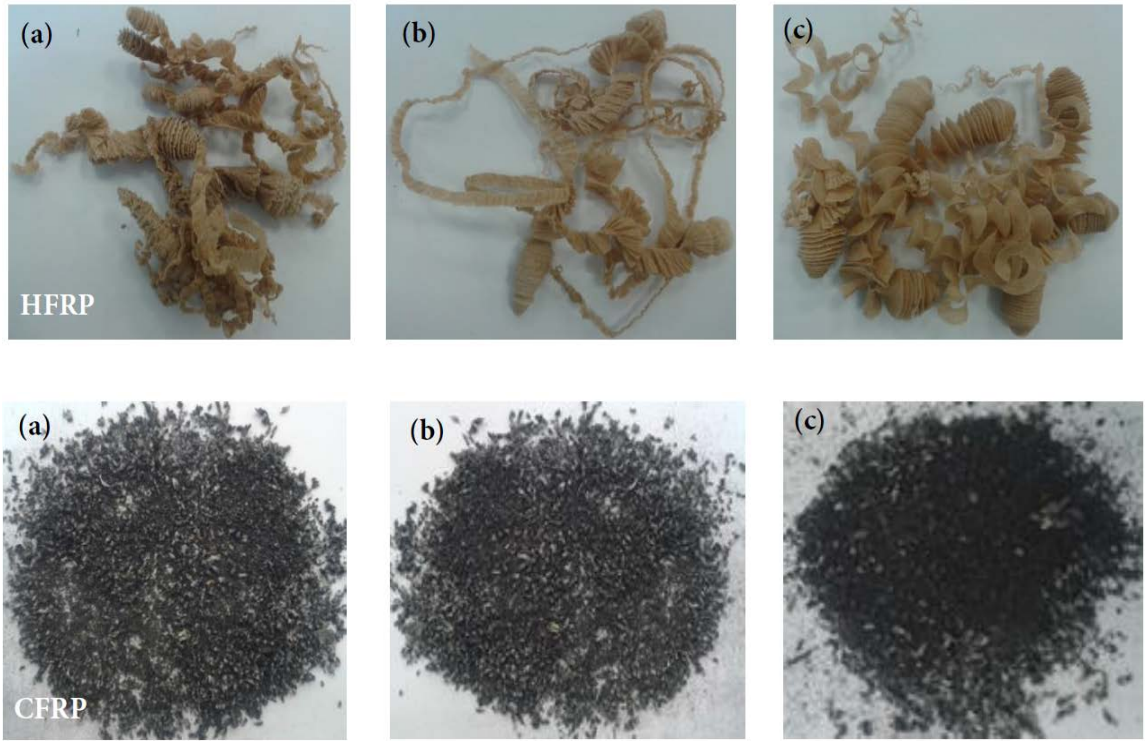

Figure 7.16: Chips morphology at different increasing order of drilling parameters: (a) f = 0.05 & v = 10;(b) f = 0.15 & v = 30; (c) f = 0.20 mm/rev & v = 40 m/mm (ismail et al., 2016c)

7.1.2.6 Other drilling-induced damage

Further non-destructive examinations on the specimens were conducted with aid of X-ray micro computed tomography (X-ray micro CT) technique. In addition to the discussed defects, drilling-induced damage such as uncut-fibre and burrs formation were observed. Figure 7.17 depicts the occurrence of both small burrs and few uncut-fibres in HFRP composite specimens, especially at the entrance and exit of some of the drilled holes. The uncut-fibres damage occurred at a lower feed rate and cutting speed, whereas the minimal burrs were observed at a lower feed rate and average cutting speed. However, the CFRP composite specimens have none of these defects. These defects reduce the integrity of the holes and machinability of the HFRP specimens. There are needs for some post-machining

operations to be performed in order to remove these defects, such as de-burring and probably, reaming. Therefore, they tend to increase the total machining time and cost of manufacture. The use of the CFRP composite laminates should be encouraged when burrs are highly prohibited and cannot be compromised.

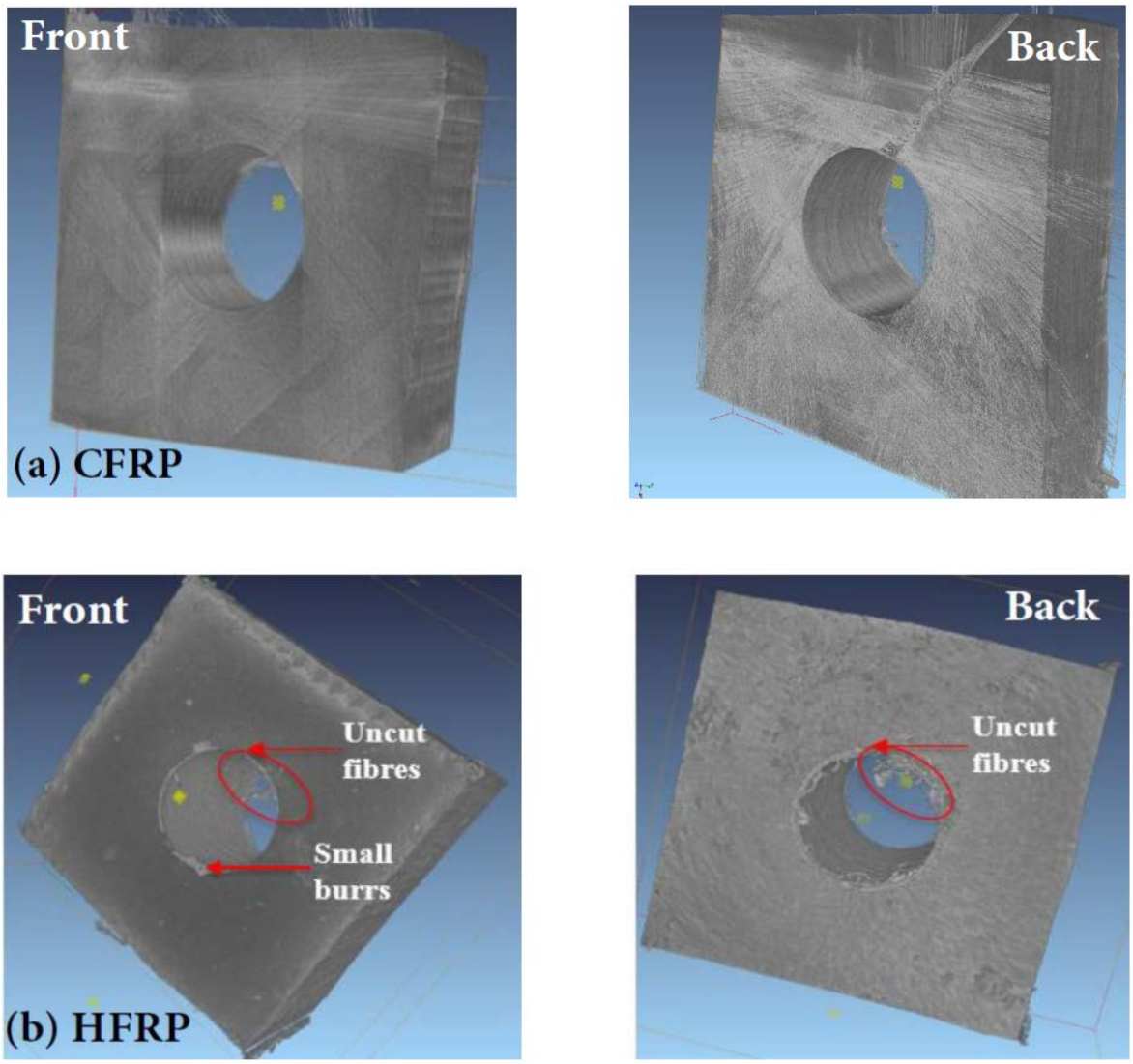

Figure 7.17: The X-ray micro CT scanning micrographs, showing: (a) CFRP -without fibre-uncut and burrs & (b) HFRP- with fibre-uncut and burrs damage ((Ismail et al., 2016c)

7.1.3 Stage 3: Machinability analysis of bio-composites: Conventional versus ultrasonically-assisted drilling techniques

This involved a novel comparative and experimental investigation into the machining of FRP bio-composite (HF/PCL and HF/VE) specimens, using both CD and UAD techniques, under the same Taguchi method of design of experiment and compressed air cooling environment. The outstanding benefit of drilling forces (thrust and torque) reduction with UAD was investigated on HF/thermoplastic PCL and HF/thermoset VE, compared with the CD technique.

7.1.3.1 Effects of thrust force and torque on the hole quality of HF/PCL bio-composite specimens

Figure 7.18 depicts that the HF/PCL composite specimens with AR of 00 (neat), 19, 23, 30 and 38 have the peak or upper thrust forces of 110 and 100 N, 90 and 75 N, 105 and 88 N, 110 and 88 N, and 120 and 110 N, using UAD and CD techniques respectively, at machining times of 40, 30, 32, 38 and 50 seconds. Also, it shows that the thrust force increased with the aspect ratios of the HF/PCL specimens. The surface quality of the HF/PCL specimens reduced as their aspect ratios increased. The heavy winding of the graphical results (Figure 7.18) was caused due to the dynamics of the vibrating drill bit, resulting into ultrasonic waves propagating in the excited drill cutting at a frequency above 20 kHz.

Evidently, both UAD and CD techniques on the HF/PCL specimen with AR 19 (19-HF/PCL) recorded the minimum values of thrust force and machining time, especially with the UAD, when compared with other aspect ratios. The 19-HF/PCL composite specimen has a peak thrust force of 90 N and 75 N during UAD and CD respectively, with the lowest machining time of 30 seconds for both drilling techniques. Consequently, the optimum drilling and best quality drilled holes were achieved on 19-HF/PCL composite specimen, in terms of a lowest thrust force reduction and drilling-induced damage, which include mainly burrs formation, fibre-uncut and surface roughness. When there is a thrust force reduction, the quality of the drilled proves better and cost of production reduces due to the lesser power

consumption rate. This UAD result is in close agreement with the results previously obtained when CD technique was only used (Ismail et al., 2016a).

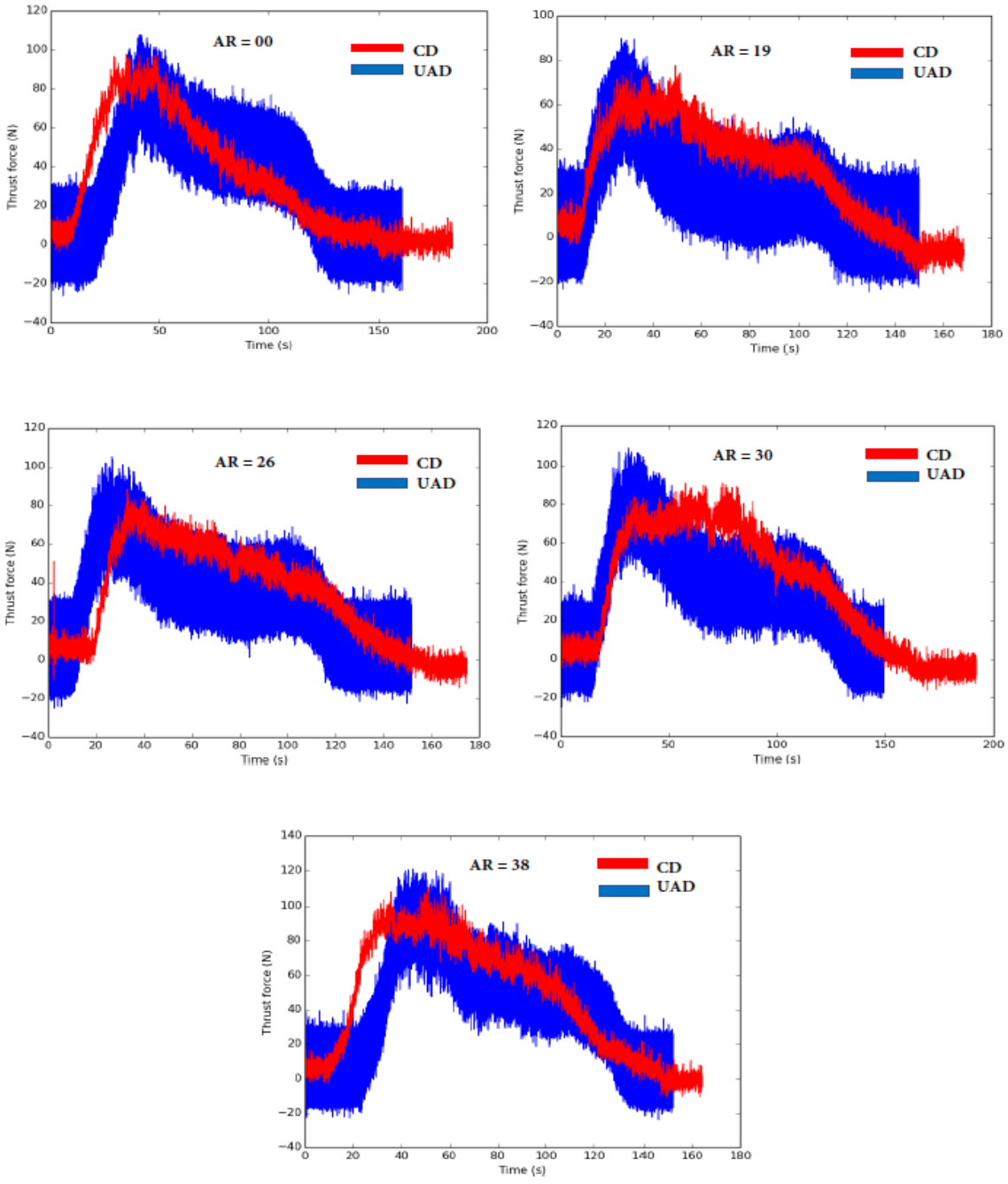

Figure 7.18: Comparison of CD and UAD techniques on HF/PCL composite specimens, showing insignificant drilling-thrust force reduction at feed rate of 0.10 mm/rev and spindle speed of 40 rev/min (Ismail et al., 2016e)

The HF/PCL composite specimens possess a high modulus of elasticity due to the presence of the ductile PCL matrix. However, the optimal specimen of 19-HF/PCL has more burnt chip-materials attached on the drilled holes during UAD than CD, which was worse at AR 38, both in physical and micrographic appearances, as depicted in Figures 7.19 (i) and (ii). The UAD effect produced a very high surface roughness (R_a), up to 13 µm. These problems occurred due to the 60 ^{o}C melting temperature of PCL resin (Rieger et al., 2012; Speranza et al., 2014), quite lower than 56-90.2 ^{o}C and 265-290.8 ^{o}C composite-tool interface temperature during CD and UAD respectively (Makhdum et al., 2014). The melting temperature of PCL is very low comparing with the decomposition temperature of around 200 ^{o}C for the 19-HF/PCL composite specimen, based on earlier discussion under sub-section 7.1.2.4 of stage 2 experiment.

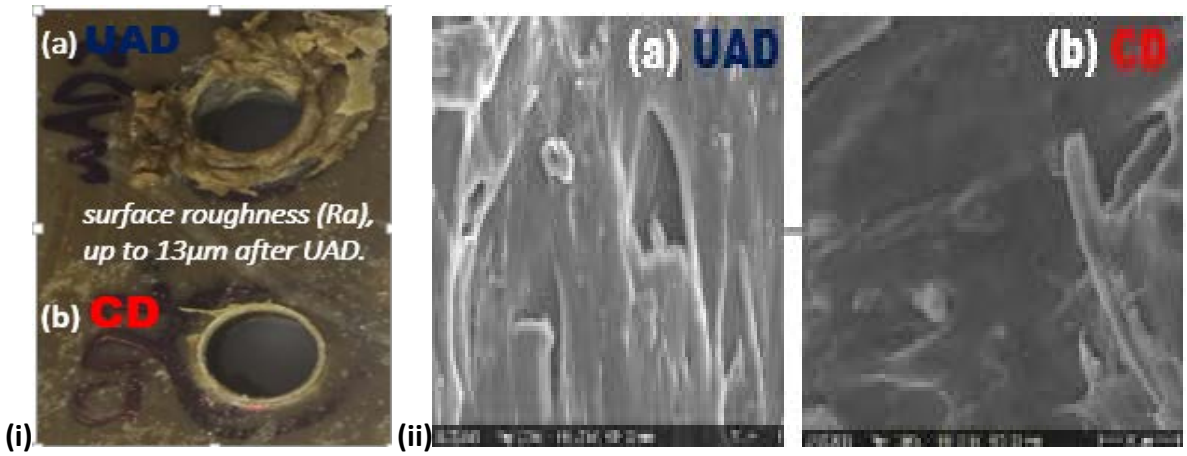

Figure 7.19: (i) Physical (visual) appearance and (ii) SEM micrographs, showing poorer surface quality after: (a) UAD of HF/PCL, when compared with (b) CD technique (Ismail et al., 2016e)

Furthermore, during drilling process at the deformation zone, the material (composite) elasticity was exceeded and converted to plastic deformation. There are nearly 90 % plastic deformation work that transformed into the heat energy which directly increased the drill-chip-workpiece interface temperature around the deformation or shearing (cutting) regions (Kapoor & Nemat-Nasser, 1998; Shetty et al.,

2014). Therefore, the PCL matrix melted and decomposed around 90.2-290.8 ^{o}C maximum surface temperature measured in CD and UAD techniques respectively (Makhdum et al., 2014). The PCL matrix has a lesser melting temperatures below the UAD workpiece-tool interface temperature, and consequently, it melted greater with UAD to give higher surface roughness.

The main benefits of a drilling-thrust force and machining time reduction using UAD technique were marginally achieved on 19-HF/PCL composite specimens, but at expense of a good quality of the drilled holes, when compared with the CD. The ultrasonic energy was absorbed and then heat generated, which made no significant force reduction and no clean cut surface. Comparatively, the use of CD technique favoured this specimen in terms of physical quality of holes produced. In addition, the full and significant benefits of UAD were difficult to obtain for the drilling of the HF/PCL composite specimens. At this juncture, it can be established that the effectiveness of the application of the UAD technique strongly depends on the properties of both the reinforcement (fibre) and the matrix (binder).

7.1.3.2 Effects of thrust force and torque on HF/VE composite specimens

The main importance connected to the invention and application of UAD technique in composite machining is the drilling forces (thrust and torque) reduction. The experimental results obtained evidently depicts that there were significant and substantial reductions in the thrust forces and the torques using UAD on HF/VE specimens, when compared with CD, as depicted in Figures 7.20 and 7.21. The maximum thrust forces and torques recorded in UAD and CD at varied feed rates are highlighted in Figure 7.21. More results are presented in Appendix E7. The average drilling forces were reduced by approximately 40 % with UAD in comparison with CD. This is significantly relevant comparing to 30 % average thrust force reduction reported by Phadnis et al. (2012b), when compared CD with UAD of CFRP. Drilling forces reduction improves the quality of the drilled holes, reduces power consumption rate and consequently total cost of production.

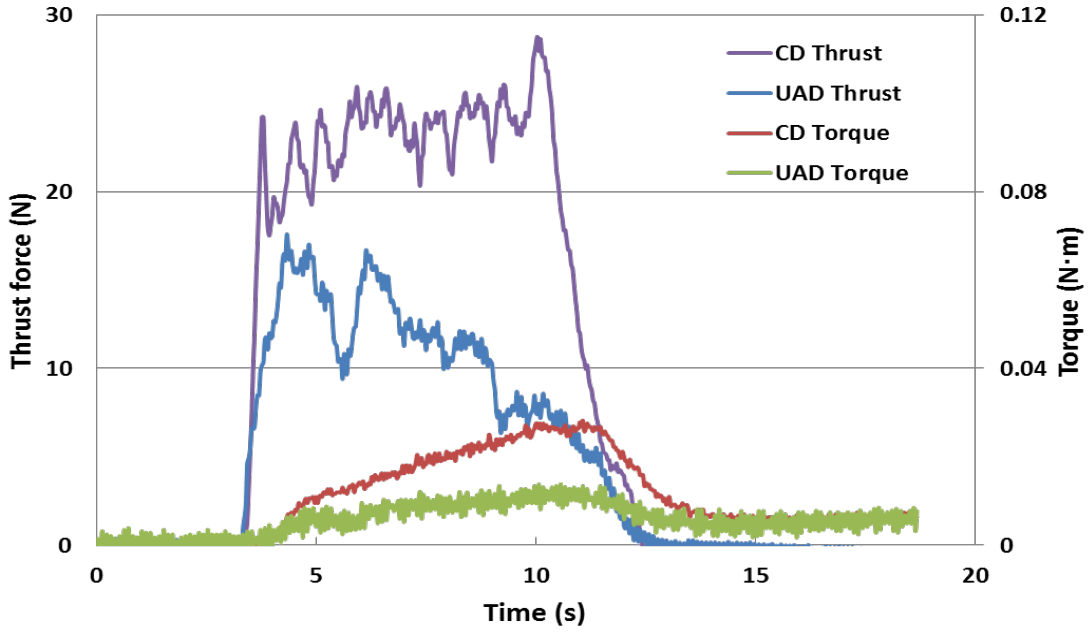

Figure 7.20: A substantial drilling (thrust and torque) forces reduction during UAD of HF/VE, compared with CD

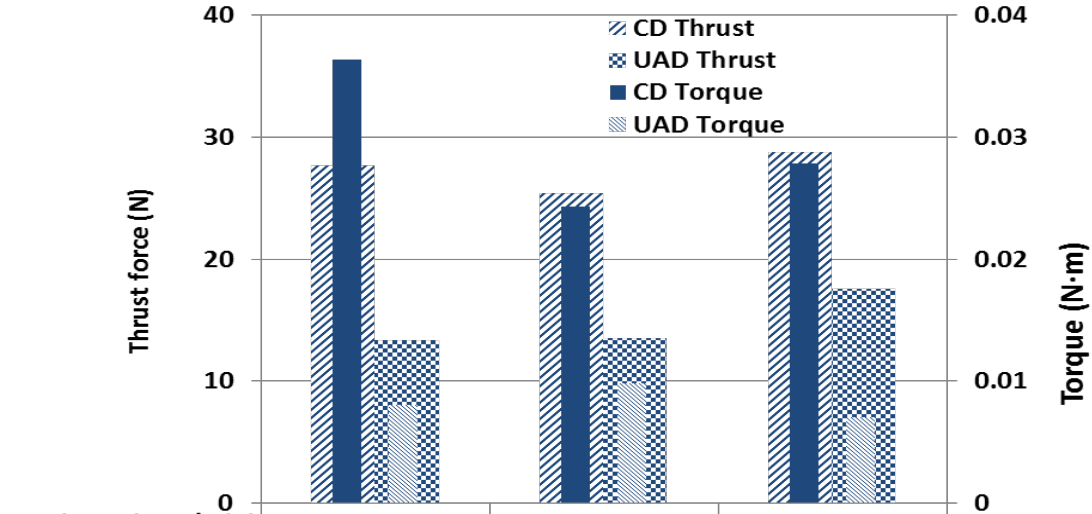

Feed rate (mm/min)	2.55	16.2	36
CD Thrust	27.65	25.35	28.75
UAD Thrust	13.36	13.54	17.58
CD Torque	3.6×10^{-2}	2.4×10^{-2}	2.8×10^{-2}
UAD Torque	8.1×10^{-3}	9.8×10^{-3}	7.0×10^{-3}

Figure 7.21: Comparison of maximum drilling (thrust and torque) forces with UAD and CD of HF/VE

7.1.3.3 Quality of holes on HF/VE composite specimens

It is evident that with forces reduction, the overall quality of drilled hole improved with UAD. A comparison on CD and UAD physical damage effects and the quality of the drilled holes produced are presented in Figure 7.22(a). This result agrees with the experimental results recently obtained by Hejjaji et al. (2016) on UD GFRP composites, using laser and conventional drilling techniques. This implies that UAD technique enhanced the machinability of HF/VE composite specimen, because the lower the drilling (thrust and torque) forces, the better the machinability of the composite material. However, fibre pull-out was detected visually on few specimens after drilling exercise using an Alicona InfiniteFocus microscope. The micrographic results are depicted in Figure 7.22(b).

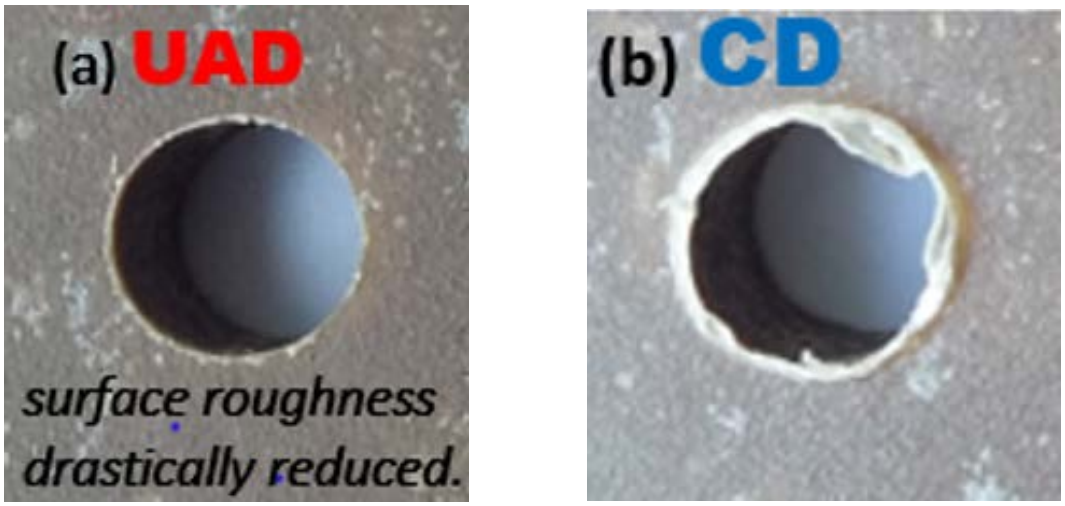

Figure 7.22(a): An improved physical surface quality with (a) UAD, compared with (b) CD of HF/VE (Ismail et al., 2016e)

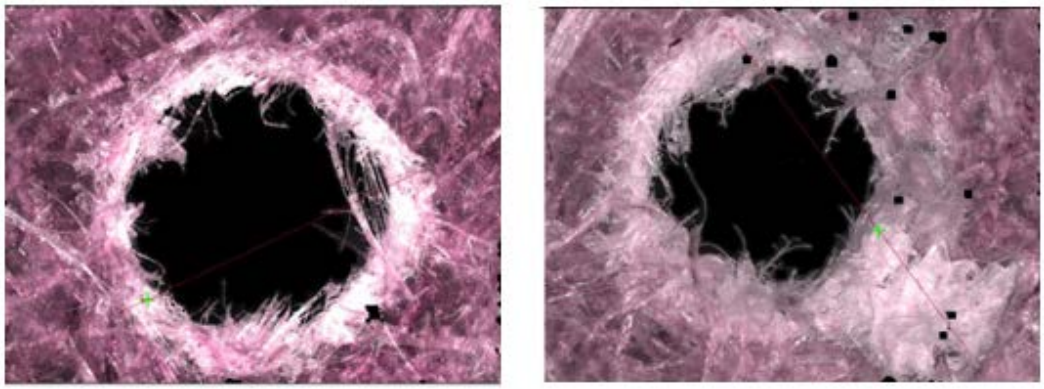

(a) **(b)**

Figure 7.22(b): Micrographs of the surface quality with (a) UAD, compared with (b) CD of HF/VE, showing specimen with CD having greater damage (light coloured surface)

Furthermore, these forces reduction, few fibre pull-out and uncut are attributed to the properties of the hemp fibre and VE matrix. The hemp fibre has a lower strength compared with some synthetic fibres, while the VE thermoset resin has a relatively higher thermal (melting) resistance compared with thermoplastic matrix such as polycaprolactone (Ismail et al., 2016a; Speranza et al., 2014; Ismail et al., 2016e). From Figures 7.20-7.26, it can be deduced that the drilled holes roundness on HF/VE specimen are more accurate with UAD. The results obtained also show that using a coolant in form of compressed air improved hole quality. The air cooling reduced the workpiece-tool interface temperature during drilling, which resultantly reduced matrix softening.

7.1.3.4 Drilling-induced damage response (push-out delamination)

From Figures 7.23(a) and (b), the measured peak fibre push-out with UAD was 381 µm, while it was 814 µm for CD. It was obvious that the push-out (exit) delamination in CD was greater than that of UAD. This is in close agreement with the previous results of recent studies (Makhdum et al., 2014; Ismail 2016b; Ismail et al., 2016e). These results further support the enhancement of machinability of HF/VE composite specimen in terms of reduced delamination drilling-induced damage, with UAD. It was clearly observed that UAD performed better twice more than CD technique. Other similar results are in Appendix E11.

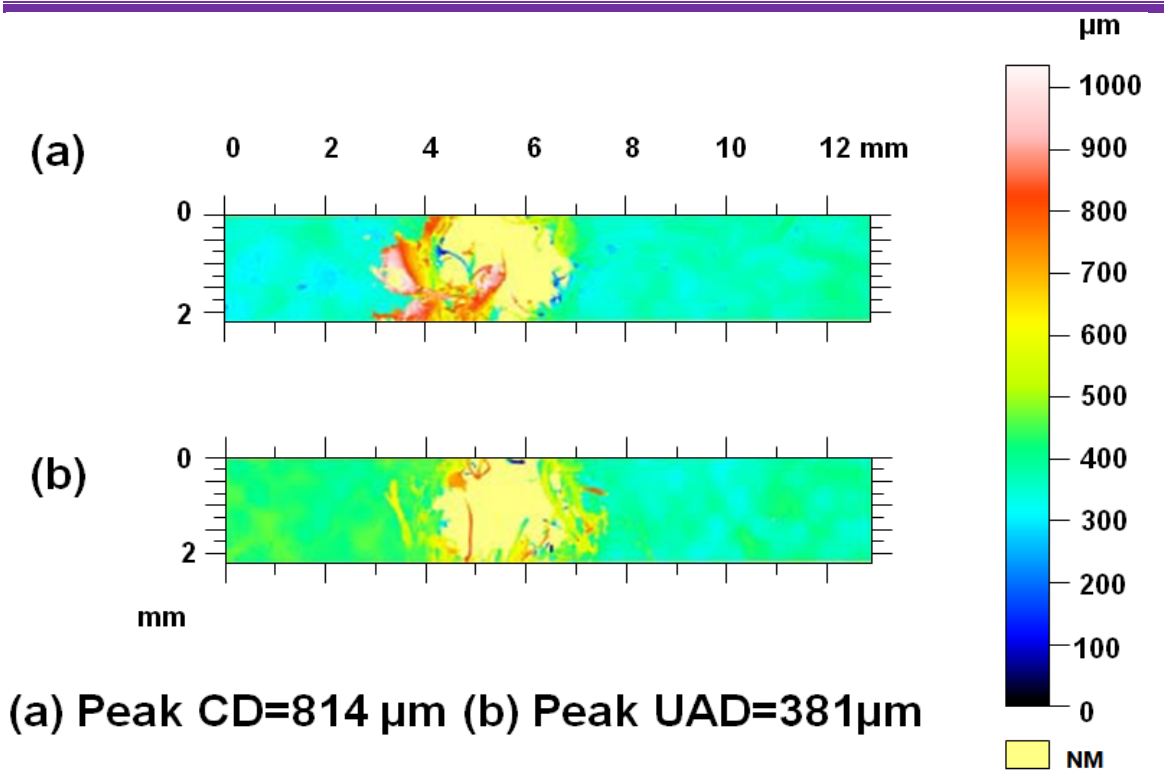

Figure 7.23: Fibre push-out damage for (a) CD (b) UAD, showing a higher value of fibre push-out damage with CD

7.1.3.5 Dimensional accuracy (hole diameter, circularity and roundness)

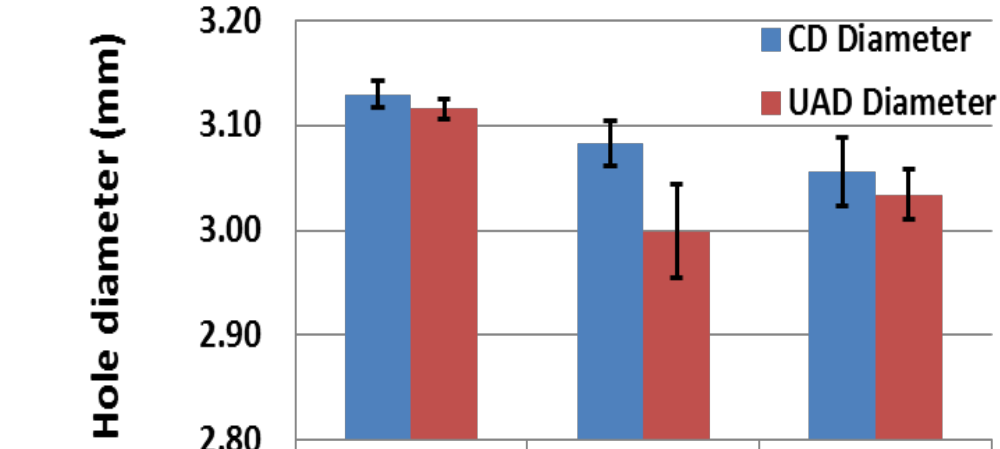

Feed rate (mm/min)	2.55	16.2	36
CD Diameter	3.13	3.08	3.06
UAD Diameter	3.12	3.00	3.03

Figure 7.24: Hole diameters in UAD and CD at varied feed rates, depicting delamination-free hole at feed rate of 16.2 mm/min with Ø 3.00 mm drill bit and UAD technique

At various feed rates, the hole diameter and circularity were measured for both CD and UAD techniques, as shown in Figures 7.24 and 7.25 respectively. Hole diameters in UAD were closer to the drill bit diameter of 3 mm than that of CD. This infers possibility of occurrence of a very little or no delamination with UAD, especially at feed rate of 16.2 mm/min (Figure 7.24). Hole circularities in UAD at lower feed rates are better than that of CD (Figure 7.25). Overall, there are better quality holes obtained from UAD than CD.

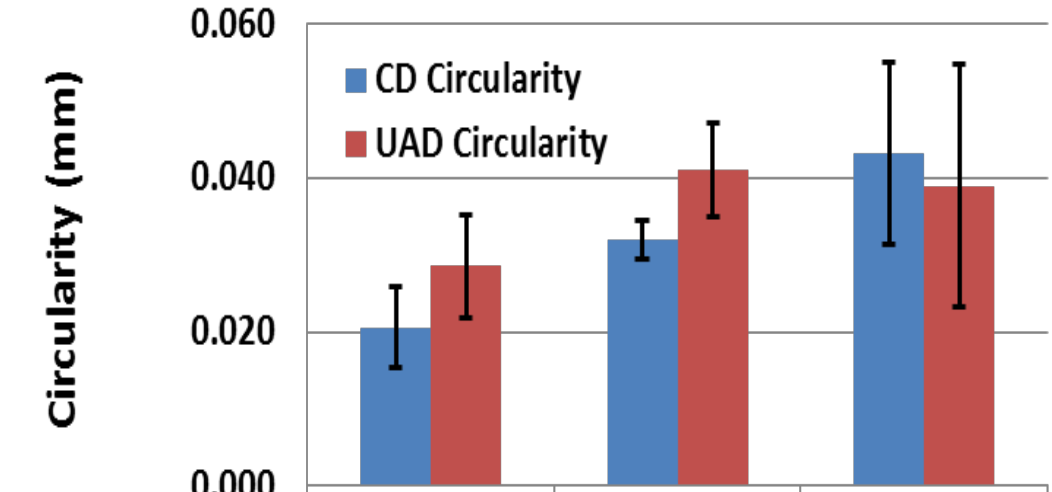

Feed rate (mm/min)	2.55	16.2	36
CD Circularity	0.021	0.032	0.043
UAD Circularity	0.029	0.041	0.039

Figure 7.25: Circularity in UAD and CD at varied feed rates, showing a better circularity at lowest feed rate

Table 7.8: Hole roundness at different depths

Sample (workpiece)	Drilling Technique	Roundness at different depths (mm)		
		0.5	2.0	3.0
HF/VE	CD	0.0273	0.0250	0.0391
	UAD	0.1036	0.0522	0.0656

From Figure 7.26, it is evident that the drilled holes roundness on HF/VE specimens with UAD technique were more accurate than CD, as the hole roundness with UAD is closer to the expected value. More results are included in appendix E8. There are many drilling factors responsible for these better quality holes. These include, but are not limited to, better chip removal and high MRR, without much melting, cratering, burrs, fibre-uncut, fuzzing and pull-out damage. Also, application of compressed air, as a coolant, enhanced the performance. The air cooling was very effective by reducing the interface temperature during the exit of the drill bit, hence reduced the matrix softening phenomenon.

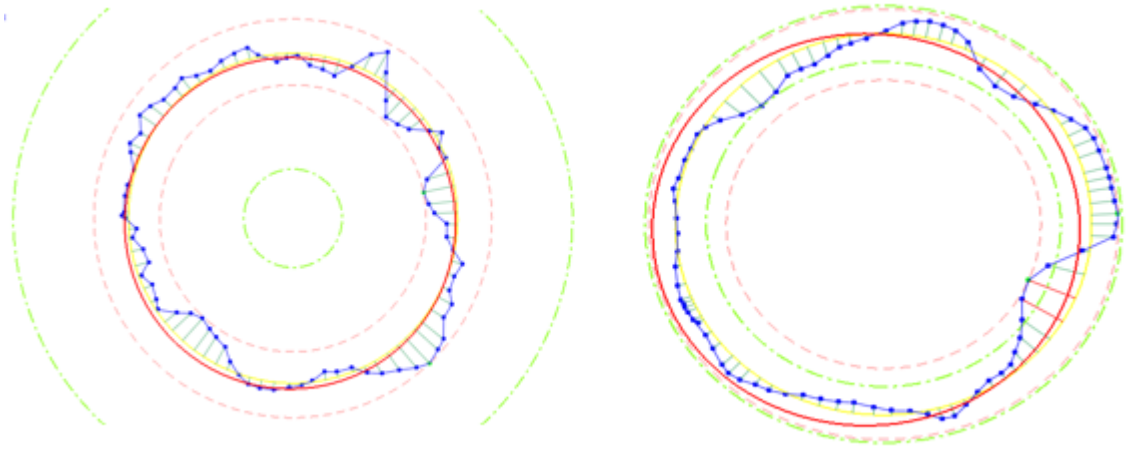

(a) CD **(b)** UAD

Figure 7.26: Hole roundness at 0.5 mm depth for HF/VE composite specimen with (a) CD and (b) UAD technique

7.1.3.6 Thermal results

The maximum temperatures of the drill bit were captured by a thermal camera (Figure 7.27) and recorded for CD and UAD with and without air cooling. The average results are shown in the Table 7.9. It was clear that more heat generated in UAD than CD. This

temperature increase was managed with air cooling, thus thermal damage of HP/VE was avoided.

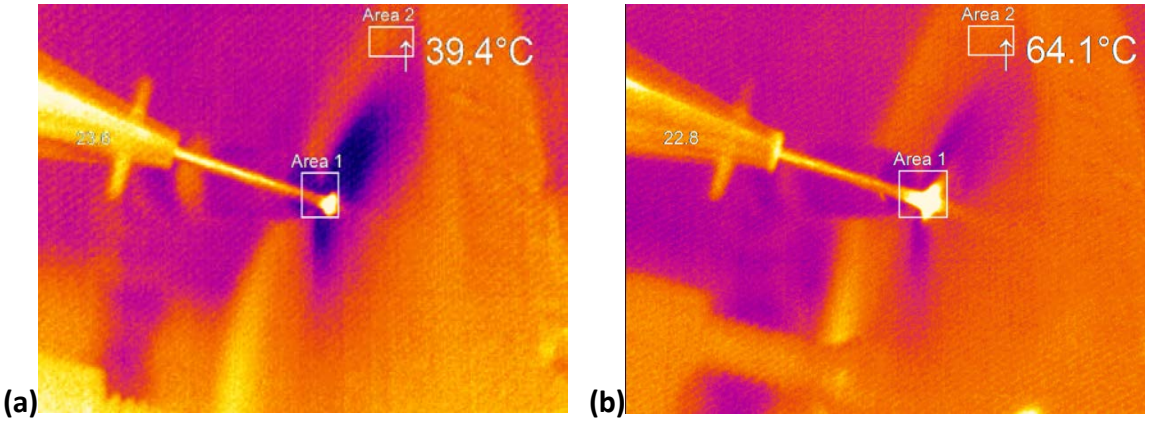

Figure 7.27: Thermal camera showing temperature difference during drilling process with (a) CD and (b) UAD techniques, at same drilling parameter

Table 7.9: Variation in maximum cutting temperature during CD and UAD

Max Temperature (°C)	CD	UAD
Without cooling	71.1	140
With cooling	43.7	65

Thermal camera results obtained indicate that during the UAD process (with cooling), the temperature at the process zone did not exceed the maximum temperature during the normal CD process. The thermo-gravimetric results previously obtained in Figures 7.15(a) and (b) depict that thermal decomposition of the first similar HF/PCL composite specimen was significantly around 200 ^{o}C, which was quite above the UAD maximum temperature of 140 ^{o}C (without cooling), though greater than CD. This implies that the thermal degradation of HF/VE specimen was prevented with application of UAD technique on the specimen, and much more prevented with cooling.

7.2 PHASE B: THEORETICAL (ANALYTICAL) WORK

This is the last part of this research, which involves application of theoretical approach to model the influence of twist drill bit geometry, critical feed rate and thrust force on drilling-induced delamination damage on FRP composite material. The choice of application of analytical approach towards solving composite drilling lies on its exact, fast and time-efficient solutions, when compared with other mathematical, theoretical and numerical methods of solving real life and practical engineering problems.

7.2.1 Thermo-mechanical modelling of FRP composite laminates drilling: Delamination damage analysis

Under the rationale for the proposed models, under sub-section 6.2 of Chapter 6 (analytical approach), it has been established that the proposed models in which their simulated results are discussed below are based on classical plate theory approach and linear elastic fracture mechanics (LEFM) mode I only. Therefore, the proposed analytical models are efficient to predict and analyse onset push-out delamination phenomenon.

7.2.1.1 Effect of ellipticity ratio on minimum critical thrust force

To demonstrate the effect of drill characteristics on the delamination of the FRP composite, a cross-ply laminate sequence consisting of 16 plies with material properties detailed in Table 7.10 is considered. Delamination is assumed to occur when the laminate is drilled so that there are n uncut plies below the drilled hole. Effect of drill characteristics (chisel edge and point angle ratios) on the critical thrust force and the critical feed rate are analysed and comparison of the proposed model with other models in the literature are also demonstrated. The underlying assumption in the analysis of the point angle is that the dependence of the critical thrust force is significant when the total thrust force is composed of part contributions due to the cutting lips and the chisel edge.

Table 7.10: The material properties of the CFRP cross-ply composite laminates (Ismail et al., 2017)

Material	E_1 (MPa)	E_2 (MPa)	v_{12}	G_{12} (MPa)	α_1 (10^{-6}/K)	α_2 (10^{-6}/K)	G_{IC} (N/mm)	h (mm)
CFRP	175.9	8.1	0.32	4.4	-0.07	30.9	0.328	0.3125

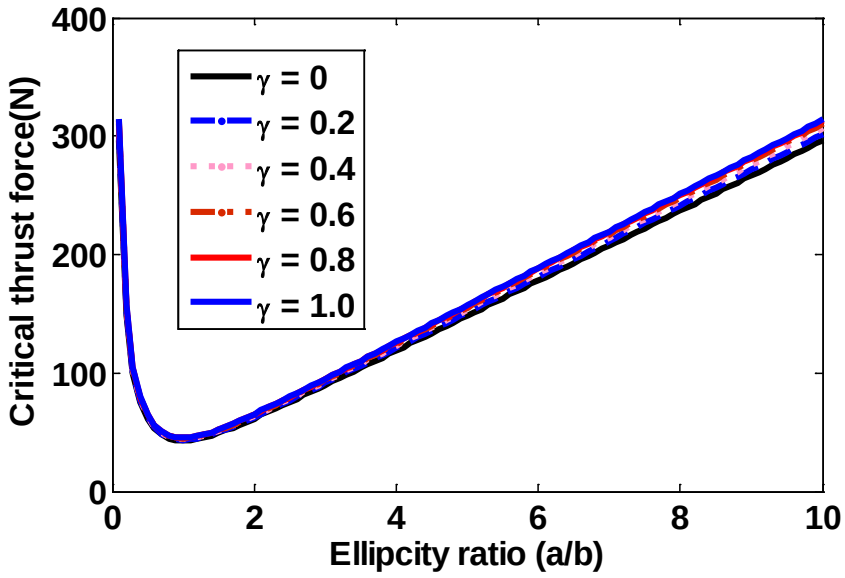

Figure 7.28: Ellipticity ratio effect on minimum critical thrust force (Ismail et al., 2017)

The critical thrust force is a function of ellipticity ratio according to Equation (6.37) in Chapter 6. Additionally, the effect of ellipticity ratio η of the critical thrust force is shown in Figure 7.28 where it is inferred that the ellipticity ratio for which the critical thrust force is minimum must be less than 1 for a range of values of chisel edge ratio, γ. At this minimum value, the possibility of delamination is quite lower. Meanwhile, immediately after ellipticity ratio of 1, ellipticity (delamination zone) increases with the critical thrust force, implies increase in delamination damage.

7.2.1.2 Effect of chisel edge load on minimum critical thrust force

Analysis of the effect of chisel edge ratio on the minimum critical thrust force in Figure 7.29 shows that the critical thrust force increases to a peak and then reduces with increasing chisel edge ratio. For a fixed value of the chisel edge ratio, the critical thrust force increases with increasing point angle ratio and this effect is more profound at low chisel edge ratio. This is an important observation since it underscores the significance of the point angles for a specific drilling operation and also confirms the findings in Langella et al. (2005). Both Figures 7.29and 7.30 depict that effective control and selection of the drill bit geometrical parameters (reduced chisel edge and point angle) could enhance possibility of delamination-free drilling of CFRP composite laminates using higher feed rate and thrust force.

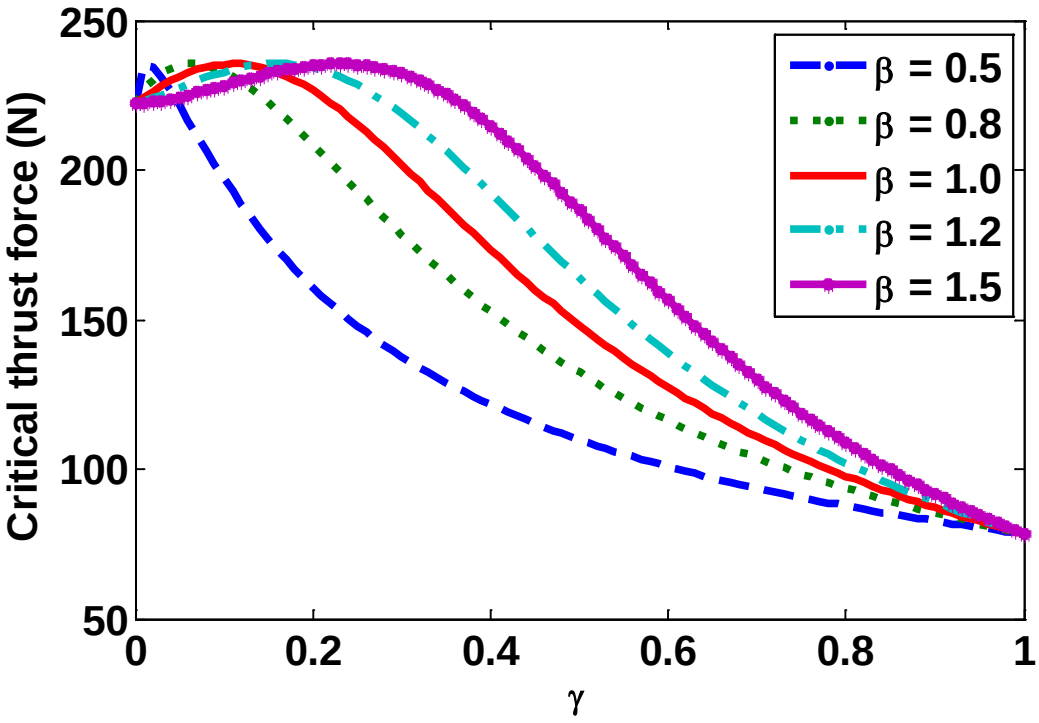

Figure 7.29: Effect of chisel edge load on minimum critical thrust force for different point angles (Ismail et al., 2017)

7.2.1.3 Effect of chisel edge load on critical feed rate for different point angles

Furthermore, it is observed in Figure 7.30 that critical feed rate dependence on the chisel edge ratio and the point angle ratio keeps the same profile like the critical force. This is expected since there is a direct proportional relationship between the thrust force and the feed rate.

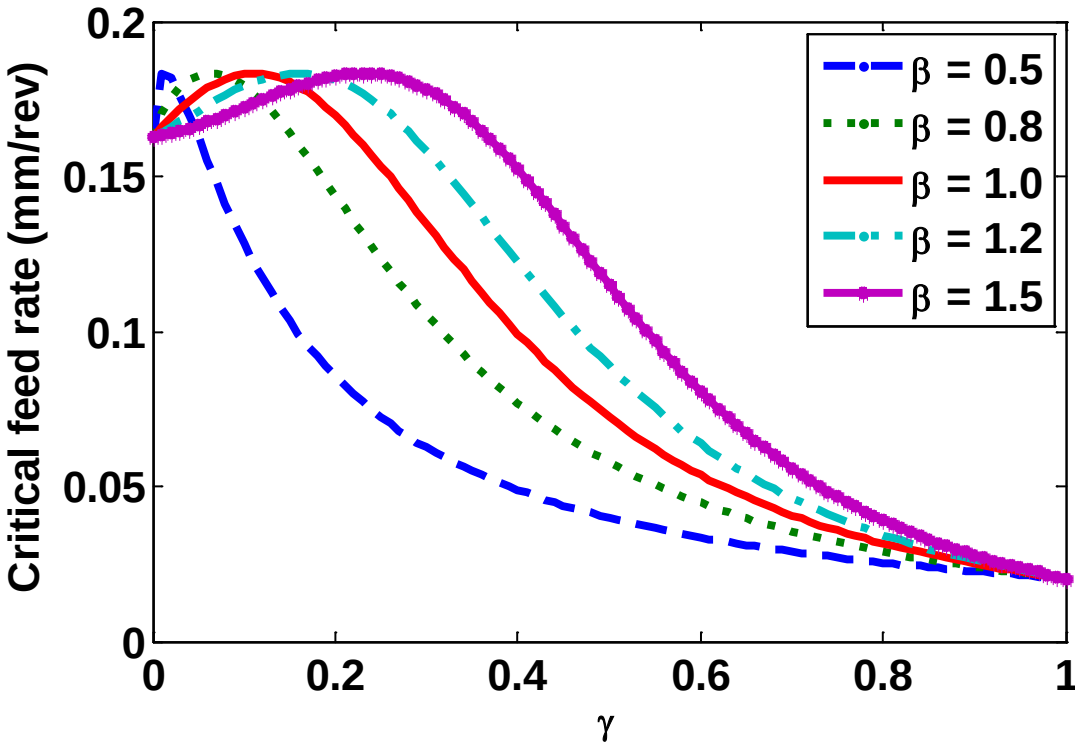

Figure 7.30: Effect of chisel edge load on critical feed rate for different point angles ($\varphi = 550$ N rev/mm) (Ismail et al., 2017)

7.2.1.4 Relationship between thrust force and feed rate

Moreover, feed rate can be related with the thrust force (Figures 7.30 and 7.31). This may be necessary in order to facilitate direct programming of feed rate into the CNC machine centre, to predict the thrust force towards having delamination-free composite drilling. This is possible because thrust force depends on feed rate. Meanwhile, the concerned feed rate is a function of feed per revolution (mm/rev), not a linear feed rate

in inches per minute (’’/min). Summarily, it is evident that a lower thrust force is a function of a lower feed rate; the thrust force increases with the feed rate.

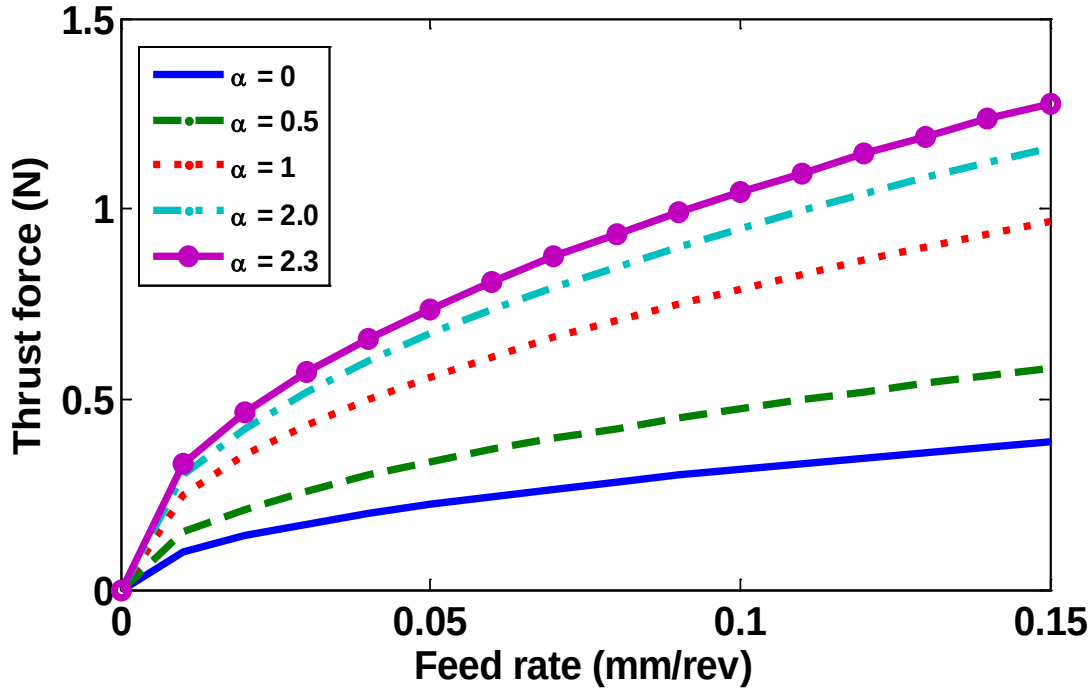

Figure 7.31: Effect of feed rate on thrust force at different α ratio (Ismail et al., 2017)

During experimental drilling of FRP composite laminate, the critical thrust force increases rapidly as the drill bit tends to gain entry into the laminate at inception. It increases to a peak before a steady state condition is maintained at full engagement of the drill inside the laminate, with nearly half number of the total plies. Immediately after this state, the drill bit approaches the exit side of the hole at a decreasing number of uncut plies, the critical thrust force is drastically reduced. The results obtained and presented in Figure 7.32 unambiguously supports the reported drilling phenomenon (Ismail et al., 2016c).

7.2.1.5 Comparison of the proposed model with existing models

Neglecting the effect of temperature, the proposed model captures contributions of distributed and concentrated loads with limiting values approaching Gururaja and Ramulu

(2009) distributed load model for $\gamma = 0$ on one hand and Jain and Yang (1993) concentrated load model for $\gamma = 1$ on the other hand, as depicted in Figure 7.32. Also, it is observed from Figure 7.32 that behavioural increase of the predicted critical thrust force as the number of the uncut ply increases.

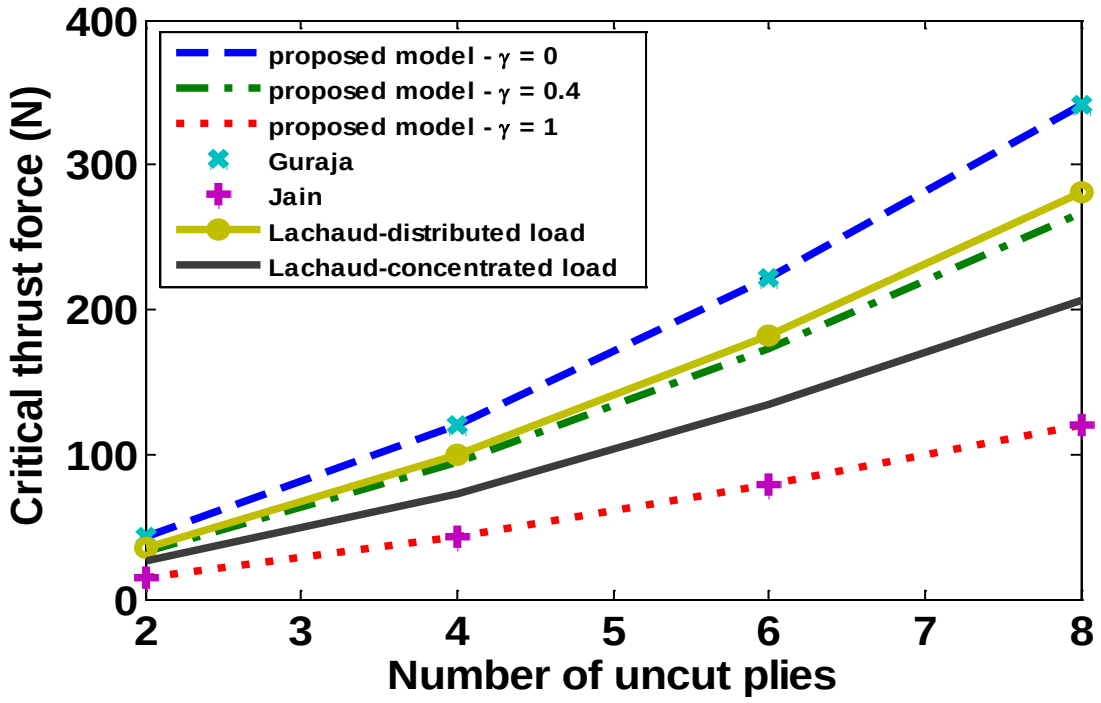

Figure 7.32: Minimum critical thrust force for different models and the proposed model (Ismail et al., 2017)

It is evident that at low number of the uncut ply, especially at 2, all the models have a very close values of predicted critical thrust forces. The proposed model with $\gamma = 0$ predicts the Gururaja and Ramulu (2009) model exactly. On this basis, the model proposed in this work is validated against existing models in the literature and specifically, Lachaud distributed and concentrated load models is compared with the proposed model with varying chisel edge ratio. It is shown in Figure 7.32 that with $\gamma = 0.4$, the result for the proposed model approaches the Lachaud distributed load model, an observation which signifies the flexibility of the proposed model based on chisel edge contribution to the total thrust force. In addition, the proposed model with $\gamma = 0.4$ predicts lower critical thrust force than the Gururaja and Lachaud distributed models.

7.3 Summary

This research has investigated and analysed the machinability and drilling-induced damage on both natural hemp fibre-reinforced polymers (thermoplastic polycaprolactone and thermoset vinyl ester) and synthetic carbon fibre-reinforced polymer (epoxy resin) composite materials. The main conclusions of this investigation are stated in the next chapter. Based on the experimental and theoretical results presented and discussed in this chapter, these subsequent summaries are hereby sequentially highlighted.

Firstly, the hemp fibre aspect ratio significantly influenced the delamination and surface roughness drilling-induced damage, among other drilling-induced damage associated with HFRP composite specimens. An increase in aspect ratio caused an increase in the delamination factor and surface roughness of the HFRP specimens. In addition, the results depict that an increase in cutting speed reduced the delamination factor, whereas increase in feed rate caused an increase in delamination factor. However, surface roughness increased with an increase in feed rate unlike the cutting speed which has a smaller effect; surface roughness decreased with an increased cutting speed. It was also observed that feed rate has a greater influence on delamination, while cutting speed has a greater effect on surface roughness of the HFRP composite specimens. These results were strongly supported by ANOVA technique. The optimal specimen and drilling parameters were 19-HFRP composite specimens and cutting speed and feed rate of 20 m/min and 0.10 mm/rev respectively. More also, few uncut fibre and fibre pull out were observed in 5.0 mm holes especially at feed rates of 0.05 and 0.10 mm/rev with cutting speeds of 10 and 20 m/min respectively. Also, minimal burrs occurred at the entrance of the 10.0 mm holes at feed rate of 0.05 mm/rev with 30 and 40 m/min cutting speeds. Moreover, short and melted chips formed at lowest feed rate and cutting speed, as depicted in Figure 7.6(a). Meanwhile, continuous ribbon-like chips formed at 0.20 mm/rev and 40 m/min feed rate and cutting speed respectively (Figure 7b); the higher the feed rate and cutting speed, the wider, longer and lighter the chips.

Secondly, there was a case of both peel –up and push-out delamination types in a single

hole of CFRP specimens when drilling at f = 0.20 mm/rev & v =10 m/min. Also, an increase in feed rate caused an increase in delamination and surface roughness of both specimens, unlike the delamination and surface roughness of both specimens which increased with a decrease in cutting speed. The delamination defect was greater in the CFRP (synthetic) composites when compared with the HFRP (Natural) composite laminates, under the same drilling conditions. But, HFRP specimens suffered greater surface roughness. These results could be traced to the clear difference in their chips formation, morphology and composite constituents or compositions. Comparatively, from the ANOVA results, it is evident and confirmed that feed rate has a greater effect (value of 0.302) on CFRP composite specimen, which consequently resulted into higher delamination factor. However, the lower value (-0.888) of effect of cutting speed on HFRP composite specimen resulted into a greater surface roughness damage. Furthermore, the MRR of both specimens has a direct proportionality to diameter, feed rate and cutting speed; it shows that the MRR increased with these drilling variables. Comparatively, the optimum drilling conditions and better hole surface quality for both specimens were associated with the use of the smaller drill diameter 5.0 mm, as bigger diameter 10.0 mm supported greater delamination and surface roughness, especially when drilling at a lowest feed rate of 0.05 mm/rev and cutting speed of 20 m/min. These results were confirmed by the SEM micrographic results obtained.

Thirdly, the optimum drilling and best quality drilled holes were achieved on 19-HF/PCL composite specimen, in terms of a relative lowest thrust force reduction and drilling-induced damage, which include mainly burrs formation, fibre-uncut and surface roughness. However, these results occurred with an insignificant drilling forces reduction using UAD and a high matrix burning or melting. Conversely, there were significant and substantial reductions in the thrust forces and the torques (drilling forces) using UAD on HF/VE specimens, when compared with CD. The average drilling forces was reduced by approximately 40 % with UAD in comparison with CD, with better material specimen integrity, hole quality in terms of lower push-out delamination and surface roughness, as well as an improved dimensional accuracy considering hole diameters, circularity and roundness.

Fourthly and theoretically, a thermo-mechanical analytical models for predicting and analysing onset push-out delamination have been successfully formulated and proposed. The chisel edge, point angle and cutting lip are very important parts of designed twist drill geometry, because the quality of drilled hole greatly depends on these geometry as both concentrated and uniformly distributed loads acted during FRP composite drilling. These loads determined the feed rate and consequently, the thrust force which is the principal factor responsible for the drilling-induced delamination damage on the composite materials. Therefore, the later part of this study explained an analytical modelling of effects of drill geometry on a delamination during composite conventional drilling. The integration of the influence of drill geometry (chisel edge and point angles/cutting lips) and mixed loads (concentrated and uniformly distributed loads) on push-out delamination enhanced the novelty, advantages and better prediction of this proposed analytical model, when compared with the existing models in literature. These two forces acting on chisel edges and cutting lips were modelled as a concentrated (point) and uniformly distributed loads. Elucidation of the results implied that an increase in chisel edge ratio caused an increase in both feed rate and thrust force. The validation of the proposed model was conducted using the models available in the previous research. The results obtained depict the flexibility of the proposed analytical model as the results of the existing models were accurately predicted.

Pen ultimately, it is evident that a good knowledge of FRP composite drilling through a well-designed drill geometry, correct selection of material specimens, drilling conditions, parameters and techniques afford better opportunity of developing drills and drilling composites with reduced or without drilling-induced damage, and resultantly producing a high quality drilled hole surface. Therefore, the possibility of reducing the delamination drilling-induced damage on the considered FRP composite specimens lies in the use of lower feed rate with higher spindle speed (Appendices E9 and E10), using smaller diameter of double-fluted and coated HSS twist drill bits. Machining operation under dry or compressed air cooling environment is preferably better for drilling of FRP composites materials because of the hydrophilic and hydrophobic natures of both fibres and matrices

respectively, of some sustainable FRP composites such as HFRP composites. Hence, drilling of better quality holes in sustainable FRP composites is possible under these machining (drilling) specifications. More detailed conclusions are given in the next chapter, as expected.

Lastly, with respects to the economic (cost) implication of this research, a huge amount of money is spent on drilling tools yearly in many developed countries. For example, industries in United State alone used close to 250 million twist drills yearly and spent in 1991 close to $1.62 billion for drill bits production (Ertunc et al., 2001). Therefore, a broad understanding of the effective drill design and application towards drastic reduction in drill bit wear and cost as well as FRP composite material delamination damage, surface roughness, fibre pull-out, fibre uncut, to mention but a few are targets that have been achieved in this research study, based on the recommended combined drilling factors (Chapter 9). Global demand for and applications of FRP composite materials are increasing exponentially, hence the need for design an optimised drill for damage-free composites machining is highly imperative. Delamination of composite materials and rapid tool wear are the main problems encountered when drilling synthetic CFRP composites, accounting for drilling-induced damage as high as 60 % (Sakthivel et al., 2015; Ismail et al., 2016b), leads to waste of capital, man-power, energy, time and other resources used in production. Furthermore, the drill bits, especially HSS type, have a widest range of application in several manufacturing, aerospace, communication, sports, marine, automobile industries, among others (Ismail et al., 2016b). These companies are vibrant sectors of the economy. Solving their difficult problems will not only lead to increase in productivity and profitability, but to national economic development and growth.

PART VI

CONCLUSIONS

&

RECOMMENDATIONS

CHAPTER EIGHT

CONCLUSIONS

8.0 Introduction

This is the concluding chapter that presents the general and detailed summary of the whole research conducted within the aims and objectives (scope) of this work. The conclusions are arranged sequentially, starting from the comprehensive review of literatures, following by the three consecutive experimental works, designated as stages 1-3 and the theoretical findings. Lastly, the overall conclusions are drawn.

8.1 On critical literature review

A highly efficient twist drill is the outcome of innovation and ingenuity. Recent advances in twist drill design with respect to composites drilling have been critically reviewed and presented. The following summaries can be drawn:

- HSS twist geometry is the most commonly used type of drilling tool due to its outstanding performance with regards to better chip removal, availability, mass production and cost effectiveness. It has a highest percentage (47 %) of applications; 24 applications out of 51 recent research works considered from more than a decade, years 2000-2012 inclusive. Other tooling materials include UCC, CCC and PCD have 13, 09 and 05 users, having 25, 18 and 10 % of applications respectively.
- The chisel edge, point and helical angles are the most important parts of twist drill designed geometry. Majority of the drilling-induced damage, especially delamination, fibre pull-out of FRP composite materials and fast drill wear are caused by these drill bits geometry. The quality of drilled hole depends greatly on the drill geometry, design, materials and selected drilling parameters. In addition, delamination of FRP composites and rapid tool wear are the two main and critical problems encountered when drilling CFRP composites accounting for drilling-induced delamination damage

as high as almost two-third of the total drilled products. These damage increased the time and cost of machining (manufacturing). Delamination decreased the assembly tolerances, reduced the bearing strength of engineering materials and reduced the components performances at a long term when subjected to fatigue loads.

- PCD provided best surface finish at high drilling parameters (cutting speed and feed rate), when compared with other tooling materials. Improved surface quality and dimensional accuracy of composite materials could be achieved using carbide especially coated types, specially designed drills and PCD drills. However, these drills are not yet commercially available. Therefore, they are more expensive when compared with HSS twist drills.
- Importantly, a good knowledge of drilling parameters, composite materials and well-designed drill geometry afford better opportunity of developing drills that will minimise delamination effect on the FRP composites, tool wear and produce a high quality drilled hole surface.

The drill design engineers and manufacturers will obtain a comprehensive understanding of the recent advances in twist drill design for fibre-reinforced composites drilling by going through the literature review parts (chapters 2 and 3) of this research, with intention of improving and optimising the efficiency of drills and solving challenges confronting composites drilling.

8.2 Phase A: Experimental works

8.2.1 Stage 1: Conventional drilling of HF/PCL composites of different aspect ratios

The achieved main aim of this stage 1 experimental study was to optimise the drilling process of HFRP composite laminates. It was achieved by determining the predictable parameters of drilling in accordance with the aspect ratio of the composites. Hence, the effects of cutting speed, feed rate and aspect ratio have been investigated on delamination and surface roughness of drilled holes of HFRP composite laminates. The following conclusions can be made:

- The effect of feed rate on delamination and surface roughness increased with the aspect ratio. An increase in cutting speed reduced the delamination factor, whereas an increase in feed rate caused a substantial increase in delamination factor. Hence, low feed rate and high cutting speed minimised delamination effect. Also, feed rate has a greater influence on delamination and surface roughness when compared with cutting speed; surface roughness increased with the feed rate unlike the cutting speed which has a small effect; increase in cutting speed caused decrease in surface roughness of the specimens.
- In addition, surface roughness increased with the lignocellulosic hemp fibre aspect ratio. This increase was greater when compared with an increase in delamination with the same aspect ratio. Delamination damage was lower in HFRP composite laminates when compared with the experimental results obtained on CFRP composite materials from extant literature.
- Significantly, the optimum result was obtained with specimen of AR 19, at cutting speed and feed rate of 20 m/min and 0.10 mm/rev respectively.

8.2.2 Stage 2: Conventional drilling of optimal HF/PCL and CF/EP composite specimens

The conventional drilling-induced damage analysis, mainly on delamination and surface integrity of drilled lignocellulosic 19/HFRP and UD MTM 44-1/CFRP OC composite specimens, has been carried out experimentally. The following results obtained are hereby summarily highlighted:

- Evidently, the drilling-induced damage were more protuberant and severe in the CFRP specimens than the HFRP composite specimens when considered under the same conditions. The SEM micrographic results obtained depict that there were more fractured carbon fibres than the hemp fibres, most importantly at an increased feed rates of 0.15 and 0.20 mm/rev.
- The damage on both FRP composite specimens significantly depended on the drilling parameters and properties of their constituents (fibres and matrices). An increase in drilling parameters affected the drilled hole quality of both HFRP and CFRP specimens, because the hemp fibre and its PCL matrix of HFRP specimens have a lower thermos

mechanical properties, in terms of matrix melting and fibre decomposition or disintegration temperatures when juxtaposed with carbon fibre and its EP matrix.

- Moreover, the SEM micrographs show that an increased drill diameter affected the surface integrity of both specimens more than causing delamination defect, because the bigger drill diameter produced greater MRR and chips, which could not be easily evacuated due to the nature of the chips generated and their morphologies from the two specimens. In addition, the X-ray micro CT examination depicts that minimal burrs formation and few uncut-fibre defects were associated with the HFRP composites drilling. However, these damage were not rampantly observed on the CFRP composite specimen due to the properties of its constituents, but CFRP specimen was mainly characterised with inter-laminar cracks and delamination.
- There was a discontinuous chips formation, which was abrasive and powder-like in nature during drilling of CFRP composite laminates, unlike a continuous chips formation, long and coiled, which characterised that of HFRP composites. These types and quantity of chips formation determined the type and severity of the drilling-induced damage occurred.
- The minimal drill wear was noticeable on CFRP composite specimens after drilling 64 holes, 32 holes using diameter 10.0 mm and 5.0 mm each, while there was an insignificant or null wear evident on the HSS twist drill used after drilling HFRP composite specimens. This was traced to the medium range of drilling parameters selected and the properties of HFRP specimens compared to CFRP.
- The minimum surface roughness and delamination factor of the two specimens for the optimum drilling were associated with a feed rate of 0.05-0.10 mm/rev and cutting speed of 30 m/min. Therefore, the optimum drilling conditions, surface finish and hole quality on the specimens appeared to occur at a low feed rate, moderate high cutting speed and a small drill diameter employed.

Lastly, based on the statistical ANOVA and other micrographic results obtained, the CFRP specimen has a lower surface roughness (better surface finish), while HFRP composite specimen exhibited a lower delamination drilling-induced damage. Both

specimens were considered and analysed within the same drilling conditions and parameters. Hence, the choice of their engineering applications should depend on their different responses to these damage.

8.2.3 Stage 3: Conventional and ultrasonically-assisted drilling techniques on HF/PCL and HF/VE composite specimens

A dry conventional drilling (CD) and a novel ultrasonically-assisted drilling (UAD) techniques have been comparatively experimented on both HF/PCL and HF/VE composite specimens. The special benefits of a significant drilling forces (thrust force and torque) reduction using UAD over CD technique have been comprehensively analysed and experimentally achieved under Taguchi method of design of experiment. Based on the results obtained, the following summaries are hereby drawn:

- The mechanical properties of the HFRP composites depended on the aspect ratio of the hemp fibres; the reinforcement and strength of the composite specimens increased with the aspect ratio. These were observed through the increased thrust force and machining time recorded during drilling of the five specimens. Therefore, an increase in aspect ratio facilitated an increase in the occurrence of flaws with reference to the drilling-induced damage which include, but are not limited to, delamination, surface roughness and matrix melting.
- The surface quality of the HF/PCL specimens decreased as their aspect ratios increased. The surface roughness of the 38-HF/PCL composite specimen was the highest and comparatively, higher with UAD than CD technique, indicating that UAD technique was not exactly suitable for the machining of natural or FRP bio-composites with higher aspect ratio and a lower thermoplastic matrix melting point or decomposition temperature. The cutting (tool-workpiece interface) temperature generated by the higher AR of the hemp fibre was too high for the PCL to withstand without occurrence of melting or burning. However, these challenges of drilling HF/PCL composite specimens with UAD were drastically reduced with thermoset VE resin, for the same optimal 19-HF specimen.

- Consequently, a nearly 40 % of an average forces reduction was observed by using UAD technique, when compared with the CD of HF/VE composite specimens under a certain drilling conditions and parameters. A low thrust and torque forces resulted in desirable delamination-free (machinability) that enhanced the structural integrity and performance of the FRP composite components.
- Notably, the outstanding performance of the UAD technique, better than the CD, can be traced to the intermittent, vibro-impact character of the operation, as well as the tendency of a decrease in frictional coefficient at the cutting interface and material hardness during UAD operation. These can also be attributed to the increase in relative sliding velocity which was translated into a significant decrease in the total drilling forces at the tool-workpiece interface. Moreover, the vibration effect on the drill bit during UAD generated an adiabatic heat transfer which further enhanced the plastic deformation and acoustic softening effect on the HF/VE specimen.
- Evidently, better total quality holes were obtained from UAD than CD technique in comparison of their hole diameter, fibre push-out/uncut, ply-exit delamination, circularity and roundness, as the cutting temperature of drill bit dropped significantly in UAD with application of compressed air cooling. Consequently, this makes UAD technique recorded a novel feasibility of drilling a bio-composite or sustainable hemp fibre-reinforced thermoset polymer composite specimen.
- Conclusively, the total quality of drilled holes of the bio-composite (19-HF/VE) specimen was greatly depended on the drilling conditions, techniques and thermo-mechanical properties of the composite (matrix and fibre).

8.3 Phase B: Theoretical (analytical) work

8.3.1 Analytical models for predicting and analysing drilling-induced delamination damage

A new thermo-mechanical models for the prediction of critical thrust force and critical feed rate has been proposed in this work. The new model takes into account the effect of drill characteristics such as the chisel edge load and the point angle. It also detailed the

thermal effect of the drilling operation. Essentially, the proposed model was formulated based on part contributions of distributed load by the cutting lips of the drill and concentrated load by the drill chisel edge. This mixed load condition allowed for the introduction of point angle variable which is a novelty with respect to existing models in the literature. Analysis of the results showed that with an increasing chisel edge ratio, the critical thrust force and the feed rate increased to a peak and then approached the limiting value of the thrust force and feed rate for a concentrated load condition. The model was validated with extant models in the literature and the results obtained show the flexibility of the proposed model to imitate the results of existing models.

8.4 Overall conclusions (summary)

The delamination defect could be either drastically reduced or totally avoided with correct selection of combination of the drilling factors including drilling parameters and conditions, drill materials and geometry, drilling technique and experimental design (with support or backup plate) as well as the proper knowledge of the tooling materials, constituents and orientations (nature and properties) of the specimen (FRP composite laminates). Hence, [1]*the best combination of drilling systems was found in aspect ratio of 19-sustainable hemp fibre-reinforced thermoset vinyl ester polymer composite with a hybrid UAD technique, using pre-drilled aluminium support or backup plate, 118^{o} point angle and Ø3 mm (small diameter) Jobber carbide TiN-coated HSS twist drill, compressed air cooling, low feed rate and high cutting speed.* [2]*Also, the proposed thermo-mechanical and analytical models have been formulated and validated to accurately predict and analyse onset push-out delamination during FRP composite drilling.* Notwithstanding, the next and last chapter gives a few recommendations both from this study and for the future improvement and optimisation of this research work.

[1] Literature & experimental works

[2] Theoretical (analytical) work

CHAPTER NINE

RECOMMENDATIONS FOR FUTURE WORKS

9.0 Introduction

This chapter suggests recommendations based on the findings of this research. It also presents a brief recommendations for future works for improvement and optimisation of the whole FRP composite drilling systems.

9.1 Recommendations from the research

According to the optimal experimental and analytical results obtained from this research, the subsequent recommendations for the FRP composite users, manufacturers (industries) and researchers (academia) are proposed, as summarily and schematically shown in Figure 9.1 for highly improved FRP composite (especially HFRP) hole quality and efficient drilling operation.

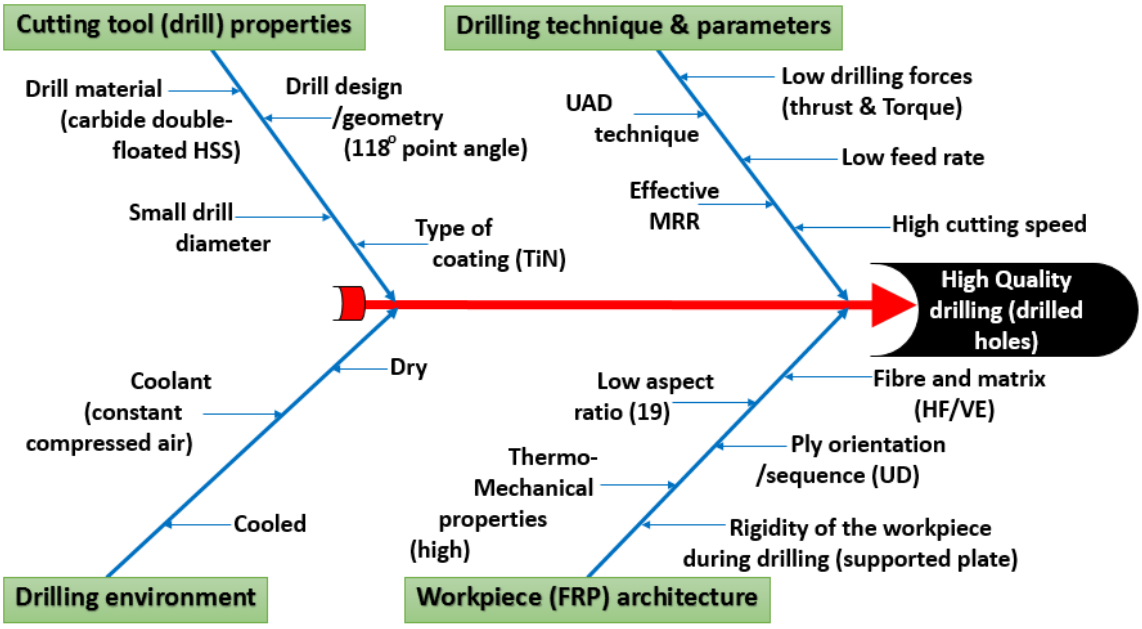

Figure 9.1: Recommended drilling systems for high quality drilling (drilled holes) of sustainable HFRP composite specimens

9.2 Recommendations for future work

Due to the limitation of time, finance and unavailability of some machines and instruments (laboratories), the following few studies are here recommended for the future improvement, betterment and optimisation of this research work.

9.2.1 Experimental works

[1] The use of other sustainable FRP composites with less than fibre aspect ratio of 19 include, but are not limited to, flax, jute, sisal and basalt fibre-reinforced polymer/matrices (both thermoplastics and thermosets) is recommended for further comparison and anticipated improvement in FRP composite drilling. These composites include woven and hybrid types of FRP composites, biodegradable (bio-based) and synthetic types such as polylactide (PLA) and polyethylene (PE) matrices respectively could also be used for the specimens fabrication before subjected to different drilling operational techniques.

[2] The following non-conventional (modern) drilling techniques: laser beam, vibratory-assisted, rotary ultrasonic-assisted, abrasive and water jet and electric discharge drillings, in addition to ultrasonically-assisted drilling are hereby suggested for the further comparative drilling of the composite specimens used within the scope of this research work and other aforementioned or recommended types of FRP composites.

[3] The application of other drill bits of various diameters include, but are not limited to, core, brad, dagger, step, saw, candle stick and special drill bits with different geometry, tooling materials as well as coated and uncoated types should be encouraged on different recommended FRP composites so that further and better comparison can be drawn from their performances, resulting to the choice of the best that is probably better than the double-fluted HSS drill bits used throughout this experimental and theoretical research works. The choice of the best drill bit should be based on ability to produce holes with lowest or no drilling-induced damage associated with FRP composites drilling. In addition, these drills could also be used on the aforementioned non-conventional (modern) drilling techniques.

[4] A trial of wet drilling with application of liquid coolant such as Cindolube V30ML can be carefully used. From literature, the use of this liquid coolant has a very little or no effect on the hydrophilic nature of FRP composite during drilling process. This coolant did not support the high water absorbability, hence it recorded a lowest damaging influence on the mechanical properties of the CFRP composite material (Turner et al., 2015). The results obtained can be compared with that of the dry machining environment.

9.2.2 Theoretical (analytical) work

[1] A future development is to validate the proposed model with experimental drilling operation which is strongly characterised by thermo-mechanical deformation. Similarly, further validation of the proposed model should be carried out using constitutive material properties of sustainable FRP composite specimens, especially that of HF/VE composite specimen.

[2] In addition, unlike the general models in the literature which derived only mode I energy release rate based on the assumption of classical laminate theory (CLPT) combined with linear elastic fracture mechanics (LEFM) mode I in the elliptic delamination zone, an improved analytical model which is derived based on first-order shear deformation theory (FSDT) is highly recommended, and it should account for mode II energy release rate in the delamination zone. This strategy will allows to activate mixed mode condition for delamination of the FRP composite laminates which is a valid assumption for laminates with layers of different orientations. Currently, a new analytical modelling work has started according to this last recommendation.

PART VII

REFERENCES

&

APPENDICES

References

Abdul Nasir, A. A., Azmi, A. I., & Khalil, A. N. M. (2015). Measurement and optimisation of residual tensile strength and delamination damage of drilled flax fibre reinforced composites. *Measurement*, *75*, 298-307.

Abele, E., & Fujara, M. (2010). Simulation-based twist drill design and geometry optimization. *CIRP Annals - Manufacturing Technology, 59*(1), 145–150.

Abilash, N., & Sivapragash, M. (2016). Optimizing the delamination failure in bamboo fiber reinforced polyester composite. *Journal of King Saud University- Engineering Sciences, 28*(1), 92-102.

Abiola, O. S., Kupolati, W. K., Sadiku, E. R., & Ndambuki, J. M. (2014). Utilisation of natural fibre as modifier in bituminous mixes: A review. *Construction and Building Materials, 54,* 305 – 312.

Abrão, A. M., Faria, P. E., Rubio, J. C. C., Reis, P., & Davim, J. P. (2007). Drilling of fibre reinforced plastics: A review. *Journal of Material Processing Technology, 186*(1-3), 1-7.

Abrão, A. M., Rubio, J. C., Faria, P. E., & Davim, J. P. (2008). The Effect of cutting tool geometry on thrust force and delamination when drilling glass fibre reinforced plastics composite. *Materials & Design*, *29*(2), 508-513.

Abrate, S., & Walton, D. (2016). Machining of composite materials. Part II: Non- traditional methods. *Composites manufacturing, 3*(2): 85-94.

Abrate, S., & Walton, D. A. (1992). Machining of composite materials Parts I: Traditional methods. *Composites Manufacturing, 3*(2), 75-83.

ACMA. (2015). *Composites manufacturing*. American Composites Manufacturers Association. Retrieved from http://compositesmanufacturingmagazine.com/2015/01/what-will-drive-composites-growth-in-2015/

Ahmadi, K., & Savilov, A. (2015). Modeling the mechanics and dynamics of arbitrary edge drills. *International Journal of Machine Tools and Manufacture, 89*, 208–220.

Alaa A. A., Kasim, T., & Mohammed, A. A. (2014). Mechanical properties for polyester resin reinforce with Fe weave wire. *International Journal of Application or*

Innovation in Engineering & Management, 3(7), 8-12.

Almansour, F. A., Dhakal, H. N., Zhang, Z. Y., & Ghasemnejad, H. (2015). Effect of hybridization on the Mode II of fracture toughness properties of flax/vinyl ester composites. *Polymer Composites,* 1-9.

Anarghya, A., Yatheesha, R. B., Gurumurthy, B. M., Rao, N., & Ranjith, B. S. (2015). Drill-ability studies of laser drilled micro holes on CFRP composites, *Proceedings on International Conference on New Developments in Biology, Biomedical & Chemical Engineering and Materials Science*, 15–17 March, Vienna, Austria.

Andrew, J. J., Arumugam, V., Bull, D. J., & Dhakal, H. N. (2016). Residual strength and damage characterization of repaired glass/epoxy composite laminates using A.E. and D.I.C. *Composite Structures, 152*, 124-139.

Armarego, E. J. A., & Kang, D. (1998). Computer –aided modelling of the flutting process for twist drill design and manufacture. *CIRP Annals - Manufacturing Technology*, *47*(1), 256-264.

Armarego, E. J. A., & Zhao, H. (1996). Predictive force models for point-thinned and circular centre edge twist drill designs. *CIRP Annals - Manufacturing Technology*, *45*(1), 65-70.

Arul, S., Vijayaraghavan, L., Malhotra, S. K., & Krishnamurthy, R. (2006). The effect of vibratory drilling on hole quality in polymeric composites. *International Journal of Machine Tools and Manufacture, 46*(3-4), 252-259.

Ashby, M. F., & Cebon, D. (1992). *Materials Selection in Mechanical Design*. (4th ed.). Oxford: Pergamon Press.

Asokan, P., Firdoous, M., & Sonal, W. (2012). Properties and potential of bio fibres, bio binders, and bio composites. *Reviews on Advanced Materials Science*, *30*(3), 254-261.

Astakhov, V. P., & Davim, J. P. (2008). Tools (geometry and material) and tool wear. In J. P. Davim (Ed.), *Machining fundamentals and recent advances* (pp. 29-57). USA: Springer.

Audy, J. (2008a). A study of computer-assisted analysis of effects of drill geometry and surface coating on forces and power in drilling. *Journal of Materials Processing Technology, 204*(1-3), 130–138.

Audy, J. (2008b). A study of dry machining performance of the TiN, Ti(Al,N) and Ti(C,N) coatings and a M35 HSS type tool substrate material assessed through basic cutting quantities generated when orthogonal turning a bisalloy 360 grade steel work-piece material. *Journal of Engineering, Annals of Faculty of Engineering Hunedoara, 6*(1), 59-70.

Azarhoushang, B., & Akbari, J. (2007). Ultrasonic-assisted drilling of Inconel 738-LC. *International Journal of Machine Tools and Manufacture, 47*, 1027-1033.

Babu, G. D., Babu, K. S., & Gowd, B. U. M. (2013a). Optimisation of machining parameters in drilling hemp fibre reinforced composites to maximise the tensile strength using design experiments. *Indian Journal of Engineering and Materials Sciences, 20*(5), 385-390.

Babu, G. D., Babu, K. S., & Gowd, B. U. M. (2013b). Effect of machining parameters on milled natural fibre-reinforced plastic composites. *Journal of Advanced Mechanical Engineering, 1*, 1-12.

Baghaei B, & Skrifvars M. (2016). Characterisation of polylactic acid biocomposites made from prepregs composed of woven polylactic acid/hemp–Lyocell hybrid yarn fabrics. *Composites Part A: Applied Science and Manufacturing*, *81*, 139–144.

Bagherpour, S. (2012). Polyester. In H. E. Salah (Ed.), *Fiber reinforced polyester composites* (pp. 135 – 166). Croatia: InTech.

Bakare, F. O., Ramamoorthy, S. K., Åkesson, D., & Skrifvars, M. (2016). Thermomechanical properties of bio-based composites made from a lactic acid thermoset resin and flax and flax/basalt fibre reinforcements. *Composites Part A: Applied Science and Manufacturing*, *83*, 176–184.

Bandhu, D., Sangwan, S. S., & Verma, M. (2014). Optimization of Drilling Parameter and Surface Roughness using different Tool Material by Drilling of CFRP Composite Material. *International Journal of Current Engineering and Technology, 4*(4), 2570-2576.

Basavarajappa, S., Chandramohan, G., & Davim, J. P. (2008). Some studies on drilling of hybrid metal matrix composites based on Taguchi techniques. *Journal of Materials Processing Technology, 196(*1-3), 332–338.

Bhattacharyya, A., Bhattacharyya, A. J., Chatterjee, A. B., & Ham, I. (1971). Modification of drill point for reducing thrust. *American Society of Mechanical Engineers Journal of Engineering for Industry, 93*(4), 1073–1078.

Bledzki, A., Sperber, V. E., & Faruk, O. (2002). *Natural wood and fibre reinforcement in polymers*. Rapra Review Reports. Shrewsbury: Rapra Technology Ltd.

Bongiorno, A., Capello, E., Copani, G., & Tagliaferri, V. (1998). Drilled hole damage and residual fatigue behaviour of GFRP, *Proceedings of the ECCM-8 Conference: Vol. II* (pp. 525 – 532). Naples, Italy.

Boyle, A. M., Martin, C. J., & Neuner, J. D., (2001). *ASM Handbook, Composites, Vol. 21.* ASM International, Hexcel Corporation-12, 79 – 89.

Brinksmeier, E., & Janssen, R. (2002). Drilling of multi-layer composite materials consisting of carbon fibre reinforced plastics (CFRP), titanium and alloys. *CIRP Annals - Manufacturing Technology, 51*(1), 87-90.

Buksnowitz, C., Adusumalli, R., Pahler, A., Sixta, H., & Gindl, W. (2010). Acoustical properties of Lyocell, hemp, and flax composites. *Journal of Reinforced Plastics and Composites, 29*(10), 3149 – 3154.

Butler-Smith, P. W., Axinte, D. A., Daine, M., Kennedy, A. R., Harper, L. T., Bucourt, J. F., & Ragueneau, R. (2015). A study of an improved cutting mechanism of composite matereials using novel design of diamond micro-core drills. *International Journal of Machine Tools and Manufacture, 88*, 175–183.

Caiazzo, F., Curcio, F., Daurelio, G., Memola, F. C. M. (2005). Laser cutting of different polymeric plastics (PE, PP and PC) by a CO2 laser beam. *Journal of Materials Processing Technology, 159(*3), 279-285.

Capello, V. E. (2004). Workpiece damping and its effect on delamination damage in drilling thin composite laminates. *Journal of Materials Processing Technology, 148*(2), 186–195.

Chambers, A., & Bishop, G. (1995). The drilling of carbon fibre polymer matrix composites, *Proceedings of the Tenth International Conference on Composite Materials: Vol. III.* (pp. 565–572). Whistler, B. C., Canada.

Chao, M., Feng, Q., Greg, S., Chou, K., & Thompson, R. (2009). Integrated design and analysis of diamond-coated drills. *Computer-Aided Design and Applications*, *6*(2), 195-205.

Che, W. (1997). Some experimental investigations in the drilling of carbon fibre-reinforced plastic (CFRP) composite laminates. *International Journal of Machine Tools and Manufacture, 37*(8), 1097-1108.

Chen, W. C. (1997). Some experimental investigation in the drilling of carbon fibre reinforced plastic (CFRP) composite laminates. *International Journal of Machine Tools and Manufacture, 37*(8), 1097–1108.

Chen, Y. R., & Ni, J. (1999). Analysis and optimisation of drill cross-sectional geometry. *Technical Paper - Society of Manufacturing Engineers. MR, (MR99-162),* pp. 1-6.

Cheung, H. Y., Ho, M. P., Lau, K. T., Cardona, F., & Hui, D. (2009). Natural fibre reinforced composites for bioengineering and environmental engineering applications. *Composites Part B: Engineering, 40*(7), 655 – 663.

Choudhury, I. A., & Shirley, S. (2010). Laser cutting of polymeric materials: An experimental investigation. *Optics & Laser Technology, 42*(3), 503-508.

Chryssolouris, G., Stavropoulos, P., & Salonitis, K. (2014). Process of laser machining. *Handbook of Manufacturing Energy and Technology*, 1–25.

Chukov, D. I., Stepashkin, A. A., Maksimkin, A. V., Tcherdyntsev, V. V., Kaloshkin, S. D., Kuskov, K. V., & Bugakov, V. I. (2015). Investigation of structure, mechanical and tribological properties of short carbon fiber reinforced UHMWPE-matrix composites. *Composites Part A: Applied Science and Manufacturing, 76*, 79 – 88.

Cong, W. L., Pei, Z. J., Feng, Q., Deines, T. W., & Treadwell, C. (2012). Rotary ultrasonic machining of CFRP: A comparison with twist drilling. *Journal of Reinforced Plastics & Composites, 31*(5), 313-321.

Coromant, S. (2011). *Close tolerance hole making in composites*, Problems, 2011. Retrieved from http://www2.coromant.sandvik.com/coromant/eBook/Composite/eng/pdf/C-2940-155.pdf.

Dandekar, C. R., & Shin, Y. C. (2012). Modeling of machining of composite materials: A review. *International Journal of Machine Tools and Manufacture, 57*, 102-121.

Davim, J. P., & Reis, P. (2003a). Study of delamination in drilling carbon fibre reinforced plastics (CFRP) using design experiments. *Composite Structures, 59*(4), 481-487.

Davim, J. P., & Reis, P. (2003b). Drilling carbon fibre reinforced plastics manufactured by auto-clave-experimental and statistical study. *Materials & Design, 24*(5), 315-324.

Davim, J. P., Barricas, N., Conceicao, M., & Oliveira, C. (2008). Some experimental studies on CO2 laser cutting quality of polymeric materials. *Journal of Materials Processing Technology, 198*(1-3), 99-104.

Davim, J. P., Reis, P., & António, C. C. (2004a). Drilling fibre reinforced plastics (FRPs) manufactured by hand lay-up- influence of matrix (Viapal VUP 9731 and ATLAC 382-05). *Journal of Materials Processing Technology, 155*(1), 1828–1833.

Davim, J. P., Reis, P., & Antonio, C. C. (2004b). Experimental study of drilling of glass fibre reinforced plastic (GFRP) manufactured by hand lay-up. *Composites Science and Technology, 64*(2), 289-297.

DeGarmo, E. P., Black, J. T., & Kohser, R. A. (2003). *Materials and processes in manufacturing* (9th ed.). New York: Wiley.

Dhakal, H. N., Sarasini, F., Santulli, C., Tirillò, J., Zhang, Z., & Arumugam, V. (2015). Effect of basalt fibre hybridisation on post-impact mechanical behaviour of hemp fibre reinforced composites. *Composites Part A: Applied Science and Manufacturing, 75*, 54–67.

Dhakal, H. N., Zhang, Z. Y., & Richardson, M. O. W. (2007). Effect of water absorption on the mechanical properties of hemp fibre reinforced unsaturated polyester composites. *Composites Science and Technology, 67*(7-8), 1674-1683.

Dharan, C. K. H., & Won, M. S. (2000). Machining parameters for an intelligent machining system for composite laminates. *International Journal of Machine Tools and Manufacture*, *40*(3), 415-426.

Dhavamani, C., & Alwarsamy, T. (2011). Review on optimization of machining operation. *International Journal of Academic Research, 3*(3), 474 – 485.

Doomra, V. K., Debnath, K., & Singh, I. (2015). Drilling of metal matrix composites: Experimental and finite element analysis. *Proceedings of the Institution of Mechanical Engineers, Part B: Journal of Engineering Manufacture, 229*(5), 886-890.

Doreswamy, D., Shivamurthy, B., Anjaiah, D., & Sharma, N. Y. (2015). An Investigation of Abrasive Water Jet Machining on Graphite/Glass/Epoxy Composite. *International Journal of Manufacturing Engineering, 2015*, 1-11.

DrillDr. (2011). *Twist drill geometry and cutting logic*, Professional tool manufacturing: Ashland. Retrieved from https://www.drilldoctor.com/files_drillbit_information/Twist_Drill_Geometry.pdf.

Durão, L. M. P. (2005). *Machining of hybrid composite*. Ph.D. Thesis. Portugal: University of Porto, Faculty of Engineering. Retrieved from https://repositorioaberto.up.pt/bitstream/10216/12507/2/Texto%20integral.pdf

Durão, L. M. P., de Moura, M. F. S. F., & Marques, A. T. (2008). Numerical prediction of delamination onset in carbon/epoxy composites drilling. *Engineering Fracture Mechanics, 75*(9), 2767–2778.

Durão, L. M. P., Goncalves, D. J. S., Trvares, J. M. R. S., de Albuquerque, V. H. C., Vieira, A. A., & Marques, A. T. (2010). Drilling tool geometry evaluation for reinforced composite laminates. *Composite Structures, 92*(7), 1545–1550.

Durão, M. L. P., Tavares, J. M. R. S., C. de Albuquerque, V. H., Marques, J. F. S., & Andrade O. N. G. (2014). Drilling damage in composite material. *Materials, 7*(5), 3802-3819.

Edie, D. D., & McHugh, J. J. (1999). High performance carbon fibers. In T. D. Burchell (Ed.), *Carbon Materials for Advanced Technologies* (pp. 119-138). Oxford, UK: Pergamon, Elsevier Science Ltd.

El-Sabbagh, A. M. M., Steuernagel, L., Meiners, D., & Ziegmann, G. (2014). Effect of extruder elements on fiber dimensions and mechanical properties of bast natural fiber polypropylene composites. *Journal of Applied Polymer Science, 131*(12), 1-15.

El-Sonbaty, I., Khashaba, U. A., & Machaly, T. (2004). Factors affecting the machinability of GFR/epoxy composite. *Composite Structures, 63*(3-4), 329-338.

Eneyew, E., & Ramulu, M. (2014). Experimental study of surface quality and damage when drilling unidirectional CFRP composites. *Journal of Materials Research and Technology, 3*(4), 354–362.

Ertunc, M. H., Loparo, K. A., & Ocak, H. (2001). Tool wear condition monitoring in drilling operations using hidden Markov models (HMMs). *International Journal of Machine Tools and Manufacture, 41*(9), 1363–1384.

FAO. (2009): *Natural fibres, hemp – International year of natural fibres*. Retrieved from http://naturalfibres2009.org/en/index.html

Faraz, A., Biermann, D., & Weinert, K. (2009). Cutting edge rounding: An innovative tool wear criterion in drilling CFRP composite laminates. *International Journal of Machine Tools and Manufacture, 49*(15), 1185-1196.

Faris, M. A., & Sapuan, S. M. (2014). Natural fiber reinforced polymer composites in industrial applications: feasibility of date palm fibers in sustainable automotive industry. *Journal of Cleaner Production*, *66,* 347 – 354.

Faruk, O., Bledzki, A. K., Fink, H. P., & Sain, M. (2012). Biocomposites reinforced with natural fibers: 2000–2010. *Progress in Polymer Science, 37*(11), 1552-1596.

Feito, N., Diaz-Álvarez, J., López-Puente, J., & Miguélez, M. H. (2016). Numerical analysis of the influence of tool wear and special cutting geometry when drilling woven CFRPs. *Composite Structures, 138*, 285–294.

Fernandes, M., & Cook, C. (2006). Drilling of carbon composites using a one shot drill bit, Part I: Five stage representation of drilling and factors affecting maximum force and torque. *International Journal of Machine Tools and Manufacture, 46(*1), 70–75.

Fetecau, C., Stan, F., & Oancea, N. (2009). Toroidal grinding method for curved cutting edge twist drills. *Journal of Materials Processing Technology, 209*(7), 3460–3468.

Forsmann, A. C., Lundgren, E. H., Dodell, A. L., Komashko, A. M., & Armas, M. S. (2007). Double pulse format for laser drilling. *Photonics Spectra*, 1-9.

Gaitonde, V. N., Karnik, S. R., Rubio, J. C., Correia, E., Abrao, A. M., & Davim, J. P. (2008). Analysis of parametric influence on delamination in high-speed drilling of carbon fibre reinforced plastic composites. *Journal of Materials Processing Technology, 203*(1-3), 431–438.

Garrick, R. (2007). Drilling advanced aircraft structures with PCD (Poly-Crystalline Diamond) drills. *SAE International Technical Paper*, pp.1-9.

Ghidossi, P., El Mansori, M., & Pierron, F. (2004). Edge machining effects on the failure of polymer matrix composite coupons. *Composites Part A: Applied Science and Manufacture, 35*, 989–999.

Gilchrist, M. D., Svensson, N., & Shishoo, R. (1998). Fracture and fatigue performance of textile mommingled yarn composites. *Journal of Material Science, 33*(16), 4049-4058.

Girisha, K. G, Anil, K. C., & Akash. (2014). Mechanical Properties of Jute and Hemp Reinforced Epoxy/Polyester Hybrid Composites. *International Journal of Research in Engineering & Technology*, *2*(4), 245 – 248.

Graf, K. (1975). Macrosonics in industry: 5. Ultrasonic machining. *Ultrasonics, 13*(3), 103-109.

Graupner, N., Herrman, A. S., & Mussig, J. (2009). Natural and man-made cellulose fibre reinforced poly (lactic acid) (PLA) composites: An overview about mechanical characteristics and application areas, *Composites Part A: Applied Science and Manufacturing*, *40*(6–7), 810 – 821.

Gupta, A., Barnes, S., McEwen, I., Kourra, N., & Williams, M. A. (2014). Study of cutting speed variation in the ultrasonic assisted drilling of carbon fibre composites, *Proceedings of the International Mechanical Engineering Congress and Exposition* (pp. 1-11). Quebec, Canada: ASME publication.

Gupta, M., & Kumar, S. (2015). Investigation of surface roughness and MRR for turning of UD-GFRP using PCA and Taguchi method. *Engineering Science and Technology, an International Journal, 18*(1), 70-81.

Gururaja, S., & Ramulu, M. (2009). Modified exit-ply delamination model for drilling FRPs. *Journal Composite Materials,* 43(5), 483-500.

Guu, Y. H., HoCheng, H., Tai, N. H., Liu, S. Y. (2001). Effect of electrical discharge machining on the characteristics of carbon fibre reinforced carbon composites. *Journal of Materials Science, 36*(8), 2037-2043.

Hajnalka, H., Racz, I., & Anandjiwala, R. D. (2008). Development of hemp fibre reinforced polypropylene composites. *Journal of Thermoplastic Composite Materials, 21*(2), 165 – 174.

Harris, B. (1999). *Engineering composite materials*. The Institute of Materials, London. Retrieved from http://www.cantab.net/users/bryanharris/Engineering%20Composites.pdf

Harris, S. G., Doyle, E. D., Vlasveld, A. C., Audy, J., & Quick, D. (2003). A study of the wear mechanisms of $Ti_{1-x}Al_xN$ and $Ti_{1-x-y}Al_xCr_yN$ coated high-speed steel twist drills under dry machining conditions. *Wear, 254*(7-8), 723–734.

Heath, P. J. (2001). Developments in applications of PCD tooling. *Journal of Materials Processing Technology, 116*(1), 31-38.

Heisel, U., & Pfeifroth, T. (2012). Influence of point angle on drill hole quality and machining forces when drilling CFRP. *Procedia CIRP, 1*, 471 – 476.

Hejjaji, A., Singh, D., Kubher, S., Kalyanasundaram, D., & Gururaja, S. (2016). Machining damage in FRPs: Laser versus conventional drilling. *Composites Part A: Applied Science and Manufacturing*, *82*, 42–52.

Hepworth, D. G., Hobson, R. N., Bruce, D. M., & Farrent, J. W. (2000). The use of unretted hemp fibre in composite manufacture. *Composite Part A: Applied Science and Manufacturing, 31*(11), 1279 – 1283.

Herbert, S., Eberhard, A., Andrea, E. K., & Carsten, S. (2002). Optimisation of the chip flute of drilling tools with methods of genetic algorithms, *Proceedings of International Science and Engineering Conference, Vol. 8* (pp. 57–68). Brijuni, Croatia.

Hinds, B. K., & Treanor, G. M. (2000). Analysis of stresses in micro-drills using the finite element method. *International Journal of Machine Tools and Manufacture, 40*(10), 1443–1456.

Hocheng, H., & Dharan, C. K. H. (1988). Delamination during drilling in composite laminates, *Proceedings of the conference on machining composites*, Winter Annual Meeting (pp. 39–44). American Society of Mechanical Engineers (PED-35/MD-12).

Hocheng, H., & Dharan, C. K. H. (1990). Delamination during drilling in composite laminates. *American Society of Mechanical Engineers Journal of Engineering for Industry, 112*(3), 236–239.

Hocheng, H., & Tsao, C. C. (2003). Comprehensive analysis of delamination in drilling of composite materials with various drill bits. *Journal of Materials Processing Technology, 140*(1-3), 335-339.

Hocheng, H., & Tsao, C. C. (2005). The path towards delamination-free drilling of composite materials. *Journal of Materials Processing Technology, 167*(2-3), 251-264.

Hocheng, H., & Tsao, C. C. (2006). Effects of special drill bits on drilling-induced delamination of composite materials. *International Journal of Machine Tools and Manufacture, 46*(12-13), 1403–1416.

Hocheng, H., & Tsao, C. C. (2007). Computerised tomography and C-scan for measuring drilling-induced delamination in composite material using twist drill and core drill. *Key Engineering Materials, 339*, 16-20.

HoCheng, H., Tai, N. H., & Liu, C. S. (2000). Assessment of ultrasonic drilling of C/SiC composite material. *Composites Part A: Applied Science and Manufacturing, 31*(2), 133-142.

Holbery, J. & Houston, D. (2006). Natural-Fiber-Reinforced Polymer Composites in Automotive Applications. *Journal of Minerals, Metals, and Materials, 58*(11), 80-86.

Holmes, M**. (**2014). *Reinforced Plastic*. Retrieved from http://www.reinforcedplastics.com/view/36341/carbon-fibre-reinforced-plastics-market-continues-growth-path-part-1/

Iliescu, D., Gehin, D., Gutierrez, M. E., & Girot, F. (2010). Modelling and tool wear in drilling of CFRP. *International Journal of Machine Tools and Manufacture, 50*(2), 204-213.

Ingrao, C., Lo Giudice, A., Bacenetti, J., Tricase, C., Dotelli, G., Fiala, M., Siracusa, V., & Mbohwa, C. (2015). Energy and environmental assessment of industrial hemp for building applications: A review. *Renewable and Sustainable Energy Reviews, 51*, 29 – 42.

Isbilir, O., & Ghassemieh, E. (2011). Finite element analysis of drilling of titanium alloy. *Procedia Engineering, 10*, 1877–1882.

Isbilir, O., & Ghassemieh, E. (2012). Delamination and wear in drilling of carbon-fibre reinforced plastic composites using TiAlN/TiN PVD-coated tungsten carbide tools. *Journal of Reinforced Plastics and Composites, 31*(10), 717-727.

Isbilir, O., & Ghassemieh, E. (2013). Numerical investigation of the effects of drill geometry on drilling induced delamination of carbon fibre reinforced composites. *Composite Structures, 105*, 126-133.

Ismail, S. O., Dhakal, H. N., Dimla, E., & Popov, I. (2016b). Recent advances in twist drill design for composites machining: A critical review, *Proceedings of the Institution of Mechanical Engineers, Part B: Journal of Engineering Manufacture,* 1-16.

Ismail, S. O., Dhakal, H. N., Dimla, E., Beaugrand, J., & Popov, I. (2016a). Effects of drilling parameters and aspect ratios on delamination and surface roughness of lignocellulosic HFRP composite laminates. *Journal of Applied Polymer Science, 133*(7), 1-8.

Ismail, S. O., Dhakal, H. N., Popov, I., & Beaugrand, J. (2016d). Analysis and impacts of chips formation on hole quality during fibre-reinforced plastic composites machining. In Y. M. Goh & K. Case (Eds.), *Advances in manufacturing technology XXX: Vol. 3 and Proceedings of the 14th international conference on manufacturing research, incorporating the 31st national conference on manufacturing research* (pp. 143 – 148). Amsterdam: IOS Press.

Ismail, S. O., Dhakal, H. N., Popov, I., & Beaugrand, J. (2015). Experimental analysis of drilling-induced damage of lignocellosic 19/hemp fibre reinforced PCL and MTM 44-1/carbon fibre reinforced epoxy resin composites, *Proceedings of 5th International Conference on Natural Fibre Composites for Industrial Applications* (pp. 1-6). Sapienza Universita de Roma, Rome, Italy.

Ismail, S. O., Dhakal, H. N., Popov, I., & Beaugrand, J. (2016c). Comprehensive study on machinability of sustainable and conventional fibre reinforced polymer composites. *Engineering Science and Technology, An international Journal*, *19*(4), 2043-2052.

Ismail, S. O., Dhakal, H. N., Roy, A., Wang, D., & Popov, I. (2016e). Machining of FRP composite laminates with CD and UAD techniques: A comparative and experimental investigation, *Proceedings of the American Society for Composites, 31st Technical Conference*, Williamsburg, Virginia, USA.

Ismail, S. O., Ojo, S. O., & Dhakal, H. N. (2017). Thermo-mechanical modelling of FRP cross-ply composite laminates drilling: Delamination damage analysis. *Composites Part B: Engineering, 108*, 45–52.

Jacob, A. (2014). Carbon fibres and cars – 2013 in review. *Reinforced Plastics, 58*(1)*,* 18 – 19.

Jain, S., & Yang, D. C. H. (1993). Effects of feed-rate and chisel edge on delamination in composite drilling. *American Society of Mechanical Engineers Journal of Engineering for Industry, 115*(4), 398–405.

Jain, S., & Yang, D. C. H. (1994). Delamination-free drilling of composite laminates. *American Society of Mechanical Engineers Journal of Engineering for Industry*, *116*(4), 475–481.

Jawaid, M., & Abdul Khalil, H. P. S. (2011). Cellulosic/synthetic fibre reinforced polymer hybrid composites: A review. *Carbohydrate Polymers, 86*(1), 1-18.

Jones, R. M. (1975). *Mechanics of Composite Materials*. (2nd ed.). Washington, D.C.: McGraw-Hill Book Company.

Kabir, M. M., Wang, H., Lau, K. T., & Cardona, F. (2012). Chemical treatments on plant based natural fibre reinforced polymer composites: An overview. *Composites Part B: Engineering, 43*(7), 2883 – 2892.

Kadivar, M. A., Akbari, J., Yousefi, R., Rahi, A., & Nick, M. G. (2014). Investigating the effects of vibration method on ultrasonic-assisted drilling of Al/SiCp metal matrix composites. *Robotics and Computer-Integrated Manufacturing, 30*(3), 344-350.

Kaldor, S., & Lenz, E. (1982). Drill point geometry and optimisation. *American Society of Mechanical Engineers Journal of Engineering for Industry, 104*(1), 84–90.

Kalpakjian, S., & Schmid, S. R. (2003). *Manufacturing processes for engineering materials* (4th ed.). USA: Prentice-Hall.

Kanno, I., Yamashita, Y., Kimura, M., & Inoue, F. (2015). Effective atomic number measurement with energy-resolved X-ray computed tomography. *Nuclear Instrument Method in Physics Research Section A: Accelerators, Spectrometers, Detectors and Associated Equipment, 787,* 121-124.

Kapoor, R. & Nemat-Nasser, S. (1998). Determination of temperature rise during high strain rate deformation. *Mechanics of Materials, 27*(1), 1-12.

Karimi, N. Z., Heidary, H., & Minak, G. (2016). Critical thrust and feed prediction models in drilling of composite laminates. *Composite Structures, 148*, 19–26.

Karnik, S. R., Gaitonde, V. N., Rubio, J. C. C., Correia, A. E., Abrao, A. M., & Davim, J. P. (2008). Delamination analysis in high speed drilling of carbon fibre reinforced plastics (CFRP) using artificial neural network model. *Materials and Design, 2008, 29*(9), 1768–1776.

Karpat, Y., Deger, B., & Bahtiyar, O. (2012). Drilling thick fabric woven CFRP laminates with double point angle drills. *Journal of Materials Processing Technology, 212*(10), 2117-2127.

Karpuschewski, B., Byelyayev, O., & Maiboroda, V. S. (2009). Magneto-abrasive machining for the mechanical preparation of high-speed steel twist drills. *CIRP Annals - Manufacturing Technology, 58*(1), 295–298.

Kavad, B. V., Pandey, A. B., Tadavi, M. V., & Jakharia, H. C. (2014). A review paper on effects of drilling on glass fibre reinforced plastic. *Procedia Technology, 14*, 457-464.

KC, B., Faruk, O., Agnelli, J. A. M., Leao, A. L., Tjong, J., & Sain, M. (2016). Sisal-glass fiber hybrid biocomposite: Optimization of injection molding parameters using Taguchi method for reducing shrinkage. *Composites Part A: Applied Science and Manufacturing, 83*, 152–159.

Keilers, C. H., & Chang, F. K. (1993). Damage detection and diagnosis of composites using built-in piezoceramics, *Proceedings of the SPIE conference: Vol.* 1917. *Smart structures and materials* (pp. 1009-1019). North American, USA.

Keilers, C. H., Chang, F. K. (1995b). Identifying delamination in composite beam using built-in piezo-electrics: Part II- an identification method. *Journal of Intelligent Material Systems and Structures, 6*(5), 664-672.

Keilers, C. K., & Chang, F. K. (1995a). Identifying delamination in composite beam using built-in piezo-electrics: Part I- experiments and analysis. *Journal of Intelligent Material Systems and Structures, 6*, 649-663.

Ketcham, R. A., & Carlson, W. D., (2001). Acquisition, optimisation and interpretation of X-ray computed tomographic imagery: Applications to the geosciences. *Computers and Geoscience, 27*, 381-400.

Kharfi, F., Yahiaoui, M., & Boussahoul, F. (2015). X-ray computed tomography system for laboratory small-object imaging: Enhanced tomography solutions. *Applied Radiation and Isotopes, 101*, 33-39.

Khashaba, U. A. (2004). Delamination in drilling GFR-thermoset composites. *Composite Structures, 63*(3-4), 313-327.

Khashaba, U. A. (2012). Drilling of a polymer matrix composites: A review. *Journal of Composite Materials, 47*(15), 1817-1832.

Khashaba, U. A., El-Sonbaty, I. A., Selmy, A. I., & Megahed, A. A. (2010b). Machinability analysis in drilling woven GFR/epoxy composites: Part II – Effect of drill wear. *Composites Part A: Applied Science and Manufacturing, 41*(9), 1130–1137.

Khashaba, U. A., El-Sonbaty, I. A., Selmy, A. I., & Megahed, A. A. (2010a). Machinability analysis in drilling woven GFR/epoxy composites: Part I – Effect of machining parameters. *Composites Part A: Applied Science and Manufacturing*, *41*, 391–400.

Kilickap, E. (2010). Optimisation of cutting parameters on delamination based on Taguchi method during drilling of GFRP composite. *Expert Systems with Applications, 37*(8), 6116-6122.

Kim, D., & Ramulu, M. (2004a). Drilling process optimisation for graphite/bismaleimide titanium alloy stacks*. Composite Structures, 63*(1), 101-114.

Kim, D., & Ramulu, M. (2004b). Frequency analysis and process monitoring in drilling of composite materials. *Advanced Composites Letters, 13*(4), 185-192.

Kim, J. K., & Mai, Y. W. (1998). *Engineered interfaces in fibre reinforced composites*. (1st ed.). Oxford: Elsevier Science Ltd.

Klocke, F., Raedt, P., & Hoppe, S. (2001). 2D-FEM simulation of the orthogonal high speed cutting process. *Machining Science and Technology, 5*(3), 323–340.

Kocsis, J., Mahmood, H., & Pegoretti, A. (2015). Recent advances in fiber/matrix interphase engineering for polymer composites. *Progress in Materials Science*, *73,* 1–43.

Komanduri, R. (1997). Machining fibre-reinforced composites. *Machining Science and Technology, 1(*1), 113-152.

König, W., & Graβ, P. (1989). Quality definition and assessment in drilling of fibre reinforced thermosets. *CIRP Annals-Manufacturing Technology, 38*(1): 119-124.

König, W., Grass, P., Heintze, A., Okcu, F., & Schmitz-Justin, C. (1984). Developments in drilling, contouring composites containing Kevlar. *Production Engineer, 63*(8), 56–61.

König, W., Wulf, Ch., Graβ, P., & Willerscheid, H. (1985). Machining of fibre-reinforced plastics. *CIRP Annals-Manufacturing Technology, 34*(2), 537–548.

Kopeliovich, D., (2012): Carbon fiber reinforced polymer composites. *Substances and Technology.* Retrieved from http://www.substech.com/dokuwiki/doku.php?id=carbon_fiber_reinforced_polymer_composites

Ku, H., Wang, H., Pattarachaiyakoop, N., & Trada, M. (2011). A review on the tensile properties of natural fibre reinforced polymer composites. *Composites Part B: Engineering, 42*(4), 856-873.

Kumar, A., Mahapatra, M. M., & Jha, P. K. (2014). Effect of machining parameters on cutting force and surface roughness of in situ Al–4.5%Cu/TiC metal matrix composites. *Measurement, 48*, 325–332.

Kumbar, S. G., Laurencin, C. T., & Deng, M. (2014). *Natural and synthetic biomedical polymers*. (1st ed.). USA: Elsevier Inc.

Kuo, C. L., Soo, S. L., Aspinwall, D. K., Bradley, S., Thomas, W., Saoubi, R. M., Pearson, D., & Leahy, W. (2014). Tool wear and hole quality when single-shot drilling of metallic-composite stacks with diamond-coated tools. *Proceedings of the Institution of Mechanical Engineers, Part B: Journal of Engineering Manufacture, 228*(10), 1314-1322.

Lachaud, F., Piquet, R., Collombet, F., & Surcin, L. (2001). Drilling of composite structures. *Composite Structures, 52*(3-4), 511-516.

Langella, A., Nele, L., & Maio, A. A. (2005). A torque and thrust prediction model for drilling of composite materials. *Composites Part A: Applied Science and Manufacturing, 36*(1), 83–93.

Lazar, M., & Xirouchakis, P. (2011). Experimental analysis of drilling fibre reinforced composites. *International Journal of Machine Tools and Manufacture, 51*(12), 937–946.

Lee, D. C., Lee, J. J., & Yun, S. J. (1995). The mechanical characteristics of smart composite structures with embedded optical fiber sensor. *Composite Structures, 32*(1-4), 39-50.

Lee, J. (2000). Free vibration analysis of delaminated composite beams. *Computers and Structures, 74*(2), 121-129.

Li, Z., Zhang, W., & Xiong, D. (2010). A practical method to determine rake angles of twist drill by measuring the cutting edge. *International Journal of Machine Tools and Manufacture, 50*(8), 747–751.

Lin, S. C., & Chen, I. K. (1996). Drilling of carbon fibre-reinforced composite material at high speed. *Wear, 194*(1-2), 156–162.

Ling, H. Y., Lau, K. T., & Cheng, L. (2004). Determination of dynamic strain profile and delamination detection of composite structures using embedded multiplexed fibre0optic sensors. *Composite Structures, 66*(1-4), 317-326.

Liu, D. F., Tang, Y. J., & Cong, W. L. (2012). A review of mechanical drilling for composite laminates. *Composite Structures, 94*(4), 1265–1279.

Liu, D., Xu, H. H., Zhang, C. Y., & Yan, H. J. (2010). Drilling force in high speed drilling carbon fibre reinforced plastics (CFRP) using half core drill. In G. Chai, C. Lu, & D. Wen (Eds.), *Advanced Materials Research, Digital Design and Manufacturing Technology* (Vol. 102-104, pp. 729-732). Switzerland: Trans Tech.

Liu, J. Y., Reni, L., Wei, Q., Wu, J. L., Liu, S., Wang, Y. J., & Li, G. Y. (2011). Fabrication and characterization of polycaprolactone/calcium sulfate whisker composites. *eXPRESS Polymer Letters, 5*(8), 742 – 752.

Liu, L., Jia, C., He, J., Zhao, F., Fan, D., Xing, L., Wang, M., Wang, F., Jiang, Z., & Yudong, H., (2015). Interfacial characterization, control and modification of carbon fiber reinforced polymer composites. *Composites Science and Technology, 121*, 1–38.

Liu, Q., & Hughes, M. (2008). The fracture behavior and toughness of woven flax fibre reinforced epoxy composites. *Composites Part A: Applied Science and Manufacture, 39*, 1644 – 1652.

Madhavan, S., & Prabu, S. B. (2012). An experimental study of influence of drill geometry on drilling of carbon fibre reinforced plastic composites. *International Journal of Engineering Research and Development, 3*(1), 36-44.

Makhdum, F., Phadnis, V. A., Roy, A., & Silberschmidt, V. V. (2014). Effect of ultrasonically-assisted drilling on carbon-fibre-reinforced plastics. *Journal of Sound and Vibration, 333*(23), 5939–5952.

Malkapuram, R., Kumar, V., & Yuvraj, S. N. (2008). Recent Development in Natural Fibre Reinforced Polypropylene Composites. *Journal of Reinforced Plastics and Composites, 28*(10), 1169 – 1189.

Mallick, P. K. (2008). *Fibre-reinforcement composites, materials, manufacturing and design*. (3rd ed.). USA: CRC Press, Taylor and Francis Group.

Marinov, V. (2010). *Manufacturing processes for metal products*. (1st ed.). Dubuque, Lowa: Kendall/Hunt Publishing Company.

Matthews, F. L., & Rawlings, R. D. (1994). *Composite materials: Engineering and science.* (1st ed.). Oxford: Chapman & Hall.

Min, S., Dornfeld, D., Kim, J., & Shyu, B. (2001). Finite element modeling of burr formation in metal cutting. *Machining Science and Technology, 5*(3), 307–322.

Mišković, A., & Koboević, N. (2011). The effect of cutting tool geometry on thrust force and delamination when drilling carbon fibre reinforced composite materials, *Proceedings of the 15th International Research/Expert Conference*: *Trends in the Development of Machinery and associated Technology* (pp. 769-772). Prague, Czech Republic.

Mohamed, A. H. (2014). Waterjet trimming and drilling of CFRP components for advanced aircraft. Flow International Corporation. *SME Technical Paper*, Kent, WA.

Mohan, N. S., Ramachandra, A., & Kulkarni, S. M. (2005). Influence of process parameters on cutting force and torque during drilling of glass-fibre polyester reinforced composites. *Composite Structures, 71*(3-4), 407-413.

Mohanty, A. K., Misra, M., & Drzal, L. T., (2005). *Natural fibers, biopolymer and biocomposites*. (1st ed.). Boca Raton, FL: CRC Press.

Murphy, C., Byrne, G., & Gilchrist, M. D. (2002). The performance of coated tungsten carbide drills when machining carbon fibre-reinforced epoxy composite materials. *Proceedings of the Institution of Mechanical Engineers, Part B: Journal of Engineering Manufacture, 216*(2), 143-152.

Nagaraja, Herbert, M. A., Shetty, D., Shetty, R., & Shivamurthy, B. (2013). Efeect of process parameters on delamination, thrust force and torque in drilling of carbon fibre epoxy composite. *Research Journal of Recent Sciences, 2*(8), 47-51.

Naveen, P. N. E, Yasaswi, M., & Prasad, R. V. (2012). Experimental investigation of drilling parameters on composite materials. *International Organisation of Scientific Research Journal of Mechanical and Civil Engineering, 2*(3), 30 -37.

NDT. (2015). *Computed tomography.* Retrieved from https://www.ndeed.org/EducationResources/CommunityCollege/Radiography/AdvancedTechniques/computedtomography.php

Nirmal, U., Hashim, J., & Ahmed, M. M. H. M. (2015). A review on the tribological performance of natural fibre polymeric composites. *Tribology International*, *83,* 77 – 104.

Ogawa, K., Aoyama, E., Inoue, H., Hirogaki, T., Nobe, H., Kitahara, Y., Katayama, T., & Gunjima, M. (1997). Investigation on cutting mechanism in small diameter drilling for GFRP (thrust force and surface roughness at drilled hole wall. *Composite Structures, 38*(1–4), 343–350.

Oguni, K., & Ravichandran, G. (2001). Dynamic compressive behavior of unidirectional E-glass/vinylester composites. *Journal of Material Science, 36*(4), 831-838.

Ojo, S. O., & Paggi, M. (2016a). Thermo-visco-elastic shear-lag model for the prediction of residual stresses in photovoltaic modules after lamination. *Composite Structures, 136*, 481-492.

Ojo, S. O., & Paggi, M. (2016b). A 3D coupled thermo-visco-elastic shear-lag formulation for the prediction of residual stresses in photovoltaic modules after lamination. *Composite Structures*, *157*, 348–359.

Oksman, K. (2000). Mechanical properties of natural fibre mat reinforced thermoplastic. *Applied Composite Materials, 7*, 403–414.

Park, K. H., Beal, A., Kim, D., Kwon, P., & Lantrip, J. (2011).Tool wear in drilling of composite/titanium stacks using carbide and polycrystalline diamond tools. *Wear, 271*(11-12), 2826–2835.

Park, K. Y., Choi, J. H., & Lee, D. G. (1995). Delamination-free and high efficiency drilling of carbon fibre reinforced plastics. *Journal of Composite Materials, 29*(15), 1988-2002.

Pattanaik, A., Satpathy, M. P., & Mishra, S. C. (2016). Dry sliding wear behavior of epoxy fly ash composite with Taguchi optimization. *Engineering Science and Technology, an International Journal, 19*(2), 710-716.

Paul, A., Kapoor, S. G., & Devor, R. E. (2005). Chisel edge and cutting lip shape optimisation for improved twist drill point design. *International Journal of Machine Tools and Manufacture, 45*(4-5), 421–431.

Paul, V., Kanny, K., & Redhi, G. C. (2015). Mechanical, thermal and morphological properties of a bio-based composite derived from banana plant source. *Composites Part A: Applied Science and Manufacturing, 68*, 90-100.

Phadnis, V. A., Makhdum, F., Roy, A., & Silberschmidt, V. V. (2013a). Drilling in carbon/epoxy composites: Experimental investigations and finite element implementation. *Composites Part A: Applied Science and Manufacturing*, *47*, 41-51.

Phadnis, V. A., Makhdum, F., Roy, A., & Silberschmidt, V. V. (2012a). Experimental and numerical investigations in conventional and ultrasonically-assisted drilling of CFRP laminate. *Procedia CIRP, 1*, 455-459.

Phadnis, V. A., Makhdum, F., Roy, A., & Silberschmidt, V. V. (2012b). Ultrasonically-assisted drilling in CFRP composites, *Proceedings of the ECCM15–15th European Conference on Composite Materials* (pp. 24-28), Venice, Italy.

Phadnis, V. A., Roy, A., & Silberschmidt, V. V. (2013b). Ultrasonic assisted drilling: A finite element model incorporating acoustic softening effects. *Journal of Physics: Conference Series, 451*, 1-9.

Pickering, K. (Ed.). (2008). *Properties and performance of natural fibre composites*. Boca Raton: CRC Press LLC.

Piquet, R., Ferret, B., Lachaud, F., & Swider, P. (2000). Experimental analysis of drilling damage in thin carbon/epoxy laminate using special drills. *Composites Part A: Applied Science and Manufacturing, 31*(10), 1107–1115.

Placet, V. (2009). Characterization of the thermo-mechanical behavior of hemp fibres intended for the manufacturing of high performance composites. *Composites Part A: Applied Science and Manufacturing, 40*(8), 1111 – 1118.

Puglia, D., Biagiotti, J., & Kenny, J. M. (2004). application of natural reinforcements in composite materials, Part II: Application of natural reinforcements in composite materials for automotive industry. *Journal of Natural Fibers*, *1*(3), 23 – 65.

Pujana, J., Rivero, A., Celaya, A., & López de Lacalle, L. N. (2009). Analysis of ultrasonic-assisted drilling of Ti6Al4V. *International Journal of Machine Tools and Manufacture, 49*(6), 500-508.

Quartus Engineering. (2016). *Composites 101: Basic laminate stacking.* Retrieved from http://www.quartus.com/resources/white-papers/composites-101/

Rahman, A. A., Mamat, A., & Wagiman, A. (2009). Effect of machining parameters on hole quality of micro drilling for brass. *Modern Applied Science, 3*(5), 221-230.

Rajasekaran, T., Palanikumar, K., & Vinayagam, B. K. (2012). Turning CFRP composites with ceramic tool for surface roughness analysis. *Procedia Engineering, 38,* 2922-2929.

Raju, K. R. C. S., Faisal, N. H., Rao, D. S., Joshi, S. V., & Sundararajan, G. (2008). Electro-spark coatings for enhanced performance of twist drills. *Surface and Coatings Technology, 202*(9), 1636–1644.

Ramesh, M., Palanikumar, K., & Reddy, K. H. (2014). Influence of tool materials on thrust force and delamination in drilling sisal-glass fiber reinforced polymer (S-GFRP) composites. *Procedia Materials Science, 5*, 1915-1921.

Ramkumar, J., Aravindan, S., Malhotra, S. K., & Krishnamurthy, R. (2004a). An enhancement of machining performance of GFRP by oscillatory assisted drilling. *International Journal of Advanced Manufacturing Technology, 23*(3), 240-244.

Ramkumar, J., Malhotra, S. K., & Krishnamurthy, R. (2004b). Effect of work piece vibration on drilling of GFRP laminates. *Journal of Materials Processing Technology, 152*(3), 329 -332.

Ramulu, M., & Arola, D. (1993). Water jet and abrasive water jet cutting of unidirectional granite/epoxy composite. *Composites 24*(4), 299-308.

Ramulu, M., Branson, T., & Kim, D. (2001). A study on the drilling of composite and titanium stacks. *Composite Structures, 54*(1), 67-77.

Rawat, S., & Attia, H. (2009). Wear mechanisms and tool life management of WC–Co drills during dry high speed drilling of woven carbon fibre composites. *Wear 267*(5–8), 1022-1030.

Rieger, B., Kunkel, A., Coates, G. W., Reichardt, R., Dinjus, E., & Zevaco, A. T. (2012). *Synthetic biodegradable polymers*. London: Springer Heidelberg Dordrecht.

Rubio, J. C. C., Abrao, A. M., Faria, P. E., Correia, A. E., & Davim, J. P. (2008). Effects of high speed in the drilling of glass fibre reinforced plastic: Evaluation of the delamination factor. *International Journal of Machine Tools and Manufacture, 48*(6), 715-720.

Rubio, J. C. C., Panzera, T. H., & Scarpa, F. (2015). Machining behaviour of three high-performance engineering plastics. *Proceedings of the Institution of Mechanical Engineers, Part B: Journal of Engineering Manufacture, 229*(1), 28-37.

Saba, N., Paridah, M. T., & Jawaid, M. (2015). Mechanical properties of kenaf fibre reinforced polymer composite: A review. *Construction and Building Materials*, *76*, 87 – 96.

Sakthivel, M., Vijayakumar, S., Channankaiah, & Rajesh, M. (2015). A review on delamination in conventional and vibrated assisted drilling in glass fibre reinforced polymer composites. *International Journal of ChemTech Research, 7*(6), 2794-2801.

Sambhav, K., Dhande, S. G., & Tandon, P. (2012b). CAD based mechanistic modeling of forces for generic drill point geometry. *Computer-Aided Design and Applications, 7*(6), 809-819.

Sambhav, K., Tandon, P., & Dhande, S. G. (2012a). Geometric modeling and validation of twist drills with a generic point profile. *Applied Mathematical. Modelling, 36*(6), 2384- 2403.

Sanjay, C. (2006). Comparative analysis of various methods of surface roughness in drilling. *Journal of Advanced Manufacturing Systems, 5*(1), 75-87.

Saoudi, J., Zitoune, R., Gururaja, S., Mezlini, S., & Hajjaji, A. A. (2016). Prediction of critical thrust force for exit ply delamination during drill composite laminates: thermo-mechanical analysis. *International Journal of Machining and Machinability of Materials, 18*(1-2), 77- 98.

Sapuan, S. M., Kho, J. Y., Zainudin, E. S., Leman, Z., Ali, B. A. A., & Hambali, A. (2011). Material selection for natural fiber reinforced polymer composites using analytical hierarchy process. *Indian Journal of Engineering and Materials Sciences*, *18*(4), 255 – 267.

Saravanos, D. A., & Hopkins, D. A. (1996). Effects of delaminations on the damped dynamic characteristics of composite laminates: Analysis and experiments. *Journal of Sound and Vibration, 192*(5), 977-993.

Sardiñas, R. Q, Reis, P., & Davim, J. P. (2006). Multi-objective optimisation of cutting parameters for drilling laminate composite materials by using genetic algorithms. *Composites Science and Technology, 66*(15), 3083–3088.

Scarponi, C., Sarasini, F., Tirillo, J., Lampani, L., Valente, T., & Gaudenzi, P. (2015). Low-velocity impact response of hemp fibre reinforced bio-based epoxy laminates, *Proceedings of 5th Conference on Natural Fibre Composites for Industrial Applications*, (pp. 1-4). Sapienza Universita de Roma, Rome: Italy.

Schapery, R. A. (1968). Thermal expansion coefficients of composite materials based on energy principles. *Journal of Composite Materials, 2*(3), 380-404.

Schulz, H., & Emrich, A. K. (2000). Optimisation of the chip flute of drilling tools using the principle of genetic algorithms, *Proceedings of the CIRP International Seminar on*

*Intelligent Computation in Manufacturing Engineering, Vol. 2 (*pp. 371–376.). Capri, Italy.

Schulz, H., & Emrich, A. K. (2001). Using the principle of genetic algorithms for the optimisation of the chip flute of drilling tools. *Production Engineering*, *8*(2), 107–110.

Seif, M. A., Khashaba, U. A., & Rojas-Oviedo, R. (2007). Measuring delamination in carbon/epoxy composites using a shadow moiré laser based imaging technique. *Composite Structures, 79*(1), 113–118.

Selvam, S. V. M., & Sujatha, C. (1995). Twist deformation and optimum drill geometry. *Computers & Structures, 57*(5), 903–914.

Shah, D. U. (2013). Developing plant fibre composites for structural applications by optimising composite parameters: a critical review. *Journal of Material Science, 48*, 6083-6107.

Shaikh, A. A. & Jain, P. S. (2012). Experimental study of various technologies for cutting polymer matrix composites. *International Journal of Advanced Engineering Technology, 2*(1), 81-88.

Shaw, M. C. (2005). *Metal cutting principles*. (2nd ed.). Oxford: University Press Incorporation.

Shetty, P. K., Shetty, R., Shetty, D., Rehaman, F. N., & Jose, T. K. (2014). Machinability study on dry drilling of titanium alloy TI-6AL-4V using L_9 orthogonal array. *Procedia Materials Science, 5,* 2605-2614.

Shunmugesh, K., & Panneerselvam, K. (2016). Machinability study of carbon fiber reinforced polymer in the longitudinal and transverse direction and optimization of process parameters using PSO–GSA. *Engineering Science and Technology, an International Journal, 19*(3), 1552-1563.

Shyha, I. S., Aspinwall, D. K., Soo, S. L., & Bradley, S. (2009). Drill geometry and operating effects when cutting small diameter holes in CFRP. *International Journal of Machine Tools and Manufacture, 49*(12-13), 1008-1014.

Shyha, I. S., Soo, S. L., Aspinwall, D. K., Bradley, S., Dawson, S., & Pretorius, C. J. (2010a). Drilling of titanium/CFRP/aluminium stacks. In J. Zhao, M. Kunieda, G. Yang, & X. M.

Yuan (Eds.), *Key Engineering Materials, Advances in Precision Engineering* (Vol. 447-448, pp. 624-633). Switzerland: Trans Tech.

Shyha, I. S., Soo, S. L., Aspinwall, D. K., Bradley, S., Perry, R., Harden, P., & Dawson, S. (2011). Hole quality assessment following drilling of metallic-composite stacks. *International Journal of Machine Tools and Manufacture, 51*(7-8), 569-578.

Shyha, I., Soo, S. L., Aspinwall, D., & Bradley, S. (2010b). Effect of laminate configuration and feed rate on cutting performance when drilling holes in carbon fibre reinforced plastic composites. *Journal on Materials Processing Technology, 210*(8), 1023 – 1034.

Signor, A. W., & Chin, J. W. (2002). Effects of ultraviolet radiation exposure on vinyl ester matrix resins: chemical and mechanical characterization, *Proceedings of National Institute of Standards and Technology, Building Materials Division* (pp. 1-12). Gaithersburg, MD.

Singh, I., & Bhatnagar, N. (2006). Drilling-induced damage in uni-directional glass fibre reinforced plastics (UD-GFRP) composite laminates. *International Journal of Advanced Manufacturing Technology, 27*(9), 877-882.

Singh, I., Bhatnagar, N., & Viswanath, P. (2008). Drilling of uni-directional glass fibre reinforced plastics: Experimental and finite element study. *Materials & Design, 29*(2), 546-553.

Singh, M. K. (2008). *Unconventional manufacturing processes.* (1st ed.). United Kingdom: New Age International.

Singla, M. & Chawla, V. (2010). Mechanical Properties of Epoxy Resin – Fly Ash Composite. *Journal of Minerals & Materials Characterization & Engineering, 9*(3), 199 – 210.

Sivarao, P. S. (2005). Tool wear investigation and surface modelling in cutting force analysis for custiomised drilling, *Proceedings of international conference on recent advances in mechanical and materials engineering* (pp. pp.27-29). University of Malaysia, Kuala Lumpur, Malaysia.

Sivarao, P. S., & Wen, C. C. (2004). Comparison of statistical and mathematical methods for determination of tool wear in drilling. *Journal of Mechanical Engineering, 55*(4), 187-198.

Sivarao, P. S., Rahim, A. S., Taufik, A. Z., & Amma, A. R. (2007). Coating characterisation of TiN and TiAlN on burr formation in drilling- Pragmatic investigation, *Proceedings of international conference on engineering and ICT,* Vol. 3. (pp. 12 -17). Universiti Teknikal Malaysia Melaka, Melaka, Malaysia.

Song, K. Y., Chung, D. K., Park, M. S., & Chu, C. N. (2009). Micro electrical discharge of tungsten carbide using deionized water. *Journal of Micromechanics and Microengineering, 19,* 1-10.

SP Systems. (2001). *The advantages of epoxy resin versus polyester in marine composite structures*, United Kingdom. Retrieved from http://www.mjmyachts.com/images/stories/pdf/sp%20advantages%20of%20epoxy%20resin.pdf

Speranza, V., Sorrentino, A., De Santis F., & Pantani, R. (2014). Characterization of the polycaprolactone melt crystallization: Complementary optical microscopy, DSC, and AFM Studies. *The Scientific World Journal, 2014*, 1-9.

Sridharan, S. (2008). *Delamination behaviour of composites* (1st ed.). Cambridge England: Woodhead Publishing Limited.

Stephenson, D. A., & Agapiou, J. S. (1996). *Metal cutting theory and practice*. (1st ed.). New York: CRC Press.

Sun, G., & Zhou, Z. (2014). Application of laser ultrasonic technique for non-contact detection of drilling-induced delamination in aeronautical composite components. *Optik, 125*(14), 3608-3611.

Svensson, N., & Gilchrist, M. D. (1998). Mixed-mode delamination of multidirectional carbon fibre/epoxy laminates. *Mechanics of Composite Materials and Structures, 5*(3), 291-307.

Swoffs, Y., Gorbatikh, L., & Verpoest, I. (2014). Fibre hybridisation in polymer composites: A review. *Composites Part A: Applied Science and Manufacturing, 67,* 181–200.

Tagliaferri, V., Caprine, G., & Diterlizzi, A. (1990). Effect of drilling parameters on the finish and mechanical properties of GFRP composites. *International Journal of Machine Tools and Manufacture, 30*(1), 77-84.

Takeda, S., Okabe, Y., & Takeda, N. (2002). Delamination detection in CFRP laminates with embedded small-diameter fiber Bragg grating sensor. *Composites Part A: Applied Science and Manufacturing, 33*(7), 971-980.

Takeda, S., Okabe, Y., Yamamoto, T., & Takeda, N. (2003). Detection of edge delamination in CFRP laminates under cyclic loading using small-diameter FBG sensors. *Composites Science and Technology, 63*(13), 1885-1894.

Tandon, P., Gupta, P., & Dhande, S. G. (2008). Modelling of twist drills in terms of 3D angles. *International Journal of Advanced Manufacturing Technology, 38*(5), 543–550.

Teboub, Y., & Hajela, P. (1992). A neural network based damage nalysis of smart composite beams. Fourth AIAA/USAF/NASA/OAI symposium on multidisciplinary analysis and optimization, AIAA paper, 92-4685.

Techtip, (2012). *Glass transition temperature for epoxies*. Epoxy Technology Inc., Retrieved from http://www.epotek.com/site/files/Techtips/pdfs/tip 23.pdf

Terzopoulou, Z. N., Papageorgio, G. Z., Papadopoulou, E., Athanassiadou, E., Alexopoulou, E., & Bikiaris, D. N. (2015). Green composites prepared from aliphatic polyesters and bast fibers. *Industrial Crops and Science*, *68,* 60 – 79.

Thomas, P. N. H., & Babitsky, V. I. (2007). Experiments and simulations on ultrasonically assisted drilling. *Journal of Sound and Vibration, 308*(3-5), 815-830.

Thomas, S., Kuruvilla, J., Malhotra, S. K., Goda, K., & Sreekala, M. S. (Eds.). (2012). *Polymer Composites* (Part one, Vol. 1, pp. 1-814). New Jersey: Wiley-VCH Verlag & Co. KGaA.

Timoshenko, S., & Woinowsky-Krieger, S. (1959). *Theory of Plates and Shells*. (2nd ed.). New York: McGraw-Hill Book Company.

Todoroki, A., & Tanaka, Y. (2002). Delamination identification of cross-ply graphite/epoxy composite beams using electric resistance change method. *Computer Science and Technology, 62*(5), 629-639.

Todoroki, A., Tanaka, Y., & Shimamura, Y. (2002). Delamination monitoring of graphite/epoxy laminated composite plate of electric resistance change method. *Composites Science and Technology, 62*(9), 1151-1160.

Tong, L., Mouritz, A. P., & Bannister, M. (2002). *3D fibre reinforced polymer composites*. (1st ed.). London: Elsevier Science.

Tonshoff, H. K., Spintig, W., Ko¨nig, W., & Neises, A. (1994). Machining of holes developments in drilling technology. *CIRP Annals- Manufacturing Technology, 43*(2), 551–561.

Toolingu. (2013). *Metal Cutting Training, Metal Removal Process 110.* Cleveland: Tooling University. Retrieved from http://www.toolingu.com/classes/department/200/Metal-Cutting.

Tsao, C. C. (2008). Experimental study of drilling composite materials with step-core drill. *Materials and Design, 29*(9), 1740–1744.

Tsao, C. C., & Hocheng, H. (2003). The effect of chisel length and associated pilot hole on delamination when drilling composite materials. *International Journal of Machine Tools and Manufacture, 43*(11), 1087–1092.

Tsao, C. C., & Hocheng, H. (2004). Taguchi analysis of delamination associated with various drill bits in drilling of composite material. *International Journal of Machine Tools and Manufacture, 44*(10), 1085-1090.

Tsao, C. C., & Hocheng, H. (2005). Computerized tomography and C-Scan for measuring delamination in the drilling of composite materials using various drills. *International Journal of Machine Tools and Manufacture, 45*(11), 1282-1287.

Tsao, C. C., & Hocheng, H. (2007). Effect of tool wear on delamination in drilling composite materials. *International Journal of Mechanical Sciences, 49*(8), 983-988.

Tsao, C. C., & Hocheng, H. (2008). Effects of peripheral drilling moment on delamination using special drill bits. *Journal of Materials Processing Technology, 201*(1-3), 471–476.

Tungjitpornkull, S., & Sombatsompop, N. (2009). Processing technique and fibre orientation angle affecting the mechanical properties of E-glass reinforced wood/PVC composites. *Journal of Materials Processing Technology, 209*(6), 3079 – 3088.

Turner, J., Scaife, R. J., & El-Dessouky, H. M. (2015). Effect of machining coolant on the integrity of CFRP composites. *Advanced Manufacturing: Polymer and Composites Science, 1*(1), 54-60.

Unde, P. D., Gayakwad, M. D., & Ghadge, R. S. (2014). Abrasive water jet machining of composite materials – A review. *International Journal of Innovative Research in Science, Engineering and Technology, 3*(4), 6-8.

Upadhyay, P. C., & Lyons, J. S. (1999). On the evaluation of critical thrust for delamination-free drilling of composite laminates. *Journal of Reinforced Plastics and Composites, 18*(14), 1287–1303.

Van Geet, M., Swennen, R., & Wevers, M., (2000). Quantitative analysis of reservoir rocks by microfocus X-ray computerised tomography. *Sedimentary Geology, 132* (1–2), 25–36.

Van Natta, F. J., Hill, J. W., & Carruthers, W. H. (1934). Polymerization and ring formation, caprolactone and its polymers. *Journal of American Chemist Society, 56*, 455 –459.

Vautard, F., & Drzal, L. T. (2009). Carbon fiber-vinyl ester interfacial adhesion improvement by the use of a reactive epoxy coating, *Proceedings of the ICCM 17, Composite Materials and Structures Centre* (pp. 1-11). Edinburgh, UK.

Vaxevanidis, N. M., Gourgouletis, K., Galanis, N. I., & Manolakos, D. E. (2006). Electrical discharge drilling of carbon fibre reinforced composite materials. *International Journal of Machining and Machinability of Materials, 10*(3), 187-201.

Velayudham, A., & Krishnamurthy, R. (2007). Effect of point geometry and influence on thrust and delamination in drilling of polymeric composites. *Journal of Materials Processing Technology, 185*(1-3), 204-209.

Velayudham, A., Krishnamurthy, R., & Soundarapandian, T. (2005a). Evaluation of drilling characteristics of high volume fraction fibre glass reinforced polymeric composite. *International Journal of Machine Tools and Manufacture, 45*(4-5), 399-406.

Velayudham, A., Krishnamurthy, R., & Soundarapandian, T. (2005b). Acoustic emission based drill condition monitoring during drilling of glass/phenolic polymeric composite using wavelet packet transform. *Materials Science and Engineering: A, 412*(1-2), 141–145.

Veniali, F., Dillio, A., & Tagliaferri, V. (1995). An experimental study of the drilling of aramid composites. *American Society of Mechanical Engineers Journal of Energy Resources Technology, 117*(4), 271–278.

Vijayaraghavan, A. (2006). *Automated drill design software*. University of California, Berkeley. Retrieved from https://people.eecs.berkeley.edu/~sequin/CS285/PAPERS/drill_modeling.pdf

Wambua, P., Ivens, J., & Verpoest, I. (2003). Natural fibres: can they replace glass in fibre reinforced plastics. *Composites Science and Technology, 63*(9), 1259 – 1264.

Wang, B., Gao, H., Cao B., Zhuang, Y., & Zhao, Z. (2014). Mechanism of damage generation during drilling of carbon/epoxy composites and titanium alloy stacks. *Proceedings of the Institution of Mechanical Engineers, Part B: Journal of Engineering Manufacture, 228*(7), 698-706.

Wang, H., Guo, Q., Yang, J., Liu, Z., Zhao, Y., Li, J., Feng, Z., & Liu, L. (2013). Microstructural evolution and oxidation resistance of polyacrylonitrile-based carbon fibers doped with boron by the decomposition of B_4C. *Carbon, 56,* 296–308.

Wang, J., & Zhang, Q. (2008). A study of high- performance plane rake faced twist drills, Part I: Geometrical analysis and experimental investigation. *International Journal of Machine Tools and Manufacture, 48*(11), 1276–1285.

Wang, Q., Ning, H., Vaidya, U., Pillay, S., & Nolen, L. (2015). Development of a carbonization-in-nitrogen method for measuring the fiber content of carbon fiber reinforced thermoset composites. *Composites Part A: Applied Science and Manufacturing*, *73*, 80 – 84.

Wang, X., Wang, L. J., & Tao, J. P. (2004). Investigation on thrust in vibration of drilling of drilling of fibre-reinforced plastics. *Journal of Materials Processing Technology*, *148*(2), 239-244.

Webb, P. M. (1993). Dynamics of the twist drilling process. *International Journal of Production Research, 31*(4), 823–828.

Wen, C. C., Soon, L. T., & Sivarao, P. S. (2004). Comparative analysis and modelling of surface roughness in drilling. *International Journal of Applied Mechanics and Engineering, 9*, 305-311.

Williams, T. O., & Addessio, F. L. (1998). A dynamic model for laminated plates with delaminations. *International Journal of Solids and Structures, 35*(1-2), 83-106.

Won, M. S, & Dharan, C. K. H. (2002). Chisel edge and pilot hole effects in drilling composite laminates. *Journal of Manufacturing Science and Engineering, 124*(2), 242–247.

Wong, T. L., Wu, S. M., & Croy, G. M. (1982). An analysis of delamination in drilling composite material, *Proceedings of the 14th National Society of Advanced Materials & Processes Engineering (SAMPE) Technology Conference* (pp. 471-483). Atlanta, USA.

Woodruff, M. A., & Hutmacher, D. W. (2010). The return of a forgotten polymer-Polycaprolactone in the 21st century. *Progress in Polymer Science, 35*(10), 1217-1256.

Xiong, L., Fang, N., & Shi, H. (2009). A new methodology for designing a curve-edged twist drill with an arbitrarily given distribution of the cutting angles along the tool cutting edge. *International Journal of Machine Tools and Manufacture, 49*(7-8), 667– 677.

Xu, C., Danielsson, M., Karlsson, S., Svensson, C., & Bornefalk, H. (2012). Preliminary evaluation of a silicon strip detector for photon-counting spectral CT. *Nuclear Instrument Method in Physics Research Section A: Accelerators, Spectrometers, Detectors and Associated Equipment, 677*, 45-51.

Yan, L., & Jiang, F. (2013). A practical optimisation design of helical geometry drill point and its grinding process. *International Journal of Advanced Manufacturing Technology, 64*(9), 1387-1394.

Yan, Z. L., Zhang, J. C., Lin, G., Zhang, H., Ding, Y., & Wang, H. (2013b). Fabrication process optimisation of hemp fibre-reinforced polypropylene composites. *Journal of Reinforced Plastics and Composites,* 1-9.

Yan, Z., Zhang, J., Zhang, H., & Wang, H. (2013a). Improvement of mechanical properties of noil hemp fiber reinforced polypropylene composites by resin modification and fiber treatment. *Advances in Materials Science and Engineering, 2013*, 1-7.

Yang, Y., & Sun, J. (2009). Finite element modelling and simulating of drilling of titanium alloy, *Proceedings of the Second International Conference on Information and Computing Science*, IEEE Computer Society (pp. 178-181), IEEE.

Zhang, L. B., Wang, L. J., & Wang, X. (2003). Study on vibration drilling of fibre reinforced plastics with hybrid variation parameters method. *Composites Part A: Applied Science and Manufacturing, 34*(3), 237-244.

Zhang, L. B., Whang, L. J., & Liu, X. Y. (2001). A mechanical model for predicting critical thrust forces in drilling composite laminates. *Proceedings of the Institution of Mechanical Engineers, Part B: Journal of Engineering Manufacture, 215*(2), 135-146.

Zitoune, R., & Collombet, F. (2007). Numerical prediction of the thrust force responsible of delamination during the drilling of the long-fibre composite structures. *Composites Part A: Applied Science and Manufacturing, 38*(3), 858-866.

Zitoune, R., Krishnaraj, V., & Collombet, F. (2010). Study of drilling of composite material and aluminium stack. *Composite Structures, 92*(5), 1246–1255.

APPENDIX A

Industrial collaborators' contact details

Upon request

APPENDIX B

Material safety data sheet (MSDS) for CAPA 6800

Polycaprolactone

1. IDENTIFICATION OF THE MATERIAL AND SUPPLIER

Product Name: CAPA 6800 POLYCAPROLACTONE

Synonym: None

Recommended uses: footwear industry, film, pharmaceuticals, automotive industry

2. HAZARDS IDENTIFICATION

NOT CLASSIFIED AS HAZARDOUS ACCORDING TO NOHSC CRITERIA

Hazard Category: None allocated

Hazard Classification: NON-HAZARDOUS SUBSTANCE, NON-DANGEROUS GOOD

RISK PHRASES

None allocated

SAFETY PHRASES

None allocated

Poison Schedule: Non Scheduled

Warning Statement:

None

3. COMPOSITION / INFORMATION ON INGREDIENTS

SUBSTANCE NAME	Proportion	CAS Number
2-Oxepanone, homopolymer	>99 %	24980-41-4

All other ingredients not hazardous according to NOHSC Criteria.

4. FIRST AID MEASURES

Swallowed:

If swallowed, DO NOT induce vomiting. If person is conscious give water to drink. Seek medical attention immediately.

Eye:

If material is splashed into eyes, immediately, flush with plenty of water for 15 minutes, ensuring eyelids are held open. If irritation persists seek medical attention.

Skin:

If material is splashed onto the skin, remove any contaminated clothing and wash skin thoroughly with water and soap.

Flush skin with water. Seek medical attention if irritation persists after washing.

Inhaled:

Remove victim to fresh air. Apply resuscitation if victim is not breathing. If trained personnel available administer oxygen if breathing is difficult.

First Aid Facilities:

Eye wash fountain, safety shower and normal washroom facilities.

Advice to Doctor:

Treat symptomatically.

In case of poisoning, contact Poisons Information Centre

In Australia call Tel: 131126

In New Zealand Tel: 034747000

5. FIRE-FIGHTING MEASURES

Fire/Explosion Hazard

If safe to do so, move undamaged containers from fire area.

HAZARDOUS DECOMPOSITION PRODUCTS: Decomposes on heating emitting toxic and/or irritating fumes including carbon monoxide and carbon dioxide.

FIRE FIGHTING PROCEDURES: Fire fighters to wear Self-Contained Breathing Apparatus (SCBA) in confined spaces, in oxygen deficient atmospheres or if exposed to products of decomposition. Full protective clothing is also recommended.

EXTINGUISHING MEDIA: Use extinguishing media suitable for surrounding fire situation. Use foam, water spray (fog), CO2 or dry powder. Use water spray to cool fire-exposed containers and for large fires.

HAZCHEM CODE: None allocated [Aust]

FLAMMABILITY

This product is not flammable.

6. ACCIDENTAL RELEASE MEASURES

Material may be slippery when spilt. Walk cautiously. Ventilate area. Wear protective equipment to prevent skin and eye contact, as outlined in Section 8 of this Material Safety Data Sheet. Bund area using sand or soil - to prevent run off into drains and waterways. Use absorbent (soil, sand, vermiculite or other inert material). Collect and seal in

7. HANDLING AND STORAGE

Store in a cool place and out of direct sunlight. Store away from sources of heat or ignition. Store away from oxidising agents. Keep containers closed when not using the product. Store in original packages as approved by manufacturer. Purge with nitrogen and close container when not in use. Do not eat, drink or smoke in the workplace.

8. EXPOSURE CONTROLS / PERSONAL PROTECTION

Exposure Standards

No exposure standards have been assigned by [NOHSC] for this product or any of the components:

****

2-Oxepanone, homopolymer

No Exposure details available

Engineering Controls

Maintain adequate ventilation at all times. In most circumstances natural ventilation systems are adequate unless the material is heated, reacted or otherwise changed in some type of chemical reaction, then the use of a local exhaust ventilation system is recommended. If exhaust ventilation is not available or inadequate, use approved respirator to Australian Standards.

Personal Protection Equipment

CLOTHING: Wear suitable protective clothing to prevent skin contact.

GLOVES: Wear impervious gloves to prevent skin contact - PVC or natural rubber.

EYES: Wear safety glasses with side shields, chemical goggles or face shield to protect eyes.

RESPIRATORY PROTECTION: Avoid breathing of vapours/gases. Select and use respirators in accordance with AS/NZS 1715/1716. The use of a respirator for organic vapours with disposable or with replaceable filters is recommended. Filter capacity and respirator type depends on exposure levels and type of contaminant. If entering spaces where the

airborne concentration of a contaminant is unknown then the use of a Self-contained breathing apparatus (SCBA) with positive pressure air supply complying with AS/NZS 1715 / 1716, or any other acceptable International Standard is recommended.

9. PHYSICAL AND CHEMICAL PROPERTIES

Appearance:	White granules/pellets
Boiling Point	Not applicable
Melting Point:	
Vapour Pressure:	[to be filled in]
Specific Gravity:	1.1 @ 60 °C
Flash Point:	275 °C (Method: Open Cup)
Flammability Limits:	No data
Solubility:	Insoluble in water
Other Properties	Souluble in aromatic solvents, chlorinated hydrocarbons
Viscosity	8000000 mPa.s @ 100 °C
Freezing Point	ca. 35 °C
Granulometry	Mean diameter. ca. 3 mm
Decomposition Temperature	ca. 200 °C

10. STABILITY AND REACTIVITY

STABILITY:

Stable under normal conditions of use.

HAZARDOUS DECOMPOSITION PRODUCTS:

Carbon monoxide, particulates of carbon, caprolactone/monomer

HAZARDOUS POLYMERIZATION:

Will not occur.

INCOMPATIBILITIES: Strong alkalis, acids.

CONDITIONS TO AVOID:

Heat, flames, ignition sources and incompatibles.

11. TOXICOLOGICAL INFORMATION

No adverse health effects are expected, if the product is handled in accordance with this Material Safety Data Sheet and the product label. Symptoms and effects that may arise if the product is mishandled and overexposure occurs are:

ACUTE HEALTH EFFECTS:

Swallowed:

May cause irritation to mouth, throat and stomach with effects including mucous build up, irritation to the tongue and lips and pains in the stomach, which may lead to nausea, vomiting and diarrhoea.

Eye:

May cause irritation to the eyes, with effects including: tearing, pain, stinging and blurred vision.

Skin:

May cause irritation to the skin, with effects including; Redness and itchiness.

Inhaled:

May cause irritation to the nose, throat and respiratory system with effects including: Dizziness, headache and loss of co-ordination.

Chronic:

Toxicological Data:

There is no other toxicological information available for this product.

12. ECOLOGICAL INFORMATION

Ecotoxity:

There is no information available for this product.

Mobility:

There is no information available for this product.

Persistence / Degradability:

There is no information available for this product.

Chemical Fate Information:

There is no ecological information available for this product, however, large quantities should not be discharged into drains, sewers or waterways.

13. DISPOSAL CONSIDERATIONS

Refer to appropriate authority in your State. Dispose of material through a licensed waste contractor. Advise flammable nature. Normally suitable for disposal by approved waste disposal agent.

14. TRANSPORT INFORMATION

Road Transport

UN Number: None allocated

Proper Shipping Name: NONE ALLOCATED

Dangerous Goods Class: None allocated

Packing Group: None allocated **Label:** None allocated

Air Transport

UN Number: None allocated

Proper Shipping Name: NONE ALLOCATED

Dangerous Goods Class: None allocated

Packing Group: None allocated **Label:** None allocated

Sea Transport

UN Number: None allocated

Proper Shipping Name: NONE ALLOCATED

Dangerous Goods Class: None allocated

Packing Group: None allocated

Label: None allocated

15. REGULATORY INFORMATION

Poison Schedule: Non Scheduled

Inventory Status:

Inventory	*Status*
Australia (AICS)	Y

Y = all ingredients are on the inventory.

16. OTHER INFORMATION

Date of Preparation:

Issue date: 12 April 2010 Supersedes: May 2008

Reasons for Update: Periodic review

Key Legend Information:

NOHSC - National Occupational Health & Safety Commission {Formerly Worksafe}[Aust]

SUSDP - Standard for the Uniform Scheduling of Drugs and Poisons [Aust]

TWA - Time Weighted Average [Int]

STEL - Short Term Exposure Limit [Int]

AICS - Australian Inventory of Chemical Substances

EPA - Environmental Protection Agency [Int]

NIOSH - National Institute for Occupational Safety and Health [US]

AS/NZS 1715 - Selection, use and maintenance of respiratory protective devices. [Aust/NZ]

AS/NZS 1716 - Respiratory protective devices. [Aust/NZ]

IATA - International Aviation Transport Authority [Int]

ICAO - International Civil Aviation Organization [Int]

IMO - International Maritime Organisation. [Int]

IMDG - International Maritime Dangerous Goods [Int]

United Nations Recommendations for the Transport of Dangerous Goods and Globally Harmonized System for the classification and labelling of Chemicals. [Int] EU - European Union

[Aust/NZ] = Australian New Zealand

[Int] = International

[US] = United States of America

Removal of the heading of *Poison Schedule [Aust]*, in section 3 and 15 of this Material Safety Data Sheet (MSDS) makes this a valid health and safety document in other international jurisdictions/countries. For full compliance please contact your Federal, State or Local regulators for further information.

Disclaimer

This MSDS summarises our best knowledge of the health and safety hazard information available on the product and the measures to be used to handle and use the product safely. Each user should read this MSDS and consider the information in connection with the way the product is intended to be handled or used.

Principal References:

Information supplied by manufacturer, reference sources including the public domain.

END OF MSDS

APPENDIX C

I. Product data sheet for HexPly®8552 Epoxy matrix

HexPly® 8552
Epoxy matrix (180°C/356°F curing matrix)
Product Data

Description

HexPly® 8552 is a high performance tough epoxy matrix for use in primary aerospace structures. It exhibits good impact resistance and damage tolerance for a wide range of applications.
HexPly® 8552 is an amine cured, toughened epoxy resin system supplied with unidirectional or woven carbon or glass fibres.
HexPly® 8552 was developed as a controlled flow system to operate in environments up to 121°C *(250°F)*.

Benefits and Features

- Toughened epoxy matrix with excellent mechanical properties
- Elevated temperature performance
- Good translation of fibre properties
- Controlled matrix flow in processing
- Available on various reinforcements
- Excellent drape and tack

Resin Matrix Properties

Rheology

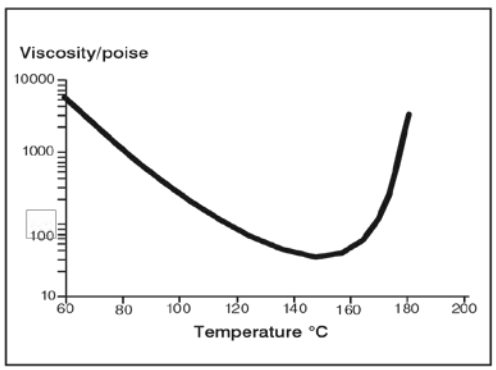

Gel Time

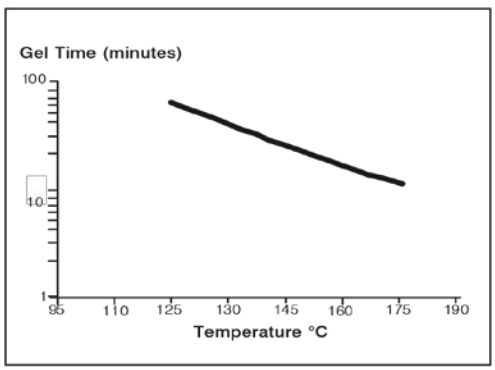

HexPly® 8552

Prepreg Properties - HexPly® 8552 UD Carbon Prepregs

Physical Properties

	Units	AS4	IM7
Fibre Density	g/cm³ *(lb/in³)*	1.79 *(0.065)*	1.77 *(0.064)*
Filiament count/tow		12K	12K
Resin density	g/cm³ *(lb/in³)*	1.30 *(0.047)*	1.30 *(0.047)*
Nominal Cured Ply Thickness 8552 /35%/134	mm *(inch)*	0.130 *(0.0051)*	0.131 *(0.0052)*
Nominal Fibre Volume	%	57.42	57.70
Nominal Laminate Density	g/cm³ *(lb/in³)*	1.58 *(0.057)*	1.57 *(0.057)*

Mechanical Properties

Test	Units	Temp °C *(°F)*	Condition	AS4	IM7
0°Tensile Strength	MPa *(ksi)*	-55*(-67)*	Dry	1903 *(267)*	2572 *(373)*
		25*(77)*	Dry	2207 *(320)*	2724 *(395)*
		91*(195)*	Dry	-	**2538 *(368)****
90°Tensile Strength	MPa *(ksi)*	-55*(-67)*	Dry	-	174 *(25.3)*
		25*(77)*	Dry	81 *(11.7)*	64 *(9.3)*
		93*(200)*	Dry	75 *(10.9)*	**92 *(13.3)****
0°Tensile Modulus	GPa *(msi)*	-55*(-67)*	Dry	134 *(19.4)*	163 *(23.7)*
		25*(77)*	Dry	141 *(20.5)*	164 *(23.8)*
		91*(195)*	Dry	-	**163 *(23.7)****
90°Tensile Modulus	GPa *(msi)*	-	-	-	-
		25*(77)*	Dry	10 *(1.39)*	12 *(1.7)*
		93*(200)*	Dry	8 *(1.22)*	**10 *(1.5)****
0°Compression Strength	MPa *(ksi)*	-55*(-67)*	Dry	1586 *(230)*	-
		25*(77)*	Dry	1531 *(222)*	1690 *(245)*
		91*(195)*	Dry	1296 *(184)*	1483 *(215)*
0°Compression Modulus	GPa *(msi)*	-55*(-67)*	Dry	124 *(18)*	-
		25*(77)*	Dry	128 *(18.6)*	150 *(21.7)*
		91*(195)*	Dry	122 *(17.7)*	162 *(23.5)*
0° ILSS (Shortbeam shear)	MPa *(ksi)*	-55*(-67)*	Dry	164 *(23.8)*	-
		25*(77)*	Dry	128 *(18.5)*	137 *(19.9)*
		91*(195)*	Dry	122 *(14.7)*	**94 *(13.6)****
		25*(77)*	Wet	117 *(16.9)*	115 *(16.7)*
		71*(160)*	Wet	84 *(12.2)*	**80 *(11.6)*****
		91*(195)*	Wet	78 *(11.3)*	-
In-plane Shear Strength	MPa *(ksi)*	25*(77)*	Dry	114 *(16.6)*	120 *(17.4)*
		93*(200)*	Dry	105 *(15.2)*	**106 *(15.4)****

Bold 93°C *(200°F)* **Bold* 104°C *(220°F)*** **Bold** 82°C *(180°F)***

Prepreg Properties - HexPly® 8552 Woven Carbon Prepregs (AS4 Fibre)

Physical Properties

	Units	AGP193 -PW	AGP 280-5H
Fibre Type	-	AS4 3K	AS4 3K
Fibre density	g/cm³ *(lb/in³)*	1.77 *(0.065)*	1.77 *(0.065)*
Weave	-	Plain	5HS
Mass	g/m² *(oz/yd²)*	193 *(5.69)*	286 *(8.44)*
Weight Ratio, Warp : Fill		50 :50	50 :50
Nominal cured ply thickness @ 37% resin content	mm *(inch)*	0.195 *(0.0076)*	0.289 *(0.0114)*
Nominal Fibre Volume	%	55.29	55.29
Nominal Laminate Density	g/cm³ *(lb/in³)*	1.57 *(0.057)*	1.57 *(0.057)*

Mechanical Properties

Test	Units	Temp°C (°F)	Condition	AGP193-PW	AGP280- 5H
0°Tensile Strength	MPa *(ksi)*	-55*(-67)*	Dry	766 *(111)*	828 *(120)*
		25*(77)*	Dry	828 *(120)*	876 *(127)*
		91*(195)*	Dry	-	903 *(131)*
90°Tensile Strength	MPa *(ksi)*	-55*(-67)*	Dry	710 *(103)*	752 *(109)*
		25*(77)*	Dry	793 *(115)*	800 *(116)*
		93*(200)*	Dry	759 *(110)*	772 *(112)*
0°Tensile Modulus	GPa *(msi)*	-55*(-67)*	Dry	66 *(9.5)*	70 *(10.2)*
		25*(77)*	Dry	68 *(9.8)*	67 *(9.7)*
		91*(195)*	Dry	-	69 *(10)*
90°Tensile Modulus	GPa *(msi)*	-55*(-67)*	Dry	66 *(9.6)*	67 *(9.7)*
		25*(77)*	Dry	66 *(9.5)*	66 *(9.5)*
		93*(200)*	Dry	68 *(9.8)*	65 *(9.4)*
0°Compression Strength	MPa *(ksi)*	-55*(-67)*	Dry	959 *(139)*	-
		25*(77)*	Dry	883 *(128)*	924 *(134)*
		91*(195)*	Dry	759 *(110)*	***752 (109)***
0°Compression Modulus	GPa *(msi)*	-55*(-67)*	Dry	60 *(8.7)*	-
		25*(77)*	Dry	60 *(8.7)*	64 *(9.3)*
		91*(195)*	Dry	61 *(8.8)*	***67(9.7)***
0° ILSS	MPa *(ksi)*	-55*(-67)*	Dry	101 *(14.6)*	-

(Shortbeam shear)		25*(77)*	Dry	84 *(12.2)*	79 *(11.4)*
		91*(195)*	Dry	70 *(10.2)*	-
		25*(77*)	Wet	75 *(10.9)*	69 *(10)*
		71*(160)*	Wet	72 *(10.4)*	-
		91*(195)*	Wet	59 *(8.5)*	-

Bold 93ºC *(200ºF)* **Bold* 104ºC *(220ºF)*** **Bold** 82ºC *(180ºF)***

Prepreg Properties - HexPly® 8552 Woven Carbon Prepregs (IM7 Fibre)

Physical Properties

	Units	**SPG 196-P**	**SPG 370-8H**
Fibre Type	-	IM7 6K	IM7 6K
Fibre density	g/cm³ *(lb/in³)*	1.77 *(0.064)*	1.77 *(0.064)*
Weave	-	Plain	8HS
Mass	g/m² *(oz/yd²)*	196 *(5.78)*	374 *(11.03)*
Weight Ratio, Warp : Fill		50 :50	49 :51
Nominal cured ply thickness @ 37% resin content	mm *(inch)*	0.199 *(0.0078)*	0.380 *(0.0150)*
Nominal Fibre Volume	%	55.57	55.57
Nominal Laminate Density	g/cm³ *(lb/in³)*	1.56 *(0.056)*	1.56 *(0.056)*

Mechanical Properties

Test	**Units**	**Temp°C (°F)**	**Condition**	**SPG 196-PW**	**SPG 370-8H**
0°Tensile Strength	MPa *(ksi)*	-55*(-67)*	Dry	979 *(142)*	965 *(140)*
		25*(77)*	Dry	1090 *(158)*	1014 *(147)*
		91*(195)*	Dry	-	-
90°Tensile Strength	MPa *(ksi)*	-55*(-67)*	Dry	862 *(125)*	903 *(131)*
		25*(77)*	Dry	945 *(137)*	959 *(139)*
		93*(200)*	Dry	***979 (142)****	***879 (130)****
0°Tensile Modulus	GPa *(msi)*	-55*(-67)*	Dry	85 *(12.3)*	86 *(12.5)*
		25*(77)*	Dry	85 *(12.3)*	86 *(12.4)*
		91*(195)*	Dry	-	-
90°Tensile Modulus	GPa *(msi)*	-55*(-67)*	Dry	80 *(11.6)*	81 *(11.7)*
		25*(77)*	Dry	80 *(11.6)*	81 *(11.7)*
		93*(200)*	Dry	***79 (11.5)****	***79 (11.5)****
0° ILSS (Shortbeam shear)	MPa *(ksi)*	-55*(-67)*	Dry	-	-
		25*(77)*	Dry	88 *(12.7)*	90 *(13)*
		91*(195)*	Dry	***69 (10)****	***74 (10.8)****
		25*(77)*	Wet	80 *(11.6)*	83 *(12.1)*
		71*(160)*	Wet	***61 (8.8)****	***63 (9.1)****
		91*(195)*	Wet	-	-

Bold 93ºC *(200ºF)* **Bold* 104ºC *(220ºF)*** **Bold** 82ºC *(180ºF)***

Typical Neat Resin Data

Colour	Yellow	
Density	1.301 g/cc	*(0.0470 lb/in³)*
Glass Transition Temperature, Tg dry	200°C	*(392°F)*
Glass Transistion Temperature, Tg wet	154°C	*(309°F)*
Tensile Strength	121 MPa	*(17.5 ksi)*
Tensile Modulus	4670 MPa	*(0.677 msi)*

CURING CONDITIONS

Cure cycle for monolithic components

1. Apply full vacuum (1 bar).
2. Apply 7 bar gauge autoclave pressure.
3. Reduce the vacuum to a safety value of 0.2 bar when the autoclave pressure reaches approximately 1 bar gauge.
4. Heat at 1- 3°C/min *(2-8°F/min)* to 110°C ± 5°C *(230°F ± 9°F)* 5. Hold at 110°C ± 5°C *(230°F ± 9°F)* for 60 minutes ± 5 minutes.
6. Heat at 1-3°C/min *(2-8°F/min)* to 180°C ± 5°C *(356°F ± 9°F)* 7. Hold at 180°C ± 5°C *(356°F ± 9°F)* for 120 minutes ± 5 minutes.
8. Cool at 2 - 5°C *(4-9°F)* per minute
9. Vent autoclave pressure when the component reaches 60°C *(140°F)* or below.

Cure cycle for honeycomb sandwich components

1. Apply full vacuum (1 bar).
2. Apply 3.2 bar gauge autoclave pressure.
3. Reduce the vacuum to a safety value of 0.2 bar when the autoclave pressure reaches approximately 1 bar gauge.
4. Heat at 1- 3°C/min *(2-8°F/min)* to 110°C ± 5°C *(230°F ± 9°F)* 5. Hold at 110°C ± 5°C *(230°F ± 9°F)* for 60 minutes ± 5 minutes.
6. Heat at 1-3°C/min *(2-8°F/min)* to 180°C ± 5°C *(356°F ± 9°F*) 7. Hold at 180°C ± 5°C *(356°F ± 9°F)* for 120 minutes ± 5 minutes.
8. Cool at 2 - 5°C *(4-9°F)* per minute
9. Vent autoclave pressure when the component reaches 60°C *(140°F)* or below.

Note: For both cure cycles – at each stage, use the temperature shown by the leading thermocouple.

Heat-up rates are dependent on component thickness, eg, slow heat-up rates should be used for thicker components and large tools. Accurate temperature measurements of the component should be made during the cure cycles by using thermocouples.

Performance testing should accompany alternative cure cycles to ensure suitability for the particular application.

CURING CYCLE FOR HONEYCOMB AND MONOLITHIC COMPONENTS

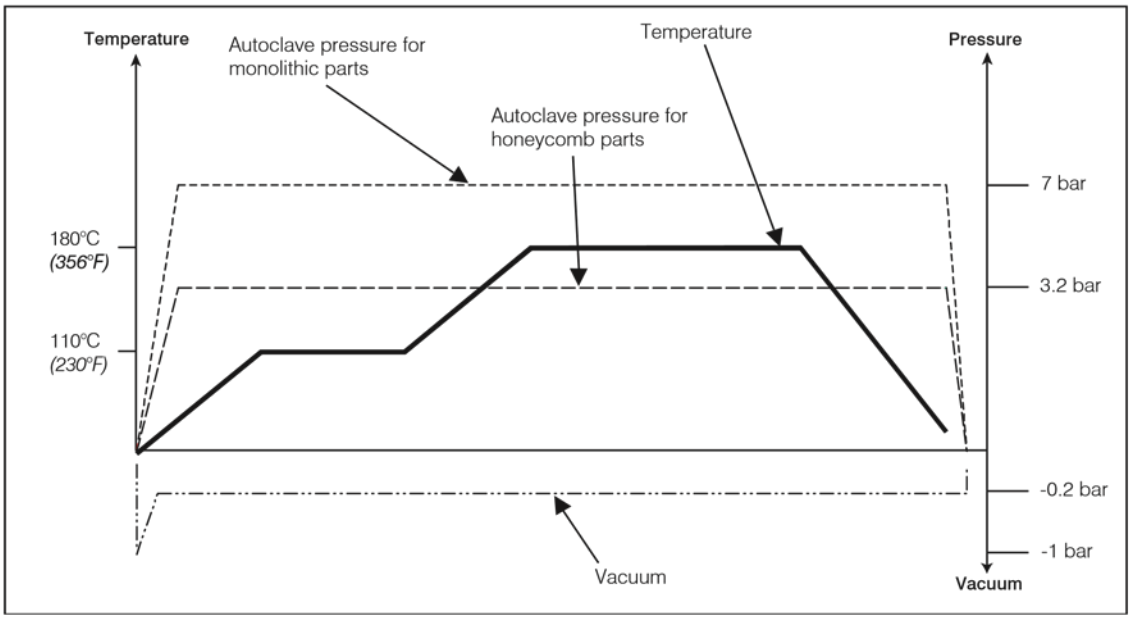

PREPREG STORAGE LIFE

Tack Life:	10 days at RT *(23°C/73°F)*
Out Life:	30 days at RT *(23°C/73°F)*
Shelf Life:	12 months at -18°C*(0°F)* (from date of manufacture)

Definitions:

Shelf Life:	The maximum storage life for HexPly® Prepreg, upon receipt by the customer, when stored continuously, in a sealed moisture-proof bag, at -18°C*(0°F)*. To accurately establish the exact expiry date, consult the box label.
Tack Life:	The time, at room temperature, during which prepreg retains enough tack for easy component lay-up.
Out Life:	The maximum accumulated time allowed at room temperature between removal from the freezer and cure.

Precautions for Use

The usual precautions when handling uncured synthetic resins and fine fibrous materials should be observed, and a Safety Data Sheet is available for this product. The use of clean disposable inert gloves provides protection for the operator and avoids contamination of material and components.

IMPORTANT

All information is believed to be accurate but is given without acceptance of liability. Users should make their own assessment of the suitability of any product for the purposes required. All sales are made subject to our standard terms of sale which include limitations on liability and other important terms.

Publication FTA 072e (Feb 2013)

FOR MORE INFORMATION

Hexcel is a leading worldwide supplier of composite materials to aerospace and other demanding industries. Our comprehensive product range includes:

- Carbon Fibre
- RTM Materials
- Honeycomb Cores
- Carbon, glass, aramid and hybrid prepregs
- HexTOOL® composite tooling material
- Structural Film Adhesives
- Honeycomb Sandwich Panels
- Engineered Core
- Reinforcement Fabrics

For US quotes, orders and product information call toll-free 1-800-688-7734

For other worldwide sales office telephone numbers and a full address list please go to:

http://www.hexcel.com/OurCompany/sales-offices

II. Safety data sheet for Epoxy Resin

Safety Data Sheet

Section 1: PRODUCT AND COMPANY IDENTIFICATION

SDS Identification Name: Hexply® 8552 Prepreg
SDS Number: 439-7737-8552-0000-15 **Date:** May 1, 2010 **Page:** 1 of 8
Supersedes SDS: 439-7737-8552-0000-14

Manufacturer:
Hexcel®
6700 West 5400 South
West Valley City, UT. 84118-0748

Emergency Telephone Number:
800-433-5072 (24-Hour) Hexcel®

Information Telephone Number:
925-551-4900 (Normal Business Hours-PT)

Product Identification Number: Hexply® 8552 Prepreg

Chemical Family: Epoxy Resin Impregnated Aramid, Carbon and Nickel Coated Carbon, Ceramic (Nextel®), Fiberglass Fabric and Fibers

Section 2: COMPOSITION/INFORMATION ON INGREDIENTS

The listed components are classified as Hazardous Chemicals as defined by the OSHA Hazard Communication Standard, 29 CFR 1910.1200.

Component	CAS® Number	% by Weight	OSHA (PEL)	ACGIH® (TLV®)
Resin Matrix Information:				
Tetra glycidyl methylene bis aniline epoxy resin	28768-32-3	8-15	Not determined	Not determined
Glycidyl amino phenol epoxy resin	5026-74-4	8-15	Not determined	Not determined
Aromatic amine	80-08-0 599-61-1	7-14	Not determined	Not determined
Substrate Information, if used:				
Fiberglass fiber, synthetic, vitreous, continuous filament	65997-17-3	35-70	15 mg/m^3 (Total) 5 mg/m^3 (Respirable)	5 mg/m^3 (Inhalable) 1 f/cc (Respirable)

Ceramic fiber	12788-79-3	35-70	15 mg/m^3 (Total) 5 mg/m^3 (Respirable)	10 mg/m^3 (Inhalable) 3 mg/m^3 (Respirable)
Nickel, metallic (for nickel coated fabric based on total fabric weight)	7440-02-0	23-34	1 mg/m^3 (TWA)	1.5 mg/m^3 (TWA)

Section 2: COMPOSITION/INFORMATION ON INGREDIENTS (Continued)

This product is classified as a Hazardous Chemical as defined by the OSHA Hazard Communication Standard, 29 CFR 1910.1200.

The exposure limits expressed are for each individual component and not for the total product.

The percentages will vary depending on product type, whether a scrim fabric or fiber is used, the individual component's variation and the resin content applied.

SECTION 3: HAZARDS IDENTIFICATION

EMERGENCY OVERVIEW:

Appearance and Odor:
Slightly tacky resin on black, white or yellow fabric or fiber, with or without a scrim fabric, on a carrier paper and / or polyethylene film with no significant odor at room temperature.

Statements of Hazard:

Warning! Dust generated from machining, grinding or sanding the product may be combustible and could result in fire and/or explosion should the necessary dust concentration in air and ignition source be present.
Warning! May cause skin, eye and respiratory tract irritation, allergic skin reaction, possible sensitization and skin absorption.

Dust from machining, grinding or sawing the cured product may cause skin, eye and upper respiratory tract irritation, allergic skin reaction and possible sensitization.

Vapor evolved during heating or curing may cause eye and respiratory tract irritation.

Primary Routes of Exposure:

Eye--Yes Skin--Yes Inhalation--Yes Ingestion--Unlikely

HMIS® Rating:

Health--2* Chronic Flammability--0 Reactivity--1 Special--None

Potential Health Effects:

Eye: Contact may cause irritation. Vapor or fumes generated from exposing this product to elevated temperatures may cause irritation. Dust from machining, grinding or sawing the cured product may cause mechanical irritation.

Skin: Contact may cause irritation, allergic skin reaction, dermatitis and possible sensitization. Dust from machining, grinding or sawing the cured product may cause mechanical irritation, sensitization and dermatitis.

Inhalation: May cause irritation to the upper respiratory tract. Vapor or fumes generated from exposing this product to elevated temperatures may cause irritation to the respiratory tract. Dust from machining, grinding or sawing the cured product may cause irritation to the upper respiratory tract.

Ingestion: The effects of ingestion are unknown. The cured product dust or particulate from machining, grinding or sawing may cause mechanical irritation.

Medical Conditions Aggravated by Exposure: Preexisting eye, skin or respiratory order may be aggravated by contact and/or exposure to this product or the dust from machining, grinding or sawing the cured product.

Section 3: HAZARDS IDENTIFICATION (Continued)

Carcinogenic Information: None of the components present in this material at concentrations equal to or greater than 0.1 % are listed or regulated by IARC, NTP, OSHA or ACGIH as a carcinogen. If Nickel coated carbon is used, (CAS® # 7440-02-0), a NTP and IARC 2B (possible human carcinogen).

Other:	**OSHA (PEL)**	**ACGIH® (TLV®)**
Exposure limits for cured product	15 mg/m^3 (Total)	10 mg/m^3 (Inhalable)
dust as [Particulate Not Otherwise Regulated (PNOR) by OSHA or Specified (PNOC) by ACGIH®]:	5 mg/m^3 (Respirable)	3 mg/m^3 (Respirable)

The exposure limits for each hazardous component of the various product types must be considered in the total exposure assessment.

Section 4: FIRST AID MEASURES

Eye: In case of eye contact, immediately flush eyes with large amounts of water for at least 15 minutes, keeping the eyelids open. Get medical attention immediately.

Skin: In case of contact with this product or the cured product dust, immediately wash skin with soap and plenty of water. Get medical attention if irritation develops.

Inhalation: If excessive inhalation of vapor, fumes, dust or particulate occurs, remove to fresh air. If breathing is difficult, get medical attention immediately.

Ingestion: Ingestion of this product or the dust from it is unlikely. If swallowed, get medical attention immediately.

Section 5: FIRE FIGHTING MEASURES

Flash Point/Method of Determination: Not determined

Means of Extinction: Use water spray, dry chemical or CO_2 to extinguish fires. Use water to keep containers cool.

Special Fire Hazards: Avoid exposure through use of a self-contained, positive-pressure breathing apparatus. Dust generated from machining, grinding or sanding the product may be combustible and could result in fire and/or explosion should the necessary dust concentration in air and ignition source be present.

Section 6: ACCIDENTAL RELEASE MEASURES

Procedures in case of Accidental Release or Leakage: Avoid contact with skin, eyes or clothing (See Section 8). Clean up material, put into suitable container and dispose of properly (See Section 13).

SECTION 7: HANDLING AND STORAGE

Precautions to be taken in Handling and Storage: See label on container for the proper temperature. Maintain sealed against contamination from dirt and moisture.

Section 8: EXPOSURE CONTROLS/PERSONAL PROTECTION

Eye/Face Protection: Avoid eye and skin contact. Wear safety glasses, chemical type goggles and a face shield, as necessary. Wear safety glasses with side shields when machining grinding or sawing the cured product.

Skin Protection: Wear protective clothing such as uniforms, coveralls or lab coats sufficient to cover skin areas. Use gloves made of impervious materials and resistant to chemicals.

Respiratory Protection: If sufficient vapor or fumes are being generated during use and/or during heating or curing the product, use a NIOSH approved organic vapor respirator. If sufficient dust or particulate are generated during machining, grinding or sawing the cured product, use a NIOSH approved dust respirator.

Ventilation: Use local exhaust sufficient to control the vapor, fumes, dust or particulate generated during use of the product or when machining, grinding or sawing the cured product. If an exhaust ventilation is not available or is inadequate, use a NIOSH approved respirator, as appropriate.

General Hygiene Recommendations: Good personal hygiene practices should be followed at all times. Before eating, drinking, smoking or using toilet facilities, wash face and hands thoroughly with soap and water. Use vacuum equipment to remove the product dust or particulate from clothing and work areas. Compressed air is not recommended.

Section 9: PHYSICAL AND CHEMICAL PROPERTIES

Appearance and Odor..... Slightly tacky resin on black, white or yellow fabric or fiber, with or without a scrim fabric, on a carrier paper and / or polyethylene film with no significant odor at room temperature.

Boiling Point (ºF/ºC)..... Not determined

Melting Point (ºF/ºC)..... Not determined

Specific Gravity (Water=1).....Not determined

pH of Undiluted Product.....Not determined

Vapor Pressure (mm Hg.).....Not determined

Vapor Density (Air=1).....Not determined

Viscosity..... Not determined

Volatile [Percent (%) by Weight].... 0-1

Percent (%) VOC..... Same as the % volatile **Solubility in Water**..... Not determined

Section 10: STABILITY AND REACTIVITY

Stability: Stable under proper handling and storage conditions.

Incompatible Materials: Avoid strong oxidizing agents.

Products evolved from Heat of Combustion or Decomposition: The products of combustion and decomposition depend on other materials present in the fire and the actual conditions of the fire. Burning will produce oxides of carbon, nickel, nitrogen, aldehydes, sulfur oxides, acrolein, phenols, amines aromatic amines and other unidentified gases and vapors that may be toxic. Avoid inhalation.

Hazardous Polymerization: Will not occur under proper conditions of use. The product, if heated improperly, heated rapidly, heated to an excessive temperature or heated in a large quantity or mass, may produce an uncontrolled exothermic reaction that may char and decompose, generating unidentified gases and vapors that may be toxic. Avoid inhalation.

Section 11: TOXICOLOGICAL INFORMATION

Component Toxicity Data:

Median Lethal Dose (Species):

Oral (LD_{50})...Tetra glycidyl methylene bis aniline epoxy resin…>10,000 mg/kg (Rat)
…Glycidyl amino phenol epoxy resin…1,000-3,000 mg/kg, (Rat)
…Aromatic amine…640 mg/kg (Rat)
…Nickel (for Nickel coated fabric), if used as the substrate…>9000 mg/kg (Rat)

Inhalation (LC_{50})...Tetra glycidyl methylene bis aniline epoxy resin…>30 mg/m^3/4H (Rat)
…Glycidyl amino phenol epoxy resin…>46.2 mg/m^3/4H max attainable (Rat)

Dermal (LD_{50})...Tetra glycidyl methylene bis aniline epoxy resin…>3,000 mg/kg (Rabbit)
…Glycidyl amino phenol epoxy resin…>3,000 mg/kg (Rat)

…Aromatic amine…>4,000 mg/kg (Rabbit)

Irritation Index, Estimation of Irritation (Species):

Skin...Glycidyl amino phenol epoxy resin…Marked (Rabbit)

Eye...Tetra glycidyl methylene bis aniline epoxy resin…Slight (Draize Score 5.4/110) (Rabbit)

Other:

Sensitization...Tetra glycidyl methylene bis aniline epoxy resin…skin sensitization reported in humans; sensitizer (Guinea pig)
…Glycidyl amino phenol epoxy resin…skin sensitizer (Guinea pig)
…Aromatic amine…severe dermal sensitization reactions in human

Mutagenic…Tetra glycidyl methylene bis aniline epoxy resin:
…Ames Tests-Positive
…E.Coli-Negative
…Mouse Lymphoma-Positive
…Cell Transformation-Negative
…Nucleus Anomaly (in vivo)-Negative
…Mouse Micronucleus Assay (in vivo)-Positive
…Sister Chromatid Exchange (in vivo)-Inconclusive/Negative
…Cytogenetic Spermatocytes-Negative
…Cytogenetic Spermatogonia-Negative
439-7737-8552-0000-15

Section 11: TOXICOLOGICAL INFORMATION (Continued)

Mutagenic (continued) …Glycidyl amino phenol epoxy resin:

…Ames Tests-Positive
…E.Coli-Positive

…Mouse Lymphoma-Positive
…Cell Transformation-Negative
…Nucleus Anomaly-Positive

…Sister Chromatid Exchange-Positive

…TSCA 8(E) Notification of mutagenicity results filed with the EPA.

Section 12: ECOLOGICAL INFORMATION

Total Product Data:

No ecological data has been determined on the total product.

Component Data:

Fish Toxicity (LC_{50})…Glycidyl amino phenol epoxy resin…4.2/mg/L/96H (Carp)
(Cyprinus carpio)

Invertebrate Toxicity (EC_{50}):

Glycidyl amino phenol epoxy resin…>10,000mg/L bacteria (Pseudomonas putida)

Biodegradability:
Glycidyl amino phenol epoxy resin…Not readily biodegradable (Modified Sturm Test)

Section 13: DISPOSAL CONSIDERATIONS

Waste Disposal Methods: Material for disposal should be placed in appropriate sealed containers to avoid potential human and environmental exposure. It is the responsibility of the generator to comply with all federal, state, provincial and local laws and regulations. We recommend that you contact an appropriate waste disposal contractor and environmental agency for relevant laws and regulations. Under the U.S., Resource Conservation and Recovery Act (RCRA), it is the responsibility of the user of the product to determine at the time of disposal, whether the product meets relevant waste classification and to assure proper disposal.

SECTION 14: TRANSPORT INFORMATION

DOT:

Proper Shipping Name….. Not regulated
Identification Number….. Not regulated
Packing Method…… Not regulated

Hazard Class……..Not regulated
Packing Group……..Not regulated
Label Required…… …..None

439-7737-8552-0000-15

SECTION 15: REGULATORY INFORMATION

SARA Title III:

Section 302/304 Extremely Hazardous Substance: None

Section 311 Hazardous Categorization:
Class 1 (Acute)
Class 2 (Chronic)

Section 313 Toxic Chemicals:
Nickel (for Nickel coated fabric), (CAS® # 7440-02-0), if used as the substrate

CERCLA Section 102(a) Hazardous Substance:
Nickel (for Nickel coated fabric), (CAS® # 7440-02-0), if used as the substrate

RCRA Information:

Currently, this product is not listed in federal hazardous waste regulations 40 CFR, Part 261.33, paragraphs (e) or (f), i.e. chemical products that are considered hazardous if they become wastes. State or local hazardous waste regulations may also apply if they are different from the federal regulation. It is the responsibility of the user of the product to determine at the time of disposal, whether the product meets relevant waste classification and to assure proper disposal.

WHMIS (Canada):
Classification

D2B

This product has been classified in accordance with hazard criteria of the "Controlled Products Regulations" and this SDS contains all the information required by the "Controlled Products Regulations."

Ingredient Disclosure List:
Fibrous Glass (CAS® # 65997-17-3), if used as the substrate
Nickel (for Nickel coated fabric), (CAS® # 7440-02-0), if used as the substrate

U.S., EPA, and TSCA Information: This product is an article as defined by TSCA and is not required to be listed in the TSCA Inventory.

Ozone Depletion Information: This product does not contain or is not manufactured with ozone depleting substances as identified in Title VI, Clean Air Act "Stratospheric Ozone Protection" and the regulations set forth in 40 CFR, Part 82.

SECTION 16: OTHER INFORMATION

Special Precautions: Airborne carbon fibers, dust or particulate may create electrical short-circuits that could result in damage to or malfunctioning of electrical equipment.

Explanation and Disclaimer: Wherever such words or phrases as “hazardous," "toxic," "carcinogen," etc. appear herein, they are used as defined or described under state employee right-to-know laws, Federal OSHA laws or the direct sources for these laws such as the International Agency for Research on Cancer (IARC), the National Toxicology Program (NTP), etc. The use of such words or phrases should not be taken to mean that we deem or imply any substance or exposure to be toxic, hazardous or otherwise harmful. 439-7737-8552-0000-15

Section 16: OTHER INFORMATION (Continued)

ANY EXPOSURE CAN ONLY BE UNDERSTOOD WITHIN THE ENTIRE CONTEXT OF ITS OCCURRENCE, WHICH INCLUDES SUCH FACTORS AS THE SUBSTANCE'S CHARACTERISTICS AS DEFINED IN THE SDS, AMOUNT AND DURATION OF EXPOSURES, OTHER CHEMICALS PRESENT AND PRE-EXISTING INDIVIDUAL DIFFERENCES IN RESPONSE TO THE EXPOSURE.

The data provided in this SDS is based on the information received from our raw material suppliers and other sources believed to be reliable. We are supplying you this data solely in compliance with the Federal OSHA Hazard Communication Standard, 29 CFR 1910.1200 and other Federal and state laws as described in Section 15: Regulatory Information.

The information contained in this SDS is proprietary and confidential to Hexcel Corporation. This SDS and the information in it are not to be used for purposes other than compliance with the Federal OSHA Hazard Communication Standard. If you have received this SDS from any source other than Hexcel Corporation or its authorized agent, the information contained in it may have been modified from the original document and it may not be the most current revision.

Liability, if any, for use of this product is limited to the terms contained in our sale terms and conditions. We do not in any way warrant (expressed or implied, including any implied warranty for merchantability or fitness for a particular purpose) the data contained or the product described in this SDS. Additionally, we do not warrant that the product will not infringe any patent or other proprietary or property rights of others.

Prepared by: Darryl Ong,
Hexcel Corporate Safety and Health,
Senior Product Safety Information Specialist

Revision History:

05/04/10 added Nickel coated fabric to the MSDS
10/12/09 added ceramic (Nextel) to the MSDS
04/17/09 added warning for combustible dust phrase in section 3 and 5.

06-09-05 Editorial on CAS number for Tetra Glycidyl 12-01-05 Deleted quartz from chemical family

III. Features and properties of MTM®44-1

MTM44-1 is a high performance, 180°C (356°F) curing, toughened epoxy resin formulated for the production of primary and secondary aircraft structures.

MTM44-1 can be processed via low pressure vacuum bag Out-of-Autoclave (OoA) moulding or autoclave moulding.

Advantages of MTM44-1 include excellent Tg retention under wet conditions, low density and a high level of damage tolerance.

MTM44-1 meets NASA outgassing requirements and can be used in space structures.

Features

- 21 days out life at 21°C (70°F)
- 12 months storage at -18°C (0°F)
- Meets NASA outgassing standards when tested to ECSS-Q-ST-70-02C
- Low density offers 2-4% weight saving compared to standard aerospace matrices
- Available in unidirectional prepreg for hand lay-up, ATL and AFP

- ☐ Available in fabric formats
- ☐ Out-of-Autoclave (OoA) or autoclave cure
- ☐ 130°C (266°F) or 180°C (356°F) initial cure
- ☐ 190°C (374°F) dry Tg following 180°C (35
- ☐ 150°C (302°F) wet Tg following 180°C (35
- ☐ Excellent damage tolerance
- ☐ Fully compatible HTA®240 OoA adhesive

RELATED DOCUMENTS

- De-bulking guidelines (TDS1036)
- MTM44-1 and MTM45-1 lay-up and bagging guidelines (TDS1043)
- Autoclave processing lay-up and bagging guidelines (TDS1037)

RELATED PRODUCTS

- HTA240 adhesive film (PDS1207)
- MTF246 surfacing film (PDS1240)

CURE CYCLE

Oven vacuum bag cure

Vacuum bag pressure	Minimum of 980 mbar (29”Hg)*
Ramp rate	1 to 2°C (1.8 to 3.6°F)/minute
Recommended cure cycle	2 hours at 130°C (266°F) + 2 hours at 180°C (356°F)
Cool down	Maximum of 3°C (5.4°F)/minute to 60°C (140°F)

*This is the ideal vacuum level, however, it is recognised that it is not always possible to attain. If in doubt, please contact our technical support staff for advice.

Autoclave cure

Vacuum bag pressure	Minimum of 980 mbar (29”Hg)*
Autoclave pressure	6.2 bar (90 psi)**
Ramp rate	1 to 2°C (1.8 to 3.6°F)/minute
Recommended cure cycle	2 hours at 130°C (266°F) + 2 hours at 180°C (
Cool down	Maximum of 3°C (5.4°F)/minute to 60°C (1

*This is the ideal vacuum level, however, it is recognised that it is not always possible to attain. If in doubt, please contact our technical support staff for advice.

**If producing sandwich panels, apply the maximum pressure allowable for the honeycomb type.

Alternative cure cycle

Temperature	Duration
130°C (266°F)	4 hours

Notes:
- The alternative cure cycle is recommended when using tooling that cannot withstand 180°C.
- Parts cured using the alternative cure cycle must be post-cured for 2 hours at 180°C (356°F)

POST-CURE

Following a 130°C (266°F) initial cure, the material will be in a relatively low state of cure. To develop full mechanical performance and maximum Tg, parts must be post-cured to 180°C (356°F) for 2 hours.

Ramp rate	0.3°C (0.5°F)/minute
Post-cure cycle	2 hours at 180°C -0/+5°C (356°F -0/+9°F
Cool down	2°C (3.6°F)/minute to 60°C (140°F)

* Temperature must be measured by the lagging thermocouple attached to the part.

Notes:
- Parts may be loaded into a pre-heated oven or heated at 3°C (5.4°F)/minute to the initial cure temperature.
- Large components should be adequately supported to avoid distortion.

PHYSICAL PROPERTIES

Test	Sample/test conditions
Cured resin density	
DMA E’ onset Tg, SACMA	Dry Wet* Skydrol*
Resin gel time	At 130°C (266°F)
Viscosity	At 80°C (176°F) At 130°C (266°F) At 140°C (284°F) At 160°C (320°F)
Moisture pick-up (cast resin)	At 25°C (77°F)/60%RH At 60°C (140°F)/60%RH

Moisture pick-up (MTM44-1/M55J 32%)	At 25°C (77°F)/60%RH At 60°C (140°F)/60%RH
Outgassing (MTM44-1/M55J 32%) Test Method ECSS-Q-ST-70-02C	Total mass loss (TML) Recovered mass loss (RML) Water vapour release (WVR) Collected volatile condensable material (CVCM)

*14 days immersion at 70°C (158°F)

Note:
All data generated on samples cured for 2 hours at 180°C (356°F)

MECHANICAL PROPERTIES

Cure cycle: 2 hours at 180°C (356°F), oven vacuum bag cure.
Test conditions: Room temperature, dry

Test	Test method	Units	145 g/m² 12k HTS5631 UD	268 g/m² 24k IMS5131 UD
0° Tensile modulus	ASTM D3039	GPa (msi)	128.9 (18.6)	174.6 (25.3)
0° Tensile strength		MPa (ksi)	2159 (313)	2738 (397)
0° Compressive modulus	ASTM D695 (MOD)	GPa (msi)	123.2 (17.8)	147.2 (21.3)
0° Compressive strength		MPa (ksi)	1330 (192.8)	1459 (211.5)
In-plane shear modulus (IPSM)	ASTM D3518	GPa (msi)	4.11 (0.6)	3.60 (0.5)
In-plane shear strength (IPSS)		MPa (ksi)	112.7 (16.3)	76 (11)
0° Flexural modulus	CRAG 200	GPa (msi)	121.9 (17.7)	154.9 (22.4)
0° Flexural strength		MPa (ksi)	1958 (238.9)	1874 (271.7)
0° Interlaminar shear strength (ILSS)	ASTM D2344	MPa (ksi)	106.6 (15.4)	109.4 (15.8)

All data, except for ILSS and IPSS & IPSM normalised to 55%Vf for fabric reinforced samples and 60%Vf for unidirectional reinforced samples.

Hot/wet laminate performance

Test	Test method	Units	Test conditions	Stitched NCF HTS5631 UD	134g/m² 12k HTS5631 UD
0° Interlaminar shear strength (ILSS)	EN2563	MPa (ksi)	RT/dry 120°C (248°F)/dry 120°C (248°F)/wet*	96 (13.9) 68 (9.86) 50 (7.25)	94 (13.6) 58 (8.4) 50 (7.25)

* Equilibrium at 70°C (158°F)/85% R.H.

Open hole compression strength

Test	Test method	Units	Test conditions	134g/m² 12k HTS5631 UD	268g/m² 24k IMS5131 UD
OHC – Quasiisotropic	LIS/MECH/280	MPa (ksi)	RT/dry	311 (45.1)	304 (44.1)

Unidirectional data normalised to 60% Vf, fabric data to 55% Vf.

Compressive strength after impact (CSAI)

Test	Test method	Units	Test conditions	32-ply 145g/m^2 12k HTS5631 UD	16-ply 268g/m^2 24k IMS5131 UD
CSAI– Quasiisotropic	SRM 2R-94 Impact 6.7J/mm	MPa (ksi)	RT/dry	259 (37.6) [32 J]	247 (35.8) [28 J]

Unidirectional data normalised to 60% Vf, and fabric data to 55% Vf. [J] = Actual impact energy for test laminate.

Availability

MTM44-1 is available as a fabric prepreg, unidirectional prepreg or slit tape.

STORAGE

Out life* at 21°C (70°F)	21 days
Storage at -18°C (0°F)	12 months from date of manufacture

*Out life refers to accumulated time out of the freezer before the part is cured.

Note:
The actual freezer storage life and out life are dependent on a number of factors, including; fibre type, format and application. For certain formats, it may be possible for the storage life and out life to be longer than stated. Please contact our technical support staff for advice.

EXOTHERM

MTM44-1 is a reactive formulation, but has a low exotherm risk and can be used for moulding thick sections. If in doubt, contact the Group's Technical support staff for advice when moulding sections greater than 50mm (2in) thick.

HEALTH & SAFETY

MTM44-1 contains epoxy resins which can cause allergic reactions by skin contact. Avoid contact with the skin. Gloves and protective clothing must be worn.

Wash skin thoroughly with soap and water or resin removing cream after handling. Do not use solvents for cleaning the skin.

Use mechanical exhaust ventilation when heat curing the resin system. Exhaust from vacuum pumps should be vented to external atmosphere and not into the work place.

For further information, consult Cytec Safety Data Sheet number:

SDS 413

IV. Safety data sheet for MTM®44-1 Epoxy Resin Prepreg

SAFETY DATA SHEET

MTM®44-1 EPOXY RESIN PREPREG

IDENTIFICATION OF THE SUBSTANCE/PREPARATION AND OF THE COMPANY/UNDERTAKING

PRODUCT NAME	MTM®44-1 EPOXY RESIN PREPREG
PRODUCT NO.	MTM44-1, ZPREG44-1, 426, 477
APPLICATION	Epoxy Resin Prepreg
SUPPLIER	Umeco Structural Materials Sinclair Close Heanor Gate Industrial Estate Heanor Derbyshire DE75 7SP e-mail: sds@umeco.com Tel: +44 (0)1773 766200 UK Office hours Only Fax: +44 (0)1773 719289 www.umeco.com

HAZARDS IDENTIFICATION

CLASSIFICATION (1999/45)	Muta Cat. 3;R68. R43. R52/53.	
CLASSIFICATION (EC 1272/2008)		
Hazards	Physical and Chemical	Not classified.
	Human health	Skin Sens. 1 - H317;Muta. 2 - H341

Environment Aquatic Chronic 3 - H412 LABEL IN ACCORDANCE WITH (EC) NO. 1272/2008

SIGNAL WORD	Warning
CONTAINS	N,N,N',N'-TETRAGLYCIDYL-4,4'-DIAMINODIPHENYLMETHANE

HAZARD STATEMENTS

H317	May cause an allergic skin reaction.
H341	Suspected of causing genetic defects.
H412	Harmful to aquatic life with long lasting effects.

SUPPLEMENTARY PRECAUTIONARY STATEMENTS

P202	Do not handle until all safety precautions have been read and understood.
P272	Contaminated work clothing should not be allowed out of the workplace.
P273	Avoid release to the environment.
P281	Use personal protective equipment as required.
P302+352	IF ON SKIN: Wash with plenty of soap and water.
P333+313	If skin irritation or rash occurs: Get medical advice/attention.
P363	Wash contaminated clothing before reuse.
P405	Store locked up.
P501	Dispose of contents/container to …

Supplemental Label Information (EU)

EUH205	Contains epoxy constituents. May p reaction.

ENVIRONMENT

Contains a substance which causes risk of hazardous effects to the environment.

PHYSICAL AND CHEMICAL HAZARDS

Potential exothermic reaction when heated.

HUMAN HEALTH

Exposure to fibres is unlikely to occur when properly used. The product contains a sensitising substance which may provoke an allergic reaction among sensitive individuals. Harmful vapours may be liberated during curing. The product contains a substance/a chemical group which is suspected of having harmful long-term effects.

COMPOSITION/INFORMATION ON INGREDIENTS

N,N,N',N'-TETRAGLYCIDYL-4,4'-DIAMINODIPHENYLMETHANE	10-25%
CAS-No.: 28768-32-3 EC No.: 249-204-3	
Classification (EC 1272/2008) Not classified.	Classification (67/548/EEC) Muta. Cat. 3; R68. N; R51/53. R43.

4,4'-METHYLENEBIS[2,6-DIETHYLANILINE] CAS-No.: 13680-35-8 EC No.: 237-185-4		5-10%
Classification (EC 1272/2008) Not classified.	Classification (67/548/EEC) Xn;R22.	
4,4'-METHYLENEBIS(2-ISOPROPYL-6-METHYLANILINE) CAS-No.: 16298-38-7 EC No.: 415-150-6		2.5-5%
Classification (EC 1272/2008) STOT Rep. 2 - H373 Aquatic Chronic 2 - H411	Classification (67/548/EEC) Xn;R48/22 N;R51/53	

The Full Text for all R-Phrases and Hazard Statements is Displayed in Section 16

FIRST-AID MEASURES

GENERAL INFORMATION

Preparation contains an epoxy resin, which may cause sensitisation and development of allergy. Exposure to fibres is unlikely to occur when properly used. Get medical attention if any discomfort continues.

INHALATION

Limited inhalation hazard at normal work temperatures. Unlikely route of exposure as the product does not contain volatile substances. General first aid, rest, warmth and fresh air. Get medical attention if any discomfort continues.

INGESTION

Not relevant, due to the form of the product.

SKIN CONTACT

Remove contaminated clothing. Wash skin thoroughly with soap and water. Get medical attention if irritation persists after washing.

EYE CONTACT

Immediately flush with plenty of water for up to 15 minutes. Remove any contact lenses and open eyes wide apart. Get medical attention promptly if symptoms occur after washing.

FIRE-FIGHTING MEASURES

EXTINGUISHING MEDIA

Fire can be extinguished using: Water spray, foam, dry powder or carbon dioxide.

SPECIAL FIRE FIGHTING PROCEDURES

Quench exotherming material with water spray Avoid breathing fire vapours. Use supplied air respirator if product is involved in a fire. Containers close to fire should be removed immediately or cooled with water. Keep run-off water out of sewers and water sources.

UNUSUAL FIRE & EXPLOSION HAZARDS

Potential exothermic reaction when heated. High temperatures generate: Acrid smoke/fumes

SPECIFIC HAZARDS

When heated and in case of fire, irritating vapours/gases may be formed.

PROTECTIVE MEASURES IN FIRE

Self contained breathing apparatus and full protective clothing must be worn in case of fire.

ACCIDENTAL RELEASE MEASURES

PERSONAL PRECAUTIONS

Wear protective clothing as described in Section 8 of this safety data sheet.

ENVIRONMENTAL PRECAUTIONS

Avoid release to the environment. Do not discharge into drains, water courses or onto the ground.

SPILL CLEAN UP METHODS

Collect in containers and seal securely. Containers with collected spillage must be properly labelled with correct contents and hazard symbol. For waste disposal, see section 13.

HANDLING AND STORAGE

USAGE PRECAUTIONS

Defrost thoroughly before use. Protective gloves are recommended. Observe good chemical hygiene practices.

STORAGE PRECAUTIONS

Keep only in the original protective bag at a temperature not exceeding - 18 °C. Do not store near heat sources or expose to high temperatures.

STORAGE CLASS

Store frozen (Product stability)

EXPOSURE CONTROLS/PERSONAL PROTECTION

INGREDIENT COMMENTS

No exposure limits noted for ingredient(s). Due to the hazardous nature of ingredients, exposure should be minimal.

PROTECTIVE EQUIPMENT

PROCESS CONDITIONS

The recommended curing procedures must be followed.

ENGINEERING MEASURES

Provide adequate general and local exhaust ventilation.

RESPIRATORY EQUIPMENT

No specific recommendation made, but protection against nuisance dust must be used when the general level exceeds 10 mg/m3. It is therefore important to take particular care to avoid inhalation exposure when mechanically processing cured material (e.g. grinding, sanding and sawing).

HAND PROTECTION

Barrier cream applied before work may make it easier to clean the skin after exposure, but does not prevent absorption through the skin. Protective gloves are recommended. Rubber (natural, latex). Nitrile. For exposure of 1 to 4 hours use gloves made of: Butyl rubber gloves are recommended, but be aware that the liquid may penetrate the gloves. Frequent change is advisable.

EYE PROTECTION

Exposure to fibres is unlikely to occur when properly used.

OTHER PROTECTION

Wear appropriate clothing to prevent any possibility of skin contact.

HYGIENE MEASURES

Wash hands after handling. Wash contaminated clothing before reuse. When using do not eat, drink or smoke. Wash at the end of each work shift and before eating, smoking and using the toilet.

PERSONAL PROTECTION

Good personal hygiene is necessary. Wash hands and contaminated areas with water and soap before leaving the work site.

SKIN PROTECTION

Wear apron or protective clothing in case of contact.

ENVIRONMENTAL EXPOSURE CONTROLS

Do not release into the environment.

PHYSICAL AND CHEMICAL PROPERTIES

APPEARANCE	Epoxy resin Impregnated fabric.
COLOUR	Orange to Brown.
ODOUR	Odourless.
SOLUBILITY	Insoluble in water
VOLATILE ORGANIC COMPOUND (VOC)	Negligible

STABILITY AND REACTIVITY

STABILITY

Stable under normal temperature conditions and recommended use.

CONDITIONS TO AVOID

Caution: Thick laminates (>10mm) may exotherm on curing. Avoid heat. Toxic gases are generated when heated. May decompose at temperatures exceeding 100 °C

HAZARDOUS POLYMERISATION

May polymerise. Potential exothermic reaction when heated.

POLYMERISATION DESCRIPTION

Systems are based on a reactive resin / curative combination and may under certain circumstances undergo a rapid rise in temperature, an exotherm. This may be accompanied by the evolution of potentially harmful fumes.

MATERIALS TO AVOID

Strong oxidising substances. Strong alkalis. Amines.

HAZARDOUS DECOMPOSITION PRODUCTS

Thermal decomposition or combustion may liberate carbon oxides and other toxic gases or vapours.

TOXICOLOGICAL INFORMATION

GENERAL INFORMATION

Cured panels often produce edges which are extremely sharp and capable of penetrating protective clothing.

INHALATION

Not relevant at normal room temperatures. When heated, harmful vapours may be formed.

INGESTION

Harmful if swallowed.

SKIN CONTACT

Risk of sensitisation or allergic reactions among sensitive individuals.

HEALTH WARNINGS

Preparation contains an epoxy resin, which may cause sensitisation and development of allergy.

ROUTE OF ENTRY

Skin and/or eye contact.

Name N,N,N',N'-TETRAGLYCIDYL-4,4'-DIAMINODIPHENYLMETHANE

Other Health Effects

Extensive in vitro and in vivo tests have been conducted with this substance in bacteria and animals in order to clarify its mutagenic potential. Interpretation of the test results in accordance with EC criteria (Directive 2001/59/EC) indicates that this substance should be classified as a Category 3 mutagen, with Risk Phrase R68.

Name 4,4'-METHYLENEBIS[2,6-DIETHYLANILINE]

Toxic Dose 1 - LD 501,901 mg/kg (oral rat)

ECOLOGICAL INFORMATION

ECOTOXICITY

The product contains substances which are toxic to aquatic organisms and which may cause long term adverse effects in the aquatic environment.

MOBILITY

The product is insoluble in water and will sediment in water systems.

BIOACCUMULATION

The product hardens to a solid immobile substance. Bioaccumulation is unlikely to be significant because of the low water solubility of this product.

DEGRADABILITY

The product is not expected to be biodegradable.

WATER HAZARD CLASSIFICATION

WGK 2

Name	N,N,N',N'-TETRAGLYCIDYL-4,4'-DIAMINODIPHENYLMETHANE
LC 50, 96 Hrs, Fish mg/l	7 mg/l (96h) (Carp)

Degradability

The product is not readily biodegradable. OECD 301 B (Mod. Sturm)

DISPOSAL CONSIDERATIONS

GENERAL INFORMATION

Waste is classified as hazardous waste. Disposal to licensed waste disposal site in accordance with the local Waste Disposal Authority.

DISPOSAL METHODS

Recover and reclaim or recycle, if practical. Waste is suitable for incineration. Dispose of waste and residues in accordance with local authority requirements.

TRANSPORT INFORMATION

GENERAL The product is not covered by international regulation on the transport of dangerous goods (IMDG, IATA, ADR/RID).
No transport warning sign required.

REGULATORY INFORMATION

UK REGULATORY REFERENCES

The Control of Substances Hazardous to Health Regulations 2002 (S.I 2002 No. 2677) with amendments.

EU DIRECTIVES

Regulation (EC) No 1272/2008 of the European Parliament and of the Council of 16 December 2008 on classification, labelling and packaging of substances and mixtures, amending and repealing Directives 67/548/EEC and 1999/45/EC, and amending Regulation (EC) No 1907/2006 with amendments. Regulation (EC) No 1907/2006 of the European Parliament and of the Council of 18 December 2006 concerning the Registration, Evaluation, Authorisation and Restriction of Chemicals (REACH), establishing a European Chemicals Agency, amending Directive 1999/45/EC and repealing Council Regulation (EEC) No 793/93 and Commission Regulation (EC) No 1488/94

as well as Council Directive 76/769/EEC and Commission Directives 91/155/EEC, 93/67/EEC, 93/105/EC and 2000/21/EC, including amendments.

APPROVED CODE OF PRACTICE

Safety Data Sheets for Substances and Preparations. Classification and Labelling of Substances and Preparations Dangerous for Supply.

NATIONAL REGULATIONS

The Chemicals (Hazard Information and Packaging for Supply) Regulations 2002. No. 1689. The Carriage of Dangerous
Goods and Use of Transportable Pressure Equipment Regulations 2007 (CDG 2007)

OTHER INFORMATION

GENERAL INFORMATION

Only trained personnel should use this material. The recommended curing procedures must be followed.

ISSUED BY

HSE Manager

REVISION DATE	03/04/2012
REV. NO./REPL. SDS	MSDS413 (Issue 8)
GENERATED	
SDS NO.	10496
SAFETY DATA SHEET STATUS	
Approved.	
DATE12/01/2009	

RISK PHRASES IN FULL

R22	Harmful if swallowed.
R48/22	Harmful: danger of serious damage to health by prolonged exposure if swallowed.
R43	May cause sensitisation by skin contact.
R68	Possible risk of irreversible effects.
R51/53	Toxic to aquatic organisms, may cause long-term adverse effects in environment.

HAZARD STATEMENTS IN FULL

H373	May cause damage to organs <<Organs>> through prolonged or repeated exposure.
H411	Toxic to aquatic life with long lasting effects.

APPENDIX D

D1: Risk assessment on drilling of HFRP composite laminates

University of Portsmouth — Health and Safety

ASSESSING OUR RISKS – GENERAL RISK ASSESSMENT FORM

Calculate: **Probability** multiplied by **severity** for No/Post control scores.
NB: For scores of 10 (High), or more contact the health & safety department for further advice.

Probability \ Severity	Minor Injury 1	Lost time/ Ill Health 2	Major / >3 days 3	Perm. Disability 4	Fatal/ Slight Loss 5
Highly Unlikely 1	1	2	3	4	5
Unlikely 2	2	4	6	8	10
Possible 3	3	6	9	12	15
Probable 4	4	8	12	16	20
Certain 5	5	10	15	20	25

Site/Department: Mechanical & Design ENGINEERING WORKSHOP.

Task/Activity/Area: Drilling of Polycaprolactone/Hemp fibre (PCLHF) composite laminates [**Non-hazardous, non-dangerous and non-flammable substance** according to National Occupational Health & Safety Commission (NOHSC) {Formerly Work safe}].

Notes: No previous record of accident on drilling of composite laminates.
(including details of previous accidents/incidents)

RA Team: Supervisory team (Dr. E. Dimla, Dr. I. Popov, Dr. H. Dhakal), S. Ismail (PhD student) & Mr. Geoff Britton.
(Mgr, Supervisor, EHS Adviser, Safety Rep, Employee, minimum is 2 people)

Date of RA: 07 -07 - 2014

People at risk: Employees and Visitors: Operator, PhD student, co-worker(s) & members of the Public (students, visitors & staff)
(e.g., visitors, contractors, hauliers, members of the public, operators, engineers, other employees etc)

Dept Manager (Print Name): Mr. Geoff Britton.

Signature:

Review Date:	07 -07 - 2014	Review Date:	07 -07 - 2014	Review Date:	07 -07- 2014		
Ref No. or Task-Step	Identified hazards or Injury causes, highlighting risks (Injury focused - see checklist)	Score -No controls (Probability x Severity = calculation)	Controls/Procedures/Key Behaviours (existing controls, information, training etc)	Score -Post Controls (Calculation)	Further action required		Action Priority (H/M/L)
01	• Exposure to hazardous fumes, gases & dust • Hazard to respiratory organ/health (asphyxiation). • When drilling the composite laminates.	1 x 1 = 1	• Wear personal protective equipment (PPE) such as nose cover, mask & breathing apparatus. • Open all windows and doors for proper ventilation. • Avoid inhalation of any fume/dust & gas	1 x 1 = 1	• Use of forced or general or local exhaust ventilation (LEV). • Reduced time exposure (Job rotation, etc).		L

Ref No. or Task-Step	Hazards identified or clear Injury causes, highlighting risks (Injury focused - see checklist)	Score -No controls (Calculation)	Controls/Procedures/Key Behaviours (existing controls, information, training etc)	Score -No controls (Calculation)	Further action required	Action Priority (H/M/L)
02	▪ Machinery entrapment, crush injuries and entanglement. ▪ When drilling the composite laminates. ▪ Permanent disability/ fatal accident.	2 x 4 = 8	• Use competent operator(s) and training • Wear suitable PPE such as smart clothing. • Avoid use of loose materials (e.g. ties, jewelleries, etc). • Avoid contact with moving parts of the machine while working. • CNC drilling machine should be in good conditions.	1 x 1 = 1	• Operation of machine within the limits of its capability.	M
03	▪ Hand burns / scalds (hot or cold, flame). ▪ When removing the composite laminates after drilling operation. ▪ Hazard to hands.	1 x 1 = 1	• Wear suitable PPE such as gloves. • Allow the drilled composite laminate to cool before it is carefully remove from the work table/machine holding device.	1 X 1 = 1	• Use of good handling tools /equipment.	L
04	▪ Eye injuries (e.g. foreign bodies & dust) ▪ When drilling the composite laminates. ▪ Hazard to human eyes.	1 x 1 = 1	• Wear suitable PPE such as goggles, visors & mask. • Avoid contact with eyes.	1 x 1 = 1	• Use of VM 10 CNC drilling machine with protective housing/guide and little or no operator-machine interface. • Reduced time exposure (Job rotation, etc)	L
05	▪ Hand cuts, injuries & bruises. ▪ When removing the composite laminates after drilling operation. ▪ Hazard to hands.	1 x 1 = 1	• Wear suitable PPE such as gloves. • Remove carefully from the work table/ Machine holding device only when the machine has stopped completely.	1 x 1 = 1	• Use appropriate tools/safety equipment. • Avoid contact with sharp edges of the composite laminate.	L

06	• Fire outbreak. • At high speed and feed rate (temperature) during drilling operation. • Permanent disability/fatal accident.	1 x 4 = 4	• Operating below the melting temperature of the composite laminate. • Use safety equipment (e.g. fire extinguisher)	1 x 1 = 1	• Effective training.	L
07	• Environmental hazard/pollution. • Co- worker(s) & members of the public (students, cleaners & other staff) • Hazard to human health.	1 x 1 = 1	• Drilling would be carried out during this summer vacation due to the absence of students and staff. • Proper channel of fumes & dust using gas chimney.	1 x 1 = 1	• Use gas suspension systems.	L

	HAZARDS LIST (Potential for Injury)		**POSSIBLE CONTROLS**
	Applies		Applies
	Slips, Trips & Low falls (e.g. from wet/contaminated floors, steps, stairs, spillage risk etc)		Prohibition or Elimination - Stop doing the job
	Struck by a falling object (lifted materials, lifting operations, overhead working, crane/tackle/beam failures etc)		Substitute with another method
	Exposure to Hazardous Substances (Chemicals, oils etc, skin/absorption, eyes, respiratory, ingestion, CIP)		Isolate job (e.g. enclose process) interlocking, fixed guarding etc or 'lock off & tag'
	Exposure to biological agents or biological hazards (bacterial, rodent, viral, legionella)		Procedures - Safety, quality, production, Safe System of Work (approved), Work Instructions
	Ergonomic/Posture Hazards (e.g. repetitive actions, over exertion/effort, awkward positions)		Maintenance and Statutory Checks (inc Planned Maintenance (PM) and PM inspections or tests)
	Manual Handling Risks - lifting, carrying, pushing, pulling + (back strains, pulled muscles etc)		Inspections and/or housekeeping
	Exposure to Gases, fumes (exhaust, solvent etc), dust, asbestos, ammonia		Training, Competent Persons, Authorised Controls, Permits or Licensing, schedules
	Noise/Vibration exposure (over 80dBA, 85dBA, 90dBA,nuisance)		Warning Notices/signs, Physical Restrictions (note-may be portable)
	Eye Injuries (e.g. foreign bodies, dust etc) and Display Screen Equipment / Visual Display Unit risks		Audible/Visual Warnings
	Radiation Exposure (substances or ionising, light - Infra Red, Ultra Violet, Laser)		Safety Equipment (i.e. Mirrors, RCDs, guarding, emergency stops, barriers, handrails, ramps)
	Electric Shock (or flash burns, static)		Reduced Time Exposure (Job rotation etc)
	Cuts & Hand tool / power tool injuries and friction injuries (inc glass & paper cuts) and bruises etc		Measurement Sensors/Alarms (inc Gas detection checks)
	Machinery Entrapment, crush injuries, entanglement (e.g. Workshop machines, plant, mechanical hazards)		Ventilation(forced or general or Local Exhaust Ventilation (LEV)), good lighting, Environmental Controls
	Fire, Highly Flammable Liquids, Pressurised gases, Explosion (inc Pressure explosions, boilers, hot work, gases)		Specialist Surveys (i.e. noise, dust, vibration, thermo graphic etc)
	Transport Risks (FLT/Pedestrian, FLT/FLT, Veh/FLT, Veh/Veh, Veh/pedestrian, trailers, mobile plant)		Manual Handling or Lifting Equipment provided
	Vehicle Manouvers (including Reversing and loading)		Emergency Procedures (for foreseeable emergency situations)
	Pressurised Systems, boilers, steam systems, pneumatics, hydraulics etc		Specific Safe System of Work (e.g. second operator, approval committees)
	Burns/Scalds (hot or cold, or flames)		Suitable PPE (Shoes, Gloves, Hi-vis clothing, goggles/visors, masks, Breathing Apparatus ,earplugs, hard hats etc)
	Falls from Height (fragile roofs/work/holes ,ladders, zip-up, scaffolding, racking, restricted access, cherrypickers)		***** Anything else that is helpful and could reduce the chance of injury**
	Asphyxiation (Confined spaces, excavations, drowning, gas suppression systems etc)		
	Lone working, restricted communications, Personal Protective Equipment (PPE) adding to risks (not fit for purpose, restricted vision etc)	tick	**OTHER RISK ASSESSMENTS OR SPECIALIST SURVEYS REQUIRED;**
	Violence / aggression / assault		Control of Substances Hazardous to Health (inc LEV) Hazardous Substances
	Striking against objects, Head Bangs, Body Bumps		Manual Handling
	Structural collapse, exposed excavations etc, Contact with underground services (water, gas, electrics)		Display Screen Equipment

	Temperature exposure (variations from normal, inc high/low temps, ventilation/humidity, heat stress/exhaustion)		Confined Spaces
			Working at Height
	PEOPLE		Noise / Vibration
	People risk groups - Young persons <18 or pregnant / nursing mothers / public / visitors		Work Equipment / Machinery - Provision and Use of Work Equipment
	People risk groups - Lone workers, night workers (Working Time Directive), customers, disabled workers		Young Persons
	People risk groups - delivery drivers, contractors, maintenance staff, agency		Pregnant Women
	***** Anything else that is foreseeable and could cause significant injury, consider emergency or abnormal activities in addition to start up, normal running and shutdown**		Lifting Operations and Lifting Equipment
NOTE: In addition Business Unit Managers may need to check local requirements and modify stds to suit these.			Fire

D2: Risk assessment on drilling of CFRP composite laminates

ASSESSING OUR RISKS – GENERAL RISK ASSESSMENT FORM

Site/Department: Mechanical & Design ENGINEERING WORKSHOP.

Task/Activity/Area: Drilling of MTM 44-1 Carbon fibre reinforced/epoxy composite laminates.

Notes: No previous record of accident on drilling of composite laminates.
(Including details of previous accidents/incidents)

RA Team: Supervisory team (Dr. E. Dimla, Dr. I. Popov, Dr. H. Dhakal), S. Ismail (PhD student) & Principal Technician (Mr. Rick)
(Mgr, Supervisor, EHS Adviser, Safety Rep, Employee, minimum is 2 people)

Date of RA: 19 -06 - 2014

People at risk: Employees and Visitors: Operator, PhD student, co-worker(s) & members of the Public (students, visitors & staff)
(e.g., visitors, contractors, hauliers, members of the public, operators, engineers, other employees etc)

Dept Manager (Print Name): Mr. Richard Baker.

Signature:

Review Date: 19 -06 - 2014

Calculate: **Probability** multiplied by **severity** for No/Post control scores.
NB: For scores of 10 (High), or more contact the health & safety department for further advice.

Probability \ Severity	Minor injury 1	Lost time/ Ill Health 2	Major / >3 days 3	Perm. Disability 4	Fatal/ Sight Loss 5
Highly Unlikely 1	1	2	3	4	5
Unlikely 2	2	4	6	8	10
Possible 3	3	6	9	12	15
Probable 4	4	8	12	16	20
Certain 5	5	10	15	20	25

Ref No. or Task-Step	Identified hazards or Injury causes, highlighting risks (Injury focused - see checklist)	Score -No controls (Probability x Severity = calculation)	Controls/Procedures/Key Behaviours (existing controls, information, training etc)	Score -Post Controls (Calculation)	Further action required	Action Priority (H/M/L)
01	▪ Exposure to hazardous fumes, gases & dust ▪ Hazard to respiratory organ/health (asphyxiation). ▪ When drilling the composite laminates.	4 x 4 = 16	• Wear personal protective equipment (PPE) such as nose cover, mask & breathing apparatus. • Open all windows and doors for proper ventilation. • Avoid inhalation of any fume/dust & gas.	2 x 2 = 4	• Use of forced or general or local exhaust ventilation (LEV). • Reduced time exposure (Job rotation, etc).	H

Ref No. or Task-Step	Hazards identified or clear Injury causes, highlighting risks (Injury focused - see checklist)	Score -No controls (Calculation)	Controls/Procedures/Key Behaviours (existing controls, information, training etc)	Score -No controls (Calculation)	Further action required	Action Priority (H/M/L)
02	▪ Machinery entrapment, crush injuries and entanglement. ▪ When drilling the composite laminates. ▪ Permanent disability/ fatal accident.	3 x 4 = 12	• Use competent operator(s) and training • Wear suitable PPE such as smart clothing. • Avoid use of loose materials (e.g. ties, jewelries, etc). • Avoid contact with machine while working. • CNC drilling machine should be in good conditions.	1 x 1 = 1	• Operation of machine within the limits of its capability.	H
03	▪ Hand burns / scalds (hot or cold, flame). ▪ When removing the composite laminates after drilling operation. ▪ Hazard to hands.	1 x 1 = 1	• Wear suitable PPE such as gloves. • Allow the drilled composite laminate to cool before it is carefully remove from the work table/machine holding device.	1 X 1 = 1	• Use of good tools /equipment.	L
04	▪ Eye injuries (e.g. foreign bodies & dust) ▪ When drilling the composite laminates. ▪ Hazard to human eyes.	2 x 2 = 4	• Wear suitable PPE such as goggles, visors & mask. • Avoid contact with eyes.	1 x 1 = 1	• Use of VM 10 CNC drilling machine with protective housing/guide and little or no operator-machine interface. • Reduced time exposure (Job rotation, etc)	L
05	▪ Hand cuts, injuries & bruises. ▪ When removing the composite laminates after drilling operation. ▪ Hazard to hands.	1 x 1 = 1	• Wear suitable PPE such as gloves. • Remove carefully from the work table/ Machine holding device only when the machine has stopped completely.	1 x 1 = 1	• Use appropriate tools/safety equipment. • Avoid contact with sharp edges of the composite laminate.	L
06	▪ Fire outbreak. ▪ At high speed and feed rate (temperature) during drilling operation. ▪ Permanent disability/fatal accident.	2 x 5 = 10	• Operating below the melting temperature of the composite laminate. • Use safety equipment (e.g. fire extinguisher)	1 x 1 = 1	• Effective training.	L
07	▪ Environmental hazard/pollution. ▪ Co- worker(s) & members of the public (students, cleaners & other staff) ▪ Hazard to human health.	2 x 1 = 2	• Drilling would be carried out during this summer vacation due to the absence of students and staff. • Proper channel of fumes & dust using gas chimney.	1 x 1 = 1	• Use gas suspension systems.	M

	HAZARDS LIST (Potential for Injury)		POSSIBLE CONTROLS
	Applies		Applies
	Slips, Trips & Low falls (e.g. from wet/contaminated floors, steps, stairs, spillage risk etc)		Prohibition or Elimination - Stop doing the job
	Struck by a falling object (lifted materials, lifting operations, overhead working, crane/tackle/beam failures etc)		Substitute with another method
	Exposure to Hazardous Substances (Chemicals, oils etc, skin/absorption, eyes, respiratory, ingestion, CIP)		Isolate job (e.g. enclose process) interlocking, fixed guarding etc or 'lock off & tag'
	Exposure to biological agents or biological hazards (bacterial, rodent, viral, legionella)		Procedures - Safety, quality, production, Safe System of Work (approved), Work Instructions
	Ergonomic/Posture Hazards (e.g. repetitive actions, over exertion/effort, awkward positions)		Maintenance and Statutory Checks (inc Planned Maintenance (PM) and PM inspections or tests)
	Manual Handling Risks - lifting, carrying, pushing, pulling + (back strains, pulled muscles etc)		Inspections and/or housekeeping
	Exposure to Gases, fumes (exhaust, solvent etc), dust, asbestos, ammonia		Training, Competent Persons, Authorised Controls, Permits or Licensing, schedules
	Noise/Vibration exposure (over 80dBA, 85dBA, 90dBA,nuisance)		Warning Notices/signs, Physical Restrictions (note-may be portable)
	Eye Injuries (e.g. foreign bodies, dust etc) and Display Screen Equipment / Visual Display Unit risks		Audible/Visual Warnings
	Radiation Exposure (substances or ionising, light - Infra Red, Ultra Violet, Laser)		Safety Equipment (i.e. Mirrors, RCDs, guarding, emergency stops, barriers, handrails, ramps)
	Electric Shock (or flash burns, static)		Reduced Time Exposure (Job rotation etc)
	Cuts & Hand tool / power tool injuries and friction injuries (inc glass & paper cuts) and bruises etc		Measurement Sensors/Alarms (inc Gas detection checks)
	Machinery Entrapment, crush injuries, entanglement (e.g. Workshop machines, plant, mechanical hazards)		Ventilation(forced or general or Local Exhaust Ventilation (LEV)), good lighting, Environmental Controls
	Fire, Highly Flammable Liquids, Pressurised gases, Explosion (inc Pressure explosions, boilers, hot work, gases)		Specialist Surveys (i.e. noise, dust, vibration, thermo graphic etc)
	Transport Risks (FLT/Pedestrian, FLT/FLT, Veh/FLT, Veh/Veh, Veh/pedestrian, trailers, mobile plant)		Manual Handling or Lifting Equipment provided
	Vehicle Manouvers (including Reversing and loading)		Emergency Procedures (for foreseeable emergency situations)
	Pressurised Systems, boilers, steam systems, pneumatics, hydraulics etc		Specific Safe System of Work (e.g. second operator, approval committees)
	Burns/Scalds (hot or cold, or flames)		Suitable PPE (Shoes, Gloves, Hi-vis clothing, goggles/visors, masks, Breathing Apparatus ,earplugs, hard hats etc)
	Falls from Height (fragile roofs/work/holes ,ladders, zip-up, scaffolding, racking, restricted access, cherrypickers)		***** Anything else that is helpful and could reduce the chance of injury**
	Asphyxiation (Confined spaces, excavations, drowning, gas suppression systems etc)		
	Lone working, restricted communications, Personal Protective Equipment (PPE) adding to risks (not fit for purpose, restricted vision etc)	tick	**OTHER RISK ASSESSMENTS OR SPECIALIST SURVEYS REQUIRED;**
	Violence / aggression / assault		Control of Substances Hazardous to Health (inc LEV) Hazardous Substances
	Striking against objects, Head Bangs, Body Bumps		Manual Handling
	Structural collapse, exposed excavations etc, Contact with underground services (water, gas, electrics)		Display Screen Equipment
	Temperature exposure (variations from normal, inc high/low temps, ventilation/humidity, heat stress/exhaustion)		Confined Spaces
			Working at Height
	PEOPLE		Noise / Vibration
	People risk groups - Young persons <18 or pregnant / nursing mothers / public / visitors		Work Equipment / Machinery - Provision and Use of Work Equipment
	People risk groups - Lone workers, night workers (Working Time Directive), customers, disabled workers		Young Persons
	People risk groups - delivery drivers, contractors, maintenance staff, agency		Pregnant Women
	***** Anything else that is foreseeable and could cause significant injury, consider emergency or abnormal activities in addition to start up, normal running and shutdown**		Lifting Operations and Lifting Equipment
NOTE: In addition Business Unit Managers may need to check local requirements and modify stds to suit these.			Fire

APPENDIX E
Additional facts and experimental results obtained

E1: Effects of drilling parameters and material removal rate on delamination of different aspect ratios of HFRP and CFRP composite specimens

Test No	Cutting Speed, v(m/min)	Feed Rate, f(mm/rev)	Delamination Factor, F_d						MRR (mm^3/min)	
			HFRP					CFRP	Drill Diameter (mm)	
			A	B	C	D	E		5.0	10.0
			0	19	26	30	38	MTM 44-1		
1	10	0.05	1.0046	1.0114	1.0154	1.0148	1.0154	1.2860	625	1250
2	10	0.10	1.0054	1.0108	1.0189	1.0166	1.0192	1.2960	1250	2500
3	10	0.15	1.0062	1.0124	1.0198	1.0216	1.0310	1.3100	1875	3750
4	10	0.20	1.0092	1.0128	1.0290	1.0422	1.0456	1.3280	2500	5000
5	20	0.05	1.0040	1.0090	1.0136	1.0138	1.0150	1.2440	1250	2500
6	20	0.10	1.0042	1.0119	1.0182	1.0186	1.0168	1.2560	2500	5000
7	20	0.15	1.0052	1.0122	1.0211	1.0196	1.0284	1.2680	3750	7500
8	20	0.20	1.0070	1.0133	1.0233	1.0396	1.0420	1.3120	5000	10000
9	30	0.05	1.0036	1.0075	1.0118	1.0080	1.0148	1.2200	1875	3750
10	30	0.10	1.0040	1.0092	1.0147	1.0158	1.0166	1.2580	3750	7500
11	30	0.15	1.0058	1.0094	1.0159	1.0182	1.0306	1.2540	5625	11250
12	30	0.20	1.0058	1.0079	1.0189	1.0234	1.0440	1.2820	7500	15000
13	40	0.05	1.0022	1.0031	1.0051	1.0074	1.0150	1.0840	2500	5000
14	40	0.10	1.0040	1.0038	1.0058	1.0090	1.0152	1.1020	5000	10000
15	40	0.15	1.0044	1.0051	1.0090	1.0176	1.0270	1.1200	7500	15000
16	40	0.20	1.0046	1.0056	1.0164	1.0190	1.0408	1.1680	10000	20000

E2: Effects of drilling parameters and material removal rate on delamination of different aspect ratios of HFRP and CFRP composite specimens

Test No	Cutting Speed, V(m/min)	Feed Rate, f(mm/rev)	Aspect Ratio (AR)						MRR (mm^3/min)	
			A	B	C	D	E			
			Surface Roughness , R_a (µm)							
			HFRP					CFRP	Drill Diameter (mm)	
			0	19	26	30	38	MTM 44-1	5.0	10.0
1	10	0.05	4.970	7.240	8.050	10.070	10.230	1.609	625	1250
2		0.10	5.320	7.330	9.100	10.300	10.390	1.250	1250	2500
3		0.15	6.230	7.690	9.180	10.980	10.440	1.664	1875	3750
4		0.20	6.430	8.300	9.960	11.050	11.140	1.160	2500	5000
5	20	0.05	4.660	7.080	7.710	8.290	8.480	2.495	1250	2500
6		0.10	5.120	7.240	7.890	8.600	8.620	1.648	2500	5000
7		0.15	5.920	7.400	8.400	9.070	9.390	1.793	3750	7500
8		0.20	6.350	8.240	8.450	9.780	9.720	1.544	5000	10000
9	30	0.05	4.020	5.650	6.310	7.540	7.450	1.546	1875	3750
10		0.10	4.320	6.700	6.940	7.400	7.620	1.298	3750	7500
11		0.15	5.570	6.950	7.090	7.910	7.920	1.762	5625	11250
12		0.20	5.750	7.090	7.240	7.990	8.010	1.197	7500	15000
13	40	0.05	4.090	5.700	6.350	7.570	7.480	1.703	2500	5000
14		0.10	4.110	6.880	6.990	7.770	7.860	1.457	5000	10000
15		0.15	5.710	7.070	7.190	7.940	8.000	1.615	7500	15000
16		0.20	5.960	7.150	7.250	8.050	8.140	1.211	10000	20000

E3: Input variables or data in the IBM SPSS tool

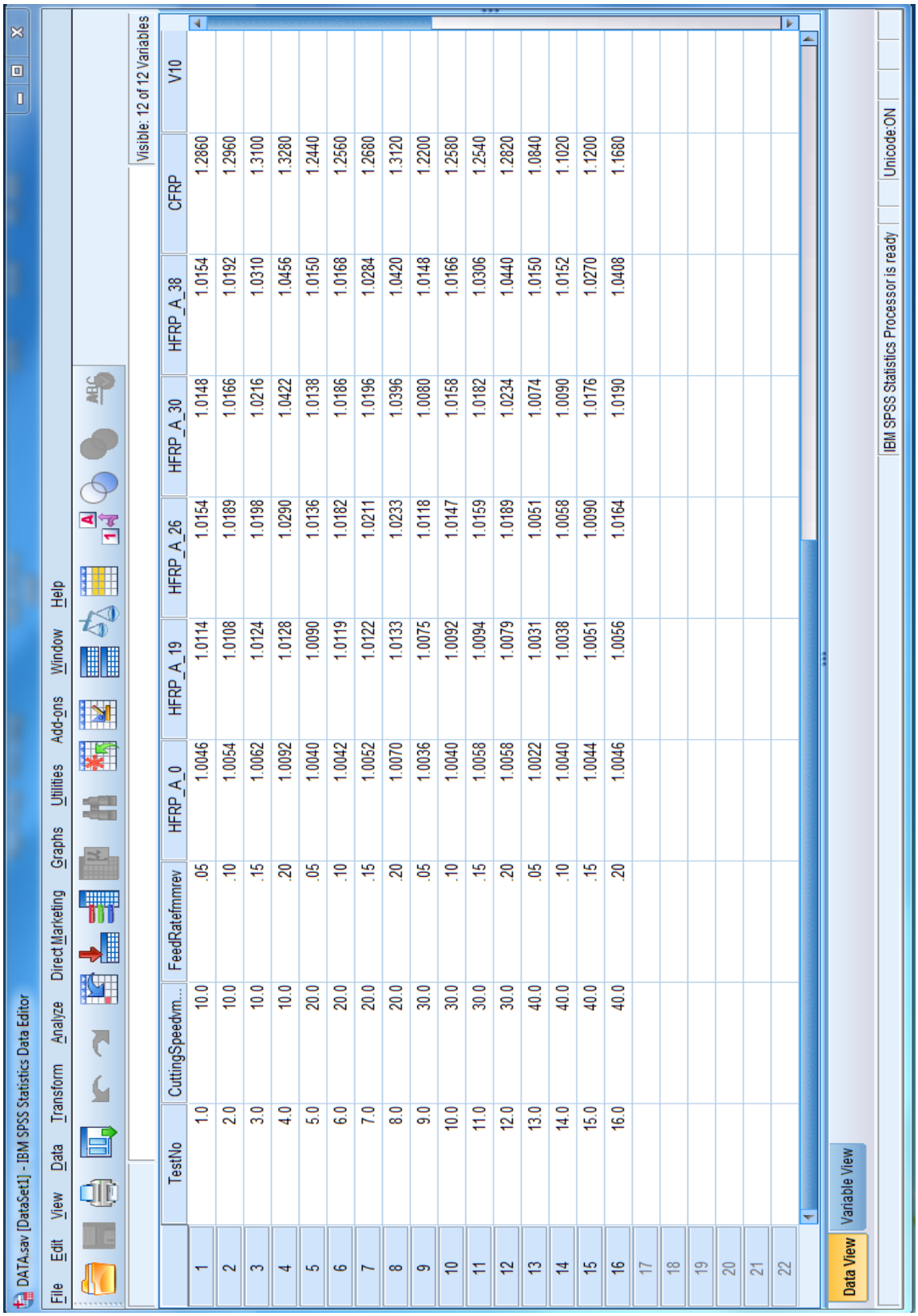

E4: ANOVA results of effects of drilling parameters (feed rate and cutting speed) on delamination of HFRP composite specimens A-E

Two-way ANOVA: A versus Feed, Speed (A)

Source	DF	SS	MS	F	P
Feed	3	0.0000208	0.0000069	13.50	0.001
Speed	3	0.0000132	0.0000044	8.60	0.005
Error	9	0.0000046	0.0000005		
Total	15	0.0000387			

S = 0.0007167 R-Sq = 88.05% R-Sq(adj) = 80.08%

Two-way ANOVA: B versus Feed, Speed (B)

Source	DF	SS	MS	F	P
Feed	3	0.0000118	0.0000039	4.74	0.030
Speed	3	0.0001450	0.0000483	58.35	0.000
Error	9	0.0000075	0.0000008		
Total	15	0.0001643			

S = 0.0009103 R-Sq = 95.46% R-Sq(adj) = 92.43%

Two-way ANOVA: C versus Feed, Speed (C)

Source	DF	SS	MS	F	P
Feed	3	0.0002321	0.0000774	25.17	0.000
Speed	3	0.0003220	0.0001073	34.91	0.000
Error	9	0.0000277	0.0000031		
Total	15	0.0005818			

S = 0.001753 R-Sq = 95.24% R-Sq(adj) = 92.07%

Two-way ANOVA: D versus Feed, Speed (D)

Source	DF	SS	MS	F	P
Feed	3	0.0009010	0.0003003	13.95	0.001
Speed	3	0.0003132	0.0001044	4.85	0.028
Error	9	0.0001938	0.0000215		
Total	15	0.0014080			

S = 0.004640 R-Sq = 86.24% R-Sq(adj) = 77.06%

Two-way ANOVA: E versus Feed, Speed (E)

Source	DF	SS	MS	F	P
Feed	3	0.0020190	0.0006730	669.83	0.000
Speed	3	0.0000236	0.0000079	7.85	0.007
Error	9	0.0000090	0.0000010		
Total	15	0.0020517			

S = 0.001002 R-Sq = 99.56% R-Sq(adj) = 99.27%

E5: ANOVA results of effects of drilling parameters (feed rate and cutting speed) on surface roughness of HFRP composite specimens A-E

Two-way ANOVA: A versus Feed, Speed (A)

Source	DF	SS	MS	F	P
Feed	3	8.2948	2.76494	95.01	0.000
Speed	3	1.9768	0.65894	22.64	0.000
Error	9	0.2619	0.02910		
Total	15	10.5335			

S = 0.1706 R-Sq = 97.51% R-Sq(adj) = 95.86%

Two-way ANOVA: B versus Feed, Speed (B)

Source	DF	SS	MS	F	P
Feed	3	3.42022	1.14007	14.21	0.001
Speed	3	3.42407	1.14136	14.23	0.001
Error	9	0.72206	0.08023		
Total	15	7.56634			

S = 0.2832 R-Sq = 90.46% R-Sq(adj) = 84.09%

Two-way ANOVA: C versus Feed, Speed (C)

Source	DF	SS	MS	F	P
Feed	3	2.7525	0.91749	16.14	0.001
Speed	3	13.0372	4.34574	76.47	0.000
Error	9	0.5115	0.05683		
Total	15	16.3012			

S = 0.2384 R-Sq = 96.86% R-Sq(adj) = 94.77%

Two-way ANOVA: D versus Feed, Speed (D)

Source	DF	SS	MS	F	P
Feed	3	1.8722	0.62406	11.67	0.002
Speed	3	21.5145	7.17151	134.13	0.000
Error	9	0.4812	0.05347		
Total	15	23.8679			

S = 0.2312 R-Sq = 97.98% R-Sq(adj) = 96.64%

Two-way ANOVA: E versus Feed, Speed (E)

Source	DF	SS	MS	F	P
Feed	3	1.6286	0.54286	12.88	0.001
Speed	3	20.3741	6.79137	161.14	0.000
Error	9	0.3793	0.04215		
Total	15	22.3820			

S = 0.2053 R-Sq = 98.31% R-Sq(adj) = 97.18%

E6: ANOVA results of effects of drilling parameters (feed rate and cutting speed) on surface roughness of optimal 19-HFRP and MTM 44-1 CFRP composite specimens

Two-way ANOVA: HFRP versus Feed, Speed

Source	DF	SS	MS	F	P
Feed	3	3.42022	1.14007	14.21	0.001
Speed	3	3.42407	1.14136	14.23	0.001
Error	9	0.72206	0.08023		
Total	15	7.56634			

S = 0.2832 R-Sq = 90.46% R-Sq(adj) = 84.09%

Two-way ANOVA: CFRP versus Feed, Speed

Source	DF	SS	MS	F	P
Feed	3	0.80214	0.267379	8.75	0.005
Speed	3	0.52583	0.175277	5.73	0.018
Error	9	0.27516	0.030573		
Total	15	1.60312			

S = 0.1749 R-Sq = 82.84% R-Sq(adj) = 71.39%

Coefficients a

Model		Unstandardized Coefficients		Standardized Coefficients	t	Sig.	95.0% Confidence Interval for B	
		B	Std. Error	Beta			Lower Bound	Upper Bound
1	(Constant)	1.014	0.001		897.869	0	1.011	1.016
	Cutting Speed, v(m/min)	0	0	-0.888	-8.359	0	0	0
	Feed Rate, f(mm/rev)	0.015	0.006	0.255	2.398	0.032	0.001	0.028

a Dependent Variable: HFRP_A_19

E7: A substantial drilling forces (thrust and torque) reduction during UAD of HF/VE, compared with CD.

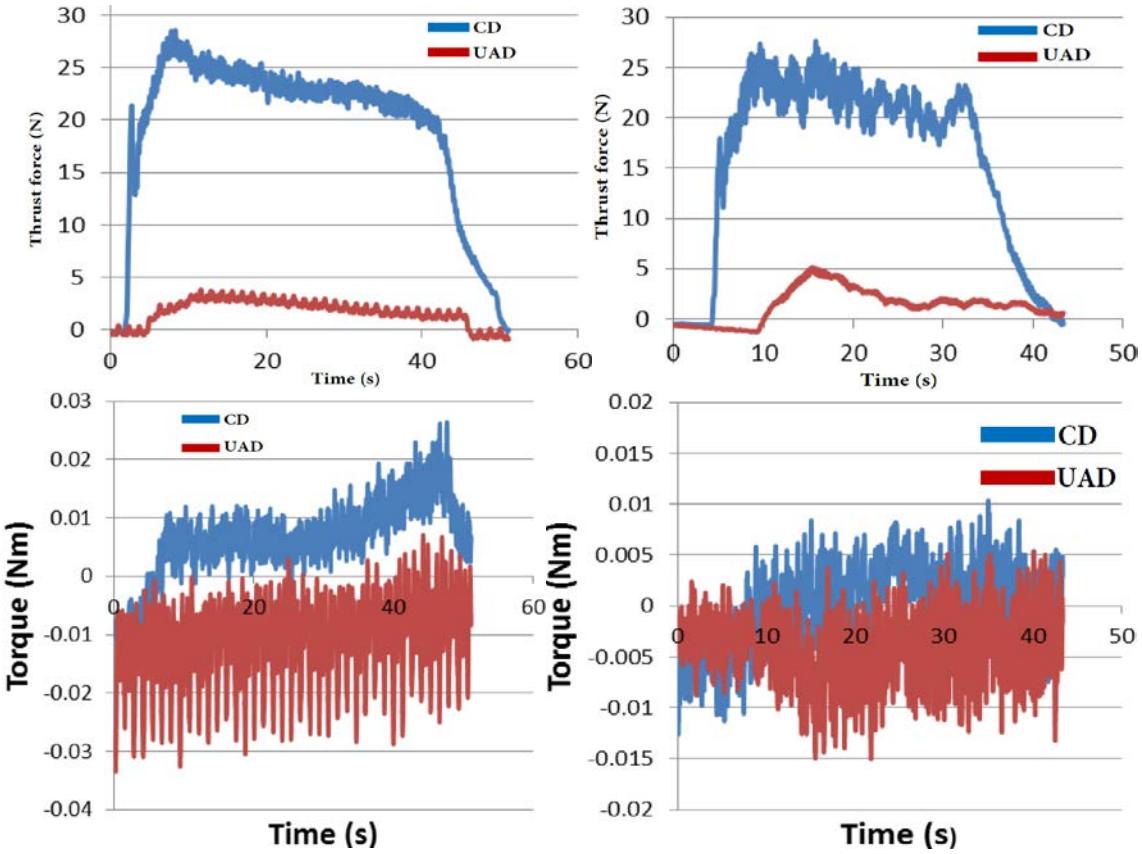

E8: Roundness at 0.5mm depth for VE (Neat) specimen with (a) CD and (b) UAD

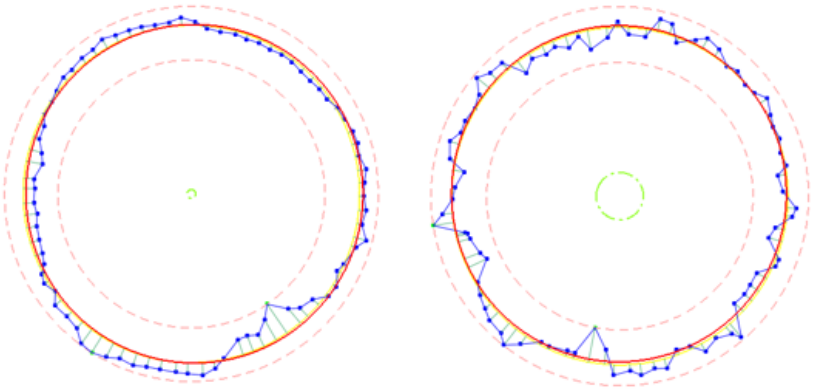

(a) **(b)**

E9: Effects of cutting speed on delamination factor of 19-HFRP

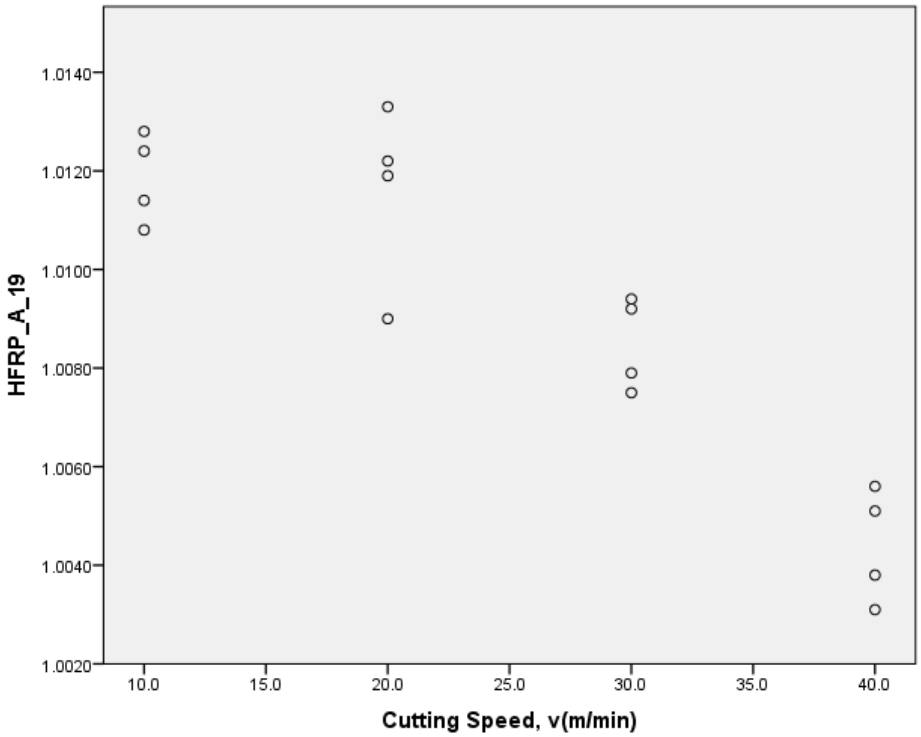

E10: Effects of cutting speed on surface roughness of 19-HFRP

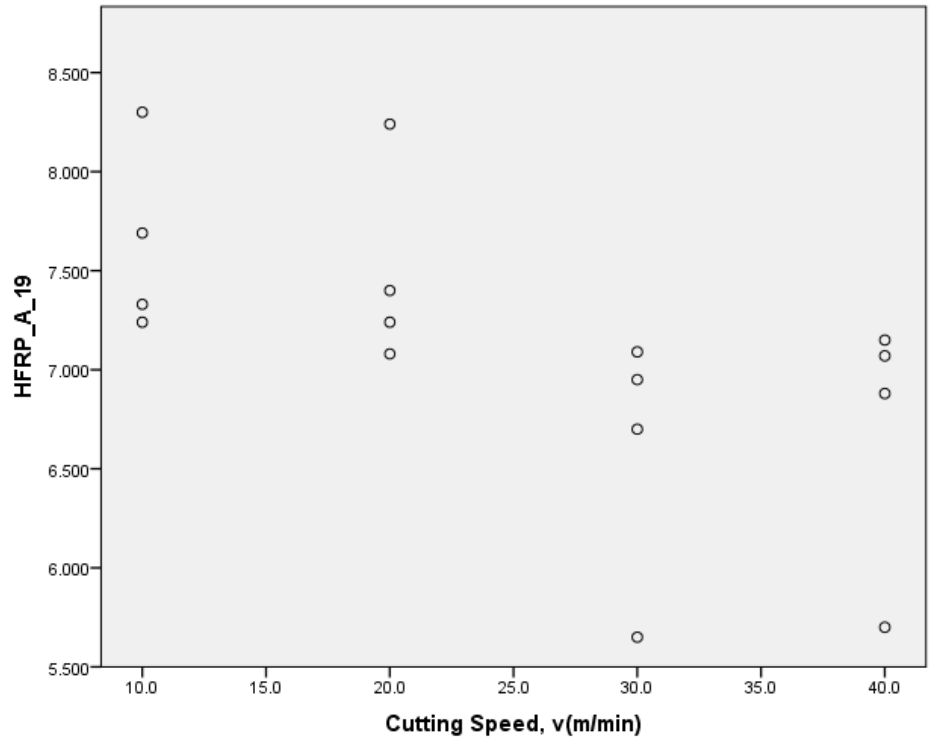

E11: Fibre push-out damage for (a) CD and (b) UAD techniques

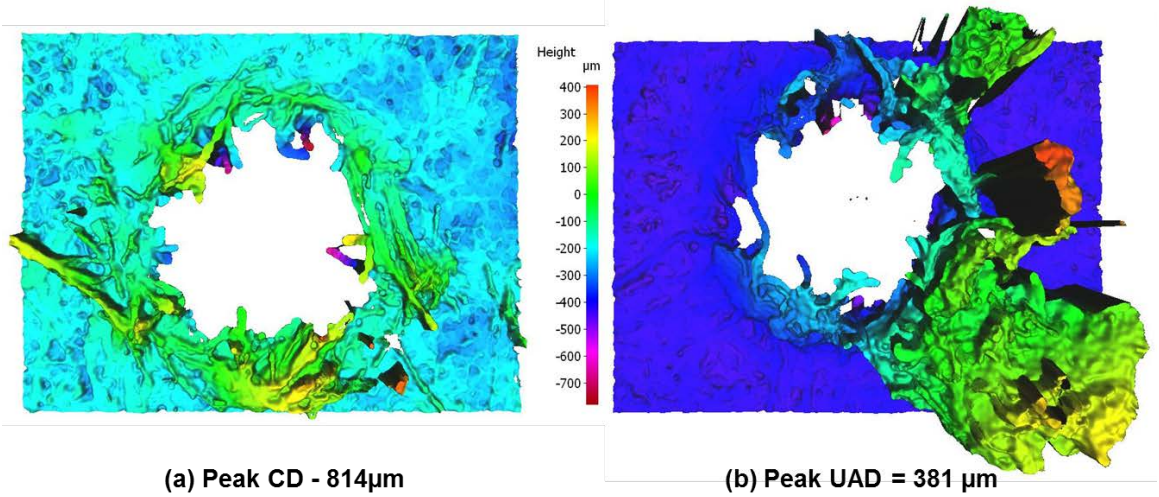

(a) Peak CD - 814µm **(b) Peak UAD = 381 µm**

APPENDIX F

List of publications, awards and relevant PhD research activities

A. Journal Articles

- **Sikiru Oluwarotimi Ismail**, Saheed Olalekan Ojo, Hom Nath Dhakal. (2017). Thermo-mechanical modelling of FRP cross-ply composite laminates drilling: Delamination damage analysis. *Composites Part B: Engineering, 108*, 45-52.

- **Sikiru Oluwarotimi Ismail**, Hom Nath Dhakal, Eric Dimla, Johnny Beaugrand, Ivan Popov. (2016). Effects of drilling parameters and aspect ratios on delamination and surface roughness of lignocellulosic HFRP composite laminates. *Journal of Applied Polymer Science, 133* (7), 1-8.

- **Sikiru Oluwarotimi Ismail**, Hom Nath Dhakal, Eric Dimla, Ivan Popov. (2016). Recent advances in twist drill design for composites machining: A critical review. *Proceedings of Institution of Mechanical Engineers, Part B: Journal of Engineering Manufacture*, 1-16.

- **Sikiru Oluwarotimi Ismail**, Hom Nath Dhakal, Ivan Popov, Johnny Beaugrand. (2016). Comparative study on machinability of sustainable and conventional fibre reinforced polymer composites. *Engineering Science and Technology, an international Journal, 19*(4), 2043-2052.

- **Sikiru Oluwarotimi Ismail**, Hom Nath Dhakal, Anish Roy, Dong Wang, Ivan Popov. (2016). Machinability analysis of bio-composite: Conventional versus ultrasonically-assisted drilling. *Composites Part A: Applied Science and Manufacturing* (under review).

B. Conference Proceedings

- **Sikiru Oluwarotimi Ismail**, Hom Nath Dhakal, Anish Roy, Dong Wang, Ivan Popov. (2016). Machining of FRP composite laminates with conventional and ultrasonically-assisted drilling techniques: A comparative and experimental investigation. *Proceedings of the ASC 31st Technical Conference and ASTM Committee D30 Meeting,* September 19-22, Williamsburg, Virginia, USA.

- **Sikiru Oluwarotimi Ismail**, Hom Nath Dhakal, Ivan Popov, Johnny Beaugrand. (2016). Analysis and impacts of chips formation on hole quality during fibre-reinforced plastic composites machining. *Proceedings of the 14th International Conference on Manufacturing Research (ICMR 2016), incorporating the 31st National Conference on Manufacturing Research,* September 6-8, 2016, pp. 143-148, Loughborough University, Loughborough, Leicester, United Kingdom.

- **Sikiru Oluwarotimi Ismail**, Hom Nath Dhakal, Ivan Popov, Johnny Beaugrand. (2015). Experimental analysis of drilling-induced damage of lignocellulosic 19/hemp fibre-reinforced polycaprolactone and MTM 44-1/carbon fibre reinforced epoxy resin composites. *Proceedings of 5th Conference on Natural Fibre Composites for Industrial Applications,* 15-16 October 2015, pp. 1-6, Sapienza Universiti di Roma, Rome, Italy.

C. Edited Book Chapter

- **Sikiru** Oluwarotimi Ismail & Hom Nath Dhakal. (2017). Philosophical study on composites and their drilling techniques. *Functional Biopolymers.* Berlin, Germany: Springer Publisher (final acceptance for publication).

D. Awards

- June 2017: Paper Prize - First Place, Faculty of Technology, University of Portsmouth, England, United Kingdom.
- May 2017: Best Student Paper Award in the School of Engineering, Faculty of Technology, University of Portsmouth, England, United Kingdom.

- August 2016: Doctoral Assistance Grant, awarded by Faculty of Engineering, University of Lagos, Lagos State, Nigeria.
- June 2016: Journal Paper Price-Highly Commended, awarded by the Faculty of Technology at the Annual Faculty Research Conference, University of Portsmouth, England, United Kingdom.
- June 2014 - 2016: Partial Funding as a Representative of University of Portsmouth, UK at ICONS 2014, 2015 and 2016 Conferences.
- October 2013 - September 2016: Beneficiary of Niger-Delta Development Commission (NDDC) Overseas PhD Scholarship, Federal Government of Nigeria, Nigeria.

E. Posters Presentations

- **Sikiru Oluwarotimi Ismail**, Hom Nath Dhakal, Ivan Popov. (2017). Optimised ultrasonically-assisted drilling of advanced fibre-reinforced plastic composites. *Poster Presentation at Faculty of Technology Research Conference,* University of Portsmouth, UK, Tuesday 6th June, 2017.

- **Sikiru Oluwarotimi Ismail**, Hom Nath Dhakal, Ivan Popov. (2016). Machining of FRP composites: Conventional versus ultrasonically-assisted drilling techniques. *Graduate School Research Conference/Poster Competition at Portsmouth Guildhall,* University of Portsmouth, UK, Thursday 6th October (Shortlisted for competition).

- **Sikiru Oluwarotimi Ismail**, Hom Nath Dhakal, Ivan Popov. (2016). Optimised ultrasonically-assisted drilling of advanced fibre-reinforced plastic composites. *Poster Presentation at Faculty of Technology Research Conference,* University of Portsmouth, UK, Tuesday 7th June, 2016.

- **Sikiru Oluwarotimi Ismail**, Hom Nath Dhakal, Ivan Popov, James Macule. (2015). Comparative experimental study on effects of chips formation during 19/HFRP and MTM 44-1/CFRP Composites machining. *Poster Presentation at Faculty of Technology Research Conference,* University of Portsmouth, UK, Wednesday 3rd June, 2015.

- **Sikiru Oluwarotimi Ismail**, Hom Nath Dhakal, Anish Roy, Dong Wang, Ivan Popov. (2015). Problems associated with fibre-reinforced composites ultrasonically-assisted drilling. *Proceedings of the 8th Manchester Metropolitan University (MMU) Postgraduate Research Conference (Innovation 2015),* Manchester, United Kingdom, 5th November 2015, pp 11.

- **Sikiru Oluwarotimi Ismail**, Hom Nath Dhakal, Ivan Popov. (2015). Machinability analysis and drill design optimisation for fibre-reinforced composites drilling. *Graduate School Research Poster Competition at Portsmouth Guildhall,* University of Portsmouth, UK, Thursday 8th October, 2015 (Shortlisted for competition).

F. Oral presentations

- Presentation to the supervisory team comprising Dr. Eric Dimla (Director of Study), Dr. Ivan Popov (second supervisor) and Dr. Hom Nath Dhakal (third supervisor), in preparation for Major Review Presentation.
- Major Review Official Report and Presentation to the panel comprising Dr James Buick (Chairman), Dr Gianluca Tozzi (Second assessor) and Dr. Hom Nath Dhakal (Director of Study/First Supervisor), 21st November, 2014.
- **S. O. Ismail**, H. N. Dhakal, I. Popov and James Mc. (2015). Machinability analysis and drill design optimisation for fibre-reinforced composites drilling. *A 3-Minute Thesis Competition*, Faculty of Technology Research Conference, Portland Building, University of Portsmouth, UK, Wednesday 3rd June, 2015.
- Presentation to the supervisory team comprising Dr Hom Nath Dhakal (Director of Study) and Dr Ivan Popov (second supervisor), in preparation for the Annual Review Presentation.
- **S. O. Ismail**, H. N. Dhakal, and I. Popov. (2016). Machinability analysis of fibre-reinforced polymer composites. *A 3-Minute Thesis Competition*, Faculty of Technology Research Conference, Portland Building, University of Portsmouth, UK, Tuesday 7th June, 2016.

- **S. O. Ismail**, H. N. Dhakal, and I. Popov. (2016). Machinability analysis of fibre-reinforced polymer composites. *A 3-Minute Thesis Competition*, Faculty of Technology Research Conference, Portland Building, University of Portsmouth, UK, Tuesday 7th June, 2016.

- **S. O. Ismail**, H. N. Dhakal, and I. Popov. (2016). Ultrasonically-assisted drilling of advanced composites. *A short talk delivered at the Faculty of Technology Research Conference,* Portland Building, University of Portsmouth, UK, Tuesday 7th June, 2016.

G. Special/relevant seminars, workshops and conferences attended

- Bi-monthly Research Seminar Series (Mechanical), such as ''Design of new composite crash absorbers stitched by natural fibres to improve effective crack growth resistance'', *School of Engineering*, University of Portsmouth, UK, January 22nd, 2014.
- Faculty of Technology Research Conference 2014, University of Portsmouth, UK, Thursday 3th July, 2014.
- 8th International Conference of Nigerian Students (ICONS 2014) in Diaspora, University of Central Lancashire, Preston, Lancashire, UK, June 14th - 15th, 2014.
- Annual Learning and Teaching Conference 2014 – Students as Partners, University of Portsmouth, Portsmouth, UK, Thursday 12th June, 2014.
- Research Conference 2014, University of Portsmouth, Portsmouth, UK, Wednesday 2nd April, 2014.
- ALPROF seminars – already completed the first part in 2013/2014 academic session.
- 9th International Conference of Nigerian Students (ICONS 2015) in Diaspora, at Pennine lecture theatre, Sheffield Hallam University (SHU), United Kingdom, 10th - 12th April, 2015.
- Faculty of Technology Research Conference, Lecture theatre, Portland Building, University of Portsmouth, UK, Wednesday 3th June, 2015.
- Faculty Learning and Teaching Workshop: What makes a good lecture? DS 1.12, University of Portsmouth, UK, Wednesday 18th February, 2015.

- Effective Classroom Management, DCQE Staff Development Room, Unit 3, St Andrew's Court, University of Portsmouth, Portsmouth, UK, Monday 23rd February, 2015.
- Annual Learning and Teaching Conference – Developing and Implementing Career Enhancing Activities, Department of Curriculum and Quality Enhancement (DCQE), Richmond Building, University of Portsmouth, UK, Tuesday 23 June 2015.
- Faculty of Technology Teaching and Learning mini-conference, Lion gate Building, University of Portsmouth, UK, Wednesday 24 June 2015.
- 5th Conference on Natural Fibre Composites for Industrial Applications, Sapienza Universite di Roma, Rome, Italy, 15-16 October 2015.
- 8th Manchester Metropolitan University (MMU) Postgraduate Research Conference (Innovation 2015), Manchester, United Kingdom, 5th November 2015.
- University Research and Innovation Conference, Portland Building, University of Portsmouth, Portsmouth, UK, Thursday 26th May, 2016.
- 10th International Conference of Nigerian Students (ICONS 2016) in Diaspora, University of De Montfort University, Leicester, UK, June 10th - 12th, 2016.
- Annual Learning and Teaching Conference – Delivering an engaging student experience, Department of Curriculum and Quality Enhancement (DCQE), Richmond and Portland Buildings, University of Portsmouth, UK, Friday 10th June 2016.
- Research Ethics and Governance Conference on the Ethical Challenges of Internet Mediated Research (IMR) 2016, Portland Building, University of Portsmouth, UK, Friday 24th June 2016.
- Faculty of Technology Learning and Teaching Conference on Innovations in Learning and Teaching, Lion Gate Building, Room 2.04b, University of Portsmouth, UK, Thursday 23 June, 2016.
- Annual Learning and Teaching Conference – Celebrating Success and Seizing New Opportunities, Department of Curriculum and Quality Enhancement (DCQE), Richmond and Portland Buildings, University of Portsmouth, UK, Friday 9th June, 2017.

- Faculty of Technology Research and Innovation Conference, Lecture theatre, Portland Building, University of Portsmouth, UK, Tuesday 6th June, 2017.
- International Conference for Educators, Exploring Developments in Teaching and Learning: The Scope for International Transfer, organised by Portsbridge Educational Services Ltd, Portland Building, University of Portsmouth, United Kingdom, 11-12th July, 2017.

Journal of Applied Polymer Science

Effects of drilling parameters and aspect ratios on delamination and surface roughness of lignocellulosic HFRP composite laminates

Sikiru Oluwarotimi Ismail,[1] Hom Nath Dhakal,[1] Eric Dimla,[2] Johnny Beaugrand,[3,4] Ivan Popov[1]

[1]Mechanical Engineering Department, School of Engineering, University of Portsmouth, Portsmouth PO1 3DJ, United Kingdom
[2]Mechanical Engineering Department, Institut Technologi Brunei, BE 1410, Brunei Darussalam
[3]INRA, UMR614 Fractionnement Des AgroRessourceset Environnement, Reims 51686, France
[4]Université De Reims Champagne-Ardenne, UMR614 Fractionnement Des AgroRessources Et Environnement, Reims 51100, France
Correspondence to: S. O. Ismail (E-mail: sikiru.ismail@port.ac.uk)

ABSTRACT: Hemp fibre-reinforced polycaprolactone (HFRP) composite has inherent good mechanical properties and benefits which include remarkably high specific strength and modulus, low density, and renewability. No doubt, these properties have attracted wider applications of HFRP composite in engineering applications. This paper presents an investigation on the influence of drilling parameters and fibre aspect ratios, AR (0, 19, 26, 30, and 38) on delamination damage factor and surface roughness of HFRP composite laminates utilising high speed steel twist drills under dry machining condition. Taguchi's technique was used in the design of experiment. The results obtained show that increase in cutting speed reduces delamination factor and surface roughness of drilled holes, whereas increase in feed rate causes increase in both delamination factor and surface roughness. Feed rate and cutting speed had the greatest influence on delamination and surface roughness respectively when compared with aspect ratio, while an increase in fibre aspect ratios leads to a significant increase in both delamination factor and surface roughness. The optimum results occurred at cutting speed and feed rate (drilling parameters) of 20 mm/min and 0.10 mm/rev, respectively, when drilling sample of AR 19. © 2015 Wiley Periodicals, Inc. J. Appl. Polym. Sci. **2016**, *133*, 42879.

KEYWORDS: applications; composites; fibers; mechanical properties; surfaces and interfaces

Received 1 May 2015; accepted 24 August 2015
DOI: 10.1002/app.42879

INTRODUCTION

After many decades of developments of composites manufacturing technology, the desire to improve the machining of these materials based on the numerous areas of application remains a challenge. Today, the attention of many product manufacturers has shifted to natural fibre reinforced composites (NFRC) due to the unease of production and increased tool wear from the use of synthetic fibre-reinforced composites. One of the prominent types of NFRC is HFRP (hemp fibre reinforced polycaprolactone) composite. HFRP composite comprises hemp fibre and biopolymer as the reinforcement material and as binder respectively. Hemp natural fibre (HNF) is an example of organic dicotyledonous bast plant stem fibre obtained from nonwood natural fibre while polycaprolactone (PCL) is a synthetic matrix that serves as a biobinder. Hemp is botanically referred to as *Cannabis sativa*, originated from Asia and it is one of the main sources of natural fibres.[1] The choice of HNF among other similar natural fibres depends on its great advantages. HNF is one of the strongest natural fibres, grows very well on several land appropriate for farming with huge production per year. It is suitable for the biocomposite reinforcement due to its relative high density and cellulose contents. The fibre processing of HNF requires less energy. In addition, both HNF and PCL have good mechanical properties, as shown in Table I.[2,3]

HNF has damage tolerance and impact resistance properties in addition to its nonabrasiveness, high toughness, sustainability, renewability or recyclability, good thermal properties and capability on different reinforcements when compared with synthetic fibres.[2,4] PCL has a biodegradable nature with cellulose contents. As a result of lower cost of production, higher thermal resistance and environmental superiority, NFRC have started replacing GFRC.[2,5–7] The wider applications of NFRC cut across domestic appliances, automotive, building, and food industries.[2,7]

Drilling attracts much significance and consideration among secondary machining operations, such as boring, tapping and reaming used in manufacturing industry.[8,9] However, the use of conventional metal cutting techniques in drilling composites has resulted in poor finish quality and excessive tool wear. These problems are caused due to the abrasive, heat sensitivity, heterogeneous and anisotropic nature of composite materials,[10]

Review Article

Institution of MECHANICAL ENGINEERS

Journal of ENGINEERING MANUFACTURE

Proc IMechE Part B:
J Engineering Manufacture
1–16

DOI: 10.1177/0954405416635034
pib.sagepub.com
SAGE

Recent advances in twist drill design for composite machining: A critical review

Sikiru Oluwarotimi Ismail[1], Hom Nath Dhakal[1], Eric Dimla[2] and Ivan Popov[1]

Abstract

In the field of composite technology, inefficient and poor designs of twist drills contribute immensely to the challenges facing drilling of composite materials. An attempt to report some of the drill design methods and their inherent challenges confronting composite machining necessitates the writing of this article. A critical review has been conducted to offer a clear understanding of the current advances in the field of mechanical drilling of composite materials, focusing on geometry, material and parametric tool designs. The inter-dependable effects of thrust force, cutting speed, feed rate, cutting force and torque on drill design are similarly reviewed. This article also reveals other associated issues facing composite drilling including delamination, surface roughness, rapid tool wear and drill breakage. Well-designed drill geometry and good knowledge of drilling parameters afford the producers of polycrystalline diamond, carbide and high-speed steel tooling materials better opportunity of developing a drill that will minimise delamination of the reinforced composites and tool wear and produce a high-quality surface. Twist drill manufacturers and users will benefit from this article as they seek to have well-designed and improved drills.

Keywords

Twist drill, design, composite materials, drilling, delamination, tool wear

Date received: 16 March 2015; accepted: 1 February 2016

Introduction

The kinematics of drilling is a process of using a rotating drill bit to create or enlarge existing round holes in a workpiece.[1] Drilling is one of the most frequent processes used in manufacturing industry among machining operations.[2] Tonshoff et al.[3] noted that drilling takes about 25% of the total machining time and 33% of all the total machining operations of a manufacturing process. It is a preliminary step for many other machining operations, such as reaming, tapping and boring.[4,5]

Drill, as a rotary end cutting tool, has one or more cutting lips and flutes for the release of chips and the access of a cutting fluid. Presently, drill bits are the most frequently and extensively used material cutting tools.[6] Geometrically, a twist drill is a complex material cutting tool, as depicted in Figure 1. Both the geometrical shape and dimensions of a twist drill determine the cutting performance and influence the cutting forces, tool wear, cutting dynamics and the quality and integrity of drilled holes.[9–12] These make the design of twist drill of critical importance. A poorly designed cutting edge results in an undesired distribution of the cutting angles along the drill cutting edge,[13–16] causing inefficient performance, loss of cutting ability and increase in total manufacturing cost.

This article reviews recent advances in twist drill design for machining of composite materials. The main objective is to critically review the literature, focusing on the effect of twist drill design parameters on composite drilling. An attempt is made to outline the fundamental limitations of the currently developed and applied designs. The first part of this article focuses on

[1]Mechanical Engineering Department, School of Engineering, University of Portsmouth, Portsmouth, UK
[2]Department of Mechanical Engineering, Institut Teknologi Brunei, Gadong, Brunei Darussalam

Corresponding author:
Sikiru Oluwarotimi Ismail, Mechanical Engineering Department, School of Engineering, University of Portsmouth, Portsmouth PO1 3DJ, UK.
Email: sikiru.ismail@port.ac.uk

Engineering Science and Technology, an International Journal 19 (2016) 2043–2052

HOSTED BY

Contents lists available at ScienceDirect

Engineering Science and Technology, an International Journal

journal homepage: www.elsevier.com/locate/jestch

Full Length Article

Comprehensive study on machinability of sustainable and conventional fibre reinforced polymer composites

Sikiru Oluwarotimi Ismail [a,*], Hom Nath Dhakal [a], Ivan Popov [a], Johnny Beaugrand [b,c]

[a] School of Engineering, University of Portsmouth, Portsmouth, Hampshire PO1 3DJ, United Kingdom
[b] INRA, UMR614 Fractionnement des AgroRessources et Environnement, F-51686 Reims, France
[c] Université de Reims Champagne-Ardenne, UMR614 Fractionnement des AgroRessources et Environnement, F-51100 Reims, France

ARTICLE INFO

Article history:
Received 21 February 2016
Revised 7 July 2016
Accepted 18 July 2016
Available online 21 August 2016

Keywords:
Fibre reinforced composites (FRCs)
Machinability
Drilling parameters
Delamination
Surface roughness
Optimal drilling

ABSTRACT

The conventional homogeneous materials can no longer effectively satisfy the growing demands on product capabilities and performance, due to the advancement in products design and materials engineering. Therefore, the fibre reinforced composites (FRCs) with better properties and desirable applications emerged. These enhanced qualities of the FRCs have emphasized the need for analysing their machinability for further improvement of performance. Hence, this paper presents a comprehensive investigation on the machinability effects of drilling parameters (feed rate, cutting speed and thrust force), drill diameters and chips formation mainly on delamination and surface roughness of hemp fibre reinforced polymer (19/HFRP) and carbon fibre reinforced polymer (MTM 44-1/CFRP) composite laminates, using high speed steel (HSS) drills under dry machining condition. The results obtained depict that an increase in feed rate and thrust force caused an increase in delamination and surface roughness of both samples, different from cutting speed. Also, increased drill diameter and types of chips formation caused an increase in both delamination and surface roughness of both samples, as the material removal rate (MRR) increased. Evidently, the minimum surface roughness and delamination factor of the two samples for an optimal drilling are associated with feed rates of 0.05–0.10 mm/rev and cutting speed of 30 m/min.

1. Introduction

Recently, there has been growing interest in the composites technology. The composites technology has enabled the production of outstanding FRCs with respects to better damage tolerance, impact resistance, toughness, sustainability, renewability, strength, electromagnetic transparency, biodegradability, environmental superiority, cost and ease of productions, part count reduction, stiffness, design flexibility, low weight, mechanical damping, strength properties as well as chemical, thermal, high corrosion and wear resistance when compared with the conventional metallic engineering materials [1–6]. These desirable general inherent and better properties have increased the areas of application of these heterogeneous materials as both functional and structural components. The areas of application include, but are not limited to, telecommunication, automotive, oil and gas, building and construction, sports and recreation, aviation, biomedical, marine (naval), electronics, defense or military, power generation, consumer products, food and packaging industries [1–4,7–15]. Also, the environmental and economic global treats today have called for the production of natural fibre reinforced, bio-resourced and sustainable composite materials as a substitute for a synthetic (conventional) fibre reinforced polymer (FRP) composites [5,10]. For instance, based on the directive issued by the European Union, it requires that the greatest percentage of 85%, followed by 10% and just only 5% of all new automobiles should be reusable (recyclable) by weight, for energy recovery and used in landfills respectively, starting from year 2015 [16]. However, the application of some synthetic fibre reinforced composites has not been totally replaced with the natural fibre reinforced composites in engineering structures, because of the remarkable properties of these synthetic or conventional FRCs which include, but are not limited to, relative high tensile and impact strengths, strong fibre–matrix interface adhesion and high melting points.

The hemp fibre is a bast lignocellulosic natural fibre, which reinforced a fully biodegradable thermoplastic matrix, known as polycaprolactone (PCL), while the carbon fibre is an inorganic and synthetic fibre, which reinforced a non-biodegradable

* Corresponding author.
E-mail addresses: sikiruismail@port.ac.uk (S.O. Ismail), hom.dhakal@port.ac.uk (H.N. Dhakal), ivan.popov@port.ac.uk (I. Popov), johnny.beaugrand@reims.inra.fr (J. Beaugrand).

Peer review under responsibility of Karabuk University.

http://dx.doi.org/10.1016/j.jestch.2016.07.010
2215-0986/

Composites Part B 108 (2017) 45–52

Contents lists available at ScienceDirect

Composites Part B

journal homepage: www.elsevier.com/locate/compositesb

Thermo-mechanical modelling of FRP cross-ply composite laminates drilling: Delamination damage analysis

Sikiru Oluwarotimi Ismail [a, *], Saheed Olalekan Ojo [b], Hom Nath Dhakal [a]

[a] School of Engineering, University of Portsmouth, Portsmouth, England, PO1 3DJ, United Kingdom
[b] IMT School for Advanced Studies Lucca, Piazza San Francesco 19, 55100 Lucca, Italy

ARTICLE INFO

Article history:
Received 13 August 2016
Accepted 29 September 2016
Available online 1 October 2016

Keywords:
Laminate
Delamination
Fracture
Thermo-mechanical
Mix loads condition

ABSTRACT

Among other factors, thrust force, feed rate, twist drill bit chisel edge and point angle are the principal factors responsible for delamination drilling-induced damage during thermo-mechanical deformation. Hence, in this paper, an analytical thermo-mechanical model is proposed to predict critical feed rate and critical thrust force at the onset of delamination crack on CFRP composite cross-ply laminates, using the principle of linear elastic fracture mechanics (LEFM), classical plate theory, cutting mechanics and energy conservation theory. The delamination zone (crack opening Mode I) is modelled as an elliptical plate. The advantages of this proposed model over the existing models in literature are that the influence of drill geometry (chisel edge and point angle) on push-out delamination are incorporated, and mix loads condition are considered. The forces on chisel edges and cutting lips are modelled as a concentrated (point) and uniformly distributed loads, resulting into a better prediction. The model is validated with models in the literature and the results obtained show the flexibility of the proposed model to imitate the results of existing models.

1. Introduction

Fibre reinforced polymer (FRP) composite laminates possess attractive characteristics like chemical resistance, low weight, design flexibility, high strength and high stiffness-to-weight ratio [1–4]. These properties account for manufacturing of structural parts with FRP composite in the aircraft and spacecraft industries, where drilling of the structural parts is frequently encountered for manufacturing either riveted assemblies or structural repairs [1,5,6]. Due to inherent anisotropy and structural inhomogeneity in the FRP composite laminates [3], drilling operation may cause delamination in the structural parts which in turns lowers the bearing strength and stiffness of the structure [7,8]. This consequently impairs the load bearing capacity of the structure. In this context, exit-ply delamination has been identified as the most critical damage phenomenon for structural components [7,9].

Drilling takes an indispensable role among the principal machining operations which include, but are not limited to, milling, turning and boring [10]. It attracts an average of 50% of the total material removal operations [11,12]. The drilling operation is performed by a cutting tool, commonly known as a drill bit. Drill bit, such as twist drill has a multi-cutting parts with different designed complex geometry [10]. The geometric design of drills determines their efficiency and durability (tool life). Consequently, the total quality of the drilled holes depends on the geometry of the drill used. The geometric parts of drill include the point angle, chisel edge/angle, cutting lip [13–16], helix angle, diameter, and web [10]. The resultant effects of these parts are directly on the drilling variables or parameters. These parameters include, but are not limited to, drilling forces such as thrust force and torque [17], cutting force [18], cutting speed, feed rate [10], material removal rate (MRR) and depth of cut [19–21]. Among these variables, feed rate plays a crucial role in determining the quality of drilled holes of FRP composite laminates. It determines the magnitude of a thrust force during drilling operation; thrust force mainly depends on feed rate and chisel edge [22].

To eliminate the problem of delamination in drilling, calculation of the critical thrust force below which no damage occurs is important. To achieve this, classical plate theory approach is employed and assumption of linear elastic fracture mechanics (LEFM) mode I is invoked to determine the amount of work required to initiate and cause propagation of delamination drilling-induced damage in the composite laminates [5–7,9,23–27]. In an

* Corresponding author.
E-mail address: sikiru.ismail@port.ac.uk (S.O. Ismail).

http://dx.doi.org/10.1016/j.compositesb.2016.09.100
1359-8368/

Proceedings of the American Society for Composites 31st Technical Conference, Williamsburg, Virginia, USA, Sept 19-21, 2016

Machining of FRP Composite Laminates with CD and UAD Techniques: A Comparative and Experimental Investigation

S. O. ISMAIL, H. N. DHAKAL, A. ROY, D. WANG and I. POPOV

ABSTRACT

The enhanced properties and increased application of a natural hemp fibre-reinforced polymer (HFRP) composites have emphasized the need for an innovative and a deeper understanding of their machinability in order to further improve their functionality and applicability. Hence, this paper presents a comparative and experimental investigation of the effects of a dry conventional drilling (CD) and hybrid ultrasonically-assisted drilling (UAD) techniques on both hemp fibre-reinforced/polycaprolactone and vinyl ester (HF/PCL and HF/VE) composite samples. The results obtained depict that HF/PCL composite sample of 19 aspect ratio (AR) has a minimum values of peak thrust force of 90N and 75N during UAD and CD respectively, with the lowest machining time of 30seconds for both techniques, among other ARs. These values produced an optimum drilling and best quality drilled holes, in terms of lowest thrust force and resultant drilling-induced damage. It is observed that there was a very little or no thrust force reduction between UAD and CD when drilling the HF/PCL composites. Consequently, PCL was replaced with VE, to produce another sample of HF/VE composites. Therefore, a substantial reduction in drilling forces (thrust force and torque) was obtained during HF/VE drilling, using UAD technique, when compared with the dry CD technique. Comparatively, the percentage of the forces reduction is approximately 70. The quality of the drilled sample depended on these primary forces. In addition, a significant lower ply delamination defect, burr formation, fibre-uncut/pull-out and surface roughness were observed, as well as an improved chip expulsion, hole roundness, material removal rate and surface finish (hole quality) were obtained with UAD, when compared with CD technique. Evidently, a non-traditional hybrid machining technique, UAD, has enhanced machinability (drilling) of HF/VE composite compared with the CD and HF/PCL composite samples.

Keywords: Natural hemp fibre-reinforced polymer (HFRP), Drilling techniques, Thrust force reduction, Hole quality.

Ismail S. Oluwarotimi, Hom N. Dhakal & Ivan Popov, School of Engineering, Faculty of Technology, University of Portsmouth, Portsmouth, Hampshire, PO1 3DJ, United Kingdom.
Anish Roy & Dong Wang, Wolfson School of Mechanical and Manufacturing Engineering, Loughborough University, Loughborough, LE11 3TU, United Kingdom.

Advances in Manufacturing Technology XXX
Y.M. Goh and K. Case (Eds.)
IOS Press, 2016

doi:10.3233/978-1-61499-668-2-143

Analysis and Impacts of Chips Formation on Hole Quality During Fibre-Reinforced Plastic Composites Machining

Sikiru Oluwarotimi ISMAIL[a,1], Hom Nath DHAKAL[a], Ivan POPOV[a] and Johnny BEAUGRAND[b, c]
[a] *Department of Mechanical and Design Engineering, University of Portsmouth, Anglesea Building, Anglesea Road, PO1 3DJ, United Kingdom.*
[b] *INRA, UMR614 Fractionnement des AgroRessourcesetEnvironnement, F-51686 Reims, France*
[c] *Université de Reims Champagne-Ardenne, UMR614 Fractionnement des AgroRessources et Environnement, F-51100 Reims, France*

Abstract. This work presents the effect of chips formation types on the quality of drilled holes of a natural and conventional hemp and carbon fibre-reinforced plastic (HFRP and CFRP) composites respectively. The results depict that variation in chips morphology depends on drilling parameters, drill geometry and compositions of composites (matrix and fibre properties). HFRP samples produced continuous brown ribbon-like chips, which were short and melted at lower feed rate and cutting speed, implying that higher feed rate and cutting speed produced wider, longer and lighter chips. CFRP samples generated discontinuous black powder-like chips, with small and abrasive chips at the same applied drilling parameters. These formations and morphology affected quality of drilled holes: lower surface roughness in CFRP, but lower delamination and drill wear in HFRP samples. Evidently, an increased feed rate, cutting speed and drill diameter caused an increase in chips formation, validating the material removal rate (MRR) model results.

Keywords. Reinforced plastics, drilling parameters, chips formation types, quality of drilled holes.

1. Introduction

The increasing applications of different types of fibre-reinforced plastic (FRP) composite materials in a various sectors of engineering has necessitated a wider and detailed research on machining of these composites. The FRP composites have some inherent desirable and outstanding physical and mechanical properties that attracted for numerous applications. However, the combination of a softer polymer (matrix) and harder reinforcement (fibre) makes the machining of FRP composite materials quite different from the drilling of a conventional metals and their alloys, as reported by Lin

[1] Corresponding Author. sikiru.ismail@port.ac.uk

5th Conference on Natural Fibre Composites for Industrial Applications, Rome 15-16 October 2015

Experimental analysis of drilling-induced damage of lignocellulosic 19/hemp fibre reinforced polycaprolactone and MTM 44-1/carbon fibre reinforced epoxy resin composites

Sikiru Oluwarotimi Ismail[1, a], Hom Nath Dhakal [1, b], Ivan Popov [1, c], Johnny Beaugrand [2, 3, d]

[1]Department of Mechanical and Design Engineering, University of Portsmouth,

Anglesea Building, Anglesea Road, PO1 3DJ, United Kingdom.

[2]INRA, UMR614 Fractionnement des AgroRessourcesetEnvironnement, F-51686 Reims, France

[3]Université de Reims Champagne-Ardenne, UMR614 Fractionnement des AgroRessources et Environnement, F-51100 Reims, France

[a]sikiru.ismail@port.ac.uk, [b]hom.dhakal@port.ac.uk, [c]ivan.popov@port.ac.uk, [d]johnny.beaugrand@reims.inra.fr

Keywords: Fibre reinforced composites (FRCs); machinability; Drilling parameters; Delamination; Surface roughness.

Abstract. The conventional homogeneous materials cannot longer satisfy the growing demands on product capabilities and performance effectively due to the advancement in products design and materials engineering. Therefore, the fibre reinforced composites (FRCs) with better properties and desirable applications emerged. These enhanced qualities of the FRCs have emphasized the need for analysing their machinability for further improvement of performance. Hence, this paper presents a comparative investigation on the effects of drilling parameters on delamination and surface roughness of 19/HFRP and MTM 44-1/CFRP composite laminates, using HSS drills under dry machining. The results obtained depict that increase in feed rate caused an increase in delamination and surface roughness of both specimens, unlike cutting speed. Generally, the minimum surface roughness and delamination factor of the two specimens for the optimum drilling were associated with feed rates of 0.05-0.10mm/rev and cutting speed of 30m/min.

Introduction

The composites technology came up to produce outstanding fibre reinforced composites (FRCs) with respects to better damage tolerance, impact resistance, toughness, sustainability, renewability, strength, electromagnetic transparency, biodegradability, environmental superiority, cost and ease of productions, part count reduction, stiffness, design flexibility, low weight, mechanical damping, strength properties as well as chemical, thermal, corrosion and wear resistance when compared with the conventional metallic engineering materials [1, 2]. These desirable general inherent and better properties have increased the areas of application of these anisotropic materials as both functional and structural components. The areas of application include telecommunication, automotive, power, oil and gas, building and construction, sports and recreation, aviation, biomedical, marine, electronics, defense, food and packaging industrials [1, 2, 3, 4]. Also, the environmental and economic global treats today have called for the production of natural fibre reinforced, bio-resourced and sustainable composite materials. For instance, based on the directive gave by the European Union that the greatest percentage of 85%, followed by 10% and just only 5% of all new automobiles should be reusable (recyclable) by weight, for energy recovery and used in landfills respectively, starting from year 2015 [5]. The hemp fibre reinforced polymer (HFRP) is an example of a natural fibre reinforced composite, while carbon fibre reinforced polymer (CFRP) is synthetic.

The quality and the integrity of the holes obtained during drilling of various fibre reinforced composite laminates are quite different from that of drilled metals. The drilled metal surfaces are

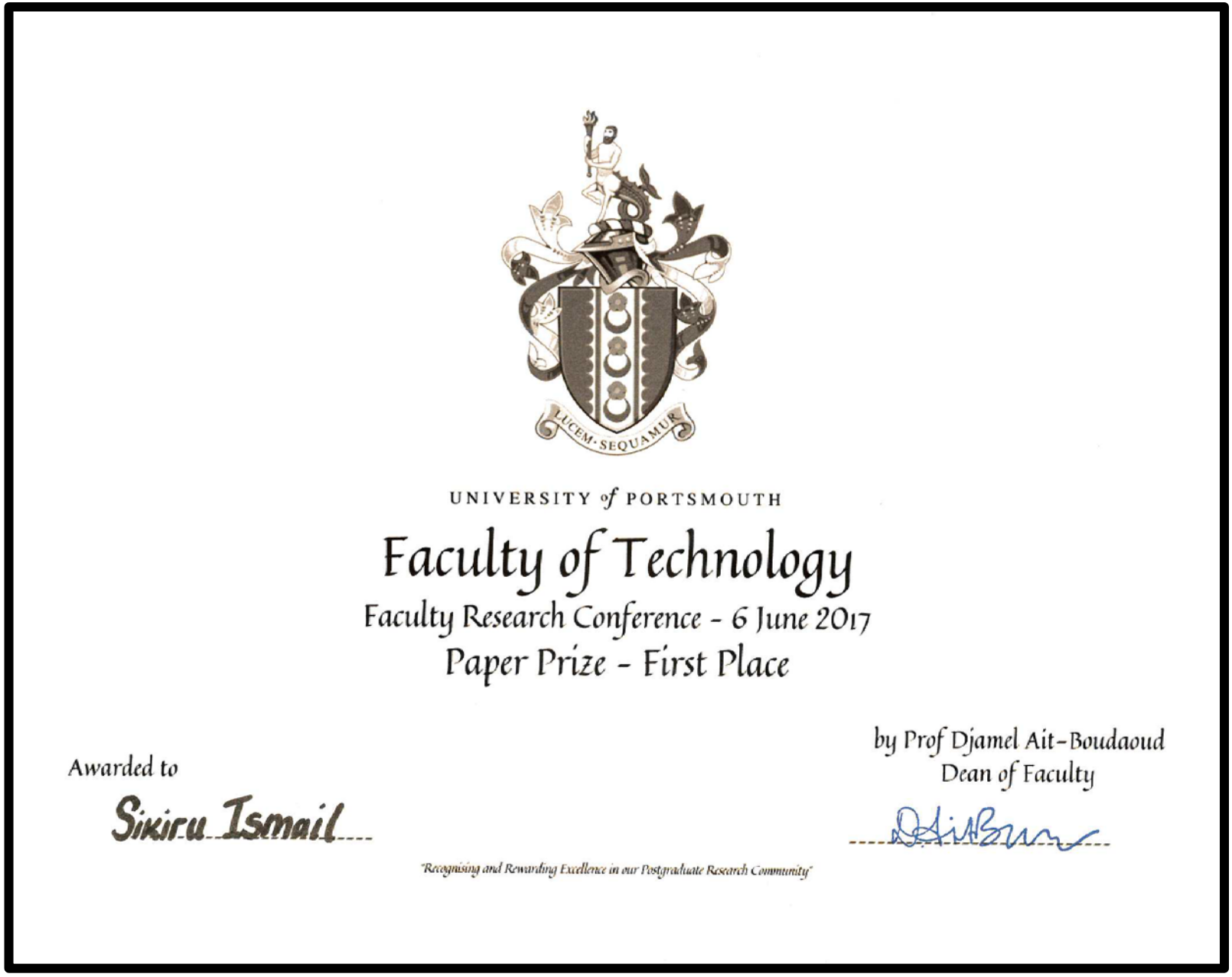

UNIVERSITY of PORTSMOUTH

Faculty of Technology

Faculty Research Conference - 6 June 2017

Paper Prize - First Place

Awarded to

Sikiru Ismail

by Prof Djamel Ait-Boudaoud
Dean of Faculty

"Recognising and Rewarding Excellence in our Postgraduate Research Community"

UNIVERSITY of PORTSMOUTH

FACULTY OF TECHNOLOGY
SCHOOL OF ENGINEERING

ACADEMIC YEAR 2016/2017

Best Student Paper in the School of Engineering

Awarded to

Sikiru O Ismail

Professor Asa Barber
Head of School

Dr David Sanders TD
Research Degrees Coordinator

UNIVERSITY of PORTSMOUTH

Faculty of Technology

Faculty Research Conference – 7 June 2016

Paper Prize – Highly commended

by Prof Djamel Ait-Boudaoud
Dean of Faculty

Awarded to

Sikiru Ismail

"Recognising and Rewarding Excellence in our Postgraduate Research Community"

INTRODUCTION

- ❑ Drilling is a process of using a rotating multi-point tool or drill bit to create or enlarging existing round holes in a workpiece as shown in Fig. 1.
- ❑ In a manufacturing industry, drilling is one of the most regularly used machining processes.
- ❑Drilling takes about 1/4 of the total machining time and 33% of all the total machining operations of a manufacturing process.
- ❑ Twist drill bits are the most frequently and extensively used material cutting tools.
- ❑ Due to the complex geometry of the twist drill (Fig.2) and rapid invention of various workpieces (composites) the design of an efficient and powerful twist drill still remains a very difficult task even after twenty decades of invention.

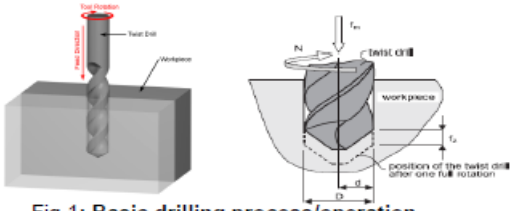

Fig.1: Basic drilling process/operation

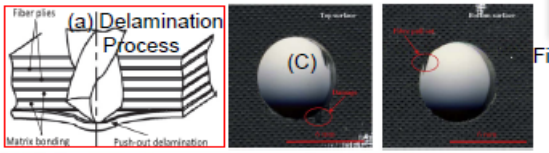

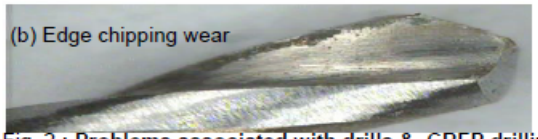

Fig. 2 : Problems associated with drills & CRFP drilling.

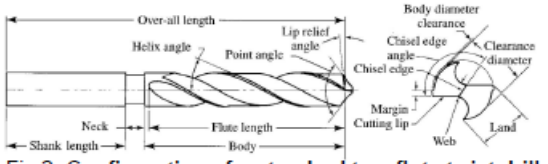

Fig.2: Configuration of a standard two-flute twist drill.

MATERIALS AND METHODS

- ❑ **Geometric Design** as shown in Fig. 2.
- ❑ **Drill Material Design (coated & uncoated types)** as depicted in Figs.4 & 5.
  - **Problems associated with twist drills** as shown in Fig. 2 (b).
  - **Problems associated with composite drilling** as shown in Fig. 2 (a) & (c).
- ❑ **Parametric Design(Drilling variables** as shown in Figs. 3 & 6.

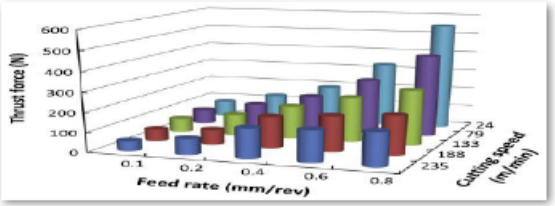

Fig. 3: Parametric effect of Speed & feed on thrust force.

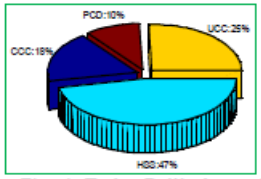

Fig. 4: Twist Drills by applications.

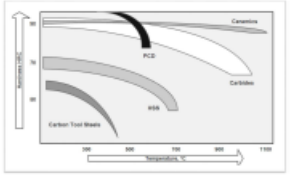

Fig. 5: Drill material hardness and temperature relationship.

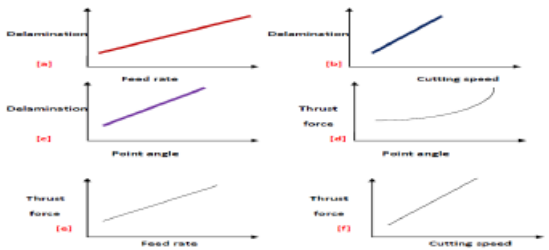

Fig.6: Effect of input variables on delamination ([a], [b] & [c]) and thrust force ([d], [e] & [f]) .

Table 1: Maximum interface normal stresses for different twist drill point and helix angles.

Point angle(°)	90	118	135
σ_{rmax}(GPa)	1.217	1.227	1.234
$\sigma_{\theta max}$(GPa)	2.78	2.89	2.94
Helical angle (°)	20	30	40
σ_{rmax}(GPa)	1.24	1.23	1.21
$\sigma_{\theta max}$(GPa)	3.05	2.89	2.73

CONCLUSION

❑Drilled hole quality and twist drill life depend significantly on cutting parameters and drill designs (material and geometry).

❑ Delamination of composites and rapid tool wear are typical main problems encountered when drilling CFRP accounting for drilling-induced damages as high as 60%.

❑ PCD provides good surface finish at high cutting speed and feed rate.

❑ Improved surface quality and dimensional accuracy of composite materials could be achieved using carbide especially coated types and PCD drills.

University of Portsmouth

RECENT ADVANCES IN TWIST DRILL DESIGN: A CRITICAL REVIEW

Course: **PhD Mechanical Engineering**

Name: Sikiru Oluwarotimi ISMAIL, 642881

Supervisory Team: Dr. Eric Dimla, Dr. Ivan Popov & Dr. H. Dhakal

School of Engineering

GRADUATE SCHOOL RESEARCH POSTER COMPETITION 2015

INTRODUCTION

- Chips are generated immediately the composite materials undergo a **plastic deformation**, generally at the drill-material slipping interface within a **shearing region**
- During the chip formation, neither dust-like nor very long continuous chips are encouraged during drilling operations.
- The powdery chips from the CFRP composites are not easily evacuated from the drill flutes causing **chip clogging** due to high friction and forces while the long **continuous chips** often results into serious chip evacuation predicaments.
- These problems have high propensity of causing decrease in **drilled holes quality**, tool (**drill**) **life** and **drill breakage** if they are not properly managed.

MATERIALS AND METHODS

- **Materials**
  - ❑ 19/Hemp fibre-reinforced polymer (**HFRP**), extruded composite laminate, with aspect ratio of 19.
  - ❑ MTM 44-1/Carbon fibre-reinforced polymer (**CFRP**) composite laminate, UD, oven cure & OoA moulding.
- **Experimental Methods**
  - ❑ L_{16} 4^2 orthogonal array of Taguchi method of design of experiment, under dry machining condition.

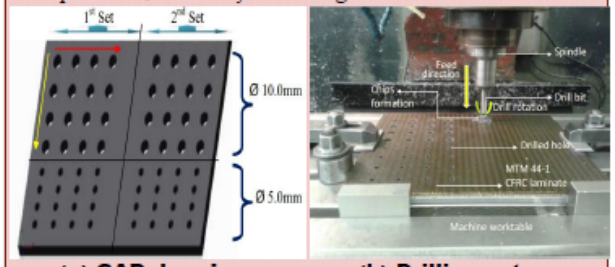

(a) CAD drawing **(b) Drilling set-up**

Fig.1.0: **Machining experimental procedures.**

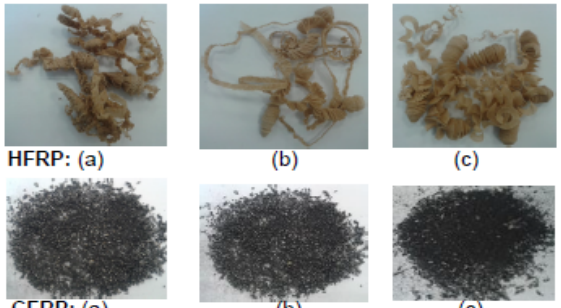

Fig.2.0: **Chips morphology at: (a) f = 0.05 & v = 10; (b) f = 0.15 & v = 30; (c) f = 0.20mm/rev & v = 40m/mm**

RESULTS AND DISCUSSION

❑ The chips formation increased during drilling of the specimens at increased feed rate & cutting speed, which was well prominent at 0.20mm/rev and 40m/min feed rate & cutting speed resp.; the higher the feed rate & cutting speed, the wider, longer & lighter the chips. In 19/HFRP, short & melted chips formed at lower feed rate & cutting speed (Fig. 2.0a), but finer & dusty in MTM 44-1/CFRP comp.

❑ **Material Removal Rate (MRR) Model formulation**

- $N_i = \frac{1000V}{\pi D}$ & $MRR = \frac{\pi D^2 f N_i}{4}$
- $MRR = 250\,DfV$

Where N= spindle revolution (rpm), V= Cutting speed (m/min), f = feed rate (mm/rev), i = D= drill diameters (5.0 and 10.0mm), and π = a constant. *Table 1.0 shows the model results.*

Table 1.0: Experimental drilling parameters and Material Removal Rate performance.

Test No	Cutting Speed, V(m/min)	Feed Rate, f(mm/rev)	Material Removal Rate, MRR (mm^3/min) Diameter (mm) 5.0	10.0
1	10	0.05	625	1250
2		0.10	1250	2500
3		0.15	1875	3750
4		0.20	2500	5000
5	20	0.05	1250	2500
6		0.10	2500	5000
7		0.15	3750	7500
8		0.20	5000	10000
9	30	0.05	1875	3750
10		0.10	3750	7500
11		0.15	5625	11250
12		0.20	7500	15000
13	40	0.05	2500	5000
14		0.10	5000	10000
15		0.15	7500	15000
16		0.20	10000	20000

CONCLUSION

❑ A **continuous brown ribbon-like chips** formed during the drilling of 19/HFRP specimen, while the size of the MTM 44-1/CFRP **discontinuous black chips** generated was very small, fine, powdery and abrasive in nature, due to the properties of their matrices.

❑ These produced a lower **surface roughness** in the CFRP, **delamination** & **drill wear** in 19/HFRP.

❑ The chips formed increased when the **drill diameter**, **cutting speed** and **feed rate** were increased, but significantly characterised by the feed rate, which agreed with the MRR model results, as depicted in Table 1.0.

❑ The black chips formation in MTM 44-1/CFRP has a less strain, with a better surface finish as a brittle material

University of Portsmouth

COMPARATIVE EXPERIMENTAL STUDY ON EFFECTS OF CHIPS FORMATION DURING 19/HFRP AND MTM 44-1/CFRP COMPOSITES MACHINING.

Course: **PhD Mechanical Engineering**
Name: Sikiru Oluwarotimi ISMAIL, 642881
Supervisory Team: Dr. Hom N. Dhakal, Dr. Ivan Popov.
Faculty of Technology

GRADUATE SCHOOL RESEARCH POSTER COMPETITION 2015

INTRODUCTION

- **Composites** have become attractive materials today with various **desirable properties** and **applications**.
- After many decades of developments of composites manufacturing technology, the desire to improve the machining of these materials based on the numerous areas of application remains a quest.
- **Drilling** of composite laminates has several *common problems*. These defects include delamination, surface scorching, excessive tool wear, fibre cratering, matrix-melting and softening (poor hole quality).
- This study aims at analysing two of these problems.

MATERIALS AND METHODS

❑ Materials

- 19/Hemp fibre-reinforced polymer (**HFRP**), extruded composite laminate with aspect ratio (AR) of 19.
- **MTM 44-1**/Carbon fibre-reinforced polymer (**CFRP**) composite laminate, unidirectional (UD), oven cure & OoA moulding.

❑ Experimental Methods

- $L_{16}4^2$ orthogonal array of **Taguchi method** of design of experiment, under dry machining condition.

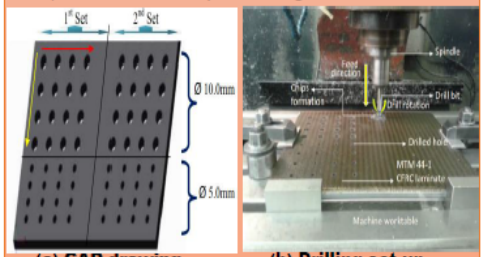

(a) CAD drawing (b) Drilling set-up

Fig.1.0: **Machining experimental procedures.**

❑ Measurement Procedures

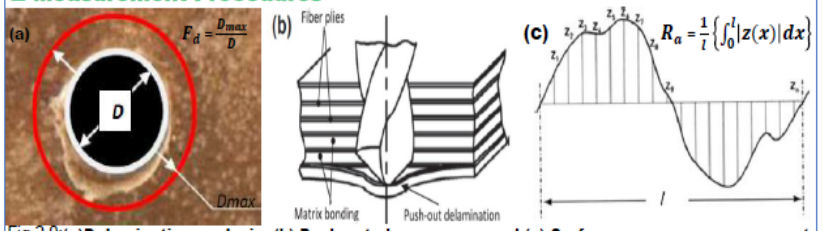

Fig.2.0: **(a)Delamination analysis; (b) Push-out phenomenon; and (c) Surface response measurement**

RESULTS AND DISCUSSION

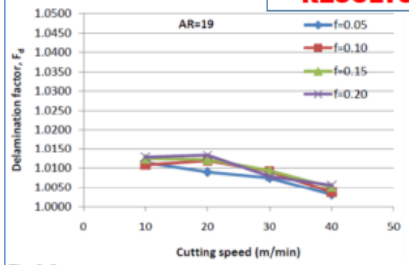

Fig.3.0: **Effects of drilling parameters & *AR* on F_d**

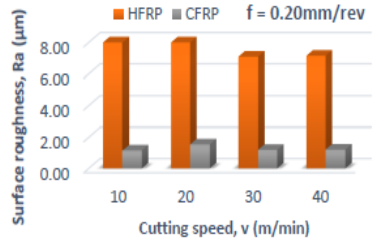

Fig.4.0: **Effects of drilling parameters & mtl on R_a**

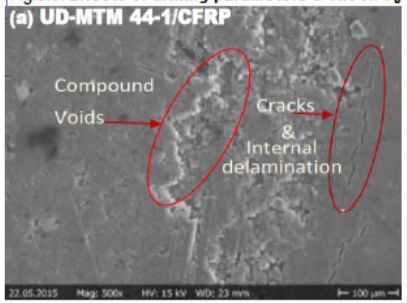

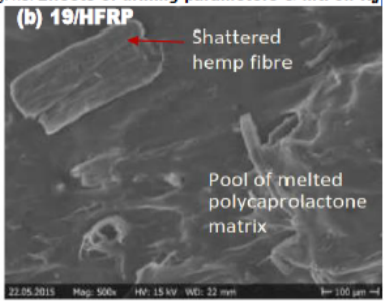

Fig.5.0: **SEM of the specimens holes of 5.0mm diameter drilled at f = 0.15mm/rev and v = 30m/min**

- The SEM (Fig.5.0) depicts that the waved peaks and deep valleys observed in the profile of the drilled surfaces of both HFRP & CFRP laminates were caused as a result of **matrix melting**. This melting is more significant in the HFRP, probably due to the lower glass transition temperature of HFRP matrix (*polycaprolactone*) compared with that of CFRP (*epoxy resin*).

CONCLUSIONS

- The increase in **feed rate** caused an increase in delamination & surface roughness of both specimens. Conversely, the increase in **cutting speed** decreased the delamination of both specimens. But, the increase in cutting speed caused an increase in the surface roughness of the CFRP composite & decrease in the surface roughness of the HFRP composite specimen.
- Feed rate has the greatest significant effect on both surface roughness & delamination, tailed by the cutting speed & **drill bit diameter**. The CFRP composite has a better surface roughness, while the HFRP composite exhibited lower delamination defect. These responses determine the choice of their applications.

FUTURE WORKS

- Conduct Ultrasonic Assisted Drilling (UAD) for comparison;
- Statistical and geometric modelling of the experimental data & drill design respectively;
- Publication of journal, conference articles & Writing of thesis/doctoral Viva Voce examination.

University of Portsmouth

MACHINABILITY ANALYSIS AND DRILL DESIGN OPTIMISATION OF FIBRE-REINFORCED COMPOSITES DRILLING

Course: **PhD Mechanical Engineering**
Name: **Sikiru Oluwarotimi ISMAIL, 642881**
Supervisory Team: **Dr. Hom N. Dhakal, Dr. Ivan Popov.**
Faculty of Technology

PROBLEMS ASSOCIATED WITH FIBRE-REINFORCED COMPOSITES ULTRASONICALLY-ASSISTED DRILLING

University of Portsmouth

Course: **PhD Mechanical Engineering**

Presenter: Sikiru Oluwarotimi ISMAIL

Co-authors: Dr Hom Nath Dhakal, Dr Ivan Popov.

Faculty of Technology

INTRODUCTION

- **Composites,** particularly the natural fibre-reinforced composites such as hemp fibre-reinforced polymer/polycaprolactone **(HFRP/PCL)** have become attractive materials today with various **desirable properties** and **applications** (Ismail et al., 2015).
- The ultrasonically-assisted drilling **(UAD)** has remarkable advantages over the conventional drilling **(CD)**, especially in achieving high drilling-force reduction and excellent drilled surface finish.
- These advantages are contributing factors for the quality of the drilled holes.
- This study revealed that the benefits of UAD are difficult to obtain for the drilling of the HFRC/PCL.

MATERIALS AND METHODS

❑ Materials (workpiece/sample)

- HFRP/PCL, extruded composite laminate with aspect ratios (AR) of 00 (neat), 19, 26, 30 and 38 (Fig. 1.0b).

❑ Experimental Methods/Design.

- $L_{16}4^2$ orthogonal array of **Taguchi method** (Fig. 1.0a).
- UD and UAD techniques, using high speed steel (HSS) drill bit.

Table 1.0: Drilling Parameters and Conditions.

Drilling Parameter	Symbol	Machining Technique CD	Machining Technique UAD	Unit
Drill bit diameter	Ø	6.00	6.00	mm
Spindle speed	N	40.00	40.00	rev/min
Feed rate	f	0.1 (10%)	0.1 (10%)	mm/rev
Cutting speed	v	0.75	0.75	m/min
Vibration frequency	F	-----	24.75	kHz
Vibration amplitude (peak to peak) at the tip of drill bit	α	-----	8.00	µm
Condition	----	Dry	Dry	-----

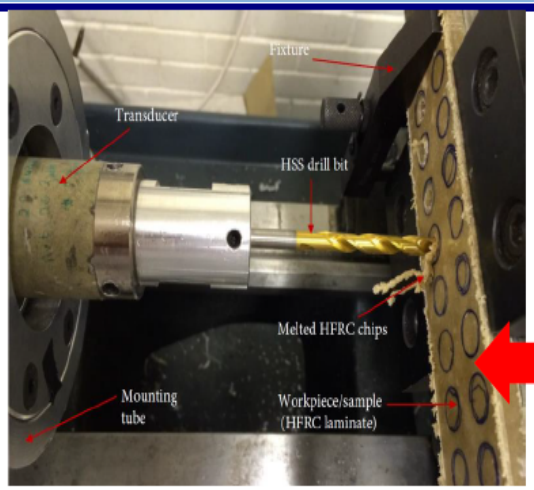

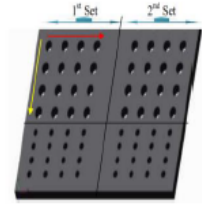

(a) CAD drawing

(b) HFRP/PCL laminate

Fig. 1.0: The CD and UAD (machining) experimental set-up and (a) & (b) samples.

RESULTS AND DISCUSSIONS

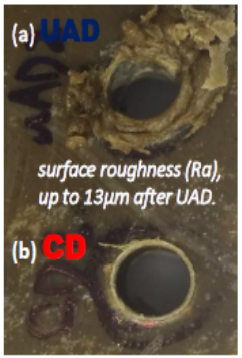

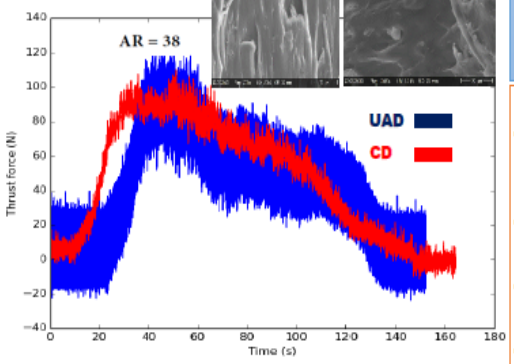

Fig. 2.0: Poor surface quality and insignificant force reduction during UAD of HFRP/PCL (natural/biodegradable composites with polycaprolactone matrix).

- In addition to the **expensiveness of set-up, unpredictable results** and **drill bit chipping effects** of UAD, Figure 2.0a depicts greater **poor surface quality** during UAD when compared with the CD (Fig. 2.0b), even at variable drilling parameters (Table 1.0) and AR.
- A huge occurrence of matrix-melting was observed, resulting into poor burnt-chip evacuation, due to the 60°C melting temperature of PCL (Speranza et al., 2014), quite lower than 56-90.2°C & 265–290.8°C composite-tool interface temperature during CD & UAD respectively (Makhdum et al., 2014), and above 200°C thermal degradation or decomposition of natural fibres including hemp fibres (Mallick, 2008).

CONCLUSIONS

- The two observable effects produced a very high average surface roughness (Ra), up to 13µm.
- Evidently, the drilling-induced damage on HFRP/PCL composite depends greatly on the composite constituents (fibres and matrix) and drilling techniques.
- Hence, the choice of drilling technique and engineering applications of the drilled HFRC/PCL laminates should depend on their responses to these damage, as UAD techniques could not benefit significantly.

REFERENCES

- Ismail S.O., Dhakal H.N., Dimla E., Beaugrand J., Popov I. (2016). The effects of drilling parameters & aspect ratios on delamination & surface roughness of lignocellulosic HFRP composites. *J. of Applied Polymer Science, 133 (7), 1-8,* DOI:10.1002/app.42879, published early view/on-line.
- Speranza V., Sorrentino A., De Santis F., Pantani R.(2014). Characterization of PCL melt crystallization: Complementary optical micros., DSC&AFM studies. *Scient. World J.*, 2014, 1-9.
- Makhdum, F.; Phadnis, V. A.; Roy, A.; Silberschmidt, V. V. (2014). Effect of ultrasonically-assisted drilling on carbon-fibre-reinforced plastic. *J. Sound Vibration*, 333, 5939–5952.
- Mallick, P. K. (2008). Fibre-reinforcement composites, materials, manufacturing and design. Third edition, CRC Press, Taylor and Francis Group, USA, pp. 1- 619.

Poster Presentations 2

Elizabeth Buckingham-Jeffery e.m.buckingham-jeffery@warwick.ac.uk	Syndromic Surveillance	University of Warwick
James Cameron j.cameron@mmu.ac.uk	Changes in Muscle Size and Function During a 5 Year Longitudinal Study in Older Men and Women	Manchester Metropolitan University
Lin Charlston lin.charlston@stu.mmu.ac.uk	Investigating Plant-Related Signs in an Urban Context through Multimodal Book-Art: A Practice-Based Ecosemiotic Approach	Manchester Metropolitan University
Julie Connolly j.connolly@ljmu.ac.uk	Surviving Carbon Monoxide Poisoning	Liverpool John Moores University
Sikiru Oluwarotimi Ismail sikiru.ismail@port.ac.uk	Problems Associated with Fibre-Reinforced Composites Ultrasonically-Assisted Drilling	University of Portsmouth
Aveen Haji Mam p100004263@myemail.dmu.ac.uk	The Effect of an Educational Program on Pregnancy Outcomes among Obese Women in Kurdistan Region.	De Montfort University
Tracy Hayes tracy.hayes@cumbria.ac.uk	A Creative Exploration of Young People's Relationship with Nature	University of Cumbria
Peri Korshed peri.korshed@postgrad.manchester.ac.uk	The Molecular Mechanism of Antimicrobial Properties of Laser Processed Nano-Particles	University of Manchester
Elizabeth Lewis Elizabeth.lewis2@stu.mmu.ac.uk	Managing Adult Social Care Effectively: Are Human Resource Management and Development Integral?	Manchester Metropolitan University
Luz Helena Loguercio luz.loguercio@stu.mmu.ac.uk	Music as a Vehicle Towards the Integration of Immigrants to the Community	Manchester Metropolitan University
Ben Marshall b.marshall@mmu.ac.uk	A Comparison of the Effects of Layered Stimulus Response Training and Combined Observation and Imagery of Golf Putting Performance, Imagery Ability and Task Self-Efficacy	Manchester Metropolitan University
Gillian Mooney ss13gsm@leeds.ac.uk	Social Class / Social Networking	University of Leeds
Niazi Nazhad niazinazhad@yahoo.co.uk	The Molecular Mechanism of Antimicrobial Properties of Laser Processed Nano-Particles	Manchester Metropolitan University
Nicholas Opiyo elno@leeds.ac.uk	Modelling Factors Affecting Temporal Diffusion of PV Microgeneration Systems in a Rural Developing Community	University of Leeds
Sevendy Patchamuthu sp2e12@soton.ac.uk	Critical Thinking Skills for ESAP Engineering: A Research into Theory, Practice and the Development of Critical Thinking Skills Within Foundation Engineering Programme	University of Southampton
Zaynab Rabbee zaynabrabee@hotmail.co.uk	Skype: An Innovative Method of Data Collection for Qualitative Interviews?	Manchester Metropolitan University

University of Portsmouth

Certificate of Ethics Review

Project Title:	MACHINABILITY ANALYSIS OF DRILLING-INDUCED DAMAGE ON FIBRE-REINFORCED POLYMER COMPOSITE LAMINATES
User ID:	642881
Name:	Sikiru Oluwarotimi Ismail
Application Date:	26/10/2016 13:06:55

You must download your certificate, print a copy and keep it as a record of this review.

It is your responsibility to adhere to the University Ethics Policy and any Department/School or professional guidelines in the conduct of your study including relevant guidelines regarding health and safety of researchers and University Health and Safety Policy.

It is also your responsibility to follow University guidance on Data Protection Policy:

- General guidance for all data protection issues
- University Data Protection Policy

You are reminded that as a University of Portsmouth Researcher you are bound by the UKRIO Code of Practice for Research; any breach of this code could lead to action being taken following the University's Procedure for the Investigation of Allegations of Misconduct in Research.

Any changes in the answers to the questions reflecting the design, management or conduct of the research over the course of the project must be notified to the Faculty Ethics Committee. **Any changes that affect the answers given in the questionnaire, not reported to the Faculty Ethics Committee, will invalidate this certificate.**

This ethical review should not be used to infer any comment on the academic merits or methodology of the project. If you have not already done so, you are advised to develop a clear protocol/proposal and ensure that it is independently reviewed by peers or others of appropriate standing. A favourable ethical opinion should not be perceived as permission to proceed with the research; there might be other matters of governance which require further consideration including the agreement of any organisation hosting the research.

GovernanceChecklist
A1-BriefDescriptionOfProject: The aims of this present research was to experimentally and analytically analyse the machinability of a natural (hemp) and conventional (carbon) fibre-reinforced polymer (FRP) composites as well as the causes of their drilling-induced damage, for the purpose of optimising the FRP composites drilling.
A2-Faculty: Technology
A3-VoluntarilyReferToFEC: No
A5-AlreadyExternallyReviewed: No

Certificate Code: 160B-0165-5010-035F-29DD-7D66-6BBF-12CC Page 1

B1-HumanParticipants: No
HumanParticipantsDefinition
B2-HumanParticipantsConfirmation: Yes
B4-InvolvesNHSPatients: No
B5-NoConsentOrDeception: No
B7-InvolvesUninformedOrDependents: No
B9-FinancialInducements: No
C1-DrugsPlacebosOrOtherSubstances: No
C2-BloodOrTissueSamples: No
C3-PainOrMildDiscomfort: No
C4-PsychologicalStressOrAnxiety: No
C5-ProlongedOrRepetitiveTesting: No
C6-SafetyRisksBeyondAssessment: No
D2-PhysicalEcologicalDamage: No
PhysicalEcologicalDamageWarning
D4-HistoricalOrCulturalDamage: No
HistoricalOrCulturalDamageWarning
E1-ContentiousOrIllegal: No
ContentiousOrIllegalWarning
E2-SociallySensitiveIssues: No
SociallySensitiveWarning
F1-InvolvesAnimals: No
InvolvesAnimalsWarning
F2-HarmfulToThirdParties: No
HarmfulToThirdPartiesWarning
G1-ConfirmReadEthicsPolicy: Confirmed
G2-ConfirmReadUKRIOCodeOfPractice: Confirmed
G3-ConfirmReadConcordatToSupportResearchIntegrity: Confirmed
G4-ConfirmedCorrectInformation: Confirmed

Certificate Code: 160B-0165-5010-035F-29DD-7D66-6BBF-12CC Page 2

FORM UPR16

Research Ethics Review Checklist

University of Portsmouth

Please include this completed form as an appendix to your thesis (see the Postgraduate Research Student Handbook for more information

Postgraduate Research Student (PGRS) Information			Student ID:	642881
PGRS Name:	SIKIRU OLUWAROTIMI ISMAIL			
Department:	ENGINEERING	First Supervisor:	DR. HOM NATH DHAKAL	
Start Date: (or progression date for Prof Doc students)	OCTOBER, 2013			
Study Mode and Route:	Part-time ☐ Full-time ☒	MPhil ☐ PhD ☒	MD ☐ Professional Doctorate ☐	

Title of Thesis:	MACHINABILITY ANALYSIS OF DRILLING-INDUCED DAMAGE ON FIBRE-REINFORCED POLYMER COMPOSITES
Thesis Word Count: (excluding ancillary data)	56,891

If you are unsure about any of the following, please contact the local representative on your Faculty Ethics Committee for advice. Please note that it is your responsibility to follow the University's Ethics Policy and any relevant University, academic or professional guidelines in the conduct of your study

Although the Ethics Committee may have given your study a favourable opinion, the final responsibility for the ethical conduct of this work lies with the researcher(s).

UKRIO Finished Research Checklist:
(If you would like to know more about the checklist, please see your Faculty or Departmental Ethics Committee rep or see the online version of the full checklist at: http://www.ukrio.org/what-we-do/code-of-practice-for-research/)

a)	Have all of your research and findings been reported accurately, honestly and within a reasonable time frame?	YES ☒ NO ☐
b)	Have all contributions to knowledge been acknowledged?	YES ☒ NO ☐
c)	Have you complied with all agreements relating to intellectual property, publication and authorship?	YES ☒ NO ☐
d)	Has your research data been retained in a secure and accessible form and will it remain so for the required duration?	YES ☒ NO ☐
e)	Does your research comply with all legal, ethical, and contractual requirements?	YES ☒ NO ☐

Candidate Statement:

I have considered the ethical dimensions of the above named research project, and have successfully obtained the necessary ethical approval(s)

Ethical review number(s) from Faculty Ethics Committee (or from NRES/SCREC):	160B-0165-5010-035F-29DD-7D66-6BBF-12CC

If you have *not* submitted your work for ethical review, and/or you have answered 'No' to one or more of questions a) to e), please explain below why this is so:

Signed *(PGRS)*:		Date: 30 - 11 - 2016

UPR16 – August 2015